

Distribution Agreement

In presenting this thesis or dissertation as a partial fulfillment of the requirements for an advanced degree from Emory University, I hereby grant to Emory University and its agents the non-exclusive license to archive, make accessible, and display my thesis or dissertation in whole or in part in all forms of media, now or hereafter known, including display on the world wide web. I understand that I may select some access restrictions as part of the online submission of this thesis or dissertation. I retain all ownership rights to the copyright of the thesis or dissertation. I also retain the right to use in future works (such as articles or books) all or part of this thesis or dissertation.

Signature:

Michael A. Martin

Date

Leveraging genomic and genetic diversity to gain insights into viral evolution and spread

By

Michael A. Martin
Doctor of Philosophy

Population Biology, Ecology, and Evolution

Katharina Koelle, Ph.D.
Advisor

Anice Lowen, Ph.D.
Committee Member

Anne Piantadosi, M.D., Ph.D.
Committee Member

Timothy Read, Ph.D.
Committee Member

Daniel Weissman, Ph.D.
Committee Member

Accepted:

Kimberly Jacob Arriola, Ph.D.
Dean of the James T. Laney School of Graduate Studies

Date

Leveraging genomic and genetic diversity to gain insights into viral evolution and spread

By

Michael A. Martin
B.A., Johns Hopkins University, 2013
M.S., Harvard T.H. Chan School of Public Health, 2018

Advisor: Katharina Koelle, Ph.D.

An abstract of
A dissertation submitted to the Faculty of the
James T. Laney School of Graduate Studies of Emory University
in partial fulfillment of the requirements for the degree of
Doctor of Philosophy
in Population Biology, Ecology, and Evolution
2022

Abstract

Leveraging genomic and genetic diversity to gain insights into viral evolution and spread

By Michael A. Martin

As viral pathogens replicate within host species, errors by the viral polymerase introduce differences between the original and replicated genomes. Even when these errors do not alter viral function, their accumulation over time leaves characteristic patterns representative of the biological context in which they arose. Fitting quantitative models to these data provides a way for researchers to interrogate these patterns. Here, we analyze influenza A and SARS-CoV-2 sequence data to better understand the dynamics of these pathogens across biological scales. We show that the within-host evolution of influenza genomic diversity is highly stochastic, that transmission bottlenecks of SARS-CoV-2 between hosts are extremely small, and that population level SARS-CoV-2 transmission is characterized by rapid undetected geographic dispersion and a high degree of transmission heterogeneity between infected hosts. Our results as a whole add to the growing body of literature regarding the ecology and evolution of human RNA viruses and in particular highlight how these populations are shaped by cross-scale dynamics.

Leveraging genomic and genetic diversity to gain insights into viral evolution and spread

By

Michael A. Martin

B.A., Johns Hopkins University, 2013

M.S., Harvard T.H. Chan School of Public Health, 2018

Advisor: Katharina Koelle, Ph.D.

A dissertation submitted to the Faculty of the
James T. Laney School of Graduate Studies of Emory University
in partial fulfillment of the requirements for the degree of
Doctor of Philosophy
in Population Biology, Ecology, and Evolution
2022

Acknowledgments

This work would not have been possible without the village who have supported me both before and during my PhD. There are too many people to thank, but there are a few I'd like to specifically mention.

First, I would like to acknowledge all of the patients who donated samples which have made this research possible. In the abstract it is easy to lose sight of the fact that our primary goal in research is learning about the natural world to better the lives of people, animals, plants, and the planet.

I would also like to thank my parents, who have supported me emotionally and (at times) financially throughout this process. They've always pushed me to work hard and do my best, but have never openly questioned me for still being in school at the age of 30.

I wouldn't be here today without the opportunities I was given during my time at the Harvard T.H. Chan School of Public Health. Particularly, Dr. Bill Hanage, Dr. Lauren Cowley, Dr. Robyn Lee, and Dr. Joseph Lewnard were played a crucial role in getting me started in this general field of research and shaping my scientific viewpoints.

It goes without saying that my advisor, Dr. Katia Koelle, has been instrumental in the completion of this dissertation. She has gone above and beyond in guiding me and providing me with opportunities to collaborate and publish. I'm not sure what I did to give her so much confidence in me, but I am forever grateful. I will probably spend the rest of my career trying to develop her sense of decomposing complex natural processes into tractable mathematical descriptions.

Much of the research in this dissertation has been collaborative in nature and I thank the collaborators who have allowed me to assist in their research projects, primarily Dr. Adi Stern at Tel Aviv University and Dr. Anne Piantadosi at Emory University.

Beyond formal collaborators, my committee has helped to shape the research in this dissertation and guide my views of science as a whole over the past years. Each one of you (Dr. Anice Lowen, Dr. Anne Piantadosi, Dr. Tim Read, and Dr. Daniel Weissman) offer a

unique scientific perspective that has made me a more well rounded scientist and person. A particular thanks to Tim Read who encouraged me to come to Emory for my PhD.

I have also had the pleasure of being lab mates with an incredible group of talented and interesting scientists. The Koelle lab has a tendency to recruit individuals with varied, yet complementary, professional and personal experiences and skills, which fosters a dynamic and vibrant laboratory environment. You've all made me a better scientist and person and I hope you have also found my perspective valuable. This includes: Brent Allman, Nicolas Berg, Lisa Bono, Amber Coats, Baptiste Elie, Molly Gallagher, Jeremy Harris, Jack Lin, Ellie Mainou, Yeongseon Park, Ananya Saha, Dave VanInsberghe, Diana Vera Cruz, and Julie Zhu. While not technically a lab mate, Matt Malishev was a reliable source of laughs in RRC1161 during the early years of my PhD.

I'd also like to thank all of the staff who work tirelessly to keep the academic machine running smoothly. Particularly Miss Judy who is endlessly sweet to everyone she sees and is a true gem of the Rollins Research Center community.

Unfortunately, COVID induced working from home and my subsequent move really limited our ability to bond, but my PBEE cohort has been a particularly strong source of support throughout this process. You all have an incredibly diverse and interesting set of scientific and professional experiences, interests, and goals and I'm honored to have been your classmate.

And finally, my fiancée Molly, who I met during the completion of this degree. I'm extremely grateful that you decided to relive the PhD experience by my side nearly immediately after finishing your own degree. You've been there for me on the hardest days of the past four years, joined me on endless adventures when I needed them the most, and always reminded me to celebrate my successes when they came. I love you and would not have been as balanced and happy of a person throughout the completion of this degree without you.

Contents

1	Introduction	1
1.1	Generation of viral diversity	3
1.2	Processes which shape viral diversity	5
1.3	Characterizing viral diversity	8
1.4	Cross-scales analysis of acute viral diversity	12
2	Leveraging genomic diversity to gain insights into within host influenza dynamics	29
2.1	Abstract	30
2.2	Introduction	30
2.3	Materials and methods	35
2.3.1	Data source	35
2.3.2	Transmission analyses	35
2.3.3	DVG identification	36
2.3.4	DVG quality filtering	37
2.3.5	BlastN analysis	38
2.3.6	Statistical analyses and visualization	39
2.4	Results	39
2.4.1	Limited DVGs in plasmid controls	39
2.4.2	DVGs observed readily in clinical samples	40

2.4.3	Nearly ubiquitous NS DVG	42
2.4.4	DVG populations are dynamic	43
2.4.5	Limited evidence for the transmission of DVGs	46
2.5	Discussion	48
2.6	Supplementary	53
2.6.1	Supplementary Figures	53
2.6.2	Supplementary Tables	87
3	Insights from SARS-CoV-2 sequences	97
3.1	M.A.M Contributions	97
3.2	Published Manuscript	97
4	Comment on “Genomic epidemiology of superspreading events in Austria reveals mutational dynamics and transmission properties of SARS-CoV-2”	101
4.1	M.A.M Contributions	102
4.2	Published Manuscript	102
4.3	Supplement	108
5	Full genome viral sequences inform patterns of SARS-CoV-2 spread into and within Israel	162
5.1	M.A.M. Contributions	162
5.2	Published Manuscript	163
5.3	Supplement	174
6	Unrecognized introductions of SARS-CoV-2 into the US state of Georgia shaped the early epidemic	207
6.1	M.A.M. Contributions	208
6.2	Published Manuscript	208
6.3	Supplement	222

List of Figures

*Figures for which M.A.M. is directly responsible are indicated with an * symbol*

- Chapter 1
 - None

- Chapter 2
 - **2.1***: DVGs identified in the plasmid controls.
 - **2.2***: DVGs identified in clinical samples.
 - **2.3***: Nearly ubiquitous NS DVG.
 - **2.4***: Polymerase DVG dynamics over the course of infection.
 - **2.5***: Polymerase DVGs shared between pairs of patients.
 - **S2.6***: Observed junction locations for all PB2, PB1, and PA DVGs observed in all clinical samples.
 - **S2.7***: Number of deleted nucleotides for each DVG identified in the PB2, PB1, and PA segments.
 - **S2.8***: Relative read support of DVGs identified in the PB2, PB1, and PA segments of all patients with longitudinal samples.
 - **S2.9***: Relative read support of all DVGs identified in longitudinal samples taken 0, 1, 2, 3, 4, and 6 days apart, stratified by whether those DVGs are persistent (P) or non persistent (NP) between t_0 and t_1 .

- Chapter 3
 - **3.1***: Uses for viral sequence data

- Chapter 4

- **3.S1***: Transmission bottleneck size estimates for each of the 39 transmission pairs analyzed in Popa et al
- **3.S2***: All iSNVs observed in either donor and/or recipient of all 39 epidemiologically confirmed transmission pairs
- **3.S3***: Allele frequencies for all iSNVs observed in at least 3 of the 43 samples involved in the 39 transmission pairs
- **3.S4***: Number of occurrences for all iSNVs observed in at least 3 of the 43 samples involved in the 39 transmission pairs
- **3.S5***: Read depth across the SARS-CoV-2 genome (Wuhan/Hu-1) for each of the 43 samples involved in the 39 transmission pairs calculated after adjusting for overlapping reads and trimming amplicon primers from the publicly available BAM files (black lines)
- **3.S6***: Number of iSNVs (read frequency 1-99%) per amplicon that were observed in at least 10 (black), at least 20 (red), or at least 40 (blue) of the 43 samples involved in the 39 transmission pairs
- **3.S7***: Patterns of shared viral genetic diversity between transmission pairs under the assumption of a large bottleneck of $N_b = 3000$ (red dots)

- Chapter 5

- **4.1**: Variation found in sequenced samples from Israel
- **4.2**: Deletions found in Israeli samples
- **4.3**: Patterns of SARS-CoV-2 introduction into Israel
- **4.4**: Spread of SARS-CoV-2 into and within Israel
- **4.5***: Estimated epidemiological parameters and cumulative incidence across different levels of transmission heterogeneity

- **4.6***: Epidemiological dynamics inferred using phylodynamic analysis
- **4.S1**: Inferred regions responsible for clade introductions into six focal countries
- **4.S2**: Cumulative number of importations throughout time
- **4.S3**: Distribution of importations into Israel
- **4.S4***: Compartmental model used in the phylodynamic analysis
- **4.S5***: Sensitivity of phylodynamic analyses to the overall magnitude of the importation/exportation rate η
- **4.S6***: Sensitivity of phylodynamic analyses to the overall magnitude of the importation/exportation rate η , when h is assumed to be constant
- **4.S7***: Time-aligned maximum clade credibility phylogeny
- **4.S8**: Distribution of importation dates into Israel
- **4.S9***: Distribution of importation dates into Israel assumed in our phylodynamic analysis
- **4.S10***: Probabilities of a new infection being due to importation rather than local infection under different magnitudes of the importation rate, assuming a functional form of η based on inferred timing of clade importations
- **4.S11***: Probabilities of a new infection being due to importation rather than local infection under different magnitudes of the importation rate, assuming a constant η

- Chapter 6

- **5.1***: Temporal and spatial distribution of SARS-CoV-2 cases and sequences in the state of Georgia
- **5.2***: Presence of multiple clades and maximum likelihood phylogenetic analysis indicate multiple introductions of SARS-CoV-2 into Georgia

- **5.3***: Bayesian phylogenetic analysis of genetically related Georgia 19B sequences and their phylogenetic neighbors reveals undetected circulation in February 2020
- **5.4***: Analysis of SARS-CoV-2 whole genome sequences from EHC patients with recent travel provides examples of travel-associated infections of SARS-CoV-2 coming into Georgia
- **5.5***: Shared mutations between related Georgia 19B sequences and global sequences harboring this mutational profile indicate its decline in early 2020
- **5.S1**: SARS-CoV-2 diagnostic rRT-PCR tests performed by the EHC Molecular and Microbiology Laboratories between 2020-03-15 and 2020-03-31
- **5.S2**: Associations between CT value and SARS-CoV-2 sequencing parameters
- **5.S3***: Number of sequences from Georgia per lineage, per week included in the phylogenetic analysis
- **5.S4***: Root-to-tip regression of global sequences selected using weighted downsampling
- **5.S5***: Maximum likelihood divergence tree of sequences selected using weighted downsampling
- **5.S6***: Presence of multiple clades and maximum likelihood phylogenetic analysis indicates multiple introductions of SARS-CoV-2 into Georgia (temporally and geographically homogeneous downsampling)
- **5.S7***: Root-to-tip regression of select 19B sequences
- **5.S8***: Maximum likelihood divergence tree of select 19B sequences with U.S. sequences highlighted
- **5.S9***: Maximum likelihood divergence tree of select 19B sequences with non-U.S. sequences highlighted
- **5.S10***: Downsampled Bayesian phylogenetic analysis of genetically related Georgia 19B sequences and their phylogenetic neighbors

- **5.S11***: Comparison of SARS-CoV-2 genomes from returning travelers
- **5.S12**: SARS-CoV-2 rRT-PCR CT value by spike position 614 residue for 47 Nasopharyngeal (NP) samples
- **5.S13**: Associations between molecular results and clinical parameters
- **5.S14***: Root-to-tip regression of global sequences selected using temporally and geographically homogeneous downsampling

List of Tables

*Tables for which M.A.M. is directly responsible are indicated with an * symbol*

- Chapter 1
 - None
- Chapter 2
 - **S2.1***: Logistic Regression of the probability of polymerase DVG persistence between t_0 and t_1 as a function of relative DVG read support
 - **S2.2***: Logistic Regression of the probability of polymerase DVG persistence between t_0 and t_1 as a function of time between samples and relative DVG read support
 - **S2.3***: Logistic Regression of the number of shared DVGs between sample pairs as a function of the type of pair
- Chapter 3
 - None
- Chapter 4

- None

- Chapter 5

- **4.1**: Summary of samples successfully sequenced.

- **4.S1**: Global samples belonging to the S2430R clade that contain short unique deletions.

- **4.S2**: Details of samples sequenced.

- **4.S3***: Model parameter priors and estimated values ($\theta = 0.8$)

- **4.S4***: Model parameter priors and estimated values ($\theta = 0.9$)

- **4.S5***: Model parameter priors and estimated values ($\theta = 1.0$)

- **4.S6***: Model parameter priors and estimated values ($\theta = 1.1$)

- **4.S7***: Model parameter priors and estimated values ($\theta = 1.2$)

- **4.S8***: Model parameter priors and estimated values ($\eta = 10$)

- **4.S9***: Model parameter priors and estimated values ($\eta = 100$)

- **4.S10***: Model parameter priors and estimated values ($\eta = 1000$)

- **4.S11***: Model parameter priors and estimated values ($\eta = 2500$)

- **4.S12***: Model parameter priors and estimated values ($\eta = 5000$)

- **4.S13**: Sequencing primer list

- Chapter 6

- **5.1**: Demographic and clinical data from fifty-four EHC patients

- **5.S1**: Detailed SARS-CoV-2 sequencing metrics

- **5.S2**: Detailed clinical data for 54 EHC patients with SARS-CoV-2 infection in March 2020

- **5.S3***: GISAID acknowledgements table for all sequences used in travel and phylogenetic analyses
 - **5.S4**: County data for non-EHC sequences
 - **5.S5***: Sequence names and accession numbers for sequences included in the weighted downsampling maximum likelihood analysis
 - **5.S6***: Sequence names and accession numbers for sequences included in the Bayesian phylogenetic analysis
 - **5.S7***: Select parameter prior and posterior estimates from the Bayesian phylogenetic analysis
 - **5.S8***: Travel data and mutational profile for 9 patients who had traveled in the 2 weeks preceding symptom onset
 - **5.S9***: Sequence names and accession numbers for sequences which match the mutational profile of the 69 closely related 19B Georgia sequences
 - **5.S10***: Sequence names and accession numbers for sequences included in the temporally homogeneous downsampling maximum likelihood analysis
- Chapter 7
 - None

Chapter 1

Introduction

Viral pathogens are a significant cause of human morbidity and mortality worldwide [1, 2, 3, 4]. While there are a number of viral life history characteristics which exacerbate their ability to readily spread between humans, RNA viruses with short generation times and high mutation rates pose a particular challenge because the ecological and evolutionary processes acting on these populations occur on similar time scales and often on time scales observable by humans [5]. Consequently, evolution can act to evade the ecological constraints on viral fitness and changing ecological contexts can simultaneously shift the fitness landscape on which evolution acts.

Because viruses require a host species to replicate, the primary ecological processes acting on viral populations concern the interaction between viruses and their corresponding host species. These include the transmission mode for a given viral pathogen in a given host population [6], heterogeneity in host susceptibility to infection (due to e.g. immunity) [7], spatial or contact structure in the host population [8, 9], and viral life history traits in a given host species [10]. Many viral species are able to infect multiple host species, which introduces yet another layer of ecological interactions to consider [11]. Here I will primarily be considering the circulation of viral pathogens amongst human hosts.

Evolution is able to interact with these ecological processes due to the diversity in vi-

ral populations that is generated when the RNA polymerase makes mistakes during viral replication. The fate of this diversity depends, in part, on its impact on viral fitness. Laboratory studies have attempted to quantify the so-called distribution of fitness effects in model systems [12]. These studies have found that 40% of mutations in viral genomes are so deleterious to fitness that selection will readily purge them from the population. These mutations, therefore, are unlikely to be observed in natural systems. On the contrary, roughly 4% of mutations are beneficial, that is, they increase viral fitness. Selection will act to increase the frequency of these mutations in the viral population, so long as they continue to be beneficial in a given ecological context. Finally, the majority (>50%) of mutations are neutral or slightly deleterious, meaning they have no or limited impact on viral fitness. Selection will not act strongly on this subset of mutations, however, genetic drift may alter their frequency in a given population over time. As viral populations evolve, the fixation of beneficial mutations may act to counteract ecological constraints in viral fitness (e.g. the acquisition of mutations which evade host immunity [13] or improve transmissibility [14]) and these ecological process will leave characteristic patterns in the viral population diversity [15]).

Consequently, there is considerable interest in monitoring changes in viral genomes as they spread throughout host populations. There is interest in both early detection of mutations which increase fitness and in interrogating the patterns of acquired neutral or nearly-neutral mutations to uncover the ecologic contexts governing their evolution. Viral genome sequencing, in which the genomic diversity of viral pathogens within a given host can be measured, is a crucial tool in monitoring these changes. These data are generated from individual hosts and can be compared in a longitudinal fashion to determine the relative contributions of selection and drift during single infections [16, 17], between transmission pairs to determine how transmission bottlenecks shape diversity [16, 18], and at the host population scale to observe e.g. selective sweeps of lineages with fitness advantages (such as SARS-CoV-2 variants of concern [19]) and to estimate the impact of epidemiological inter-

ventions on viral spread [20]. As evidenced by these examples, fitting quantitative models to deep sequencing data can be particularly insightful to test competing biological hypotheses about the forces acting on viral populations.

1.1 Generation of viral diversity

As stated above, the diversity in viral populations is generated due to mistakes in the viral polymerase. These mistakes, however, can take multiple forms. These forms are generated through distinct biological processes and have distinct consequences for viral fitness.

Point mutations, in which one nucleotide in the genome is replaced by another, are the most commonly studied. These are commonly categorized as either non-synonymous, which affect the translated amino acid sequence, and synonymous which do not affect the makeup of viral proteins. While changes in translated protein sequences have clear potential fitness implications, it is increasingly being recognized that even the synonymous mutations in coding regions can affect viral fitness [21]. Furthermore, synonymous mutations in non-coding regions that are involved in e.g. genome packaging into virions can have significant fitness effects [22]. Some viruses feature proof-reading mechanisms which help to correct for the introduction of errors into the replicated viral genome by the viral polymerase [23]. For example, the exonuclease capabilities of the Nsp14 protein in SARS-CoV as well as other coronaviruses has been shown to reduce the number of accumulated mutations by more than an order of magnitude [24]. Other viral families, such as the Orthomyxoviridae family, to which influenza viruses belong, lack this proof reading capability. These families therefore generally generate more mistakes during viral replication. Importantly, observing mutations in empirical data depends on both the rate at which mutations are generated as well as their impact on viral fitness. As an extreme example, the roughly 40% of lethal mutations described above are never observed because they are readily purged from the viral population.

Additionally, larger-scale mistakes made by the viral polymerase during genome replication can also occur. One of these, recombination, occurs when the viral polymerase jumps between template strands during replication [25]. Homologous recombination, in which the portion of the genome from one template strand is swapped for a template strand from the same species (and in the case of segmented viruses, the same segment) can occur when a single cell is co-infected with multiple progenitor viruses. This process produces a distinct novel genotype, with genetic material from both donor genotypes. Often this novel genotype includes the same set of genes as the progenitor viruses however this process can also produce genomes with the deletion and duplication of genetic material. Evolutionary important recombination (e.g. those which produce functionally novel progeny viruses) is a function both of how likely a given virus is to recombine as well as the likelihood of co-infection of a single host with two distinct parental genomes. Thus, the rate at which homologous recombinant genomes are generated may provide a signal as to the epidemiological context in which a virus is circulating. Non-homologous, or heterologous, recombination occurs when the polymerase either skips between host and viral template strands leading to viral integration into the host genome [26]. However, we expect heterologous recombination to be much rarer than homologous recombination and will not consider it further here.

Genome deletions generated by polymerase skipping can be functionally categorized by the number of deleted nucleotides. Small deletions of only one or a handful of amino acids are observed relatively frequently in both influenza [27] and SARS-CoV-2 [28] and often do not result in non-viable viral progeny. In fact, the Δ H69/V70 deletion in SARS-CoV-2 may actually increase viral infectivity [29]. Additionally, polymerase skipping can generate large (on the order of hundreds of nucleotides) deletions in the viral genome. When these deletions render the virus incapable of replicating without the presence of a helper virus they are commonly referred to as defective viral genomes (DVGs). In influenza, deletion DVGs of this type retain the 5' and 3' ends of the DVG segment, as those regions are crucial for packaging into new virions [30]. In rare cases, specific DVGs can actually interfere with the

replication of wild type virus, acting as genomic parasites of their wild-type counterparts. These are referred to as defective interfering particles (DIPs) and were first described by Von Magnus in 1954 [31, 32]. Since then they have been recognized as common features of influenza viral populations during high multiplicity of infection (MOI) passage studies and have previously been identified during natural human infections [33], although their role in disease dynamics in natural infections is largely unknown. In influenza, DIPs are commonly found on the three polymerase segments and have been proposed as a putative antiviral therapy due to their predatory nature on wild-type virus [34].

Changes in the genomic make up of viral populations can also be generated even when no replication mistakes are made. This is particularly common in the case of segmented viruses, such as influenza, in which the genome is broken up into multiple segments. In such cases, when two virions coinfect the same host cell, progeny virion can harbor genetic material from both parental viruses in a process known as reassortment [35]. This process is responsible for the generation of novel influenza sub-types, such as the pandemic H1N1 sub-type, which harbored segments from multiple parental sub-types [36]. Influenza reassortment which results in novel sub-types is much more likely to occur in host species which can be infected with many subtypes (e.g. swine). While it is generated in the absence of polymerase errors, it is evolutionary analogous to homologous recombination in that it shuffle portions of the genome from multiple donor viruses without changing the gene composition of the progeny virus.

1.2 Processes which shape viral diversity

Once genetic and genomic diversity has been generated during viral genome replication and packaged into progeny virions, the ultimate fate of that diversity is governed by the contrasting forces of selection and genetic drift and gene flow between distinct viral and host populations.

These processes first act within single-hosts, where viral diversity is originally generated. As the process of transmission inherently introduces a significant bottleneck in the viral population size (see below), the impact of genetic drift will be exacerbated early in infection [16]. Selection, primarily in well-adapted endemic viruses with large amounts of pre-existing population immunity such as influenza, is largely due to the host immune response. However, in acute infections this immune response is lagged relative to rapid viral population growth [37], such that selection is relatively weak on immune-escape mutations. Thus, the analysis of deep sequencing data from acute infections does not reveal positive selection acting on immune escape variants [16, 38]. Specifically, known antigenic sites in the influenza A genome do not appear to have an elevated number of non-synonymous mutations or an elevated number of high frequency minor variants during acute infections. Similarly, within-host evolutionary dynamics are similar between vaccinated and non-vaccinated hosts, even when looking specifically at known antigenic mutations. On the contrary, longitudinal analyses of chronically infected hosts has revealed the parallel fixation of specific putatively-antigenic mutations in multiple hosts, strongly indicative of positive selection. These same mutations have also been observed to be under positive selection at the host population scale, providing further evidence that they confer a fitness advantage, likely through antigenic escape, to the virus [17]. Selection will also act on variants that increase the inherent transmissibility of a given virus, particularly in viruses that are poorly adapted to their host. For example, the SARS-CoV-2 D614G mutation which increase between-host transmissibility [39] evolved within hosts multiple times soon after the viruses spillover into human populations [40]

Regardless of the dynamics within individual hosts, the viral population is shaped by the process of transmission between hosts [41]. This process limits the amount of genetic diversity that seeds infection in the new host, relative to what is present in the donor host. If the bottleneck is sufficiently small this provides an opportunity for rare variants in the donor host or *de novo* variants which arise soon after transmission to fix in the recipient host. On the contrary, under a large bottleneck the genetic diversity in the recipient will more closely

mimic that in the donor host, allowing selection to more efficiently act across transmission chains. As such, the transmission bottleneck is an important quantity that modulates the strength of genetic drift during transmission and the degree to which transmission itself promotes the fixation of novel mutations. Estimates of the bottleneck size in influenza virus are on the order of one to three virions [16], implying that very little of the within host diversity is transmitted to recipient hosts.

Finally, as viruses transmit throughout host populations, processes which act on this scale shape the diversity that was generated within single hosts. Selection at this scale will primarily act to fix mutations which either increase the ability of a virus to transmit between hosts (e.g. those which increase transmissibility given infection) or increase the size of the susceptible host population (e.g. immune escape variants). A poignant example of evolution acting at this scale can be seen in pandemic influenza A H1N1 [42]. This virus emerged following zoonotic spillover into human hosts and therefore in the years following its emergence most observed mutation is attributed to host adaptation, not antigenic evolution. However, as immunity to the virus built in the human population, selection began to act primarily on immune escape variants, which replenish the susceptible host population. How selection shapes a viral population therefore depends both on the biology of a given viral species as well as the ecological context in which it is circulating. Genetic drift may also shape diversity at the host population scale and its impact is amplified by epidemiological factors. Seasonality, for example in influenza [43], often results in reduced viral population sizes and genetic bottlenecks during the epidemiological troughs. Assuming the lineages which persist through the trough are selected at random from the preceding peak, this will exacerbate genetic drift and may lead to the fixation of neutral mutations in the viral population. Superspreading, in which certain infected individuals or certain types of social contacts are particularly prone to transmission [44], will also amplify genetic drift at the host population scale. This process skews the offspring distribution of infected hosts, which reduces the effective population size (N_E) [45], accentuating drift.

As an additional level of complexity, host populations are often not well mixed and more closely resemble a metapopulation, or a population of populations. This metapopulation can either be a spatial one (e.g. countries [9]) or an epidemiological one (e.g. contact networks [8]). Host, and therefore pathogen, flow between subpopulations introduces yet another ecological force that shapes viral populations. The evolution of influenza A H3N2 presents a relevant example [46]. Seasonality of influenza in temperate regions and annual epidemics are thought to be reseeded by continual transmission in tropics. This process introduces a bottleneck in the circulating genetic diversity which seeds seasonal epidemics in temperate regions and there is limited reseeding of these drifted populations back to the source regions. As such, the metapopulation structure of influenza evolution exacerbates transient effects of genetic drift within a given season, however, selection is efficient at fixing beneficial mutations in the temperate regions over longer time scales. Metapopulation structure therefore can have disparate effects on shaping viral diversity, dependent on the movement between demes, seasonal dynamics within demes, and selective landscape within and between demes.

1.3 Characterizing viral diversity

Genome sequencing data from infected hosts is a transformative tool for characterizing viral diversity within host populations. These technologies generate thousands of sequenced fragments of the input genetic material [47]. To make inferences about the biological sample these fragments must be either aligned to a given reference genome by finding the region of the reference with the best match to each read or assembled into a contiguous genome in a *de novo* manner. By comparing the assembled genome to a known reference, changes relative to that reference can be identified. Deep sequencing data, in which there are on the order of 10^3 reads aligned to each site in the genome can be used to measure the genetic and genomic diversity within a clinical sample. The accuracy of these estimates, however, depends critically on the quality of the input sample, particular the quantity of input viral

RNA [48].

The relative impacts of selection and drift acting on viral populations within host can be teased apart by comparing viral populations within single hosts across multiple time points. Mutations in the viral genome which are under positive selection will increase in frequency over time, often leading to an elevated ratio of the number of non-synonymous to synonymous substitutions [17, 16]. The accumulation of neutral or mildly deleterious mutations, as is expected under genetic drift, is not expected to produce an elevated number of non-synonymous mutations. Computational models of this process can be used to provide a quantitative estimate of the selection coefficient of specific viral mutations [49, 50].

Deep sequencing data can also provide insight into the presence of recombinant genomes within hosts. In practice, recombination is often identified by comparing a sampled virus to a reference set of viral genomes (e.g. using [51]). Canonically, recombinant genomes harbor genome portions most similar to multiple distinct viral lineages. For example, by identifying the defining mutations for the major circulating clades of SARS-CoV-2, viruses which simultaneously harbored subsets of the clade defining mutations from distinct clades were identified early in the pandemic as recombinant viruses [52]. The resolution to identifying recombinants therefore depends in part on how genetically similar the coinfecting viruses are. One cannot identify recombinant genomes between two identical parental genomes using sequence data alone.

Similarly, the presence of DVGs within hosts also leave characteristic signatures in deep sequencing data. These signatures are found in the reads which span the deletion site in a given DVG. When these reads are aligned to the reference genome they align either to one end of the genome or another with the remainder of the read clipped, or are aligned in a “split” fashion, depending on the mapping algorithm used. The development of algorithms specifically for the purpose of identifying genomic variants which iteratively align chunks of the read to the reference genome have significantly aided in the bioinformatic analysis of DVGs [53, 54]. Additionally, samples with large amounts of DVGs relative to wild-type

virus will characteristically have much higher sequencing depth on the 5' and 3' ends of the segments harboring DVGs, with very few reads coming from the deleted internal nucleotide of the segments. This produces a so-called “bat ear” pattern in the sequencing depth across the genome (e.g. [33]). Differentiating between DVGs and DIPs from sequencing alone is not possible and laboratory experiments must be conducted to confirm the interfering nature of genuine DIPs (e.g. [55]).

Finally, reassortant viral genomes can be identified by comparing the sample from a single host to a set of reference samples. This is often done by comparing the independent evolutionary history of each segment of the genome. Evolutionary histories which are inconsistent may indicate the presence of historical reassortment [56]. These analyses are occasionally visualized using a “tanglegram” in which the order of tips in multiple genealogies are directly compared (e.g. [57]). However, tanglegrams can be misleading as they only show differences in the evolutionary history if those difference affect the ultimate ordering of the tips [58].

By comparing deep sequencing data between epidemiologically linked donors and recipients, the size of the transmission bottleneck can be estimated. In general, under a large transmission bottleneck the viral population in the recipient host will more closely mimic that of the donor host than under a tight bottleneck. While a number of methods for this procedure exist, the most commonly used method is known as the beta-binomial approach [18]. This approach accounts for binomial sampling of the mutations within the donor host, stochastic replication within the recipient host, and the presence of variants which may be present but are unable to be identified due to limitations in the resolution of the sequence data.

Across many individual hosts, the processes of selection and drift within hosts, drift between hosts, and selection and drift at the host population scale all leave characteristic signatures in viral genomes. We can leverage the signal in this diversity to make inferences about virus ecology and evolution from collections of viral sequences. These methods most commonly rely on phylogenetic and phylodynamic approaches. In short, by combining se-

quence and epidemiological data with models for evolution and spread, we can identify the processes which gave rise to the data that are best supported by that model. Specifically, with a model of sequence evolution, i.e. a transition rate matrix between nucleotide states we can identify the genealogical relationships between sampled viruses [59]. Through a process called ancestral state reconstruction (ASR) the nucleotide states of unsampled ancestral viruses can be estimated [60].

Furthermore, the branch lengths of this estimated genealogy can be scaled to be in unit of calendar time, instead of genetic distance, using an estimate for the rate at which substitutions are accumulated [61, 62]. When population sizes change over time, an underlying model for the demographic history of the population can be jointly considered using either a coalescent [63] or a birth-death [64] prior. Under a coalescent prior, the rate at which two lineages merge, or coalesce, looking backwards in time depends on the inverse of the population size. Parametric (e.g. constant, exponential growth/decline) or non-parametric (e.g. skyline [65], skyride [66], or skygrid [67]) models for changes in the population size over time can be fit to the sequence and sampling date data. Recent developments in so-called structured coalescent models allow users to define dynamical models for the underlying population structure (e.g. susceptible - infectious - recovered (SIR) models) and assign each sampled sequence to a given deme [68, 69, 70]. These models therefore allow epidemiological parameters (e.g. R_0) to be directly fit to the data. Alternatively, birth-death models for the underlying demographic dynamics take a forward-in-time approach in which lineages in the tree transmit (branching events), are sampled (tips), or go extinct (unobserved) at certain rates [64]. These rates can then be used to derive parameters of epidemiological interest.

By incorporating additional metadata about the sampled sequences (e.g. sampling location) ASR can also be used to reconstruct changes in a given trait over the genealogy. This process is often used to estimate the spatial location of ancestral sequences either in a discrete [71] or continuous [72] fashion. Looking over the phylogeny as a whole, the relative rates of transmission between different deems can also be quantified. This process allows for

the identification of source and sink populations in e.g. influenza [73].

Implementing these methods in a Bayesian framework [74, 75] provides users with posterior distributions for estimated parameters and genealogical histories. These posterior estimates can be interrogated to test biological hypothesis such as the time to most recent common ancestor (tMRCA) of a given clade, changes in the local substitution rate throughout the genealogical history, and the number of introductions of a given population into a specific geographic region.

1.4 Cross-scales analysis of acute viral diversity

Here, I (M.A.M) present a comprehensive analysis of acute viral diversity across biological scales. I start by analyzing within host deep sequencing data from natural infections of influenza A H3N2 (**Chapter 2**). Previous analyses have revealed that genetic diversity in the form of point mutations is extremely limited in this context [16]. As a result, I focus on the dynamics of genomic diversity in the form of defective viral genomes, a largely unstudied aspect of influenza diversity in natural infections. As the remainder of the chapters focus on the analysis of SARS-CoV-2 sequence data, **Chapter 3** provides the reader with a primer on the insights which have been gained about the SARS-CoV-2 pandemic using sequencing data and open questions and challenges in conducting these analyses. In **Chapter 4** I fit a model of the transmission process to deep sequencing data from epidemiologically linked SARS-CoV-2 transmission pairs to estimate the size of the transmission bottleneck. Finally, in **Chapter 5** and **Chapter 6** I use phylogenetic and phylodynamic analyses to better understand the spread of SARS-CoV-2 into Israel and Georgia, USA, respectively. I attempt to summarize over arching findings from these works with an eye towards future studies in **Chapter 7**.

My specific contributions for each chapter are listed according to the CRediT author statement guidelines (<https://casrai.org/credit/>), with additional detail where applicable.

As multiple chapters are made up of published works, a separate **References** section is listed for each chapter. Supplementary data files are not included, however, they are readily available from the publisher or online repositories.

Chapter 1 References

- [1] J. Paget, P. Spreuwenberg, V. Charu, R. J. Taylor, A. D. Iuliano, J. Bresee, L. Simonsen, and C. Viboud, “Global mortality associated with seasonal influenza epidemics: New burden estimates and predictors from the GLaMOR Project,” *Journal of Global Health*, vol. 9, p. 020421, Dec. 2019.
- [2] A. Karlinsky and D. Kobak, “Tracking excess mortality across countries during the COVID-19 pandemic with the World Mortality Dataset,” *eLife*, vol. 10, p. e69336, June 2021.
- [3] “Fact Sheet - World AIDS Day 2021,” tech. rep., UNAIDS, 2021.
- [4] M. Jefferies, B. Rauff, H. Rashid, T. Lam, and S. Rafiq, “Update on global epidemiology of viral hepatitis and preventive strategies,” *World Journal of Clinical Cases*, vol. 6, pp. 589–599, Nov. 2018.
- [5] A. J. Drummond, O. G. Pybus, A. Rambaut, R. Forsberg, and A. G. Rodrigo, “Measurably evolving populations,” *Trends in Ecology & Evolution*, vol. 18, pp. 481–488, Sept. 2003.
- [6] J. S. Kutter, M. I. Spronken, P. L. Fraaij, R. A. Fouchier, and S. Herfst, “Transmission routes of respiratory viruses among humans,” *Current Opinion in Virology*, vol. 28, pp. 142–151, Feb. 2018.
- [7] R. Hickson and M. Roberts, “How population heterogeneity in susceptibility and infec-

- tivity influences epidemic dynamics,” *Journal of Theoretical Biology*, vol. 350, pp. 70–80, June 2014.
- [8] S. Messinger and A. Ostling, “The Consequences of Spatial Structure for the Evolution of Pathogen Transmission Rate and Virulence,” *The American Naturalist*, vol. 174, pp. 441–454, Oct. 2009.
- [9] R. M. May, “Network structure and the biology of populations,” *Trends in Ecology & Evolution*, vol. 21, pp. 394–399, July 2006.
- [10] L. P. Villarreal, V. R. Defilippis, and K. A. Gottlieb, “Acute and Persistent Viral Life Strategies and Their Relationship to Emerging Diseases,” *Virology*, vol. 272, pp. 1–6, June 2000.
- [11] S. Cleaveland, M. Laurenson, and L. Taylor, “Diseases of humans and their domestic mammals: pathogen characteristics, host range and the risk of emergence,” *Philosophical Transactions of the Royal Society of London. Series B: Biological Sciences*, vol. 356, pp. 991–999, July 2001.
- [12] R. Sanjuan, A. Moya, and S. F. Elena, “The distribution of fitness effects caused by single-nucleotide substitutions in an RNA virus,” *Proceedings of the National Academy of Sciences*, vol. 101, pp. 8396–8401, June 2004.
- [13] D. J. Smith, A. S. Lapedes, J. C. de Jong, T. M. Bestebroer, G. F. Rimmelzwaan, A. D. M. E. Osterhaus, and R. A. M. Fouchier, “Mapping the Antigenic and Genetic Evolution of Influenza Virus,” *Science*, vol. 305, pp. 371–376, July 2004.
- [14] Y. J. Hou, S. Chiba, P. Halfmann, C. Ehre, M. Kuroda, K. H. Dinno, S. R. Leist, A. Schäfer, N. Nakajima, K. Takahashi, R. E. Lee, T. M. Mascenik, R. Graham, C. E. Edwards, L. V. Tse, K. Okuda, A. J. Markmann, L. Bartelt, A. de Silva, D. M. Margolis, R. C. Boucher, S. H. Randell, T. Suzuki, L. E. Gralinski, Y. Kawaoka, and R. S. Baric,

“SARS-CoV-2 D614G variant exhibits efficient replication ex vivo and transmission in vivo,” *Science*, Nov. 2020.

- [15] B. T. Grenfell, O. G. Pybus, J. R. Gog, J. L. N. Wood, J. M. Daly, J. A. Mumford, and E. C. Holmes, “Unifying the Epidemiological and Evolutionary Dynamics of Pathogens,” *Science*, vol. 303, no. 5656, pp. 327–332, 2004.
- [16] J. T. McCrone, R. J. Woods, E. T. Martin, R. E. Malosh, A. S. Monto, and A. S. Lauring, “Stochastic processes constrain the within and between host evolution of influenza virus,” *eLife*, vol. 7, pp. 1–19, 2018.
- [17] K. S. Xue, T. Stevens-Ayers, A. P. Campbell, J. A. Englund, S. A. Pergam, M. Boeckh, and J. D. Bloom, “Parallel evolution of influenza across multiple spatiotemporal scales,” *eLife*, vol. 6, pp. 1–16, 2017.
- [18] A. Sobel Leonard, D. B. Weissman, B. Greenbaum, E. Ghedin, and K. Koelle, “Transmission Bottleneck Size Estimation from Pathogen Deep-Sequencing Data, with an Application to Human Influenza A Virus,” *Journal of Virology*, vol. 91, July 2017.
- [19] R. P. Walensky, H. T. Walke, and A. S. Fauci, “SARS-CoV-2 Variants of Concern in the United States—Challenges and Opportunities,” *JAMA*, vol. 325, p. 1037, Mar. 2021.
- [20] S. Dellicour, G. Baele, G. Dudas, N. R. Faria, O. G. Pybus, M. A. Suchard, A. Rambaut, and P. Lemey, “Phylogenetic assessment of intervention strategies for the West African Ebola virus outbreak,” *Nature Communications*, vol. 9, p. 2222, Dec. 2018.
- [21] J. M. Cuevas, P. Domingo-Calap, and R. Sanjuán, “The Fitness Effects of Synonymous Mutations in DNA and RNA Viruses,” *Molecular Biology and Evolution*, vol. 29, pp. 17–20, Jan. 2012.
- [22] E. C. Hutchinson, H. M. Wise, K. Kudryavtseva, M. D. Curran, and P. Digard, “Charac-

- terisation of influenza A viruses with mutations in segment 5 packaging signals,” *Vaccine*, vol. 27, pp. 6270–6275, Oct. 2009.
- [23] F. Robson, K. S. Khan, T. K. Le, C. Paris, S. Demirbag, P. Barfuss, P. Rocchi, and W.-L. Ng, “Coronavirus RNA Proofreading: Molecular Basis and Therapeutic Targeting,” *Molecular Cell*, vol. 79, pp. 710–727, Sept. 2020.
- [24] L. D. Eckerle, M. M. Becker, R. A. Halpin, K. Li, E. Venter, X. Lu, S. Scherbakova, R. L. Graham, R. S. Baric, T. B. Stockwell, D. J. Spiro, and M. R. Denison, “Infidelity of SARS-CoV Nsp14-Exonuclease Mutant Virus Replication Is Revealed by Complete Genome Sequencing,” *PLoS Pathogens*, vol. 6, p. e1000896, May 2010.
- [25] M. Pérez-Losada, M. Arenas, J. C. Galán, F. Palero, and F. González-Candelas, “Recombination in viruses: Mechanisms, methods of study, and evolutionary consequences,” *Infection, Genetics and Evolution*, vol. 30, pp. 296–307, Mar. 2015.
- [26] E. Holmes, “The Evolution of Endogenous Viral Elements,” *Cell Host & Microbe*, vol. 10, pp. 368–377, Oct. 2011.
- [27] O. Stech, J. Veits, E.-S. M. Abdelwhab, U. Wessels, T. C. Mettenleiter, and J. Stech, “The Neuraminidase Stalk Deletion Serves as Major Virulence Determinant of H5N1 Highly Pathogenic Avian Influenza Viruses in Chicken,” *Scientific Reports*, vol. 5, p. 13493, Oct. 2015.
- [28] D. Miller, M. A. Martin, N. Harel, O. Tirosh, T. Kustin, M. Meir, N. Sorek, S. Gefen-Halevi, S. Amit, O. Vorontsov, A. Shaag, D. Wolf, A. Peretz, Y. Shemer-Avni, D. Roif-Kaminsky, N. M. Kopelman, A. Huppert, K. Koelle, and A. Stern, “Full genome viral sequences inform patterns of SARS-CoV-2 spread into and within Israel,” *Nature Communications*, vol. 11, p. 5518, Dec. 2020.
- [29] B. Meng, S. A. Kemp, G. Papa, R. Datir, I. A. Ferreira, S. Marelli, W. T. Harvey, S. Lytras, A. Mohamed, G. Gallo, N. Thakur, D. A. Collier, P. Mlcochova, L. M. Dun-

can, A. M. Carabelli, J. C. Kenyon, A. M. Lever, A. De Marco, C. Saliba, K. Culap, E. Cameroni, N. J. Matheson, L. Piccoli, D. Corti, L. C. James, D. L. Robertson, D. Bailey, R. K. Gupta, S. C. Robson, N. J. Loman, T. R. Connor, T. Golubchik, R. T. Martinez Nunez, C. Ludden, S. Corden, I. Johnston, D. Bonsall, C. P. Smith, A. R. Awan, G. Bucca, M. E. Torok, K. Saeed, J. A. Prieto, D. K. Jackson, W. L. Hamilton, L. B. Snell, C. Moore, E. M. Harrison, S. Goncalves, D. J. Fairley, M. W. Loose, J. Watkins, R. Livett, S. Moses, R. Amato, S. Nicholls, M. Bull, D. L. Smith, J. Barrett, D. M. Aanensen, M. D. Curran, S. Parmar, D. Aggarwal, J. G. Shepherd, M. D. Parker, S. Glaysher, M. Bash-ton, A. P. Underwood, N. Pacchiarini, K. F. Loveson, K. E. Templeton, C. F. Langford, J. Sillitoe, T. I. de Silva, D. Wang, D. Kwiatkowski, A. Rambaut, J. O'Grady, S. Cottrell, M. T. Holden, E. C. Thomson, H. Osman, M. Andersson, A. J. Chauhan, M. O. Hassan-Ibrahim, M. Lawniczak, A. Alderton, M. Chand, C. Constantinidou, M. Unnikrishnan, A. C. Darby, J. A. Hiscox, S. Paterson, I. Martincorena, E. M. Volz, A. J. Page, O. G. Pybus, A. R. Bassett, C. V. Ariani, M. H. S. Chapman, K. K. Li, R. N. Shah, N. G. Jesu-dason, Y. Taha, M. P. McHugh, R. Dewar, A. S. Jahun, C. McMurray, S. Pandey, J. P. McKenna, A. Nelson, G. R. Young, C. M. McCann, S. Elliott, H. Lowe, B. Temperton, S. Roy, A. Price, S. Rey, M. Wyles, S. Rooke, S. Shaaban, M. de Cesare, L. Letchford, S. Silveira, E. Pelosi, E. Wilson-Davies, M. Hosmillo, . O'Toole, A. R. Hesketh, R. Stark, L. du Plessis, C. Ruis, H. Adams, Y. Bourgeois, S. L. Michell, D. Gram-atopoulos, J. Edgeworth, J. Breuer, J. A. Todd, C. Fraser, D. Buck, M. John, G. L. Kay, S. Palmer, S. J. Peacock, D. Heyburn, D. Weldon, E. Robinson, A. McNally, P. Muir, I. B. Vipond, J. Boyes, V. Sivaprakasam, T. Salluja, S. Dervisevic, E. J. Meader, N. R. Park, K. Oliver, A. R. Jeffries, S. Ott, A. da Silva Filipe, D. A. Simpson, C. Williams, J. A. Masoli, B. A. Knight, C. R. Jones, C. Koshy, A. Ash, A. Casey, A. Bosworth, L. Ratcliffe, L. Xu-McCrae, H. M. Pymont, S. Hutchings, L. Berry, K. Jones, F. Halstead, T. Davis, C. Holmes, M. Iturriza-Gomara, A. O. Lucaci, P. A. Randell, A. Cox, P. Madona, K. A. Harris, J. R. Brown, T. W. Mahungu, D. Irish-Tavares, T. Haque, J. Hart, E. Witele,

M. L. Fenton, S. Liggett, C. Graham, E. Swindells, J. Collins, G. Eltringham, S. Campbell, P. C. McClure, G. Clark, T. J. Sloan, C. Jones, J. Lynch, B. Warne, S. Leonard, J. Durham, T. Williams, S. T. Haldenby, N. Storey, N.-F. Alikhan, N. Holmes, C. Moore, M. Carlile, M. Perry, N. Craine, R. A. Lyons, A. H. Beckett, S. Goudarzi, C. Fearn, K. Cook, H. Dent, H. Paul, R. Davies, B. Blane, S. T. Girgis, M. A. Beale, K. L. Bellis, M. J. Dorman, E. Drury, L. Kane, S. Kay, S. McGuigan, R. Nelson, L. Prestwood, S. Rajatileka, R. Batra, R. J. Williams, M. Kristiansen, A. Green, A. Justice, A. I. Mahanama, B. Samaraweera, N. F. Hadjirin, J. Quick, R. Poplawski, L. M. Kermack, N. Reynolds, G. Hall, Y. Chaudhry, M. L. Pinckert, I. Georgana, R. J. Moll, A. Thornton, R. Myers, J. Stockton, C. A. Williams, W. C. Yew, A. J. Trotter, A. Trebes, G. MacIntyre-Cockett, A. Birchley, A. Adams, A. Plimmer, B. Gatica-Wilcox, C. McKerr, E. Hilvers, H. Jones, H. Asad, J. Coombes, J. M. Evans, L. Fina, L. Gilbert, L. Graham, M. Cronin, S. Kumziene-Summerhayes, S. Taylor, S. Jones, D. C. Groves, P. Zhang, M. Gallis, S. F. Louka, I. Starinskij, C. Jackson, M. Gourtovaia, G. Tonkin-Hill, K. Lewis, J. M. Tovar-Corona, K. James, L. Baxter, M. T. Alam, R. J. Orton, J. Hughes, S. Vattipally, M. Ragonnet-Cronin, F. F. Nascimento, D. Jorgensen, O. Boyd, L. Geidelberg, A. E. Zarebski, J. Raghvani, M. U. Kraemer, J. Southgate, B. B. Lindsey, T. M. Freeman, J.-P. Keatley, J. B. Singer, L. de Oliveira Martins, C. A. Yeats, K. Abudahab, B. E. Taylor, M. Menegazzo, J. Danesh, W. Hogsden, S. Eldirdiri, A. Kenyon, J. Mason, T. I. Robinson, A. Holmes, J. Price, J. A. Hartley, T. Curran, A. E. Mather, G. Shankar, R. Jones, R. Howe, S. Morgan, E. Wastenge, M. R. Chapman, S. Mookerjee, R. Stanley, W. Smith, T. Peto, D. Eyre, D. Crook, G. Vernet, C. Kitchen, H. Gulliver, I. Merrick, M. Guest, R. Munn, D. T. Bradley, T. Wyatt, C. Beaver, L. Foulser, S. Palmer, C. M. Churcher, E. Brooks, K. S. Smith, K. Galai, G. M. McManus, F. Bolt, F. Coll, L. Meadows, S. W. Attwood, A. Davies, E. De Lacy, F. Downing, S. Edwards, G. P. Scarlett, S. Jeremiah, N. Smith, D. Leek, S. Sridhar, S. Forrest, C. Cormie, H. K. Gill, J. Dias, E. E. Higginson, M. Maes, J. Young, M. Wantoch, D. Jamrozy, S. Lo, M. Patel, V. Hill, C. M. Bew-

shea, S. Ellard, C. Auckland, I. Harrison, C. Bishop, V. Chalker, A. Richter, A. Beggs, A. Best, B. Percival, J. Mirza, O. Megram, M. Mayhew, L. Crawford, F. Ashcroft, E. Moles-Garcia, N. Cumley, R. Hopes, P. Asamaphan, M. O. Niebel, R. N. Gunson, A. Bradley, A. Maclean, G. Mollett, R. Blacow, P. Bird, T. Helmer, K. Fallon, J. Tang, A. D. Hale, L. R. Macfarlane-Smith, K. L. Harper, H. Carden, N. W. Machin, K. A. Jackson, S. S. Ahmad, R. P. George, L. Turtle, E. O'Toole, J. Watts, C. Breen, A. Cowell, A. Alcolea-Medina, T. Charalampous, A. Patel, L. J. Levett, J. Heaney, A. Rowan, G. P. Taylor, D. Shah, L. Atkinson, J. C. Lee, A. P. Westhorpe, R. Jannoo, H. L. Lowe, A. Karamani, L. Ensell, W. Chatterton, M. Pusok, A. Dadrah, A. Symmonds, G. Sluga, Z. Molnar, P. Baker, S. Bonner, S. Essex, E. Barton, D. Padgett, G. Scott, J. Greenaway, B. A. Payne, S. Burton-Fanning, S. Waugh, V. Raviprakash, N. Sheriff, V. Blakey, L.-A. Williams, J. Moore, S. Stonehouse, L. Smith, R. K. Davidson, L. Bedford, L. Coupland, V. Wright, J. G. Chappell, T. Tsoleridis, J. Ball, M. Khakh, V. M. Fleming, M. M. Lister, H. C. Howson-Wells, L. Berry, T. Boswell, A. Joseph, I. Willingham, N. Duckworth, S. Walsh, E. Wise, N. Moore, M. Mori, N. Cortes, S. Kidd, R. Williams, L. Gifford, K. Bicknell, S. Wyllie, A. Lloyd, R. Impey, C. S. Malone, B. J. Cogger, N. Levene, L. Monaghan, A. J. Keeley, D. G. Partridge, M. Raza, C. Evans, K. Johnson, E. Betteridge, B. W. Farr, S. Goodwin, M. A. Quail, C. Scott, L. Shirley, S. A. Thurston, D. Rajan, I. F. Bronner, L. Aigrain, N. M. Redshaw, S. V. Lensing, S. McCarthy, A. Makunin, C. E. Balcazar, M. D. Gallagher, K. A. Williamson, T. D. Stanton, M. L. Michelsen, J. Warwick-Dugdale, R. Manley, A. Farbos, J. W. Harrison, C. M. Samples, D. J. Studholme, A. Lackenby, T. Mbisa, S. Platt, S. Miah, D. Bibby, C. Manso, J. Hubb, G. Dabrera, M. Ramsay, D. Bradshaw, U. Schaefer, N. Groves, E. Gallagher, D. Lee, D. Williams, N. Ellaby, H. Hartman, N. Manesis, V. Patel, J. Ledesma, K. A. Twohig, E. Allara, C. Pearson, J. K. Cheng, H. E. Bridgewater, L. R. Frost, G. Taylor-Joyce, P. E. Brown, L. Tong, A. Broos, D. Mair, J. Nichols, S. N. Carmichael, K. L. Smollett, K. Nomikou, E. Aranday-Cortes, N. Johnson, S. Nickbakhsh, E. E. Vamos,

M. Hughes, L. Rainbow, R. Eccles, C. Nelson, M. Whitehead, R. Gregory, M. Gemmell, C. Wierzbicki, H. J. Webster, C. L. Fisher, A. W. Signell, G. Betancor, H. D. Wilson, G. Nebbia, F. Flaviani, A. C. Cerda, T. V. Merrill, R. E. Wilson, M. Cotic, N. Bayzid, T. Thompson, E. Acheson, S. Rushton, S. O'Brien, D. J. Baker, S. Rudder, A. Aydin, F. Sang, J. Debebe, S. Francois, T. I. Vasylyeva, M. E. Zamudio, B. Gutierrez, A. Marchbank, J. Maksimovic, K. Spellman, K. McCluggage, M. Morgan, R. Beer, S. Affi, T. Workman, W. Fuller, C. Bresner, A. Angyal, L. R. Green, P. J. Parsons, R. M. Tucker, R. Brown, M. Whiteley, J. Bonfield, C. Puethe, A. Whitwham, J. Liddle, W. Rowe, I. Siveroni, T. Le-Viet, A. Gaskin, R. Johnson, I. Abnizova, M. Ali, L. Allen, R. Anderson, C. Ariani, S. Austin-Guest, S. Bala, J. Barrett, A. Bassett, K. Battle-day, J. Beal, M. Beale, S. Bellany, T. Bellerby, K. Bellis, D. Berger, M. Berriman, P. Bevan, S. Binley, J. Bishop, K. Blackburn, N. Boughton, S. Bowker, T. Brendler-Spaeth, I. Bronner, T. Brooklyn, S. K. Buddenborg, R. Bush, C. Caetano, A. Cagan, N. Carter, J. Cartwright, T. C. Monteiro, L. Chapman, T.-J. Chillingworth, P. Clapham, R. Clark, A. Clarke, C. Clarke, D. Cole, E. Cook, M. Coppola, L. Cornell, C. Cornwall, C. Corton, A. Crackett, A. Cranage, H. Craven, S. Craw, M. Crawford, T. Cutts, M. Dabrowska, M. Davies, J. Dawson, C. Day, A. Densem, T. Dibling, C. Dockree, D. Dodd, S. Dogga, M. Dorman, G. Dougan, M. Dougherty, A. Dove, L. Drummond, M. Dudek, L. Durrant, E. Easthope, S. Eckert, P. Ellis, B. Farr, M. Fenton, M. Ferrero, N. Flack, H. Fordham, G. Forsythe, M. Francis, A. Fraser, A. Freeman, A. Galvin, M. Garcia-Casado, A. Gedny, S. Girgis, J. Glover, O. Gould, A. Gray, E. Gray, C. Griffiths, Y. Gu, F. Guerin, W. Hamilton, H. Hanks, E. Harrison, A. Harrott, E. Harry, J. Harvison, P. Heath, A. Hernandez-Koutoucheva, R. Hobbs, D. Holland, S. Holmes, G. Hornett, N. Hough, L. Huckle, L. Hughes-Hallet, A. Hunter, S. Inglis, S. Iqbal, A. Jackson, D. Jackson, C. J. Verdejo, M. Jones, K. Kallepally, K. Kay, J. Keatley, A. Keith, A. King, L. Kitchin, M. Kleanthous, M. Klimekova, P. Korlevic, K. Krasheninikova, G. Lane, C. Langford, A. Laverack, K. Law, S. Lensing, A. Lewis-Wade, J. Liddle, Q. Lin,

S. Lindsay, S. Linsdell, R. Long, J. Lovell, J. Lovell, J. Mack, M. Maddison, A. Makunin, I. Mamun, J. Mansfield, N. Marriott, M. Martin, M. Mayho, J. McClintock, S. McHugh, L. MapcMinn, C. Meadows, E. Mobley, R. Moll, M. Morra, L. Morrow, K. Murie, S. Nash, C. Nathwani, P. Naydenova, A. Neaverson, E. Nerou, J. Nicholson, T. Nimz, G. G. Noell, S. O’Meara, V. Ohan, C. Olney, D. Ormond, A. Oszlanczi, Y. F. Pang, B. Pardubska, N. Park, A. Parmar, G. Patel, M. Payne, S. Peacock, A. Petersen, D. Plowman, T. Preston, M. Quail, R. Rance, S. Rawlings, N. Redshaw, J. Reynolds, M. Reynolds, S. Rice, M. Richardson, C. Roberts, K. Robinson, M. Robinson, D. Robinson, H. Rogers, E. M. Rojo, D. Roopra, M. Rose, L. Rudd, R. Sadri, N. Salmon, D. Saul, F. Schwach, P. Seekings, A. Simms, M. Sinnott, S. Sivadasan, B. Siwek, D. Sizer, K. Skeldon, J. Skelton, J. Slater-Tunstall, L. Sloper, N. Smerdon, C. Smith, C. Smith, J. Smith, K. Smith, M. Smith, S. Smith, T. Smith, L. Sneade, C. D. Soria, C. Sousa, E. Souster, A. Sparkes, M. Spencer-Chapman, J. Squares, R. Stanley, C. Steed, T. Stickland, I. Still, M. Stratton, M. Strickland, A. Swann, A. Swiatkowska, N. Sycamore, E. Swift, E. Symons, S. Szluha, E. Taluy, N. Tao, K. Taylor, S. Taylor, S. Thompson, M. Thompson, M. Thomson, N. Thomson, S. Thurston, D. Toombs, B. Topping, J. Tovar-Corona, D. Ungureanu, J. Uphill, J. Urbanova, P. J. Van, V. Vancollie, P. Voak, D. Walker, M. Walker, M. Waller, G. Ward, C. Weatherhogg, N. Webb, A. Wells, E. Wells, L. Westwood, T. Whipp, T. Whiteley, G. Whitton, S. Widaa, M. Williams, M. Wilson, and S. Wright, “Recurrent emergence of SARS-CoV-2 spike deletion H69/V70 and its role in the Alpha variant B.1.1.7,” *Cell Reports*, vol. 35, p. 109292, June 2021.

- [30] M. Gerber, C. Isel, V. Moules, and R. Marquet, “Selective packaging of the influenza A genome and consequences for genetic reassortment,” *Trends in Microbiology*, vol. 22, pp. 446–455, Aug. 2014.
- [31] P. von Magnus, “Incomplete forms of influenza virus,” *Advances in virus research*, vol. 2, pp. 59–79, 1954.

- [32] F. G. Alnaji and C. B. Brooke, “Influenza virus DI particles: Defective interfering or delightfully interesting?,” *PLOS Pathogens*, vol. 16, p. e1008436, May 2020.
- [33] K. Saira, X. Lin, J. V. DePasse, R. Halpin, A. Twaddle, T. Stockwell, B. Angus, A. Cozzi-Lepri, M. Delfino, V. Dugan, D. E. Dwyer, M. Freiberg, A. Horban, M. Losso, R. Lynfield, D. N. Wentworth, E. C. Holmes, R. Davey, D. E. Wentworth, and E. Ghedin, “Sequence Analysis of In Vivo Defective Interfering-Like RNA of Influenza A H1N1 Pandemic Virus,” *Journal of Virology*, vol. 87, no. 14, pp. 8064–8074, 2013.
- [34] L. Pelz, D. Rüdiger, T. Dogra, F. G. Alnaji, Y. Genzel, C. B. Brooke, S. Y. Kupke, and U. Reichl, “Semi-continuous Propagation of Influenza A Virus and Its Defective Interfering Particles: Analyzing the Dynamic Competition To Select Candidates for Antiviral Therapy,” *Journal of Virology*, vol. 95, pp. e01174–21, Nov. 2021.
- [35] H. Tao, J. Steel, and A. C. Lowen, “Intrahost Dynamics of Influenza Virus Reassortment,” *Journal of Virology*, vol. 88, pp. 7485–7492, July 2014.
- [36] R. J. Garten, C. T. Davis, C. A. Russell, B. Shu, S. Lindstrom, A. Balish, W. M. Sessions, X. Xu, E. Skepner, V. Deyde, M. Okomo-Adhiambo, L. Gubareva, J. Barnes, C. B. Smith, S. L. Emery, M. J. Hillman, P. Rivaller, J. Smagala, M. de Graaf, D. F. Burke, R. A. M. Fouchier, C. Pappas, C. M. Alpuche-Aranda, H. López-Gatell, H. Olivera, I. López, C. A. Myers, D. Faix, P. J. Blair, C. Yu, K. M. Keene, P. D. Dotson, D. Boxrud, A. R. Sambol, S. H. Abid, K. St. George, T. Bannerman, A. L. Moore, D. J. Stringer, P. Blevins, G. J. Demmler-Harrison, M. Ginsberg, P. Kriner, S. Waterman, S. Smole, H. F. Guevara, E. A. Belongia, P. A. Clark, S. T. Beatrice, R. Donis, J. Katz, L. Finelli, C. B. Bridges, M. Shaw, D. B. Jernigan, T. M. Uyeki, D. J. Smith, A. I. Klimov, and N. J. Cox, “Antigenic and Genetic Characteristics of Swine-Origin 2009 A(H1N1) Influenza Viruses Circulating in Humans,” *Science*, vol. 325, pp. 197–201, July 2009.

- [37] D. H. Morris, V. N. Petrova, F. W. Rossine, E. Parker, B. T. Grenfell, R. A. Neher, S. A. Levin, and C. A. Russell, “Asynchrony between virus diversity and antibody selection limits influenza virus evolution,” *eLife*, vol. 9, p. e62105, Nov. 2020.
- [38] K. Debbink, J. T. McCrone, J. G. Petrie, R. Truscon, E. Johnson, E. K. Mantlo, A. S. Monto, and A. S. Lauring, “Vaccination has minimal impact on the intrahost diversity of H3N2 influenza viruses,” *PLoS Pathogens*, vol. 13, no. 1, pp. 1–18, 2017.
- [39] E. M. Volz, V. Hill, J. T. McCrone, A. Price, D. Jorgensen, A. O’Toole, J. A. Southgate, R. Johnson, B. Jackson, F. F. Nascimento, S. M. Rey, S. M. Nicholls, R. M. Colquhoun, A. da Silva Filipe, J. G. Shepherd, D. J. Pascall, R. Shah, N. Jesudason, K. Li, R. Jarrett, N. Pacchiarini, M. Bull, L. Geidelberg, I. Siveroni, I. G. Goodfellow, N. J. Loman, O. Pybus, D. L. Robertson, E. C. Thomson, A. Rambaut, T. R. Connor, and The COVID-19 Genomics UK Consortium, “Evaluating the effects of SARS-CoV-2 Spike mutation D614G on transmissibility and pathogenicity,” *Cell*, vol. 184, Aug. 2020.
- [40] G. Tonkin-Hill, I. Martincorena, R. Amato, A. R. Lawson, M. Gerstung, I. Johnston, D. K. Jackson, N. Park, S. V. Lensing, M. A. Quail, S. Gonçalves, C. Ariani, M. Spencer Chapman, W. L. Hamilton, L. W. Meredith, G. Hall, A. S. Jahun, Y. Chaudhry, M. Hosmillo, M. L. Pinckert, I. Georgana, A. Yakovleva, L. G. Caller, S. L. Caddy, T. Feltwell, F. A. Khokhar, C. J. Houldcroft, M. D. Curran, S. Parmar, The COVID-19 Genomics UK (COG-UK) Consortium, A. Alderton, R. Nelson, E. M. Harrison, J. Sillitoe, S. D. Bentley, J. C. Barrett, M. E. Torok, I. G. Goodfellow, C. Langford, D. Kwiatkowski, and Wellcome Sanger Institute COVID-19 Surveillance Team, “Patterns of within-host genetic diversity in SARS-CoV-2,” *eLife*, vol. 10, p. e66857, Aug. 2021.
- [41] J. T. McCrone and A. S. Lauring, “Genetic bottlenecks in intraspecies virus transmission,” *Current Opinion in Virology*, vol. 28, pp. 20–25, 2018. Publisher: Elsevier B.V.
- [42] Y. C. F. Su, J. Bahl, U. Joseph, K. M. Butt, H. A. Peck, E. S. C. Koay, L. L. E.

- Oon, I. G. Barr, D. Vijaykrishna, and G. J. D. Smith, “Phylogenetics of H1N1/2009 influenza reveals the transition from host adaptation to immune-driven selection,” *Nature Communications*, vol. 6, p. 7952, Nov. 2015.
- [43] E. Lofgren, N. H. Fefferman, Y. N. Naumov, J. Gorski, and E. N. Naumova, “Influenza Seasonality: Underlying Causes and Modeling Theories,” *Journal of Virology*, vol. 81, pp. 5429–5436, June 2007.
- [44] J. O. Lloyd-Smith, S. J. Schreiber, P. E. Kopp, and W. M. Getz, “Superspreading and the effect of individual variation on disease emergence,” *Nature*, vol. 438, pp. 355–359, Nov. 2005.
- [45] C. Fraser and L. M. Li, “Coalescent models for populations with time-varying population sizes and arbitrary offspring distributions,” *BioRxiv*, Apr. 2017.
- [46] C. A. Russell, T. C. Jones, I. G. Barr, N. J. Cox, R. J. Garten, V. Gregory, I. D. Gust, A. W. Hampson, A. J. Hay, A. C. Hurt, J. C. De Jong, A. Kelso, A. I. Klimov, T. Kageyama, N. Komadina, A. S. Lapedes, Y. P. Lin, A. Mosterin, M. Obuchi, T. Odagiri, A. D. Osterhaus, G. F. Rimmelzwaan, M. W. Shaw, E. Skepner, K. Stohr, M. Tashiro, R. A. Fouchier, and D. J. Smith, “The global circulation of seasonal influenza A (H3N2) viruses,” *Science*, vol. 320, no. 5874, pp. 340–346, 2008.
- [47] B. E. Slatko, A. F. Gardner, and F. M. Ausubel, “Overview of Next-Generation Sequencing Technologies,” *Current Protocols in Molecular Biology*, vol. 122, Apr. 2018.
- [48] J. T. McCrone and A. S. Lauring, “Measurements of Intra-host Viral Diversity Are Extremely Sensitive to Systematic Errors in Variant Calling,” *Journal of Virology*, vol. 90, pp. 6884–6895, Aug. 2016.
- [49] C. J. Illingworth, “Fitness Inference from Short-Read Data: Within-Host Evolution of a Reassortant H5N1 Influenza Virus,” *Molecular Biology and Evolution*, vol. 32, pp. 3012–3026, Nov. 2015.

- [50] H. Zhu, B. E. Allman, and K. Koelle, “Fitness Estimation for Viral Variants in the Context of Cellular Coinfection,” *Viruses*, vol. 13, p. 1216, June 2021.
- [51] D. P. Martin, B. Murrell, M. Golden, A. Khoosal, and B. Muhire, “RDP4: Detection and analysis of recombination patterns in virus genomes,” *Virus Evolution*, vol. 1, Mar. 2015.
- [52] D. VanInsberghe, A. Neish, A. C. Lowen, and K. Koelle, “Identification of SARS-CoV-2 recombinant genomes,” *bioRxiv*, Aug. 2020.
- [53] A. Routh and J. E. Johnson, “Discovery of functional genomic motifs in viruses with ViReMa—a virus recombination mapper—for analysis of next-generation sequencing data,” *Nucleic Acids Research*, vol. 42, no. 2, pp. 1–10, 2014.
- [54] F. G. Alnaji, J. R. Holmes, G. Rendon, J. C. Vera, C. Fields, B. E. Martin, and C. B. Brooke, “Sequencing framework for the sensitive detection and precise mapping of defective interfering particle-associated deletions across influenza A and B viruses.,” *Journal of Virology*, vol. 93, May 2019.
- [55] N. J. Dimmock, E. W. Rainsford, P. D. Scott, and A. C. Marriott, “Influenza Virus Protecting RNA: an Effective Prophylactic and Therapeutic Antiviral,” *Journal of Virology*, vol. 82, no. 17, pp. 8570–8578, 2008.
- [56] M. I. Nelson, C. Viboud, L. Simonsen, R. T. Bennett, S. B. Griesemer, K. St. George, J. Taylor, D. J. Spiro, N. A. Sengamalay, E. Ghedin, J. K. Taubenberger, and E. C. Holmes, “Multiple Reassortment Events in the Evolutionary History of H1N1 Influenza A Virus Since 1918,” *PLoS Pathogens*, vol. 4, p. e1000012, Feb. 2008.
- [57] S. M. Bell and T. Bedford, “Modern-day SIV viral diversity generated by extensive recombination and cross-species transmission,” *PLOS Pathogens*, vol. 13, p. e1006466, July 2017.

- [58] J. Lees, “Tanglegrams can be misleading,” Feb. 2017.
- [59] J. Felsenstein, “Evolutionary trees from DNA sequences: A maximum likelihood approach,” *Journal of Molecular Evolution*, vol. 17, pp. 368–376, Nov. 1981.
- [60] Z. Yang, S. Kumar, and M. Nei, “A new method of inference of ancestral nucleotide and amino acid sequences.,” *Genetics*, vol. 141, pp. 1641–1650, Dec. 1995.
- [61] A. Rambaut, “Estimating the rate of molecular evolution: incorporating non-contemporaneous sequences into maximum likelihood phylogenies,” *Bioinformatics*, vol. 16, pp. 395–399, Apr. 2000.
- [62] A. D. Yoder and Z. Yang, “Estimation of Primate Speciation Dates Using Local Molecular Clocks,” *Molecular Biology and Evolution*, vol. 17, pp. 1081–1090, July 2000.
- [63] J. Kingman, “The Coalescent,” *Stochastic Processes and their Applications*, vol. 13, pp. 235–248, 1982.
- [64] T. Stadler, D. Kühnert, S. Bonhoeffer, and A. J. Drummond, “Birth–death skyline plot reveals temporal changes of epidemic spread in HIV and hepatitis C virus (HCV),” *Proceedings of the National Academy of Sciences*, vol. 110, pp. 228–233, Jan. 2013.
- [65] A. J. Drummond, “Bayesian Coalescent Inference of Past Population Dynamics from Molecular Sequences,” *Molecular Biology and Evolution*, vol. 22, pp. 1185–1192, Feb. 2005.
- [66] V. N. Minin, E. W. Bloomquist, and M. A. Suchard, “Smooth Skyride through a Rough Skyline: Bayesian Coalescent-Based Inference of Population Dynamics,” *Molecular Biology and Evolution*, vol. 25, pp. 1459–1471, Apr. 2008.
- [67] M. S. Gill, P. Lemey, N. R. Faria, A. Rambaut, B. Shapiro, and M. A. Suchard, “Improving Bayesian Population Dynamics Inference: A Coalescent-Based Model for Multiple Loci,” *Molecular Biology and Evolution*, vol. 30, pp. 713–724, Mar. 2013.

- [68] E. M. Volz, “Complex Population Dynamics and the Coalescent Under Neutrality,” *Genetics*, vol. 190, pp. 187–201, Jan. 2012.
- [69] D. A. Rasmussen, E. M. Volz, and K. Koelle, “Phylogenetic Inference for Structured Epidemiological Models,” *PLoS Computational Biology*, vol. 10, p. e1003570, Apr. 2014.
- [70] E. M. Volz and I. Siveroni, “Bayesian phylogenetic inference with complex models,” *PLOS Computational Biology*, vol. 14, p. e1006546, Nov. 2018.
- [71] P. Lemey, A. Rambaut, A. J. Drummond, and M. A. Suchard, “Bayesian Phylogeography Finds Its Roots,” *PLoS Computational Biology*, vol. 5, p. e1000520, Sept. 2009.
- [72] P. Lemey, A. Rambaut, J. J. Welch, and M. A. Suchard, “Phylogeography Takes a Relaxed Random Walk in Continuous Space and Time,” *Molecular Biology and Evolution*, vol. 27, pp. 1877–1885, Aug. 2010.
- [73] T. Bedford, S. Riley, I. G. Barr, S. Broor, M. Chadha, N. J. Cox, R. S. Daniels, C. P. Gunasekaran, A. C. Hurt, A. Kelso, A. Klimov, N. S. Lewis, X. Li, J. W. McCauley, T. Odagiri, V. Potdar, A. Rambaut, Y. Shu, E. Skepner, D. J. Smith, M. A. Suchard, M. Tashiro, D. Wang, X. Xu, P. Lemey, and C. A. Russell, “Global circulation patterns of seasonal influenza viruses vary with antigenic drift,” *Nature*, vol. 523, no. 7559, pp. 217–220, 2015.
- [74] A. J. Drummond and A. Rambaut, “BEAST: Bayesian evolutionary analysis by sampling trees,” *BMC Evolutionary Biology*, vol. 7, no. 1, p. 214, 2007.
- [75] R. Bouckaert, J. Heled, D. Kühnert, T. Vaughan, C.-H. Wu, D. Xie, M. A. Suchard, A. Rambaut, and A. J. Drummond, “BEAST 2: A Software Platform for Bayesian Evolutionary Analysis,” *PLoS Computational Biology*, vol. 10, p. e1003537, Apr. 2014.

Chapter 2

Leveraging genomic diversity to gain insights into within host influenza dynamics

Michael A. Martin^{1,2}, Nicolas Berg ², Katia Koelle^{2,3}

¹Graduate Program in Population Biology, Ecology, and Evolution, Emory University, Atlanta, GA 30322, USA.

²Department of Biology, Emory University, Atlanta, GA 30322, USA.

³Emory-UGA Center of Excellence for Influenza Research and Surveillance (CEIRS), Atlanta GA 30322, USA.

add credit statements

M.A.M Contributions

Conceptualization, Methodology, Validation, Formal analysis, Investigation, Data Curation, Writing - Original Draft, Writing - Review & Editing, Visualization, Supervision

2.1 Abstract

Infection with influenza virus results in considerable public health and economic impacts each year. One of the contributing factors to influenza's continued spread within the human population is its ability to evade acquired immunity through continual antigenic evolution. Understanding the evolutionary forces that act within and between hosts is therefore crucial to understanding the generation of new antigenic variants. Many studies have analyzed the longitudinal patterns of genetic diversity within individual hosts to assess the relative contributions of selection and drift on evolution. However, most infected individuals harbor very few point mutations in their infecting viral genomes, limiting our resolution in understanding the forces acting on these populations. Further, because of this limited within host genetic diversity we have limited resolution to infer the extent of drift across transmission events. We here propose to use genomic diversity as an alternative signal to better understand the within and between host evolution of influenza virus. Specifically, we focus on the dynamics of defective viral genomes (DVGs), or those genomes harboring a large internal deletion in at least one segment, in natural human infections. By comparing DVG populations across time points and between donor and recipient hosts we show that DVG populations are highly dynamic within hosts and rarely appear to be transmitted along with wild-type virus. Our findings are consistent with the predominance of genetic drift shaping within host populations of influenza A virus and the presence of tight bottlenecks occurring at the point of transmission.

2.2 Introduction

Influenza A virus is one of the most common viral pathogens worldwide. Despite relatively widespread vaccination, influenza infection results in over 20,000 deaths and \$3.7 billion in direct medical costs each year in the United States alone [1]. One of the contributing factors to the virus's continued widespread circulation is its ability to rapidly evolve to

evade natural and vaccine-derived immunity [2, 3, 4, 5, 6]. This so-called “antigenic drift” allows the virus to continually replenish its pool of susceptible hosts by reinfecting hosts who harbor immunity to previously circulating strains. Understanding how new antigenic variants evolve within single hosts and ultimately sweep the population is important for vaccine strain selection [7, 8, 9] and informing the development of vaccines that are more robust to viral evolution [10].

The evolution of antigenically diverse lineages of influenza virus is possible because there is diversity in the viral population on which selection can act. This diversity exists because of errors made by the viral polymerase during replication within single hosts. This diversity is shaped by the evolutionary forces within hosts and the population bottlenecks that occur during transmission between hosts [11]. Analyzing the dynamics of this diversity, therefore, can provide insights into the evolution acting within- and between hosts.

Deep sequencing data can be used to quantify the diversity of viral populations within hosts. Sequencing reads generated from a single host can be aligned to the reference genome and used to estimate the frequency of each nucleotide at each site of the viral genome. By comparing variant frequencies across multiple time points one can determine whether selection is acting on specific mutations or whether genetic drift dominates within host evolution [12]. Finally, by comparing variant frequencies in donor and recipient hosts in transmission pairs one can estimate how many virions seeded infection in the recipient [13].

Previous analyses of this type have revealed that selection during natural influenza infection within individual human hosts is relatively weak. For example, it has been shown that there is no signal of elevated dN/dS within hosts, no evidence for selection on known antigenic escape mutants, and the presence of prior immunity has little impact on the amount of observed within host diversity [14, 11]. It has been suggested that this may be due to mismatch in the timing between viral population growth and the immune response [15]. Alternatively, during chronic infections in which there are more viral generations for selection to act, the within host generation of beneficial antigenic variants is readily observed [16].

However, within any given acute infection, there is a relatively limited amount of genetic diversity in the form of single nucleotide polymorphisms (SNPs). In any individual host, there are generally fewer than 15 sites in the viral genome with detectable diversity and those mutations that are present are present at low frequency, rarely shared between hosts, and often not shared between multiple time points from the same subject [14, 11]. This limited diversity hinders our ability to robustly characterize the evolutionary forces acting on these populations and results in considerable uncertainty in our inferred contributions of selection and drift to within and between host evolution. Here we propose using an alternative signal to study the evolutionary dynamics of viral populations within and between hosts. Specifically, we propose focusing on the *genomic* diversity that is generated during infection, in the form of influenza defective viral genomes (DVGs).

DVGs (here used synonymously with deletion-containing viral genomes, DelVGs [17]) harbor a large internal deletion in at least one of the eight segments of the influenza genome. As a result, virions with a DVG are incapable of replicating on their own. However, through coinfection of a cell with wild-type virus, they can proliferate throughout an infection [17]. The process by which coinfection rescues cellular infection with DVGs is similar to the process by which coinfection can rescue infection by virions with incomplete genomes [18, 19] except that instead of missing them entirely, DVGs harbor truncated copies of some segments. Due to this reliance on coinfection, we expect the evolutionary forces acting on DVG populations to mirror those acting on the wild-type viral population. For example, if positive selection is acting on a specific viral mutations, then DVG species that coinfect with wild-type viruses harboring this mutation will appear to have an evolutionary advantage over the DVG species which coinfect with cells lacking this beneficial mutation. This is roughly analogous to the process of genetic hitchhiking, in which neutral loci that co-occur with beneficial ones will increase in frequency due to this linkage [20].

We know from theoretical models of hitchhiking that the apparent selective advantage of a neutral gene linked to a beneficial one is dependent on the rate of recombination, or in the case

of influenza, reassortment, between the neutral and beneficial gene. Given viral reassortment occurs readily during cellular coinfection [21], we might expect the linkage between DVGs and their co-infecting helper viruses to be quite weak. However, within host influenza infections are highly spatially structured [22] and this spatial structure may help to counteract the effects of reassortment by increasing the likelihood that a given DVG species coinfects the same cells with a given wild-type genome over multiple cellular replication cycles. Thus, DVGs may offer a complimentary signal to that which is present in the dynamics of SNPs on wild-type viral genomes.

It has been proposed that DVGs may also be transmitted between hosts [23], although these findings have not yet been substantiated elsewhere. Similarly to at the within-host scale, this process in theory relies on coinfection of recipient hosts cells by both wild-type and DVG virions. *A priori*, this is expected to be unlikely if you assume wild-type and DVG virions infect host cells at random during transmission, given the large number of susceptible host cells. However, it is thought that some viruses, influenza included, may form so-called collective infectious units [24]. In these collective units, virions aggregate together, presumably increasing the probability of cellular coinfection. This may play a role in how influenza viruses are able to transmit at all, given the high prevalence of virions harboring incomplete genomes [18, 19]. While their role in between-host transmission remains putative, it has been shown *in vitro* that influenza viruses can in fact form aggregates [25]. If viral aggregates play a role in host to host transmission, we might expect that they act to increase the probability of coinfection early in infection. In addition to physical aggregation with a wild-type virus, the putative transmission of DVGs is made more likely by the fact that DVG RNA can persist in cells for more than two weeks [26]. This finding increases the chance that DVG RNA from a donor host coinfects with wild-type virus in the recipient host as wild-type virus spreads throughout the susceptible recipient host cells.

A subset of DVGs are able to interfere with the replication of wild-type virus during coinfection. This subset of the larger collection of DVGs are referred to as defective interfering

particles (DIPs). DIPs were first identified due to the fact that their interfering properties result in cycles of wild-type virus population expansion and contraction in high-multiplicity of infection passages [27, 28]. For that reason exogenous DIPs have been proposed as potential therapeutic for viral pathogens [29, 30]. It is not well understood which of the many possible DVGs harbor interfering capabilities and if there are any common features of the DVGs which are interfering [28]. In some viral species the presence of DVGs may actually be beneficial for establishing persistent infection [31]. Influenza DIPs have been intensively studied in cell culture [32, 33, 17], and, to a lesser extent, animal models [34, 35]. They have been identified directly from human clinical samples [23]., however, their longitudinal and host to host dynamics in natural human infections is still under investigation. Thanks to recent bioinformatic developments, DVGs can be reliably identified from short read sequencing data. The identification of DVG reads hinges on the fact that when these reads are aligned to a wild-type reference genome, each end of the read will best align to distinct portions of the reference genome. Depending on the algorithm used this will either result in the read not being aligned at all, being heavily “clipped,” or aligning in a “split” fashion which allows for many deleted reference nucleotides in the alignment. We here use a slightly modified version of a recently developed pipeline [36] that uses the ViReMa algorithm [37] to identify DVG supporting reads. By iteratively aligning portions of the read, the ViReMa algorithm allows distinct portions of a given sequencing read to align to different locations in the reference genome.

Here, we apply this workflow to previously published deep sequencing data from 217 clinical samples of influenza A H3N2 infections taken from 168 patients [11]. Within these data there are 49 subjects with samples from multiple time points and 47 epidemiologically linked transmission pairs allowing us to look at aggregate dynamics across all subjects, longitudinal dynamics within single-subjects, and dynamics between transmission pairs. This analysis therefore provides a comprehensive view of the generation, evolution, and transmission of influenza DVGs during natural human infections.

2.3 Materials and methods

2.3.1 Data source

All clinical and sequencing data were previously published as part of [11] and all epidemiological and laboratory methods are described in detail in the original publication. In short, the HIVE cohort at the UM School of Public Health queries participating households weekly during the months of October through May for symptoms of respiratory illness. Individuals with symptoms were sampled via a combined nasal and throat swab by the research team. During the 2014-2015 season individuals were also instructed to take a self- or parent-collected nasal swab at symptom onset.

cDNA was amplified from samples testing positive for influenza virus using the SuperScript III One-Step RT-PCR Platinum Taq HiFi Kit and the universal influenza A primers [38]. Sequencing libraries were prepared from 300-400bp sheared cDNA fragments and bar-coded libraries were further purified by isolation of a 300-500 bp band using gel isolation. Sequencing reads were generated on an Illumina HiSeq 2500 with 2×125 nucleotide paired end reads. Samples with input titers between 10^3 and 10^5 genomes/ μ l were sequenced in replicate. For each sequencing run PCR amplicons derived from eight clonal plasmids of the circulating strain were sequenced on the same HiSeq flow cell as the patient samples.

Influenza A H3N2 (as identified by a library labelled “perth,” “hk,” or “vic”) sequencing reads were downloaded from the National Library of Medicine (NLM) National Center for Biotechnology Information (NCBI) Sequencing Read Archive (SRA) BioProject PRJNA412631 using the fasterq-dump utility available as part of the SRA Toolkit (<https://github.com/ncbi/sra-tools>).

2.3.2 Transmission analyses

We used the same household and community pairings reported in [11]. Pairs of epidemiologically unlinked samples (“community pairs”) were generated by randomly assigning pairs of

samples within each season, excluding samples from the same household. Epidemiologically linked pairs (“transmission pairs”) were identified as in [11] from pairs of individuals from the same household who were infected with influenza viruses more similar than 95% of random community pairs, as measured by the L1-norm.

2.3.3 DVG identification

DVGs were identified using a modified version of the pipeline presented in [36]. Reference genomes were used in accordance with those used in [11]: GenBank CY121496-503 was used for samples collected as part of the 2010-2011 or 2011-20112 season, GenBank KJ942680-8 was used for samples collected during the 2012-2013 season, and GenBank CY207731-8 used for samples collected during the 2014-2015 season. To aid in the identification of DVGs with breakpoints near the 5’ or 3’ end of a segment we added a 210nt poly-A pad to the 5’ and 3’ end of each segment. The analysis pipeline was run in Nextflow v19.01.0 [39].

For quality control sequencing reads were first trimmed using Trimmomatic v0.39 [40] in Phred33 mode using the TruSeq3-PE-2 adapters allowing for 2 seed mismatches, a palindromeClipThreshold of 15, and a simpleClipThreshold of 10, scanning the read with a 3 base sliding window and cutting when the average quality falls below 20, removing leading and trailing bases with quality less than 28, and removing reads less than 75 nucleotides in length. Next Kraken2 v.2.0.7-beta [41] with the k2_pluspf_16gb database in paired end mode was used to categorize each read. The `extract_kraken_reads.py` script from Kraken Tools (<https://github.com/jenniferlu717/KrakenTools>) was used to filter only for reads assigned to influenza A virus (taxonomic id 11320) or any children taxa. Quality control on the filtered reads was conducted with FastQc v0.11.9 [42].

The paired end reads were concatenated into a single fastq file and aligned using Bowtie2 v.2.4.2 [43] in end-to-end mode with a minimum scoring scheme of L,0,-0.3. End-to-end mode disallows soft-clipping of reads which is needed to align reads that span DVG junction sites. Therefore, reads which do align in end-to-end mode include all wild-type viral reads

as well as reads from the 5' and 3' ends of DVGs which do not span the deletion junction site (hereby referred to as non-DVG supporting reads). The number of reads that aligned to each segment in the step was calculated using Samtools v1.13 with htslib v.1.13 [44] by first sorting by name, then adding mate score tags with fixmate, sorting again by coordinates, marking and removing duplicates with markdup and finally tabulating reads using idxstats.

Sequencing reads which did not align in end-to-end mode include the DVG deletion spanning reads and were thus used as input to ViReMa v0.25 [37] with a seed length of 25 nucleotides, tolerating 1 mismatch in the seed alignment, and allowing up to 8 mismatches at the 5' and 3' end of an alignment. To exclude small indels we removed any DVG-supporting reads which support a deletion of less than 20 nucleotides. Duplicate DVG supporting reads were also removed with ViReMa. Bowtie v1.0.0 [45] was used within ViReMa.

As discussed in [36] identifying the precise DVG breakpoint from sequencing data can be impossible when there are nucleotide repeats on either side of the deletion junction, as is prone to occur [17]. ViReMa includes a “DeFuzz” feature which allows users to force the reported junction site to either the 5' or 3' end of a given read. However, because DVGs may be supported by reads either in the forward or reverse direction, this behavior results in disparate reporting for the same DVG depending on the supporting read direction. Therefore, we slightly modified ViReMa’s underlying AddToDict function to force the reported junction sites to the 5' or 3' end of the reference genome, instead of the supporting read. All DVG junctions reported here have been DeFuzz’d to the 3' end of the reference genome. ViReMa results were parsed in Perl v5.26.2 using the summary scripts included as part [36].

2.3.4 DVG quality filtering

DVGs for each clinical sample as well as the plasmid control for each sequencing run were further parsed using Python v3.9.4 [46] with Pandas v1.1.4 [47] and Numpy v1.19.4 [48]. The reported junction breakpoints from the three sets of reference genomes were reconciled by pairwise aligning the segments from each reference using MAFFT v7.6.4 [49] and creating

a mapping between the coordinates for each individual reference and a universal coordinate system. DVGs breakpoints are reported in the universal coordinate system. For each identified DVG we calculated its relative read support by normalizing the number of DVG supporting reads by the sum of the DVG supporting reads and the non-DVG supporting reads for that segment.

Notably, this relative measure is imperfect because reads from the 5' and 3' portions of the genome which are conserved in DVGs cannot be reliably assigned to having been derived from a DVG or wild type viral genome. Furthermore, because longer segments harbor more internal coding nucleotides that can be deleted by DVGs without affecting packaging, this metric may bias the relative support of DVGs on longer segments downwards. Nevertheless, this measure should be a reasonable means of adjusting for variable sequencing depth, particularly when comparing segments of similar length (such as the three polymerase segments).

For each sequencing run, we first excluded any DVG species (as identified by their junction breakpoints) observed in their respective plasmid control. Where technical sequencing replicates from the same biological sample were available we included only DVGs present in both replicates. In these cases, the mean of the relative support values from each replicate was used in downstream analyses. Based on the read support of DVGs present in the plasmid controls, we included only DVGs supported by at least 10 sequencing reads in downstream analyses.

2.3.5 BlastN analysis

Nucleotide Blast (BlastN) analysis [50] was run on the NLM NCBI website (<https://blast.ncbi.nlm.nih.gov/Blast.cgi>) on May 16th, 2022 using the standard database with the nucleotide collection optimized for highly similar sequences (megablast [51]).

2.3.6 Statistical analyses and visualization

All statistical analyses were done in Python. Statistical tests were conducted using Scipy v1.8.0 [52] and regression modeling was done using statsmodels v0.13.2 [53]. All visualization was done in Python using Matplotlib v3.5.1.

2.4 Results

2.4.1 Limited DVGs in plasmid controls

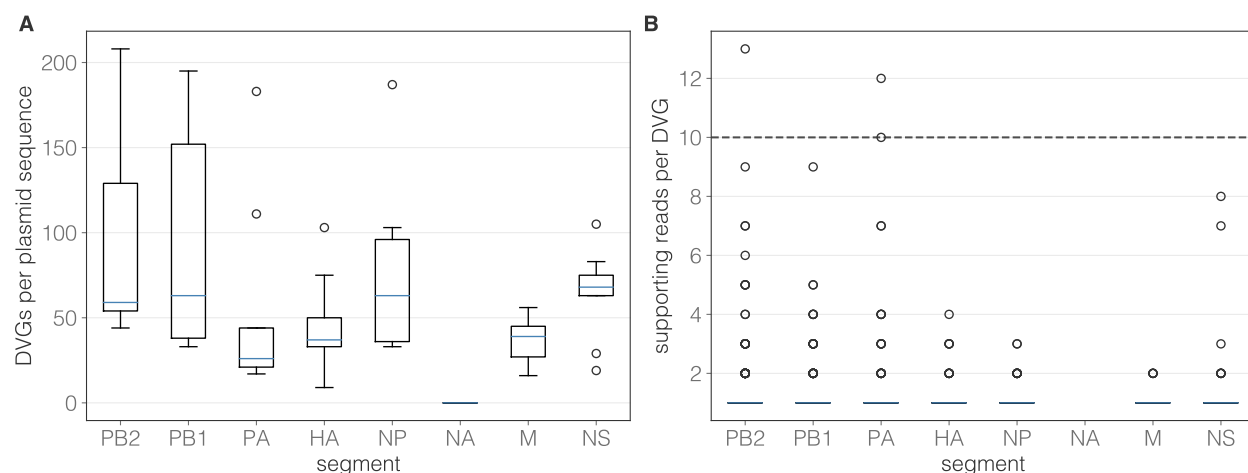


Figure 2.1: DVGs identified in the plasmid controls. Blue line represents the median value for a given dataset, box extends to the limits of the inter-quartile range (IQR), and whiskers extend to 1.5 IQR below and above the 1st and 3rd quartile, respectively. Outliers are shown as dots beyond the range of the whiskers. A) Number of unique DVGs identified per sequenced plasmid per genome segment. B) Number of supporting reads per DVG per sequenced plasmid per genome segment. Dotted horizontal line at $N = 10$ reads represent threshold used for downstream analyses.

To determine the number of spurious DVGs introduced by the sequencing protocol, we first queried the reads generated from the plasmid controls for each sequencing run for DVGs. This analysis acts as a negative control as these DVG reads are generated from clonal plasmids containing full-length viral genome segments and thus should not contain any DVGs. While we observed many (median [sd]: 44.00 [49.54]) unique DVGs in each plasmid control, encouragingly, these DVGs were almost exclusively present at very low read

support (**Figure 2.1**, 1.00 [0.52]). The vast majority (>99.9%) of DVGs identified in plasmid controls are supported by <10 reads. Consequently, we required DVGs to be supported by a minimum of 10 sequencing reads for all downstream analyses to remove spurious DVGs introduced by the sequencing protocol.

2.4.2 DVGs observed readily in clinical samples

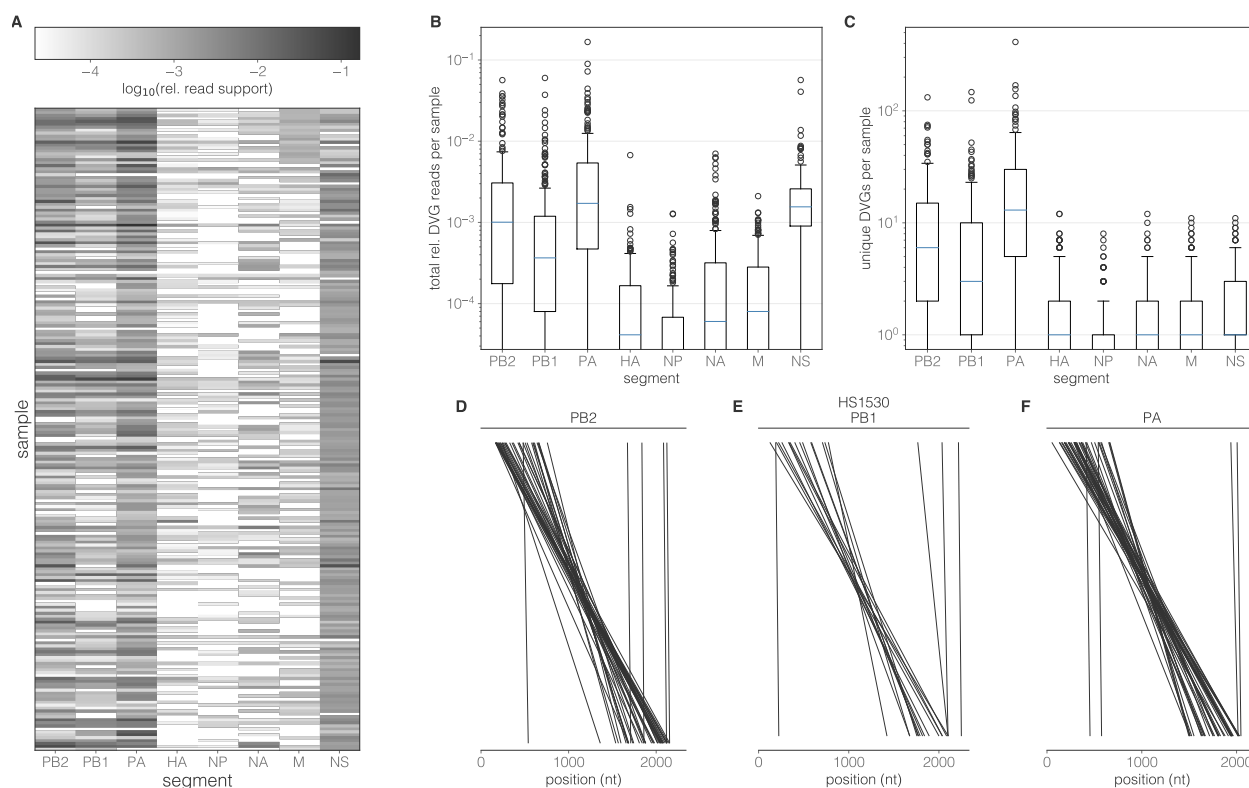


Figure 2.2: DVGs identified in clinical samples. In all boxplots (B, C) blue line represents the median value for each segment, box extends to the limits of the IQR, and whiskers extend to 1.5 IQR below and above the 1st and 3rd quartile, respectively. Outliers are shown as dots beyond the range of the whiskers. A) Heatmap showing the total relative DVG reads in each sample (rows) in each segment (columns). B) Total relative DVG reads per sample per segment. C) Number of unique DVGs per sample per segment. D,E,F) Breakpoints of all PB2 (D), PB1 (E), and PA (F) DVGs identified in representative sample HS1530. Each line connects the last undeleted base on the 5' end of the DVG and the first undeleted base on the 3' end of the DVG.

As opposed to the plasmid controls described above, DVGs are observed readily in the clinical samples (**Figure 2.2**). We observe at least one quality filtered DVG in all 217 of the clinical samples (**Figure 2.2A**). DVGs are observed most abundantly on the PB2, PB1,

PA, and NS segments (**Figure 2.2A,B**, unequal variance T-test with 1000 permutations comparing the relative read support of PB2, PB1, PA, and NS DVGs v. HA, NP, NA, and M DVGs p value $< 1e-4$). However, when looking at the number of unique DVGs (**Figure 2.2C**), as defined by their junction breakpoints, we see a slightly different pattern: PB2, PB1, and PA harbor many more unique DVG species than other segments. NS, compared to the relative read support analysis, contains very few unique DVGs (unequal variance T-test with 1000 permutations comparing the number of DVGs per sample observed on the PB2, PB1, PA segments v. on the HA, NP, NA, M, and NS segments p value $< 1e-4$). This pattern is consistent with the presence of one or very few unique NS DVGs which are abundantly supported (**subsection 2.4.3**). Our finding that DVGs primarily proliferate on the polymerase segment is consistent with previous *in vitro* [17, 33] and *in vivo* [23] analyses. Based on our finding that (with the exception of NS), most observed DVGs are on the polymerase segments and previous work in the field, we here focus only on DVGs observed in the polymerase segment for downstream analyses.

Canonically, the generation of influenza DVGs results in the deletion of the internal coding region for each segment and the conservation of the 5' and 3' regions of each segment, which are thought to be needed for virion packaging [30]. To assess whether our identified DVGs followed this pattern we mapped the deletion junction sites onto the reference genome (**Figure 2.2D,E,F**, **Figure S2.6**). This analysis reveals that the majority of observed DVGs do in fact result in the deletion of the internal portion of each segment, providing confidence that our analysis pipeline is accurately identifying defective genomes, that is, those which are incapable of establishing productive infection in the absence of wild-type virus. Nevertheless, despite our small indel filter which removes any reads supporting a deletion of less than 20 nucleotides, our analysis identified a small number of polymerase DVGs harboring relatively small deletions. A comprehensive analysis of the number of deleted nucleotides in each of the observed polymerase DVGs reveals a highly bi-modal pattern (**Figure S2.7**). To ensure that our analyses were based solely on truly defective genomes and not those harboring small

indels with minimal fitness effects we implemented an additional empirical filtering step to remove any DVGs which support the deletion of less than 500 nucleotides.

Importantly, these identified DVG patterns are likely influenced by the sequencing protocol used to generate these data. The universal influenza A primers [38] used to amplify the input genetic material are designed to amplify based on binding to the conserved regions at the 5' and 3' termini. As such, any genetic material in the input sample lacking these regions would not be amplified. Furthermore, size filters in the sequencing protocol limited our resolution to identify DVGs with less than 300 nucleotides in the resulting segment.

2.4.3 Nearly ubiquitous NS DVG

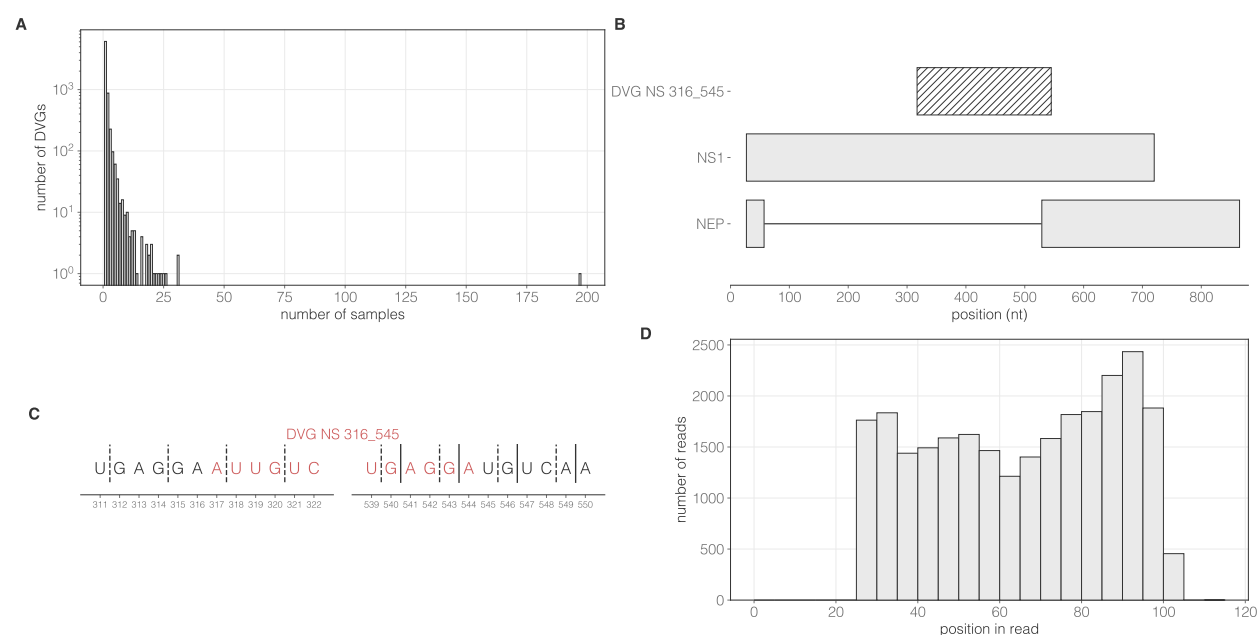


Figure 2.3: Nearly ubiquitous NS DVG. A) Number of DVGs (y-axis) observed in N samples (x-axis). DVG NS 316_545 is found in 197/217 clinical samples. B) Mapping of DVG NS 316_545 onto a schematic of coding portions of the NS segment. The DVG spans the 3' NEP splice site. C) Mapping of DVG NS 316_545 onto the NS segment. Nucleotides in red are deleted as part of DVG NS 316_545. Dashed vertical lines delineate the codons of NS1 in the wild-type protein and dashed solid lines delineate the codons of NEP in the wild-type protein. D) Break point position in the supporting sequencing read for all reads supporting DVG NS 316_545.

In our analysis most individual DVG species were unique, with 99% of all identified DVGs observed in seven or fewer or clinical samples. However, a single NS DVG, DVG NS

316_545 was observed in 197/217 samples (**Figure 2.3A**). This DVG tends to be present at slightly higher relative read support than others in NS ($1.1e-3$ [$9.2e-4$] v. $3.1e-4$ [$3.8e-3$]), although the difference is non-significant (unequal variance T-test with 1000 permutations p value=0.09). The breakpoints of this DVG occur within a 11 nucleotide repeat that is present twice in NS: once between nucleotides 306 and 316 and once between 534 and 544 which spans the splice site of NEP (**Figure 2.3B**). Notably, we can not identify the precise breakpoint within this 11-nucleotide region and reported breakpoints were artificially pushed to the 3' end of the reference genome. Because NEP splicing occurs prior to translation [54], we would therefore not expect proper splicing of the DVG mRNA to occur. An analysis of where the DVG breakpoints occur in relation to the codons of NS1 reveals that this DVG would maintain the open reading frame of this protein (**Figure 2.3C**).

To ensure that this DVG is not a computational artifact we first used BLASTN ([50]) optimized for highly similar sequences to query a DVG NS 316_545 supporting read against the NCBI's standard nucleotide database. The top 100 matches (sorted by E-value) were to influenza A NS segments with nucleotide alignments consistent with the DVG alignment reported here. Furthermore, when mapping the DVG breakpoint onto the supporting reads we did not observe any bias in the read position of the DVG breakpoint on supporting reads **Figure 2.3D**. Nevertheless, we cannot rule out for certain that the reads supporting this breakpoint are not due to contamination or bioinformatic artifact.

2.4.4 DVG populations are dynamic

Our primary goal in this study was to assess how polymerase DVG populations change over time during the course of single infections and during transmission between hosts. To assess the former of these two goals, we first analyzed both the total relative polymerase DVG read support as well as the number of unique polymerase DVGs on a per sample basis as a function of the days post symptom onset, which is used in the absence of data on time since infection (**Figure 2.4A,B**). Our results indicate that both the total relative DVG reads and

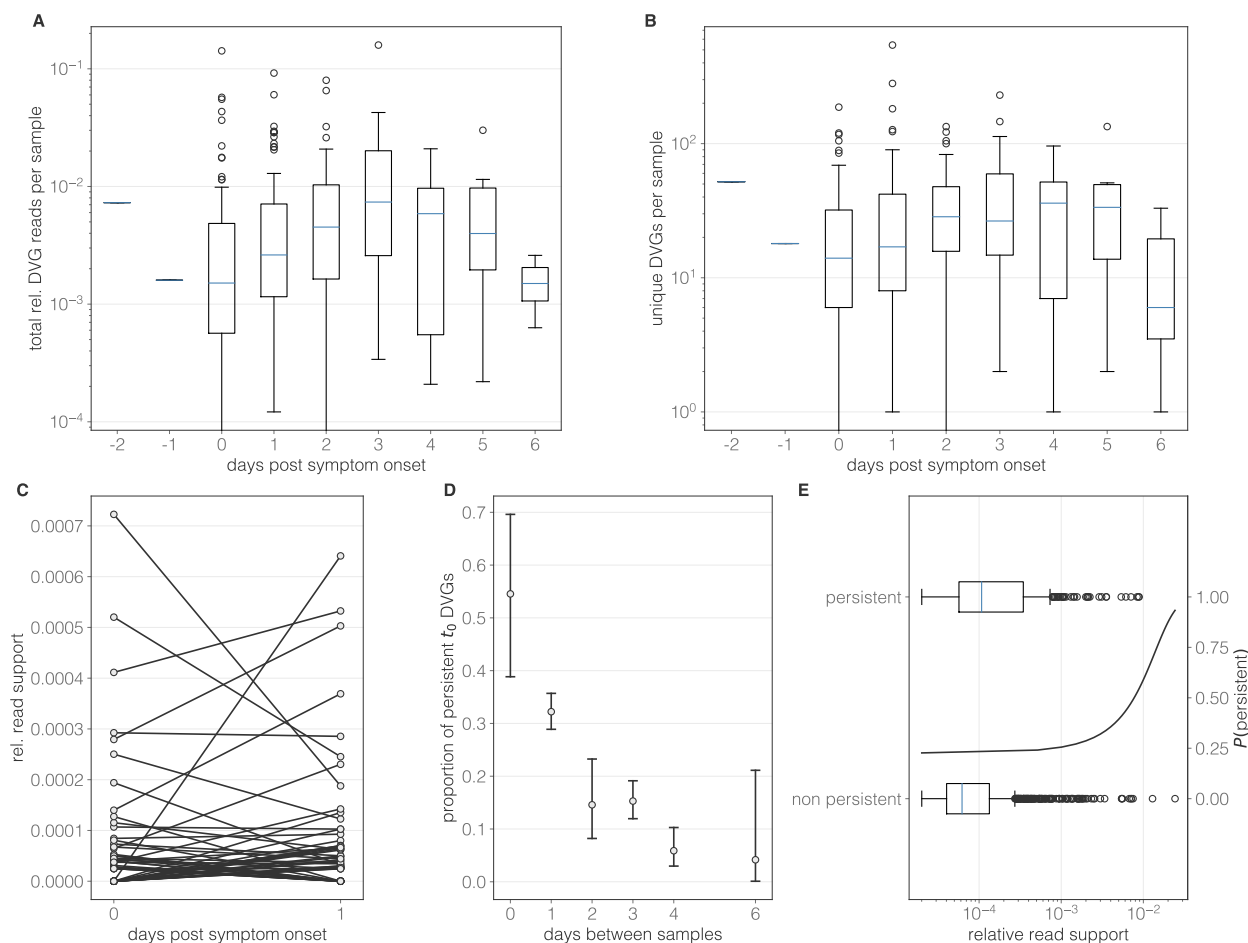


Figure 2.4: Polymerase DVG dynamics over the course of infection. In all boxplots (A, B, E) Blue line represents the median value for each segment, box extends to the limits of the IQR, and whiskers extend to 1.5 IQR below and above the 1st and 3rd quartile, respectively. Outliers are shown as dots beyond the range of the whiskers. A) Total relative polymerase DVG reads per sample as a function of the number of days post symptom onset that a given sample was taken. B) Number of unique polymerase DVGs per sample as a function of the number of days post symptom onset that a given sample was taken. C) Longitudinal DVG dynamics in a representative sample. Lines connect the relative read support of a given polymerase DVG in each of the two samples taken. D) Proportion of all DVGs observed in a given t_0 sample which is also observed in the corresponding t_1 sample as a function of the number of days between when those samples were taken. Whiskers extend to the exact binomial confidence intervals for a given proportion. E) Relative read support of t_0 DVGs which do and do not persist in the t_1 . Solid line represents the estimated probability of a DVG with a given read support persisting from a logistic regression.

the number of unique DVG reads per sample do not vary based on the number of days post symptom onset (Kruskal-Wallis H-test p value=0.08 and 0.06, respectively). Qualitatively, samples taken six days post symptom onset appeared to harbor fewer DVG reads and fewer unique DVG reads compared to samples taken earlier in the course of infection ($1.50e-3$

[8.05e−4] v. 3.18e−3 [1.94e−2] and 6.00 [14.06] v. 19.00 [53.52], respectively). However, there are only three samples taken six days post symptom onset.

This lack of temporal pattern indicates that either DVG populations are generated prior to the earliest samples in this dataset and then persist throughout infection or that there is continual turn over (generation and loss) of novel DVG species throughout infection. This lack of temporal pattern in the quantity of DVGs is consistent with observed in the number of SNPs in these data [11].

To specifically analyze how DVG populations change over time within single hosts, we compared the DVG populations present at multiple time points, when those data were available. In general, DVG populations are highly dynamic over time (**Figure 2.4C**, **Figure S2.8**) and many DVGs do not persist across time points. This implies that there is continuous *de novo* DVG generation and extinction of previously generated DVGs during infections. To assess the factors which may influence the probability that DVGs are able to persist across time points, we first looked at the proportion of DVGs present at the first time point (t_0 DVGs) with those present at the second time point (t_1 DVGs). This analysis reveals that the proportion of DVGs present at t_0 that are also observed at t_1 is significantly dependent on the number of days which have elapsed between t_0 and t_1 (χ^2 test of independence p value=1.20e−22). Specifically, DVG populations are more similar between samples which were taken at similar time points. Samples taken on the same day share roughly 55% of DVGs whereas those which were taken six days apart tend to share less than 5% of DVGs (**Figure 2.4D**). As genetic drift predicts that the probability of a given mutation fixing within a population depends on the frequency of that mutation in the given population, we next tested whether the probability that a t_0 DVG is also present at t_1 depends on the relative read support of that DVG at t_0 . Our analyses reveal that DVG persistence does depend on its relative read support: t_0 DVGs supported by more reads were more likely to be observed at t_1 (logistic regression of persistence as a function of relative read support coefficient p value=0.01, **Table S2.1**). However, we do note that the modeled

fit to our data is relatively flat over the range of relative read supports in which most DVGs are observed. In other words, the 99th percentile of observed relative read support ($3.33e-3$) would be predicted to only have a 33% probability of persisting between time points based on our regression coefficients. These results were further supported by a multivariate logistic regression model incorporating both relative read support and categorical time between samples (relative read support coefficient p value= $1e-3$, $t=1,2,3,4,6$ p value= $2e-3$, $<1e-3$, $<1e-3$, $<2e-3$, respectively, **Table S2.2, Figure S2.9**). Based on the modeled coefficients a DVGs with relative read support of $1e-3$ from samples taken 0,1,2,3,4,6 is predicted to have a probability of persisting between samples of 0.60, 0.36, 0.17, 0.17, 0.7, 0.5, respectively. Similarly, a DVG from samples taken 3 days apart with read supports of $1e-4$, $1e-3$, and $1e-2$ would have probabilities of persisting of 0.14, 0.17, and 0.61.

Taken together, our results are consistent with a model of genetic drift dominating within host DVG dynamics. There appears to be continual generation of novel DVGs and loss of existing ones in a manner that is both time dependent and dependent on the quantity of a DVG within a given host.

2.4.5 Limited evidence for the transmission of DVGs

Viral evolution is shaped not just by the dynamics which operate within hosts but also by those which operate between hosts, including at the stage of transmission. Previous analyses based on genetic variation have revealed that the transmission bottleneck of influenza A is quite small, on the order of one to three virions [11]. This results in a significant loss of genetic diversity during transmission such that nearly all genetic variation observed within a host is generated *de novo* following transmission.

To determine whether genomic diversity supports these conclusions, we wished to evaluate how DVG populations compare between known donor and recipient pairs. To do this, for each identified transmission pair we identified all DVGs present in both donor and recipient and determined which are present in both hosts. When multiple time points were available

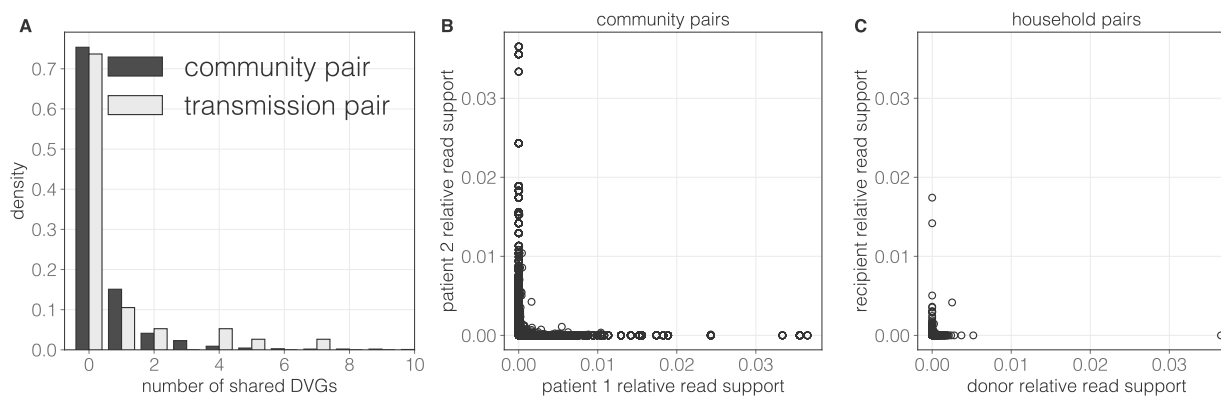


Figure 2.5: Polymerase DVGs shared between pairs of patients. A) Histogram showing the number of DVGs shared between epidemiologically unlinked community pairs (dark grey) and epidemiologically linked transmission pairs (light grey). X-axis has been truncated to 10 for visualization purposes, despite a long tail on the community pair distribution. B) Relative read support in patient 1 (x-axis) and patient 2 (y-axis) of all DVGs identified in at least one patient in all random community pairs. C) Relative read support in the donor patient (x-axis) and recipient patient (y-axis) of all DVGs identified in at least one patient in all epidemiologically linked transmission pairs.

for a given host, we included all DVGs identified at all time points to account for the fact that DVGs present at earlier time points may be present, but at sufficiently low frequency that they can not be identified in the later sample. We compared this to a null distribution generated from community pairs to account for the *de novo* generation of identical DVGs within each host.

We found that epidemiologically unlinked samples generally share very few polymerase DVGs, on the order of zero to one (0.39 [1.03] (**Figure 2.5A**)). This indicates that *de novo* DVG generation on polymerase segments is likely random and there is no evidence for preferential generation of specific DVG species. Amongst transmission pairs, we similarly found that generally very few DVGs are shared between individuals (0.54 [1.22]). In a negative binomial regression with the type of pair (unlinked/linked) as a predictor and number of shared DVGs as an outcome, the coefficient on the type of pair was non-significant (p value=0.727), indicating that epidemiologically linked transmission pairs are no more likely to share DVGs than unlinked random community pairs. Finally, to determine whether DVGs that were shared between known transmission pairs were distinct from those shared between commu-

nity pairs we compared the relative read support of DVGs shared between these two groups of pairs. For each DVG shared between each pair, we took the maximum read support from all samples for both patients in the pair. We found no significant difference between these two distributions (**Figure 2.5B, C, Table S2.3**, unequal variance T-test with 1000 permutations comparing the maximum relative read support of polymerase DVGs shared between community pairs and known transmission pairs p value=0.424).

Taken together, these results indicate that there is no discernible difference between how often DVGs are shared, and the relative read frequency of the small number of DVGs which are shared by transmission pairs and community pairs. Therefore, because known transmission pairs do not share more DVGs than community pairs we can conclude that there is no supporting evidence for the transmission of DVGs in these data, implying that there is a very small bottleneck size for genomic diversity.

2.5 Discussion

Understanding how influenza viral populations evolve within and between hosts is key to understanding how viral evolution proceeds on the host population scale. This is relevant, for example, in learning how new antigenic variants arise and ultimately sweep the host population. Previous work has used genetic diversity, or diversity in the form of single nucleotide polymorphisms, to better understand the evolutionary forces acting within hosts, i.e. the relative contribution of selection and drift in shaping viral populations. These analyses have found that selection is weak within hosts, e.g. known antigenic escape mutants do not appear to be under selection, and drift in the form of transient low frequency SNPs predominates [14, 11]. Furthermore, the size of the transmission bottleneck, or the number of virions transmitted between donor and recipient hosts, has been estimated to be on the order of one to three virions [11], which will introduce an additional source of genetic drift at the point of transmission. However, the resolution of these studies is inherently limited

by the low levels of genetic diversity which exist within acute human infections of influenza: generally less than 15 observable mutations per host at any given time [14, 11].

Analyses based solely on SNPs do not incorporate the *genomic* diversity that is generated during infection in the form of defective viral genomes. These genomes feature large internal deletions in at least one segment and are therefore incapable without of establishing productive infection without coinfection of a cell with a wild type virus. Due to this reliance on coinfection and the spatial structure of within-host infections that may retain linkage between specific wild-type genotypes and their corresponding DVG species, we expect the ecological and evolutionary dynamics of DVGs to mirror those of the wild-type viral population.

At present, little is known about the *in vivo* dynamics of influenza DVGs. The vast majority of our understanding of influenza DVGs come from *in vitro* studies [32, 33, 17] and existing *in vivo* studies offer only a cross sectional view of DVGs within a host population [23]. How DVG populations change over time, and what those dynamics tell us about the forces shaping the entire collection of influenza viral particles within and between hosts in natural human infections therefore remains an open question.

Here, we attempt to address this gap in the literature by identifying DVGs from deep sequencing data collected as part of a longitudinal influenza household cohort study [11]. We identify at least some quality-filtered DVGs in all samples in the dataset, primarily on the PB2, PB1, PA, and NS segments. These DVGs largely harbor the canonical motif in which the majority of the coding portion of each segment is deleted but the packaging signals at either end of the segment are maintained. These large deletions almost certainly render the affected segments incapable of replicating without a wild-type helper virus.

We observe a novel NS DVG that is nearly ubiquitous in our data. This DVG contains a smaller deletion than many others, only 228 of NS's 879 nucleotides. It's formation looks to be driven by the repetition of an 11 nucleotide motif in two places within NS, within which the DVG breakpoints fall. Based on a BlastN analysis as well as an analysis of supporting

read alignment we feel confident that this DVG is not a bioinformatic artifact. However, its biological importance and whether this DVG is also observed in other human deep sequencing is an avenue for future research.

Our primary interests in this study was in assessing changes in DVG populations over the course of infection and across transmission chains. From a cross sectional perspective we do not observe any significant changes in the quantity of DVGs relative to the quantity of wild-type virus. This implies that either DVG populations are relatively stable over the course of infection or that DVGs are continually being lost and regenerated at similar relative rates. Importantly, we know based on previous analyses of these data [11] that viral titers are the highest in the earliest available time points. Therefore, the relative quantity of DVGs early in infection, when viral population sizes are growing rapidly is unobserved in these data.

To differentiate between the two possible explanations for the relative stability of DVG quantity over the range of days post infection included in this study, we turned to longitudinal samples from single patients within the dataset. When looking at specific DVGs over time within single hosts, we observe highly dynamic populations. Between time points there is considerable loss of DVGs which were present at one time and *de novo* generation of novel DVG species at the following sampling time. We find that this process is dependent on at least two factors: the time between samples and the relative read support of a given DVGs. DVGs are more likely to persist between time points when samples are taken at more similar time points and DVGs are present at a higher relative frequency.

The strength of genetic drift acting on a given population can be quantified by the effective population size, N_E . Regardless of census population sizes, drift will be stronger in populations with small N_E whereas the ability of stochastic changes to considerably affect evolutionary dynamics will be minimal in populations with large N_E . Quantifying the within-host N_E of influenza A using genetic data is difficult, given the rapidly changing population sizes, noise in the SNP frequency estimates, and the number of evolutionary assumptions required of existing models. When it has been attempted, the estimates tend to be on the

order of $< 1e2$ [55]. While here we do not attempt to quantify N_E , our observations that DVG populations are highly dynamic and change rapidly between time points is consistent with a relatively small N_E as populations with a large N_E would be expected to be more stable. Given the apparent lack of intrinsic differentiating characteristics between DVGs which persistent across time points and those which do not we would not expect selection to be responsible for these rapid changes in DVG population composition. Furthermore, we do not observe selection acting on any specific polymerase DVGs given the fact that most random pairs of samples share almost no DVG species.

As discussed above, the viral diversity which is present within host is also shaped by the process of transmission between hosts. The size of the transmission bottleneck can be quantified to guide our understanding of how this process shapes viral diversity. To guide our knowledge of the transmission bottleneck based on the DVGs within a sample we compared DVG populations between known transmission pairs. We find that known transmission pairs, on average, share almost no DVGs and do not share more than random community pairs. This finding indicates that any DVGs which are shared are likely due to *de novo* generation.

This finding is unsurprising given the small estimated bottleneck size from genetic diversity and the fact that DVGs require coinfection with wild-type virions to establish infection. Thus, the probability that a wild-type and DVG virion coinfect the same cell early in infection when is rare. However, non-replicating DVGs can persist in cells *in vitro* for several weeks [26], increasing the likelihood that theoretically transmitted DVGs are able to find a wild-type helper virus sometime during the course of infection. Furthermore, it is thought that viruses may transmit not independently, but in collective infectious units of multiple viral particles, which would make it more likely that a DVG and a wild-type virus from the same collective infectious unit find the same host cell [24]. Our findings, therefore, are insightful in reconciling these conflicting *a priori* expectations regarding the transmission of DVGs.

We believe, based on that fact that there is limited to no evidence of DVG transmission

between known transmission pairs that human to human transmission of natural influenza infection is likely mediated by a very small bottleneck. This finding implies that the vast majority of the within host genetic and genomic diversity is not transmitted and is generated *de novo* within each infected hosts. This process constrains the ability of selection to act across transmission chains and accentuates the force of genetic drift on host population level evolution.

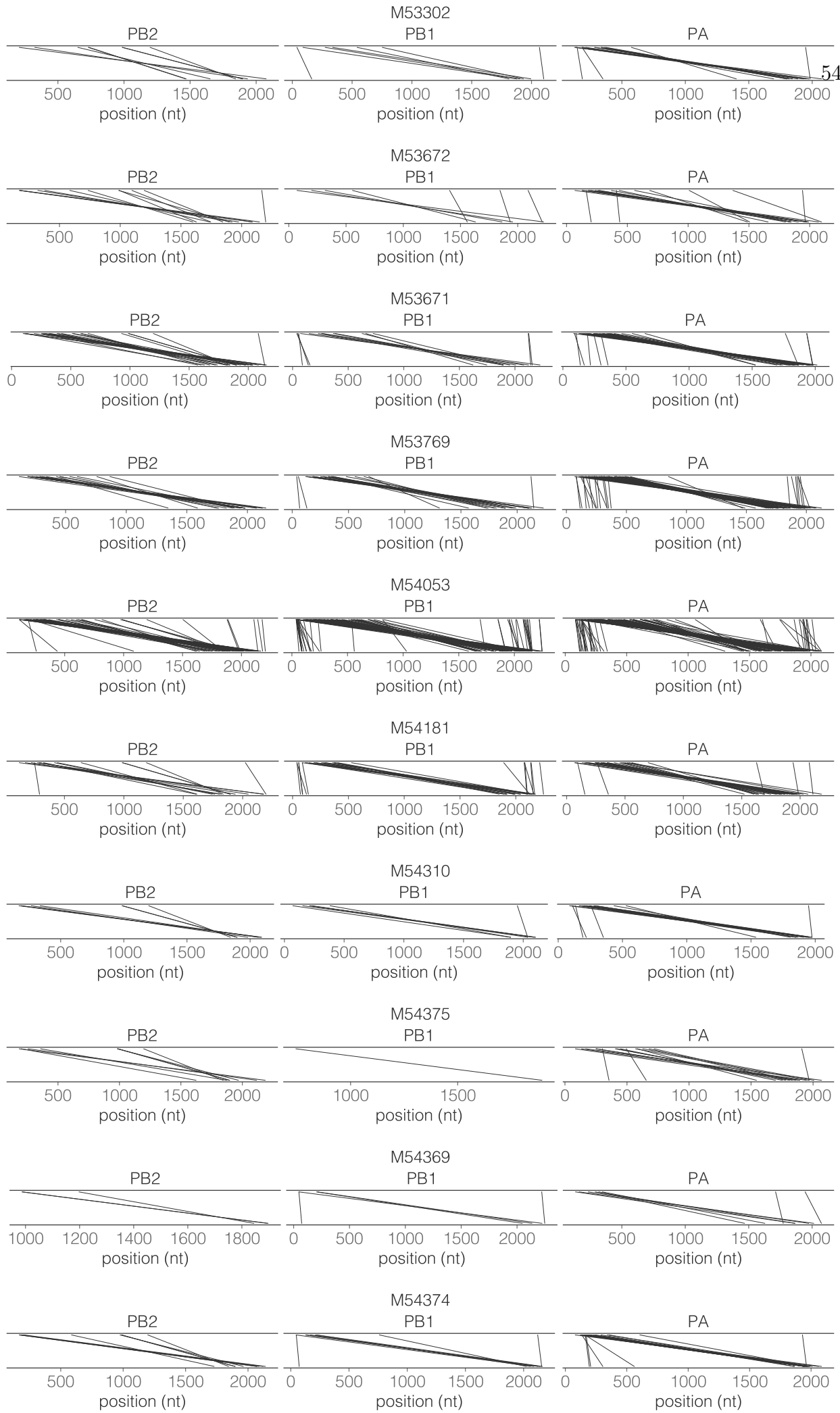
There are some important limitations to this work. Primarily, it is difficult to reliably quantify the amount of DVGs within a sample using sequencing data. Here we have relied on a relative measure of the number of reads spanning a given junction site to the total number of reads mapped to a given segment. This method is slightly biased, however, because we cannot assign reads from the 5' and 3' termini as belonging to either a wild type or DVG segment. Furthermore, this metric will be biased downwards in longer segments as there are more coding nucleotides which can be deleted in a DVG without affecting the packaging signals. However, without additional laboratory measurements, we feel this metric represents a suitable attempt to account for varying sequencing depth between samples. Furthermore, our set of identified DVGs will be affected by the amplification and sequencing protocol used to generate these data. Genetic material was amplified based on primers which bind to the terminal regions of the wild-type segments and there are several size-filtering steps which eliminate smaller DVG segments. But, there is reason to expect that DVGs without the terminal packaging signals would be unlikely to be efficiently packaged into virions, even if they were generated by the polymerase [56]. Nevertheless, the fact that the plasmid controls harbor very low relative amounts of DVGs provides confidence that the DVGs reported here represent a subset of true biological DVGs. Additionally, we are unable to computationally determine which, if any, of our DVGs genuinely have interfering properties with regards to their effect on wild-type viral populations. Identifying interference requires monitoring the relative quantity of DVG and wild-type material through cell culture passages (e.g. [57]). Finally, as with any *in vivo* deep sequencing based analysis we are unable to determine the

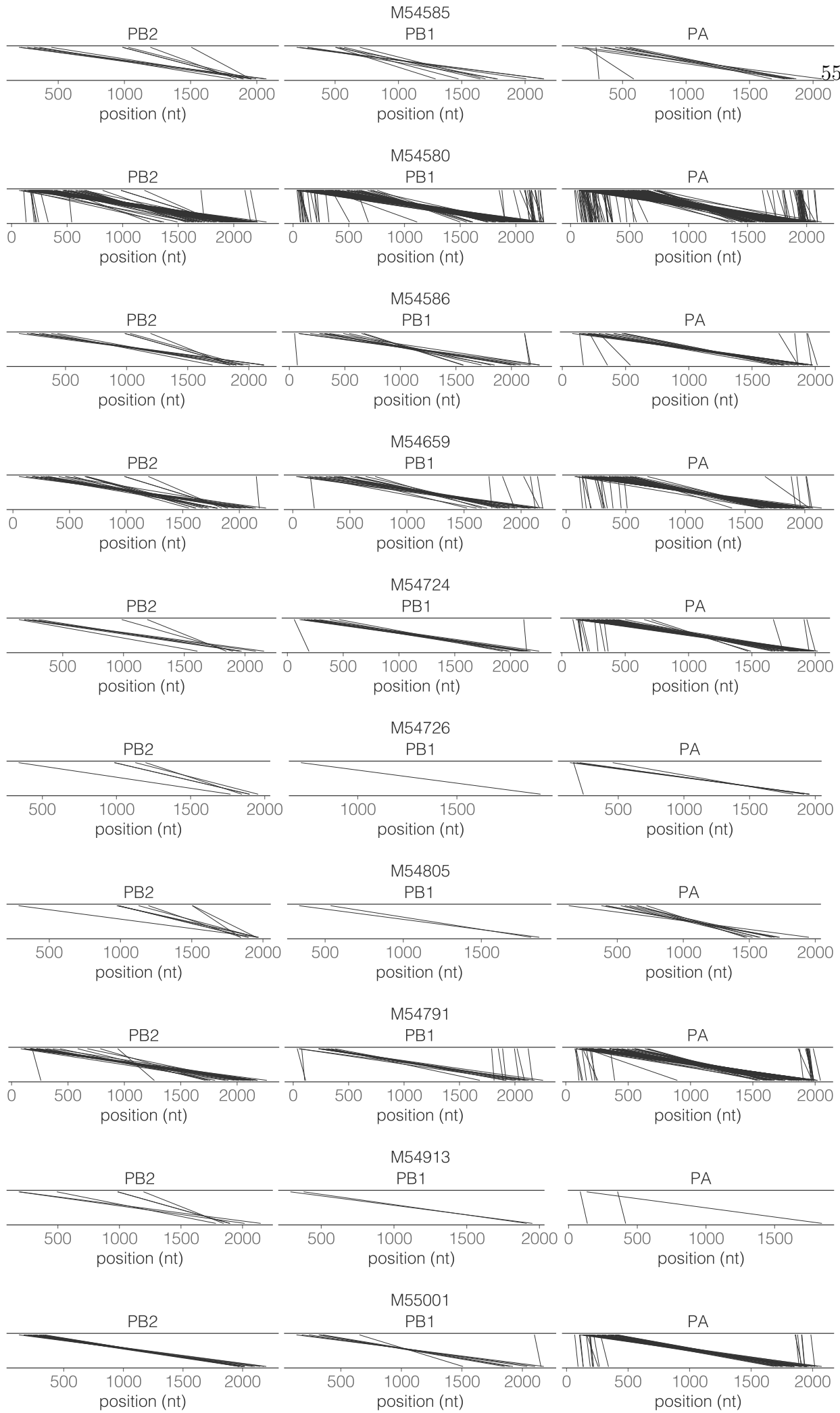
extent to which are measured viral populations mirror the genuine population within a host. Sub-compartmentalization of the within host viral population may bias the viral diversity which is detected in throat and nasal swabs.

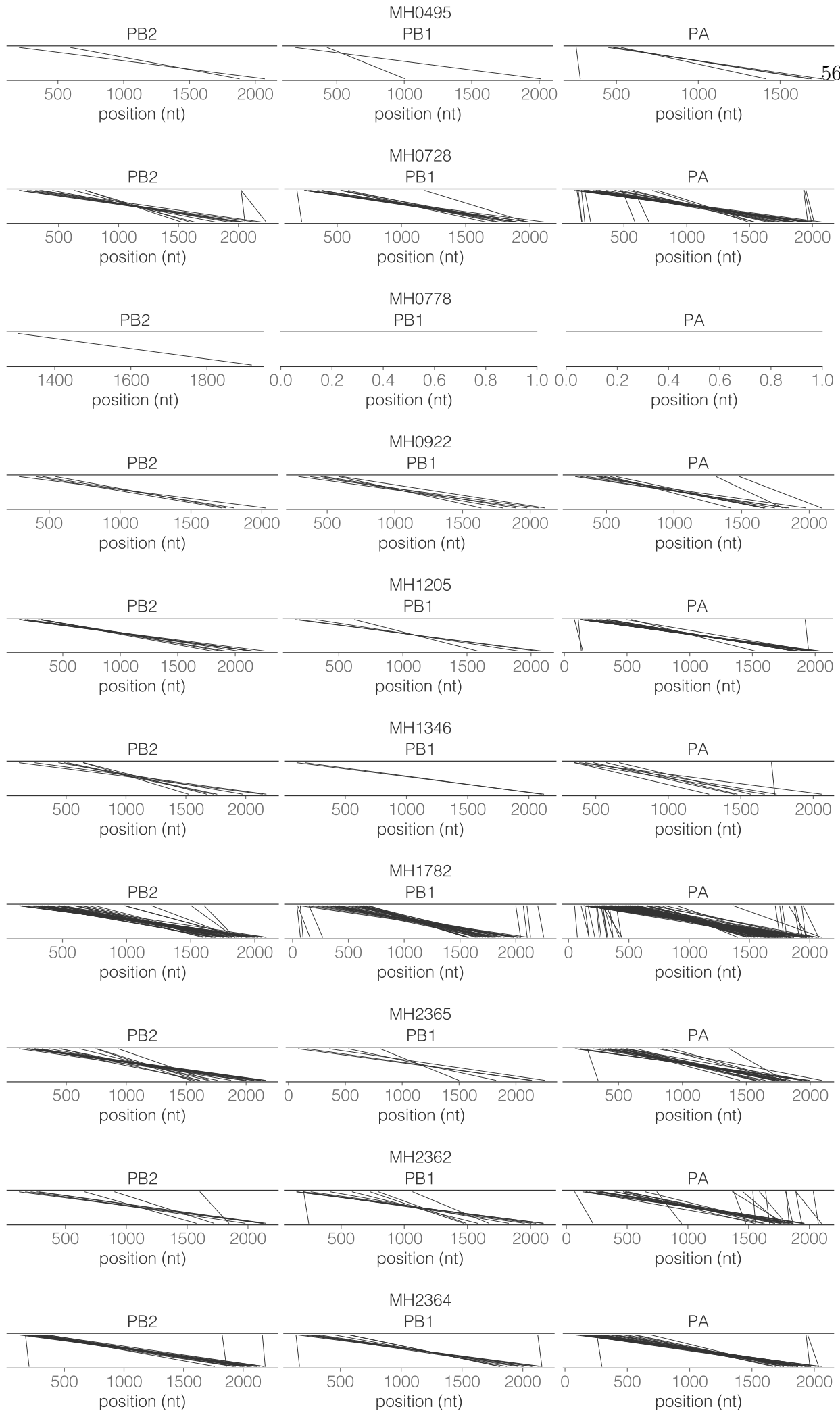
Despite these caveats our our results further add to the growing body of evidence that viral populations harbor considerable diversity beyond what is observed in SNPs. This diversity is accentuated in a segmented virus such as influenza as virions can, in addition to wild-type virions and DVGs, also harbor genomes with segments that are missing segments entirely [18]. Fully understanding the ecological and evolutionary dynamics within natural systems requires analyzing how these forces shape the full suite of genetic and genomic diversity that is generated during replication.

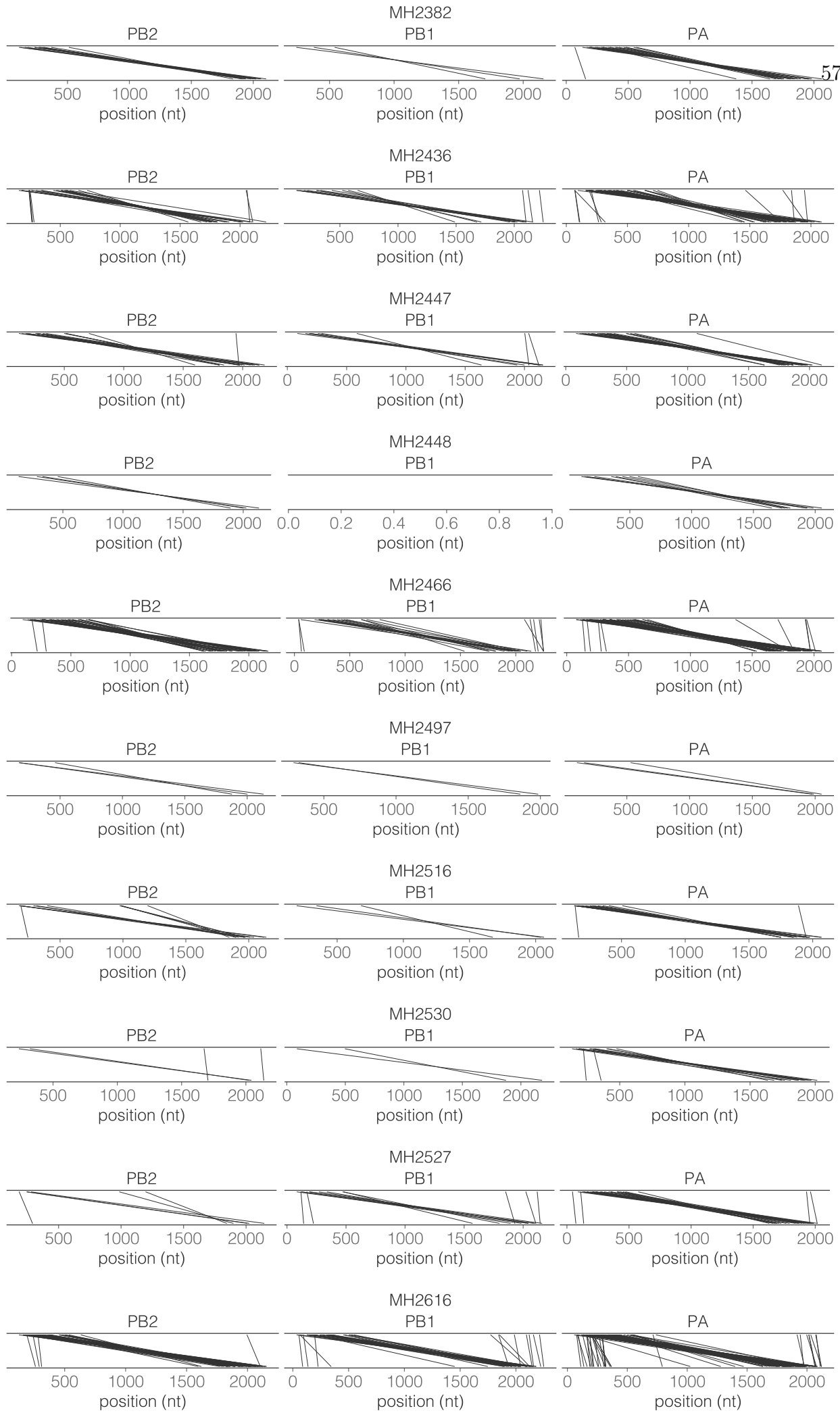
2.6 Supplementary

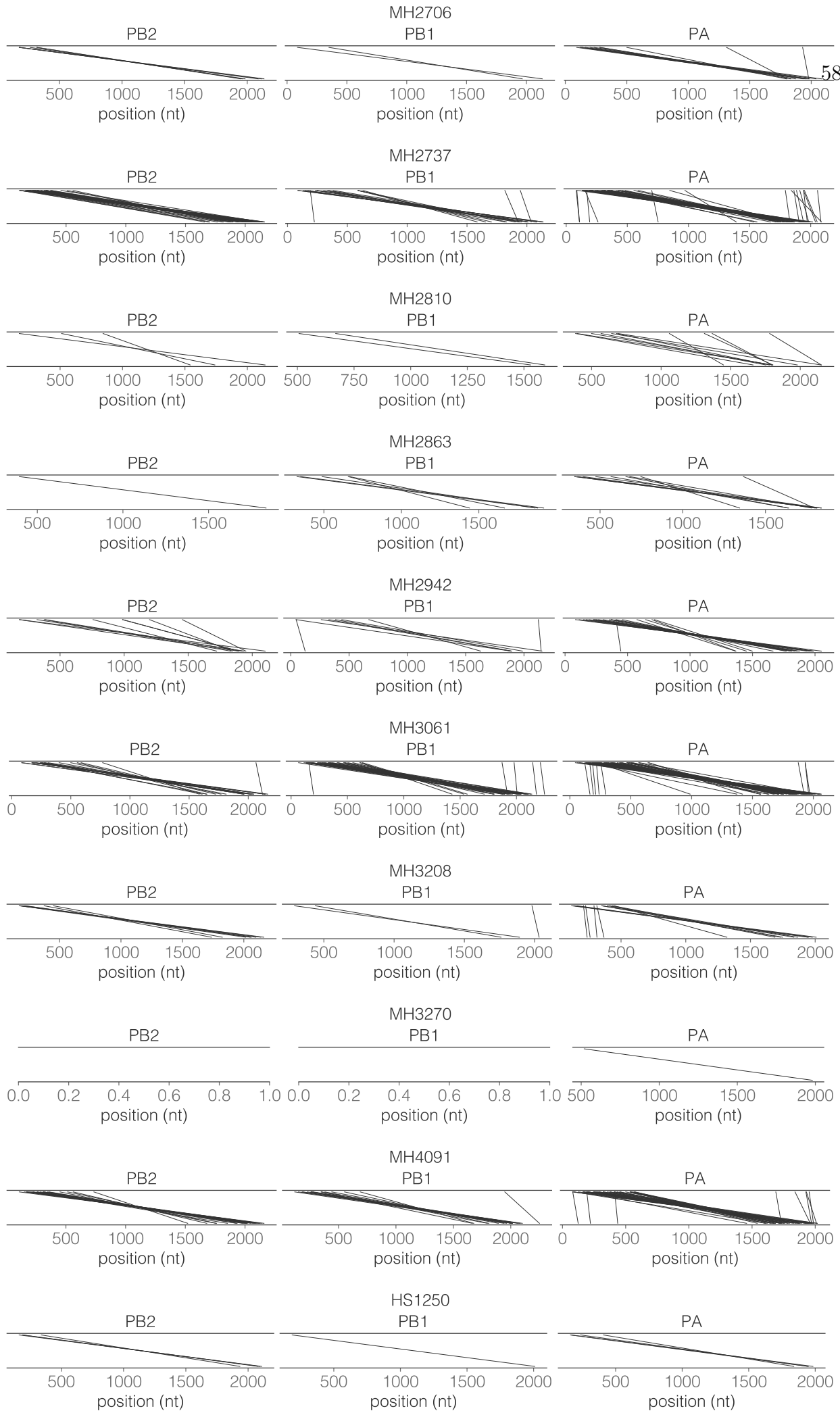
2.6.1 Supplementary Figures

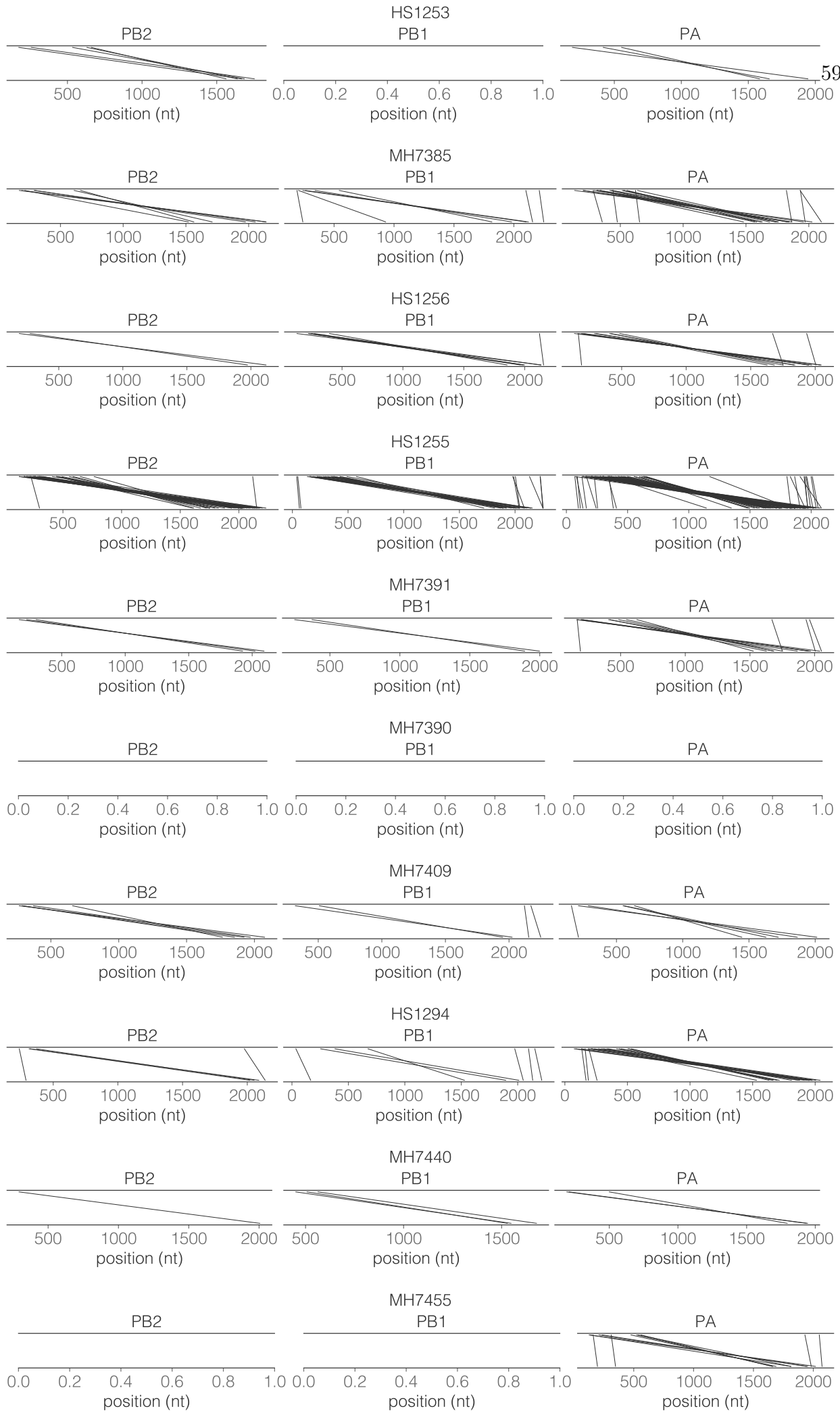


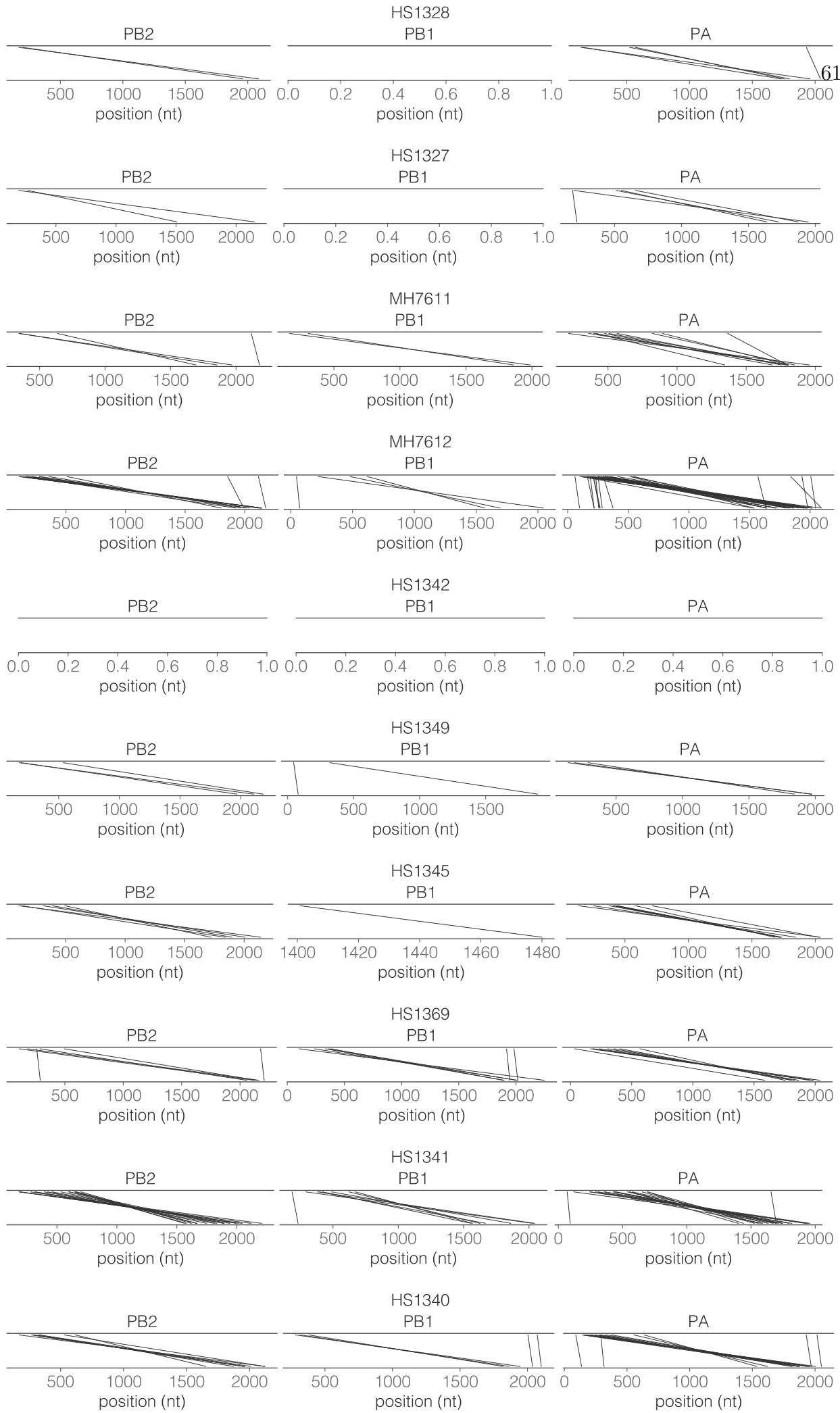


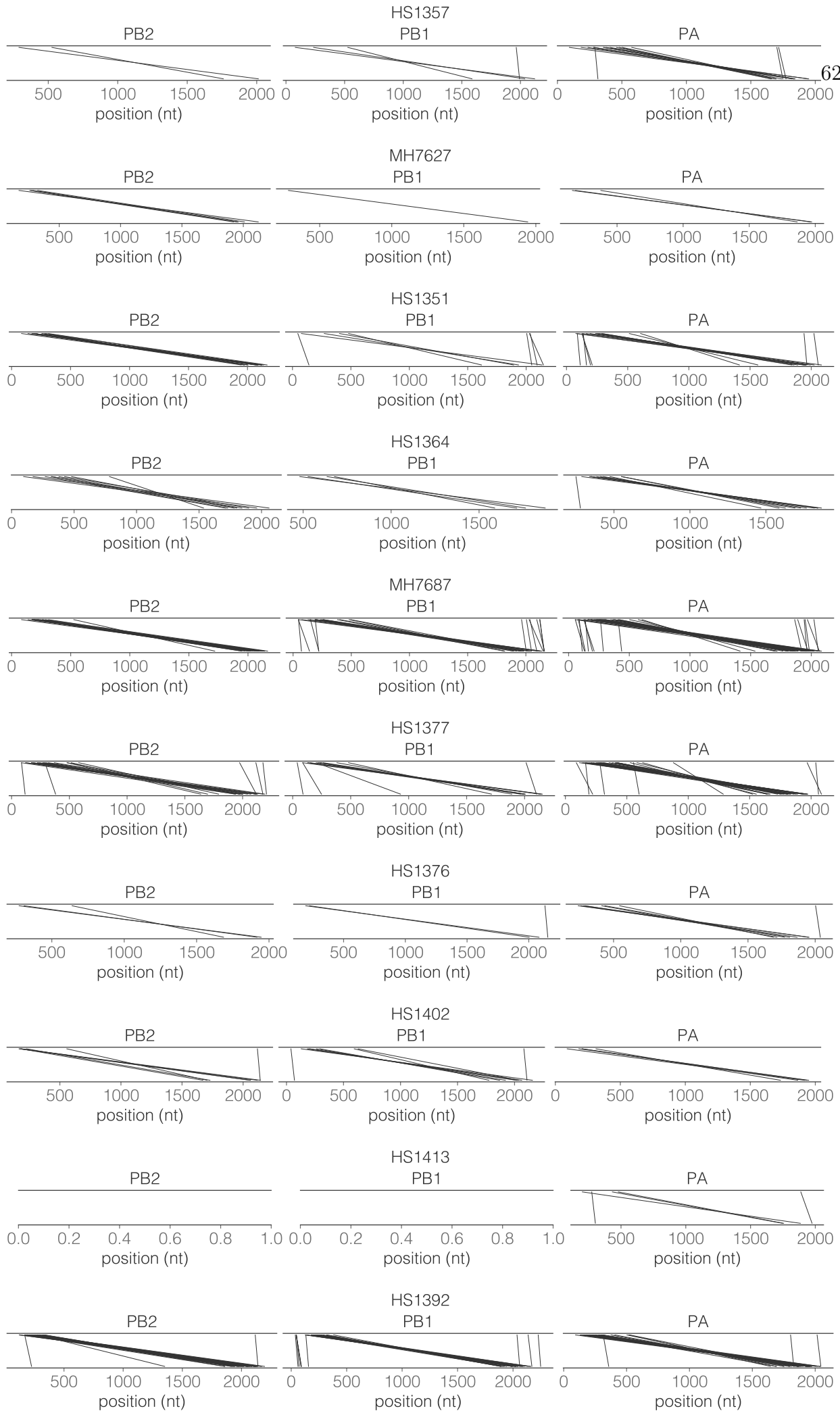


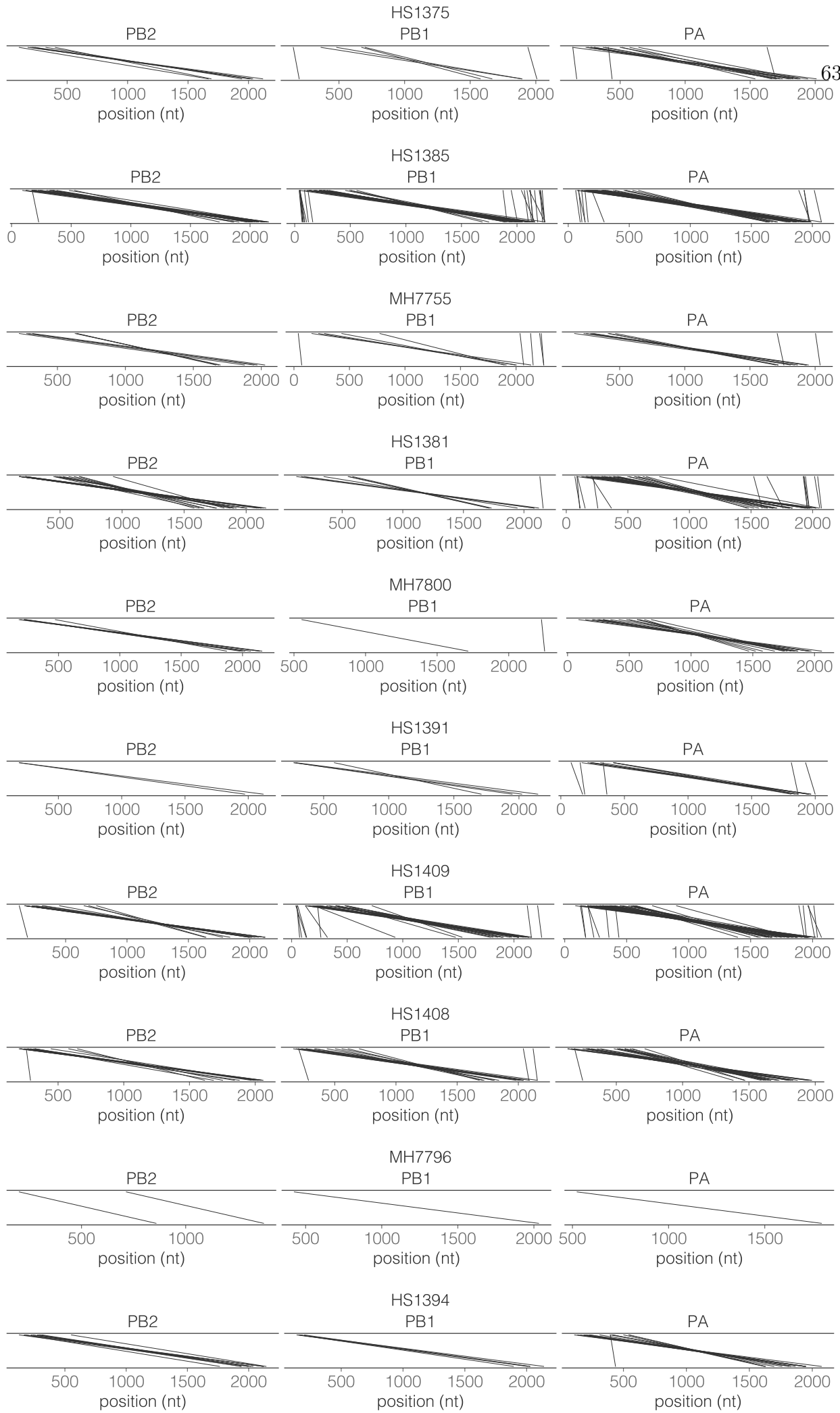


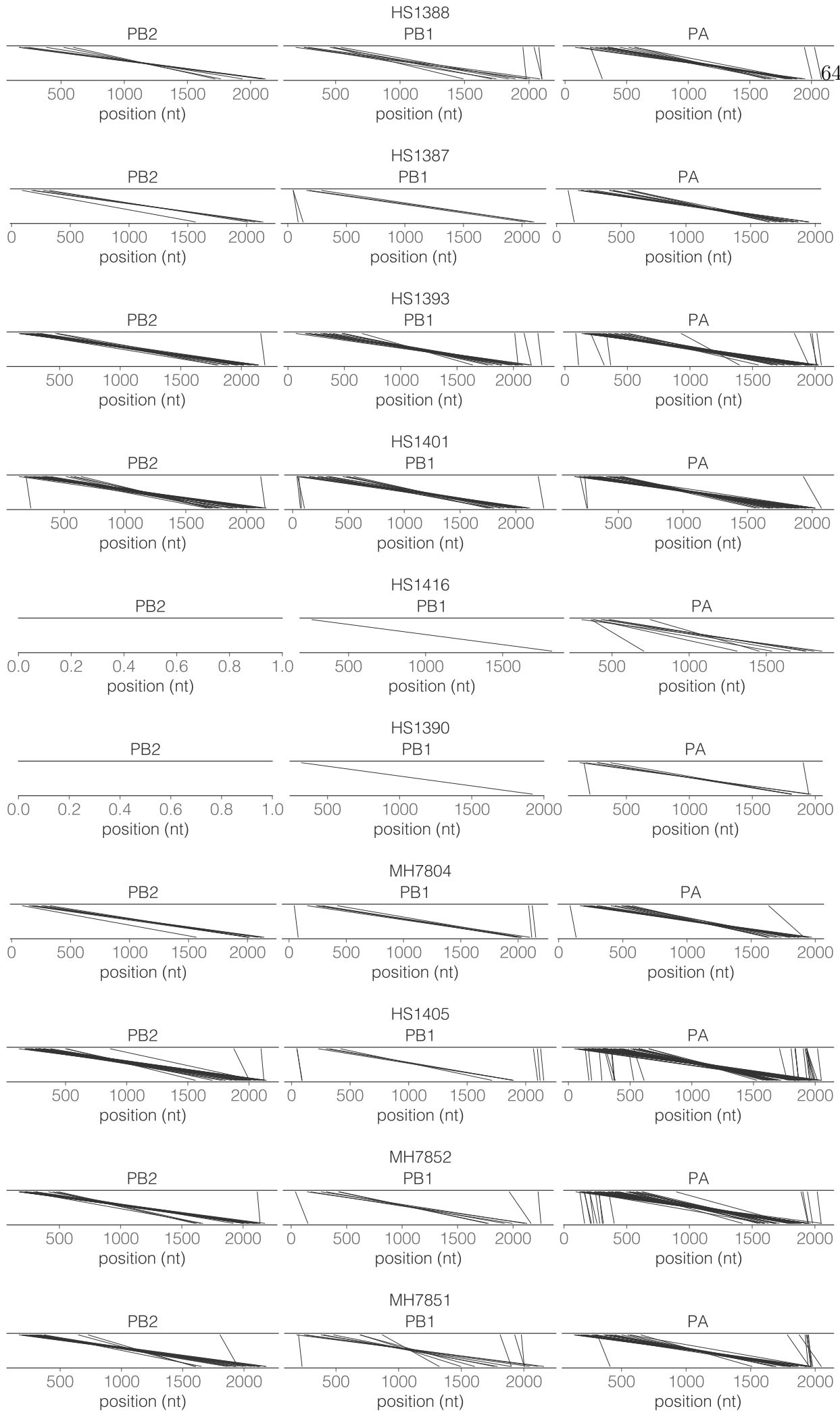


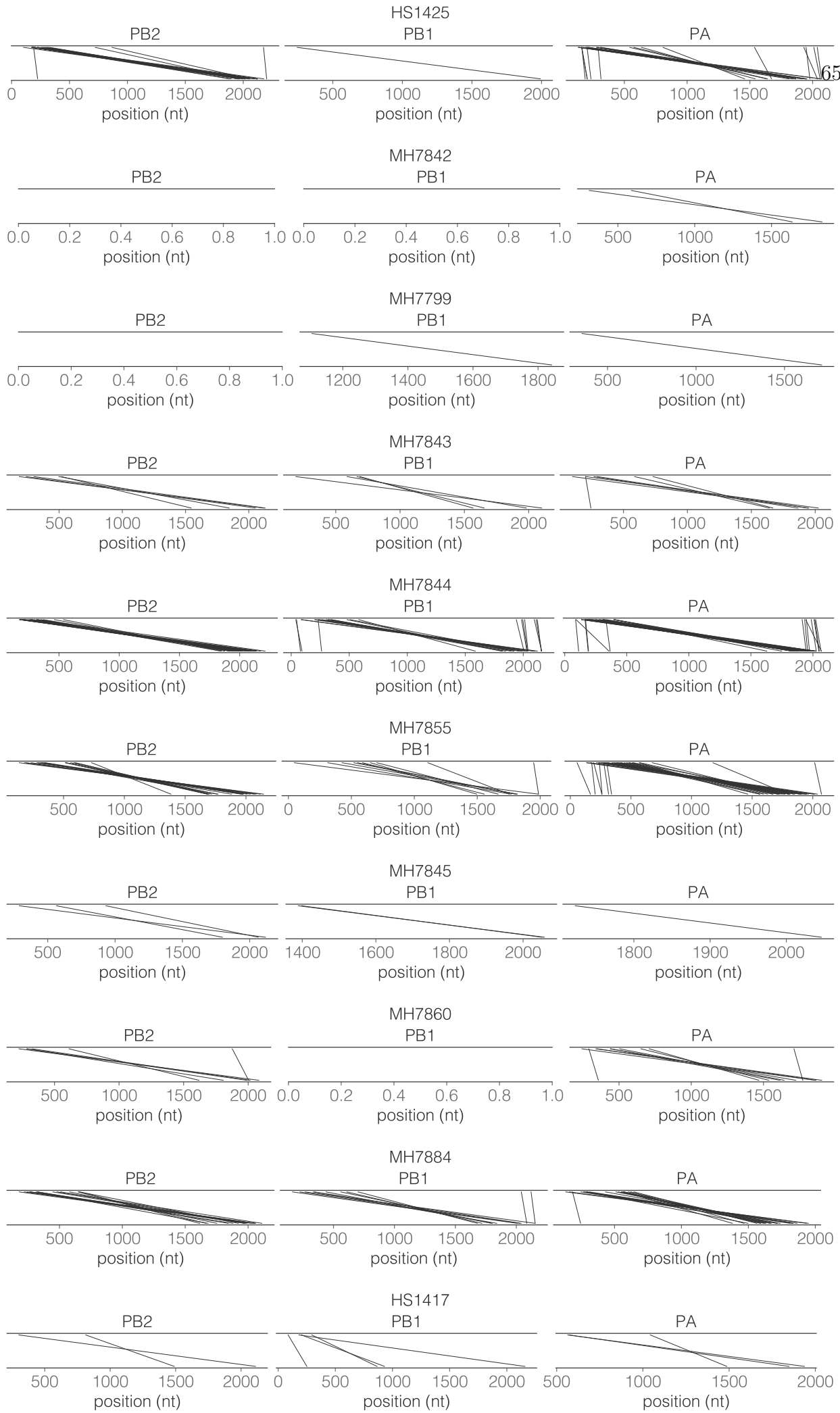


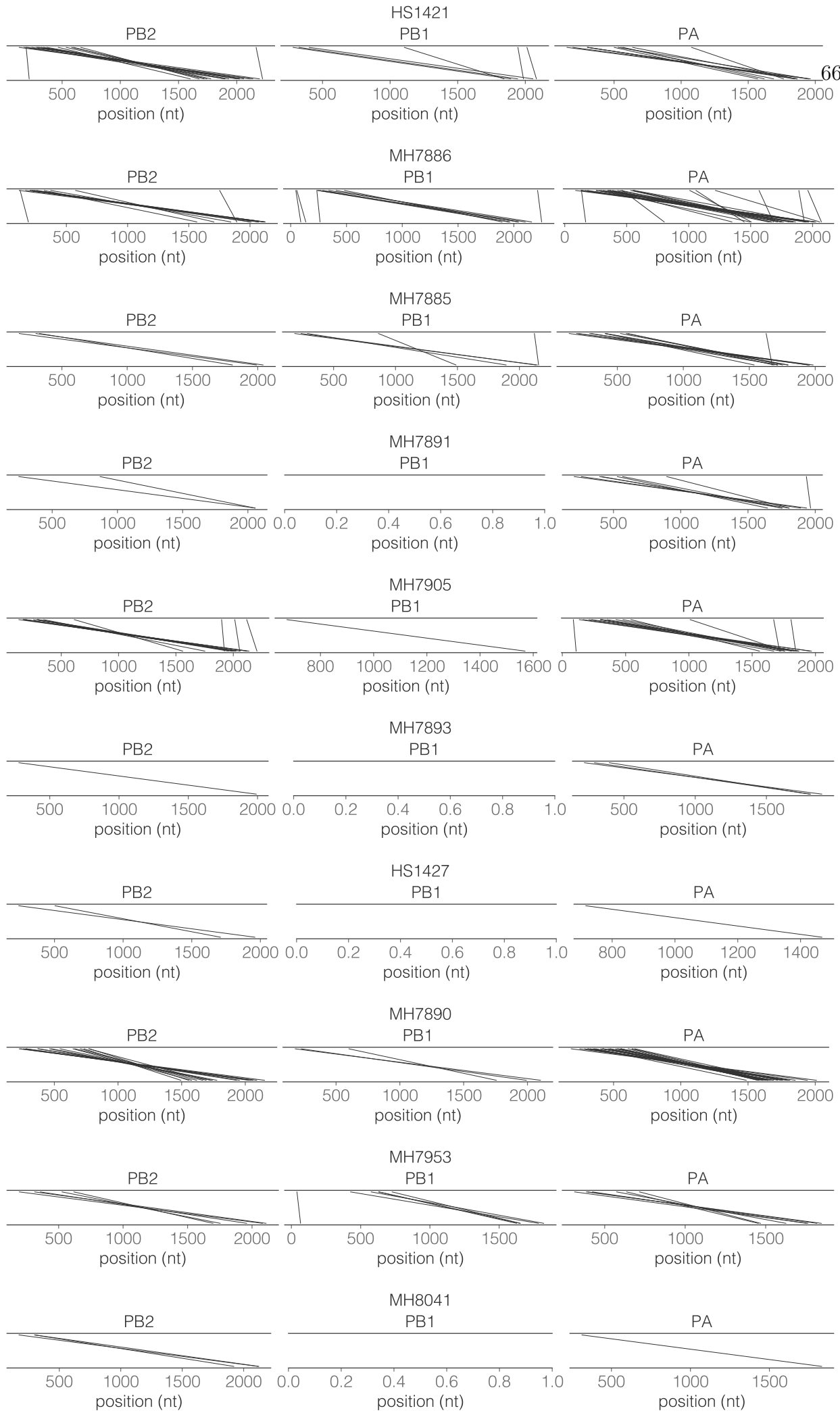


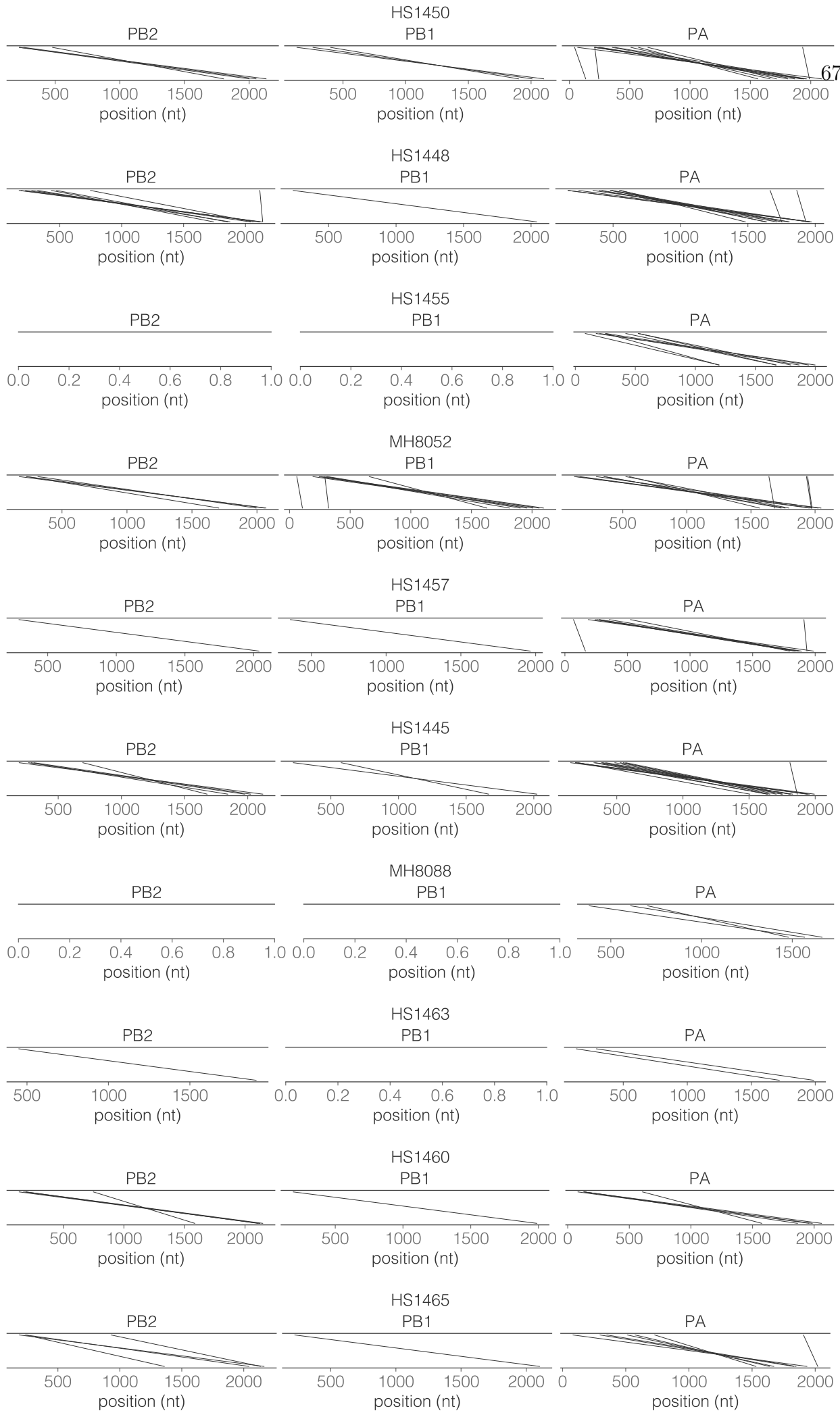


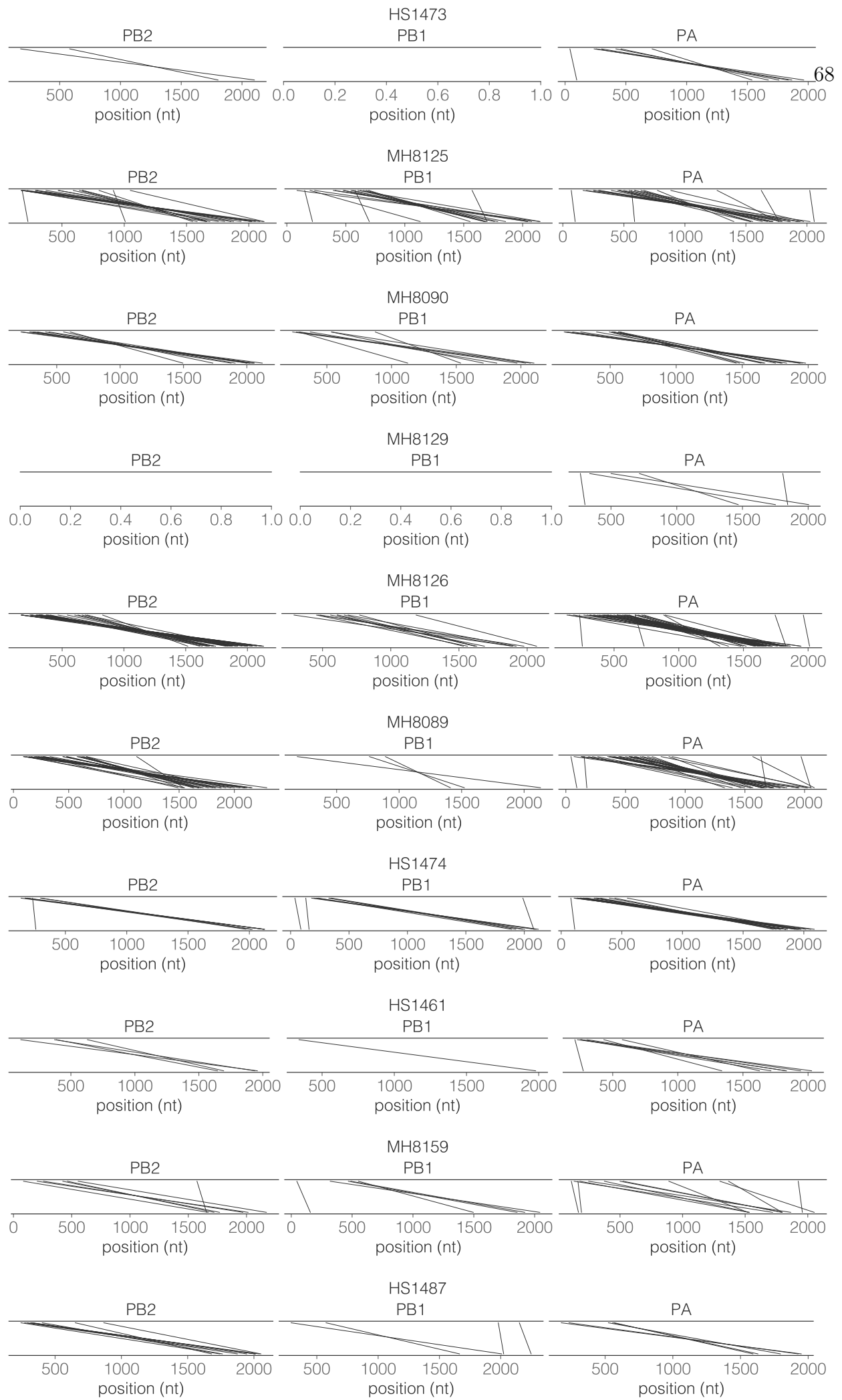


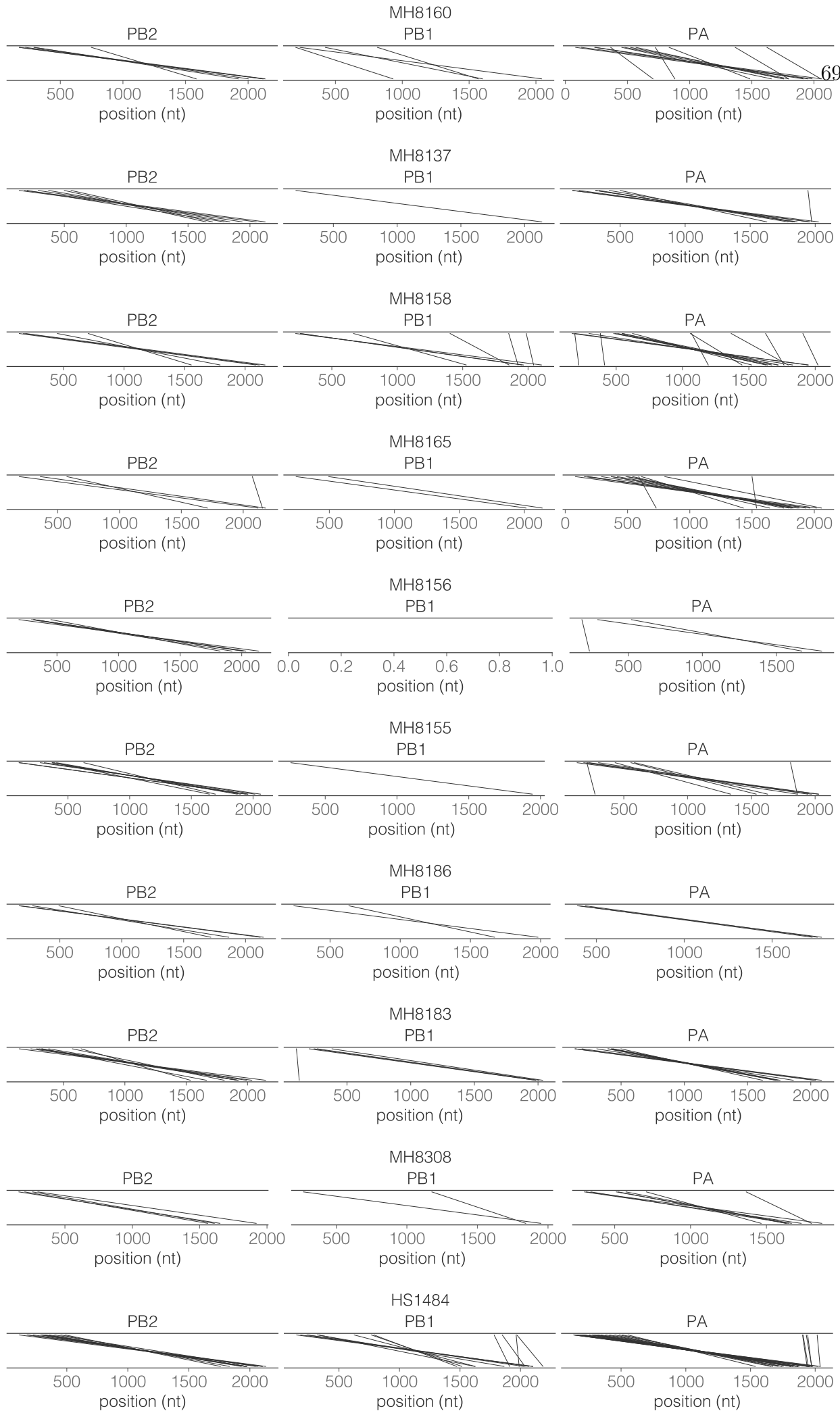


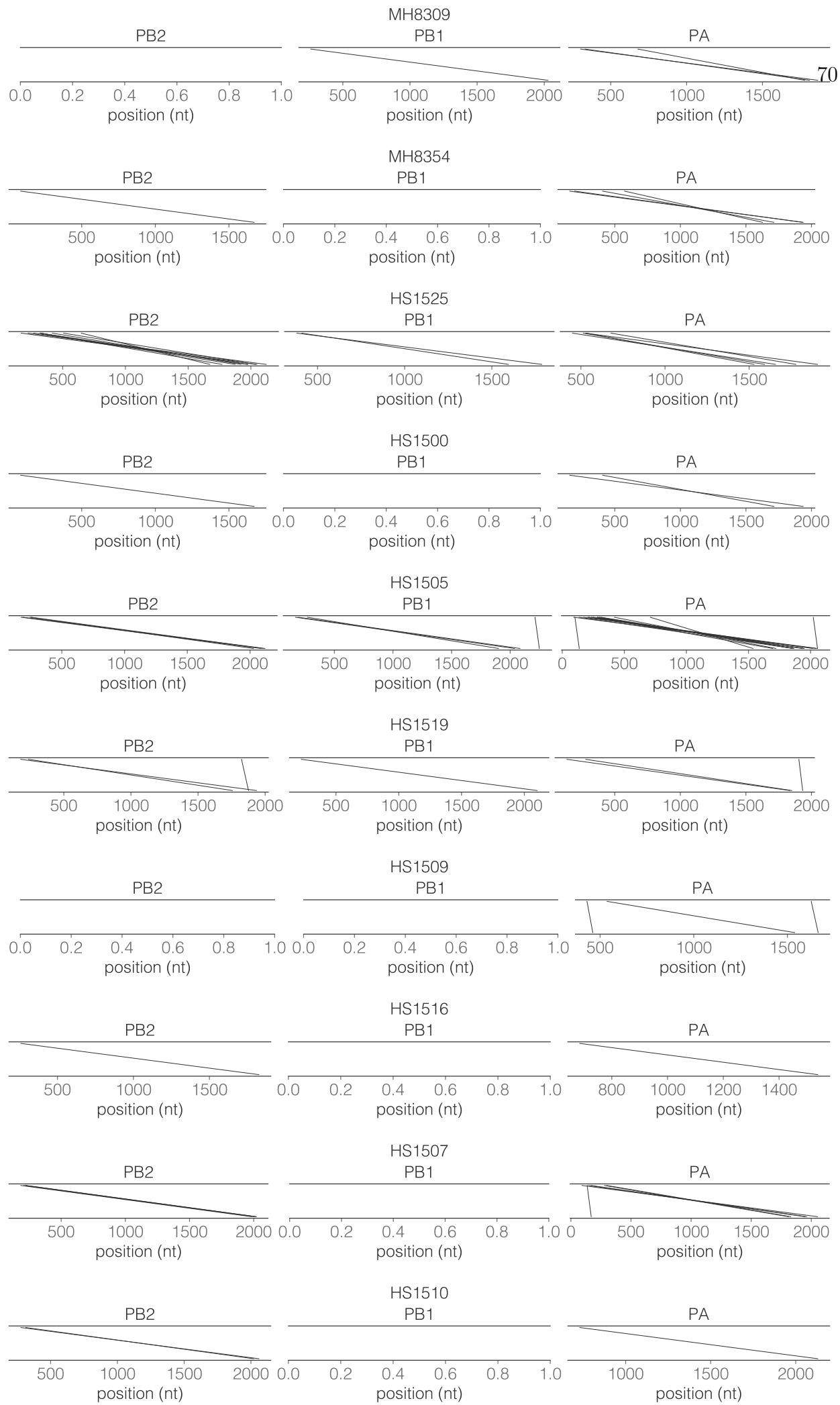


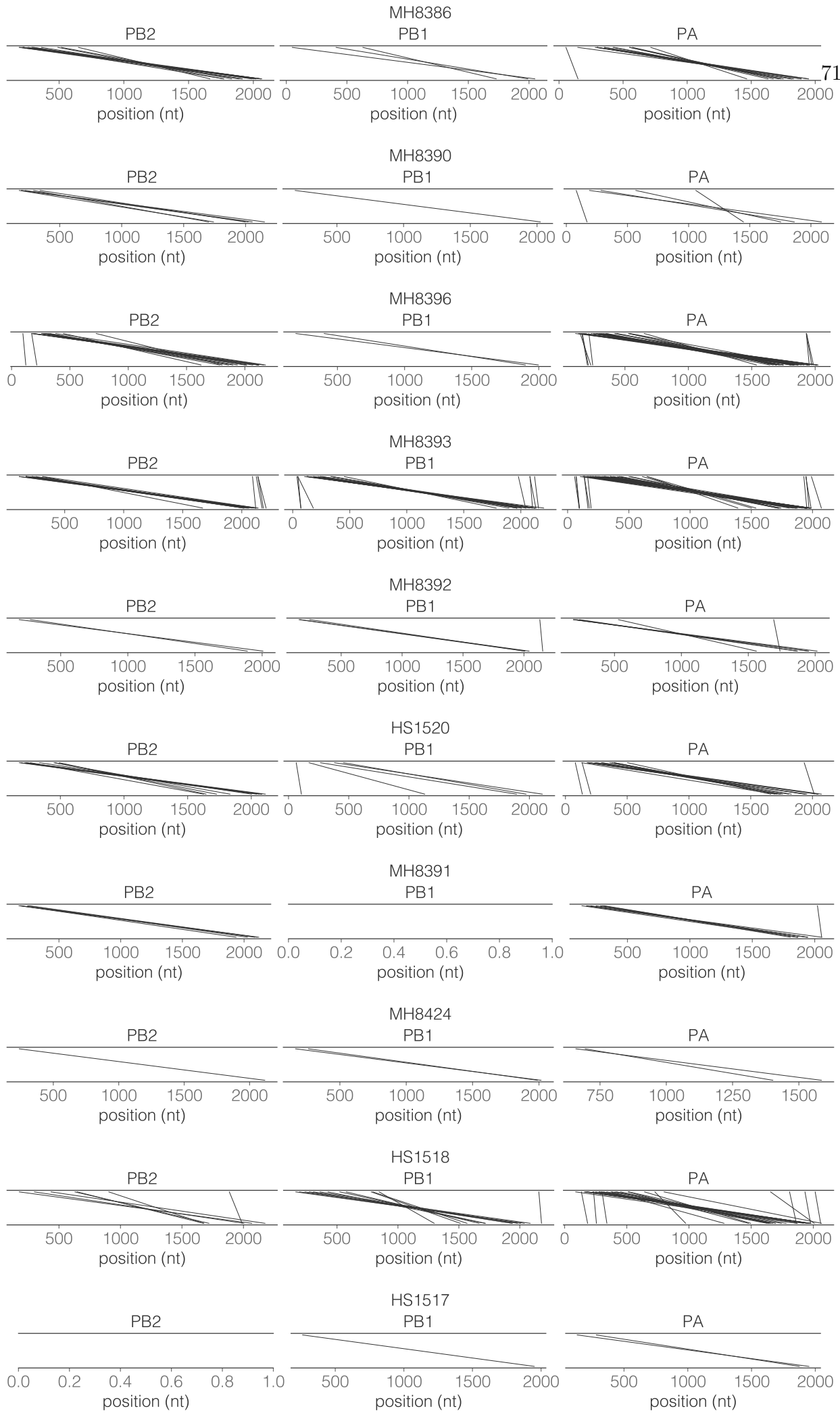


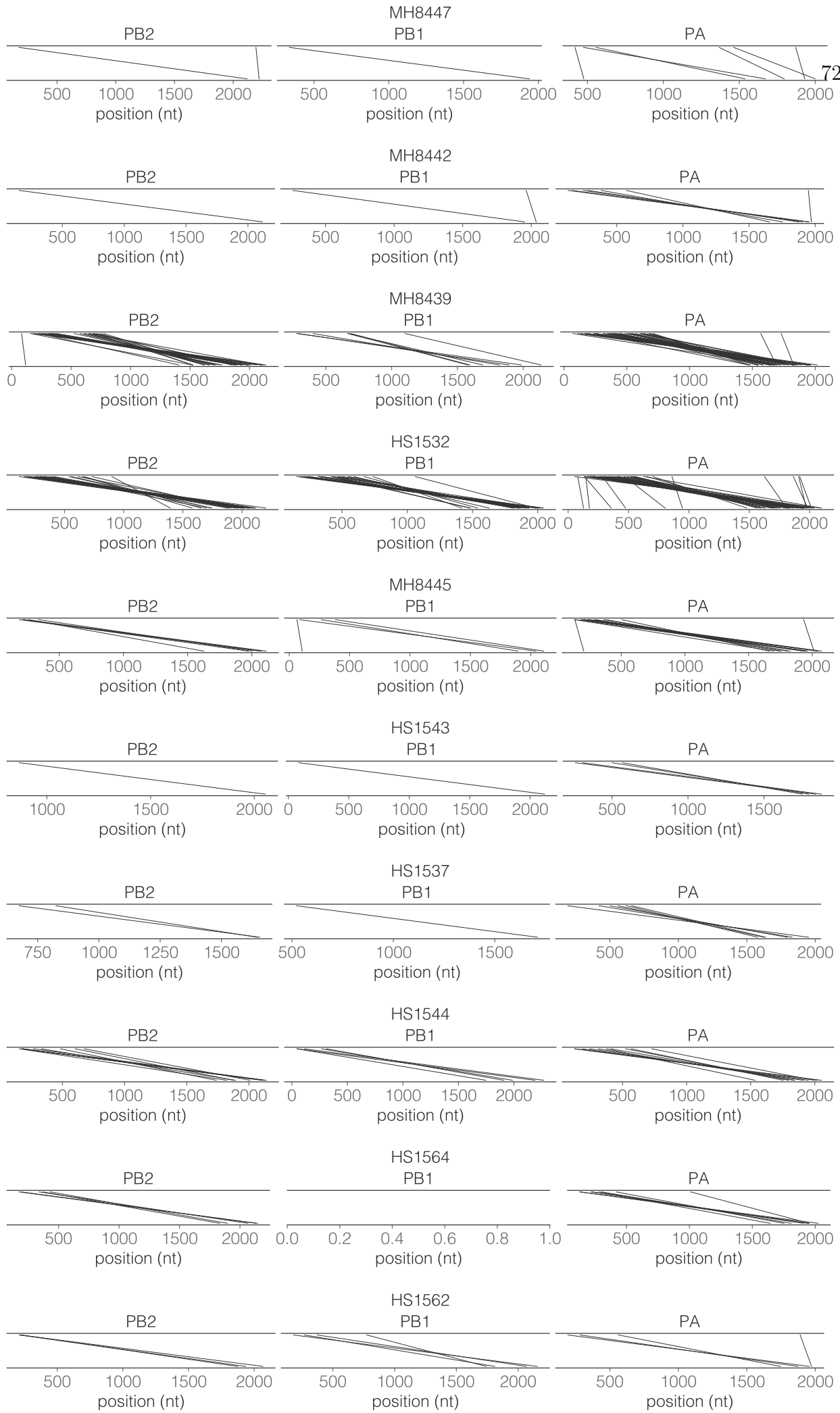


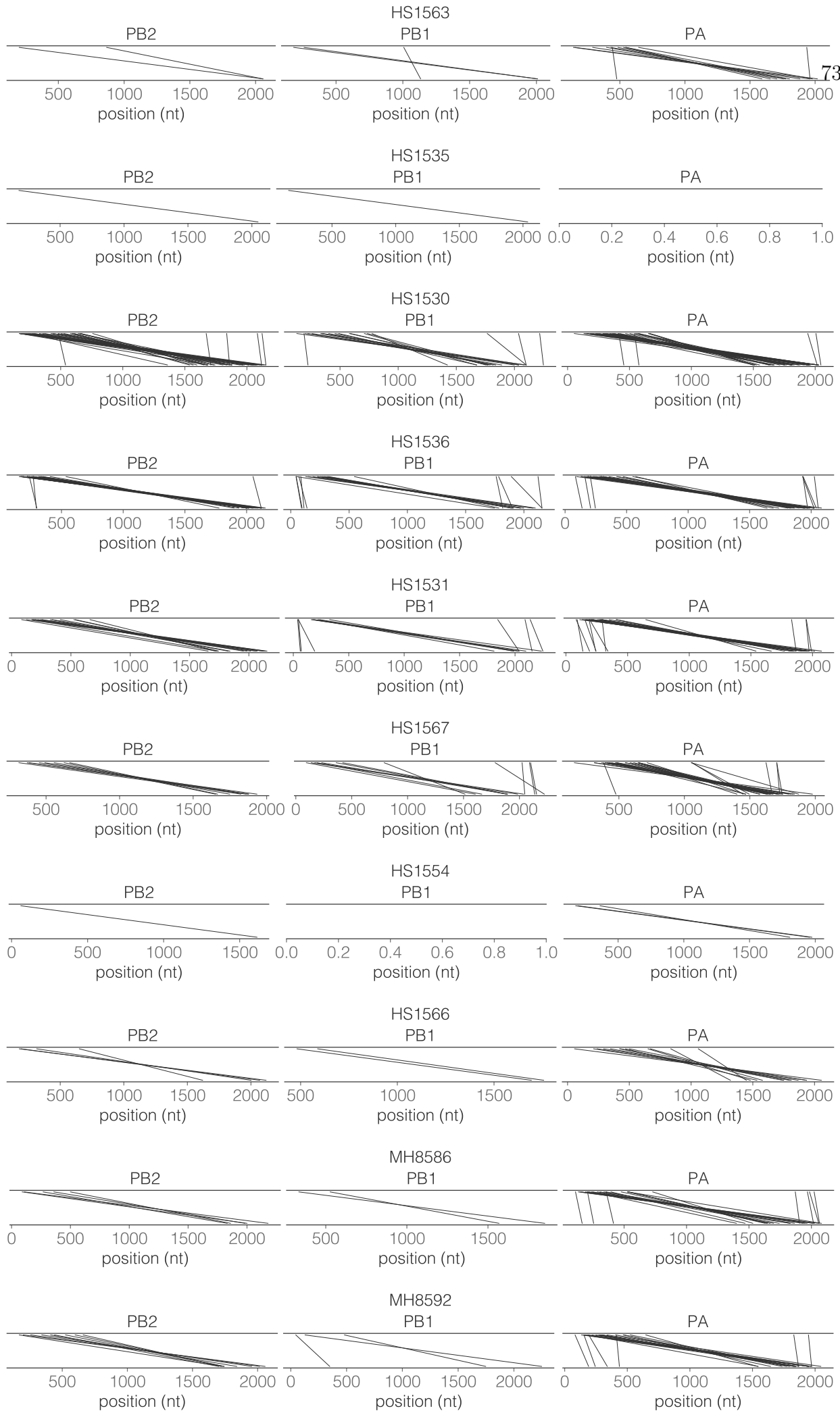


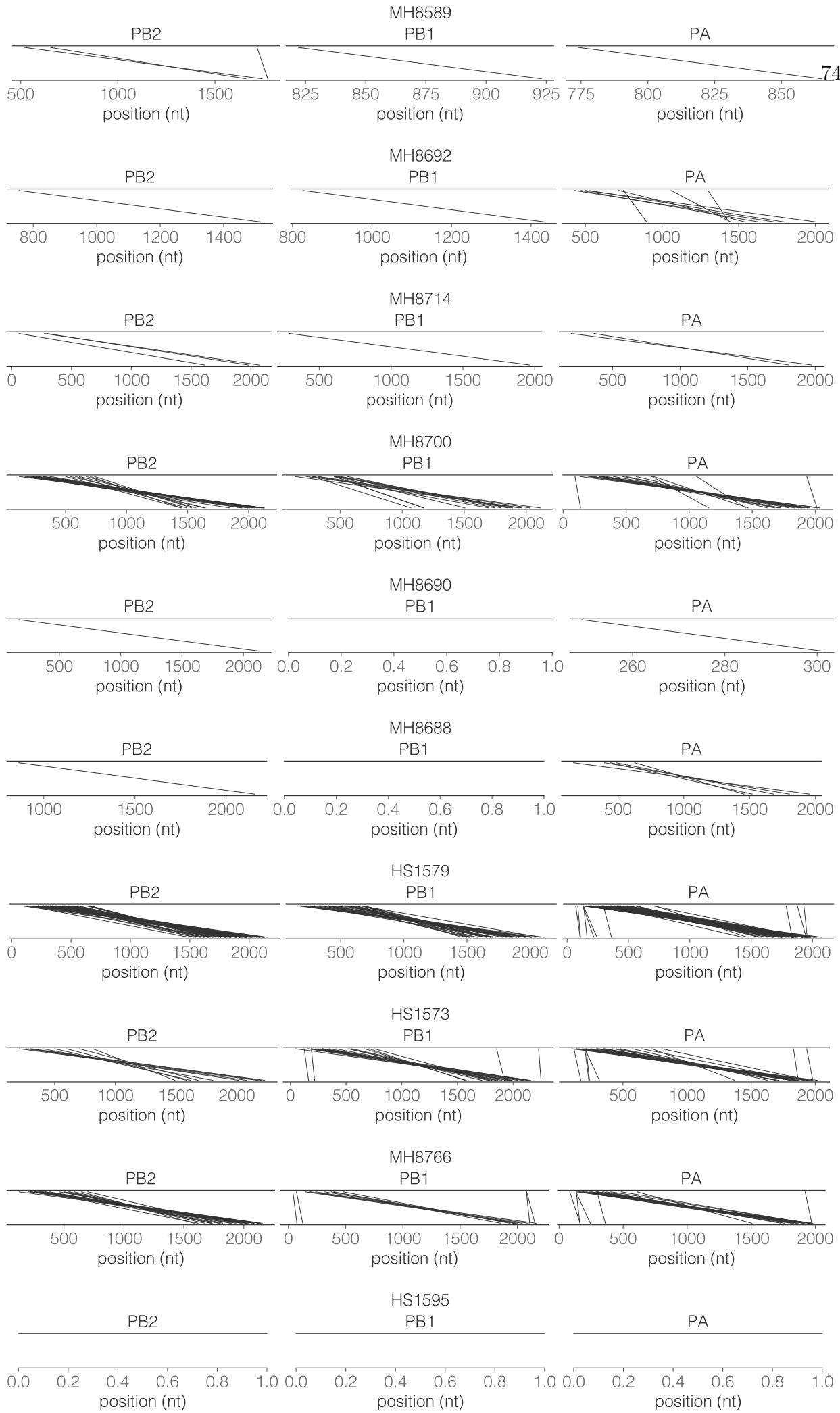












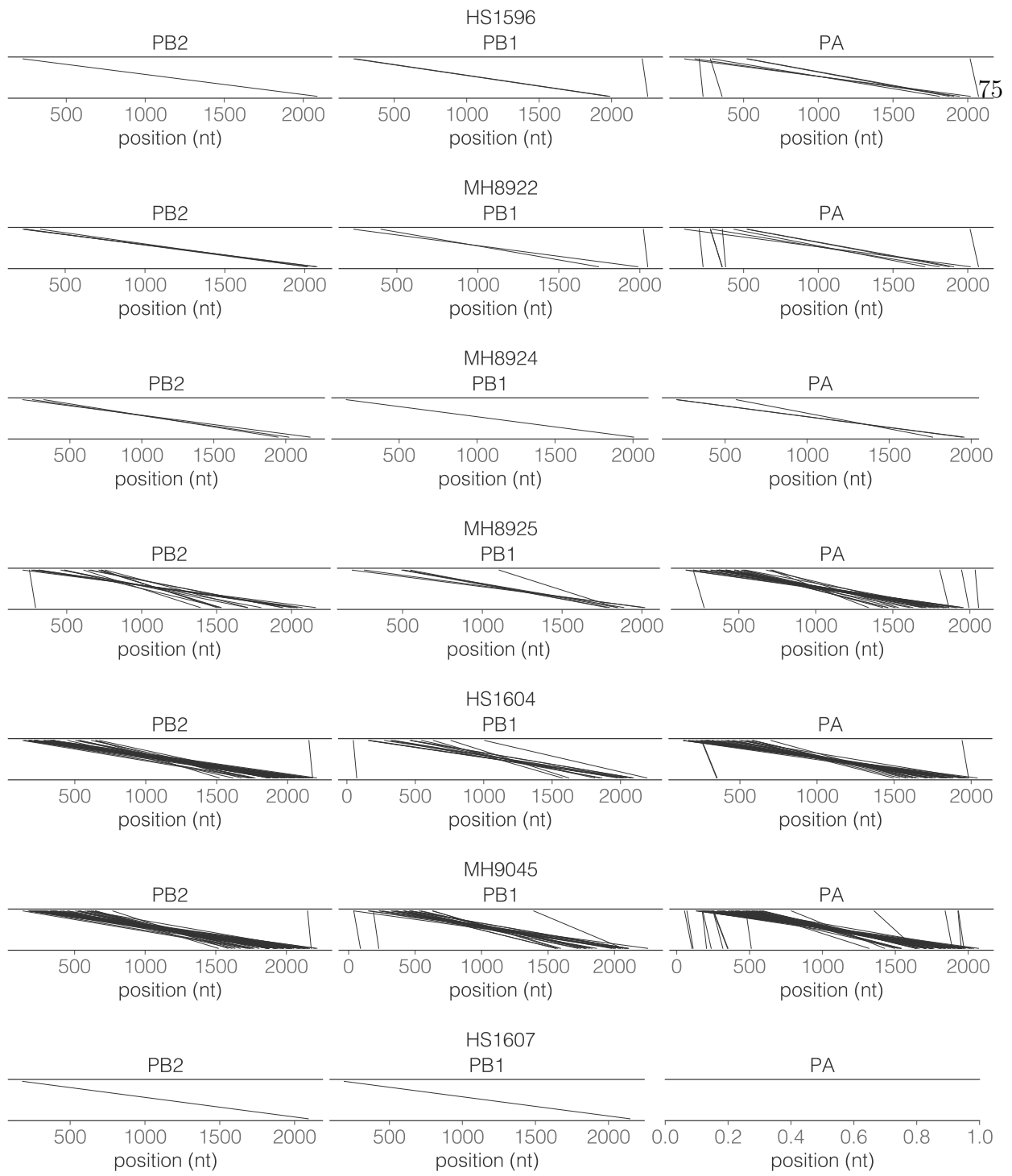


Figure S2.6: Observed junction locations for all PB2, PB1, and PA DVGs observed in all clinical samples. Lines connect the nucleotides flanking the deleted nucleotides for each identified DVG.

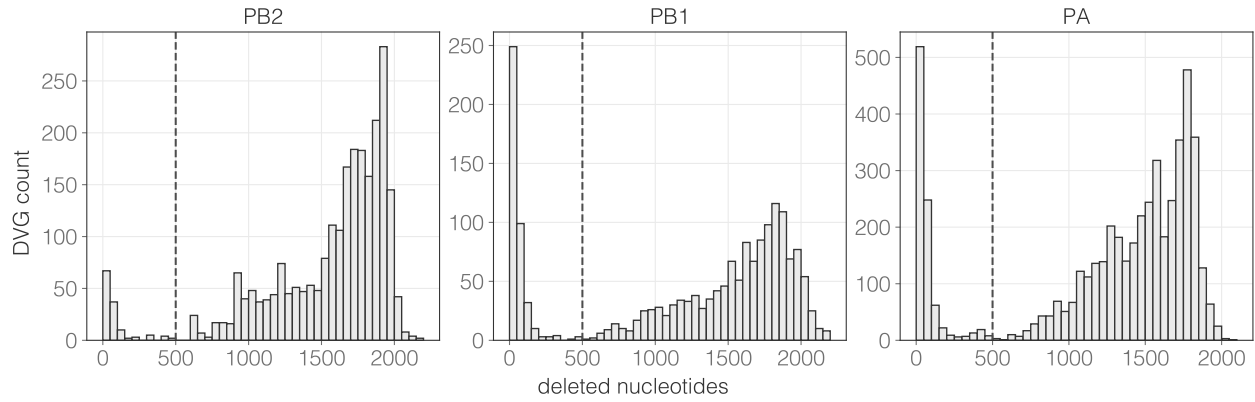
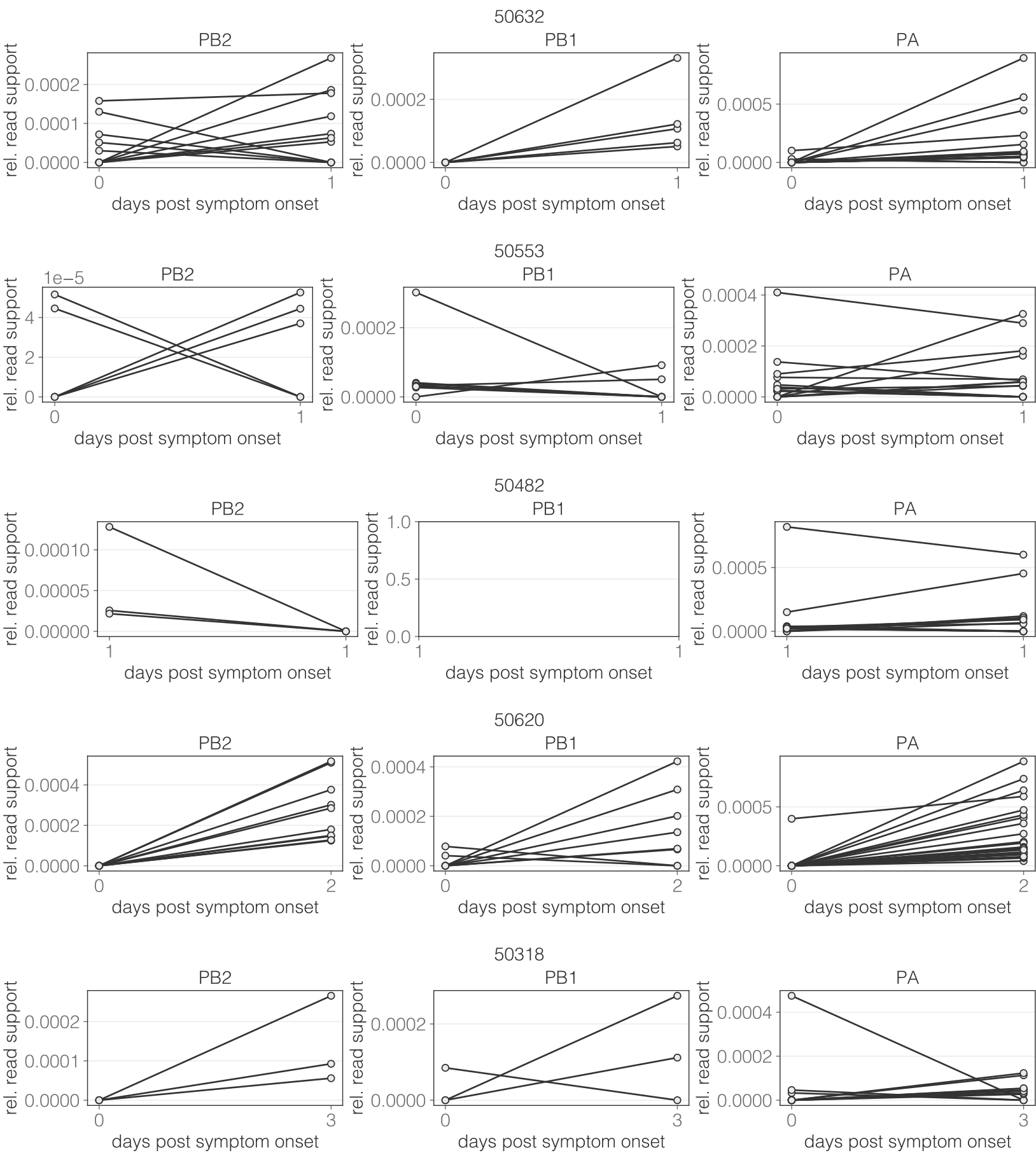
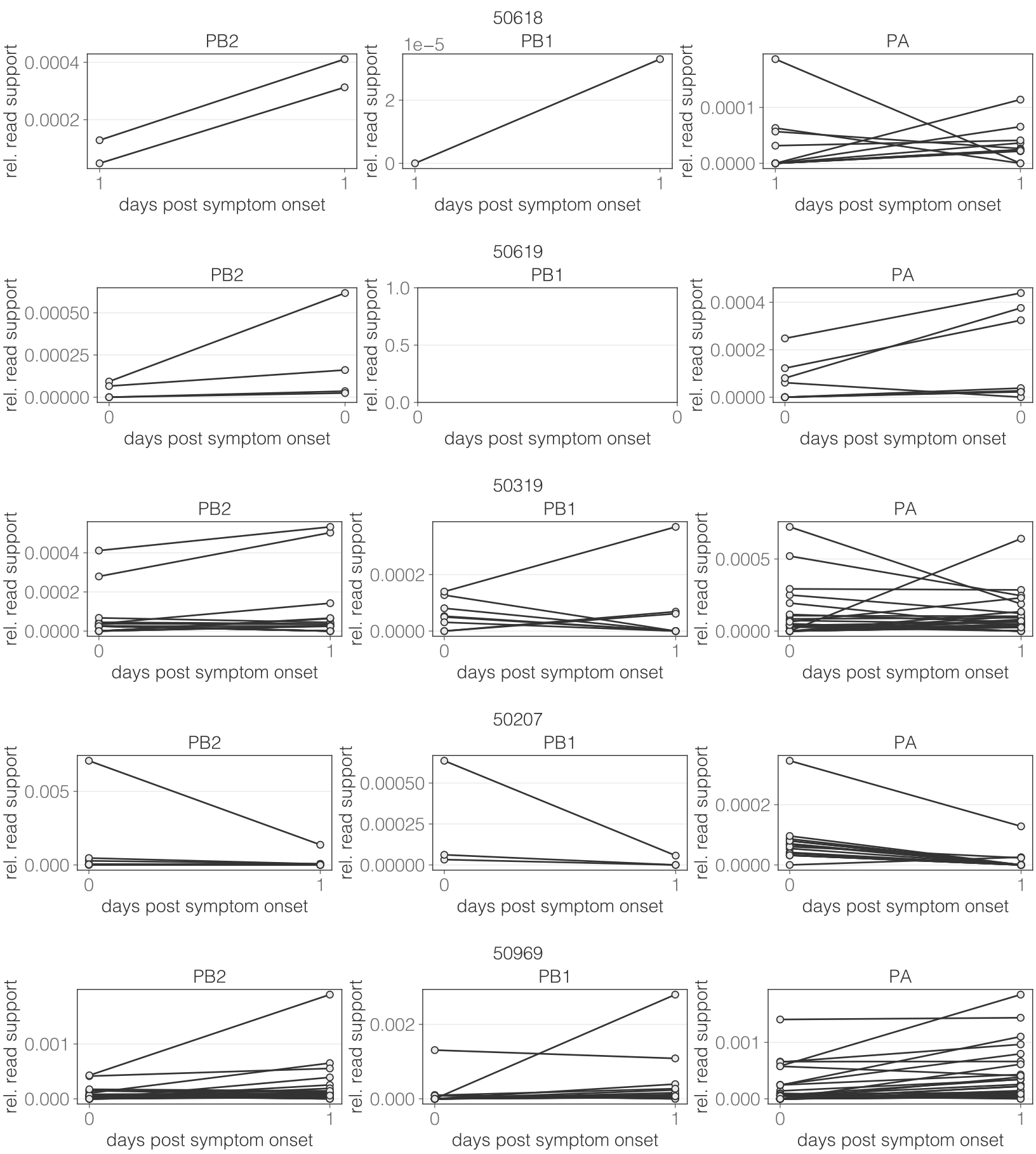
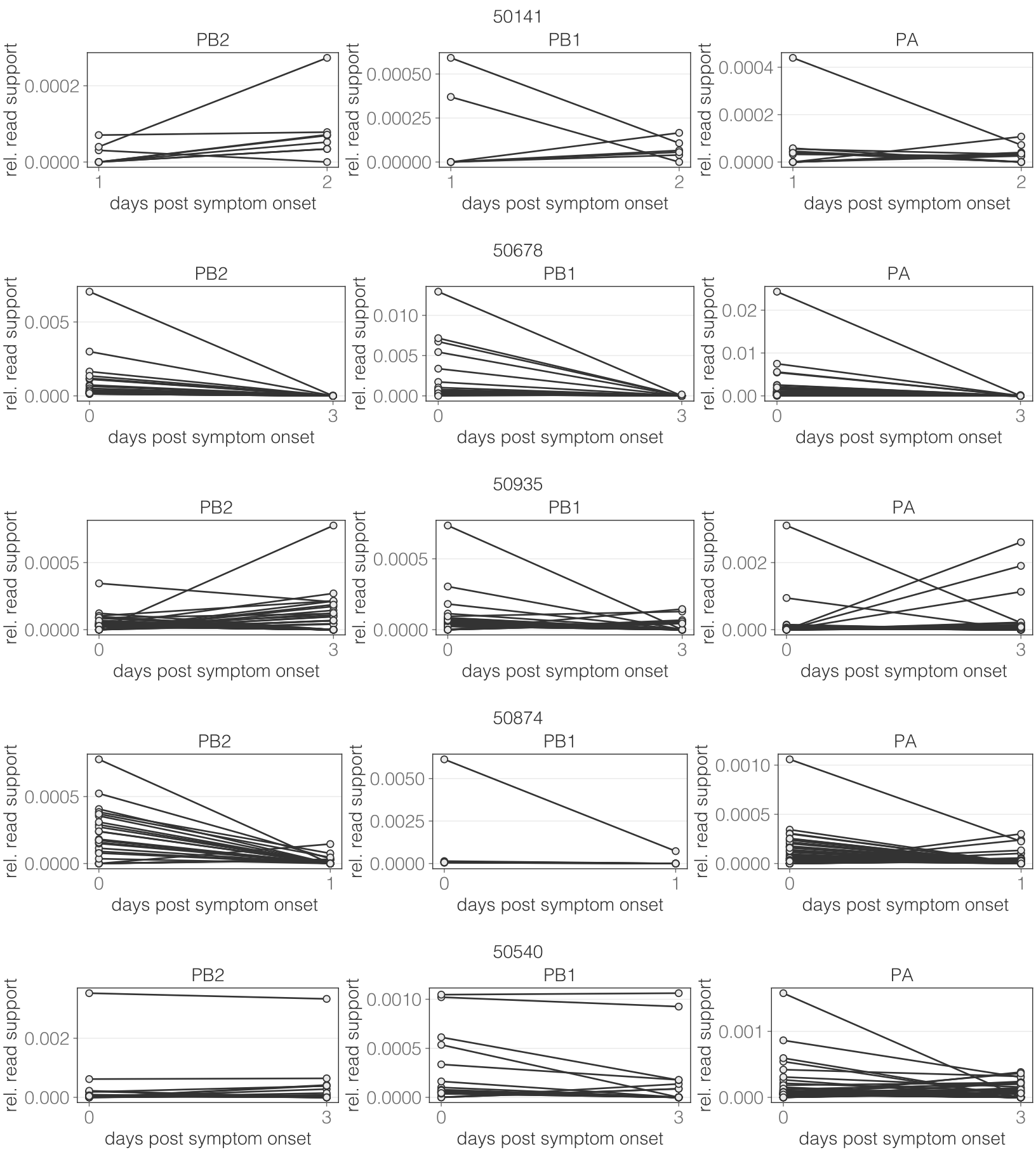


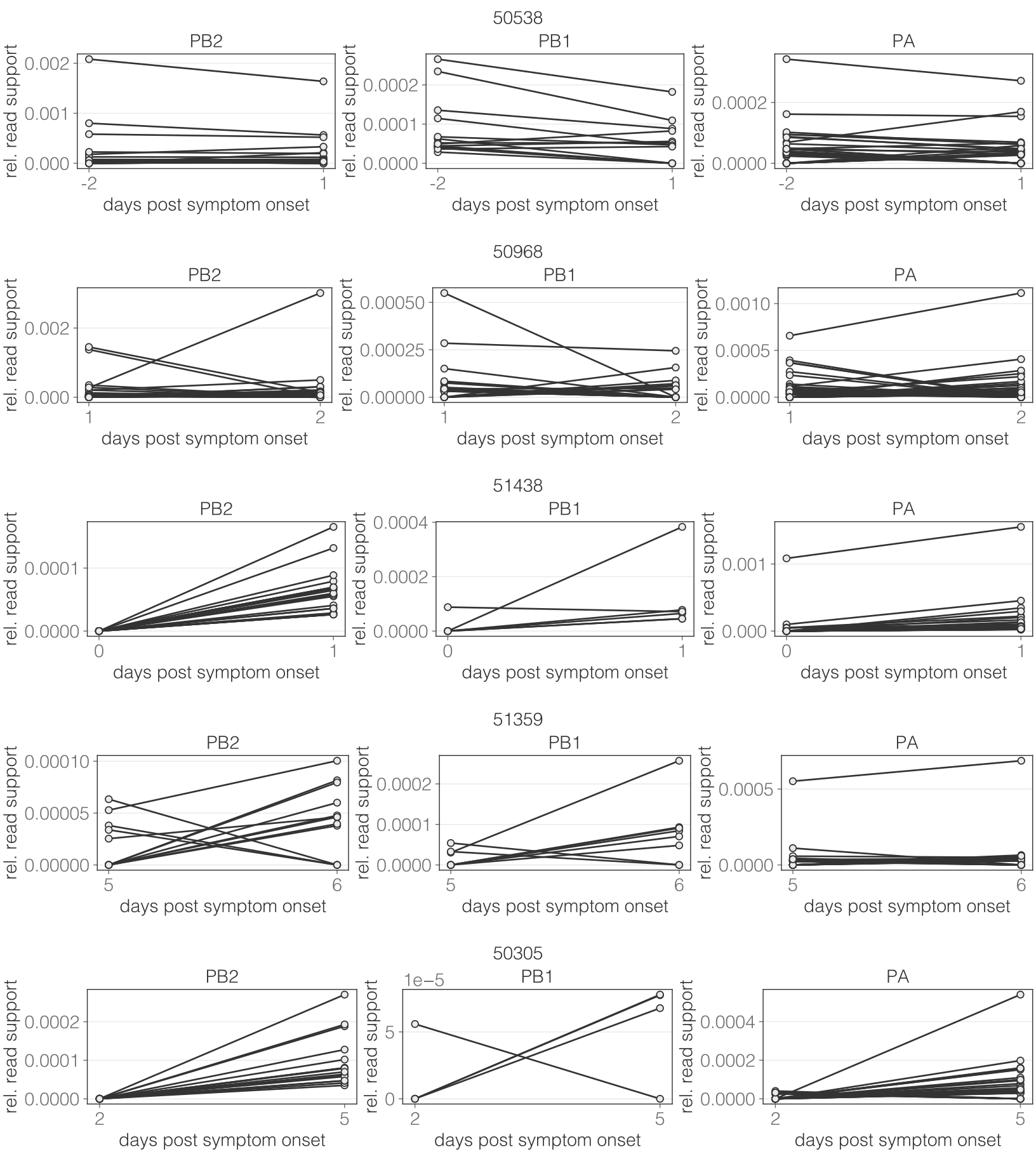
Figure S2.7: Number of deleted nucleotides for each DVG identified in the PB2 (A), PB1 (B), and PA (C) segments. Dashed line at 500 nucleotides represents our empirical filtering threshold.

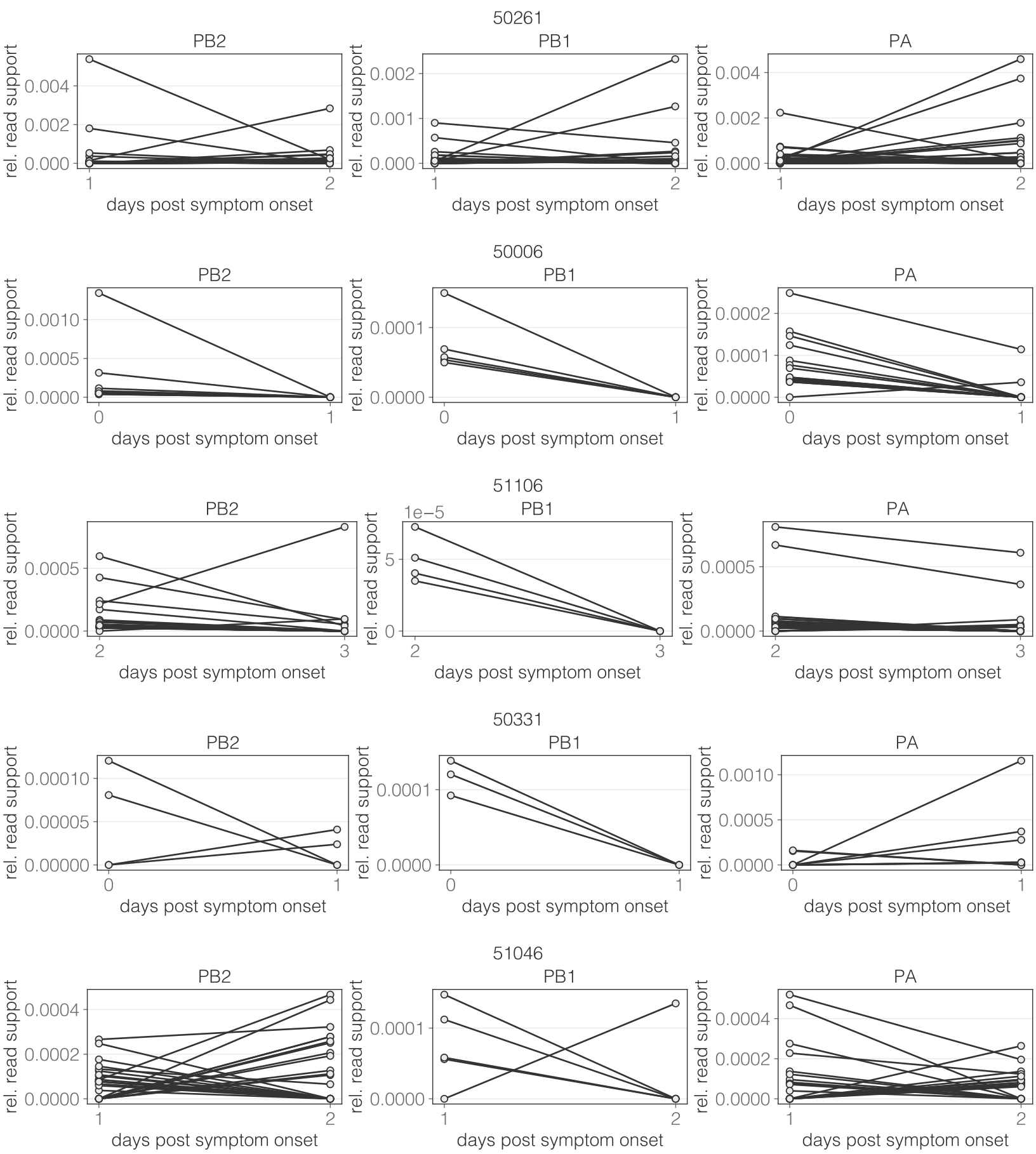


78

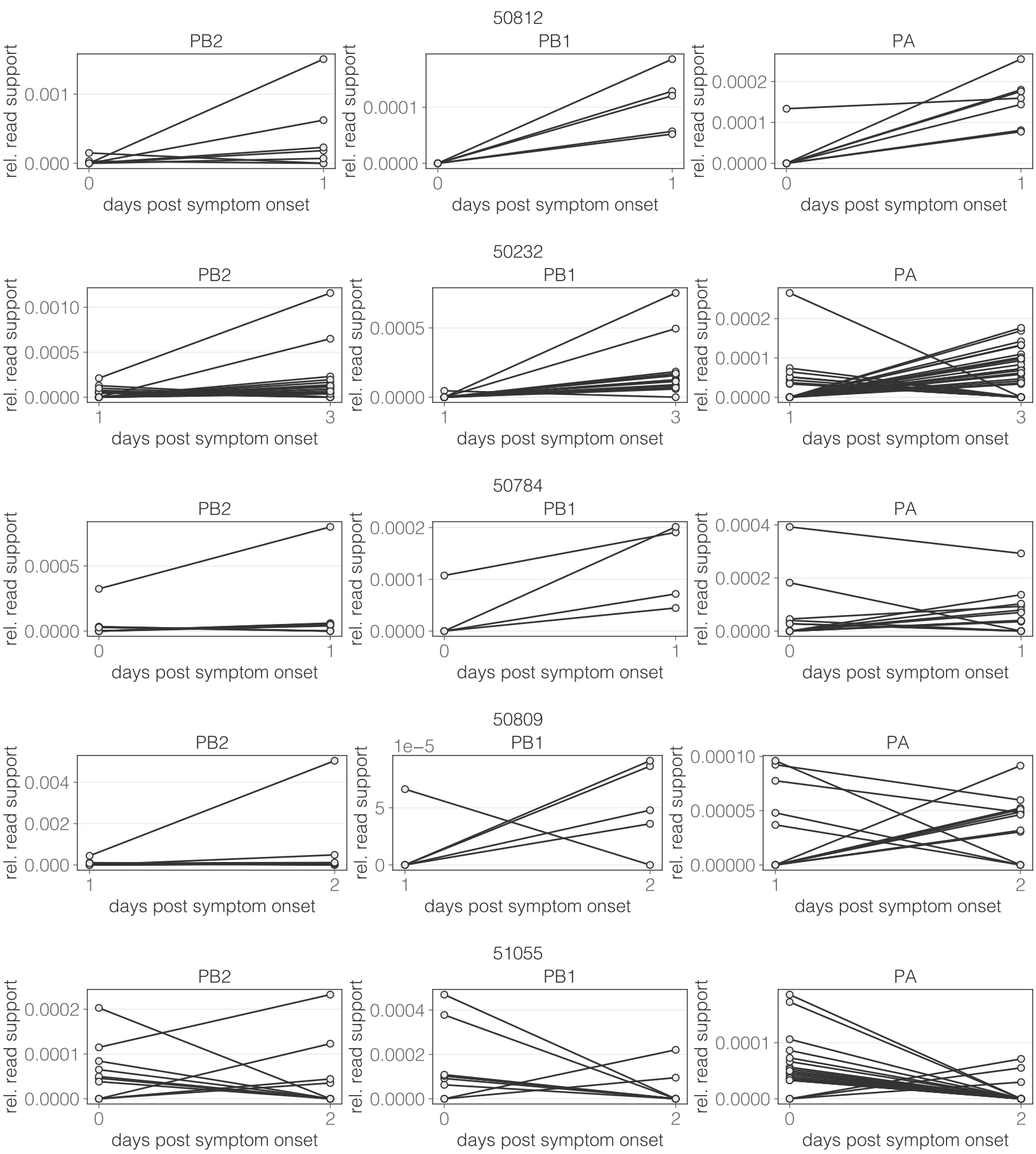


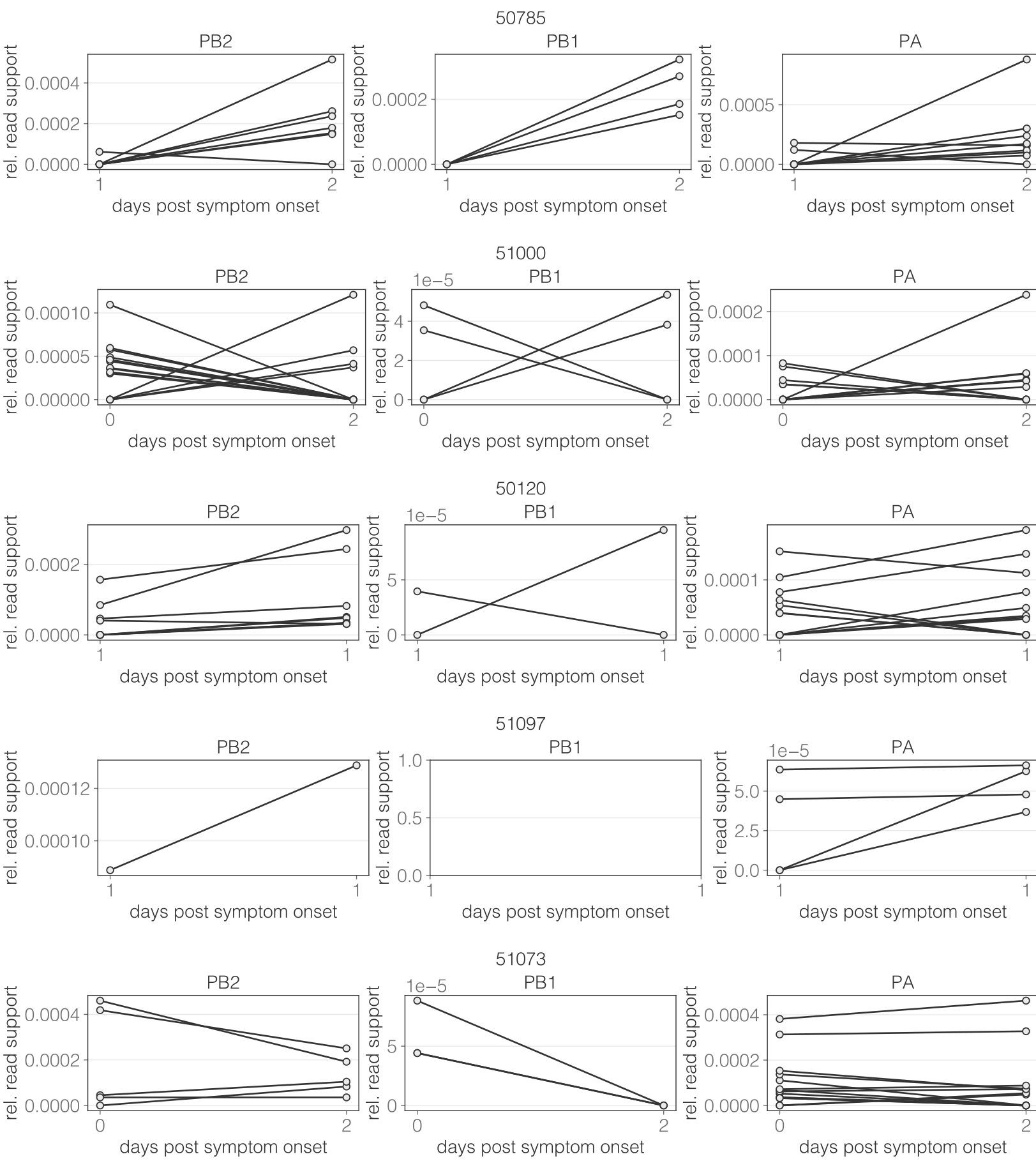


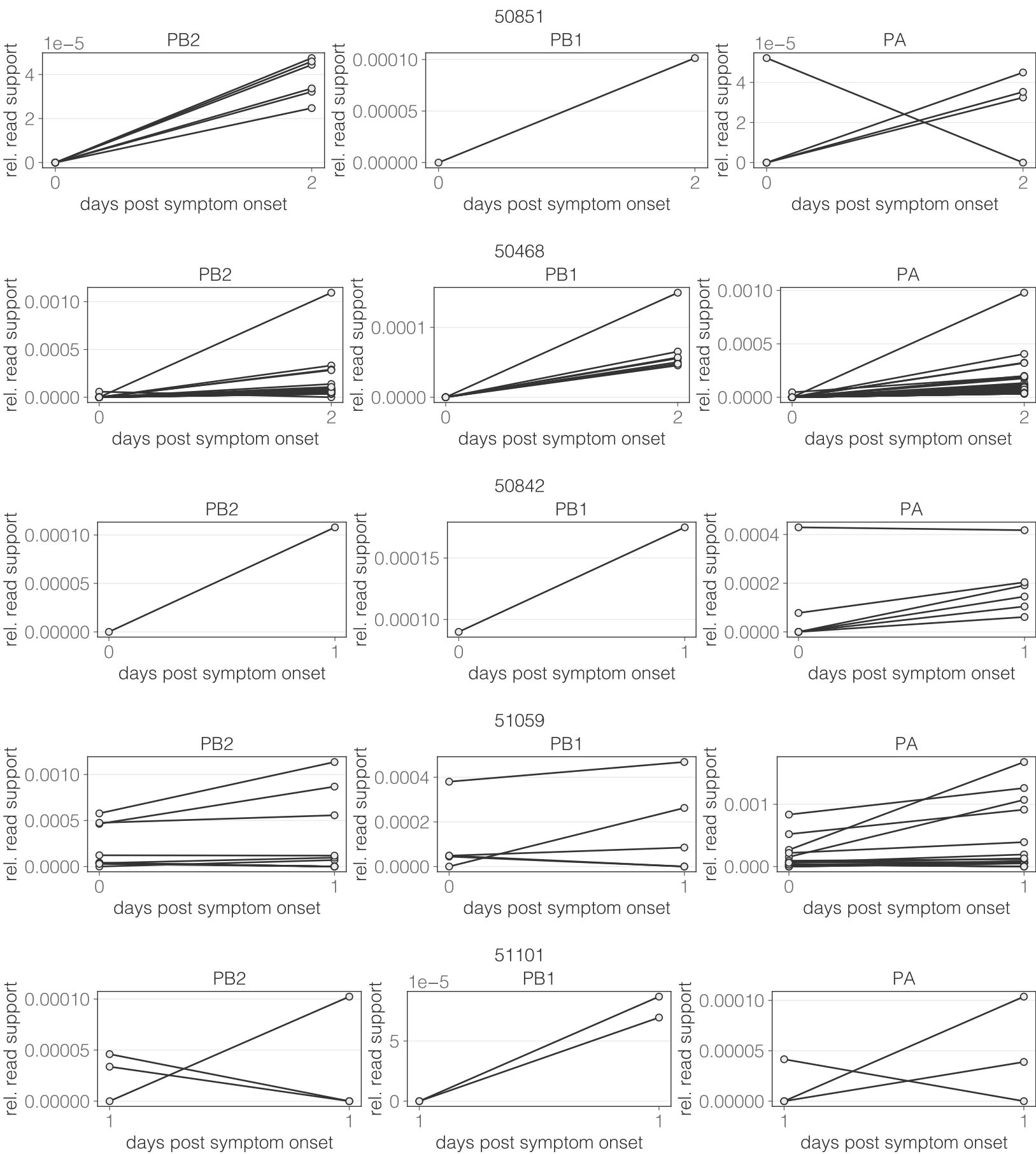


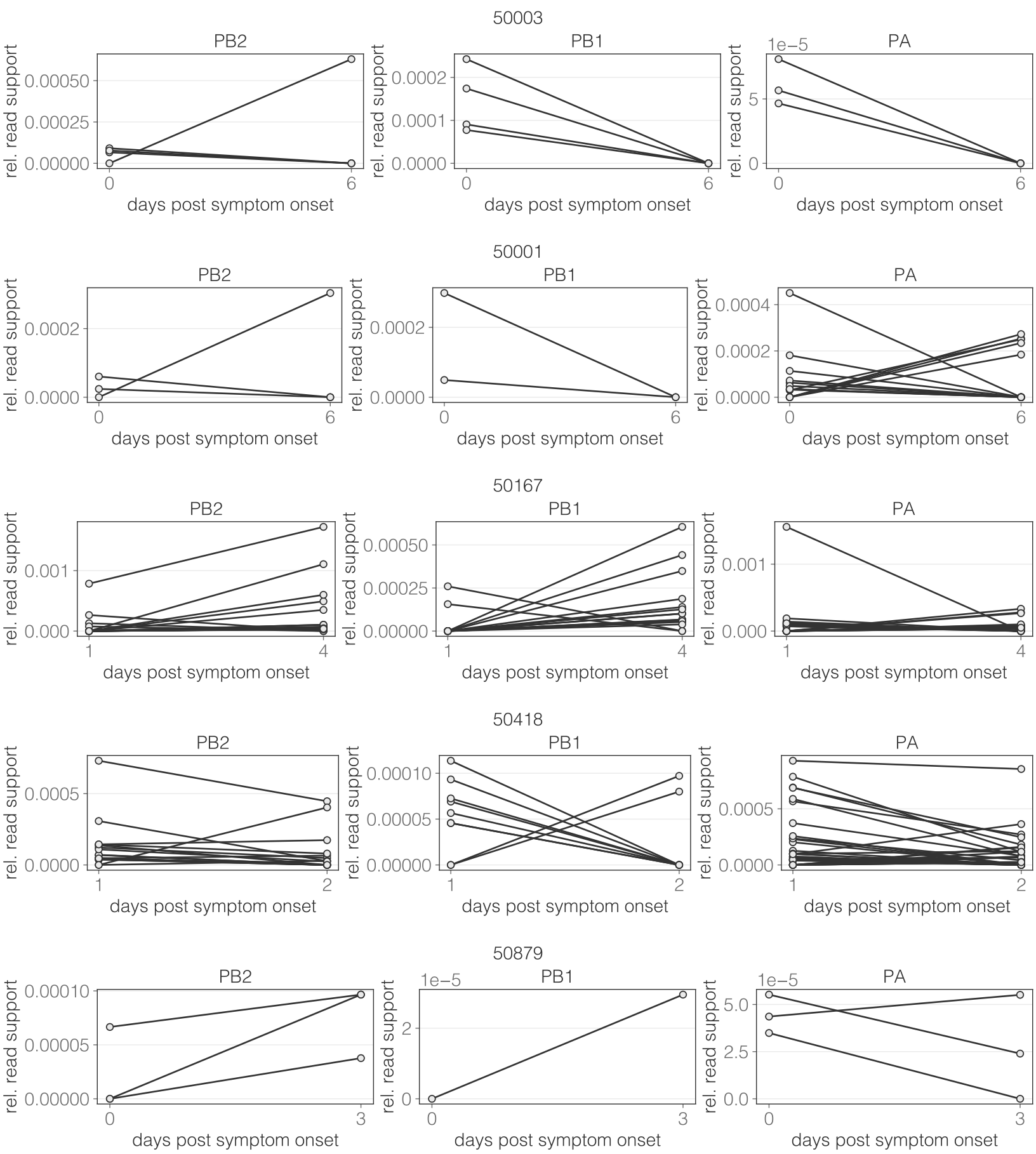


82









86

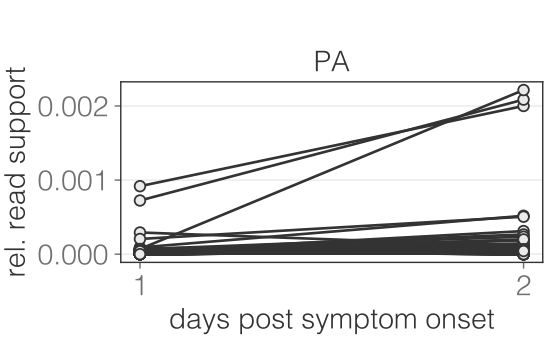
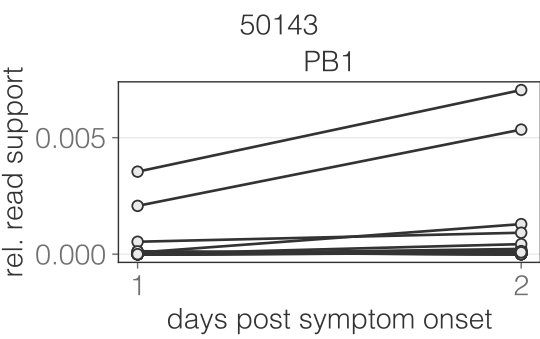
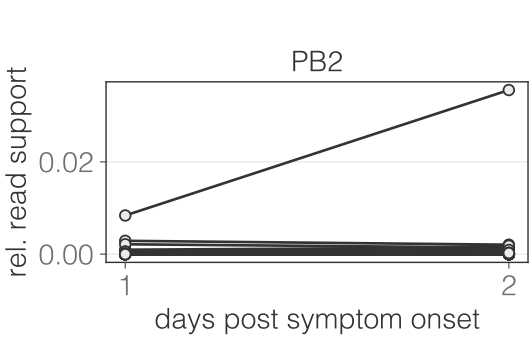
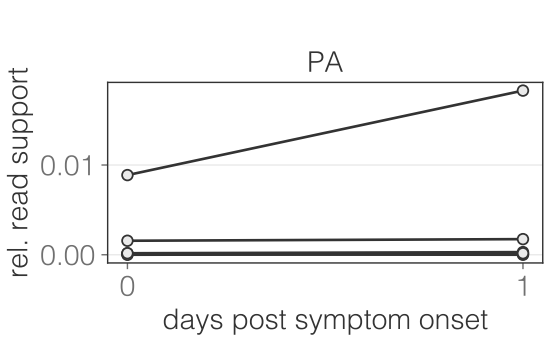
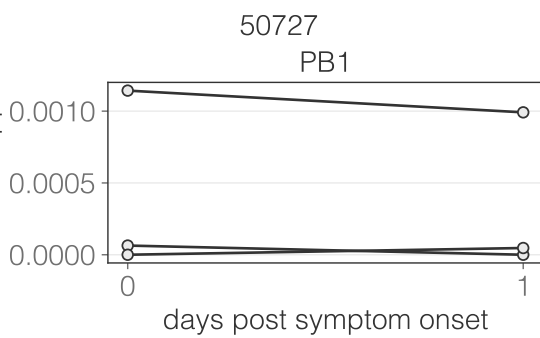
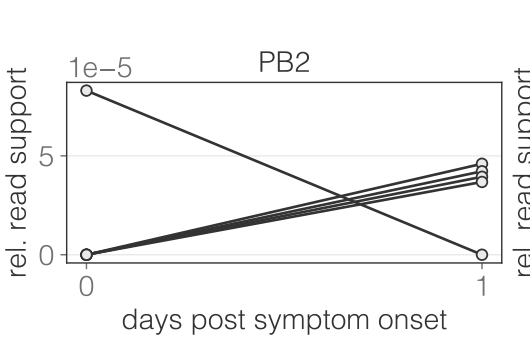
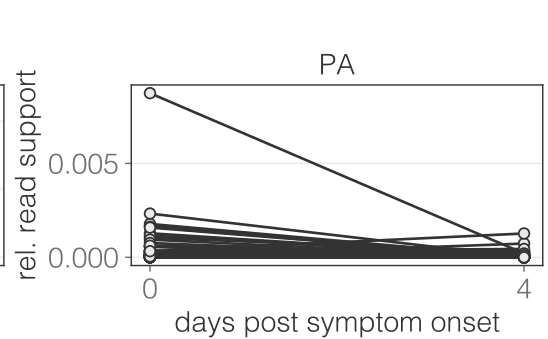
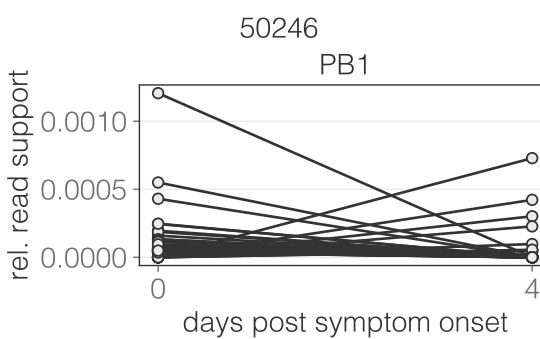
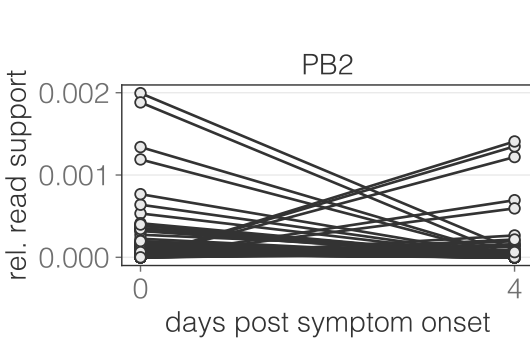


Figure S2.8: Relative read support of DVGs identified in the PB2, PB1, and PA segments of all patients with longitudinal samples.

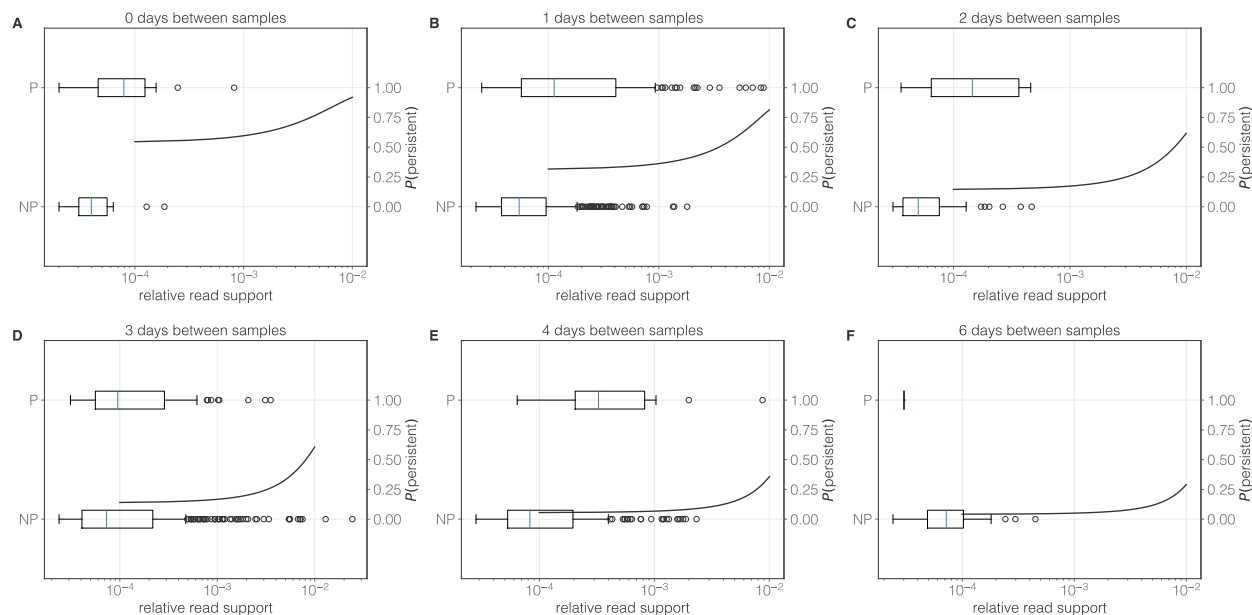


Figure S2.9: Relative read support of all DVGs identified in longitudinal samples taken 0, 1, 2, 3, 4, and 6 days apart, stratified by whether those DVGs are persistent (P) or non persistent (NP) between t_0 and t_1 . In all box plots blue line represents the median value for a given dataset, box extends to the limits of the inter-quartile range (IQR), and whiskers extend to 1.5 IQR below and above the 1st and 3rd quartile, respectively. Outliers are shown as dots beyond the range of the whiskers. Curve is the predicted probability of persistence from a multivariate logistic regression with relative read support and time between samples (categorical) as predictors.

2.6.2 Supplementary Tables

Table S2.1: Logistic Regression of the probability of polymerase DVG persistence between t_0 and t_1 as a function of relative DVG read support

Variable	Coefficient	Std Err	<i>p</i> value	0.025	0.975
Intercept	-1.2295	0.064	0.000	-1.354	-1.105
Relative support	159.0822	62.526	0.011	36.534	281.630

Table S2.2: Logistic Regression of the probability of polymerase DVG persistence between t_0 and t_1 as a function of time between samples and relative DVG read support

Variable	Coefficient	Std Err	p value	0.025	0.975
Intercept	0.1628	0.303	0.591	-0.431	0.756
$C(t_{span} = 1)$	-0.9543	0.313	0.002	-1.568	-0.341
$C(t_{span} = 2)$	-1.9514	0.419	0.000	-2.772	-1.131
$C(t_{span} = 3)$	-1.9988	0.335	0.000	-2.655	-1.343
$C(t_{span} = 4)$	-3.0189	0.435	0.000	-3.872	-2.166
$C(t_{span} = 6)$	-3.3221	1.065	0.002	-5.410	-1.234
Relative support	226.5670	70.198	0.001	88.981	364.153

Table S2.3: Logistic Regression of the number of shared DVGs between sample pairs as a function of the type of pair

Variable	Coefficient	Std Err	p value	0.025	0.975
Intercept	-0.9545	0.022	0.000	-0.998	-0.911
$C(\text{type})$	0.3354	0.272	0.217	-0.197	0.868

Chapter 2 References

- [1] J. Paget, P. Spreeuwenberg, V. Charu, R. J. Taylor, A. D. Iuliano, J. Bresee, L. Simonsen, and C. Viboud, “Global mortality associated with seasonal influenza epidemics: New burden estimates and predictors from the GLaMOR Project,” *Journal of Global Health*, vol. 9, p. 020421, Dec. 2019.
- [2] K. Koelle, S. Cobey, B. Grenfell, and M. Pascual, “Epochal Evolution Shapes the Phylodynamics of Interpandemic Influenza A (H3N2) in Humans,” *Science*, vol. 314, no. 5807, pp. 1898–1903, 2006.
- [3] M. F. Boni, “Vaccination and antigenic drift in influenza,” *Vaccine*, vol. 26, pp. C8–C14, July 2008.
- [4] D. J. Smith, A. S. Lapedes, J. C. de Jong, T. M. Bestebroer, G. F. Rimmelzwaan, A. D. M. E. Osterhaus, and R. A. M. Fouchier, “Mapping the Antigenic and Genetic Evolution of Influenza Virus,” *Science*, vol. 305, pp. 371–376, July 2004.
- [5] T. Bedford, M. A. Suchard, P. Lemey, G. Dudas, V. Gregory, A. J. Hay, J. W. McCauley, C. A. Russell, D. J. Smith, and A. Rambaut, “Integrating influenza antigenic dynamics with molecular evolution,” *eLife*, vol. 3, pp. 1–26, 2014.
- [6] T. Bedford, S. Riley, I. G. Barr, S. Broor, M. Chadha, N. J. Cox, R. S. Daniels, C. P. Gunasekaran, A. C. Hurt, A. Kelso, A. Klimov, N. S. Lewis, X. Li, J. W. McCauley, T. Odagiri, V. Potdar, A. Rambaut, Y. Shu, E. Skepner, D. J. Smith, M. A. Suchard,

- M. Tashiro, D. Wang, X. Xu, P. Lemey, and C. A. Russell, "Global circulation patterns of seasonal influenza viruses vary with antigenic drift," *Nature*, vol. 523, pp. 217–220, July 2015.
- [7] R. A. Neher, T. Bedford, R. S. Daniels, C. A. Russell, and B. I. Shraiman, "Prediction, dynamics, and visualization of antigenic phenotypes of seasonal influenza viruses," *Proceedings of the National Academy of Sciences*, vol. 113, Mar. 2016.
- [8] J. Huddleston, J. R. Barnes, T. Rowe, X. Xu, R. Kondor, D. E. Wentworth, L. Whitaker, B. Ermetal, R. S. Daniels, J. W. McCauley, S. Fujisaki, K. Nakamura, N. Kishida, S. Watanabe, H. Hasegawa, I. Barr, K. Subbarao, P. Barrat-Charlaix, R. A. Neher, and T. Bedford, "Integrating genotypes and phenotypes improves long-term forecasts of seasonal influenza A/H3N2 evolution," *eLife*, vol. 9, p. e60067, Sept. 2020.
- [9] L. A. Castro, T. Bedford, and L. Ancel Meyers, "Early prediction of antigenic transitions for influenza A/H3N2," *PLOS Computational Biology*, vol. 16, p. e1007683, Feb. 2020.
- [10] C. Viboud, K. Gostic, M. I. Nelson, G. E. Price, A. Perofsky, K. Sun, N. Sequeira Trovão, B. J. Cowling, S. L. Epstein, and D. J. Spiro, "Beyond clinical trials: Evolutionary and epidemiological considerations for development of a universal influenza vaccine," *PLOS Pathogens*, vol. 16, p. e1008583, Sept. 2020.
- [11] J. T. McCrone and A. S. Lauring, "Genetic bottlenecks in intraspecies virus transmission," *Current Opinion in Virology*, vol. 28, pp. 20–25, 2018. Publisher: Elsevier B.V.
- [12] K. S. Xue, L. H. Moncla, T. Bedford, and J. D. Bloom, "Within-Host Evolution of Human Influenza Virus," *Trends in Microbiology*, vol. 26, pp. 781–793, Sept. 2018.
- [13] A. Sobel Leonard, D. B. Weissman, B. Greenbaum, E. Ghedin, and K. Koelle, "Transmission Bottleneck Size Estimation from Pathogen Deep-Sequencing Data, with an Application to Human Influenza A Virus," *Journal of Virology*, vol. 91, July 2017.

- [14] K. Debbink, J. T. McCrone, J. G. Petrie, R. Truscon, E. Johnson, E. K. Mantlo, A. S. Monto, and A. S. Luring, “Vaccination has minimal impact on the intrahost diversity of H3N2 influenza viruses,” *PLoS Pathogens*, vol. 13, no. 1, pp. 1–18, 2017.
- [15] D. H. Morris, V. N. Petrova, F. W. Rossine, E. Parker, B. T. Grenfell, R. A. Neher, S. A. Levin, and C. A. Russell, “Asynchrony between virus diversity and antibody selection limits influenza virus evolution,” *eLife*, vol. 9, p. e62105, Nov. 2020.
- [16] K. S. Xue, T. Stevens-Ayers, A. P. Campbell, J. A. Englund, S. A. Pergam, M. Boeckh, and J. D. Bloom, “Parallel evolution of influenza across multiple spatiotemporal scales,” *eLife*, vol. 6, pp. 1–16, 2017.
- [17] F. G. Alnaji, W. K. Reiser, and J. Rivera-Cardona, “Influenza A Virus Defective Viral Genomes Are Inefficiently Packaged into Virions Relative to Wild-Type Genomic RNAs,” vol. 12, no. 6, p. 12, 2021.
- [18] N. T. Jacobs, N. O. Onuoha, A. Antia, J. Steel, R. Antia, and A. C. Lowen, “Incomplete influenza A virus genomes occur frequently but are readily complemented during localized viral spread,” *Nature Communications*, vol. 10, no. 1, 2019. Publisher: Springer US.
- [19] C. B. Brooke, W. L. Ince, J. Wrammert, R. Ahmed, P. C. Wilson, J. R. Bennink, and J. W. Yewdell, “Most Influenza A Virions Fail To Express at Least One Essential Viral Protein,” *Journal of Virology*, vol. 87, no. 6, pp. 3155–3162, 2013.
- [20] N. H. Barton, “Genetic hitchhiking,” *Philosophical Transactions of the Royal Society of London. Series B: Biological Sciences*, vol. 355, pp. 1553–1562, Nov. 2000.
- [21] H. Tao, L. Li, M. C. White, J. Steel, and A. C. Lowen, “Influenza A Virus Coinfection through Transmission Can Support High Levels of Reassortment,” *Journal of Virology*, vol. 89, pp. 8453–8461, Aug. 2015.

- [22] M. E. Gallagher, C. B. Brooke, R. Ke, and K. Koelle, “Causes and Consequences of Spatial Within-Host Viral Spread,” *Viruses*, vol. 10, no. 11, pp. 1–23, 2018.
- [23] K. Saira, X. Lin, J. V. DePasse, R. Halpin, A. Twaddle, T. Stockwell, B. Angus, A. Cozzi-Lepri, M. Delfino, V. Dugan, D. E. Dwyer, M. Freiberg, A. Horban, M. Losso, R. Lynfield, D. N. Wentworth, E. C. Holmes, R. Davey, D. E. Wentworth, and E. Ghedin, “Sequence Analysis of In Vivo Defective Interfering-Like RNA of Influenza A H1N1 Pandemic Virus,” *Journal of Virology*, vol. 87, no. 14, pp. 8064–8074, 2013.
- [24] R. Sanjuán, “Collective Infectious Units in Viruses,” *Trends in Microbiology*, vol. 25, pp. 402–412, May 2017.
- [25] C. Wallis and J. L. Melnick, “Virus Aggregation as the Cause of the Non-neutralizable Persistent Fraction,” *Journal of Virology*, vol. 1, pp. 478–488, June 1967.
- [26] C. Cane, L. McLain, and N. J. Dimmock, “Intracellular stability of the interfering activity of a defective interfering influenza virus in the absence of virus multiplication,” *Virology*, vol. 159, pp. 259–264, Aug. 1987.
- [27] D. P. Nayak, K. Tobita, J. M. Janda, a. R. Davis, and B. K. De, “Homologous interference mediated by defective interfering influenza virus derived from a temperature-sensitive mutant of influenza virus.,” *Journal of virology*, vol. 28, no. 1, pp. 375–86, 1978.
- [28] F. G. Alnaji and C. B. Brooke, “Influenza virus DI particles: Defective interfering or delightfully interesting?,” *PLOS Pathogens*, vol. 16, p. e1008436, May 2020.
- [29] A. C. Marriott and N. J. Dimmock, “Defective interfering viruses and their potential as antiviral agents: Defective interfering viruses,” *Reviews in Medical Virology*, vol. 20, pp. 51–62, Jan. 2010.

- [30] N. J. Dimmock and A. J. Easton, “Defective Interfering Influenza Virus RNAs: Time To Reevaluate Their Clinical Potential as Broad-Spectrum Antivirals?,” *Journal of Virology*, vol. 88, pp. 5217–5227, May 2014.
- [31] J. Xu, Y. Sun, Y. Li, G. Ruthel, S. R. Weiss, A. Raj, D. Beiting, and C. B. López, “Replication defective viral genomes exploit a cellular pro-survival mechanism to establish paramyxovirus persistence,” *Nature Communications*, vol. 8, p. 799, Dec. 2017.
- [32] M. A. Wasik, L. Eichwald, Y. Genzel, and U. Reichl, “Cell culture-based production of defective interfering particles for influenza antiviral therapy,” *Applied Microbiology and Biotechnology*, vol. 102, pp. 1167–1177, Feb. 2018.
- [33] L. Pelz, D. Rüdiger, T. Dogra, F. G. Alnaji, Y. Genzel, C. B. Brooke, S. Y. Kupke, and U. Reichl, “Semi-continuous Propagation of Influenza A Virus and Its Defective Interfering Particles: Analyzing the Dynamic Competition To Select Candidates for Antiviral Therapy,” *Journal of Virology*, vol. 95, pp. e01174–21, Nov. 2021.
- [34] N. J. Dimmock, E. W. Rainsford, P. D. Scott, and A. C. Marriott, “Influenza Virus Protecting RNA: an Effective Prophylactic and Therapeutic Antiviral,” *Journal of Virology*, vol. 82, pp. 8570–8578, Sept. 2008.
- [35] N. J. Dimmock, B. K. Dove, B. Meng, P. D. Scott, I. Taylor, L. Cheung, B. Hallis, A. C. Marriott, M. W. Carroll, and A. J. Easton, “Comparison of the protection of ferrets against pandemic 2009 influenza A virus (H1N1) by 244 DI influenza virus and oseltamivir,” *Antiviral Research*, vol. 96, pp. 376–385, Dec. 2012.
- [36] F. G. Alnaji, J. R. Holmes, G. Rendon, J. C. Vera, C. Fields, B. E. Martin, and C. B. Brooke, “Sequencing framework for the sensitive detection and precise mapping of defective interfering particle-associated deletions across influenza A and B viruses.,” *Journal of Virology*, vol. 93, May 2019.

- [37] A. Routh and J. E. Johnson, “Discovery of functional genomic motifs in viruses with ViReMa—a virus recombination mapper—for analysis of next-generation sequencing data,” *Nucleic Acids Research*, vol. 42, no. 2, pp. 1–10, 2014.
- [38] B. Zhou, M. E. Donnelly, D. T. Scholes, K. St. George, M. Hatta, Y. Kawaoka, and D. E. Wentworth, “Single-Reaction Genomic Amplification Accelerates Sequencing and Vaccine Production for Classical and Swine Origin Human Influenza A Viruses,” *Journal of Virology*, vol. 83, no. 19, pp. 10309–10313, 2009.
- [39] P. Di Tommaso, M. Chatzou, E. W. Floden, P. P. Barja, E. Palumbo, and C. Notredame, “Nextflow enables reproducible computational workflows,” *Nature Biotechnology*, vol. 35, pp. 316–319, Apr. 2017.
- [40] A. M. Bolger, M. Lohse, and B. Usadel, “Trimmomatic: A flexible trimmer for Illumina sequence data,” *Bioinformatics*, vol. 30, no. 15, pp. 2114–2120, 2014.
- [41] D. E. Wood, J. Lu, and B. Langmead, “Improved metagenomic analysis with Kraken 2,” *Genome Biology*, vol. 20, p. 257, Dec. 2019.
- [42] S. Andrews, “FastQC: a quality control tool for high throughput sequence data.,” 2010.
- [43] B. Langmead and S. L. Salzberg, “Fast gapped-read alignment with Bowtie 2,” *Nature Methods*, vol. 9, pp. 357–359, Apr. 2012.
- [44] H. Li, B. Handsaker, A. Wysoker, T. Fennell, J. Ruan, N. Homer, G. Marth, G. Abecasis, and R. Durbin, “The Sequence Alignment/Map format and SAMtools,” *Bioinformatics*, vol. 25, no. 16, pp. 2078–2079, 2009.
- [45] B. Langmead, C. Trapnell, M. Pop, and S. L. Salzberg, “Ultrafast and memory-efficient alignment of short DNA sequences to the human genome,” *Genome Biology*, vol. 10, no. 3, p. R25, 2009.
- [46] “Python Language Reference, version 3.9.”

- [47] Pandas Development Team, “Pandas,” tech. rep., NumFocus, Oct. 2020.
- [48] C. R. Harris, K. J. Millman, S. J. van der Walt, R. Gommers, P. Virtanen, D. Cournapeau, E. Wieser, J. Taylor, S. Berg, N. J. Smith, R. Kern, M. Picus, S. Hoyer, M. H. van Kerkwijk, M. Brett, A. Haldane, J. F. del Río, M. Wiebe, P. Peterson, P. Gérard-Marchant, K. Sheppard, T. Reddy, W. Weckesser, H. Abbasi, C. Gohlke, and T. E. Oliphant, “Array programming with NumPy,” *Nature*, vol. 585, pp. 357–362, Sept. 2020.
- [49] K. Katoh, K. Misawa, K.-i. Kuma, and T. Miyata, “MAFFT: a novel method for rapid multiple sequence alignment based on fast Fourier transform.,” *Nucleic acids research*, vol. 30, no. 14, pp. 3059–3066, 2002.
- [50] Z. Zhang, S. Schwartz, L. Wagner, and W. Miller, “A Greedy Algorithm for Aligning DNA Sequences,” *Journal of Computational Biology*, vol. 7, pp. 203–214, Feb. 2000.
- [51] A. Morgulis, G. Coulouris, Y. Raytselis, T. L. Madden, R. Agarwala, and A. A. Schäfer, “Database indexing for production MegaBLAST searches,” *Bioinformatics*, vol. 24, pp. 1757–1764, Aug. 2008.
- [52] SciPy 1.0 Contributors, P. Virtanen, R. Gommers, T. E. Oliphant, M. Haberland, T. Reddy, D. Cournapeau, E. Burovski, P. Peterson, W. Weckesser, J. Bright, S. J. van der Walt, M. Brett, J. Wilson, K. J. Millman, N. Mayorov, A. R. J. Nelson, E. Jones, R. Kern, E. Larson, C. J. Carey, . Polat, Y. Feng, E. W. Moore, J. VanderPlas, D. Laxalde, J. Perktold, R. Cimrman, I. Henriksen, E. A. Quintero, C. R. Harris, A. M. Archibald, A. H. Ribeiro, F. Pedregosa, and P. van Mulbregt, “SciPy 1.0: fundamental algorithms for scientific computing in Python,” *Nature Methods*, vol. 17, pp. 261–272, Mar. 2020.
- [53] S. Seabold and J. Perktold, “Statsmodels: Econometric and Statistical Modeling with Python,” (Austin, Texas), pp. 92–96, 2010.

- [54] D. Dou, R. Revol, H. Östbye, H. Wang, and R. Daniels, “Influenza A virus cell entry, replication, virion assembly and movement,” *Frontiers in Immunology*, vol. 9, no. JUL, pp. 1–17, 2018.
- [55] J. T. McCrone, R. J. Woods, A. S. Monto, E. T. Martin, and A. S. Luring, “The effective population size and mutation rate of influenza A virus in acutely infected individuals,” Oct. 2020.
- [56] M. Gerber, C. Isel, V. Moules, and R. Marquet, “Selective packaging of the influenza A genome and consequences for genetic reassortment,” *Trends in Microbiology*, vol. 22, pp. 446–455, Aug. 2014.
- [57] T. Frensing, S. Y. Kupke, M. Bachmann, S. Fritzsche, L. E. Gallo-Ramirez, and U. Reichl, “Influenza virus intracellular replication dynamics, release kinetics, and particle morphology during propagation in MDCK cells,” *Applied Microbiology and Biotechnology*, vol. 100, no. 16, pp. 7181–7192, 2016. Publisher: Applied Microbiology and Biotechnology.

Chapter 3

Insights from SARS-CoV-2 sequences

The following *Perspectives* piece, published in *Science* in January 2021, was written to provide an overview of key insights that have been derived from sequence data as well as to identify key areas of future research where sequence data may prove to be illuminating. The relatively short piece (~1,900 words) aimed to provide a high level overview of these methods and analyses and direct the reader to more detailed pieces in the literature.

3.1 M.A.M Contributions

Conceptualization, Investigation, Writing - Original Draft, Writing - Review & Editing

3.2 Published Manuscript

Reproduced with permission from the American Association for the Advancement of Science.

VIEWPOINT: COVID-19

Insights from SARS-CoV-2 sequences

Analysis of viral sequences can tell us how SARS-CoV-2 spreads and adapts

By Michael A. Martin^{1,2}, David VanInsberghe¹,
Katia Koelle^{1,3}

As severe acute respiratory syndrome coronavirus 2 (SARS-CoV-2) has spread across the globe, so have efforts to sequence its RNA genome. More than 260,000 sequences are now available in public databases, about a year after the viral genome was first sequenced (1). These sequences and their associated metadata have allowed researchers to estimate the timing of SARS-CoV-2 spillover into humans, characterize the spread of the virus, and gauge virus adaptation to its new host. Such analyses rely on interpreting patterns of nucleotide changes that have occurred in the virus population over time and are brought into focus through the reconstruction of genealogical relationships between sampled viruses that are depicted in phylogenetic trees.

Analysis of phylogenetic trees allows for conclusions to be drawn about epidemic and pandemic viruses that are important for public health (see the figure). After the emergence of a new virus, viral sequence data and sampling dates can be used to infer the rate at which the virus population evolves, along with the time of the most recent common ancestor (TMRCA) of all sampled viruses. For SARS-CoV-2, these analyses have revealed that the virus evolves at a rate of $\sim 1.1 \times 10^{-3}$ substitutions per site per year (2)—corresponding to one substitution every ~ 11 days—and a TMRCA of around late November 2019. However, owing to limited sampling early in the COVID-19 outbreak, this date likely lags behind the spillover into humans by several weeks.

Once virus circulation becomes widespread, phylodynamic analyses can give insight into how a virus spreads both spatially and temporally. Viruses from a given region can be placed in the context of those circulating globally, allowing for the number of independent virus introductions into a region to be estimated through phylogeography. These methods rely on assigning geographical states to unsampled ancestral viruses through a process called ancestral state re-

construction. Multiple applications of this approach have consistently shown that regional SARS-CoV-2 spread was ignited not by one, but by many independent introductions. This is likely due to slow or imperfect implementation of screening efforts at borders in the early stages of the pandemic. Similar types of analyses are conducted in local outbreak investigations, in what is often called genomic epidemiology. This has been used, for example, to link multiple transmission chains to a motorcycle rally in South Dakota (3).

Care must be taken, however, when interpreting phylogeographic analyses of this virus owing to the limited extent of its circulating genetic diversity. Given the evolutionary rate of SARS-CoV-2, viruses sampled weeks apart on different continents can have identical nucleotide sequences, making robust inferences more challenging. Additionally, sampling efforts are geographically heterogeneous, which can bias phylogeographic analyses. Methods have recently been developed to better accommodate the degree of undersampling across regions and the known travel history of sampled cases (4). Application of these methods has shown that later, rather than earlier, virus introductions established the first sustained transmission networks in the United States and Europe (5), highlighting the utility of genomic data in epidemiological investigations.

Once viral lineages have been introduced into a region, phylodynamic methods can also be used to infer the rate of viral spread through a host population and the basic reproduction number R_0 , defined as the average number of infections generated by an infected host in a susceptible host population. This inference can be done using coalescent-based methods, which infer changes in the underlying population size of infected individuals using the time points at which viral lineages “coalesce” (merge) backward in time. Epidemiological models can also be fit directly to viral phylogenies based on the timing of coalescent events (6). Another approach to infer R_0 from sequence data relies on a forward-in-time birth-death process, with a “birth” corresponding to a transmission event (resulting in the birth of an infected individual) and a “death” corresponding to a removal of an infected individual (7). Both methods have been applied to SARS-CoV-2 sequence data, with relatively consistent results across methods and re-

gions: At the beginning of the pandemic, R_0 fell between 2 and 3.5 (8, 9) but decreased substantially after the implementation of nonpharmaceutical interventions. Although R_0 can be, and usually is, estimated from epidemiological case data, these estimates can be biased by changes in reporting rates. The relative contributions of new introductions versus local spread are often also indistinguishable in tabulated case data. Thus, analysis of sequence data provides an alternative approach to infer R_0 that may be particularly useful in the early stages of virus circulation when a large proportion of identified cases may be new introductions and when reporting rates are likely to be low. The development of methods that integrate both epidemiological time series and sequence data is an area of active research that will improve parameter estimation.

Phylodynamic analyses can also be used to identify instances of viral adaptation. Adaptation is a particular concern because SARS-CoV-2 only recently spilled over into humans and thus may still adapt to its new host through substitutions that facilitate its spread. One emerging variant that has been implicated as being more transmissible is 614G, which replaces aspartic acid (D) with glycine (G) at amino acid site 614 in the cellular entry (spike) protein of SARS-CoV-2. This variant likely arose in China in January 2020 and has since become dominant worldwide. The D-to-G substitution results in more efficient infection and replication in vitro and enhances transmission in animal models (10). Coalescent-based phylodynamic analyses using densely sampled genomes from infections in London found trends toward higher transmissibility of 614G clusters relative to 614D clusters (11). More recently, a new SARS-CoV-2 lineage, B.1.1.7, has rapidly spread from southeast England around the globe, and early analyses indicate that it has a substantial fitness advantage over other currently circulating lineages. These recent evolutionary events indicate that SARS-CoV-2 still has the capacity to develop more efficient transmission between human hosts.

When considering viral adaptation, a commonly held fear is that a virus may evolve to become more virulent, that is, cause more severe disease and host mortality. However, natural selection acts on variation in viral transmission potential, not variation in virulence per se. More virulent strains could have

¹Department of Biology, Emory University, Atlanta, GA, USA. ²Population Biology, Ecology, and Evolution Graduate Program, Laney Graduate School, Emory University, Atlanta, GA, USA. ³Emory—University of Georgia Center of Excellence for Influenza Research and Surveillance (CEIRS), Atlanta, GA, USA. Email: katia.koelle@emory.edu

higher transmission potential if infection with a more virulent strain resulted in infected hosts shedding more virus. However, a more virulent infection may reduce contact rates of infected individuals, limiting the opportunity for viral transmission. Therefore, it is not clear whether more virulent SARS-CoV-2 strains are likely to evolve.

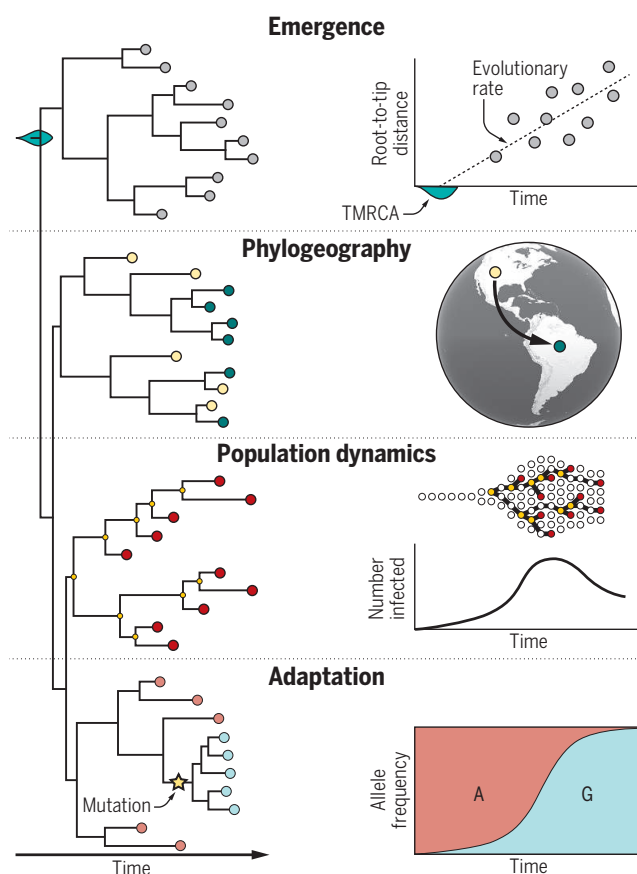
As SARS-CoV-2 continues to spread, the virus will begin to face new evolutionary pressures. Other respiratory viruses can provide insight into how SARS-CoV-2 evolution may manifest. For example, the 2009 pandemic H1N1 influenza virus started to evolve antigenically a couple of years after its emergence (12) and recent work has identified signatures of adaptive evolution in the spike protein of seasonal coronaviruses, consistent with antigenic evolution (13). Emerging evidence suggests that some SARS-CoV-2 variants may already be exhibiting antigenic evolution, and this is likely to continue as population immunity (through natural infection or vaccination) builds. Efforts by public health agencies to monitor emergent SARS-CoV-2 lineages, particularly those that may escape vaccine or natural immunity, are under way. Additionally, widespread infection of farmed mink has recently been observed, and there is evidence of transmission of mink lineages back into humans (14). Animal reservoirs may therefore contribute to the dynamics of SARS-CoV-2 evolution and adaptation.

For viral adaptation to be possible, be it through the evolution of immune escape or other viral traits, genetic (and phenotypic) variation needs to be present. Although nucleotide substitutions are the primary source of genetic variation in SARS-CoV-2, insertions and deletions of nucleotides have also been observed. Furthermore, recombination is common in coronaviruses and may potentially give rise to new SARS-CoV-2 lineages. A small number of SARS-CoV-2 recombinant genomes have already been detected (15). Because of their potential phenotypic effects, circulation of genomic insertions, deletions, and recombinants should be monitored.

The number of available SARS-CoV-2 sequences is, like many things during this pandemic, unprecedented. Gaining understanding from these data does not come without challenges. Many current methods rely not just on the sequence itself but on associated metadata that provide additional informa-

Uses for viral sequence data

Viral phylogenies, rooted at the most recent common ancestor (TMRCA), are inferred on the basis of genetic differences. These phylogenies can be used to estimate viral emergence, characterize the geographic spread of the virus, reconstruct epidemiological dynamics of viral spread within a region, and identify instances of adaptation.



tion about viral samples. Research laboratories are often limited in the metadata that can be released owing to patient privacy regulations. For similar reasons, some government health agencies, such as the U.S. Centers for Disease Control and Prevention (CDC), receive only limited metadata from state health departments. Although privacy is an important concern, the routine release of more detailed metadata would improve the power of phylodynamic methods to describe viral dynamics and evolution. Notably, sequences are often released with only coarse sampling location data. However, viral dynamics may be heterogeneous even between locations that are geographically close. Furthermore, the incorporation of travel history can improve the accuracy of phylogenetic methods (4), but this information is not commonly reported. Because phylodynamic methods often require an assumption of random sampling, when samples from individuals belonging to the same transmission chain are sequenced, it is crucial that this information be labeled in the sequence metadata to avoid biasing analyses. Despite these challenges, a

tremendous amount of SARS-CoV-2 sequence data is publicly available on GISAID's EpiCov database. Phylogenetic analyses of these sequences are conducted in near-real time and available on platforms such as Nextstrain and Microreact, allowing the ongoing evolution of SARS-CoV-2 genomes to be viewed in detail.

In many ways, the SARS-CoV-2 pandemic offers a distinct opportunity for the field of phylodynamics. Methods development over the past 10 to 15 years, the widespread availability of sequencing technologies, open data sharing, and the tireless efforts of clinicians and scientists who collect these data mean that more can be learned from viral genomes than ever before. As viral diversity continues to accumulate, SARS-CoV-2 sequence data and associated metadata can be used to answer questions focused on the longer-term evolution and adaptation of SARS-CoV-2. The volume of sequence data also presents an opportunity for methods development, because most current methods are computationally intractable when applied to hundreds of thousands of genomes. Continued efforts to collect viral sequence data and the development of efficient and scalable computational inference methods will help to further cement evolutionary analyses as a

cornerstone of the public health response to viral spread and adaptation. ■

REFERENCES AND NOTES

1. F. Wu *et al.*, *Nature* **579**, 265 (2020).
2. S. Duchene *et al.*, *Virus Evol.* **6**, veaa061 (2020).
3. M. J. Firestone *et al.*, *MMWR* **69**, 1771 (2020).
4. P. Lemey *et al.*, *Nat. Commun.* **11**, 5110 (2020).
5. M. Worobey *et al.*, *bioRxiv* 10.1101/2020.05.21.109322 (2020).
6. E. M. Volz, I. Siveroni, *PLOS Comput. Biol.* **14**, e1006546 (2018).
7. T. Stadler *et al.*, *Mol. Biol. Evol.* **29**, 347 (2012).
8. D. Miller *et al.*, *Nat. Commun.* **11**, 5518 (2020).
9. S. A. Nadeau *et al.*, *medRxiv* 10.1101/2020.06.10.20127738 (2020).
10. Y. J. Hou *et al.*, *Science* **370**, 1464 (2020).
11. E. Volz *et al.*, *Cell* **184**, 64 (2021).
12. Y. C. F. Su *et al.*, *Nat. Commun.* **6**, 7952 (2015).
13. K. E. Kistler, T. Bedford, *bioRxiv* 10.1101/2020.10.30.352914 (2020).
14. B. B. Oude Munnink *et al.*, *Science* **371**, 172 (2021).
15. D. VanInsberghe *et al.*, *bioRxiv* 10.1101/2020.08.05.238386 (2020).

ACKNOWLEDGMENTS

This work was supported by National Institute of Allergy and Infectious Diseases (NIAID) Centers of Excellence for Influenza Research and Surveillance (CEIRS) grant HHSN272201400004C and an Emory University MP3 seed grant. We thank G. Armstrong, T. Bedford, and two anonymous reviewers for feedback.

10.1126/science.abf3995

Insights from SARS-CoV-2 sequences

Michael A. MartinDavid VanInsbergheKatia Koelle

Science, 371 (6528), • DOI: 10.1126/science.abf3995

View the article online

<https://www.science.org/doi/10.1126/science.abf3995>

Permissions

<https://www.science.org/help/reprints-and-permissions>

Use of this article is subject to the [Terms of service](#)

Science (ISSN 1095-9203) is published by the American Association for the Advancement of Science, 1200 New York Avenue NW, Washington, DC 20005. The title *Science* is a registered trademark of AAAS.

Copyright © 2021 The Authors, some rights reserved; exclusive licensee American Association for the Advancement of Science. No claim to original U.S. Government Works

Chapter 4

Comment on “Genomic epidemiology of superspreading events in Austria reveals mutational dynamics and transmission properties of SARS-CoV-2”

The following *Technical Comment*, published in *Science Translational Medicine* in October 2021 was written with the goal of reconciling disparate estimates of the SARS-CoV-2 transmission bottleneck in the literature at the time. We reanalyzed deep sequencing data from 39 epidemiologically linked transmission pairs which had previously been published and used to infer a large (~ 1000 virions) transmission bottleneck. However, the original analyses did not sufficiently account for shared, non-transmitted, variants between transmission pairs. These likely spurious shared variants artificially inflate the estimated transmission bottleneck.

4.1 M.A.M Contributions

Conceptualization, Validation, Formal analysis, Investigation, Data Curation, Writing - Original Draft, Writing - Review & Editing, Visualization

4.2 Published Manuscript

Reproduced with permission from the American Association for the Advancement of Science.

CORONAVIRUS

Comment on “Genomic epidemiology of superspreading events in Austria reveals mutational dynamics and transmission properties of SARS-CoV-2”

Michael A. Martin¹ and Katia Koelle^{2,3*}

A reanalysis of SARS-CoV-2 deep sequencing data from donor-recipient pairs indicates that transmission bottlenecks are very narrow (one to three virions).

In their recent research article (1), Popa *et al.* combined epidemiological and viral genetic data to characterize the transmission dynamics of severe acute respiratory syndrome coronavirus 2 (SARS-CoV-2) in Austria between February and April 2020. The genetic data they analyzed comprised >500 deep-sequenced virus samples. Beyond using consensus-level SARS-CoV-2 sequences to infer transmission clusters within Austria and to examine the role that Austria played in seeding regional epidemics elsewhere in Europe, the authors used their sequenced samples to characterize mutational dynamics within hosts and along short transmission chains. Although we believe that the findings from their consensus-level genetic analysis are robust, we here revisit their analyses of mutational dynamics at the below-the-consensus level. Specifically, we consider their estimates of the viral transmission bottleneck size, defined as the number of virions that successfully seed infection in a recipient individual following infection from a donor individual. Equivalently, it is the number of viral particles from a person who transmits the infection that contribute genetically to the viral population in the recipient who contracts it. From our reanalysis, we conclude that transmission bottleneck sizes for SARS-CoV-2 are not on the order of 1000 virions as concluded by the authors but instead much smaller.

Our decision to revisit Popa *et al.*'s conclusions on transmission bottleneck sizes stems from certain patterns present in some of their figures. First, inferred bottleneck size estimates using a 3% variant calling threshold were bimodal, with 14 of the 39 transmission pairs having an inferred bottleneck size (N_b) of <10 and the remaining 25 pairs having N_b estimates of 115 to 5000 (their fig. S4G). Further, when a 1% variant calling threshold was used, only a single transmission pair retained an N_b estimate of <10 (their figure 5B). In an attempt to understand these patterns, we first reanalyzed their deep sequencing data and recalled variants using their pipeline. In the analyses presented below, we use these recalled variant frequencies, which appear to be highly similar to those presented in Popa *et al.* based on the plots published as part of their article that show the frequencies of called variants in donor individuals against those in recipient individuals in their identified transmission pairs (10.5281/zenodo.4247401).

As expected, re-estimation of transmission bottleneck sizes at variant calling thresholds of 1 and 3% yielded similar results to

those shown in (1) (Fig. 1A, fig. S1, A and B, and data file S1). During this analysis, we noticed that bottleneck size estimates dropped, sometimes precipitously, when going from a 1 to a 3% cutoff for each of the 13 transmission pairs that had donors with a maximum intra-host single-nucleotide variant (iSNV) frequency of >6% ($P = 0.004$, paired t test; Fig. 1A). Because increasing the variant calling threshold would remove low-frequency iSNVs from the analysis, these consistent decreases in N_b estimates could come about if low-frequency donor iSNVs pointed toward bottleneck sizes being large, whereas high-frequency donor iSNVs instead pointed toward bottleneck sizes being small. Examination of low-frequency iSNVs across donor-recipient pairs indicates a high degree of congruence between their frequencies (Fig. 1B, inset, and fig. S2 in data file S2), which would suggest wide transmission bottlenecks. In contrast, high-frequency donor iSNVs rarely appeared to be transmitted to their corresponding recipient (fig. S2), suggesting narrow transmission bottlenecks.

To come to terms with these conflicting patterns, we considered genetic variation that appeared *de novo* in recipient hosts. This genetic variation appears in the donor-against-recipient variant frequency plots as iSNVs that are absent from a donor but present in a corresponding recipient. When a *de novo* variant is observed as fixed in a recipient sample, we should not observe any shared iSNVs between a donor and a recipient that are present in the recipient at subclonal (that is, not fixed) frequencies unless within-host recombination occurred extremely rapidly or the fixed *de novo* variant arose multiple times in different genetic backgrounds. However, in the transmission pairs analyzed in Popa *et al.*, shared subclonal iSNVs are observed in several transmission pairs where there is also a fixed *de novo* variant present in the recipient. The transmission pair CoV_162 → CoV_161 provides an example (Fig. 1B). This means that the low-frequency iSNVs shared between CoV_162 and CoV_161 are either spurious or that they arose independently in the recipient (that is, they are homoplasies). Although iSNV homoplasies have been documented in a number of recent SARS-CoV-2 studies (2, 3), we believe that these low-frequency iSNVs in the Popa *et al.* transmission pairs are likely spurious, potentially arising from systematic issues related to the sequencing protocol. This is because these low-frequency iSNVs occur at extremely similar frequencies between the donor sample and the recipient sample (Fig. 1B, inset, and fig. S2), which is unlikely if the iSNVs were homoplasies. In either case, however, the low-frequency shared iSNVs in transmission pair CoV_162 → CoV_161 and in other transmission pairs with fixed *de novo* variants in the recipient could only constitute transmitted genetic variation under scenarios that are highly implausible from a biological perspective and as such

¹Graduate Program in Population Biology, Ecology, and Evolution, Emory University, Atlanta, GA 30322, USA. ²Department of Biology, Emory University, Atlanta, GA 30322, USA. ³Emory-UGA Center of Excellence for Influenza Research and Surveillance (CEIRS), Atlanta GA 30322, USA.

*Corresponding author. Email: katia.koelle@emory.edu

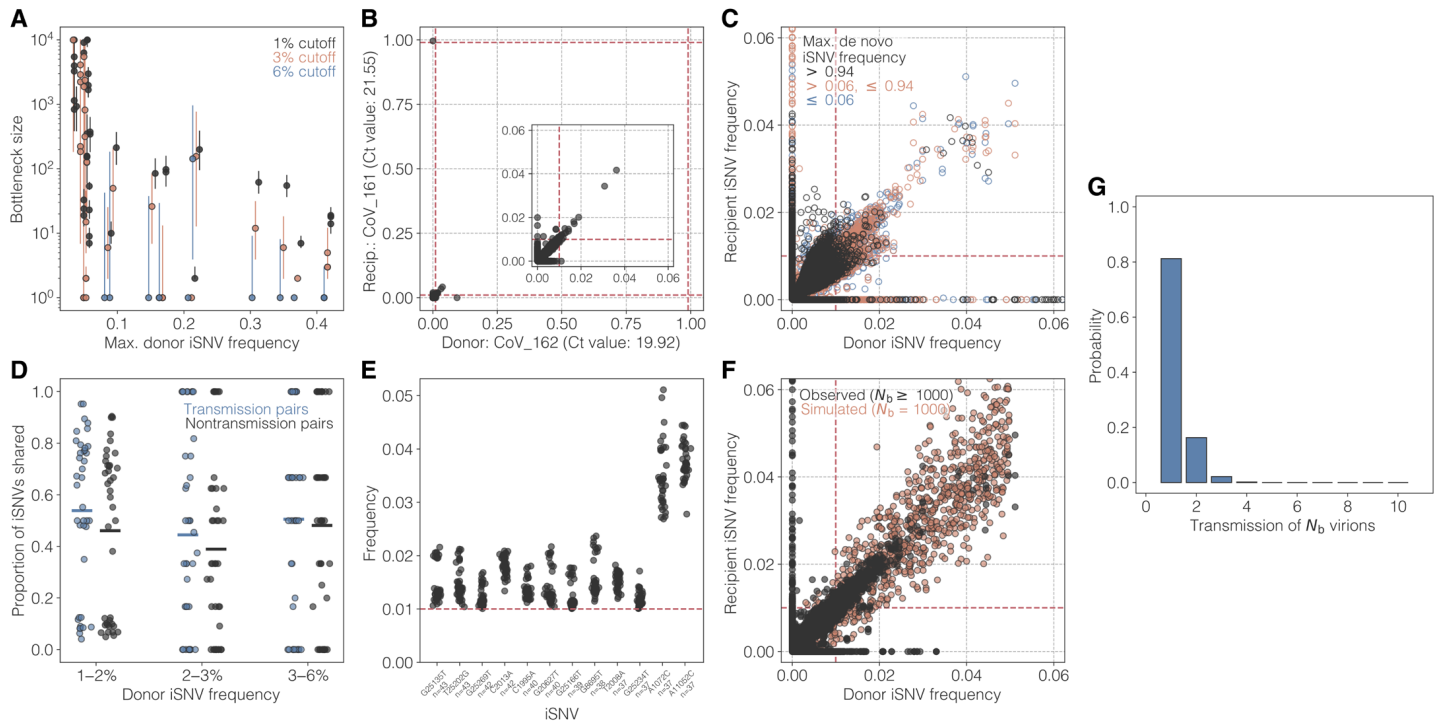


Fig. 1. Transmission bottleneck sizes and patterns of shared viral genetic diversity between the transmission pairs studied in Popa *et al.* (A) Bottleneck size estimates for 39 epidemiologically confirmed SARS-CoV-2 transmission pairs using variant calling thresholds of 1% ([0.01, 0.99]), 3% ([0.03, 0.97]), and 6% ([0.06, 0.94]). Estimates are based on all iSNVs that passed the quality-filtering thresholds. Maximum likelihood estimates are indicated by a colored circle and vertical lines show 95% CIs. Estimates are plotted according to the maximum iSNV frequency observed in the donor of the transmission pair. Estimates from the same transmission pair are offset slightly on the x axis to aid in visualization. iSNV frequencies are based on variant calling relative to donor-specific reference sequences. (B) All iSNVs observed in either the donor or the recipient of the epidemiologically confirmed CoV_162 → CoV_161 transmission pair. Note the de novo variant in the recipient (C26894U) that is fixed within individual 161 and absent from individual 162. Inset highlights low-frequency iSNVs. Red dashed lines show the 1% variant calling threshold. iSNV frequencies are based on variant calling relative to donor-specific reference sequences. Here, all iSNVs that passed quality filtering thresholds are shown, regardless of whether they fell above or below the 1% variant calling threshold. (C) Low-frequency iSNVs observed across transmission pairs. Transmission pairs are classified as belonging to one of three groups according to the maximum de novo iSNV frequency observed in the recipient. Red dashed lines show the 1% variant calling threshold, and iSNV frequencies are based on variant calling relative to donor-specific reference sequences. (D) Proportion of iSNVs identified in a donor that are shared with a recipient host. Blue dots show proportions for epidemiologically linked pairs, whereas black dots show proportions for random, epidemiologically unlinked donor-recipient pairs. Random pairs were generated such that the random recipient was not a member of the same family as the focal donor or recipient and was not a known recipient of that donor sample. iSNVs were binned on the basis of their frequency in the donor: [0.01, 0.02], [0.02, 0.03], and [0.03, 0.06]. Allele frequencies are based on variant calling relative to Wuhan/Hu-1 (9). Differences between the epidemiologically linked and unlinked distributions were assessed using the Kolmogorov-Smirnov test. This test failed to find significant differences between these distributions in the 1 to 2% donor frequency group ($P = 0.389$), 2 to 3% donor frequency group ($P = 0.752$), and 3 to 6% frequency group ($P > 0.999$). (E) Top 12 most abundantly shared iSNVs among the 43 samples involved in the 39 transmission pairs. iSNVs are ordered by the number of samples in which they were found (n). Each dot represents the allele frequency of that iSNV in a given sample. Red dotted line shows the 1% variant calling threshold. Allele frequencies are based on variant calling relative to Wuhan/Hu-1. (F) Patterns of shared viral genetic diversity between transmission pairs under the assumption of a large bottleneck of $N_b = 1000$ (red dots). Black dots show all iSNVs observed in either the donor or recipient for all transmission pairs with an estimated bottleneck size of ≥ 1000 at a variant calling threshold of 1%. (G) Probability of a transmission bottleneck of size N_b based on bottleneck size estimation using a variant calling threshold of 6% and data from all 13 transmission pairs with one or more iSNVs above this 6% threshold. The probability that a transmission involves a bottleneck size of 1, 2, or 3 virions exceeds 99%.

should be excluded from a transmission bottleneck analysis involving these transmission pairs.

A comprehensive analysis of all transmission pairs identified in Popa *et al.* indicates that patterns of low-frequency shared genetic variation are quantitatively highly similar across transmission pairs. To illustrate this, we categorized transmission pairs into three groups: transmission pairs with de novo fixed variants in the recipient (here defined as $>94\%$ in frequency), transmission pairs with de novo high-frequency (6–94%) variants in the recipient, and transmission pairs with only low-frequency de novo variants ($\leq 6\%$). Figure 1C shows that the shared low-frequency iSNVs across these three groups are quantitatively extremely similar: Most shared iSNVs

in each of these groups have frequencies falling between 1 and 2% in the donor, although some have frequencies of up to 6%. Whereas we should expect no transmitted subclonal genetic variation for the transmission pairs falling in the first group, we expect any shared iSNVs between transmission pairs belonging to the second group to have markedly different frequencies between the donor and the recipient because of genetic linkage with the high-frequency de novo variant in the recipient. The third group in principle could have very similar iSNV frequencies if bottleneck sizes were sufficiently large. In contrast to these expectations, Fig. 1C shows that all shared iSNVs (regardless of which group is being considered) are highly congruent in their frequencies between donors and recipients, indicating

again that these iSNVs are very likely spurious. When we calculate the proportion of the low-frequency donor iSNVs that are observed in a corresponding recipient (at $\geq 1\%$) versus observed in an epidemiologically unlinked recipient, we find that the distribution of these proportions are highly similar (Fig. 1D). This finding again suggests that these shared low-frequency iSNVs do not constitute true shared genetic variation within transmission pairs; if these shared iSNVs were transmitted, we would expect the proportion of shared low-frequency variants to be higher for the corresponding recipient compared to an epidemiologically unlinked one.

Given these findings that shed doubt on low-frequency iSNVs constituting transmitted genetic variation, we decided to quantify the extent to which particular iSNVs were present across the samples used in the transmission pair analyses. We found that 5 iSNVs were present in ≥ 40 of the 43 samples analyzed at frequencies that fell into a very narrow range (1 to 2.2%) (Fig. 1E). Many other iSNVs were also present across numerous samples (Fig. 1E, fig. S3 in data file S3, and fig. S4), with the frequencies of any particular iSNV being highly similar across the samples that it appears in. This similarity in iSNV frequencies again argues against these low-frequency iSNVs being homoplasies and strongly argues for these iSNVs being spurious. To assess the evidence for this, we plotted the genome location of all variants observed in between 1 and 99% of reads in at least 10 samples against the read depth at those positions (fig. S5). Although these variants do not tend to appear in areas of particularly low sequencing coverage, they do cluster within a small number of sequenced amplicons, which are distributed across the genome (fig. S6).

Last, a comparison between observed patterns of iSNV frequencies between donors and recipients versus those expected under large transmission bottleneck sizes as inferred in Popa *et al.* further argues against the transmission of the low-frequency shared iSNVs. Specifically, observed iSNV frequencies from transmission pairs with inferred bottleneck sizes of $N_b \geq 1000$ show that iSNVs are present in both donor and recipient at highly similar frequencies or are observed exclusively in the donor or recipient (Fig. 1F). On this figure, we overlaid simulated iSNV frequencies under the assumption of a bottleneck size of $N_b = 1000$. Juxtaposition of the observed versus theoretically predicted iSNV frequencies highlights an inconsistency: at N_b values of ~ 1000 , we should expect almost all (at least 96.1%) of the iSNVs present in the donor at $\geq 2\%$ to be transmitted and also observed above the variant calling threshold of 1% in the recipient. However, only 77.5% of donor iSNVs within the 2 to 6% frequency range were observed in the corresponding recipients at $\geq 1\%$ frequency. This inconsistency indicates that the low-frequency iSNVs themselves show patterns that cannot be parsimoniously explained by large transmission bottleneck sizes. Moreover, bottleneck sizes of around $N_b = 3000$ are needed to quantitatively reproduce patterns of shared iSNV frequencies (fig. S7); at this bottleneck size, nearly 100% of iSNVs present in the donor at $\geq 2\%$ should be transmitted to the recipient, but this is not the case.

Given our finding that the shared low-frequency iSNVs called in Popa *et al.* are likely spurious, we re-estimated transmission bottleneck sizes using the beta-binomial method (4) at a conservative variant calling threshold of 6% (Fig. 1A, fig. S1C, and data file S1). Increasing the variant calling threshold does not bias bottleneck size estimates, but it does increase statistical uncertainty in the estimated values. At this 6% cutoff, only 13 transmission pairs had one or more donor iSNVs remaining, such that bottleneck sizes could only

be estimated for these pairs. The maximum likelihood estimate for N_b was 1 for 12 of these 13 transmission pairs [with the largest upper bound of the 95% confidence interval (CI) being $N_b = 181$ virions]; for the remaining transmission pair (CoV_198 \rightarrow CoV_230), the estimate was $N_b = 143$ virions (95% CI = 4 to 951). This transmission pair was the only one where a donor iSNV (at a frequency of $\sim 22\%$) was transmitted to a recipient but remained subclonal (at a frequency of $\sim 17\%$). Because the confidence intervals around these estimates were large, we also estimated an overall transmission bottleneck size using the data from these 13 transmission pairs. We arrived at an estimate of a mean bottleneck size of 1.21, with three or fewer viral particles successfully seeding infection in $>99\%$ of successful transmissions (Fig. 1G). Of note, this estimate depends on patterns of genetic variation observed between donors and recipients of transmission pairs. We here relied on the transmission pairs specified in Popa *et al.*; misspecification of these pairs could result in erroneously small bottleneck estimates.

Our finding of a very tight transmission bottleneck from a reanalysis of the viral deep sequencing data from Popa *et al.* is consistent with conclusions from other recent studies that have quantified SARS-CoV-2 transmission bottleneck sizes in humans (3, 5) and other mammals (6). These results indicate that SARS-CoV-2 has a narrow transmission bottleneck, similar in size to that of influenza A viruses (7). Small bottleneck sizes also mean that infections generally start off with very little, if any, viral genetic diversity, such that acute infections will likely be characterized by low levels of viral diversity except in instances of superinfection, consistent with other recent studies (2, 8). Our reanalysis thus parsimoniously adds to a growing understanding of SARS-CoV-2 evolution between and within infected individuals.

SUPPLEMENTARY MATERIALS

www.science.org/doi/10.1126/scitranslmed.abh1803

Materials and Methods

Figs. S1 to S7

Data files S1 to S3

REFERENCES AND NOTES

1. A. Popa, J.-W. Genger, M. D. Nicholson, T. Penz, D. Schmid, S. W. Aberle, B. Agerer, A. Lercher, L. Endler, H. Coloço, M. Smyth, M. Schuster, M. L. Grau, F. Martínez-Jiménez, O. Pich, W. Borena, E. Pawelka, Z. Keszei, M. Senekowitsch, J. Laine, J. H. Aberle, M. Redlberger-Fritz, M. Karolyi, A. Zoufaly, S. Maritschnick, M. Borkovec, P. Hufnagl, M. Nairz, G. Weiss, M. T. Wolfinger, D. von Laer, G. Superti-Furga, N. Lopez-Bigas, E. Puchhammer-Stöckl, F. Allerberger, F. Michor, C. Bock, A. Bergthaler, Genomic epidemiology of superspreading events in Austria reveals mutational dynamics and transmission properties of SARS-CoV-2. *Sci. Transl. Med.* **12**, eabe2555 (2020).
2. A. L. Valesano, K. E. Rumfelt, D. E. Dimcheff, C. N. Blair, W. J. Fitzsimmons, J. G. Petrie, E. T. Martin, A. S. Lauring, Temporal dynamics of SARS-CoV-2 mutation accumulation within and across infected hosts. *PLoS Pathog.* **17**, e1009499 (2021).
3. K. A. Lythgoe, M. Hall, L. Ferretti, M. de Cesare, G. MacIntyre-Cockett, A. Trebes, M. Andersson, N. Otecko, E. L. Wise, N. Moore, J. Lynch, S. Kidd, N. Cortes, M. Mori, R. Williams, G. Vernet, A. Justice, A. Green, S. M. Nicholls, M. A. Ansari, L. Abeler-Dörner, C. E. Moore, T. E. A. Peto, D. W. Eyre, R. Shaw, P. Simmonds, D. Buck, J. A. Todd; Oxford Virus Sequencing Analysis Group (OVSG), T. R. Connor, S. Ashraf, A. da Silva Filipe, J. Shepherd, E. C. Thomson; COVID-19 Genomics UK (COG-UK) Consortium, D. Bonsall, C. Fraser, T. Golubchik, SARS-CoV-2 within-host diversity and transmission. *Science* **372**, eabg0821 (2021).
4. A. Sobel Leonard, D. B. Weissman, B. Greenbaum, E. Ghedin, K. Koelle, Transmission bottleneck size estimation from pathogen deep-sequencing data, with an application to human influenza A virus. *J. Virol.* **91**, e00171-17 (2017).
5. K. Braun, G. K. Moreno, C. Wagner, M. A. Accola, W. M. Rehrauer, D. A. Baker, K. Koelle, D. H. O'Connor, T. Bedford, T. C. Friedrich, L. H. Moncla, Acute SARS-CoV-2 infections

- harbor limited within-host diversity and transmit via tight transmission bottlenecks. *PLoS Pathog.* **17**, e1009849 (2021).
6. K. M. Braun, G. K. Moreno, P. J. Halfmann, E. B. Hodcroft, D. A. Baker, E. C. Boehm, A. M. Weiler, A. K. Haj, M. Hatta, S. Chiba, T. Maemura, Y. Kawaoka, K. Koelle, D. H. O'Connor, T. C. Friedrich, Transmission of SARS-CoV-2 in domestic cats imposes a narrow bottleneck. *PLoS Pathog.* **17**, e1009373 (2021).
 7. J. T. McCrone, R. J. Woods, E. T. Martin, R. E. Malosh, A. S. Monto, A. S. Luring, Stochastic processes constrain the within and between host evolution of influenza virus. *eLife* **7**, e35962 (2018).
 8. G. Tonkin-Hill, I. Martincorena, R. Amato, A. R. J. Lawson, M. Gerstung, I. Johnston, D. K. Jackson, N. R. Park, S. V. Lensing, M. A. Quail, S. Gonçalves, C. Ariani, M. S. Chapman, W. L. Hamilton, L. W. Meredith, G. Hall, A. S. Jahun, Y. Chaudhry, M. Hosmillo, M. L. Pinckert, I. Georgana, A. Yakovleva, L. G. Caller, S. L. Caddy, T. Feltwell, F. A. Khokhar, C. J. Houldcroft, M. D. Curran, S. Parmar; COVID-19 Genomics UK (COG-UK) Consortium, A. Alderton, R. Nelson, E. Harrison, J. Sillitoe, S. D. Bentley, J. C. Barrett, M. E. Torok, I. G. Goodfellow, C. Langford, D. Kwiatkowski; Wellcome Sanger Institute COVID-19 Surveillance Team, Patterns of within-host genetic diversity in SARS-CoV-2. *eLife* **10**, e66857 (2021).
 9. F. Wu, S. Zhao, Y.-M. Chen, W. Wang, Z.-G. Song, Y. Hu, Z.-W. Tao, J.-H. Tian, Y.-Y. Pei, M.-L. Yuan, Y.-L. Zhang, F.-H. Dai, Y. Liu, Q.-M. Wang, J.-J. Zheng, L. Xu, E. C. Holmes, Y.-Z. Zhang, A new coronavirus associated with human respiratory disease in China. *Nature* **579**, 265–269 (2020).

Acknowledgments: We thank A. Bergthaler and his group for providing clarification on the SARS-CoV-2 deep sequencing data submitted as part of their research article. We also thank C. Bergstrom for a clear definition of transmission bottleneck size and three anonymous reviewers for their insightful recommendations to improve this work. **Funding:** The research reported in this technical comment was supported by National Institute of Allergy and Infectious Diseases Centers of Excellence for Influenza Research and Surveillance (CEIRS) grant HHSN272201400004C and by the NIH National Institute of General Medical Sciences grant 1R01 GM124280-03S1. **Competing interests:** K.K. consults for Moderna on SARS-CoV-2 epidemiology and evolution. **Data and materials availability:** All raw sequencing data used in this study are available from the National Center for Biotechnology Information (NCBI) Sequencing Read Archive (SRA) BioProject #PRJEB39849. Associated metadata and analysis code to recreate the analysis are available at <https://doi.org/10.5281/zenodo.5224640>.

Submitted 20 February 2021

Accepted 26 September 2021

Published 27 October 2021

10.1126/scitranslmed.abh1803

Citation: M. A. Martin, K. Koelle, Comment on "Genomic epidemiology of superspreading events in Austria reveals mutational dynamics and transmission properties of SARS-CoV-2". *Sci. Transl. Med.* **13**, eabh1803 (2021).

Comment on “Genomic epidemiology of superspreading events in Austria reveals mutational dynamics and transmission properties of SARS-CoV-2”

Michael A. MartinKatia Koelle

Sci. Transl. Med., 13 (617), eabh1803. • DOI: 10.1126/scitranslmed.abh1803

View the article online

<https://www.science.org/doi/10.1126/scitranslmed.abh1803>

Permissions

<https://www.science.org/help/reprints-and-permissions>

Use of this article is subject to the [Terms of service](#)

Science Translational Medicine (ISSN) is published by the American Association for the Advancement of Science. 1200 New York Avenue NW, Washington, DC 20005. The title *Science Translational Medicine* is a registered trademark of AAAS. Copyright © 2021 The Authors, some rights reserved; exclusive licensee American Association for the Advancement of Science. No claim to original U.S. Government Works

4.3 Supplement

Reproduced with permission from the American Association for the Advancement of Science.

Supplementary Materials for

Comment on “Genomic epidemiology of superspreading events in Austria reveals mutational dynamics and transmission properties of SARS-CoV-2”

Michael A. Martin and Katia Koelle

Corresponding author: Katia Koelle, katia.koelle@emory.edu

Sci. Transl. Med. **13**, eabh1803 (2021)
DOI: 10.1126/scitranslmed.abh1803

The PDF file includes:

Methods and materials
Figs. S1 to S7
Legends for data files S1 to S3

Other Supplementary Material for this manuscript includes the following:

Data files S1 to S3

Materials and Methods

Aligned viral reads in the form of BAM files for all samples involved in the 39 transmission pairs described in Popa *et al.* (1) were downloaded from the National Center for Biotechnology Information (NCBI) Sequencing Read Archive (SRA) BioProject #PRJEB39849. Variants were called from these BAM files using a modified version of the variant calling pipeline used in (1) which was downloaded from https://github.com/Bergthalerlab/SARSCoV2_Code. Modified ARTIC (<https://artic.network/>) v2 primers were trimmed using iVar v. 1.3 with a four base sliding window, no minimum quality threshold, and a minimum length of 20. Overlapping read pairs were clipped using the clipOverlap utility available in bamUtil v. 1.0.14. SAMtools v. 1.10 depth was used to calculate the read depth of each viral BAM file after adjusting for overlapping read pairs. LoFreq v. 2.1.5 was used to realign reads to correct mapping errors with the viterbi function and to insert indel quality scores using the indelqual function. Last, LoFreq was used to call variants relative to Wuhan/Hu-1 (NC_045512.2) (9) requiring a minimum of 75 reads. Variant positions with a phred quality score < 90 were marked with LoFreq filter and indels with with an HRUN > 4 were marked with BCFtools v. 1.10.2 (using HTSlib v. 1.10.2) filter. BCFtools norm was used to left-align and normalize indels and split bi-allelic records. The variant calling pipeline was run in Python v. 3.7.3 (<http://www.python.org>) using PyPiper v. 0.12.1 (Databio; <http://pypiper.databio.org/en/latest/faq/>).

For each donor sample, BCFtools view and BCFtools consensus were used to generate a donor-specific reference sequence based on the Wuhan/Hu-1 reference and any variants identified with an allele frequency > 50%. SAMtools v. 1.10 was used to sort the viral BAM files by name and generate FASTQ files. FASTQ files for each transmission pair were realigned to the donor specific reference sequence using bwa mem v. 0.7.17-r1188 (<http://bio-bwa.sourceforge.net>) with a seed length of 17, looking for internal seeds longer than 17×1.25 , and marking shorter split hits as secondary as in (1). The same pipeline as above was used to recall variants relative to the donor reference sequences.

For each transmission pair we identified the variants present in the donor at frequencies of $\geq 1\%$, $\geq 3\%$ and $\geq 6\%$. These donor allele frequencies and the corresponding recipient allele frequencies were used to estimate the transmission bottleneck as described in (10) using MATLAB R2020A. Estimated transmission bottleneck sizes at these variant calling thresholds are shown in Figure S1.

Transmission pairs in Figure 1C were categorized based on the maximum *de novo* (that is, present in less than 1% of the reads in the donor) allele frequency in the recipient.

We further calculated the transmission for these low frequency alleles by first identifying all variants present in donor samples at the following frequencies: [0.01, 0.02), [0.02, 0.03), and [0.03, 0.06) and then identifying the proportion of these variants that were identified in the recipient samples (at a frequency ≥ 0.01). To generate a comparison distribution, we sampled non-epidemiologically linked (i.e. not a known recipient of the focal donor sample and not in the same family as the focal donor or recipient) “recipients” for each donor sample without replacement and calculated the proportion of shared variants belonging to each category. The proportions of shared variants between transmission pairs, as well as between epidemiological unlinked samples, are shown in Figure 1D.

To compare patterns of observed iSNV frequencies against those expected under bottleneck sizes of 1000 and 3000 (Figure 1F, S7), we first generated a large set ($n = 1000$) of low-frequency donor iSNVs by drawing their frequencies from a uniform distribution of 0 to 6%. For each of these donor iSNVs, we create a stochastic realization of the iSNV’s frequency in the recipient based on the forward model on which the beta-binomial method that estimates transmission bottleneck sizes is based. Specifically, for each iSNV, we first drew a random variable k from a binomial distribution with $N_b = 1000$ or $N_b = 3000$ number of

trials and success probability given by the donor iSNV frequency. This random variable k gives a stochastic realization of the number of virions in the founding population size of N_b that carrying the variant allele. We then determined the frequency of the iSNV in the recipient by drawing a random variable from a beta distribution with parameters k and $(N_b - k)$. Following this procedure for each of the 1000 iSNVs gives rise to the data points shown in orange in Figure 1F and S7.

Overall transmission bottleneck sizes were estimated based on the assumption that transmission bottleneck sizes were distributed according to a zero-truncated Poisson-distribution. To arrive at a maximum likelihood estimate for the mean N_b , given the available iSNV frequency data for the 13 transmission pairs that had donor iSNVs that exceeded 6%, we first use the beta-binomial method to infer, for each of the 13 transmission pairs, log-likelihood values for each bottleneck size from 1 to 50. We then considered a broad range of λ values (0 to 10) for this Poisson distribution. At any value of λ , the mean N_b is given by $\frac{\lambda}{(1-e^{-\lambda})}$. At each value of λ considered, we calculated the probability mass of k virions initiating an infection, with $p_k = \frac{\lambda^k}{(e^\lambda - 1)k!}$, and $k = 1, 2, 3$, etc. The likelihood of any given value of λ was evaluated via the following equation:

$$L(\lambda) = \sum_{n=1}^{13} \sum_{k=1}^{\infty} p_k e^{\log L_{n,k}}$$

where n indexes the transmission pairs and k indexes the number of virions initiating infection. $\log L_{n,k}$ is the log-likelihood of a bottleneck size of k in transmission pair n . The likelihood of λ peaked at a value of 0.402, corresponding to a mean N_b of 1.21. Figure 2 shows the probability mass function of the zero-truncated Poisson distribution parameterized with a λ of 0.402.

Two out of the 13 transmission pairs have donor samples with an unusually large number of high-frequency iSNVs. These are donor CoV_187 and donor Cov_273 (see figure S2). Both of these donors also have high Ct values (>34). Due to the possibility of transmission pairs associated with these donors biasing the mean N_b to a low value, we re-estimated the mean N_b again after removing these two transmission pairs. Based on the remaining 11 transmission pairs, we find that the maximum likelihood estimate for $\lambda = 0.659$, for the mean $N_b = 1.37$, yielding a similar conclusion that over 99% of successful SARS-CoV-2 infections result from 3 or fewer virions.

Unless otherwise noted, data were analyzed in Python v. 3.9.1 (<http://www.python.org>) using Pandas v. 1.1.4 (<https://pandas.pydata.org>) and Numpy v. 1.19.4 and all figures were generated using Matplotlib v. 3.3.3. All code to replicate the analysis is available at <https://doi.org/10.5281/zenodo.5224640>. All data are also available at this repository, accessible in the supplementary data from (1), or accessible from NCBI SRA BioProject # PRJEB39849.

Supplementary Figures

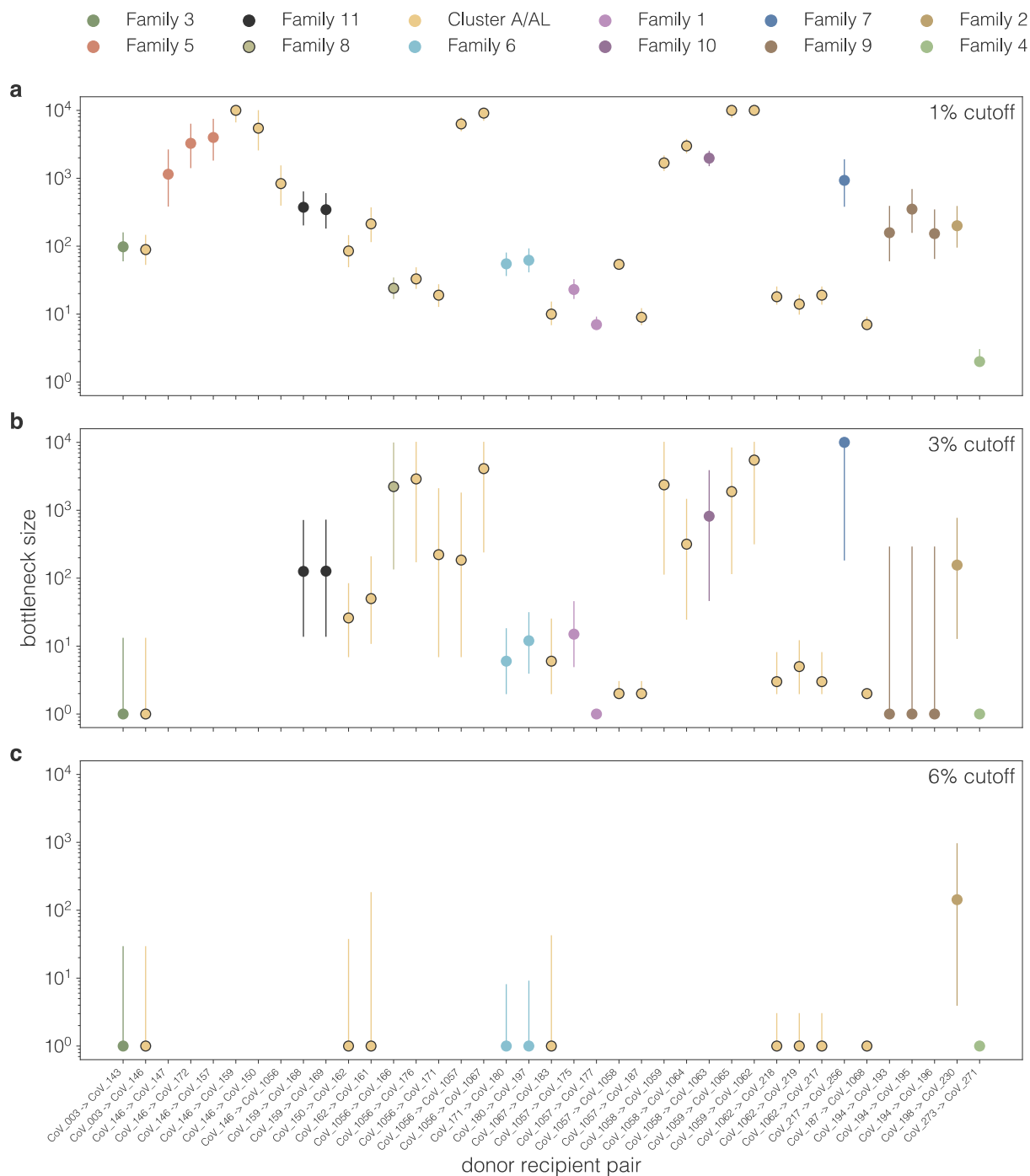
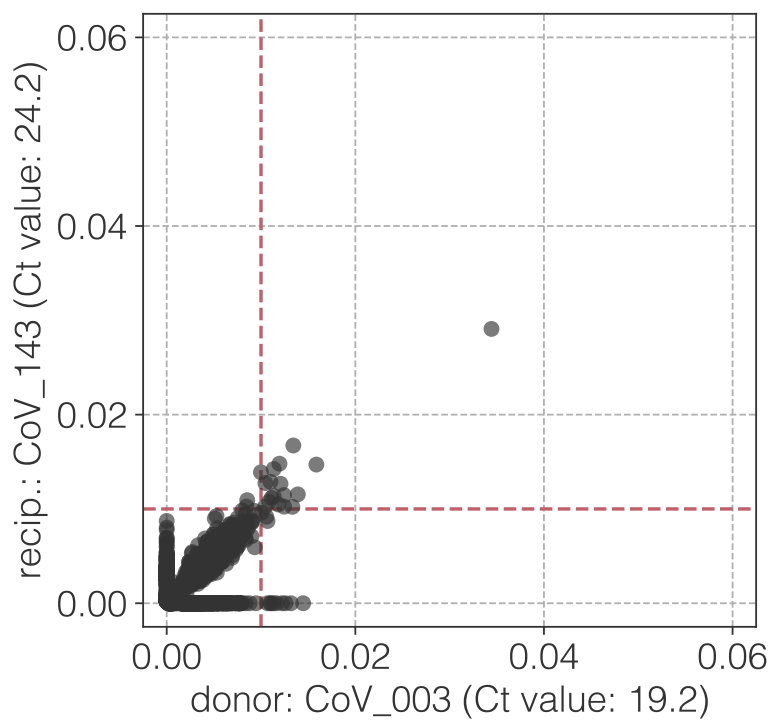
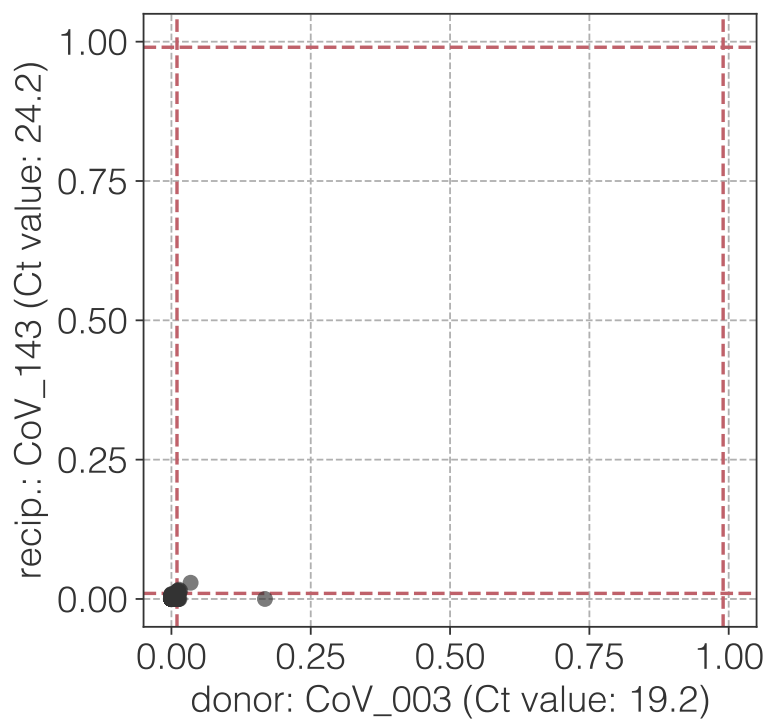
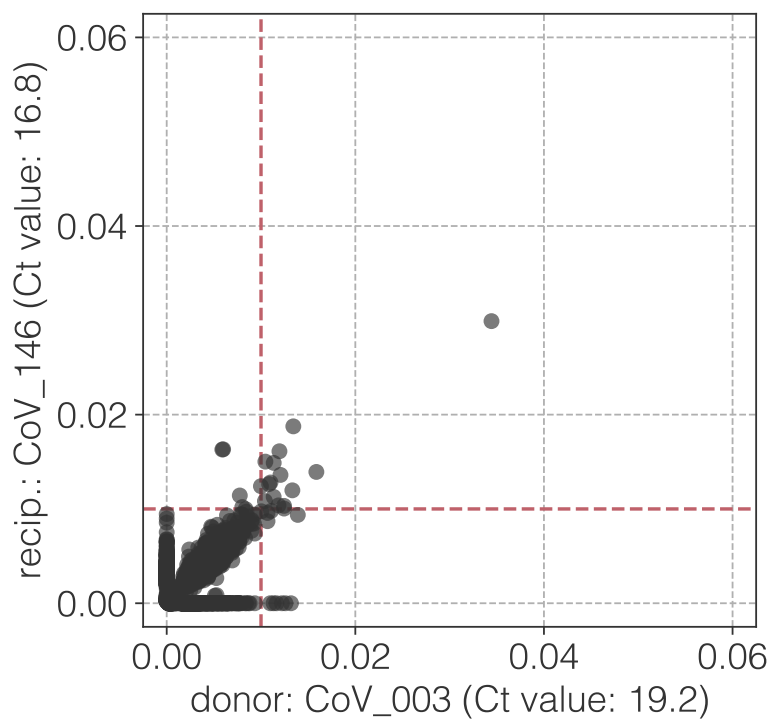
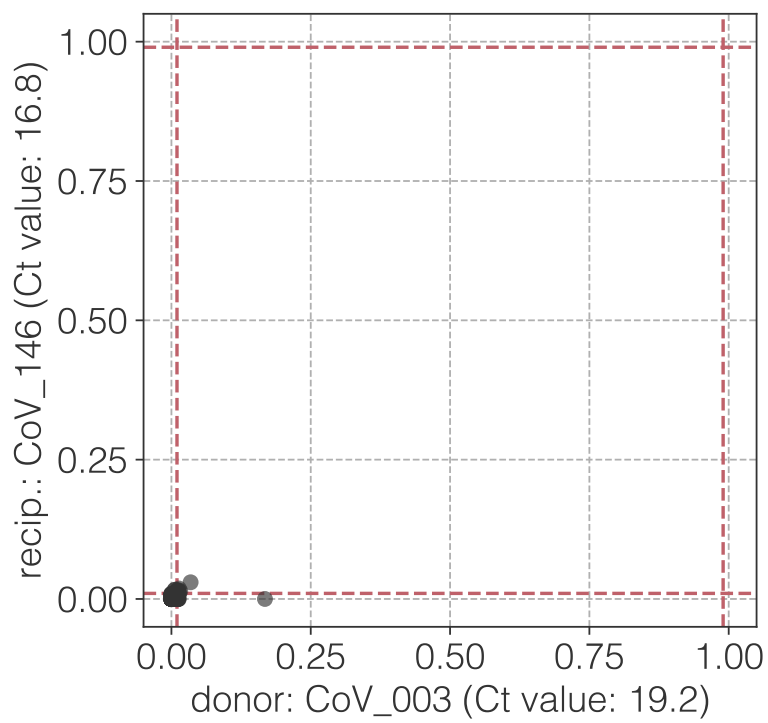
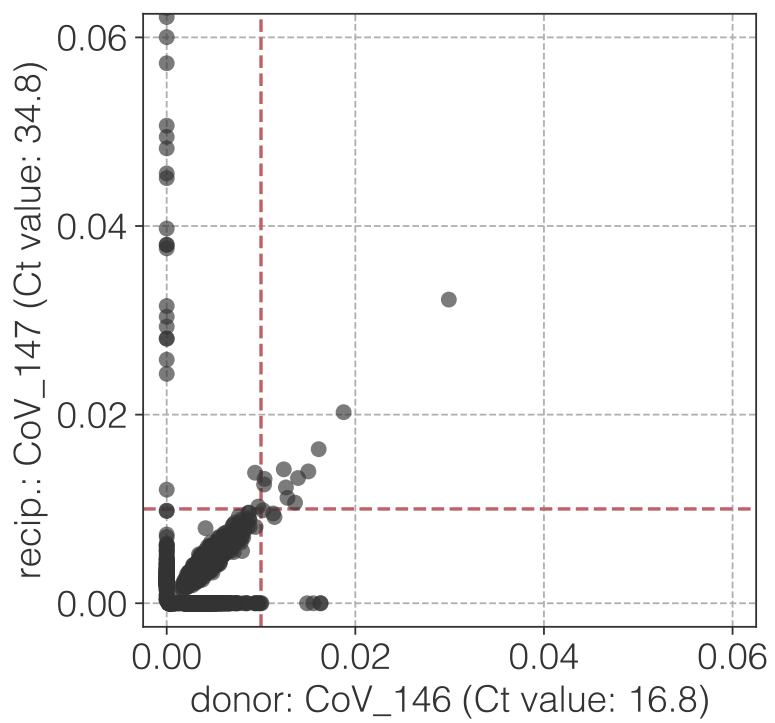
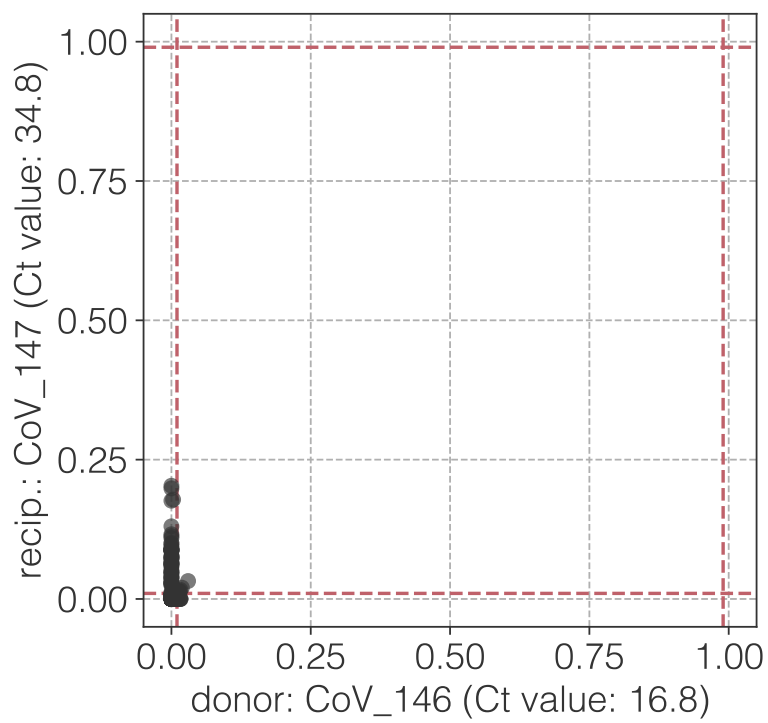


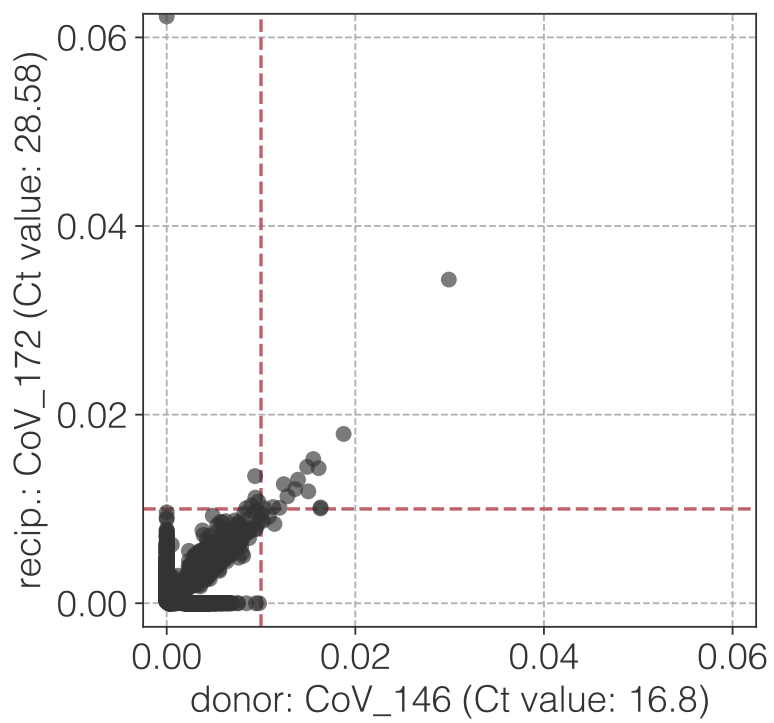
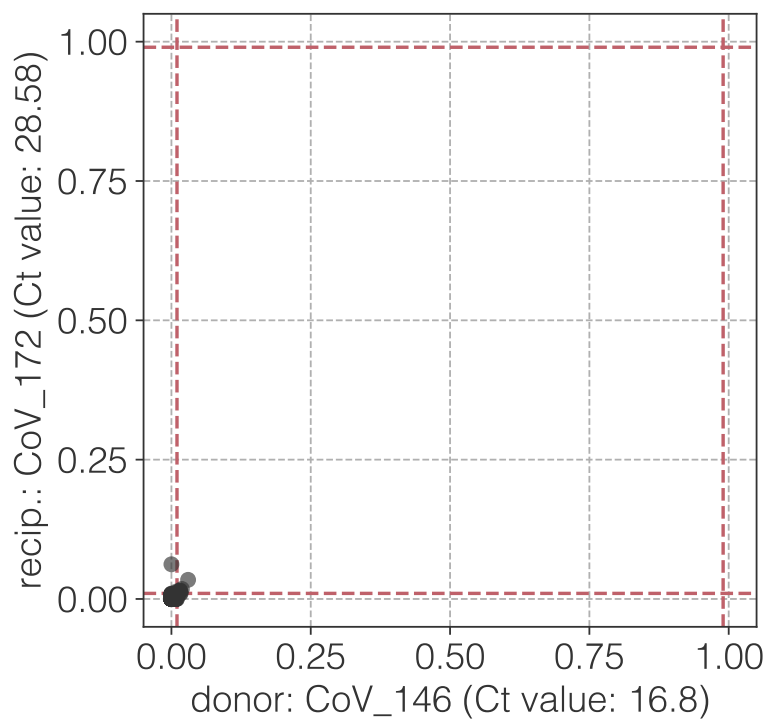
Figure S1. Transmission bottleneck size estimates for each of the 39 transmission pairs analyzed in Popa *et al.* Bottleneck sizes were estimated using A) a 1% variant calling threshold [0.01 0.99], B) a 3% variant calling threshold [0.03 0.97], and C) a 6% variant calling threshold [0.06 0.94]. Frequencies of iSNVs are based on variant calling relative to donor-specific reference sequences. Color coding of transmission pairs is as in Popa *et al.* for ease of comparison. Maximum likelihood estimates are indicated by a colored circle and vertical lines show the 95% confidence intervals. (We allowed a maximum bottleneck size of 10,000

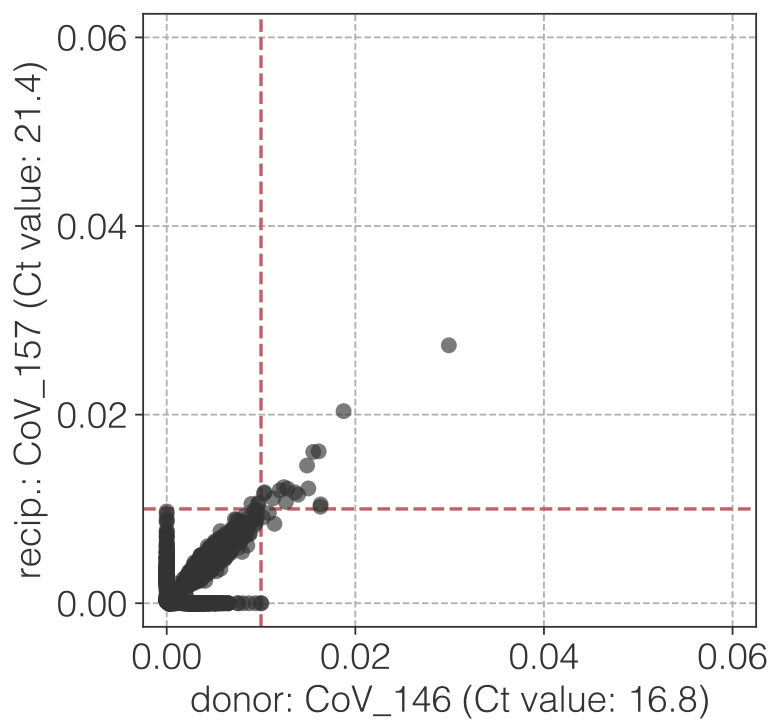
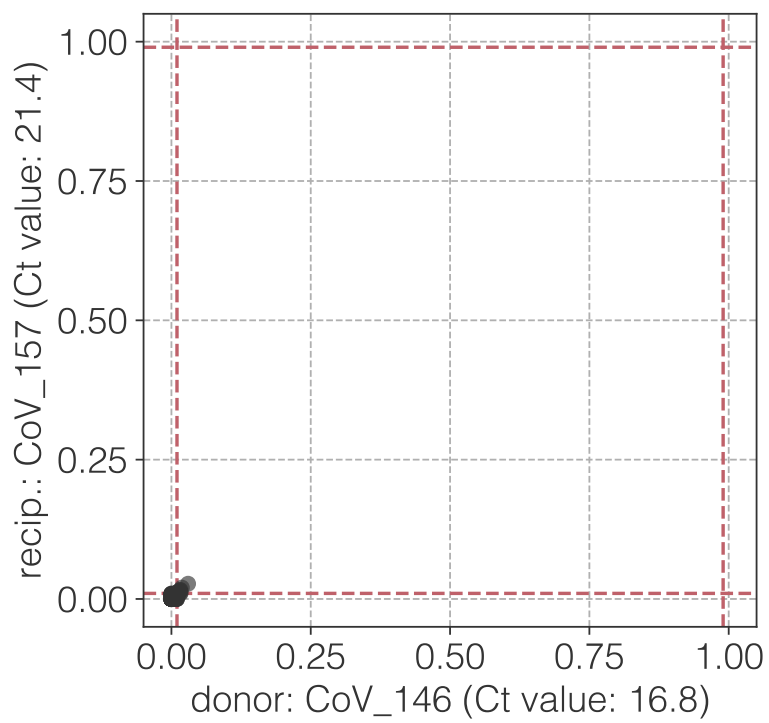
virions, whereas Popa *et al.* allowed a maximum bottleneck size of 5,000 virions, but this difference was inconsequential to the interpretation of the results.) Note that in (B), we do not have transmission bottleneck size estimates for pairs with individual 146 as donor because the maximum iSNV frequency we found in this sample was 0.0299.

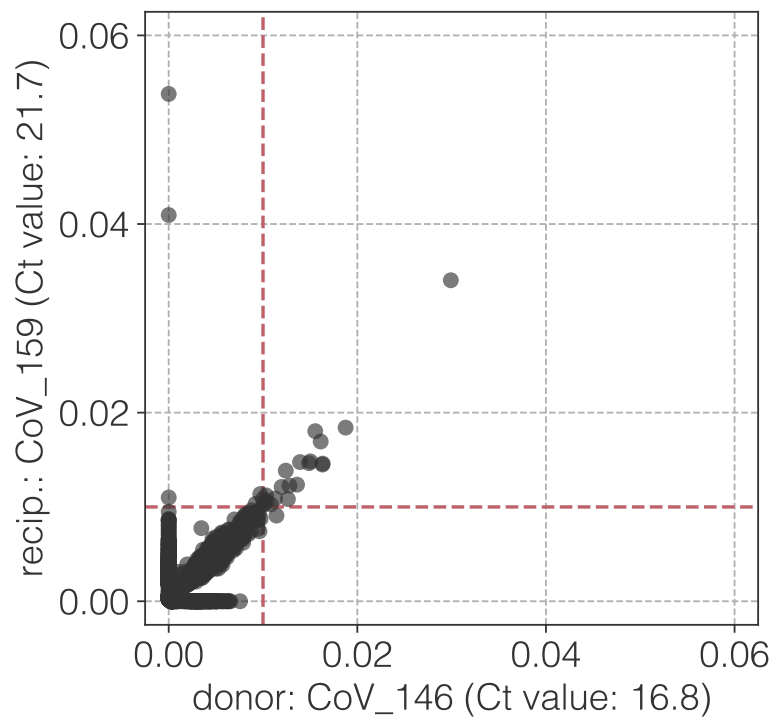
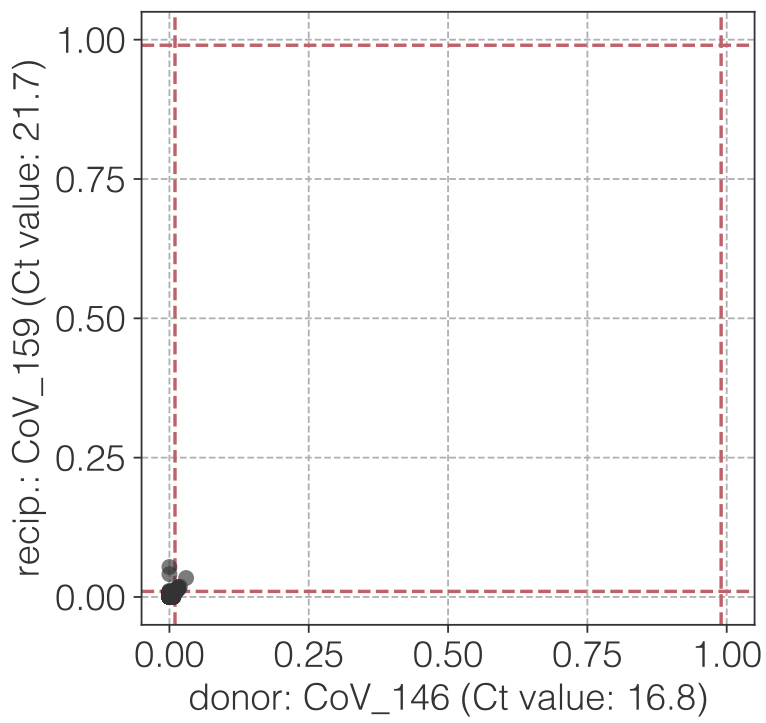
aa

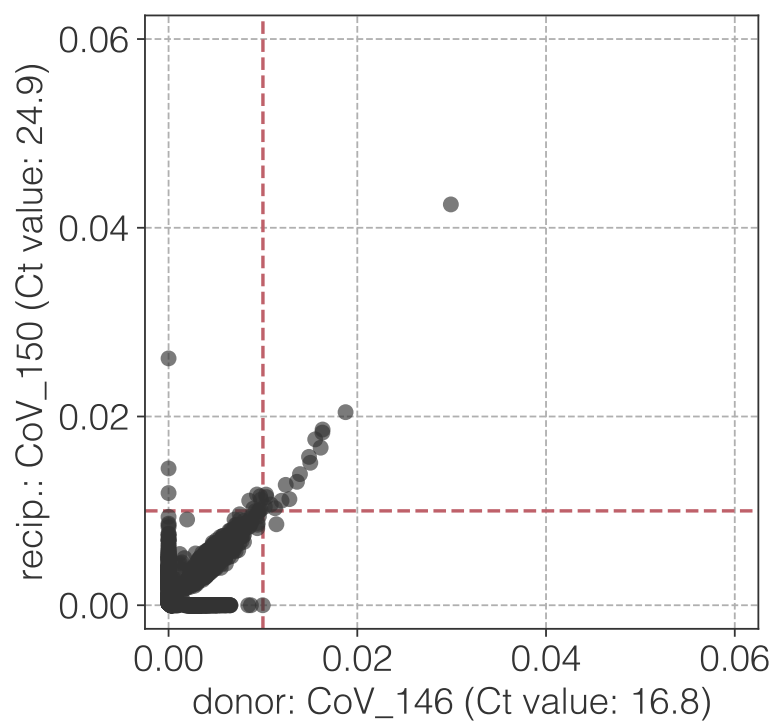
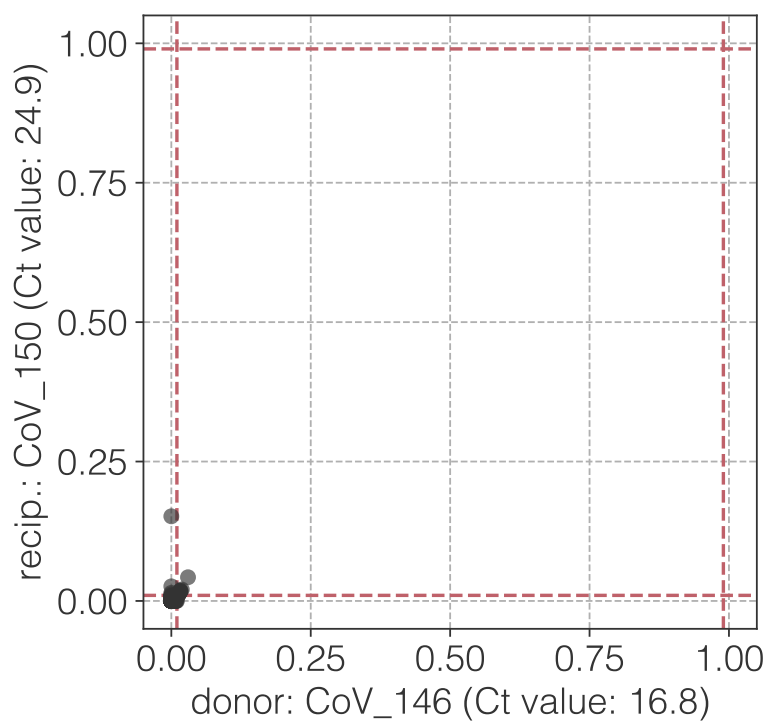
ab

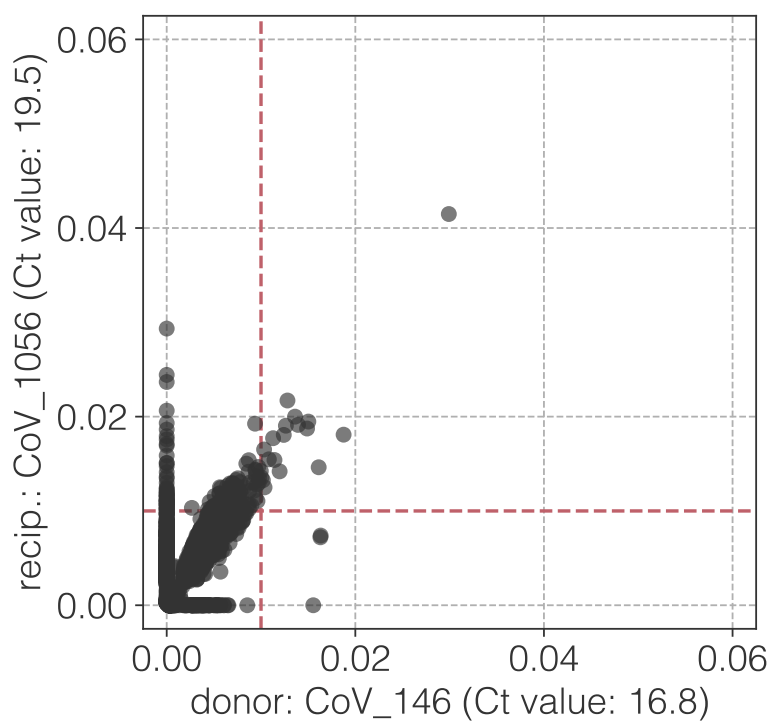
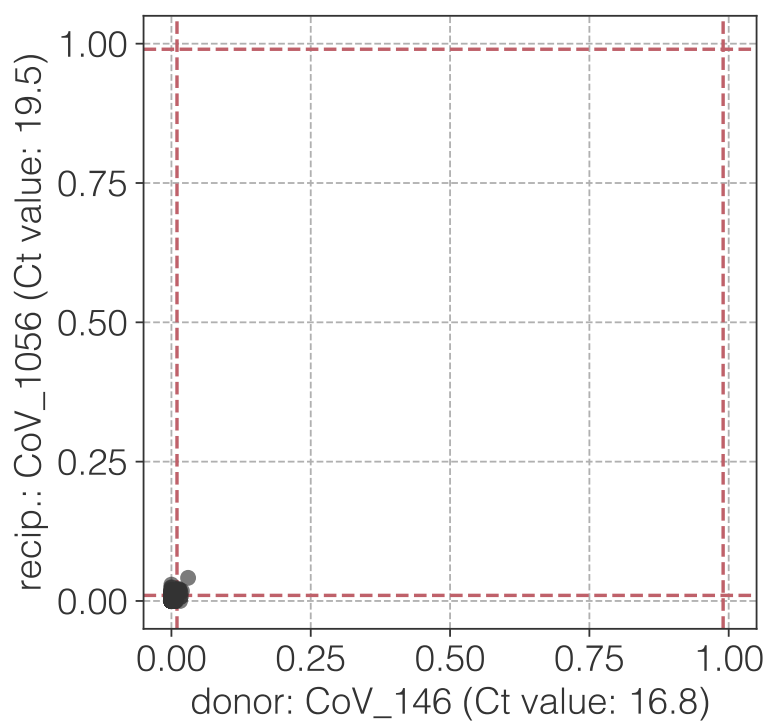
ac

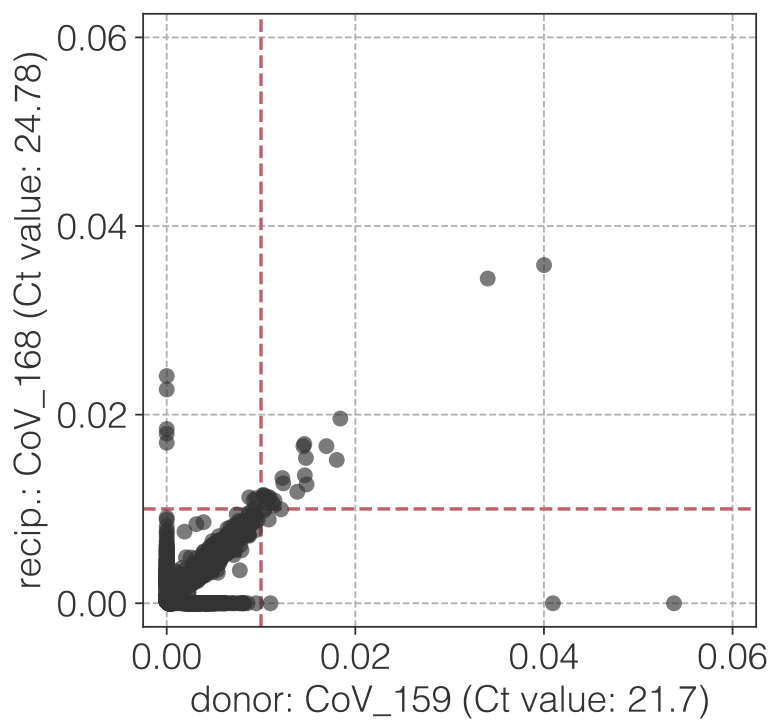
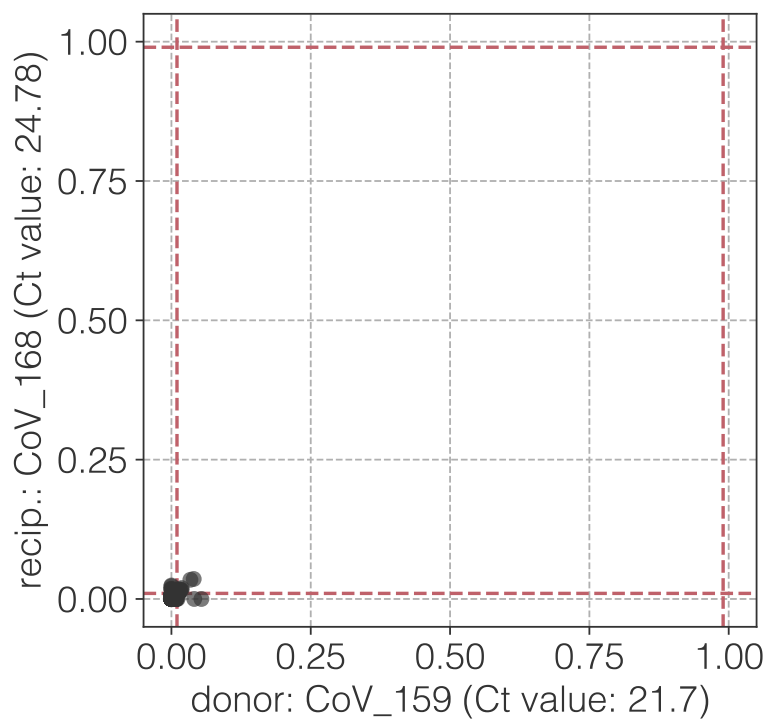
ad

ae

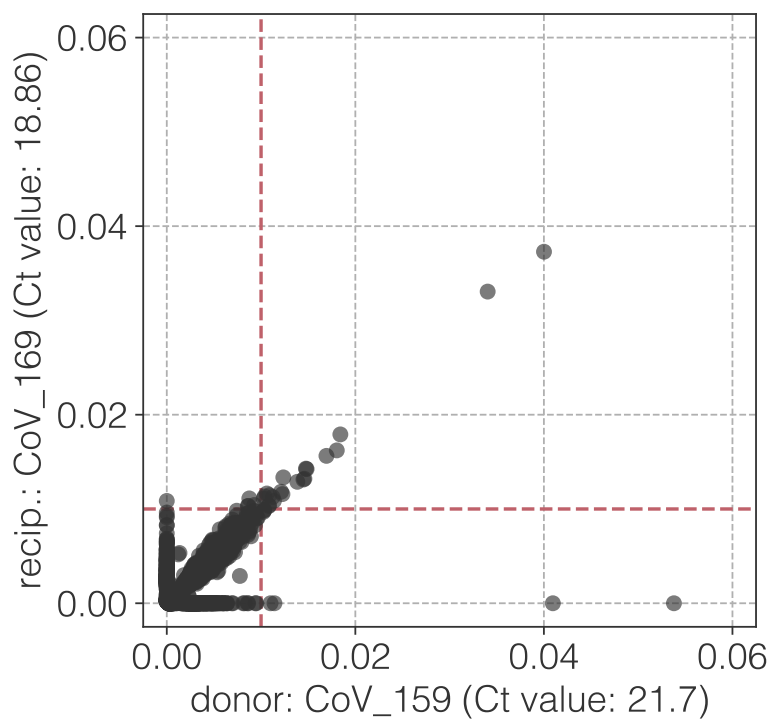
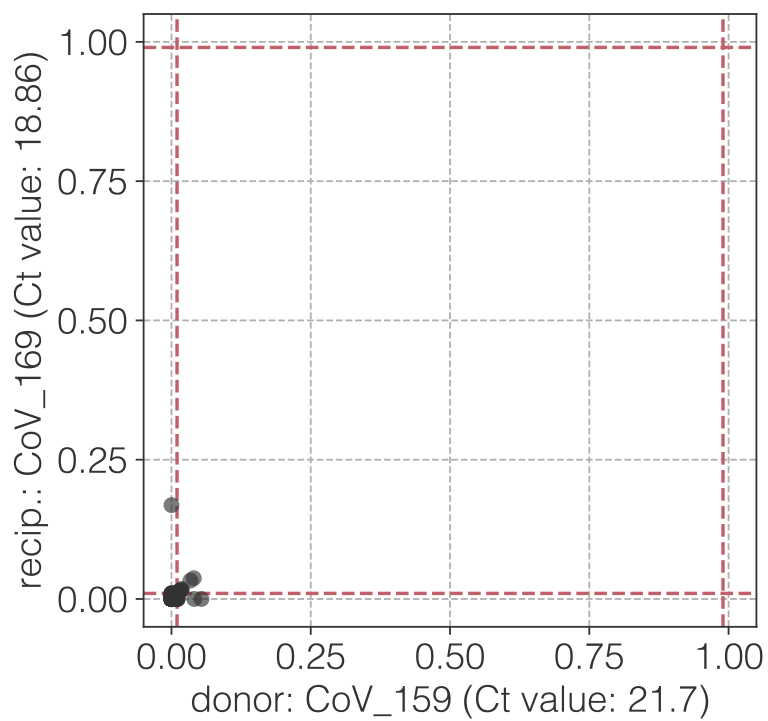
af

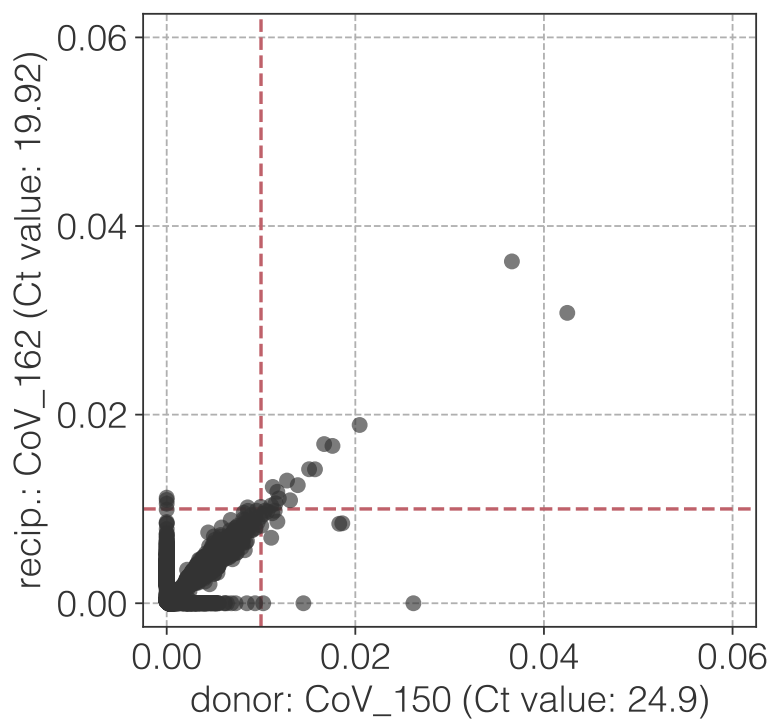
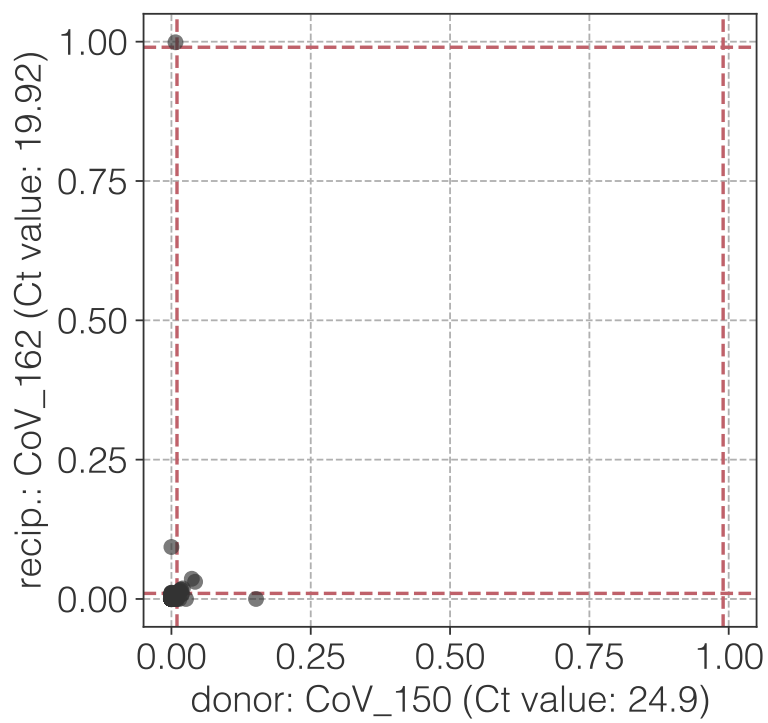
ag

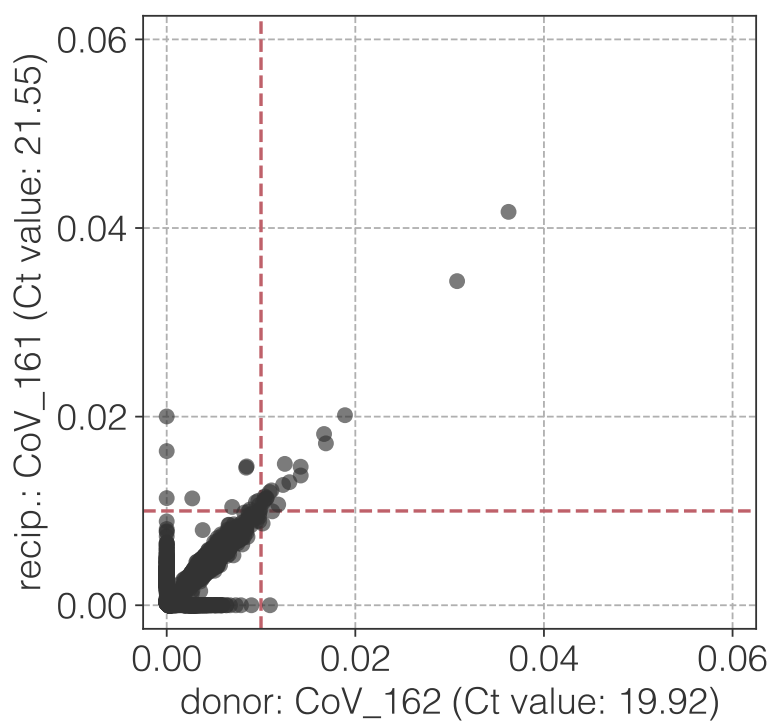
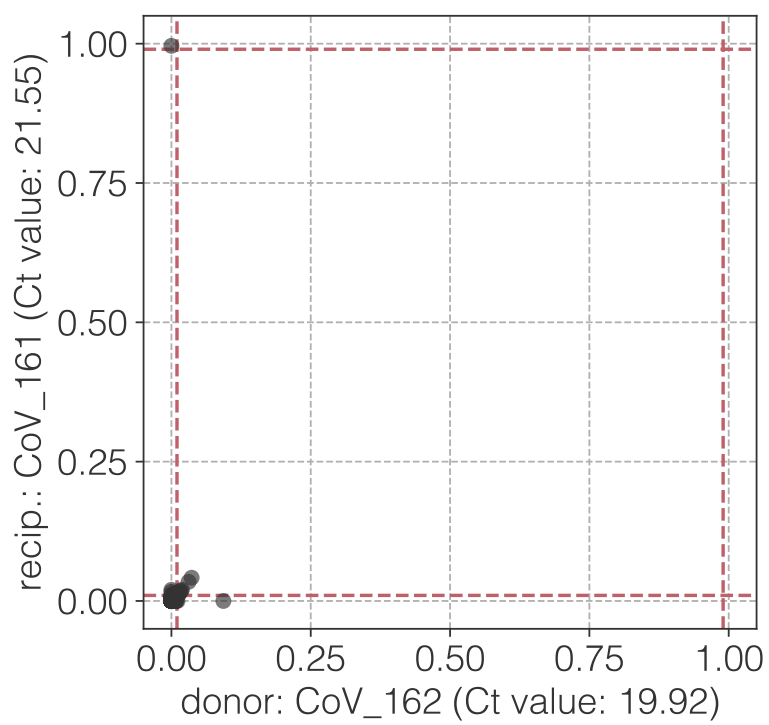
ah

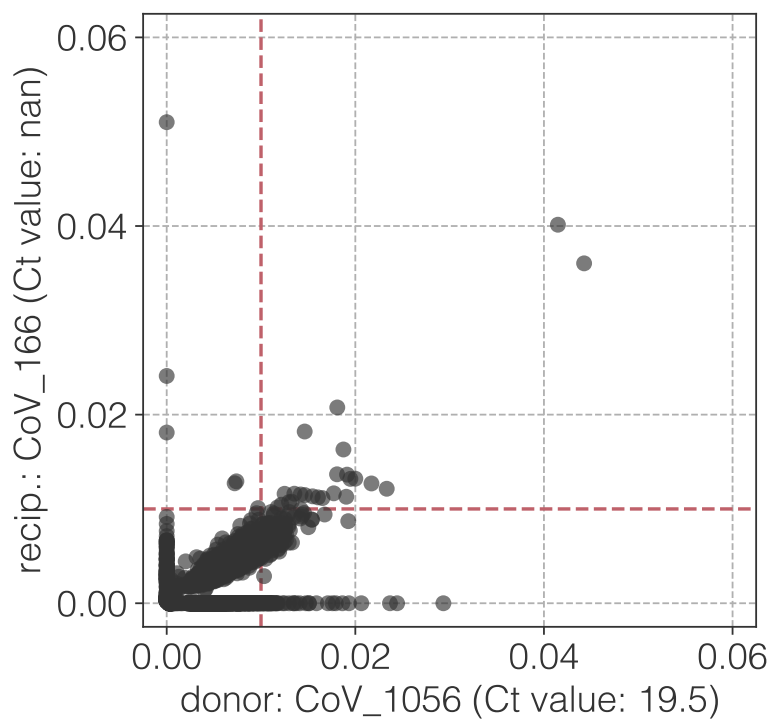
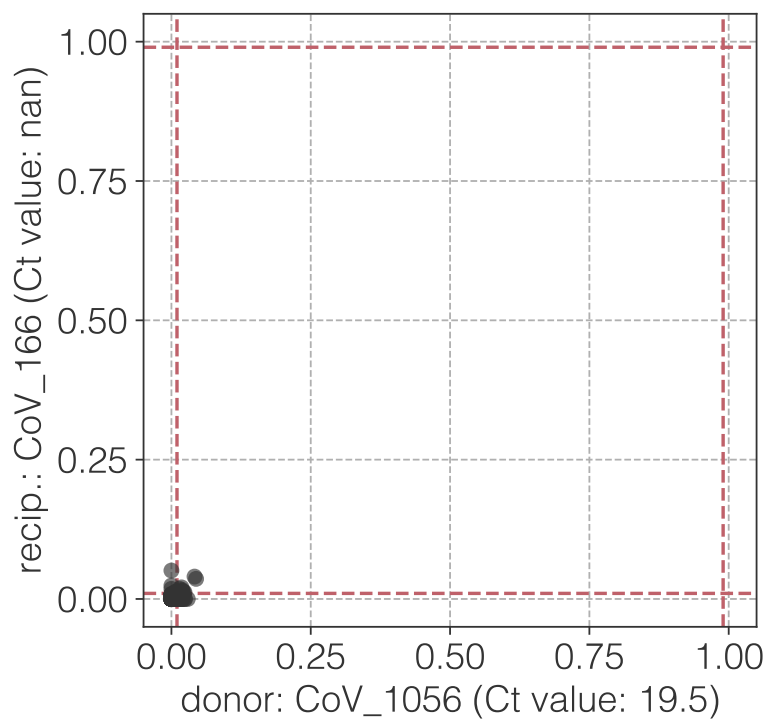
ai

aj

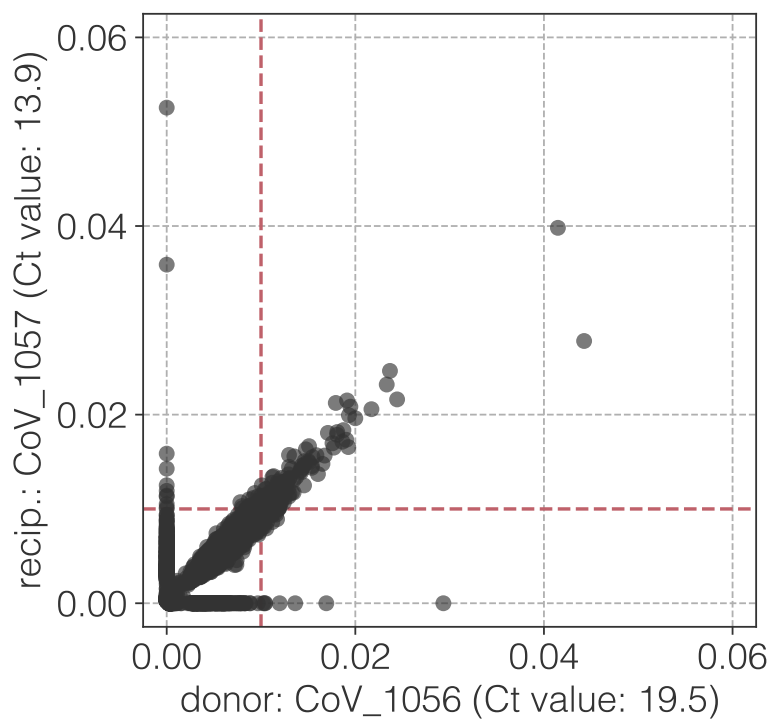
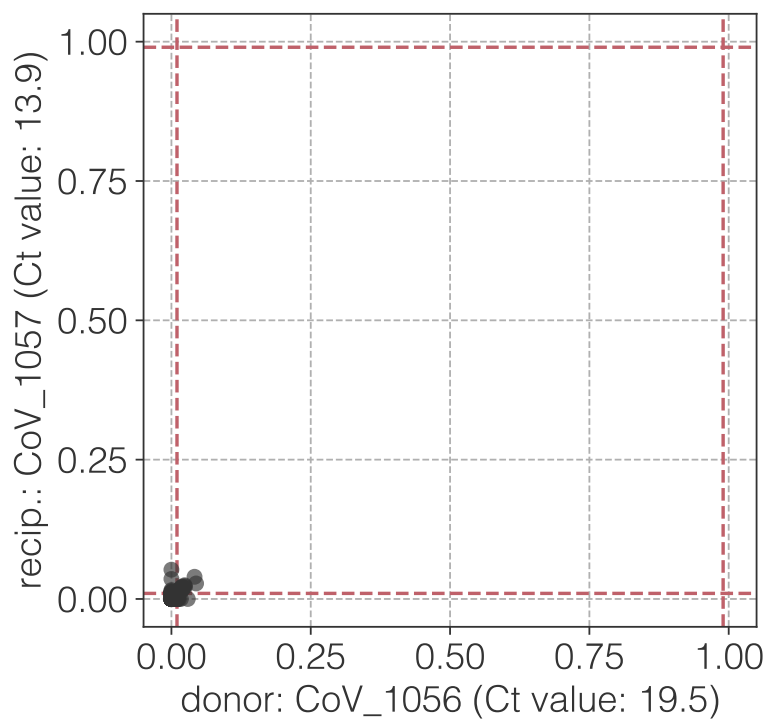


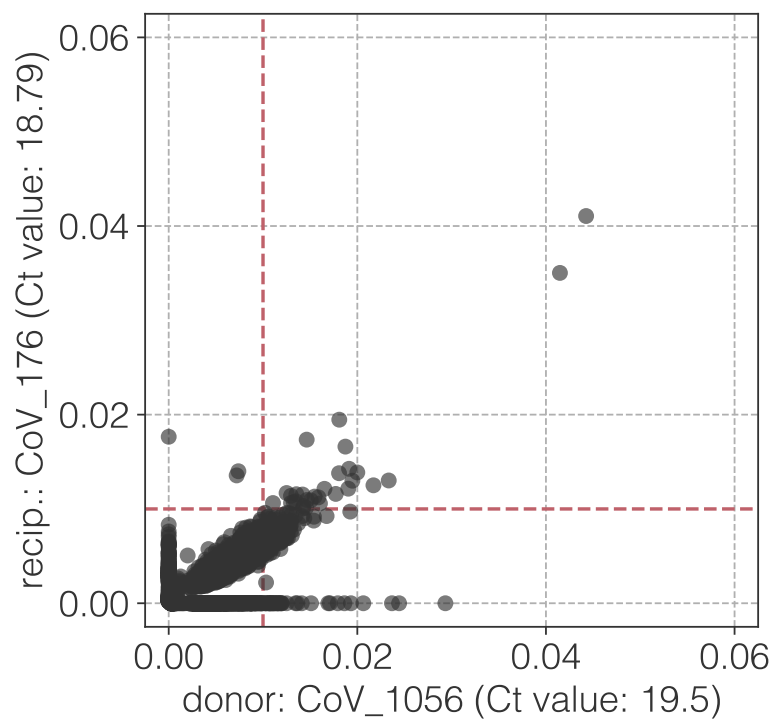
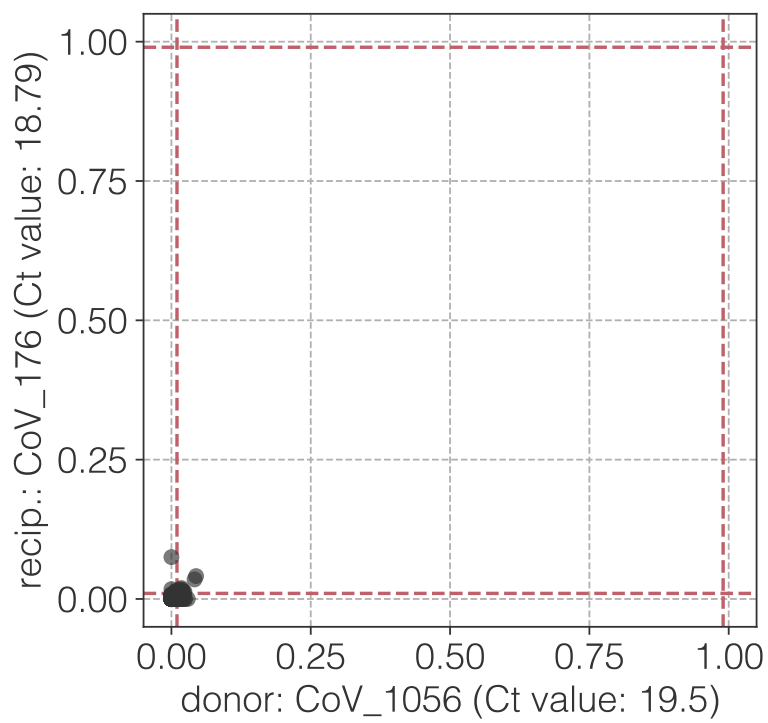
ak

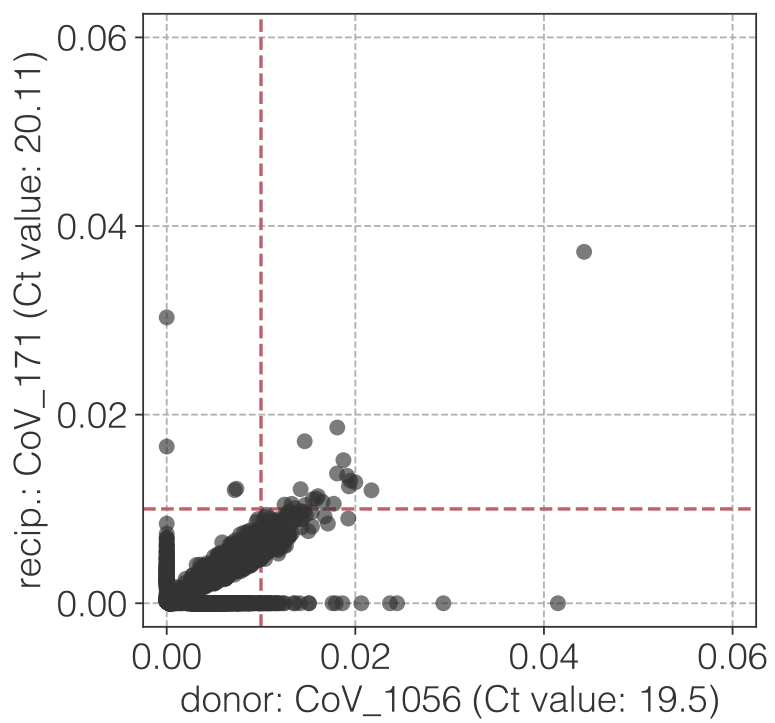
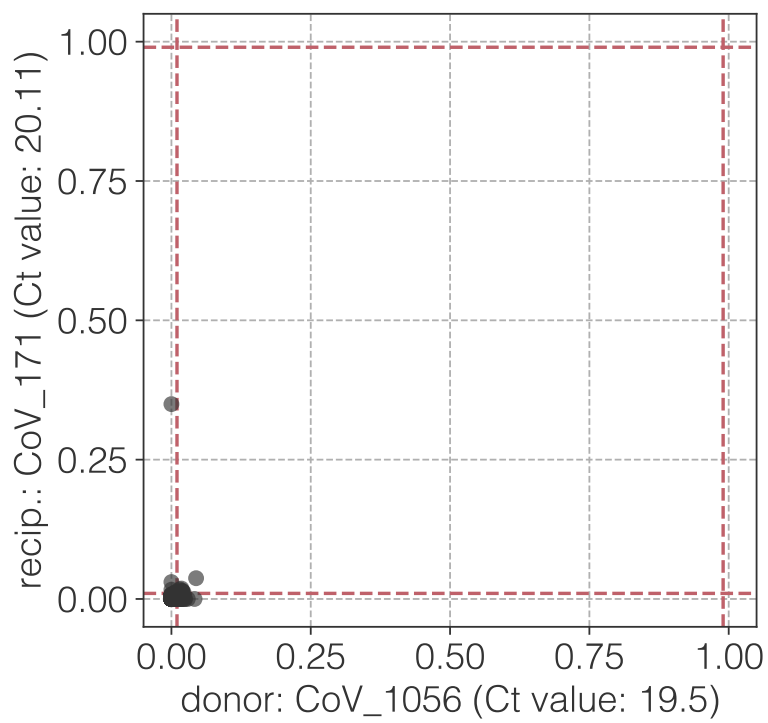
al

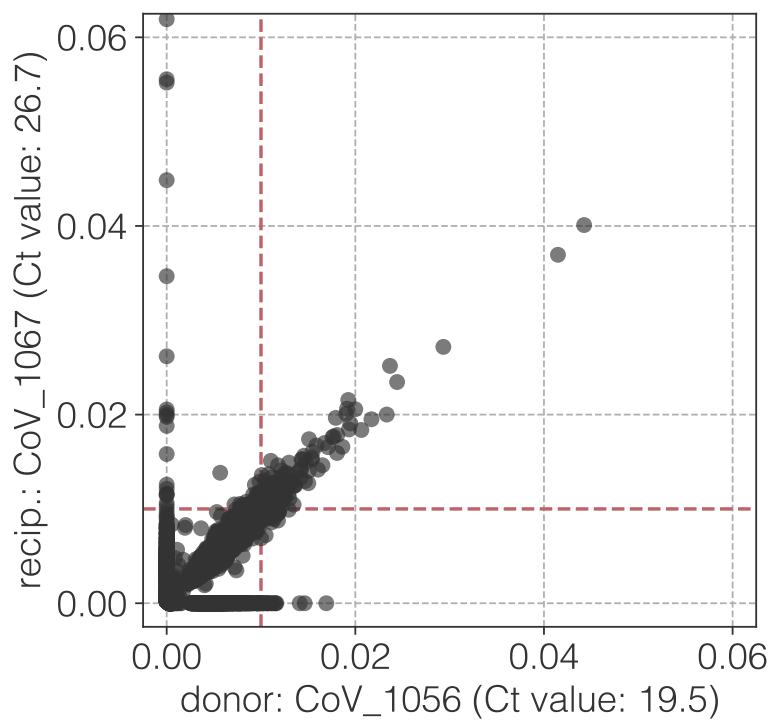
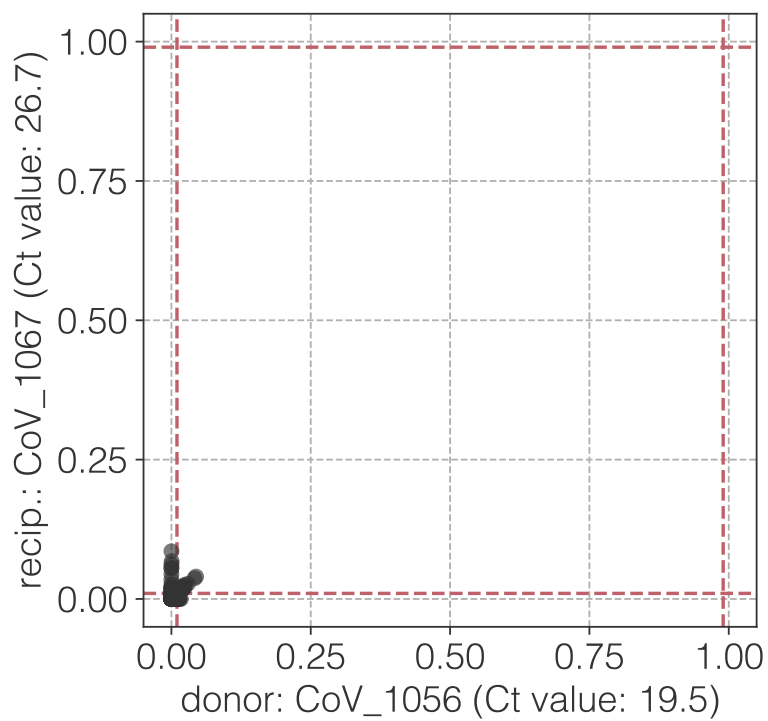
am

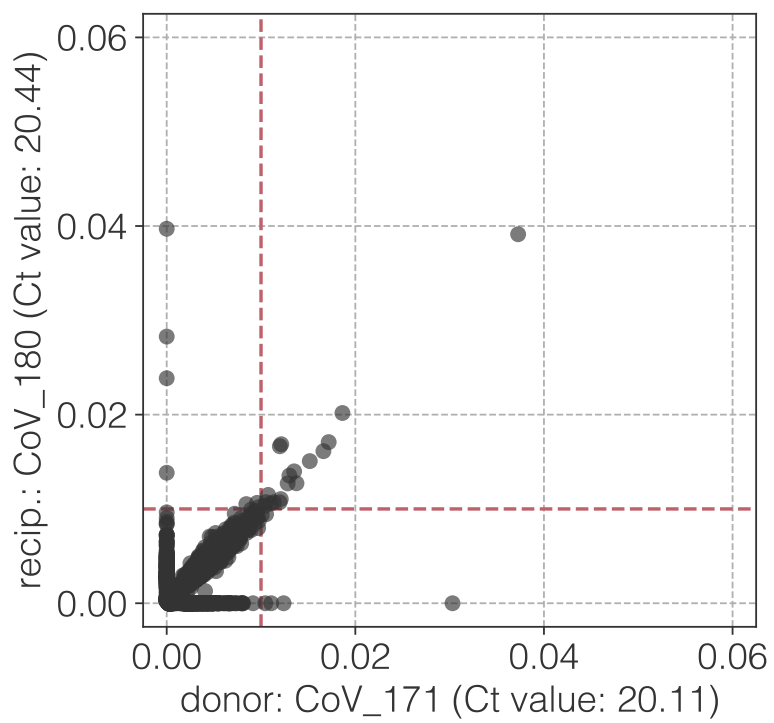
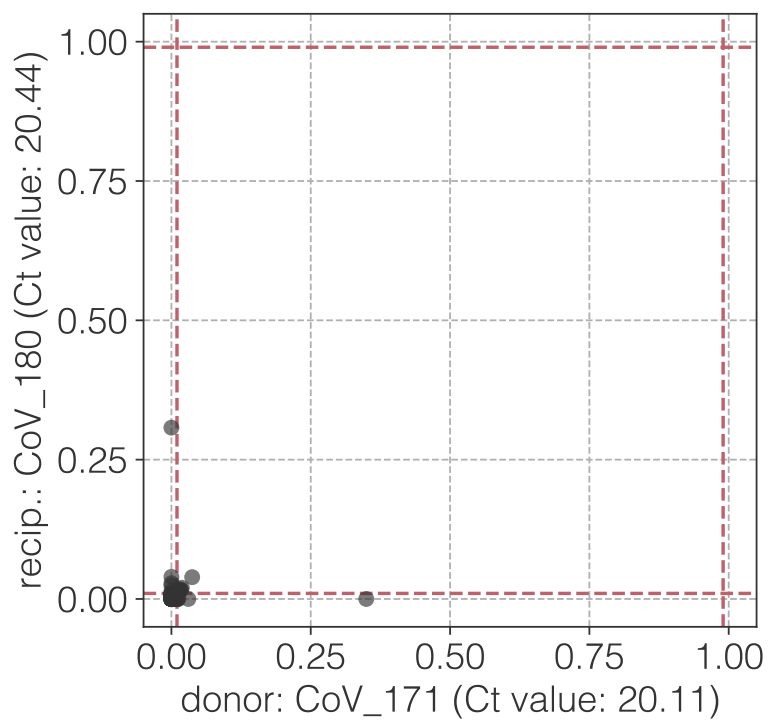
an

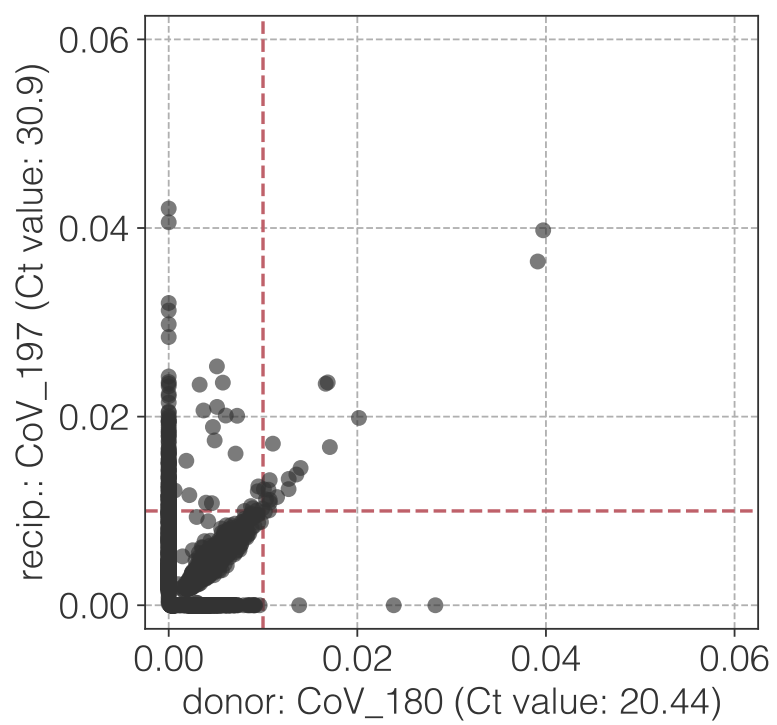
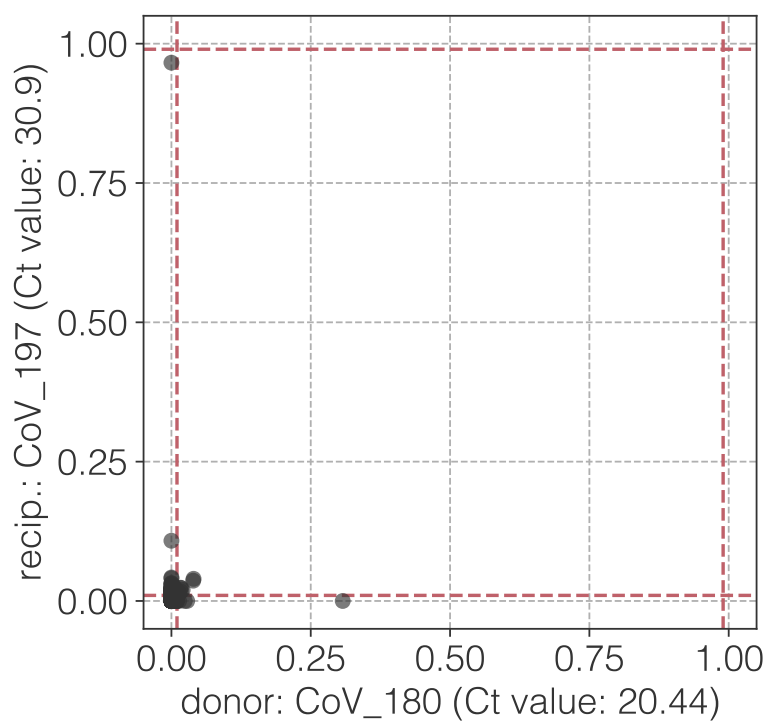


ao

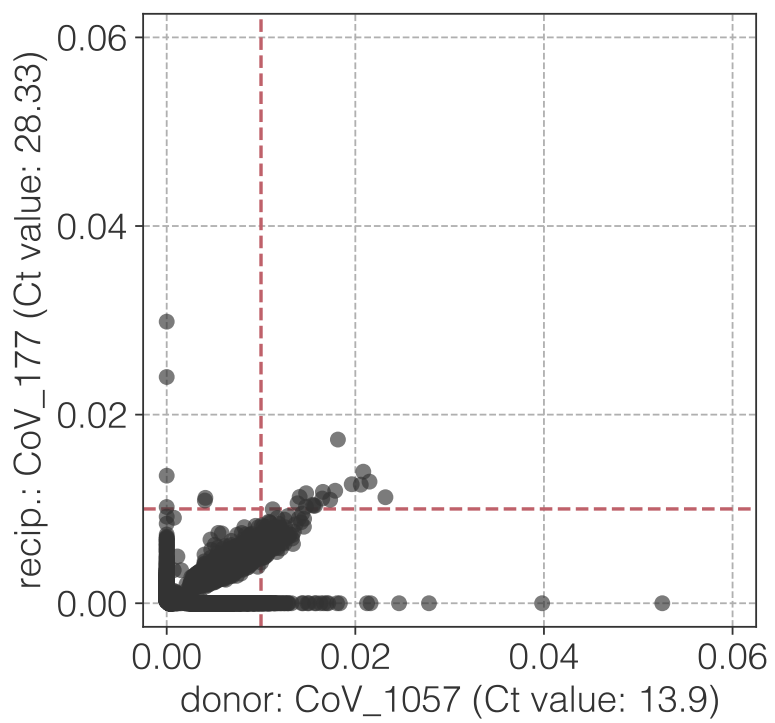
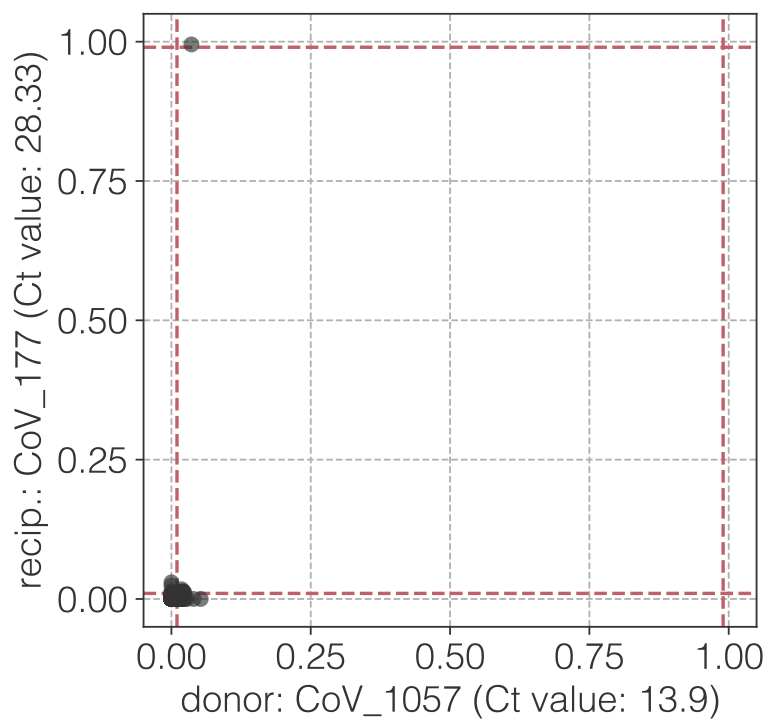
ap

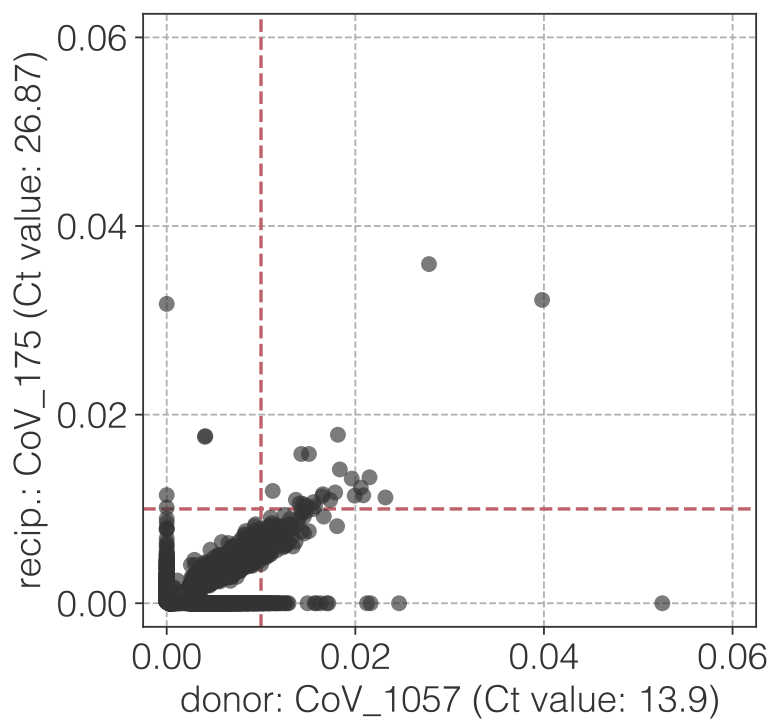
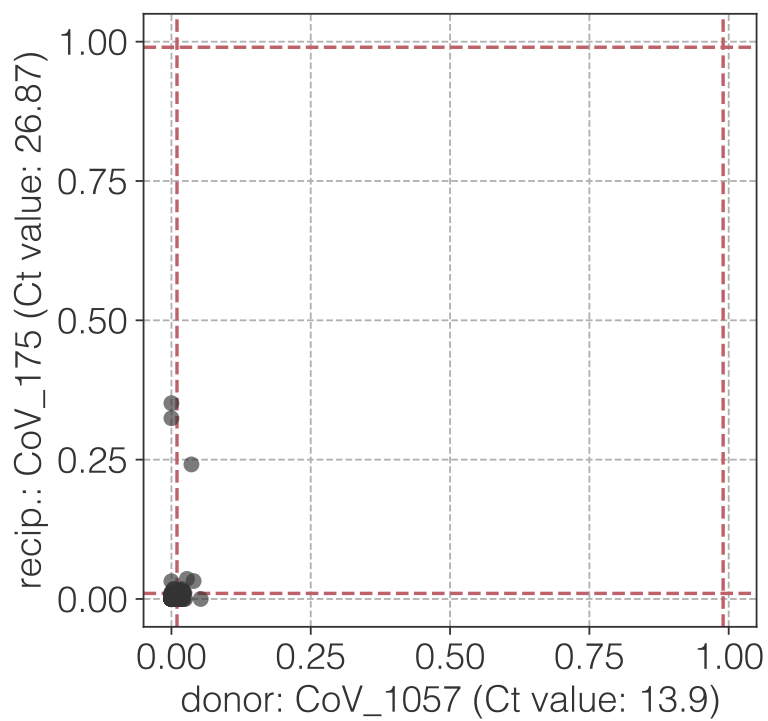
aq

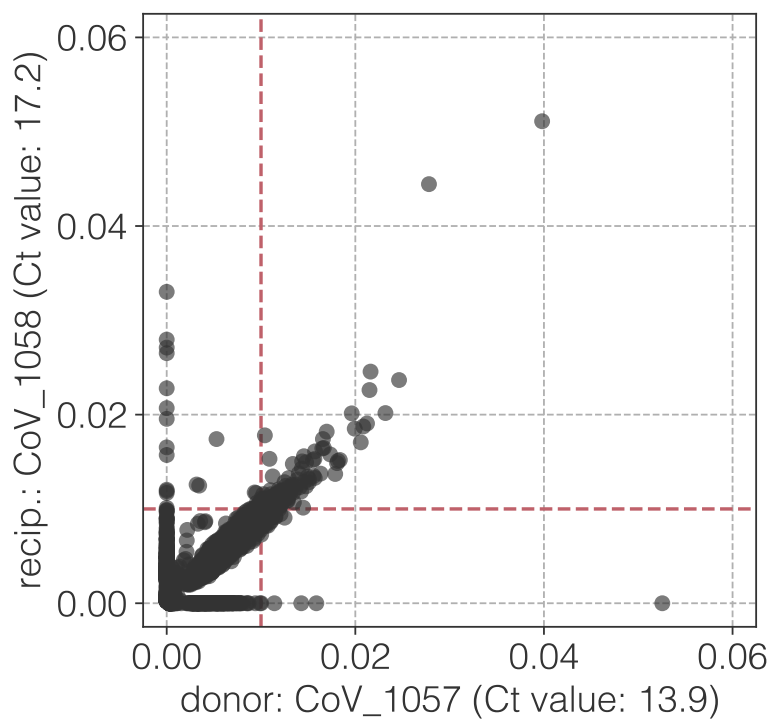
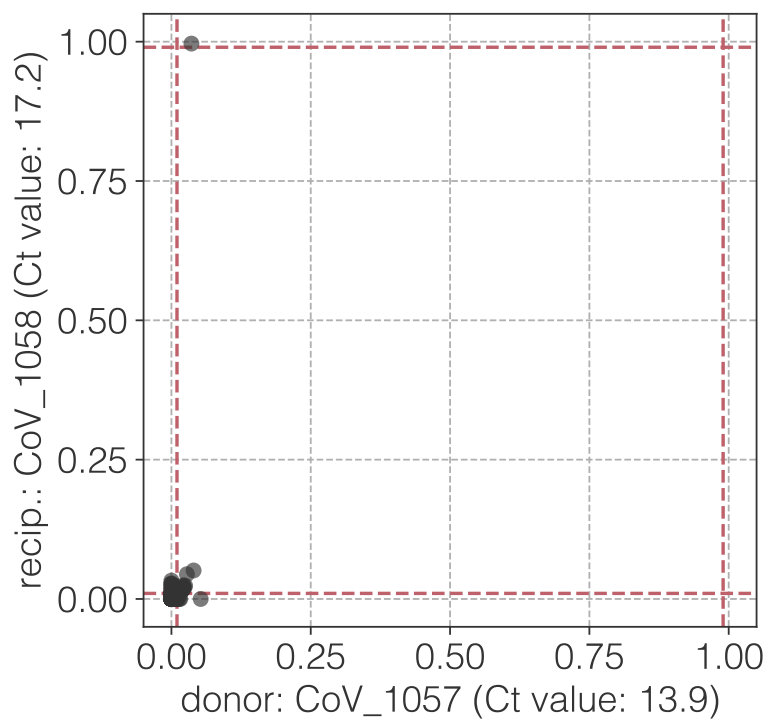
ar

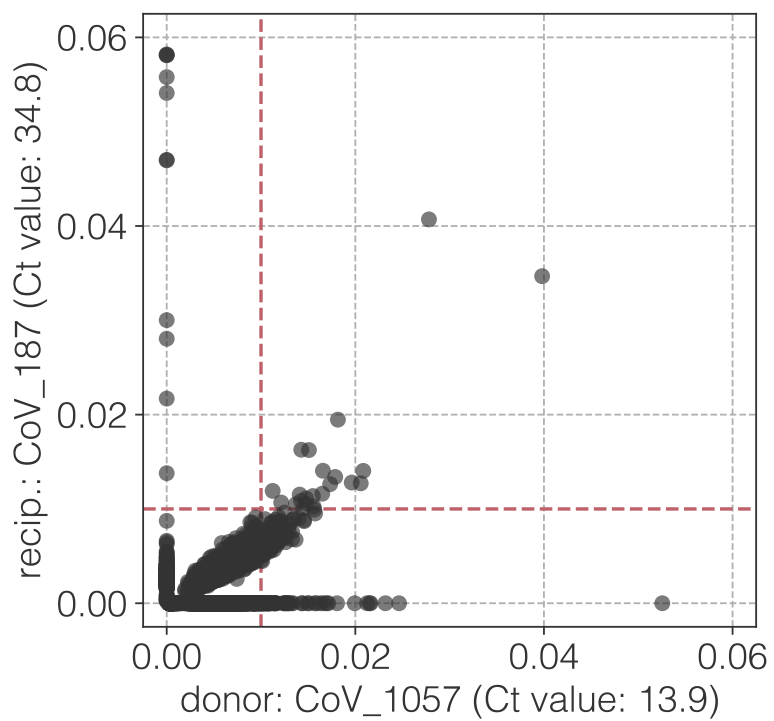
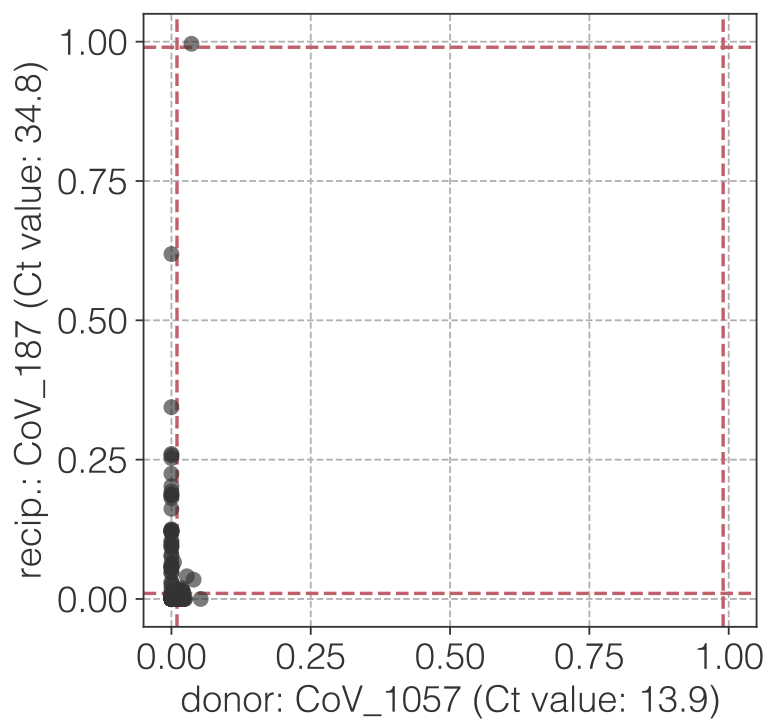
as

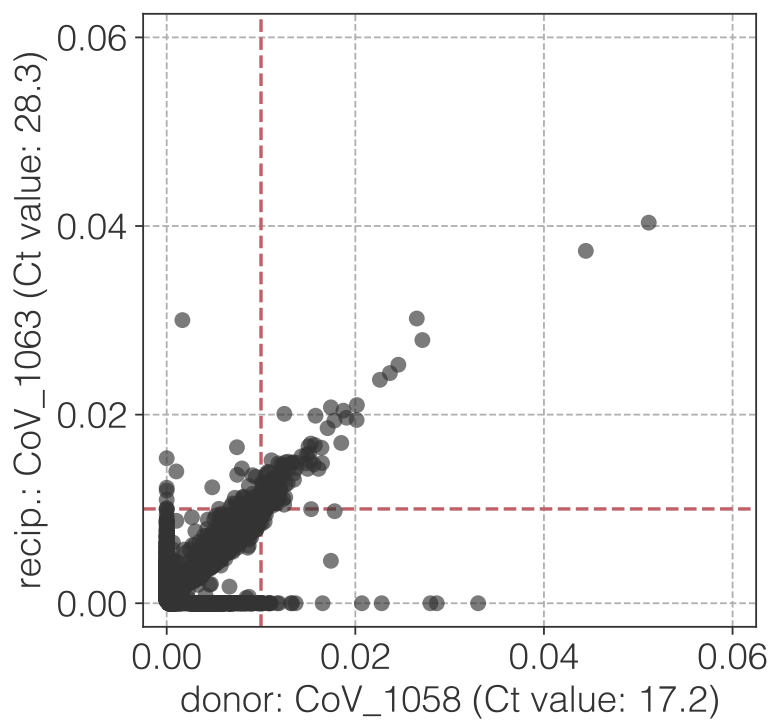
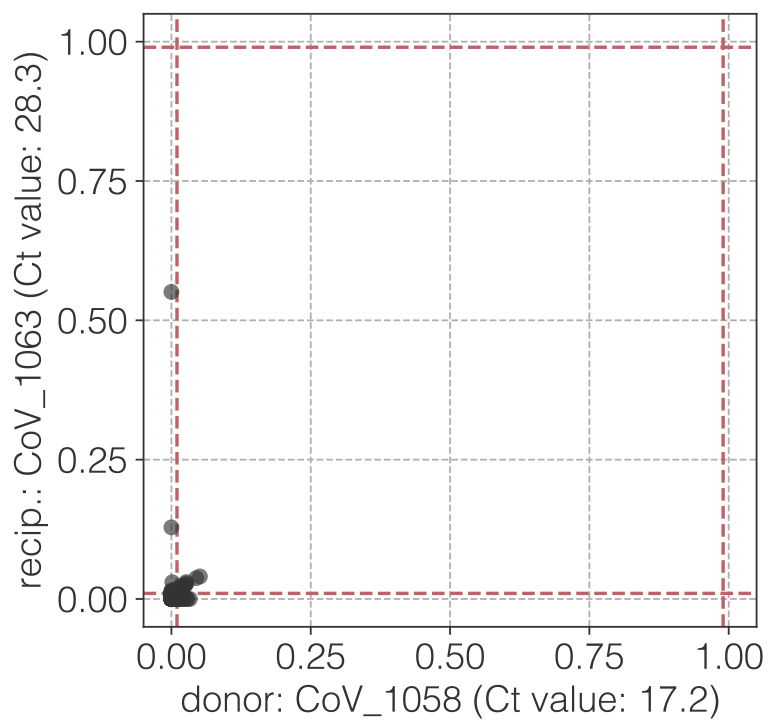
at



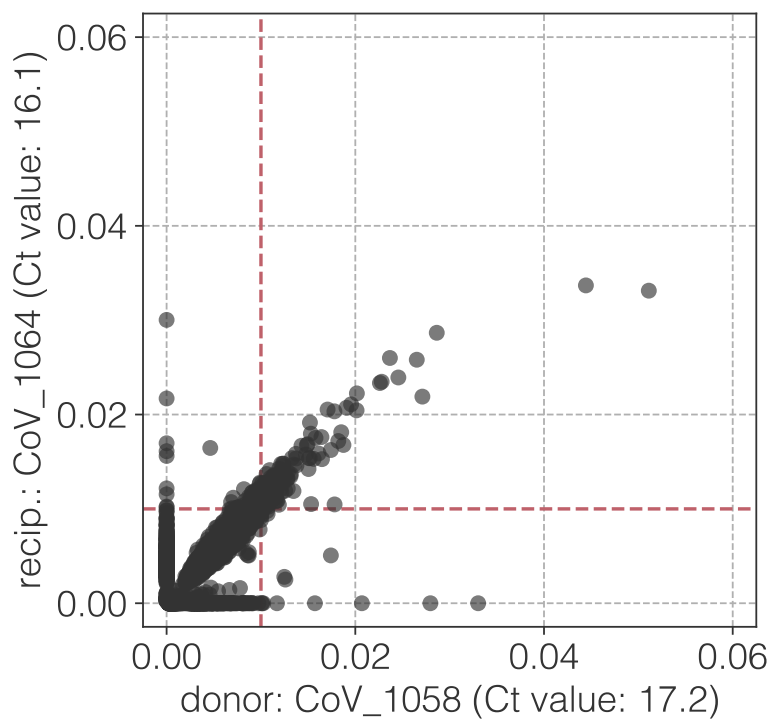
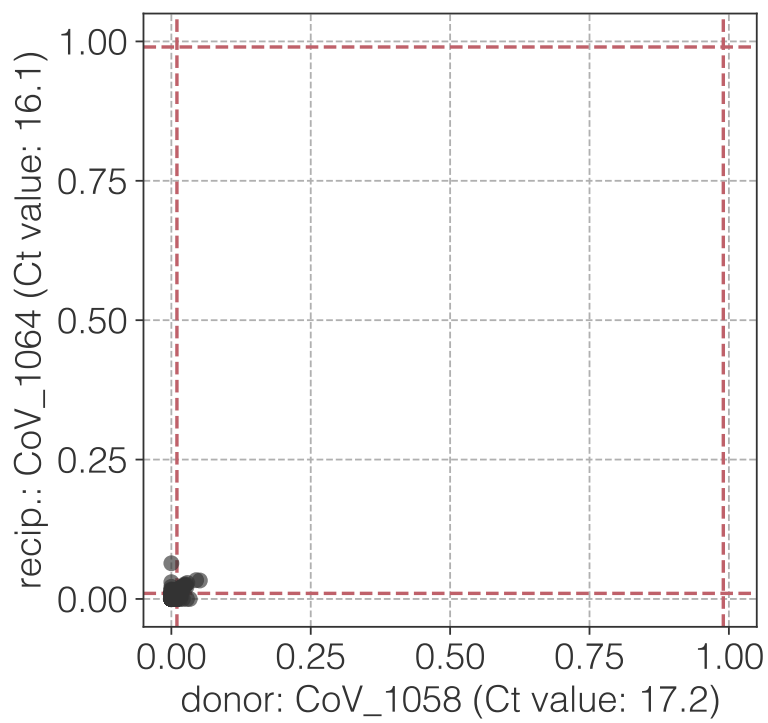
au

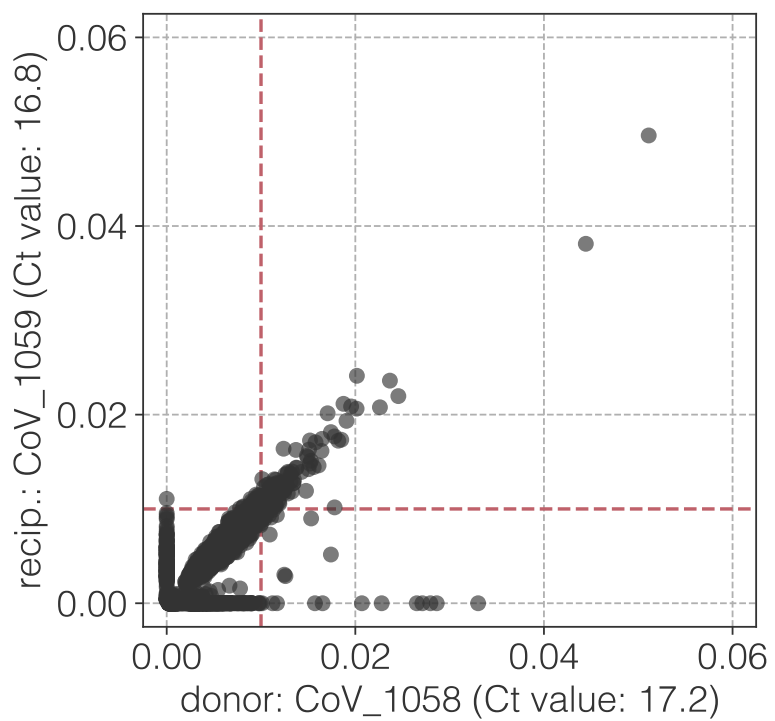
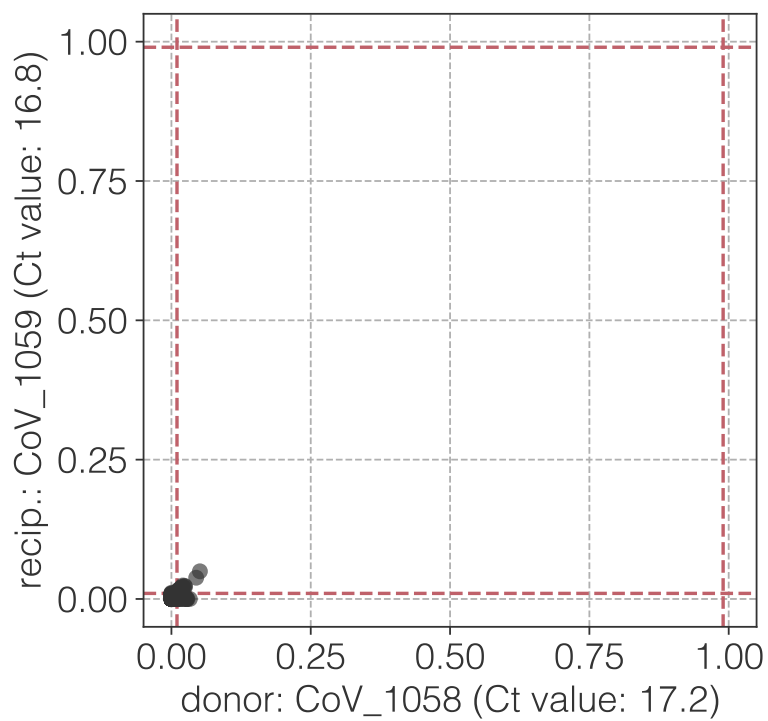
av

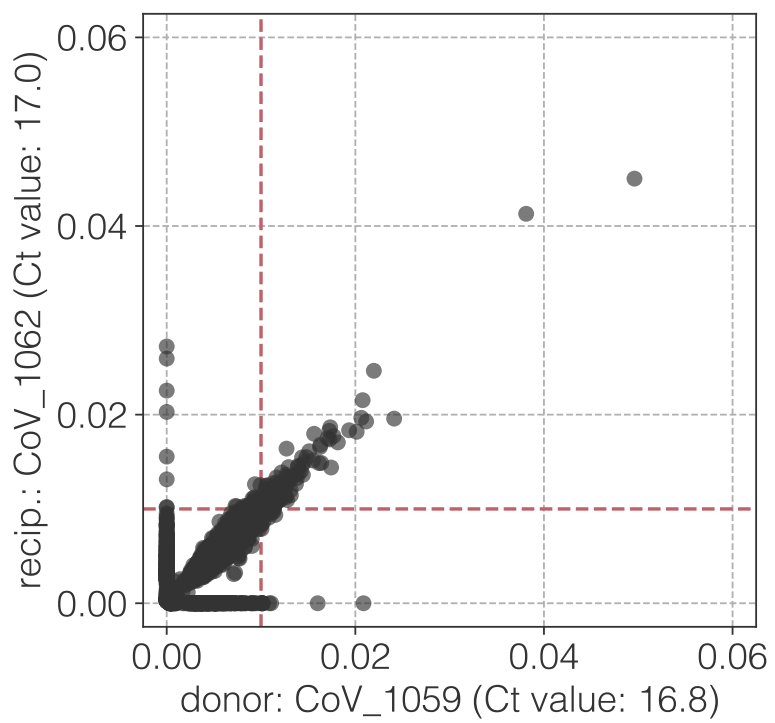
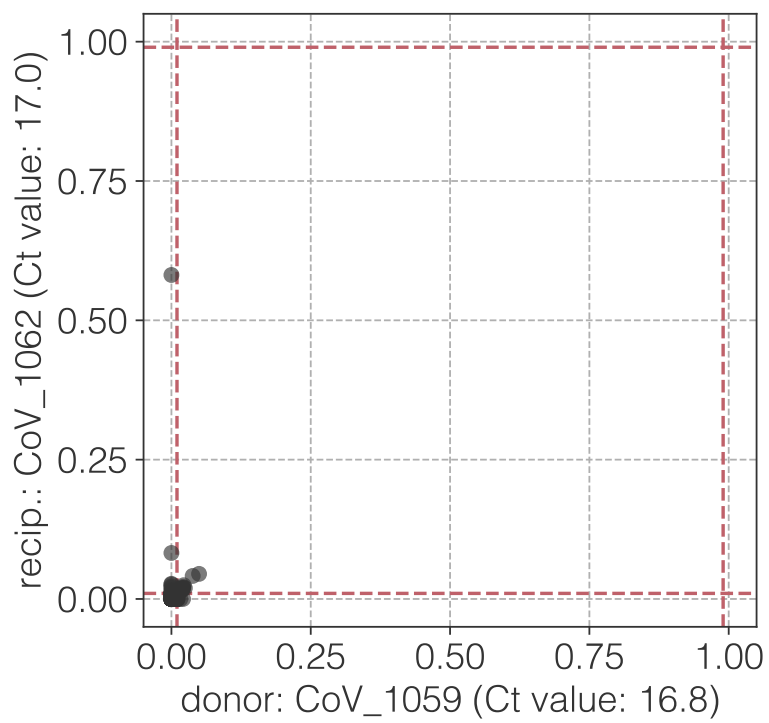
aw

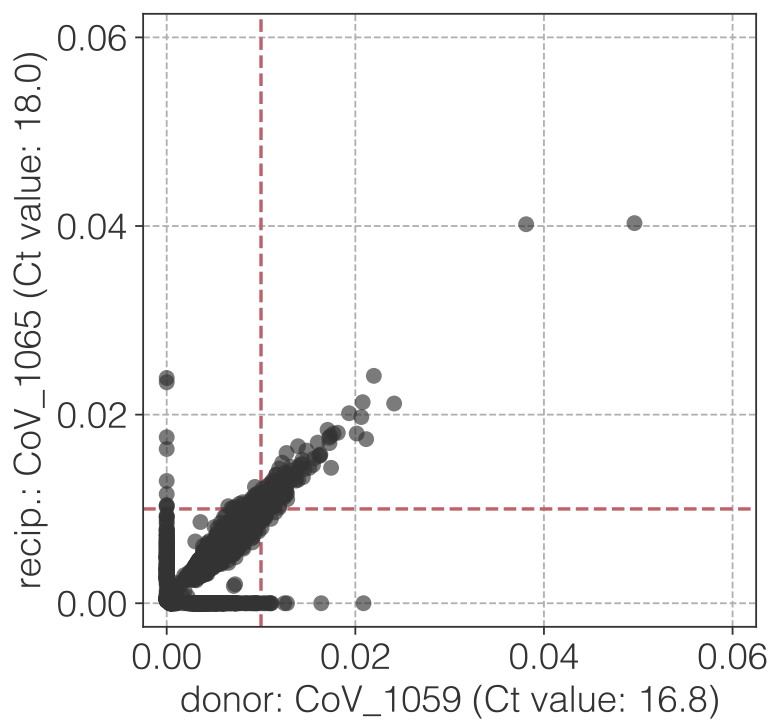
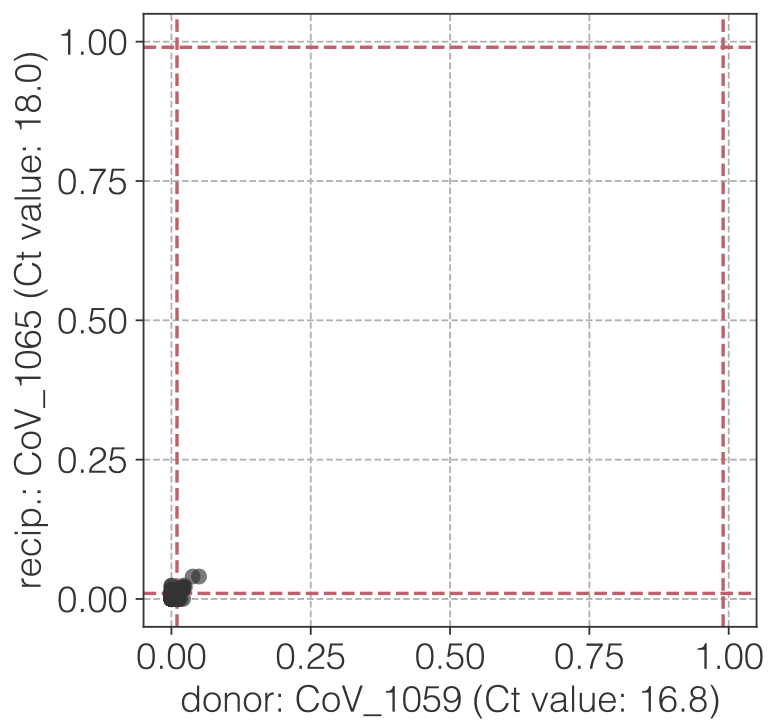
ax

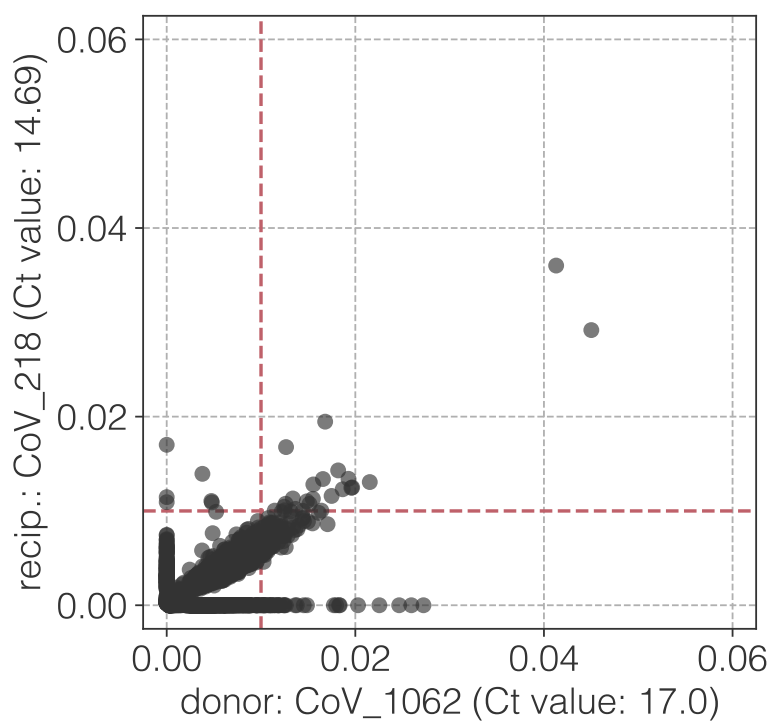
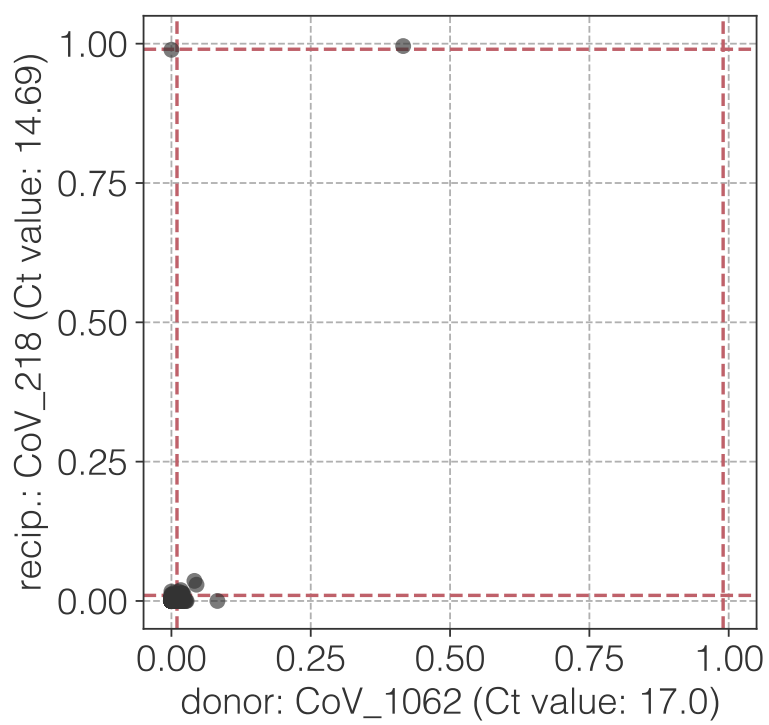
ay

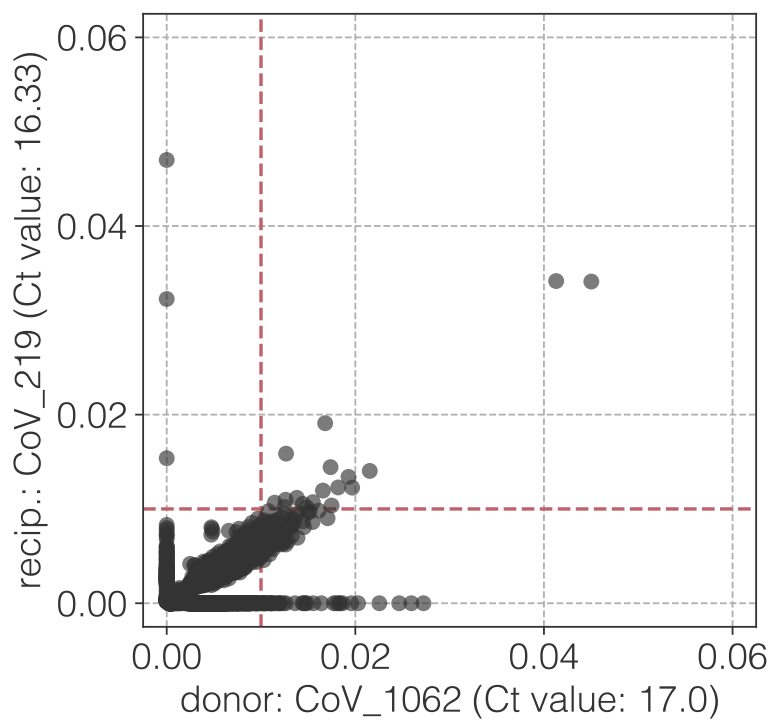
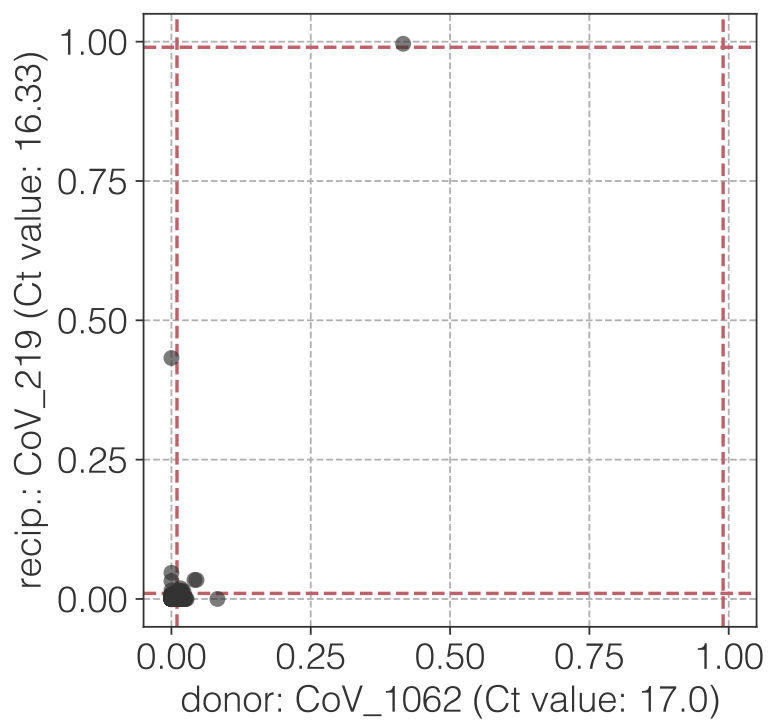


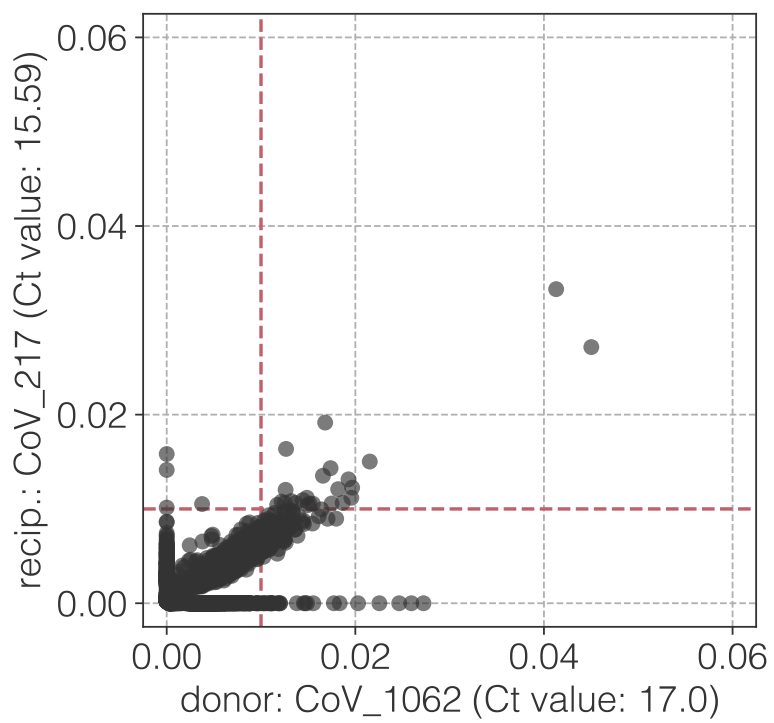
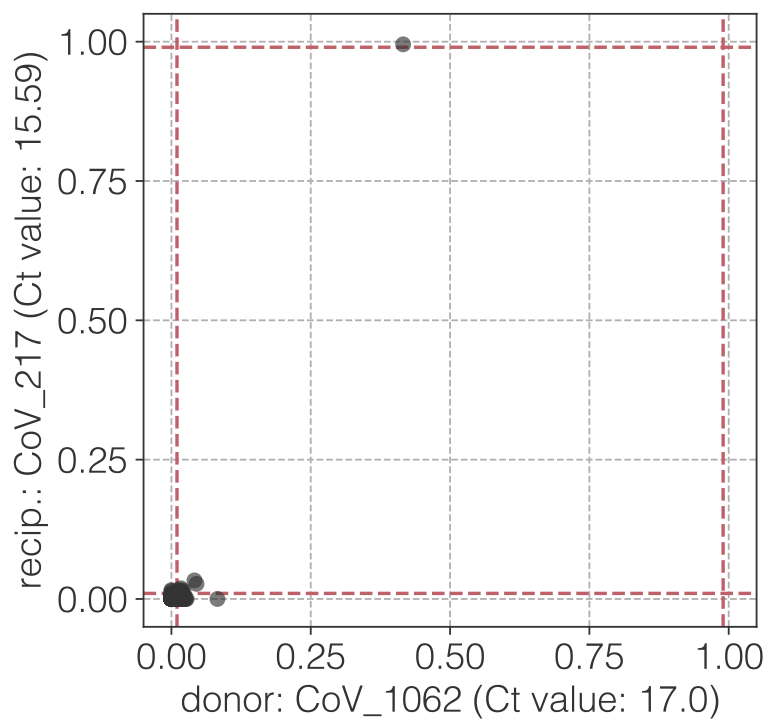
az

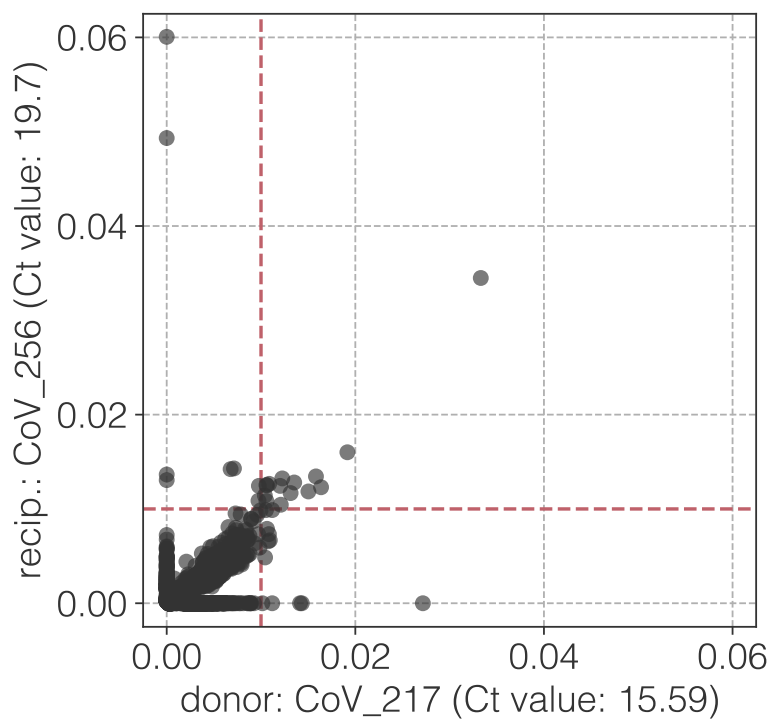
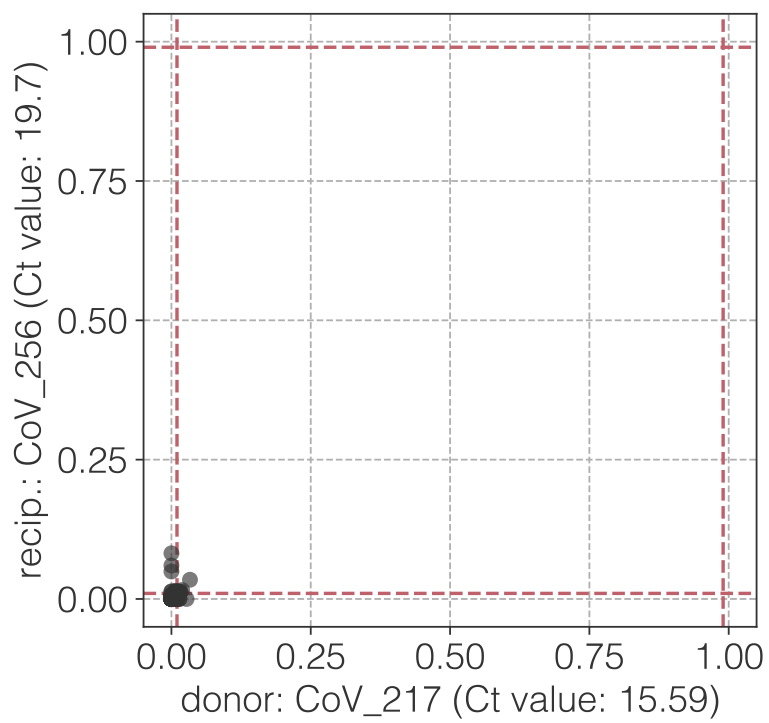
ba

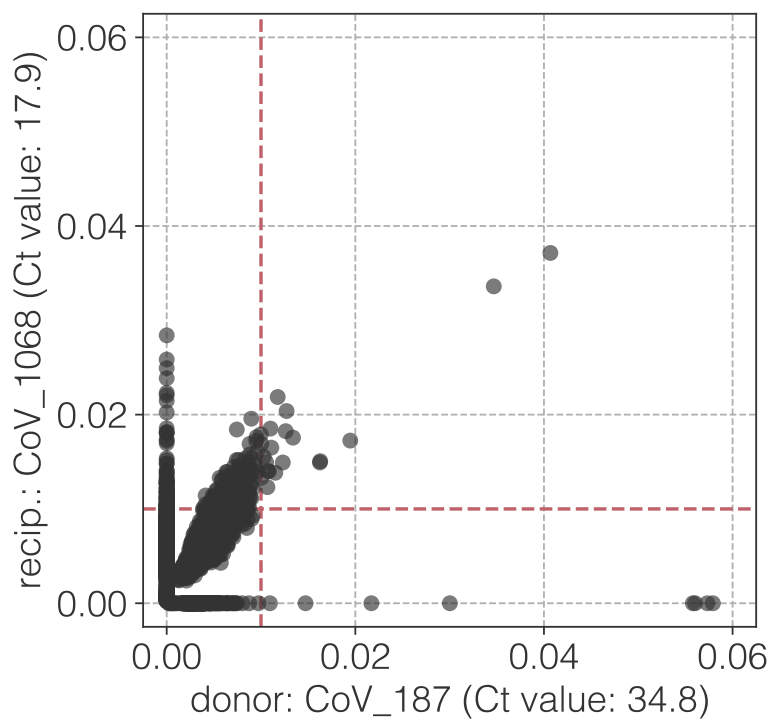
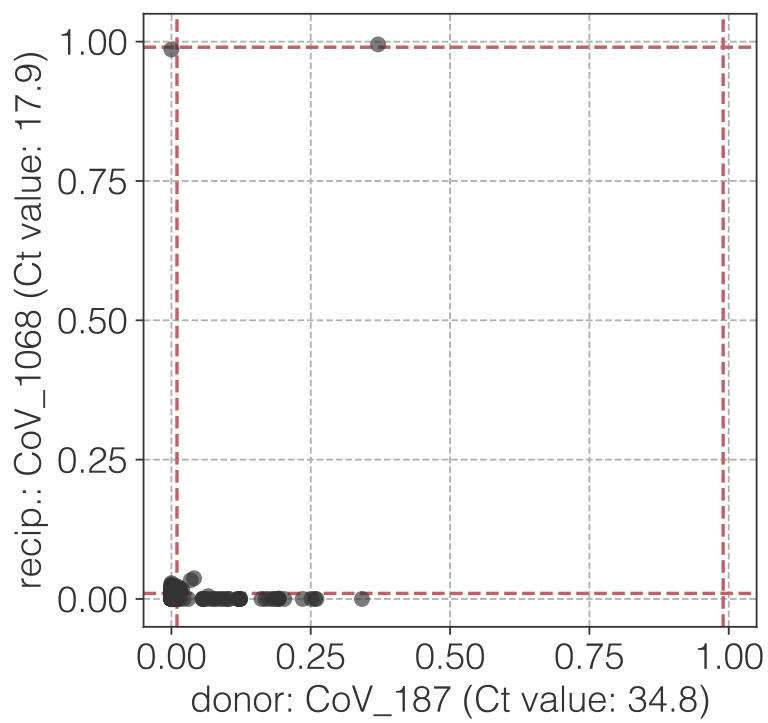
bb

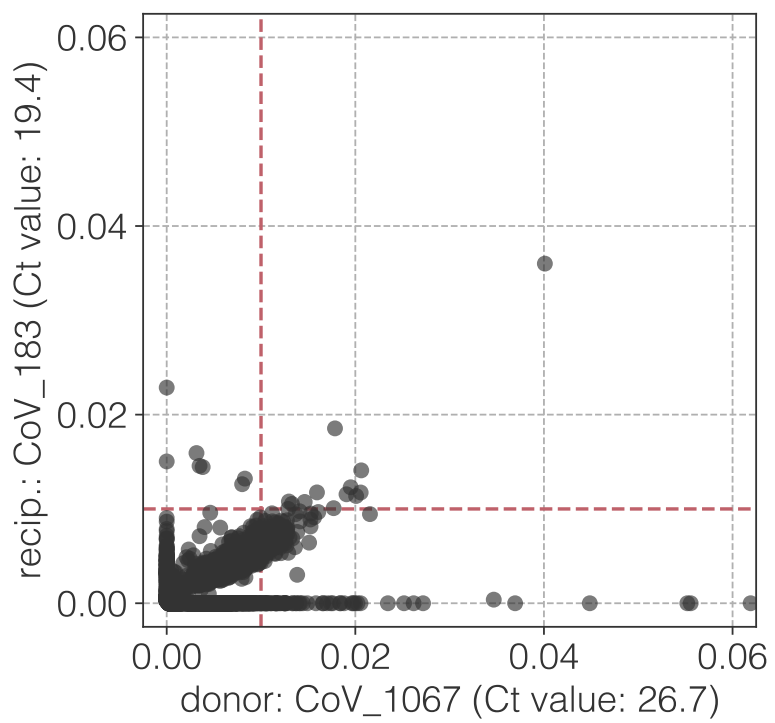
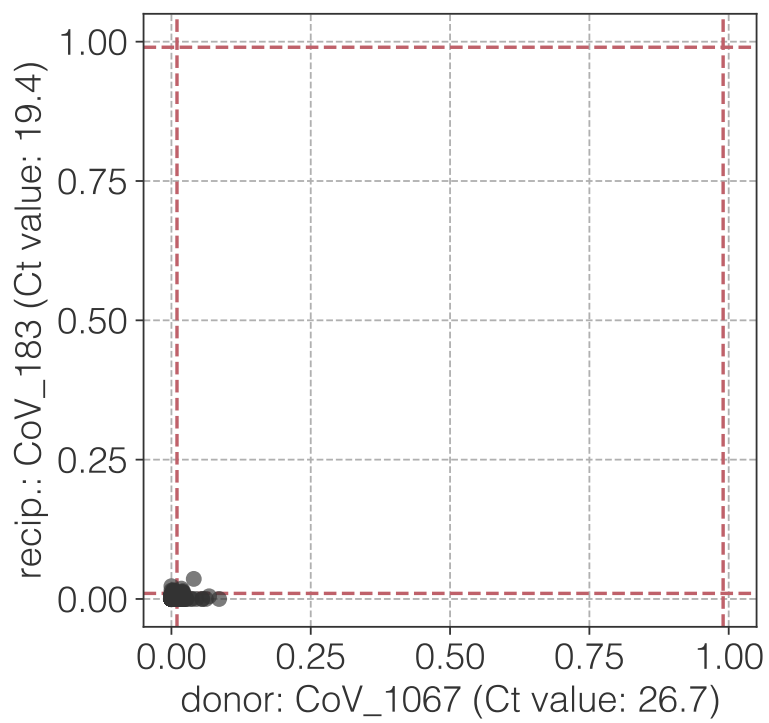
bc

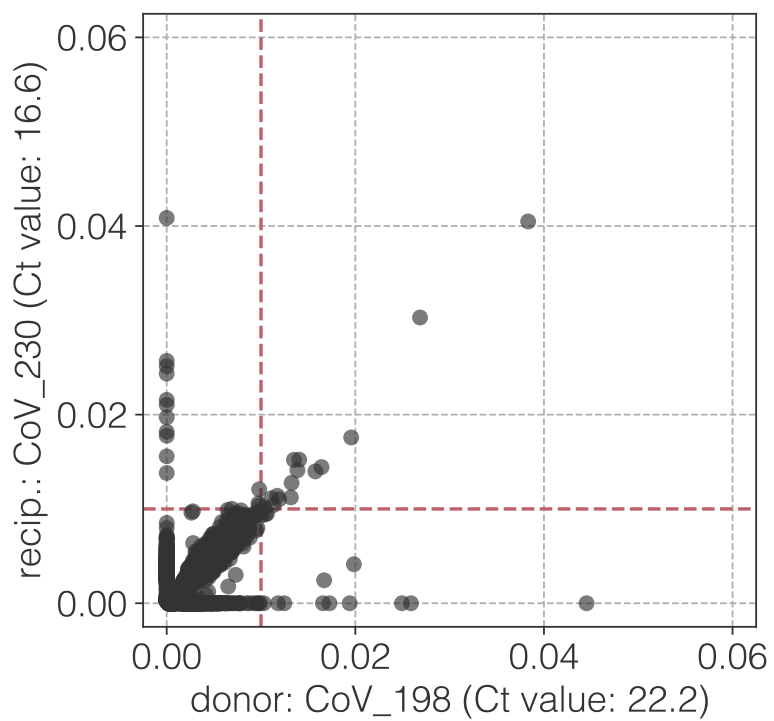
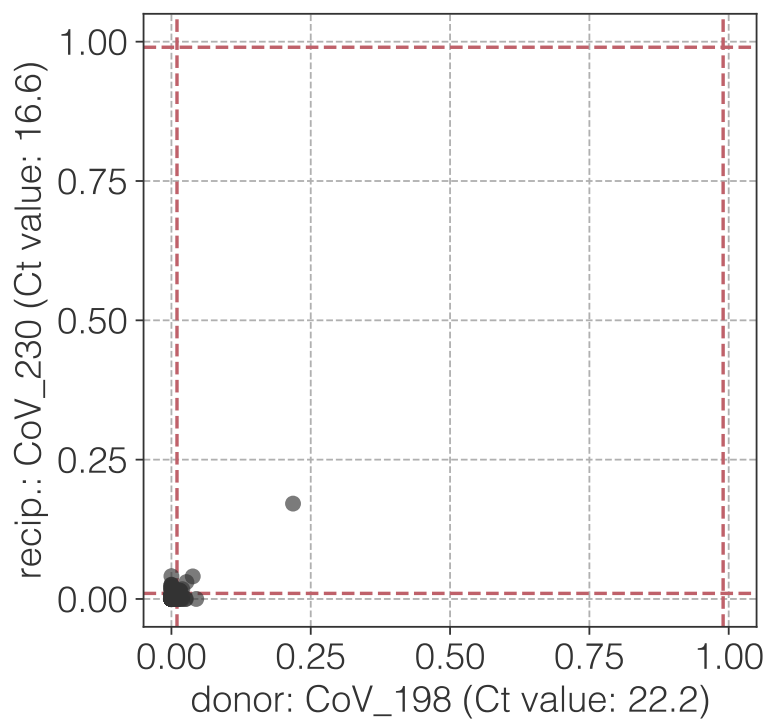
bd

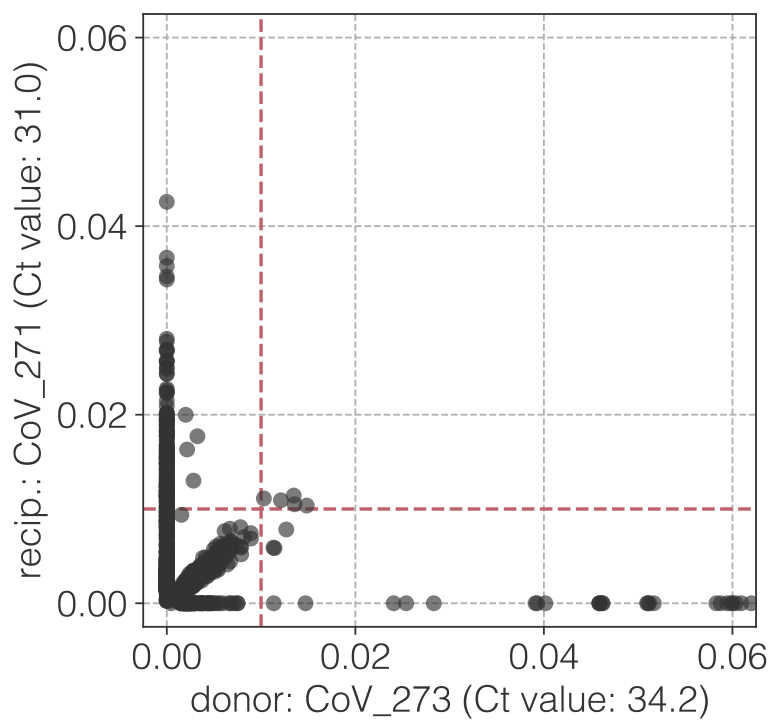
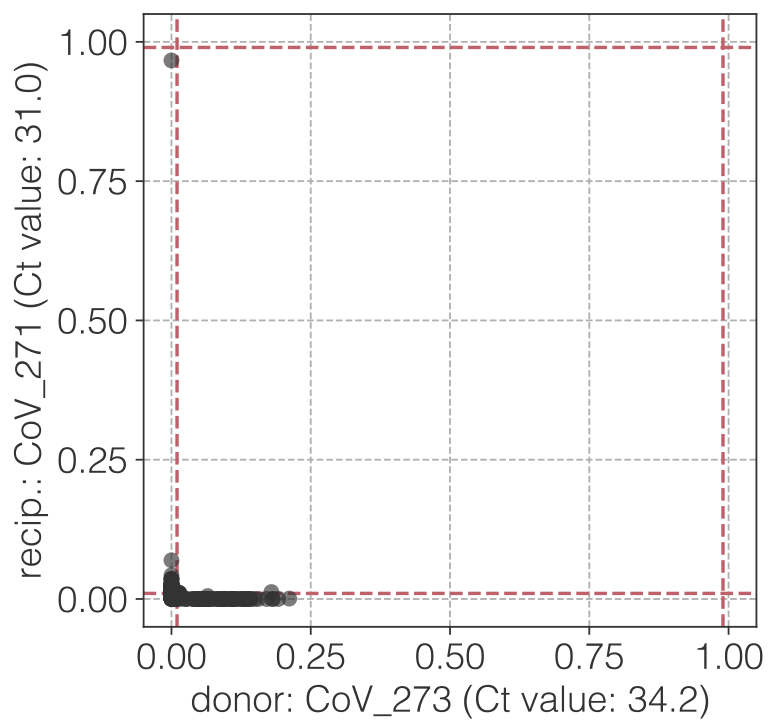
be

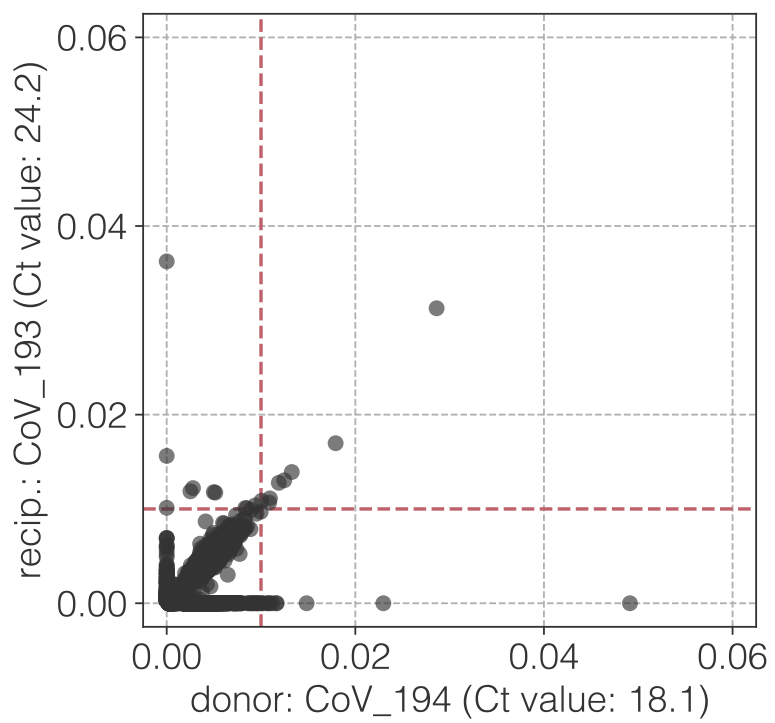
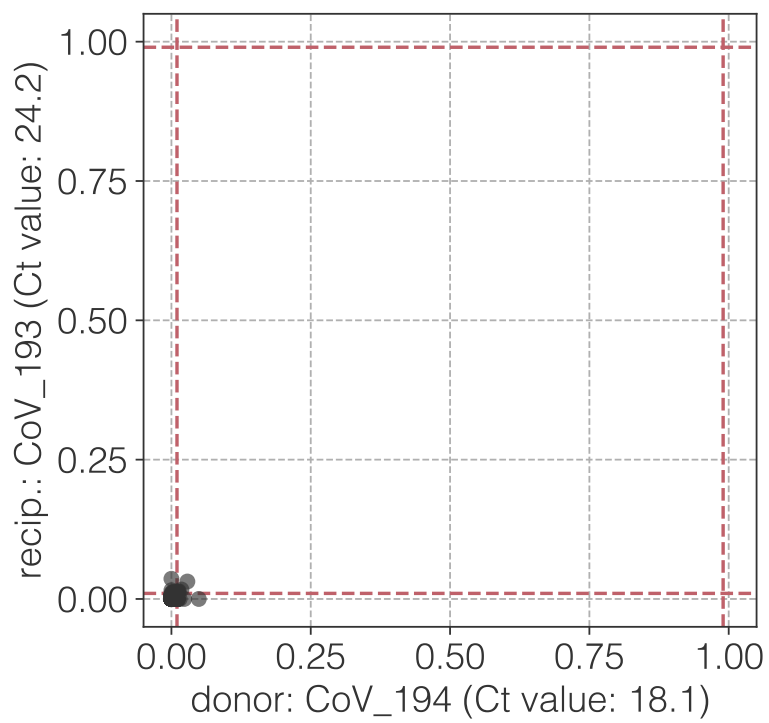
bf

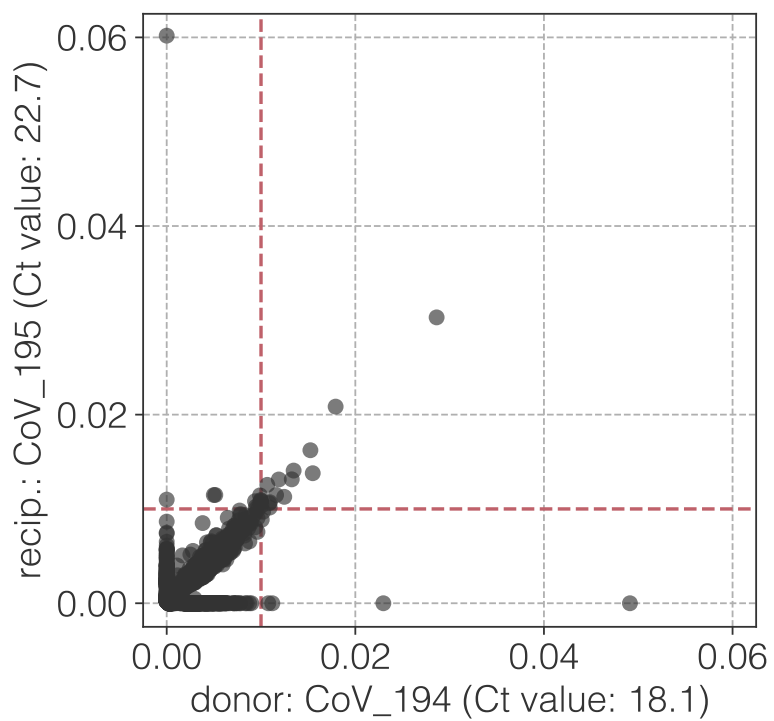
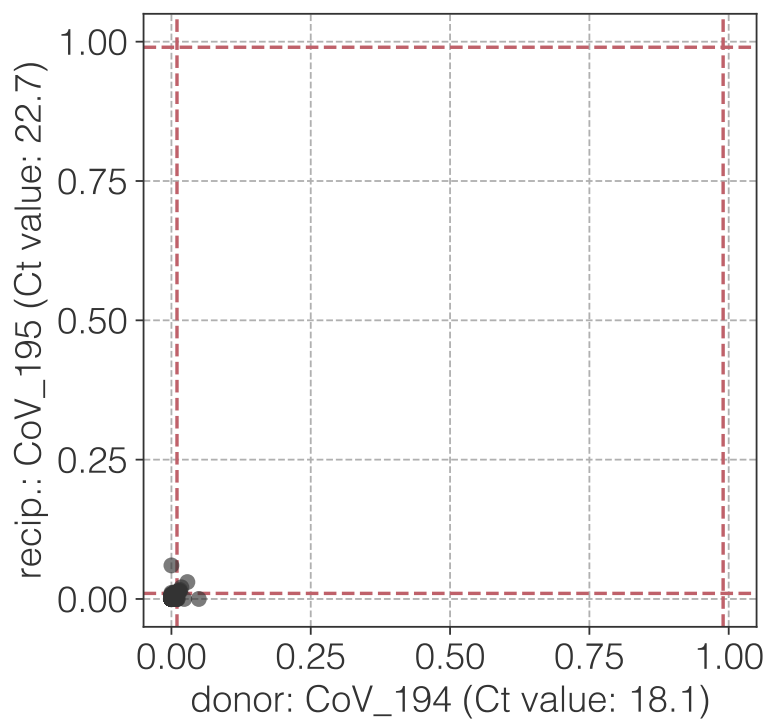
bg

bh

bi

bj

bk

bl

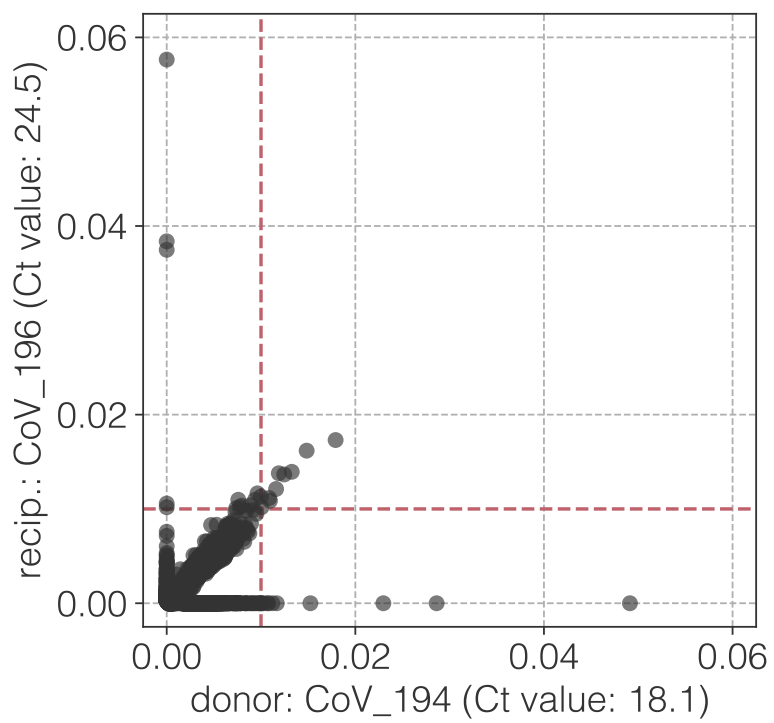
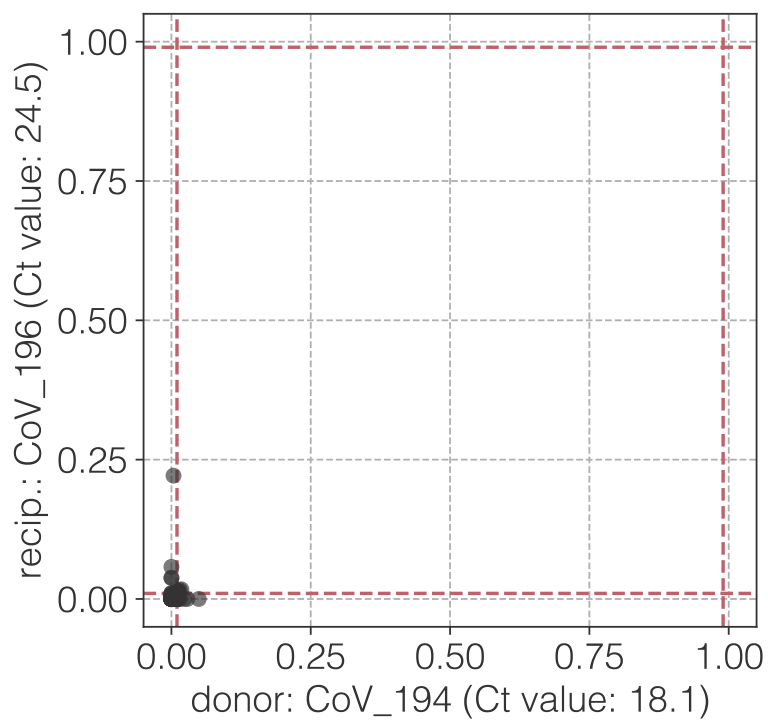
bm

Figure S2. All iSNVs observed in either donor and/or recipient of all 39 epidemiologically confirmed transmission pairs. Donor iSNV frequency is shown on the x-axis and recipient iSNV frequency is shown on the y-axis. Low-frequency iSNVs are highlighted in the panels on the right. Red-dashed lines show the 1% variant calling threshold. iSNV frequencies are based on variant calling relative to donor-specific reference sequences. Cycle threshold (Ct) values associated with the donor and recipient samples are provided when available. Note that high Ct samples tend to have a large number of high-frequency iSNVs, while low Ct samples only have few, if any iSNVs that exceed 6%.

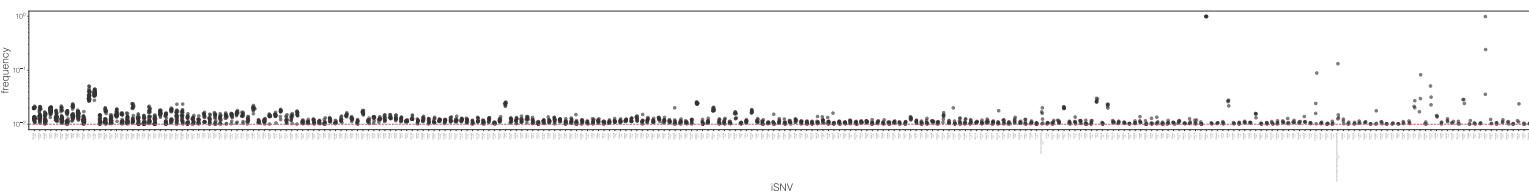
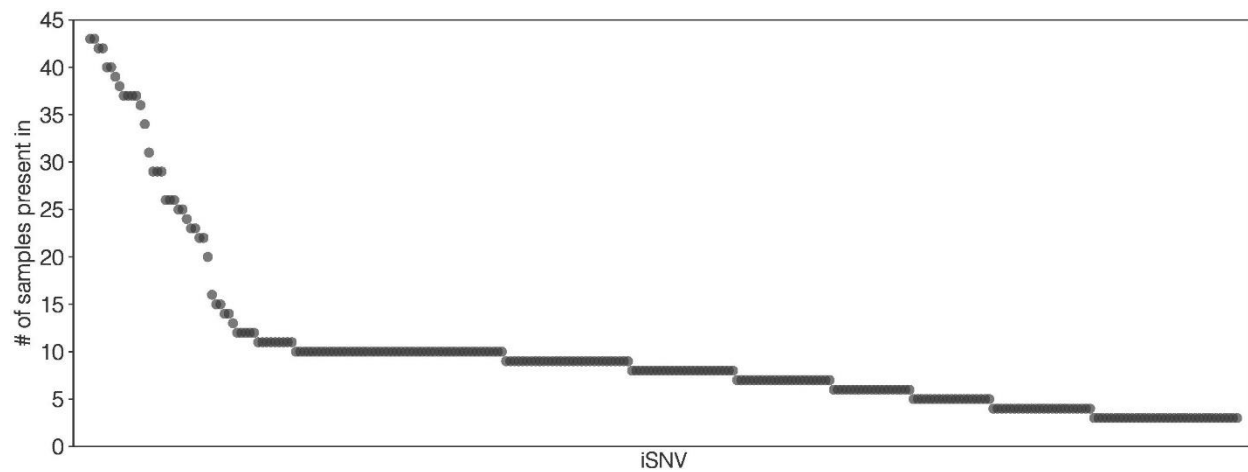


Figure S3. Allele frequencies for all iSNVs observed in at least 3 of the 43 samples involved in the 39 transmission pairs. iSNVs are ordered by the number of samples they are found in. Each dot shows the allele frequency of that iSNV in a given sample. Red dashed line shows the 1% variant calling threshold. Allele frequencies are based on variant calling relative to Wuhan/Hu-1.



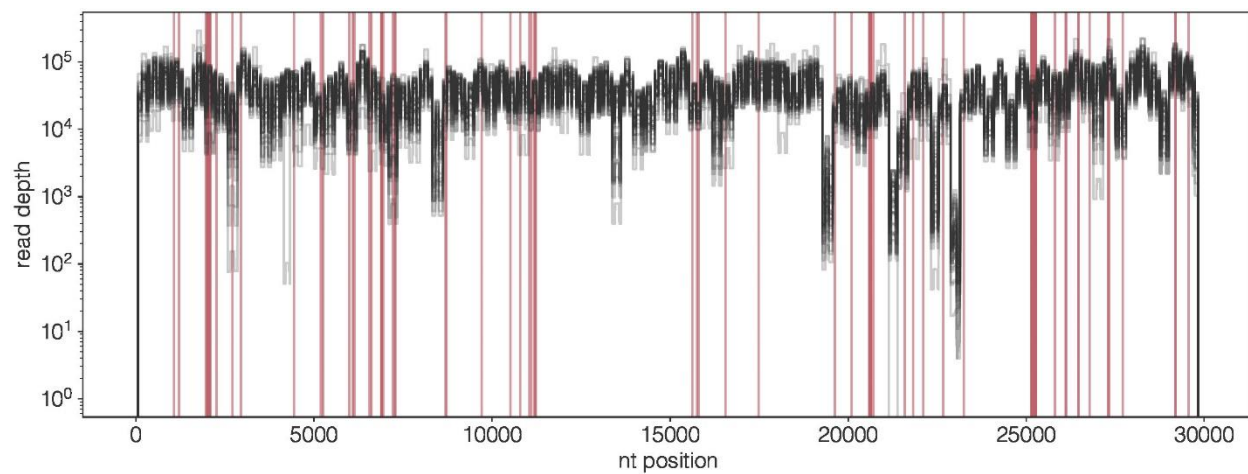


Figure S5. Read depth across the SARS-CoV-2 genome (Wuhan/Hu-1) for each of the 43 samples involved in the 39 transmission pairs calculated after adjusting for overlapping reads and trimming amplicon primers from the publicly available BAM files (black lines). Vertical red lines indicate the position in the genome of each iSNV (read frequency 1-99%) observed in at least 10 of the 43 samples.

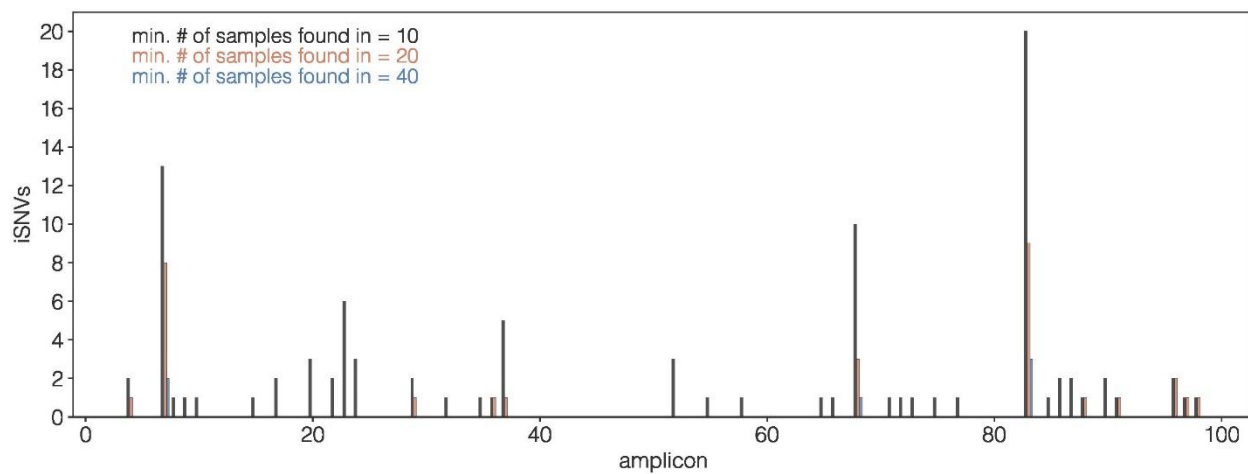


Figure S6. Number of iSNVs (read frequency 1-99%) per amplicon that were observed in at least 10 (black), at least 20 (red), or at least 40 (blue) of the 43 samples involved in the 39 transmission pairs. Amplicon assignments were based on the genome region between the end of the positive strand amplicon and the beginning of the negative strand amplicon. Variants falling in a genome region assigned to multiple amplicons were counted in both.

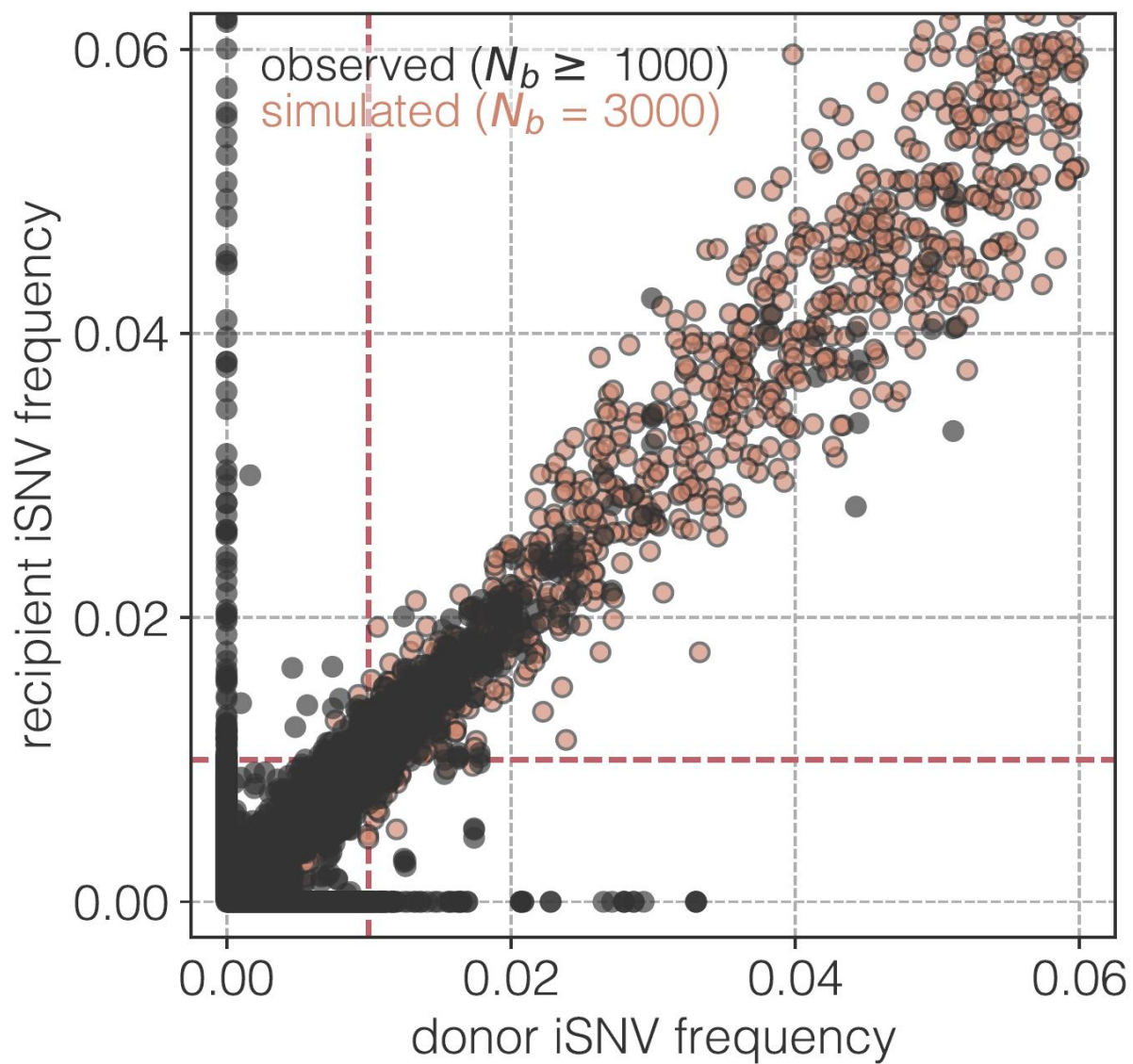


Figure S7. Patterns of shared viral genetic diversity between transmission pairs under the assumption of a large bottleneck of $N_b = 3000$ (red dots). As in Figure 1F, black dots show all iSNVs observed in either the donor and/or recipient for all transmission pairs with an estimated bottleneck size of ≥ 1000 at a variant calling threshold of 1%.

donor	recipient	1%BottleneckSize_mle	1%BottleneckSize_lower95	1%BottleneckSize_upper95	3%BottleneckSize_mle	3%BottleneckSize_lower95	3%BottleneckSize_upper95	6%BottleneckSize_mle	6%BottleneckSize_lower95	6%BottleneckSize_upper95
3	143	98	61	157	1	1	13	1	1	29
3	146	89	54	144	1	1	13	1	1	29
146	147	1147	390	2605 NaN	NaN	NaN	NaN	NaN	NaN	
146	150	5457	2619	9864 NaN	NaN	NaN	NaN	NaN	NaN	
146	157	3988	1856	7358 NaN	NaN	NaN	NaN	NaN	NaN	
146	159	10000	6765	10000 NaN	NaN	NaN	NaN	NaN	NaN	
146	172	3268	1438	6250 NaN	NaN	NaN	NaN	NaN	NaN	
146	1056	835	403	1519 NaN	NaN	NaN	NaN	NaN	NaN	
150	162	85	50	143	26	7	83	1	1	37
159	168	374	206	628	126	14	706 NaN	NaN	NaN	
159	169	345	185	593	127	14	715 NaN	NaN	NaN	
162	161	213	117	366	50	11	206	1	1	181
171	180	55	37	79	6	2	18	1	1	8
180	197	62	42	91	12	4	31	1	1	9
187	1068	7	6	9	2	2	2	1	1	1
194	193	158	61	385	1	1	287 NaN	NaN	NaN	
194	195	351	160	681	1	1	287 NaN	NaN	NaN	
194	196	153	66	341	1	1	287 NaN	NaN	NaN	
198	230	200	97	384	156	13	760	143	4	951
217	256	931	388	1864	10000	186	10000 NaN	NaN	NaN	
273	271	2	2	3	1	1	1	1	1	1
1056	166	24	17	34	2228	137	9773 NaN	NaN	NaN	
1056	171	19	13	27	222	7	2076 NaN	NaN	NaN	
1056	176	33	24	48	2897	175	9999 NaN	NaN	NaN	
1056	1057	6304	5021	7792	185	7	1790 NaN	NaN	NaN	
1056	1067	9109	7158	9999	4105	244	9999 NaN	NaN	NaN	
1057	175	23	17	32	15	5	45 NaN	NaN	NaN	
1057	177	7	6	9	1	1	1 NaN	NaN	NaN	
1057	167	9	7	12	2	2	3 NaN	NaN	NaN	
1057	1058	54	48	62	2	2	3 NaN	NaN	NaN	
1058	1059	1681	1305	2125	2370	115	9999 NaN	NaN	NaN	
1058	1063	1978	1538	2497	818	47	3830 NaN	NaN	NaN	
1058	1064	2994	2372	3719	317	25	1447 NaN	NaN	NaN	
1059	1062	10000	8600	10000	5483	322	9999 NaN	NaN	NaN	
1059	1065	10000	7892	10000	1885	117	8267 NaN	NaN	NaN	
1062	217	19	14	25	3	2	8	1	1	3
1062	218	18	14	25	3	2	8	1	1	3
1062	219	14	10	19	5	2	12	1	1	3
1067	183	10	7	15	6	2	25	1	1	42

Data file S1. CSV file providing transmission bottleneck size estimates for each of the 39 transmission pairs analyzed by Popa *et al.* Transmission bottleneck size estimates are provided using a 1% variant calling threshold, a 3% variant calling threshold, and a 6% variant calling threshold. At each threshold, the maximum likelihood estimate for N_b is provided, along with the lower and upper bounds of the 95% confidence interval.

Chapter 5

Full genome viral sequences inform patterns of SARS-CoV-2 spread into and within Israel

The following *Article*, published in *Nature Communications* in November 2020 was written in collaboration with Dr. Adi Stern at Tel Aviv University. Our goal was to leverage consensus sequence data to better understand the spread of SARS-CoV-2 into and within Israel. Primarily, our role in the project was to conduct the phylodynamic analyses used to infer the epidemiological parameters of SARS-CoV-2 in Israel in early 2020. Particularly, we highlighted the association between the implementation of non-pharmaceutical interventions and a decrease in the reproductive number in the region. Additionally, we showed that the epidemiological dynamics were dominated by superspreading, such that <10% of infected individuals were responsible for 80% of observed transmissions.

5.1 M.A.M. Contributions

Conceptualization, Validation, Formal analysis (**Figure 4-6, Figure S4-S7, S9-11, Table S3-S12**), Investigation (**Figure 4-6, Figure S4-S7, S9-11, Table S3-S12**), Writing -

Original Draft, Writing - Review & Editing, Visualization (**Figure 4-6, Figure S4-S7, S9-11**).

5.2 Published Manuscript

Reproduced with permission from Springer Nature.

ARTICLE

<https://doi.org/10.1038/s41467-020-19248-0>

OPEN

Full genome viral sequences inform patterns of SARS-CoV-2 spread into and within Israel

Danielle Miller^{1,16}, Michael A. Martin^{2,3,16}, Noam Harel^{1,16}, Omer Tirosh^{1,16}, Talia Kustin^{1,16}, Moran Meir¹, Nadav Sorek⁴, Shiraz Gefen-Halevi⁵, Sharon Amit⁵, Olesya Vorontsov⁶, Avraham Shaag⁶, Dana Wolf⁶, Avi Peretz^{7,8}, Yonat Shemer-Avni⁹, Diana Roif-Kaminsky¹⁰, Naama M. Kopelman¹¹, Amit Huppert^{12,13}, Katia Koelle^{2,14} & Adi Stern^{1,15}✉

Full genome sequences are increasingly used to track the geographic spread and transmission dynamics of viral pathogens. Here, with a focus on Israel, we sequence 212 SARS-CoV-2 sequences and use them to perform a comprehensive analysis to trace the origins and spread of the virus. We find that travelers returning from the United States of America significantly contributed to viral spread in Israel, more than their proportion in incoming infected travelers. Using phylodynamic analysis, we estimate that the basic reproduction number of the virus was initially around 2.5, dropping by more than two-thirds following the implementation of social distancing measures. We further report high levels of transmission heterogeneity in SARS-CoV-2 spread, with between 2-10% of infected individuals resulting in 80% of secondary infections. Overall, our findings demonstrate the effectiveness of social distancing measures for reducing viral spread.

¹The Shmunis School of Biomedicine and Cancer Research, George S. Wise Faculty of Life Sciences, Tel Aviv University, Tel Aviv, Israel. ²Department of Biology, Emory University, Atlanta, GA, USA. ³Population Biology, Ecology, and Evolution Graduate Program, Laney Graduate School, Emory University, Atlanta, GA, USA. ⁴Microbiology Laboratory, Assuta Ashdod University-Affiliated Hospital, Ashdod, Israel. ⁵Clinical Microbiology Laboratory, Sheba Medical Center, Ramat-Gan, Israel. ⁶Clinical Virology Unit, Hadassah Hebrew University Medical Center, Jerusalem, Israel. ⁷The Azrieli Faculty of Medicine, Bar-Ilan University, Safed, Israel. ⁸Clinical Microbiology Laboratory, The Baruch Padeh Medical Center, Poriya, Tiberias, Israel. ⁹Clinical Virology Laboratory, Soroka Medical Center and the Faculty of Health Sciences, Ben-Gurion University of the Negev, Beer-Sheva, Israel. ¹⁰Microbiology Division, Barzilai University Medical Center, Ashkelon, Israel. ¹¹Department of Computer Science, Holon Institute of Technology, Holon, Israel. ¹²Bio-statistical and Bio-mathematical Unit, The Gertner Institute for Epidemiology and Health Policy Research, Chaim Sheba Medical Center, 52621 Tel Hashomer, Israel. ¹³School of Public Health, The Sackler Faculty of Medicine, Tel-Aviv University, 69978 Tel Aviv, Israel. ¹⁴Emory-UGA Center of Excellence of Influenza Research and Surveillance (CEIRS), Atlanta, GA, USA. ¹⁵Edmond J. Safra Center for Bioinformatics, Tel Aviv University, Tel Aviv, Israel. ¹⁶These authors contributed equally: Danielle Miller, Michael A. Martin, Noam Harel, Omer Tirosh, Talia Kustin. ✉email: sternadi@tauex.tau.ac.il

In December 2019, an outbreak of severe respiratory disease was identified in Wuhan, China¹. Shortly later, the etiological agent of the disease was identified as severe acute respiratory syndrome coronavirus 2 (SARS-CoV-2)^{2,3}, and the disease caused by the virus was named coronavirus disease 19 (COVID-19). The virus has since spread rapidly across the globe, causing a WHO-declared pandemic with social and economic devastation in many regions of the world⁴. The infectious disease research community has quickly stepped up to the task of characterizing the virus and its replication dynamics, describing its pathogenesis, and tracking its movement through the human population. Parameterized epidemiological models have been particularly informative of how this virus has spread with and without control measures in place, e.g., ref. 5, and have been used to project viral spread both in the short-term⁶ and in the more distant future⁷.

Along with epidemiological analysis based on case reports and COVID-19 death data, sequencing of viral genomes has become a powerful tool in understanding and tracking the dynamics of infections^{8,9}. So-called genomic epidemiology allows for effective reconstruction of viral geographical spread as well as estimation of key epidemiological quantities such as the basic reproduction number of a virus, its growth rate and doubling time, and patterns of disease incidence and prevalence. Such insights have been used to inform policy makers during various pathogen outbreaks, as occurred for example in the 2014–2016 outbreak of Ebola virus in West Africa^{10,11} and during this current SARS-CoV-2 pandemic^{12,13}.

Here, we set out to sequence SARS-CoV-2 from samples across the state of Israel, with the aim of gaining a better understanding of introductions of the virus into Israel, spread of the virus inside the country, and the epidemiology of the disease, including (a) the basic reproduction number of the virus before and after social distancing measures were implemented, and (b) the extent of viral superspreading within Israel. As pointed out recently¹⁴, caution should be exercised when interpreting viral dynamics based on genetic data only. We thus incorporated here extensive, high-resolution epidemiological data that exist regarding the outbreak in Israel.

The first confirmed cases of SARS-CoV-2 infection in Israel were reported in mid-February, followed by many identified SARS-CoV-2 cases in travelers returning to Israel mainly from Europe and the United States. Growth in the number of verified

cases rapidly ensued, which led to increased measures of social distancing, including the cessation of passenger flights to Israel, school closure, and eventually a near complete lockdown across the entire state of Israel. Quarantining of returning travelers from Europe was implemented between February 26 and March 4, 2020, and subsequently all incoming travel to Israel (including from the U.S.) was arrested on March 9. In the meantime, the rate of testing was ramped up, eventually reaching a rate of more than 1500 tests per million people per day. The reported daily incidence and reported numbers of daily severe cases peaked around mid-April and dropped steadily up to the time of this manuscript's initial submission (May 2020). Despite this knowledge, many questions remain: Which of the multiple SARS-CoV-2 introductions resulted in sustained local transmission? How did the virus spread across the state? What was the magnitude of the virus's reproduction potential within Israel, and to what extent did control measures mitigate its spread through March–April?

Here, through a comprehensive set of phylogenetic and phylodynamic analyses, we quantitatively address these questions. We show that travelers from the U.S. contributed significantly more to viral spread as compared to their proportion in incoming infected travelers. We use a phylodynamic approach to estimate the basic reproduction number of the virus, and show a substantial reduction in viral spread following the implementation of social distancing measures. Finally, we report high levels of transmission heterogeneity in SARS-CoV-2 spread, with between 2% and 10% of infected individuals resulting in 80% of secondary infections.

Results and discussion

To gain a better understanding of the dynamics of SARS-CoV-2 spread into and within Israel, we sequenced the virus from a cohort of patients representing a random sample across Israel, resulting in 212 full-genome SARS-CoV-2 sequences (Methods). A total of 224 unique single nucleotide variants (SNVs) were identified between the Wuhan reference sequence and this set of sequences from Israel. Figure 1 shows the distribution of identified SNVs along the genome and their counts in the sequenced samples. Of these SNVs, 141 were non-synonymous, 72 were synonymous, and the remaining 11 were in non-coding regions. One of the most abundantly detected SNVs was a non-synonymous variant D614G found in the spike protein, which

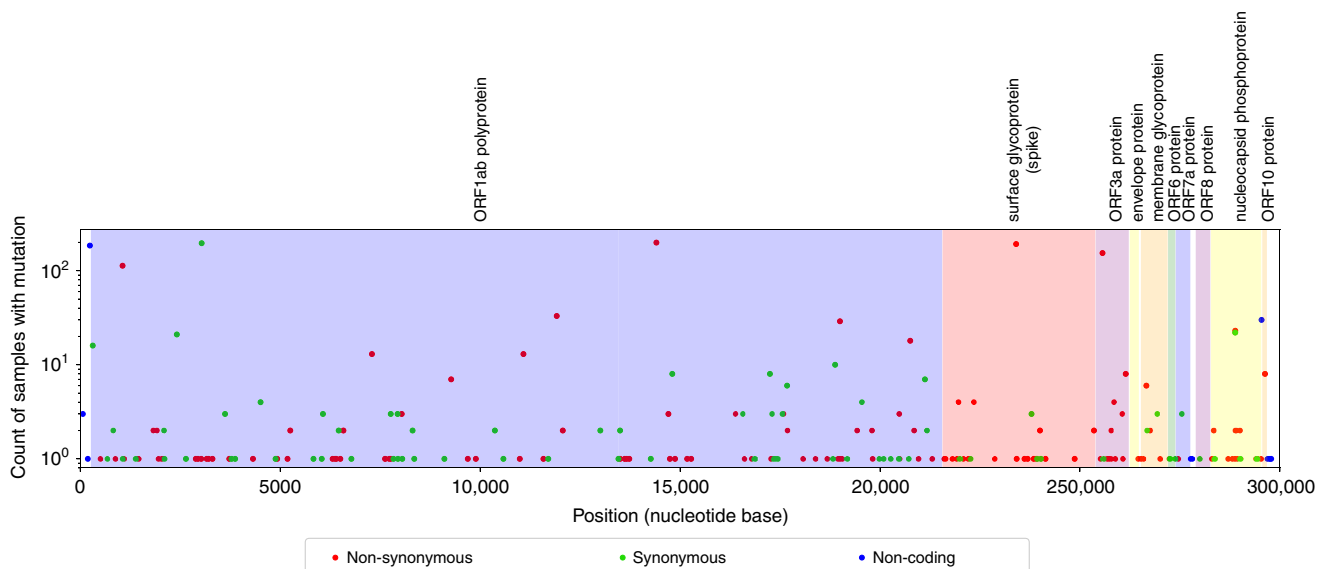


Fig. 1 Variation found in sequenced samples from Israel. The x-axis corresponds to the SARS-CoV-2 genome and the y-axis provides counts of identified SNVs across the viral genome. Source data are provided as a Source Data file.

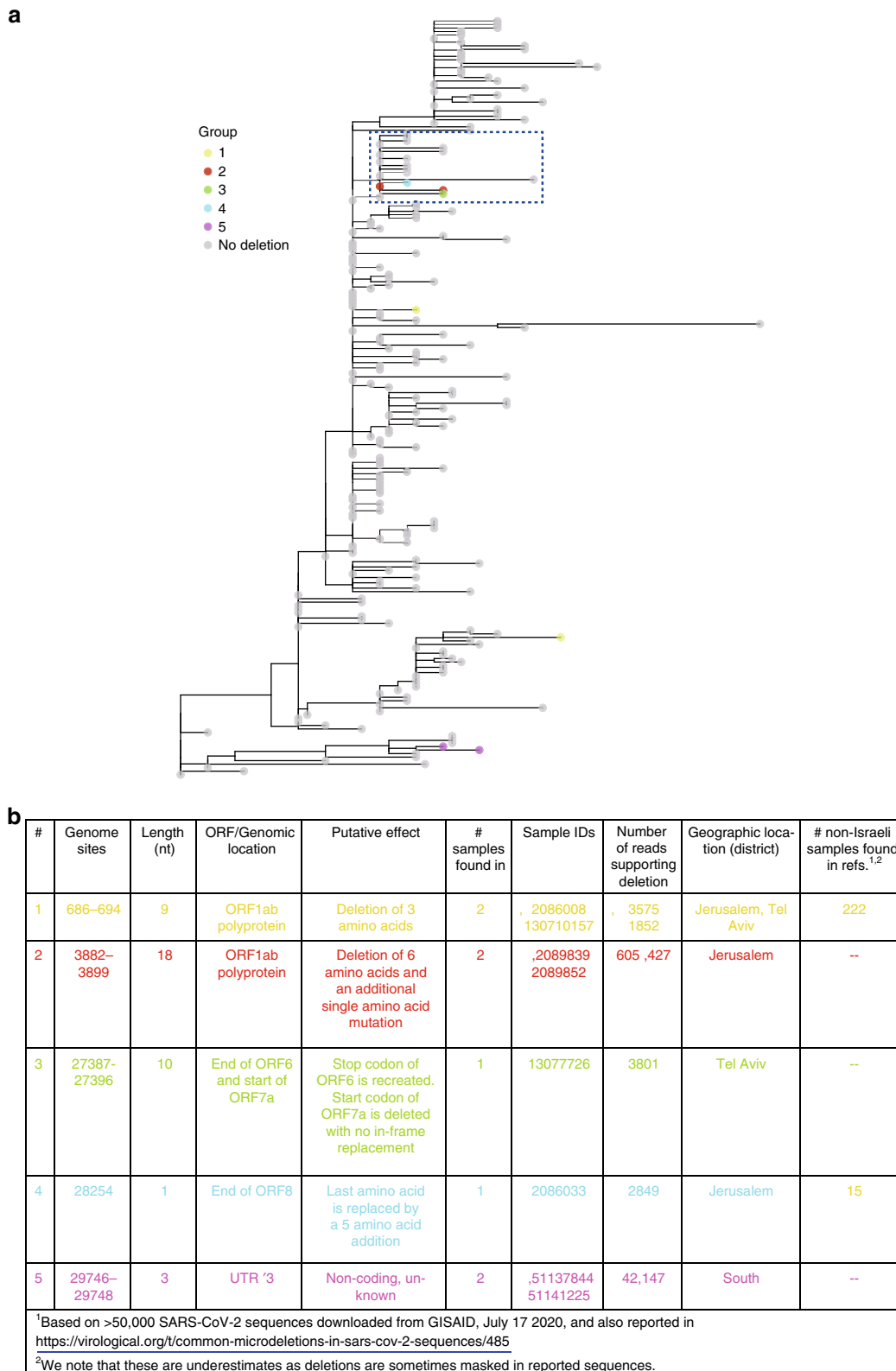


Fig. 2 Deletions found in Israeli samples. **a** Maximum-likelihood tree of Israeli sequences highlighting sequences found with deletions. Sequences are color-coded by the groups described in **b**. A clade with three independent deletions occurring in four samples is boxed. Source data are provided as a Source Data file.

was present in 90% of the sequences. This variant has generated much interest as it has been reported to potentially increase the transmissibility of the virus¹⁵. However, additional analyses have suggested that the observed increase in this variant’s frequency may be due to stochastic effects¹⁶.

We also found five different high confidence genomic deletions, spanning between 1 and 18 nucleotides (Fig. 2) (Methods). Each of these deletions was found in one to two samples. Three of the five deletions occur in multiples of three and are in-frame deletions or affect non-coding regions. Of the remaining two

deletions, deletion #3 spans ten nucleotides, and likely prevents the translation of ORF7a. Deletion #4 occurs at the end of ORF8 and causes the replacement of the last amino acid with an additional five amino acids. Notably, an 81-nucleotide in-frame deletion in ORF7a has been previously reported¹⁷, as has a 382-nucleotide deletion in ORF8 (ref. 18), suggesting that the virus is to some extent tolerant to deletions in these ORFs.

When focusing on deletions that occurred in two samples, we noted that deletion #5 was present in two related samples that were sampled 5 days apart from each other. Deletion #1, on the other hand, appeared in two samples located in very remote clades of the phylogeny. This deletion has been observed multiple times in various sequences with diverse genetic backgrounds, including sequences from many different countries across the world, suggesting that it has arisen multiple independent times (Fig. 2b). Deletions #2, #3, and #4 revealed an intriguing pattern: three independent deletions (one of which was present in two samples) were all part of the same clade that included 18 samples (Fig. 2). One non-synonymous SNV defined this clade: S2430R in ORF1b, which affects the non-structural protein NSP16. This protein has been reported to be a 2′O-methyltransferase that enhances evasion of the innate immune system¹⁹. To follow up on our finding of deletions in this clade, we examined a set of over 50,000 global sequences, and found that 137 sequences likely belong to the clade defined by S2340R, with eight of these sequences bearing short deletions (Supplementary Table 1). Interestingly, we found that the proportion of these unique deletions observed in the S2340R-defined clade was 5%, significantly higher than the proportion of unique deletions observed across the entire global tree (1.8%) ($P=0.01$; hypergeometric test), leading us to cautiously suggest that S2340R is associated with a higher rate of deletions.

While further in-depth investigation of SARS-CoV-2 indels is clearly needed, at this point we conjecture that the deletions we detected are neutral or to some extent deleterious, and that deletions in SARS-CoV-2 are likely to occur frequently given the number of deletions detected in our samples.

Origins and transmission patterns in Israel. We next set out to explore patterns of SARS-CoV-2 introduction into Israel. Figure 3 shows the time-resolved phylogeny inferred using 214 Israeli sequences (the 212 sequenced here and two additional ones sequenced previously) in addition to 4693 representative sequences from across the world. This phylogeny allowed us to characterize the major viral clades circulating within Israel and to infer the geographic sources and timing of virus introductions into the state. We found multiple introductions into Israel from both the U.S. and Europe, the latter including mainly the U.K., France, and Belgium. Over 70% of the clade introductions into Israel were inferred to have occurred from the U.S., while the remaining were mainly from Europe. To rule out that this result is due to biases in geographic sampling, we first note that in our sample, the number of sequences from Europe ($n=1991$) was higher than the number from the U.S. ($n=1195$). We further quantified sampling noise by bootstrapping the Israeli samples and exogenous samples, leading to confidence intervals ranging between 50% and 80% for U.S. clade importations (Methods). We noted considerably lower proportions of importations from the U.S. into other countries we examined (Supplementary Fig. 1), making it unlikely that our results arise from systematic biases of U.S. sequences relative to sequences from other regions. We validated the robustness of our inference to changes in underlying evolutionary model parameters and possible biases in ancestral state assignments, and found that any biases stemming from uncertainty in phylogenetic reconstruction are negligibly small

(Supplementary Fig. 2). Finally, we note that attribution¹⁶⁷ of an Israeli sequence to a U.S. clade was normally based on two to four shared mutations, making it exceedingly unlikely that parallel independent substitutions occurred that could alternatively explain these patterns. However, we acknowledge that additional sequencing may change some of the inferences we make here, as has been shown elsewhere²⁰.

Throughout the epidemic in Israel, very close monitoring of all incoming infected travelers was imposed, and reports show that only ~27% of infected returning travelers were from the U.S. (Supplementary Fig. 3). There is a strong discrepancy between this 27% estimate and the 70% estimate for clade introductions, and this discrepancy holds even when considering our lower bound bootstrap estimate of 50% for clade importations (mentioned above). This suggests that the travelers returning from the U.S. contributed substantially more to the spread of the virus in Israel than would be proportionally expected. This may have occurred due to the gap in policy that allowed returning non-European travelers to avoid quarantine until March 9, or due to different contact patterns of those who returned from the U.S. Moreover, by examining the timing of viral importation events from the U.S. into Israel, we found that up to 55% of the transmission chains in Israel (118 out of 214; Methods) could have been prevented had flights from the U.S. been arrested at the same time that flights from Europe were arrested (between February 26 and March 4, instead of by March 9).

As the pandemic spread, entry into Israel was restricted, and local transmission became dominant. Transmission patterns into and between five geographical regions in Israel (North district, Tel Aviv district, South coast district, Jerusalem district, and South district) are shown in Fig. 4. While most transmission occurred inside defined regions, transmission between distinct regions was also observed, such as, for example, movement between Jerusalem and the north district of Israel.

Phylodynamic modeling of viral spread in Israel. To estimate the basic reproduction number of SARS-CoV-2 in Israel initially and then following the implementation of social distancing measures, we performed coalescent-based phylodynamic inference using the PhyDyn program implemented in BEAST2 (Methods). We note that existing phylodynamic analyses of SARS-CoV-2, focusing on a number of different geographic regions across the world, have shown that the effective reproduction number of the virus has decreased over time, as quarantine and social distancing measures have been implemented^{21–23}. However, many of these analyses have to date modeled reductions in the reproduction number as stemming from the depletion of susceptible individuals²³, rather than from reductions in the basic reproduction number R_0 , the latter of which would be consistent with lowering of contact rates. Other analyses, particularly those that use the birth–death model approach for phylodynamic inference, have allowed for changes in R_0 over time^{21,22}, but cannot as easily accommodate structure in the infected host population (e.g., that some individuals are exposed but not yet infectious, and that transmission heterogeneity exists between infected individuals). Our phylodynamic analysis here, based heavily on existing coalescent-based model structures that have been applied to SARS-CoV-2²⁴, instead allows for this structure to be accommodated and for R_0 to change in a piecewise fashion over time.

Our phylodynamic analysis assumes an underlying susceptible–exposed–infected–recovered (SEIR)-type epidemiological model for SARS-CoV-2 transmission dynamics and explicitly incorporates transmission heterogeneity (Supplementary Fig. 4, Methods). Recent epidemiological analyses have estimated considerable

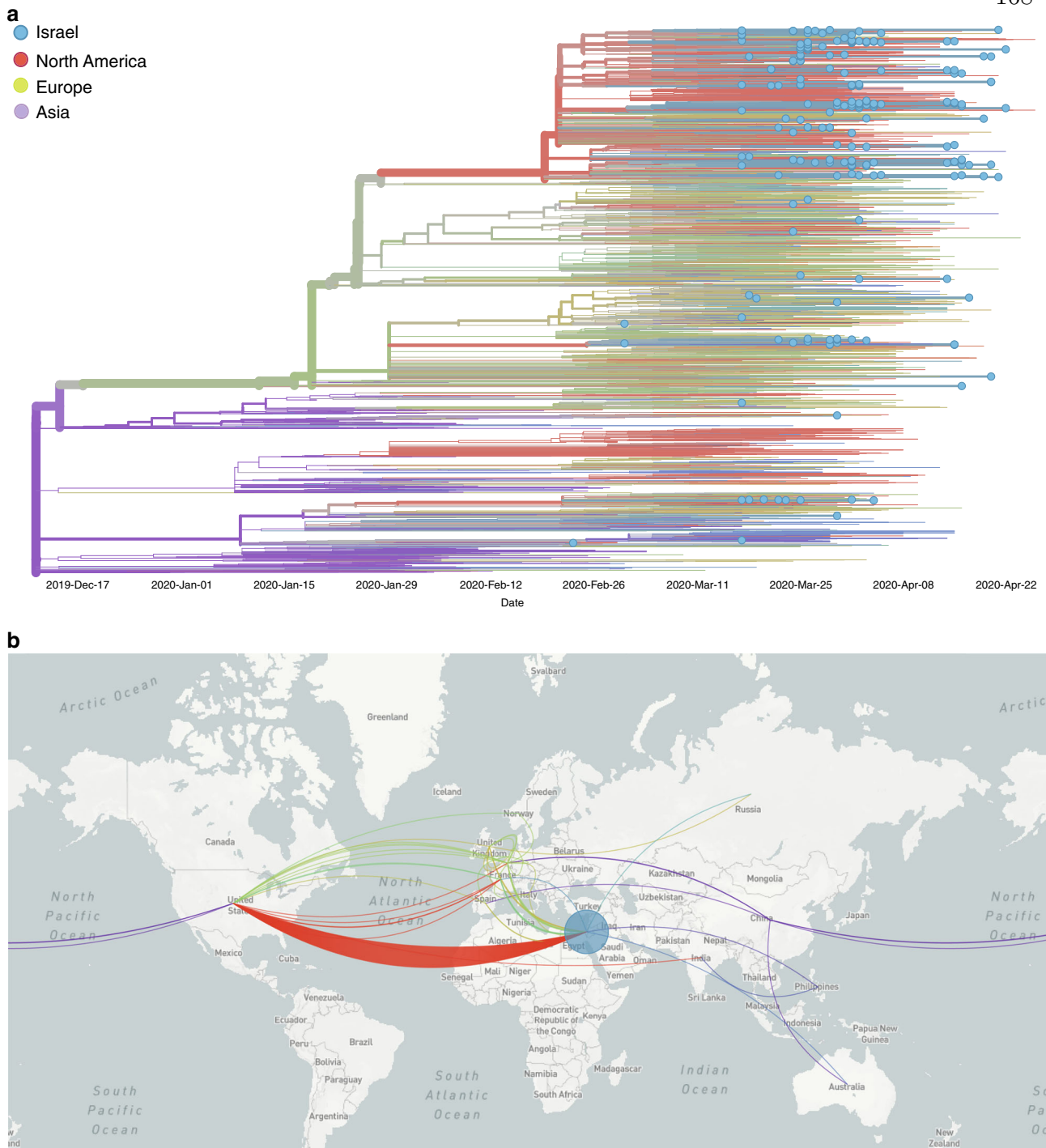


Fig. 3 Patterns of SARS-CoV-2 introduction into Israel. **a** Time-resolved phylogeny inferred using viral sequences from Israel (blue tips) and around the world (tips without dots). Lineages are colored by inferred region of circulation. Phylogeographic analysis reveals multiple introductions into Israel, mainly from the U.S. **b** Map of phylogenetically inferred introductions into Israel highlighting the dominance of the U.S. and to a lesser extent Europe as the geographic sources of SARS-CoV-2 introductions into Israel. Figure (including map) generated using NextStrain³². Source data are provided as a Source Data file.

levels of SARS-CoV-2 transmission heterogeneity, with ~7–10% of infected individuals estimated to be responsible for 80% of secondary infections^{25,26}. Instead of assuming a given level of transmission heterogeneity for Israel, we instead performed phylodynamic inference for the SEIR model across a range of transmission heterogeneities. Specifically, the SEIR-type model implemented two classes of infectious individuals, corresponding to a highly infectious subset of individuals (I_h) and a less

infectious subset of individuals (I_l). Exposed (E) individuals transitioned to I_h with a probability given by the parameter p_h , and transitioned to I_l with a probability given by $(1 - p_h)$. The relative transmission rate of I_h to I_l individuals was set such that the highly infectious class (I_h) was responsible for 80% of secondary cases. As such, we were able to modify the extent of transmission heterogeneity by modifying p_h . A p_h value of 0.8 implements a model with no transmission heterogeneity (as 80%

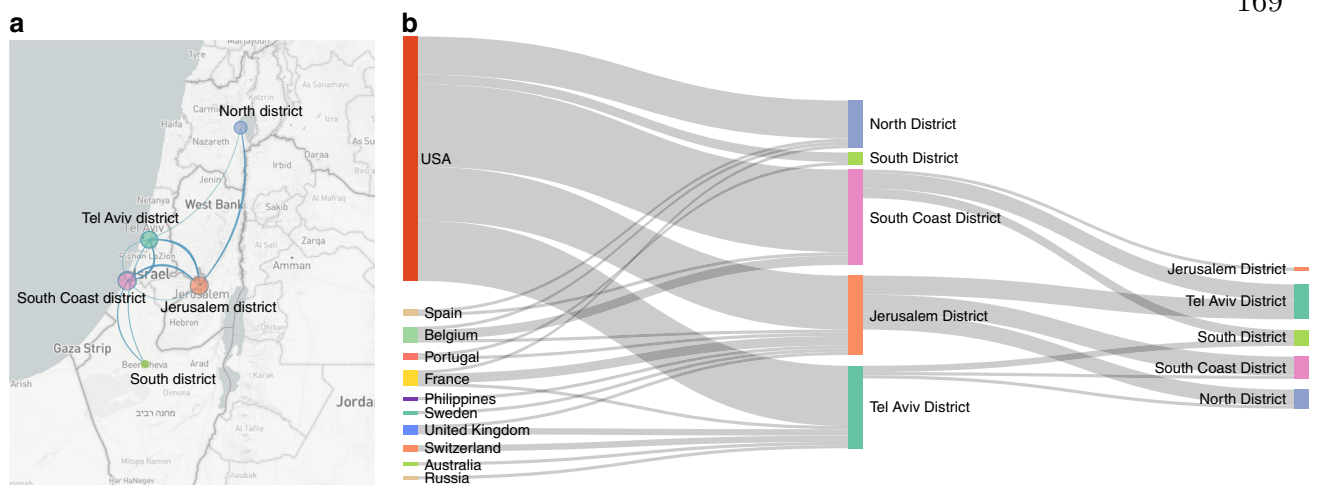


Fig. 4 Spread of SARS-CoV-2 into and within Israel. **a** Map of Israel with geographic locations of samples, and inferred spread inside Israel (blue lines). Figure generated using NextStrain³². **b** Inferred viral spread into and inside Israel, with directionality (left to right). Each line represents a transmission event inferred based on the phylogeny. Thicker lines indicate multiple transmission events. Source data are provided as a Source Data file.

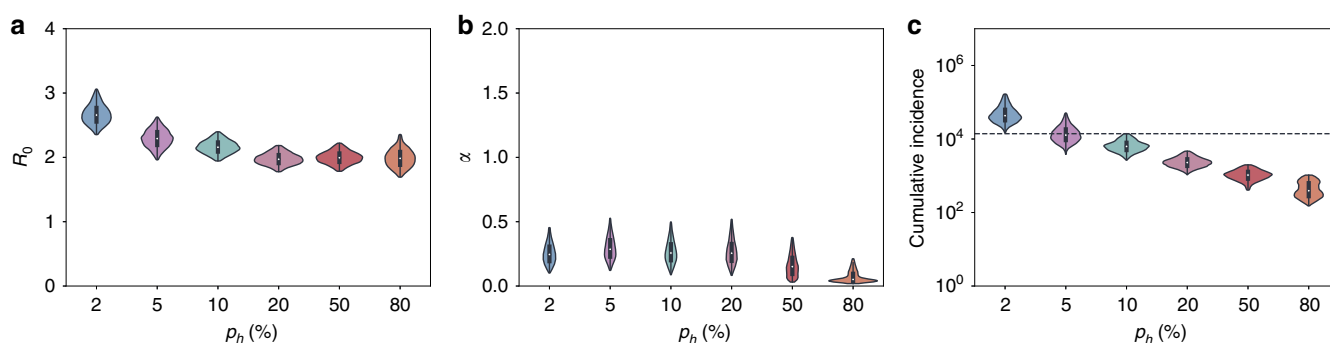


Fig. 5 Estimated epidemiological parameters and cumulative incidence across different levels of transmission heterogeneity. The parameter p_h gives the fraction of infected individuals that are responsible for 80% of secondary infections. Higher p_h values correspond to less transmission heterogeneity. **a** Estimated R_0 in Israel prior to March 19, 2020. **b** Estimated factor by which R_0 in Israel changed after March 19. **c** Estimated cumulative number of infected individuals in Israel on the date of the last sampled sequence (April 22, 2020). Horizontal dotted line at $N = 13,942$ shows the cumulative number of reported cases on April 22, 2020, as given by the ECDC (<https://opendata.ecdc.europa.eu/covid19/casedistribution/csv>). In **a–c**, only values that fall within the 95% highest posterior density intervals from the main MCMC chain are shown (total of 4751 data points). Violin plots show the kernel density estimation of the underlying distribution. The median value is denoted by a white dot and the black bar in the center of the violin defines the interquartile range. The black line stretched from the bar extends to the range of data that are not more than 1.5 times the interquartile range above the upper or below the lower quartile. Density is only plotted over the range of observed values. Results shown assume a time-varying migration rate estimated from a global maximum-likelihood phylogeny. Source data are provided as a Source Data file.

of the infected individuals are responsible for 80% of secondary infections), whereas a p_h value of 0.2 implements a model consistent with the 20/80 superspreading rule²⁷ with 20% of individuals being responsible for 80% of secondary infections. Values of p_h under 0.2 implement a model with even more extreme levels of transmission heterogeneity. The SEIR-type model we implemented further included terms for migration into and out of Israel; these terms enabled lineages in the phylogeny to transition out of Israel going backward in time (as would happen, in forward time, during an importation event). We considered two different functional forms for this migration term, one based on phylogenetically inferred timing of importations and the other assuming a simpler, constant rate of migration (Methods).

Using the migration rate form based on inferred importation times, we estimated R_0 prior to March 19 to be between 2.1 and 2.3 across the range of $p_h = 0.1–0.8$ (that is, 10–80%) with estimates increasing toward $R_0 = 3.0$ at high levels of superspreading ($p_h = 2\%$) (Fig. 5a). Across the full range of $p_h = 2–80\%$, we robustly estimated that quarantine measures had the effect of reducing R_0 by more than two-thirds ($\alpha = \sim 25\%$, where

R_0 following quarantine measures was given by α times R_0 prior to the implementation of these measures; Fig. 5b).

Figure 5c shows the cumulative number of SARS-CoV-2 cases by April 22, estimated by our phylodynamic analyses across the considered range of transmission heterogeneity. Estimates of the cumulative number of cases is highly sensitive to the level of assumed transmission heterogeneity, particularly at high levels of superspreading ($p_h = 2–10\%$). Comparison between these inferred cumulative cases and reported case numbers (dotted lines in Fig. 5c) indicates that SARS-CoV-2 transmission dynamics were driven by a high level of viral superspreading. Specifically, if we assume almost complete case reporting, our phylodynamic analysis indicates that between 5% and 10% of infections are responsible for 80% of secondary infections. With lower assumed levels of case reporting, less than 5% of infections would be responsible for 80% of secondary infections. Findings from the phylodynamic analyses were shown to be robust to the specific functional form of the migration rate that was assumed, as well as to the overall magnitude of migration across a broad range of values (Supplementary Figs. 5 and 6).

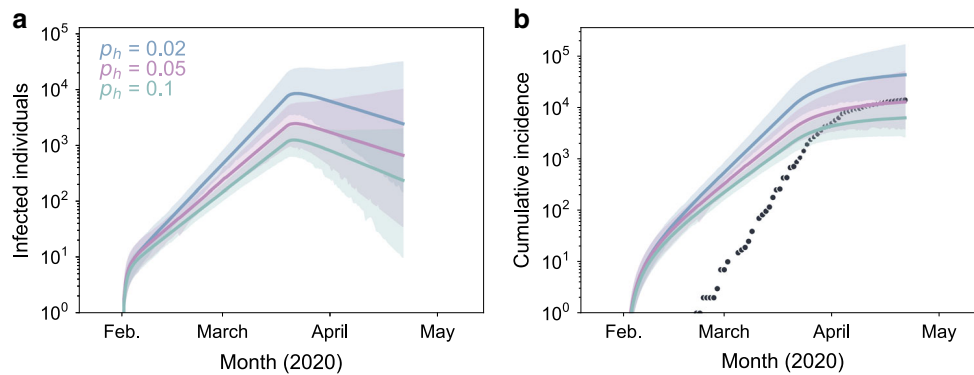


Fig. 6 Epidemiological dynamics inferred using phylodynamic analysis. **a** Estimated number of currently infected individuals ($I_t + I_n$) over time. **b** Estimated cumulative number of infected individuals. An infected individual is assumed to contribute to cumulative incidence at the end of their infectious period. Black dots show the cumulative number of reported cases in Israel over time. In **a** and **b**, lines show median estimates of models with different levels of transmission heterogeneity. Shaded regions represent the 95% highest posterior density region. Source data are provided as a Source Data file.

Phylodynamic analysis further allows us to visualize inferred epidemiological dynamics. In Fig. 6, we show inferred patterns of prevalence (Fig. 6a) and incidence (Fig. 6b) for three different assumed levels of viral superspreading. Inferred patterns of prevalence corroborate epidemiological findings that the number of cases started to decline in early April. Inferred patterns of cumulative incidence indicate that reporting rates were initially low but improved considerably over the time course of viral spread. The leveling off of cumulative incidence around late March/early April is observed in both the reported case data and in our inferred epidemiological dynamics, ground-truthing the results of our phylodynamic analyses.

Overall, our findings highlight the use of genomic data to effectively track the spread of an emerging virus using phylogenetic and phylodynamic approaches that have been developed to study viral outbreaks. We have found a relatively high proportion of genomes with short deletions, suggesting that such deletions arise frequently during SARS-CoV-2 replication and are to some extent tolerated by the virus. We succeeded in tracking the main transmission chains that led to SARS-CoV-2 spread in Israel, and applied phylodynamic analysis to infer the key epidemiological parameters governing its spread. Our results indicate that superspreading events drive the transmission dynamics of SARS-CoV-2, suggesting that focused measures to reduce contacts of select individuals/social events could mitigate viral spread. Finally, our results highlight how global connectivity allows for massive introductions of a virus and emphasize how border control and shelter-in-place restrictions are crucial for halting viral spread. Addendum September 2020: the authors would like to note that unfortunately, following the relaxation of social distance measures in May, case counts have substantially climbed and Israel has entered a second lockdown.

Methods

Ethics statement. An exemption from institutional review board approval was determined by the Israeli Ministry of Health as part of an active epidemiological investigation, based on the use of retrospective anonymous data only and no medical intervention. This included exemption from informed consent. The study was further approved by the Tel-Aviv University ethics committee (approval 0001274-1).

Details of samples and virus genome sequencing. With the aim of generating a random sample of viral infections across the entire country, a total of 213 samples were retrieved from six major hospitals in Israel spanning the entire geography of Israel from south to north (Table 1 and Supplementary Table 2).

We obtained RNA extracted from nasopharyngeal samples. Sequencing was performed based on the V3 Artic protocol (<https://artic.network/ncov-2019>).

Table 1 Summary of samples successfully sequenced.		
a		
Age group		
Age group	Number of samples	
0-9	8	
10-19	17	
20-29	42	
30-39	28	
40-49	26	
50-59	29	
60-69	31	
70-79	15	
80-89	11	
90 and up	3	
Unknown	2	
b		
Location and hospital		
Hospital	Geographic region	Number of samples
Barzilai Medical Center	South coast district	30
Samson Assuta Ashdod	South coast district	23
University Hospital		
Hadassah University Hospital - Ein Kerem	Jerusalem district	62
Poria Medical Center	North district	26
Sheba Medical Center	Tel-Aviv district	51
Soroka Medical Center	South district	20
c		
Sex		Number of samples
Female	101	
Male	111	
The table is divided by metadata information (a-c). Source data are provided as a Source Data file.		

Briefly, reverse transcription and multiplex PCR of 109 amplicons was performed, and adapters were ligated to allow for sequencing. All samples were run on an Illumina Miseq using 250-cycle V2 kits in the Technion Genome Center (Israel). Supplementary Table 13 contains all primer names and sequences as described in the Artic protocol.

Determining genome consensus sequences. Sequencing reads were trimmed using pTrimmer, a multiplexing primer trimming tool²⁸, and then aligned to the reference genome of SARS-CoV-2 (GenBank ID MN908947) using our AccuNGS pipeline²⁹, which is based on BLAST³⁰, using an e -value of 10^{-9} . The pipeline allows for consensus determination and variant calling. We considered substitutions at the consensus sequence (as compared to the reference) only if a given base was present in 80% of the aligned reads, and five or more reads aligned to the reference; bases where the majority of reads showed a substitution but that did not fulfill these two conditions were deemed uncertain. Similarly, positions to which no reads were mapped were also deemed uncertain, and such positions were assigned with an “N”. All deletions were manually verified: (a) over 98% of the reads covering the deletion site mapped to both ends of the deletion (i.e., bore evidence of the deletion), (b) the deletion was based on over 40 independent reads (on average >1000 reads), and (c) coverage was high at both ends of the deleted region. Only sequences that spanned 90% of the reference genome were retained, leading to the removal of one sequence (Supplementary Table 2), and hence a new set of 212 Israeli sequences was generated here. Another two Israeli sequences already available on GISAID were added to the phylogenetic analysis, leading to a total of 214 sequences from Israel.

The collection dates of the 214 Israeli sequences used in our analysis ranged from February 23 through April 22, 2020. The number of sequences is thus ~1.5% of the total number of reported cases on April 22.

Phylogenetic analyses. All available full-length SARS-CoV-2 genomes from outside of Israel (a total of 16,403 sequences) were retrieved from GISAID on May 5, 2020. All sequences from a non-human host as well as sequences with incomplete sampling date (YYYY-MM or YYYY-MM-XX) or a high level of uncertainty (>10% ambiguous bases marked as N) were removed. All available sequences were then down-sampled to 4693 representative sequences across the globe using the latest build of NextStrain ncov pipeline^{31,32} (<https://github.com/nextstrain/ncov>); 1195 of these 4693 sequences were from the U.S., while 1991 were from Europe. The 212 new Israeli sequences were added to the tree.

Down-sampling of global tree for phylodynamic analysis. Following the initial sampling of the global tree described above, we applied a second sampling specifically for the phylodynamic analysis. The down-sampling was inspired by the recommended guidelines described for SARS-CoV-2 ([sarscov2phylogenetics.org](https://www.sarscov2phylogenetics.org)), and thus we applied two sampling techniques:

- Random time stratified sampling—We sampled a total of 100 sequences from outside of Israel across $v = 5$ time intervals such that each time interval contained ~20 sequences.
- Closest sequence match—Defining S_{ISR} as the set of all sequences from Israel, we sample the exogenous set of sequences from the global tree with the minimal cophenetic distance between each Israeli sequence belonging to S_{ISR} as based on the maximum-likelihood phylogeny. This results in sequences closely related to sequences from Israel to be included in the analysis.

We next manually curated the sequences from Israel to ensure they represent a random sample across Israel. To this end, we removed samples suspected to be from the same household, samples with consecutive identifiers, or identical samples with similar identifiers and similar dates. Only one sample from a given household was chosen randomly. This led to a removal of six sequences.

Following down-sampling and manual curation, a phylogenetic tree was inferred using the NextStrain pipeline³². The tree topology was validated as a legitimate representative of the global tree by performing 1000 random samples containing 373 sequences from the global tree. The Kendall–Colijn metric³³ was used to assess the distance between each random sample and the original tree, allowing us to create a null distribution. The λ parameter, which determines the trade-off between topology and branch length, was set to zero, thus accounting for the tree topology alone. The significance of the topology of the down-sampled tree as compared to the global tree was thus obtained by comparing the Kendall–Colijn metric of the down-sampled tree to the null distribution ($P = 0.003$).

Timing and distribution of importations. Given a time-resolved global tree (after the initial down-sampling from GISAID database and before down-sampling for phylodynamic analysis; 4693 sequences total), we assigned a country to each internal node using NextStrain’s maximum-likelihood ancestral state reconstruction. We defined an importation event into Israel as a transition from a non-Israeli node to an Israeli node. We then used the dates associated with the internal nodes to generate a distribution of importation dates, which was used to parameterize the phylodynamic migration rate (Supplementary Fig. 8), as described below. Moreover, we inferred that the first introductions to Israel occurred already in late January/early February, as further supported by data from epidemiological investigations.

The internal nodes and their associated dates were further used to infer the number of transmission chains that could have been prevented by arresting flights from the U.S. earlier. Out of a total of 214 clade importations from the U.S., 118 (55%) were inferred to have occurred between February 26 and March 9, 103

between March 1 and March 9 (48%), and 42 between March 4 and March 9 (20%).

Confidence in numbers and fractions of importation events. Confidence in the relative number of importation events from the U.S. vs. Europe was assessed using two measures of confidence intervals. These were aimed at testing whether the set of exogenous (non-Israeli) sequences was biased, or whether the set of Israeli sequences was biased. First, we generated 1000 samples of the exogenous sequences using a bootstrap approach: we sampled N sequences with replacement, where N is the number of exogenous sequences. We then determined the fraction of importation events into Israel for each set. Second, we similarly bootstrapped only the local (Israeli) sequences using a similar approach and assessed the fraction of importation events into Israel for each bootstrapped set. The reported confidence interval includes the lower bound and higher bound of both bootstrapping schemes. We describe below our approach for inferring the timing of importation events.

Phylodynamic analysis. Phylodynamic analyses were conducted using BEAST2 v2.6.2 (ref. 34) and PhyDyn v1.3.6 (ref. 35). An HKY substitution model with a lognormal prior for κ with mean $\log(\kappa) = 1.0$ and standard deviation of $\log(\kappa) = 1.25$ was used. We assumed no sites to be invariant and used an exponential prior for γ with a mean of 1.0. A strict molecular clock with a uniform prior between 0.0007 and 0.002 substitutions/site/year was used. A uniform prior was used for nucleotide frequencies. The down-sampled maximum-likelihood tree generated using IQ Tree was used as a starting tree.

PhyDyn is a coalescent-based inference approach implemented in BEAST2, allowing for the integration over phylogenetic uncertainty^{35,36}. The program requires specification of an underlying epidemiological model, as well as any priors on parameters that will be estimated. In line with recent analyses³⁷, we assumed that the epidemiological dynamics of SARS-CoV-2 were governed by SEIR dynamics. Transmission heterogeneity has previously been described for viral pathogens including SARS-CoV-1 (ref. 38) and appears to be important in the transmission dynamics of SARS-CoV-2 (refs. 25,26). To account for the possibility of transmission heterogeneity, as in previous work³⁷, we modeled two classes of infected individuals: one with low transmissibility I_l and one with high transmissibility I_h . Mathematically, the epidemiological model is given by Eqs. (1)–(5):

$$\frac{dS}{dt} = -\beta_l I_l \cdot \left(\frac{S}{N}\right) - \beta_h I_h \cdot \left(\frac{S}{N}\right) \quad (1)$$

$$\frac{dE}{dt} = \beta_l I_l \cdot \left(\frac{S}{N}\right) + \beta_h I_h \cdot \left(\frac{S}{N}\right) - \gamma_E E \quad (2)$$

$$\frac{dI_l}{dt} = (1 - p_h) \gamma_E E - \gamma_l I_l \quad (3)$$

$$\frac{dI_h}{dt} = p_h \gamma_E E - \gamma_l I_h \quad (4)$$

$$\frac{dR}{dt} = \gamma_l I_l + \gamma_l I_h \quad (5)$$

We set as fixed the host population size to the population size of Israel, according to the European Centre for Disease Prevention and Control ($N = 8,883,800$), the average duration of time an individual spends in the exposed class ($1/\gamma_E = 3$ days), and the average duration of time an individual spends in the infected (infectious) class ($1/\gamma_l = 5.5$ days). These durations are based on a study that inferred transmissibility over the course of infection using data from established SARS-CoV-2 transmission pairs³⁹. R_0 in this model is given by $(\beta_h p_h + \beta_l (1 - p_h)) / \gamma_b$, where p_h is the fraction of exposed individuals who transition to the I_h class instead of to the I_l class. In our model, we estimated a piecewise R_0 by estimating an initial R_0 that was in effect until March 19, 2020, when strong social distancing measures were implemented, along with a factor α by which R_0 changed on March 19.

Instead of independently parameterizing β_h and β_l , we defined (as in previous work³⁷) the relative transmissibility of infected individuals in the I_h and I_l classes by the parameter $\tau = \beta_h / \beta_l$, and simplify notation by defining $\beta \equiv \beta_l$. We further defined a parameter P as the fraction of secondary infections that were caused by a fraction p_h of the most transmissible infected individuals and set P to 0.8. Based on set values of P and p_h , we calculated τ as $(\frac{1-P}{p_h}) / (\frac{1}{P} - 1)$. As such, we could easily parameterize the model across various levels of transmission heterogeneity, with a fraction p_h of infected individuals being responsible for 80% of secondary infections. Existing epidemiological analyses indicate that p_h is approximately 0.07–0.1 (7–10%)^{25,26} indicative of even more transmission heterogeneity than given by the 20/80 rule²⁷. We considered a range of p_h between 2% and 80% in our phylodynamic analyses to allow for a broad range of transmission heterogeneity, from extreme superspreading ($p_h = 2$ –10%) to no transmission heterogeneity ($p_h = 80\%$).

Again, based on existing analyses ([sarscov2phylogenetics.org](https://www.sarscov2phylogenetics.org))³⁷, we included an external reservoir in our analysis to allow for multiple introduced clades into

Israel to be jointly considered. Instead of modeling both exposed (E) and infected (I) individuals in the external reservoir, we assume a single infected class Y undergoing exponential growth. We fix the duration of infection of this class of individuals to be 8.5 days ($= 1/\gamma_E + 1/\gamma_I$). We attempted to estimate both the growth rate of the infected class Y and its initial size at time $t = 2019.7$, but found that these parameters were practically unidentifiable. We thus set the growth rate of the infected class to 24 person⁻¹ year⁻¹ (resulting in an R_0 of 1.56 in the reservoir) and estimated only the initial size of the infected class Y . An exponential prior with mean 1.0 was used for the initial size of Y .

Migration into and out of Israel occurred at an overall migration rate of $\eta(t)$ and we assumed for simplicity that all migrations involved exposed (E class) individuals, rather than also implementing migration of the infected (I_i and I_h) classes. As migration is assumed to be symmetrical into and out of Israel, it does not affect the focal SEIR model dynamics. However, it does influence the probability that a given lineage's geographic state is assigned to Israel. We considered two different functional forms of the migration rate $\eta(t)$. The first form for $\eta(t)$ was generated using the timing of inferred importation events (described above in "Timing and distribution of importations"). Inferred importation events were grouped into 3-day windows and a piecewise exponential function fit to the data using the Nelder–Mead algorithm as implemented in SciPy⁴⁰. The curve was fixed to change from growth to decay at the end of the time window with the peak number of importations (Supplementary Fig. 9A) and assumed to be 0 until the date at which the best fit curve was ≥ 1 . Model fitting resulted in an importation rate given by the curve $\exp(57(t - 2020.05))$ between 2020.05 and 2020.18 and declined from 2020.18 with the curve $1680 \exp(-52(t - 2020.18))$. To assess the robustness of our results to the magnitude of this curve, we also scaled the growth and decay rates (57 and -52 , respectively) by $\theta = 0.8, 0.9, 1.0, 1.1$, and 1.2 and modified the initial value of the importation rate at 2020.18 accordingly (Supplementary Figs. 5 and 9B and Supplementary Tables 3–7). Over the time series in our model, this translates to a total of 17, 33, 62, 118, and 228 migrations into and out of Israel that result in established clades. The second form for $\eta(t)$ assumed a constant migration rate ($\eta = 10, 100, 1000, 2500, 5000$ year⁻¹) (Supplementary Fig. 5 and Supplementary Tables 8–12) which translates to 6, 61, 607, 1518, and 3037 migrations over the time course of our model.

With a given functional form for $\eta(t)$ and with the parameterization of this form, we used our parameter estimates to infer the time-varying probability that an exposed individual in Israel migrated into Israel versus became infected locally (Supplementary Figs. 10 and 11). This time-varying probability is given by $\eta(t) / (\eta(t) + \frac{\beta S(I_i + \tau I_h)}{N})$. At high migration rates ($\theta = 1.2, \eta \geq 2500$), this probability remained unrealistically high throughout the epidemic. At reasonable values of θ and η (0.9–1.1 and 100–1000, respectively), the parameter estimates were relatively insensitive to η (Supplementary Figs. 5 and 6). PhyDyn simultaneously estimates model parameters and phylogenies and thus integrates over phylogenetic uncertainty. Our extensive sensitivity analysis involving the importation/exportation rate η was done to ensure the robustness of our inferred epidemiological parameters. The choice and magnitude of η will affect not only the probability that viral lineages are inside or outside of Israel but the overall topology of the phylogenies and thus has the potential to impact epidemiological parameter estimation.

Our prior on α , the factor by which R_0 changes on March 19, was a uniform prior between 0 and 2, thereby allowing R_0 to either increase, decrease, or remain unchanged after March 19. I_i and I_h were assumed to be negligibly small ($1E-8$) at the beginning of the SEIR dynamics. The PhyDyn t_0 parameter was set to 2019.7 and a constant population size coalescent model ($N_e = 0.1$) was used prior to this date when proposed trees had earlier root dates. SEIR dynamics were assumed to begin on February 1. Sequences sampled from Israel were randomly assigned to I_h with probability p_h and to I_i with probability $1 - p_h$. XML files to run both BEAST2 and PhyDyn were generated using a custom Python 3 script, which was designed to edit a template XML file originally generated with BEAUti and manually edited. To aid in mixing, we used Adaptive Metropolis Coupled MCMC⁴¹ with three chains. All MCMC chains were run for 10 million steps and convergence was assessed based on visual inspection of parameter traces. The first 50% of MCMC steps were discarded as burn-in. Maximum clade credibility trees were generated using TreeAnnotator. BEAST2 and PhyDyn outputs were visualized using Python 3, Matplotlib⁴², Seaborn, and Baltic (<https://github.com/evogytis/baltic>). The ggtree package was used to visualize the Israeli phylogeny⁴³. Supplementary Fig. 7 shows the time-aligned maximum clade credibility phylogeny of the Israeli sequences along with outside-Israel sequences for the model results shown in Figs. 5 and 6.

Reporting summary. Further information on research design is available in the Nature Research Reporting Summary linked to this article.

Data availability

Data that support the findings of this study have been deposited in the relevant databases: a viral sequence per each patient sample was deposited in the GISAID database (<https://www.gisaid.org>) with accession numbers EPI_ISL_447258 – EPI_ISL_447469. The raw sequencing reads were deposited in the NCBI Sequence Read Archive (SRA) database under BioProject accession number PRJNA647529. The reference genome of SARS-CoV-2, ID MN908947, was downloaded from GenBank (<https://www.ncbi.nlm.nih.gov/>

172
genbank/). A list of all sequence accession numbers used in this study, Beast XML configurations, and outputs are available at <https://github.com/SternLabTAU/SARSCOV2NGS>. Source data are provided with this paper.

Code availability

All analysis scripts, NextStrain make file and phylodynamic model configuration scripts are available at <https://github.com/SternLabTAU/SARSCOV2NGS>. Our local NextStrain build is also available in NextStrain community at https://nextstrain.org/community/SternLabTAU/SARSCOV2NGS?f_country=Israel.

Received: 12 June 2020; Accepted: 2 October 2020;

Published online: 02 November 2020

References

- Huang, C., Wang, Y. & Li, X. Clinical features of patients infected with 2019 novel coronavirus in Wuhan, China. *Lancet* **395**, 496 (2020).
- Zhu, N. et al. A novel coronavirus from patients with pneumonia in China, 2019. *N. Engl. J. Med.* **382**, 727–733 (2020).
- Zhou, P. et al. A pneumonia outbreak associated with a new coronavirus of probable bat origin. *Nature* **579**, 270–273 (2020).
- World Health Organization. Novel Coronavirus (2019-nCoV): situation report, 51. World Health Organization. <https://www.who.int/docs/default-source/coronaviruse/situation-reports/20200311-sitrep-51-covid-19.pdf> (2020).
- Tian, H. et al. An investigation of transmission control measures during the first 50 days of the COVID-19 epidemic in China. *Science* **368**, 638–642 (2020).
- Flaxman, S. et al. Estimating the number of infections and the impact of nonpharmaceutical interventions on COVID-19 in 11 European countries. Imperial College London. <https://doi.org/10.25561/77731> (2020).
- Kissler, S. M., Tedijanto, C., Goldstein, E., Grad, Y. H. & Lipsitch, M. Projecting the transmission dynamics of SARS-CoV-2 through the postpandemic period. *Science* **368**, 860–868 (2020).
- Gardy, J. L. & Loman, N. J. Towards a genomics-informed, real-time, global pathogen surveillance system. *Nat. Rev. Genet.* **19**, 9–20 (2018).
- Volz, E. M., Koelle, K. & Bedford, T. Viral phylodynamics. *PLoS Comput. Biol.* **9**, e1002947 (2013).
- Khoury, M. J. et al. From public health genomics to precision public health: a 20-year journey. *Genet. Med.* **20**, 574–582 (2018).
- Armstrong, G. L. et al. Pathogen genomics in public health. *N. Engl. J. Med.* **381**, 2569–2580 (2019).
- Bedford, T. et al. Cryptic transmission of SARS-CoV-2 in Washington State. *Science* <https://doi.org/10.1126/science.abc0523> (2020).
- Fauver, J. R. et al. Coast-to-coast spread of SARS-CoV-2 during the early epidemic in the United States. *Cell* **181**, 990–996.e5 (2020).
- Villabona-Arenas, C. J., Hanage, W. P. & Tully, D. C. Phylogenetic interpretation during outbreaks requires caution. *Nat. Microbiol.* **5**, 876–877 (2020).
- Korber et al. Tracking Changes in SARS-CoV-2 Spike: Evidence that D614G Increases Infectivity of the COVID19 Virus. *Cell* **182**, 812–827 (2020).
- van Dorp, L. et al. No evidence for increased transmissibility from recurrent mutations in SARS-CoV-2. Preprint at <https://doi.org/10.1101/2020.05.21.108506> (2020).
- Holland, L. A. et al. An 81-Nucleotide Deletion in SARS-CoV-2 ORF7a Identified from Sentinel Surveillance in Arizona (January to March 2020). *J. Virol.* **94**, e00711-20 (2020).
- Su, Y. C. F. et al. Discovery and Genomic Characterization of a 382-Nucleotide Deletion in ORF7b and ORF8 during the Early Evolution of SARS-CoV-2. *mBio* **11**, (2020).
- Menachery, V. D., Debbink, K. & Baric, R. S. Coronavirus non-structural protein 16: evasion, attenuation, and possible treatments. *Virus Res.* **194**, 191–199 (2014).
- Worobey, M. et al. The emergence of SARS-CoV-2 in Europe and North America. *Science*, <https://doi.org/10.1126/science.abc8169> (2020).
- Danesh, G., Elie, B. & Alizon, S. Early phylodynamics analysis of the COVID-19 epidemics in France. <http://virological.org/t/early-phylodynamics-analysis-of-the-covid-19-epidemics-in-france-using-194-genomes-april-10-2020/467> (2020).
- Vaughan, T. G., Nadeau, S., Scire, J. & Stadler, T. Phylodynamic analyses of outbreaks in China, Italy, Washington State (USA), and the Diamond Princess. <http://virological.org/t/phylodynamic-analyses-of-outbreaks-in-china-italy-washington-state-usa-and-the-diamond-princess/439> (2020).

23. Volz, E. et al. Report 5: Phylogenetic analysis of SARS-CoV-2. <https://www.imperial.ac.uk/media/imperial-college/medicine/mrc-gida/2020-02-15-COVID19-Report-5.pdf> (2020). Accessed 25 May 2020.
24. Volz, E. et al. SARS Coronavirus 2 Phylodynamics. <http://sarscov2phylodynamics.org> (2020).
25. Bi, Q. et al. Epidemiology and transmission of COVID-19 in 391 cases and 1286 of their close contacts in Shenzhen, China: a retrospective cohort study. *Lancet Infect. Dis.* **20**, 911–919 (2020).
26. Endo, A. Estimating the overdispersion in COVID-19 transmission using outbreak sizes outside China. *Wellcome Open Res.* **5**, 67 (2020).
27. Woolhouse, M. E. J. et al. Heterogeneities in the transmission of infectious agents: implications for the design of control programs. *Proc. Natl Acad. Sci. USA* **94**, 338–342 (1997).
28. Zhang, X. et al. pTrimmer: an efficient tool to trim primers of multiplex deep sequencing data. *BMC Bioinformatics* **20**, 236 (2019).
29. Gelbart, M. et al. Drivers of within-host genetic diversity in acute infections of viruses. *PLoS Pathogens*, in press (2019).
30. Altschul, S. F. et al. Gapped BLAST and PSI-BLAST: a new generation of protein database search programs. *Nucleic Acids Res.* **25**, 3389 (1997).
31. Hadfield, J. et al. Twenty years of West Nile virus spread and evolution in the Americas visualized by Nextstrain. *PLoS Pathog.* **15**, e1008042 (2019).
32. Hadfield, J. et al. Nextstrain: real-time tracking of pathogen evolution. *Bioinformatics* **34**, 4121–4123 (2018).
33. Kendall, M. & Colijn, C. Mapping phylogenetic trees to reveal distinct patterns of evolution. *Mol. Biol. Evol.* **33**, 2735–2743 (2016).
34. Bouckaert, R. et al. BEAST 2.5: an advanced software platform for Bayesian evolutionary analysis. *PLoS Comput. Biol.* **15**, e1006650 (2019).
35. Volz, E. M. & Siveroni, I. Bayesian phylodynamic inference with complex models. *PLoS Comput. Biol.* **14**, e1006546 (2018).
36. Volz, E. M. Complex population dynamics and the coalescent under neutrality. *Genetics* **190**, 187–201 (2012).
37. Geidelberg, L. et al. Genomic epidemiology of a densely sampled COVID-19 outbreak in China. Preprint at <https://doi.org/10.1101/2020.03.09.20033365> (2020).
38. Lloyd-Smith, J. O., Schreiber, S. J., Kopp, P. E. & Getz, W. M. Superspreading and the effect of individual variation on disease emergence. *Nature* **438**, 355–359 (2005).
39. He, X. et al. Temporal dynamics in viral shedding and transmissibility of COVID-19. *Nat. Med.* **26**, 672–675 (2020).
40. Virtanen, P. et al. SciPy 1.0: fundamental algorithms for scientific computing in Python. *Nature methods* **17**, 261–272. (2020).
41. Müller, N. F. & Bouckaert, R. R. Adaptive parallel tempering for BEAST 2. Preprint at <https://doi.org/10.1101/603514> (2020).
42. Hunter, J. D. Matplotlib: a 2D graphics environment. *Comput. Sci. Eng.* **9**, 90–95 (2007).
43. Yu, G. C., Smith, D. K., Zhu, H. C., Guan, Y. & Lam, T. T. Y. GGTREE: an R package for visualization and annotation of phylogenetic trees with their covariates and other associated data. *Methods Ecol. Evol.* **8**, 28–36 (2017).

Acknowledgements

We wish to thank Dr. Erik Volz for helpful discussions, as well as Dr. Boaz Lev at the Israeli Ministry of Health, Dr. Tal Katz-Ezov at the Technion Genome Center, and Stern

lab members for their support during an ongoing pandemic and various stages of lockdown. This work was funded by the Israeli Science Foundation (1333/16), by the NIAID Centers of Excellence for Influenza Research and Surveillance (CEIRS) grant HHSN272201400004C, and by a generous donation from the Milner foundation and from AppsFlyer. This study was supported in part by a fellowship to D.M., T.K., and O.T. from the Edmond J. Safra Center for Bioinformatics at Tel-Aviv University. The phylodynamic analysis presented as part of this work used the High Performance Computing Environment provided by the MIDAS Coordination Center, supported by NIGMS grant 5U24GM132013 and the NIH STRIDES program.

Author contributions

D.M., M.A.M., N.H., O.T., and T.K. performed all the analyses and drafted the paper. M.M. coordinated the sample sequencing. N.S., S.G.H., S.A., O.V., A.Sh., D.W., A.P., Y.S.A., and D.R.K. contributed clinical samples. N.M.K., A.H., and A.S. conceived and coordinated the study. A.S. and K.K. supervised and led the study.

Competing interests

The authors declare no competing interests.

Additional information

Supplementary information is available for this paper at <https://doi.org/10.1038/s41467-020-19248-0>.

Correspondence and requests for materials should be addressed to A.S.

Peer review information *Nature Communications* thanks Matthew Hall and the other, anonymous reviewer(s) for their contribution to the peer review of this work. Peer review reports are available.

Reprints and permission information is available at <http://www.nature.com/reprints>

Publisher's note Springer Nature remains neutral with regard to jurisdictional claims in published maps and institutional affiliations.



Open Access This article is licensed under a Creative Commons Attribution 4.0 International License, which permits use, sharing, adaptation, distribution and reproduction in any medium or format, as long as you give appropriate credit to the original author(s) and the source, provide a link to the Creative Commons license, and indicate if changes were made. The images or other third party material in this article are included in the article's Creative Commons license, unless indicated otherwise in a credit line to the material. If material is not included in the article's Creative Commons license and your intended use is not permitted by statutory regulation or exceeds the permitted use, you will need to obtain permission directly from the copyright holder. To view a copy of this license, visit <http://creativecommons.org/licenses/by/4.0/>.

© The Author(s) 2020

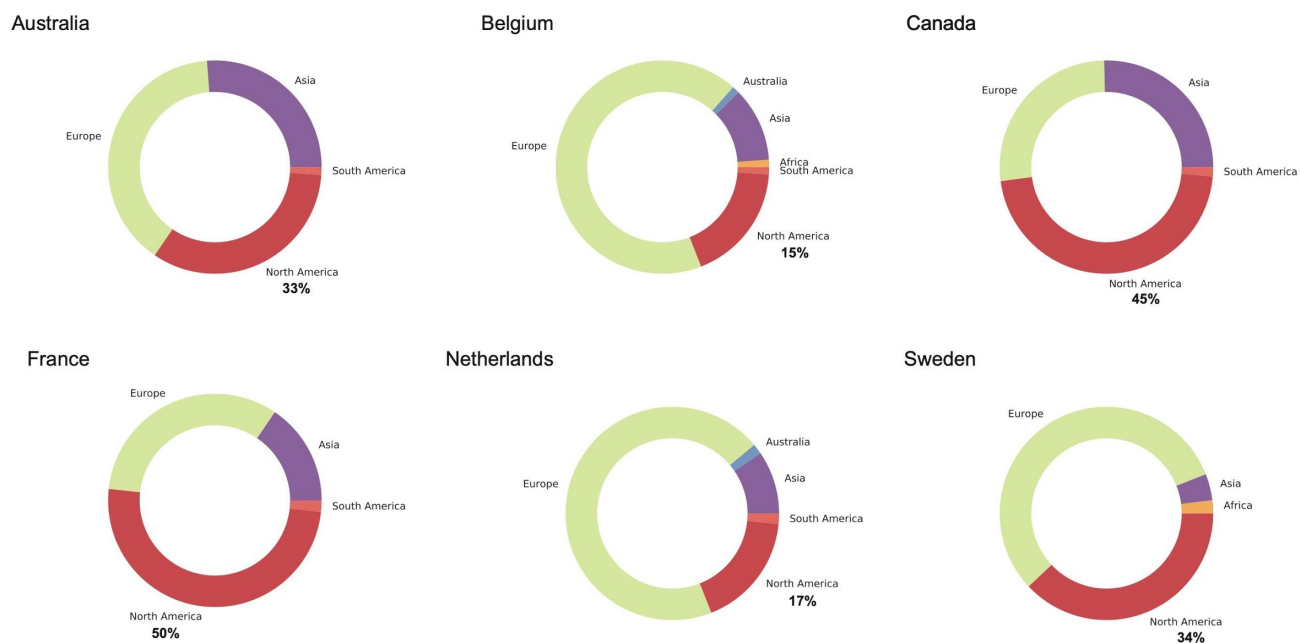
5.3 Supplement

Reproduced with permission from Springer Nature.

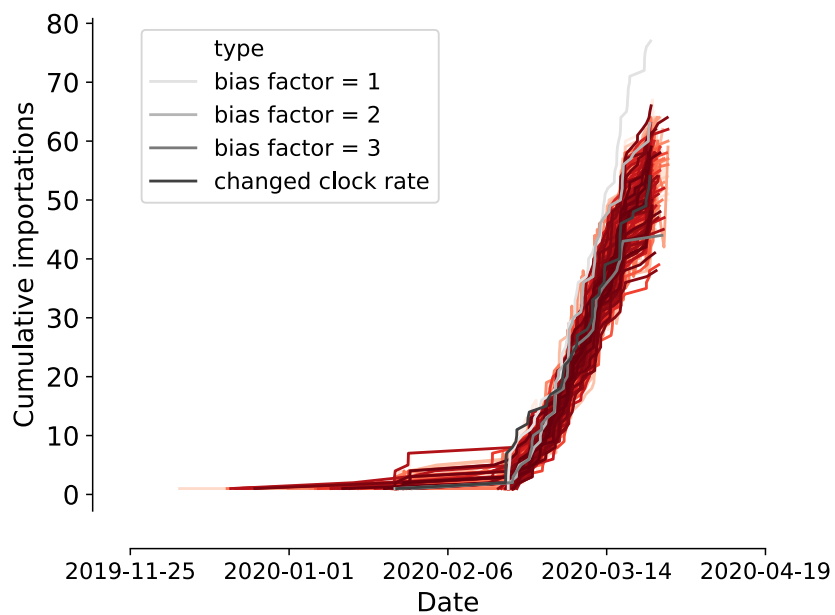
Full genome viral sequences inform patterns of SARS-CoV-2 spread into and within Israel

Danielle Miller*, Michael A. Martin*, Noam Harel*, Omer Tirosh*, Talia Kustin*, Moran Meir, Nadav Sorek, Shiraz Gefen-Halevi, Sharon Amit, Olesya Vorontsov, Avraham Shaag, Dana Wolf, Avi Peretz, Yonat Shemer-Avni, Diana Roif-Kaminsky, Naama M. Kopelman, Amit Huppert, Katia Koelle, Adi Stern

Supplementary Information



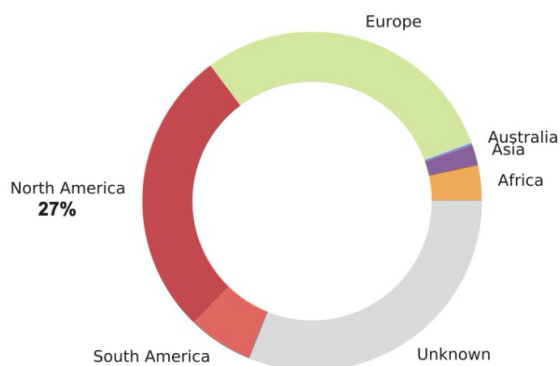
Supplementary Fig. 1. Inferred regions responsible for clade introductions into six focal countries. Each of the six countries shown had > 100 sequences available for analysis. Sectors in each pie chart show the proportion of clade introductions that were inferred to originate from the labeled regions. North America is highlighted in bold, and includes almost exclusively sequences from the U.S. For each country, we excluded local transmission (e.g., the Europe sector in the Netherlands excluded the Netherlands).



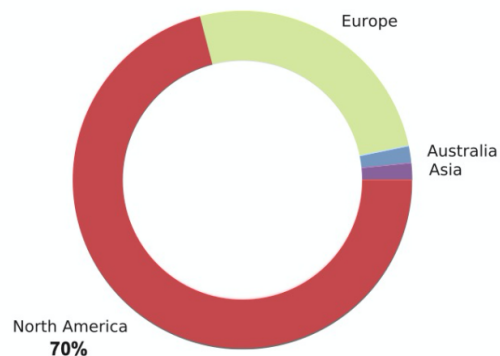
Supplementary Fig. 2. Cumulative number of importations throughout time. Cumulative sum of importation events into Israel for 1,000 bootstrap replicates are presented in red spectra. Changes in the sampling correction bias and clock rate are presented in greyscale. Bias factor of 1 means no sampling correction to the GTR matrix of the TreeTime model.

A

Infected returning travelers

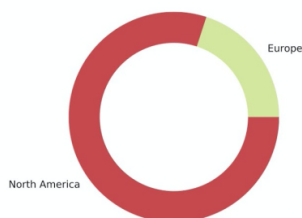


Inferred clade importations

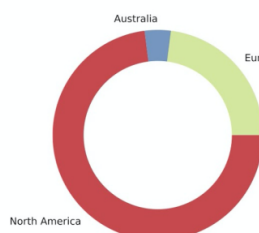


B

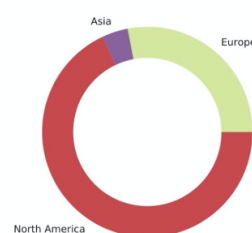
North district



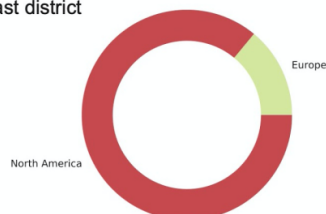
Tel Aviv district



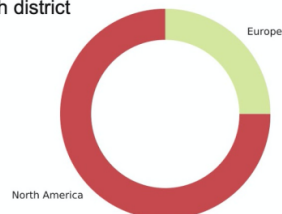
Jerusalem district



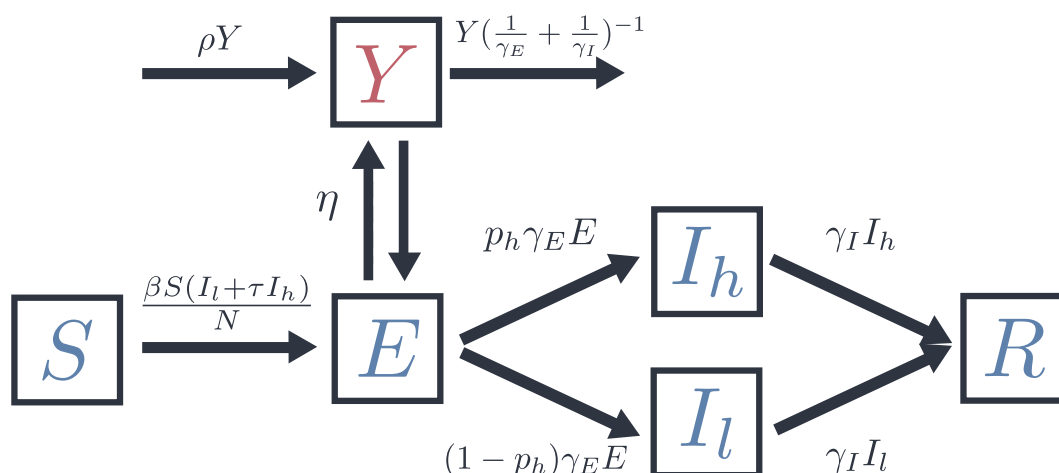
South Coast district



South district

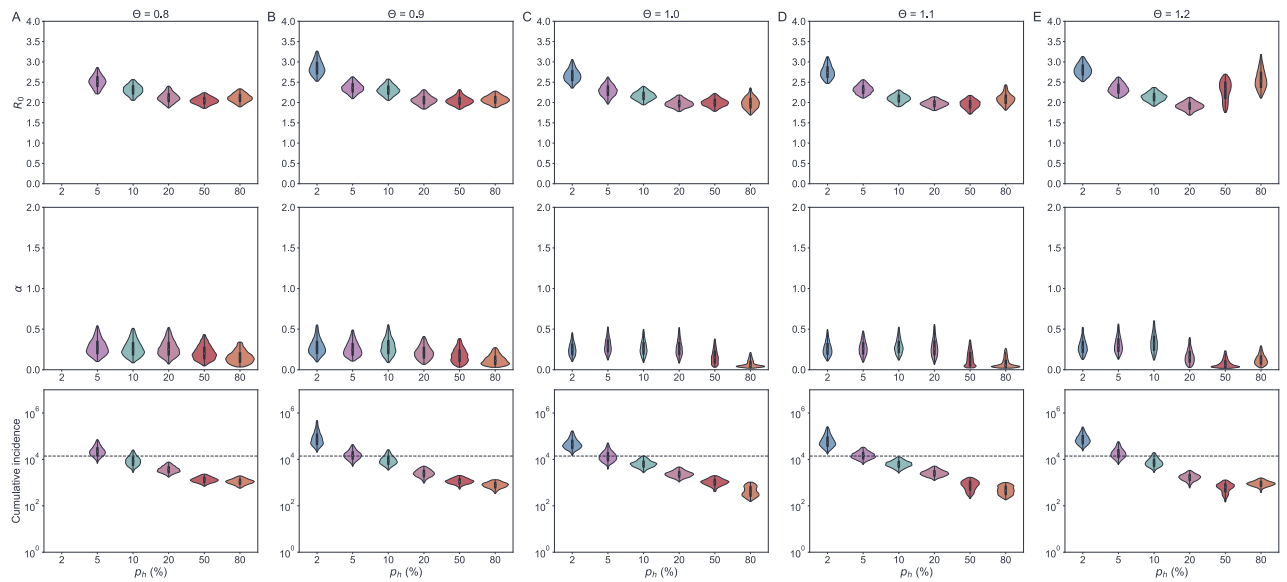


Supplementary Fig. 3. Distribution of importations into Israel. (A) Comparison of viral importations into Israel according to epidemiological data (the number of infected travelers reported) versus viral genetic data (inferred clade introductions). (B) Inferred proportion of clade introductions, by district within Israel. As in Figure S1, local transmissions were excluded from the analysis.

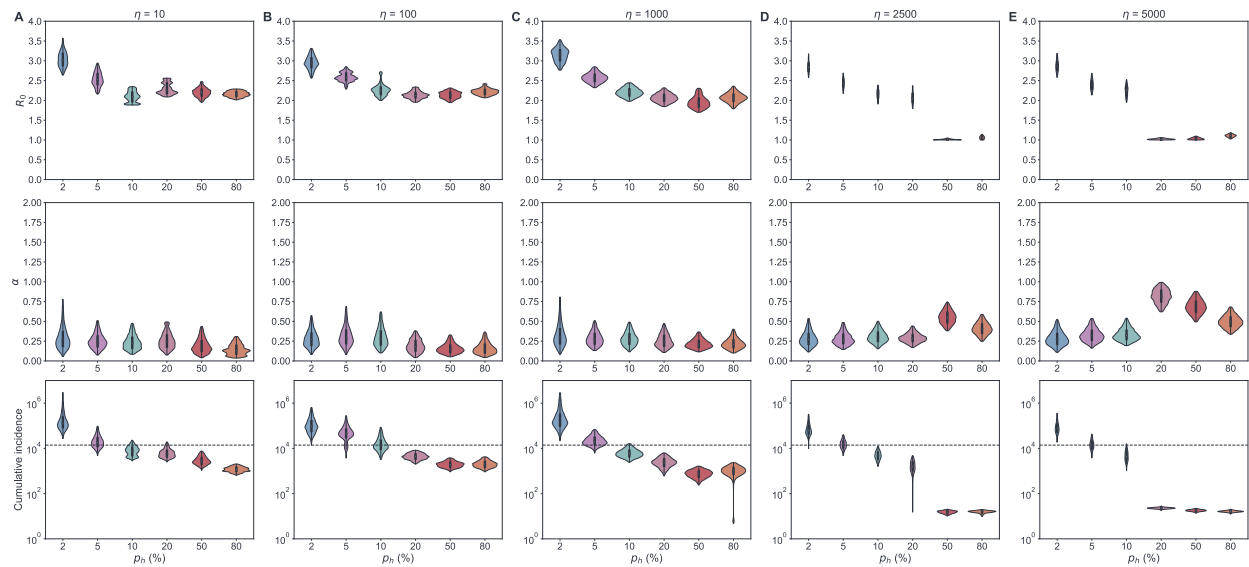


Supplementary Fig. 4. Compartmental model used in the phylodynamic analysis.

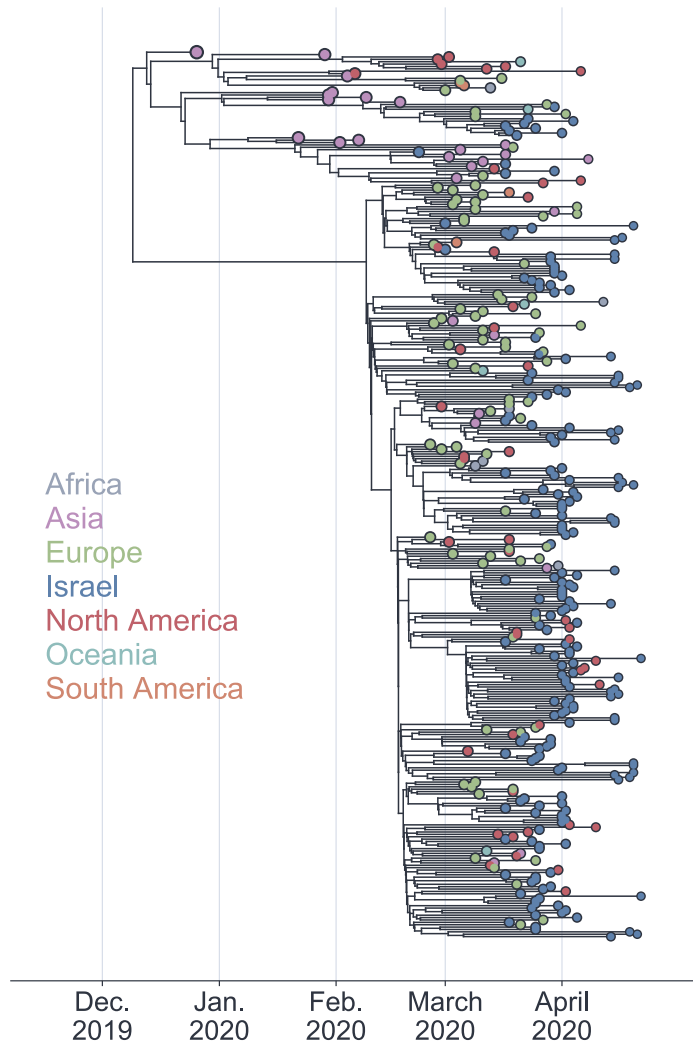
Compartments shown in blue (S, E, I_h, I_l, R) represent classes of individuals within Israel. Compartment shown in red (Y) represents a single class of infected individuals outside of Israel. The transmission term within Israel is given by $\frac{\beta S(I_l + \tau I_h)}{N}$ where τ is a factor by which highly infectious individuals (I_h) are more infectious than those with lower infectiousness (I_l). The parameter p_h is the probability that an individual transition to the highly infectious (I_h) class. The parameter τ is given by $(\frac{1-p_h}{p_h}) / (\frac{1}{0.8} - 1)$, such that individuals in I_h are responsible for 80% of secondary infections. Infected individuals remain exposed for $\gamma_E^{-1} = 3$ days and remain infectious for $\gamma_I^{-1} = 5.5$ days. Exposed individuals migrate into and out of Israel at an overall rate of η , which we consider can change over time (discussed in more detail elsewhere in the text). Infected individuals in the exogenous reservoir (Y) reproduce at a per capita rate of ρ and individuals remain in this reservoir for an average of 8.5 days.



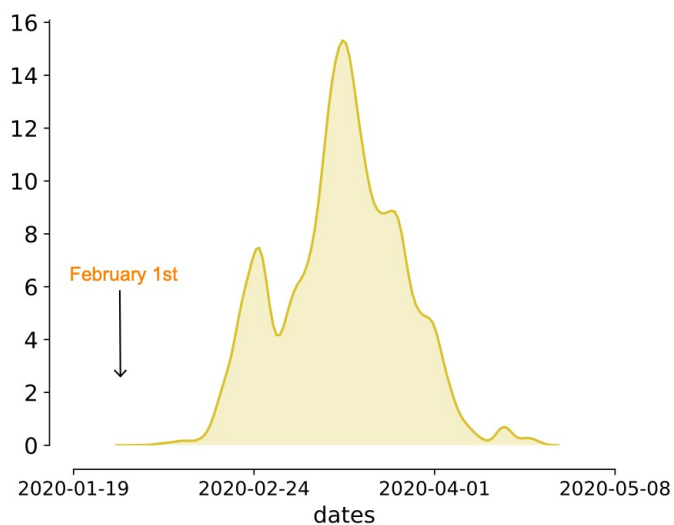
Supplementary Fig. 5. Sensitivity of phylodynamic analyses to the overall magnitude of the importation/exportation rate η . The parameter θ scales the importation/exportation rate $\eta(t)$ (see Methods). Estimated values of R_0 , α , and cumulative incidence using the migration rate form based on phylogenetically-informed timing of clade introductions. Columns shown correspond to (A) $\theta = 0.8$, (B) $\theta = 0.9$, (C) $\theta = 1.0$ (as shown in Figure 5), (D) $\theta = 1.1$, (E) $\theta = 1.2$. Horizontal dotted lines at $N = 13,942$ in the bottom row show the cumulative number of reported cases on April 22, 2020 as given by the ECDC. Only values which fall within the 95% highest posterior density (HPD) from the main MCMC chain are shown (total of 4,751 data points). Violin plots show the kernel density estimation of the underlying distribution. Median value is denoted by a white dot and the black bar in the center of the violin defines the interquartile range. The upper/lower adjacent values (the black line stretched from the bar) is defined as 1.5 times the width of the interquartile range past the first and third quartiles respectively. Density is only plotted over the range of observed values. Results for $p_h = 0.02$, $\theta = 0.8$ are excluded due to poor mixing of the MCMC chain for this set of parameters.



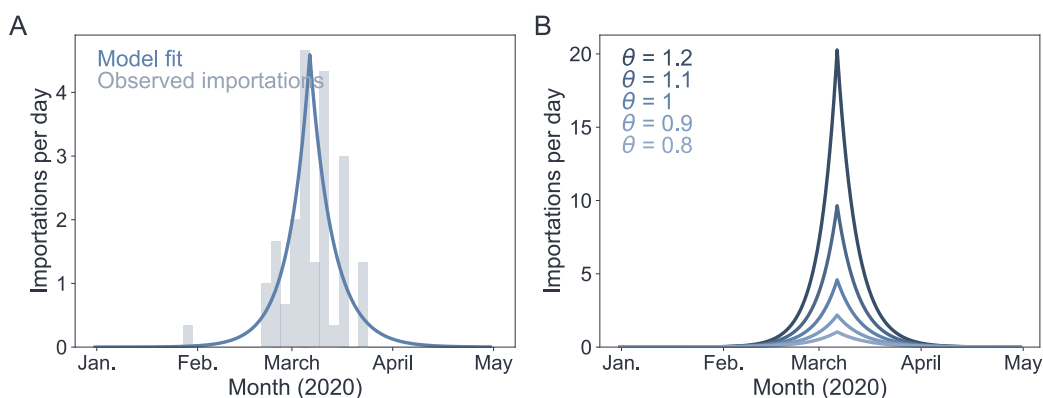
Supplementary Fig. 6. Sensitivity of phylodynamic analyses to the overall magnitude of the importation/exportation rate η , when η is assumed to be constant. Columns shown correspond to (A) $\eta = 10$ (B) $\eta = 100$, (C) $\eta = 1000$, (D) $\eta = 2500$, (E) $\eta = 5000$. Horizontal dotted lines at $N = 13,942$ in the bottom row show the cumulative number of reported cases on April 22, 2020 as given by the ECDC. Only values which fall within the 95% highest posterior density (HPD) from the main MCMC chain are shown (total of 4,751 data points). Violin plots show the kernel density estimation of the underlying distribution. Median value is denoted by a white dot and the black bar in the center of the violin defines the interquartile range. The upper/lower adjacent values (the black line stretched from the bar) is defined as 1.5 times the width of the interquartile range past the first and third quartiles respectively. Density is only plotted over the range of observed values.



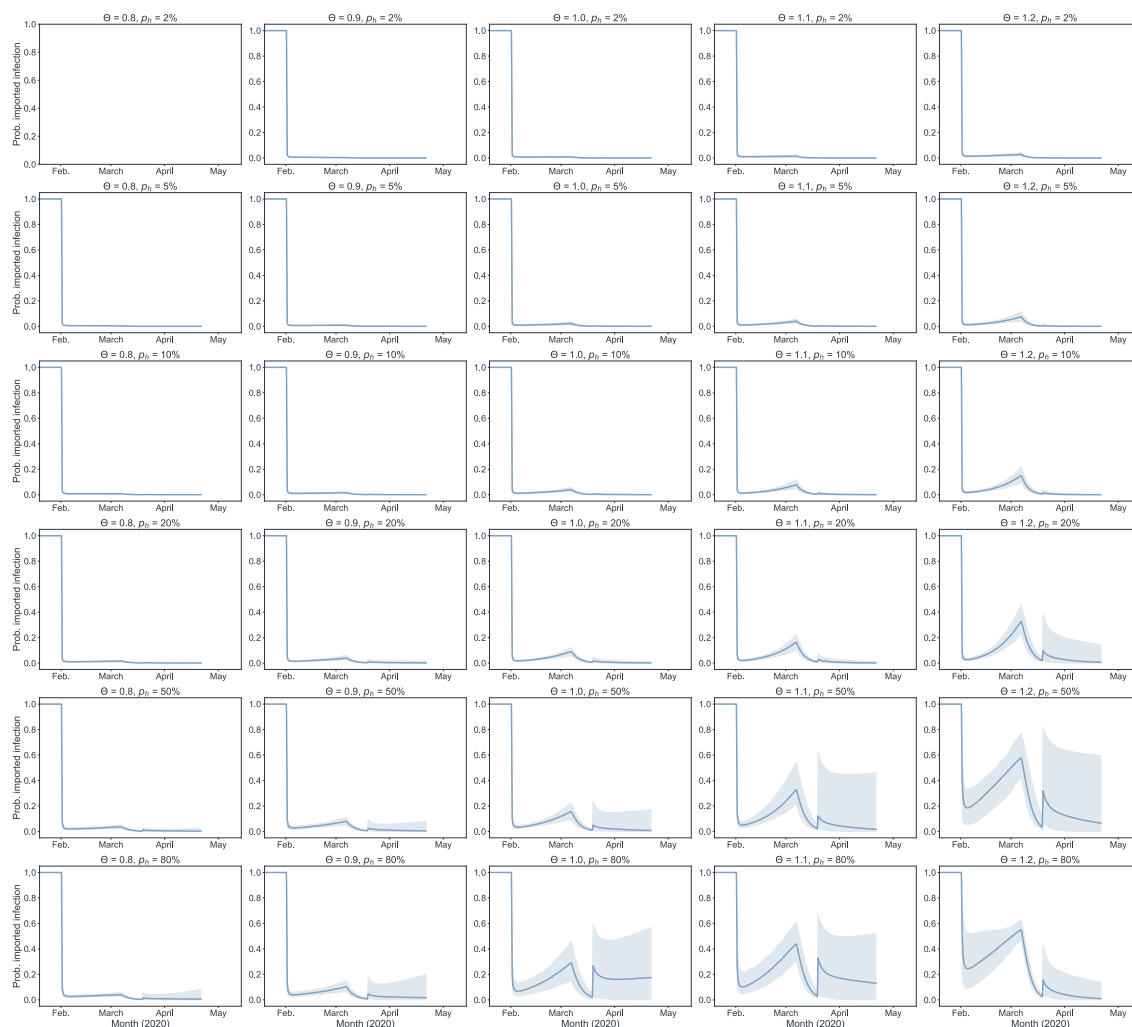
Supplementary Fig. 7. Time-aligned maximum clade credibility phylogeny. Phylogeny was estimated using both genetic and epidemiological parameters under an *SEIR* model implemented in BEAST2 and PhyDyn, under $p_h = 5\%$ and $\theta = 1.0$. Tips are colored by sampling location with Israel tips shown in blue.



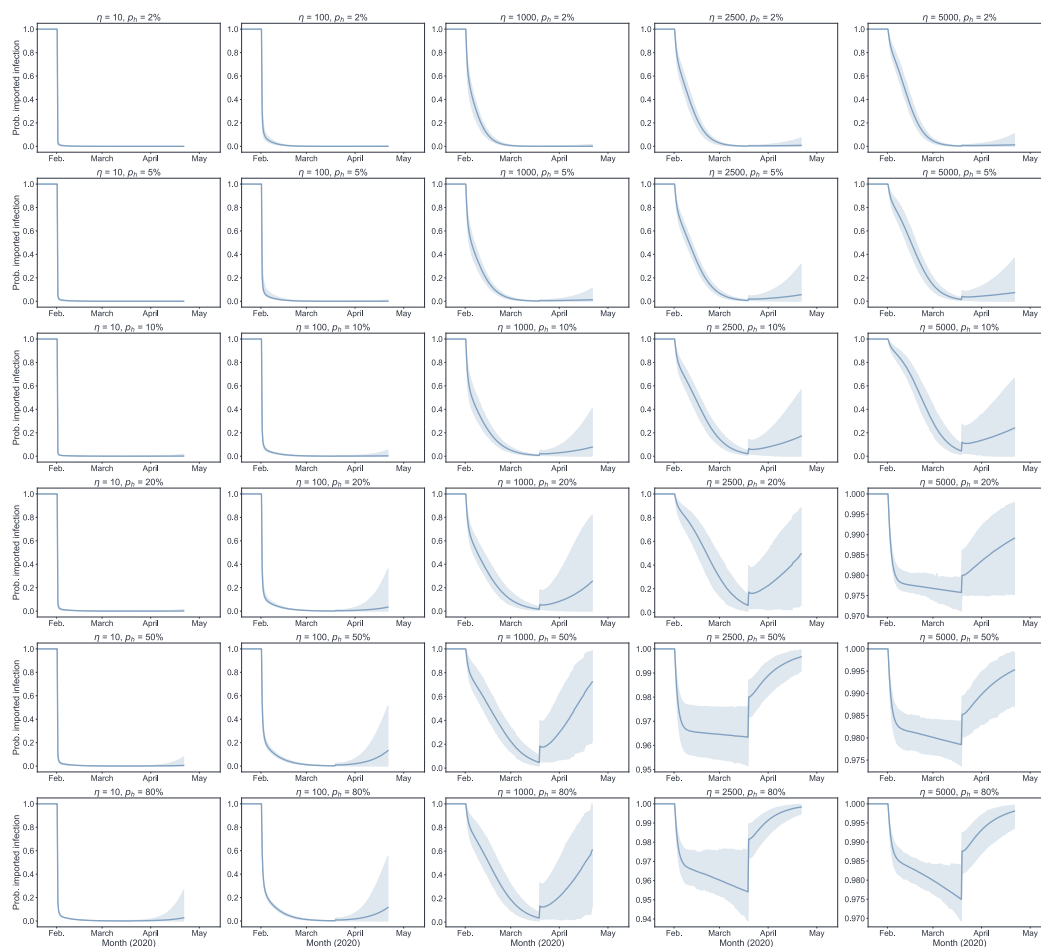
Supplementary Fig. 8. Distribution of importation dates into Israel. Density plot of all importation dates inferred from the phylogeny. Earliest importation is around February 1st (marked with an arrow). The highest peak of the distribution is around March 19th, ten days after the official date of airport closure (March 9th).



Supplementary Fig. 9. Distribution of importation dates into Israel assumed in our phylodynamic analysis. (A) Distribution of importation dates into Israel estimated using ancestral state reconstruction of a global phylogeny. Dates were grouped into non-overlapping three day windows and a piecewise exponential function fit to the data. (B) The growth and decay rates of the inferred importation curve were scaled by a range of θ values (0.8, 0.9, 1.0, 1.1, 1.2).



Supplementary Fig. 10. Probabilities of a new infection being due to importation rather than local infection under different magnitudes of the importation rate, assuming a functional form of η based on inferred timing of clade importations. Estimated state probabilities are shown across a range of θ (columns) and p_h (rows) values. Line represents the median estimate of the 95% HPD and shaded regions represent the limits of the 95% HPD. Results for $p_h = 0.02$, $\theta = 0.8$ are excluded due to poor mixing of the MCMC chain.



Supplementary Fig. 11. Probabilities of a new infection being due to importation rather than local infection under different magnitudes of the importation rate, assuming a constant η . Estimated state probabilities are shown across a range of η values (columns) and p_h values (rows). Line represents the median estimate of the 95% HPD and shaded regions represent the limits of the 95% HPD.

Supplementary Table 1: Global samples belonging to the S2430R clade that contain short unique deletions.

A sample was defined as belonging to the S2340R clade if it bore all 6 mutations that define the S2340R clade ('A20755C', 'A23403G', 'C1059T', 'C14408T', 'C3037T', 'G25563T'). The coordinates of the deletions are specified (coordinates based on the Wuhan ancestral sequences, see Methods), as is the country of origin of each sequence.

EPI_ID	deletion start	deletion end	deletion length	country
EPI_ISL_418202	26531	26531	1	USA
EPI_ISL_428377	510	518	9	USA
EPI_ISL_447362	3881	3898	18	Israel
EPI_ISL_447363	3881	3898	18	Israel
EPI_ISL_447377	28254	28254	1	Israel
EPI_ISL_447426	27387	27396	10	Israel
EPI_ISL_450084	23555	23582	28	USA
EPI_ISL_460096	29555	29602	48	Russia

Supplementary Table 2. Details of samples sequenced.

Sample ID	Ct E	Ct RdRp	Ct N	Ct average	Sex	Age	Date	Genome coverage	Geog. location of sample
1639953	28.5	30.5	32	30.18	M	10-19	26/3/20	0.996	North
1639996	23.1	24.4	26	24.45	M	20-29	26/3/20	0.996	North
2020038	22.5			22.46	F	50-59	17/3/20	0.994	Tel Aviv
2020051	30.9			30.87	M	40-49	17/3/20	0.976	Tel Aviv
2020063	28.4			28.39	F	20-29	17/3/20	0.985	Jerusalem
2020068	24.8			24.78	F	20-29	17/3/20	0.986	Jerusalem
2020069	28.2			28.24	F	30-39	17/3/20	0.987	Jerusalem
2020078	21.5			21.5	M	50-59	17/3/20	0.989	Jerusalem
2020084	24.9			24.87	M	60-69	17/3/20	0.994	Jerusalem
2020087	21.5			21.48	M	20-29	17/3/20	0.996	Jerusalem
2023920	18.6			18.56	M	40-49	17/3/20	0.996	Jerusalem
2023922	28			28	F	20-29	17/3/20	0.979	Jerusalem
2046129	23.1	24.2	27	24.88	M	20-29	31/3/20	0.996	North
2046171	29.6	30.8	33	31.24	F	50-59	31/3/20	0.954	North
2046434	19.5	20.6	24	21.28	F	50-59	1/4/20	0.996	North
2046548	28.5	31.1	34	31.01	M	40-49	1/4/20	0.991	North
2046614	24.4	26.2	28	26.24	F	30-39	2/4/20	0.996	North
2046616	20.5	22.3	25	22.47	F	70-79	2/4/20	0.996	North
2046815	13.8	16.5	18	16.08	F	80-89	4/4/20	0.994	North
2047004	23	24.5	27	24.81	M	30-39	27/3/20	0.996	North
2047011	28.5	30.2	32	30.24	M	20-29	26/3/20	0.952	North
2047016	25.7	26.7	29	26.99	F	0-9	26/3/20	0.996	North
2047145	10.3	11.8	15	12.38	F	30-39	26/3/20	0.996	North
2047188	13.6	15.3	18	15.48	M	20-29	26/3/20	0.996	North
2047189	9.75	11.7	14	11.87	M	20-29	26/3/20	0.996	North
2047364	20.8	22.8	25	22.68	F	60-69	28/3/20	0.996	North
2047392	27.6	29.9	31	29.42	F	30-39	29/3/20	0.966	North
2047418	24	25.4	28	25.67	M	0-9	29/3/20	0.996	North
2047567	26.8	28.7	31	28.97	F	30-39	29/3/20	0.978	North
2047586	22.8	24.1	27	24.71	F	20-29	29/3/20	0.996	North
2047604	22.7	24	26	24.32	M	50-59	29/3/20	0.996	North
2047738	20	22.1	25	22.21	M	10-19	30/3/20	0.996	North
2047749	19.3	20.7	23	21.03	F	40-49	30/3/20	0.996	North
2047772	23.8	25.7	26	25.3	F	30-39	30/3/20	0.996	North
2047883	21.1	22.9	25	22.87	M	60-69	31/3/20	0.996	North
2047927	32	33.7	36	33.74	F	60-69	31/3/20	0.918	North
2086001	28.4			28.4	F	10-19	1/4/20	0.988	Jerusalem
2086004	24.6			24.63	F	20-29	1/4/20	0.993	Jerusalem
2086008	20.2			20.24	M	90+	1/4/20	0.996	Jerusalem
2086012	24.4			24.39	M	20-29	1/4/20	0.988	Jerusalem
2086022	27.9			27.88	M	20-29	1/4/20	0.986	Jerusalem
2086033	28.8			28.79	F	60-69	1/4/20	0.991	Jerusalem
2086034	30			30.01	F	20-29	1/4/20	0.981	Jerusalem

2086045	20			19.99	M	50-59	1/4/20	0.996	Jerusalem
2089366	20.4			20.36	M	20-29	1/4/20	0.996	Jerusalem
2089368	25.6			25.62	M	60-69	1/4/20	0.985	Jerusalem
2089375	27.5			27.54	M	10-19	1/4/20	0.992	Jerusalem
2089380	30.1			30.14	F	60-69	1/4/20	0.979	Jerusalem
2089383	29.8			29.79	M	30-39	1/4/20	0.989	Jerusalem
2089697	28.3			28.27	F	20-29	1/4/20	0.989	Jerusalem
2089698	28.6			28.58	F	50-59	1/4/20	0.984	Jerusalem
2089712	25.5			25.52	M	20-29	1/4/20	0.989	Jerusalem
2089718	20.6			20.6	F	30-39	1/4/20	0.996	Jerusalem
2089723	28.6			28.55	M	30-39	1/4/20	0.992	Jerusalem
2089812	23.3			23.29	F	20-29	1/4/20	0.995	Jerusalem
2089839	25.5			25.5	M	60-69	1/4/20	0.989	Jerusalem
2089852	25.5			25.53	F	60-69	1/4/20	0.989	Jerusalem
2089861	18.3			18.31	M	70-79	1/4/20	0.996	Jerusalem
2089863	18.8			18.8	M	30-39	1/4/20	0.996	Jerusalem
2089866	20.7			20.7	M	30-39	1/4/20	0.996	Jerusalem
2099018	30.3			30.34	F	60-69	2/4/20	0.980	Jerusalem
2099019	27.5			27.48	M	20-29	2/4/20	0.992	Jerusalem
2099159	27.3			27.3	F	10-19	2/4/20	0.988	Jerusalem
2099251	23			22.98	F	20-29	2/4/20	0.996	Jerusalem
2099416	29			28.98	M	20-29	2/4/20	0.983	Jerusalem
2099421	20.5			20.45	M	50-59	2/4/20	0.996	Jerusalem
2107132	29.9			29.91	F	50-59	14/4/20	0.996	Jerusalem
2107137	19.6			19.6	F	10-19	14/4/20	0.996	Jerusalem
2107681	22.3			22.3	F	30-39	14/4/20	0.996	Jerusalem
2113155	25.6			25.55	M	0-9	15/4/20	0.996	Jerusalem
2113161	25.9			25.92	M	70-79	15/4/20	0.996	Jerusalem
2113173	29.8			29.78	M	10-19	15/4/20	0.996	Jerusalem
2113174	26.4			26.42	M	70-79	15/4/20	0.996	Tel Aviv
2113178	26.6			26.62	M	20-29	15/4/20	0.996	Jerusalem
2113255	29.1			29.14	F	60-69	14/4/20	0.994	Jerusalem
2113256	29.7			29.65	F	10-19	14/4/20	0.996	Jerusalem
2113601	25.1			25.07	M	0-9	15/4/20	0.996	Jerusalem
2113603	21.7			21.72	M	70-79	15/4/20	0.996	Jerusalem
2113678	29.8			29.78	M	0-9	15/4/20	0.996	Tel Aviv
2115701	26			25.96	F	10-19	16/4/20	0.996	Jerusalem
2115964	28.4			28.35	M	10-19	16/4/20	0.996	Tel Aviv
2115968	26.8			26.83	F	20-29	16/4/20	0.996	Tel Aviv
2115976	28.2			28.17	M	60-69	16/4/20	0.985	Tel Aviv
2115980	24.5			24.49	F	20-29	16/4/20	0.912	North
2115990	30.2			30.15	F	50-59	16/4/20	0.996	Jerusalem
2116859	29.6			29.6	F	10-19	20/4/20	0.953	Jerusalem
2123853	28.1			28.05	M	70-79	20/4/20	0.996	Jerusalem
2123863	27.5			27.47	M	80-89	20/4/20	0.996	Jerusalem
13075703	24	25.6	28	25.98	F	20-29	29/3/20	0.996	Tel Aviv
13075719	27.7	28.9	31	29.16	F	20-29	29/3/20	0.996	Tel Aviv
13075735	26.8	28.4	30	28.47	M	40-49	30/3/20	0.996	Tel Aviv
13075782	29.1	30.5	33	30.85	F	40-49	30/3/20	0.992	Tel Aviv

13075788	27.8	29.3	31	29.4	F	40-49	30/3/20	0.996	Tel Aviv
13075790	27.2	28.8	30	28.7	M	50-59	30/3/20	0.996	Tel Aviv
13075832	17.5	18.6	20	18.7	M	30-39	30/3/20	0.996	Tel Aviv
13075879	18.6	20	22	20.27	M	50-59	30/3/20	0.993	Tel Aviv
13075882	18.6	20.4	21	20.1	F	20-29	30/3/20	0.996	Tel Aviv
13075914	17.1	18.5	20	18.39	F	50-59	30/3/20	0.996	Tel Aviv
13077377	27	29	29	28.33	M	40-49	2/4/20	0.996	Tel Aviv
13077383	26	26	28	26.67	F	40-49	2/4/20	0.984	Jerusalem
13077413	24	25	26	25	M	70-79	3/4/20	0.996	Tel Aviv
13077494	28	29	31	29.33	M	20-29	2/4/20	0.856	South Coast
13077497	21	22	24	22.33	F	60-69	2/4/20	0.996	South Coast
13077498	17	18	21	18.67	M	20-29	3/4/20	0.996	South Coast
13077510	21	22	25	22.67	M	50-59	3/4/20	0.993	Jerusalem
13077511	25	26	28	26.33	M	20-29	3/4/20	0.986	Jerusalem
13077558	19	20	22	20.33	F	30-39	3/4/20	0.996	Tel Aviv
13077560	27	28	30	28.33	F	80-89	3/4/20	0.974	Tel Aviv
13077562	15	17	19	17	F	50-59	3/4/20	0.988	Tel Aviv
13077564	22	23	25	23.33	F	50-59	3/4/20	0.992	Tel Aviv
13077711	27	28	30	28.33	F	30-39	3/4/20	0.995	Tel Aviv
13077723	22	23	25	23.33	M	?	3/4/20	0.989	Tel Aviv
13077726	20	20	22	20.67	F	60-69	3/4/20	0.996	Tel Aviv
13077803	28	29	32	29.67	F	30-39	4/4/20	0.981	South Coast
13077823	15	17	19	17	F	10-19	4/4/20	0.996	South Coast
13077840	23	25	27	25	M	20-29	4/4/20	0.991	Jerusalem
13077846	19	20	23	20.67	F	0-9	4/4/20	0.996	Tel Aviv
13077847	24	26	27	25.67	M	10-19	4/4/20	0.986	Tel Aviv
13077875	18	19	21	19.33	F	40-49	4/4/20	0.996	Tel Aviv
13077882	24	26	27	25.67	M	40-49	4/4/20	0.987	Jerusalem
51137031				18.58	M	30-39	1/3/20	0.996	Tel Aviv
51137844				27.6	F	30-39	17/3/20	0.983	South
51140028				20.56	F	50-59	17/3/20	0.996	North
51140068				22.8	M	30-39	18/3/20	0.988	South
51140271				28.16	F	40-49	18/3/20	0.971	South Coast
51140279				25.76	F	20-29	18/3/20	0.976	South Coast
51140315				23.41	M	60-69	18/3/20	0.996	South
51140539				19.4	F	50-59	19/3/20	0.996	South
51140836				24.5	M	30-39	20/3/20	0.986	South
51141014				23.08	F	90+	22/3/20	0.996	South
51141121				29.05	M	70-79	22/3/20	0.989	South
51141225				18.58	F	40-49	22/3/20	0.996	South
51144342				25.59	M	90+	30/3/20	0.976	South
51145198				25.49	M	80-89	1/4/20	0.989	South
51145482				27.92	F	40-49	5/4/20	0.992	Tel Aviv
51146355				29.24	F	80-89	4/4/20	0.989	South
51146500				21.79	M	40-49	5/4/20	0.989	Tel Aviv
51146503				23.75	F	30-39	5/4/20	0.993	Jerusalem
51146669				24.41	M	10-19	5/4/20	0.994	Tel Aviv
51146683				24.8	M	10-19	5/4/20	0.965	Tel Aviv
130710062	28	28	28	28	M	40-49	14/4/20	0.991	Tel Aviv

130710067	23	24	24	23.67	M	60-69	14/4/20	0.996	Tel Aviv
130710097	29	31	32	30.67	M	70-79	15/4/20	0.996	Tel Aviv
130710099	33	33	34	33.33	M	60-69	15/4/20	0.979	Tel Aviv
130710157	20	21	24	21.67	M	70-79	15/4/20	0.996	Tel Aviv
130710159	27	28	29	28	F	80-89	15/4/20	0.990	Tel Aviv
130710211	18	19	20	19	F	70-79	16/4/20	0.996	Tel Aviv
130710217	22	23	26	23.67	M	50-59	16/4/20	0.996	Tel Aviv
130710390	28	29	30	29	F	30-39	17/4/20	0.996	Tel Aviv
130710414	20	21	22	21	M	20-29	17/4/20	0.996	Tel Aviv
130710643	31	31	31	31	M	40-49	19/4/20	0.986	Tel Aviv
130710644	29	30	31	30	F	80-89	19/4/20	0.985	Tel Aviv
130710716	30	31	31	30.67	F	60-69	19/4/20	0.989	Tel Aviv
130711082	18.5	20	22	20.17	F	60-69	20/4/20	0.996	Tel Aviv
130711104	27	29	29	28.33	F	80-89	20/4/20	0.993	Tel Aviv
130711112	31	32	31	31.33	F	80-89	21/4/20	0.991	Tel Aviv
130711116	25	27	25	25.67	F	60-69	21/4/20	0.996	Tel Aviv
130711367	29	27	27	27.67	F	60-69	22/4/20	0.996	North
130711417	32	31	30	31	M	60-69	22/4/20	0.974	Tel Aviv
701002313				27	M	50-59	21/3/20	0.996	South Coast
701002314				21	M	20-29	21/3/20	0.996	South Coast
701002317				25	M	50-59	21/3/20	0.996	South Coast
701002327				19	M	50-59	22/3/20	0.996	South Coast
701002334				21	M	70-79	22/3/20	0.996	South Coast
701002403				31	M	40-49	23/3/20	0.996	South Coast
701002407				27	M	40-49	23/3/20	0.959	South Coast
701002426				25	M	60-69	24/3/20	0.996	South Coast
701002431				18	M	20-29	24/3/20	0.996	South Coast
701002440				26	F	20-29	24/3/20	0.996	South Coast
701002442				18	M	30-39	24/3/20	0.996	South Coast
701002455				30	F	20-29	24/3/20	0.992	South Coast
701002456				30	F	60-69	24/3/20	0.980	South Coast
701002458				21	M	40-49	24/3/20	0.996	South Coast
701002462				21	M	70-79	24/3/20	0.996	South Coast
701002489				27	M	40-49	25/3/20	0.996	South Coast
701002504				21	M	70-79	25/3/20	0.996	South Coast
701002538				28	M	70-79	25/3/20	0.996	South Coast
701002540				21	F	40-49	25/3/20	0.996	South Coast
701002550				24	M	30-39	26/3/20	0.996	South Coast
701002555				23	F	40-49	26/3/20	0.996	South Coast
701002556				22	F	60-69	26/3/20	0.996	South Coast
701002561				28	M	50-59	26/3/20	0.996	South Coast
701002591				24	F	50-59	26/3/20	0.996	South Coast
701002666				26	M	40-49	26/3/20	0.996	South Coast
701002681				24	M	60-69	27/3/20	0.996	South Coast
701002752				27	M	10-19	28/3/20	0.987	South Coast
701002768				21	M	50-59	28/3/20	0.996	South Coast
701002786				27	M	60-69	29/3/20	0.996	South Coast
701002792				25	M	50-59	29/3/20	0.995	South Coast
990059202	26.9	28.4	27	27.4	M	60-69	25/3/20	0.996	South Coast

990059203	26.5	28.6	27	27.2	F	80-89	25/3/20	0.996	South Coast
990059204	28.4	30.1	28	28.97	F	30-39	25/3/20	0.976	South Coast
990059217	29.1	31.4	32	30.9	M	60-69	25/3/20	0.995	South Coast
990059230	26.5	29.7	29	28.5	F	0-9	25/3/20	0.972	South Coast
990059231	24.9	28	28	27	M	30-39	25/3/20	0.996	South Coast
990059232	24.5	26.7	28	26.3	M	10-19	25/3/20	0.996	South Coast
990059233	19.7	21.8	23	21.43	F	50-59	25/3/20	0.996	South Coast
990059237	28.3	30.6	32	30.23	F	0-9	25/3/20	0.989	South Coast
990059238	24.3	26.3	27	25.83	F	20-29	25/3/20	0.996	South Coast
990059244	27.9	30.8	31	29.97	F	?	25/3/20	0.938	South Coast
990059251	24.7	28	28	26.9	F	50-59	25/3/20	0.996	South Coast
990059252	24.4	26.8	28	26.27	F	20-29	25/3/20	0.996	South Coast
990300681	22.9	26.4	27	25.37	F	60-69	30/3/20	0.995	South Coast
990300691	29.3	31.7	32	31	M	20-29	31/3/20	0.970	South Coast
990300724	23.7	26.6	26	25.53	M	80-89	1/4/20	0.993	South Coast
990300860	19.3	21.9	0	20.6	M	20-29	2/4/20	0.996	South Coast
990307712	26	27.3	28	26.97	F	20-29	26/3/20	0.996	South Coast
990333068	30.1	32.7	34	32.13	M	60-69	24/3/20	0.963	South Coast
990333189	29.3	31.4	32	30.9	M	50-59	26/3/20	0.950	South Coast
990333193	20.7	22.6	24	22.43	F	40-49	26/3/20	0.996	South Coast
990333263	36.4	0	0	36.4	M	30-39	31/3/20	0.660	South Coast
990430264	29.3	31.7	33	31.17	F	40-49	29/3/20	0.970	South Coast
990430265	29.6	32.2	33	31.7	F	30-39	29/3/20	0.994	South Coast

Supplementary Table 3: Model parameter priors and estimated values ($\theta = 0.8$)

Parameter	Prior	Posterior (Median (95% HPD))					
		$p_h = 0.02$	$p_h = 0.05$	$p_h = 0.10$	$p_h = 0.20$	$p_h = 0.50$	$p_h = 0.80$
Posterior							
Tree height		-46413 (-46465 -46358)	-46425 (-46483 -46357)	-46406 (-46469 -46343)	-46401 (-46462 -46347)	-46421 (-46481 -46360)	
Clock rate	Uniform(5.0e-4, 2.0e-3)	0.377 (0.326 0.443)	0.384 (0.330 0.455)	0.367 (0.323 0.434)	0.356 (0.322 0.413)	0.358 (0.323 0.426)	
κ	Lognormal(M=1.0, SD=1.25)	7.37e-04 (6.10e-04 8.83e-04)	7.36e-04 (6.07e-04 8.87e-04)	7.81e-04 (6.22e-04 9.26e-04)	8.09e-04 (6.84e-04 9.24e-04)	7.68e-04 (6.57e-04 8.87e-04)	
γ	Exponential(M=1.0)	3.719 (3.111 4.484)	3.738 (3.076 4.463)	3.702 (3.028 4.422)	3.720 (3.125 4.499)	3.710 (3.061 4.444)	
R_0	Lognormal(M=1.5, SD=0.5)	3.51e-02 (1.05e-03 8.99e-02)	3.53e-02 (1.02e-03 8.85e-02)	3.90e-02 (1.08e-03 9.32e-02)	3.78e-02 (1.59e-03 8.75e-02)	3.71e-02 (1.01e-03 8.85e-02)	
α	Uniform(0.0, 2.0)	2.52 (2.21 2.86)	2.31 (2.05 2.56)	2.11 (1.87 2.40)	2.04 (1.86 2.24)	2.11 (1.89 2.33)	
E_{mit}	Exponential(M=1.0)	0.27 (0.10 0.54)	0.25 (0.09 0.51)	0.25 (0.07 0.52)	0.20 (0.05 0.43)	0.15 (0.03 0.34)	
Y_{mit}	Exponential(M=1.0)	12.06 (6.42 19.44)	10.19 (5.80 15.62)	8.80 (4.59 13.85)	4.60 (2.52 7.46)	3.25 (1.90 5.15)	
		6.61e-03 (1.88e-03 1.64e-02)	6.72e-03 (2.34e-03 1.40e-02)	3.44e-03 (1.52e-03 1.49e-02)	2.89e-03 (1.87e-03 4.48e-03)	3.35e-03 (2.17e-03 6.23e-03)	

Supplementary Table 4: Model parameter priors and estimated values ($\theta = 0.9$)

Parameter	Prior	Posterior (Median (95% HPD))					
		$p_h = 0.02$	$p_h = 0.05$	$p_h = 0.10$	$p_h = 0.20$	$p_h = 0.50$	$p_h = 0.80$
Posterior		-46384 (-46439 -46323)	-46395 (-46458 -46334)	-46419 (-46473 -46363)	-46388 (-46454 -46326)	-46396 (-46466 -46335)	-46392 (-46451 -46325)
Tree height		0.361 (0.323 0.430)	0.370 (0.323 0.428)	0.380 (0.325 0.445)	0.362 (0.323 0.426)	0.360 (0.323 0.426)	0.360 (0.322 0.421)
Clock rate	Uniform(5.0e-4, 2.0e-3)	7.74e-04 (6.21e-04 8.97e-04)	7.84e-04 (6.63e-04 9.06e-04)	7.37e-04 (6.18e-04 8.63e-04)	8.13e-04 (6.91e-04 9.53e-04)	8.03e-04 (6.83e-04 9.24e-04)	7.98e-04 (6.94e-04 9.16e-04)
κ	Lognormal(M=1.0, SD=1.25)	3.738 (3.104 4.464)	3.743 (3.148 4.552)	3.704 (3.057 4.493)	3.694 (3.093 4.511)	3.732 (3.040 4.401)	3.712 (3.090 4.425)
γ	Exponential(M=1.0)	3.55e-02 (1.00e-03 8.73e-02)	3.80e-02 (1.16e-03 8.87e-02)	3.83e-02 (1.00e-03 8.83e-02)	3.59e-02 (1.01e-03 8.91e-02)	3.97e-02 (1.90e-03 8.98e-02)	3.84e-02 (1.02e-03 9.09e-02)
R_0	Lognormal(M=1.5, SD=0.5)	2.84 (2.52 3.26)	2.36 (2.10 2.63)	2.30 (2.05 2.57)	2.06 (1.84 2.31)	2.04 (1.83 2.31)	2.07 (1.87 2.28)
α	Uniform(0.0, 2.0)	0.27 (0.10 0.55)	0.24 (0.11 0.49)	0.27 (0.09 0.55)	0.21 (0.07 0.41)	0.17 (0.03 0.38)	0.11 (0.03 0.27)
E_{int}	Exponential(M=1.0)	12.47 (6.68 19.79)	15.30 (9.03 23.18)	10.47 (5.76 16.18)	8.42 (4.88 12.97)	4.27 (1.85 7.04)	2.90 (1.54 4.79)
Y_{int}	Exponential(M=1.0)	5.39e-03 (3.01e-03 1.23e-02)	4.56e-03 (2.50e-03 8.35e-03)	6.79e-03 (2.41e-03 1.45e-02)	3.26e-03 (1.70e-03 7.37e-03)	3.27e-03 (1.96e-03 5.16e-03)	3.35e-03 (2.24e-03 4.93e-03)

Supplementary Table 5: Model parameter priors and estimated values ($\theta = 1.0$)

Parameter	Prior	Posterior (Median (95% HPD))					
		$p_h = 0.02$	$p_h = 0.05$	$p_h = 0.10$	$p_h = 0.20$	$p_h = 0.50$	$p_h = 0.80$
Posterior		-46363 (-46426 -46311)	-46370 (-46436 -46310)	-46392 (-46441 -46330)	-46374 (-46436 -46325)	-46396 (-46455 -46339)	-46347 (-46442 -46276)
Tree height		0.368 (0.323 0.437)	0.358 (0.323 0.429)	0.360 (0.322 0.420)	0.359 (0.322 0.414)	0.361 (0.323 0.420)	0.360 (0.323 0.420)
Clock rate	Uniform(5.0e-4, 2.0e-3)	8.01e-04 (6.49e-04 9.37e-04)	8.24e-04 (6.73e-04 9.97e-04)	7.87e-04 (6.82e-04 8.98e-04)	8.41e-04 (7.21e-04 9.55e-04)	7.98e-04 (6.82e-04 9.03e-04)	8.35e-04 (7.04e-04 9.62e-04)
κ	Lognormal(M=1.0, SD=1.25)	3.770 (3.041 4.455)	3.737 (3.055 4.444)	3.743 (3.099 4.500)	3.710 (2.982 4.388)	3.704 (3.087 4.432)	3.732 (3.067 4.526)
γ	Exponential(M=1.0)	3.76e-02 (1.01e-03 9.23e-02)	3.81e-02 (1.05e-03 9.01e-02)	3.79e-02 (1.10e-03 9.37e-02)	3.91e-02 (1.04e-03 8.88e-02)	3.89e-02 (1.14e-03 8.76e-02)	3.56e-02 (1.04e-03 8.58e-02)
R_0	Lognormal(M=1.5, SD=0.5)	2.66 (2.36 3.06)	2.29 (1.96 2.62)	2.16 (1.94 2.40)	1.97 (1.78 2.18)	1.99 (1.78 2.22)	1.98 (1.69 2.35)
α	Uniform(0.0, 2.0)	0.25 (0.10 0.45)	0.29 (0.12 0.53)	0.26 (0.09 0.50)	0.26 (0.08 0.52)	0.15 (0.03 0.38)	0.05 (0.02 0.21)
E_{int}	Exponential(M=1.0)	15.33 (7.65 24.34)	15.92 (7.50 26.28)	13.07 (7.63 19.05)	9.60 (5.76 13.70)	4.79 (2.82 7.16)	2.27 (0.44 3.94)
Y_{int}	Exponential(M=1.0)	5.77e-03 (2.51e-03 1.33e-02)	4.38e-03 (2.34e-03 9.65e-03)	4.56e-03 (2.70e-03 8.19e-03)	3.22e-03 (1.98e-03 5.29e-03)	3.64e-03 (2.42e-03 5.72e-03)	3.84e-03 (2.36e-03 5.96e-03)

Supplementary Table 6: Model parameter priors and estimated values ($\theta = 1.1$)

Parameter	Prior	Posterior (Median (95% HPD))					
		$p_h = 0.02$	$p_h = 0.05$	$p_h = 0.10$	$p_h = 0.20$	$p_h = 0.50$	$p_h = 0.80$
Posterior		-46359 (-46429 -46296)	-46375 (-46426 -46320)	-46382 (-46434 -46333)	-46383 (-46439 -46335)	-46379 (-46444 -46298)	-46372 (-46434 -46305)
Tree height		0.394 (0.338 0.465)	0.375 (0.327 0.432)	0.371 (0.325 0.430)	0.363 (0.324 0.427)	0.362 (0.323 0.425)	0.369 (0.326 0.431)
Clock rate	Uniform(5.0e-4, 2.0e-3)	7.60e-04 (6.23e-04 8.93e-04)	7.83e-04 (6.87e-04 8.96e-04)	7.83e-04 (6.74e-04 9.16e-04)	8.10e-04 (6.85e-04 9.33e-04)	7.97e-04 (6.79e-04 9.12e-04)	7.72e-04 (6.74e-04 8.82e-04)
κ	Lognormal(M=1.0, SD=1.25)	3.741 (3.068 4.507)	3.739 (3.114 4.505)	3.708 (3.116 4.532)	3.704 (3.066 4.392)	3.733 (3.044 4.530)	3.765 (3.086 4.450)
γ	Exponential(M=1.0)	3.52e-02 (1.03e-03 8.89e-02)	3.61e-02 (1.02e-03 8.48e-02)	3.81e-02 (1.04e-03 8.99e-02)	3.60e-02 (1.07e-03 9.15e-02)	3.50e-02 (1.24e-03 8.81e-02)	3.51e-02 (1.02e-03 8.78e-02)
R_0	Lognormal(M=1.5, SD=0.5)	2.74 (2.47 3.13)	2.32 (2.11 2.56)	2.10 (1.90 2.31)	1.97 (1.80 2.14)	1.96 (1.71 2.17)	2.08 (1.81 2.44)
α	Uniform(0.0, 2.0)	0.25 (0.11 0.49)	0.26 (0.09 0.47)	0.28 (0.12 0.52)	0.26 (0.07 0.56)	0.12 (0.02 0.36)	0.05 (0.02 0.26)
E_{int}	Exponential(M=1.0)	14.42 (6.51 23.58)	17.19 (9.51 25.18)	16.01 (10.05 22.30)	10.34 (6.67 14.68)	4.15 (1.98 6.47)	1.77 (0.37 3.36)
Y_{int}	Exponential(M=1.0)	9.11e-03 (4.69e-03 1.67e-02)	6.40e-03 (3.83e-03 1.02e-02)	5.38e-03 (2.87e-03 8.66e-03)	4.64e-03 (2.82e-03 7.46e-03)	4.63e-03 (3.01e-03 6.83e-03)	6.03e-03 (3.66e-03 9.42e-03)

Supplementary Table 7: Model parameter priors and estimated values ($\theta = 1.2$)

Parameter	Prior	Posterior (Median (95% HPD))					
		$p_h = 0.02$	$p_h = 0.05$	$p_h = 0.10$	$p_h = 0.20$	$p_h = 0.50$	$p_h = 0.80$
Posterior		-46351 (-46400 -46310)	-46378 (-46435 -46321)	-46385 (-46436 -46331)	-46355 (-46415 -46297)	-46346 (-46427 -46274)	-46406 (-46456 -46358)
Tree height		0.422 (0.368 0.488)	0.407 (0.354 0.474)	0.392 (0.337 0.456)	0.379 (0.329 0.437)	0.367 (0.327 0.422)	0.381 (0.338 0.437)
Clock rate	Uniform(5.0e-4, 2.0e-3)	7.46e-04 (6.52e-04 8.41e-04)	7.43e-04 (6.39e-04 8.65e-04)	7.60e-04 (6.55e-04 8.94e-04)	7.82e-04 (6.78e-04 9.09e-04)	7.52e-04 (6.44e-04 8.81e-04)	6.92e-04 (5.96e-04 8.01e-04)
κ	Lognormal(M=1.0, SD=1.25)	3.686 (3.062 4.395)	3.683 (3.043 4.458)	3.713 (3.091 4.422)	3.717 (3.029 4.462)	3.689 (3.012 4.392)	3.669 (3.016 4.399)
γ	Exponential(M=1.0)	3.88e-02 (1.13e-03 8.46e-02)	3.76e-02 (1.09e-03 8.78e-02)	3.67e-02 (1.04e-03 9.03e-02)	3.75e-02 (1.01e-03 9.39e-02)	3.61e-02 (1.31e-03 8.70e-02)	3.73e-02 (1.12e-03 9.24e-02)
R_0	Lognormal(M=1.5, SD=0.5)	2.80 (2.51 3.13)	2.33 (2.11 2.62)	2.14 (1.91 2.37)	1.91 (1.69 2.13)	2.33 (1.75 2.70)	2.54 (2.11 3.18)
α	Uniform(0.0, 2.0)	0.27 (0.13 0.52)	0.30 (0.13 0.56)	0.32 (0.12 0.60)	0.15 (0.03 0.40)	0.06 (0.02 0.23)	0.12 (0.02 0.29)
E_{int}	Exponential(M=1.0)	13.47 (6.82 21.96)	17.31 (9.80 26.52)	14.30 (8.12 21.25)	10.54 (6.14 15.98)	0.98 (0.28 3.87)	0.60 (0.04 1.83)
Y_{int}	Exponential(M=1.0)	1.38e-02 (9.24e-03 1.98e-02)	1.15e-02 (6.26e-03 1.91e-02)	8.82e-03 (4.80e-03 1.35e-02)	7.10e-03 (3.68e-03 1.08e-02)	8.02e-03 (4.16e-03 1.41e-02)	9.90e-03 (5.60e-03 1.88e-02)

Supplementary Table 8: Model parameter priors and estimated values ($\eta = 10$)

Parameter	Prior	Posterior (Median (95% HPD))					
		$p_h = 0.02$	$p_h = 0.05$	$p_h = 0.10$	$p_h = 0.20$	$p_h = 0.50$	$p_h = 0.80$
Posterior		-46404 (-46444 -46360)	-46403 (-46459 -46341)	-46376 (-46428 -46302)	-46318 (-46398 -46257)	-46355 (-46406 -46301)	-46344 (-46384 -46299)
Tree height		0.394 (0.344 0.448)	0.377 (0.330 0.438)	0.407 (0.357 0.453)	0.445 (0.387 0.500)	0.473 (0.419 0.529)	0.450 (0.403 0.496)
Clock rate	Uniform(5.0e-4, 2.0e-3)	6.75e-04 (5.60e-04 7.81e-04)	7.29e-04 (5.81e-04 8.75e-04)	6.62e-04 (5.68e-04 7.53e-04)	6.16e-04 (5.34e-04 6.91e-04)	5.46e-04 (5.00e-04 6.20e-04)	6.31e-04 (5.66e-04 7.05e-04)
κ	Lognormal(M=1.0, SD=1.25)	3.709 (3.074 4.455)	3.746 (3.119 4.534)	3.727 (3.068 4.507)	3.718 (3.045 4.478)	3.694 (3.139 4.518)	3.683 (3.090 4.525)
γ	Exponential(M=1.0)	3.56e-02 (1.10e-03 8.78e-02)	3.37e-02 (1.28e-03 8.77e-02)	3.76e-02 (1.03e-03 9.27e-02)	3.76e-02 (1.00e-03 8.98e-02)	3.46e-02 (1.23e-03 8.77e-02)	3.57e-02 (1.64e-03 9.15e-02)
R_0	Lognormal(M=1.5, SD=0.5, MIN=1.0)	3.03 (2.64 3.56)	2.52 (2.16 2.94)	2.09 (1.88 2.35)	2.25 (2.09 2.56)	2.20 (1.96 2.47)	2.16 (2.02 2.29)
α	Uniform(0.0, 2.0)	0.26 (0.06 0.78)	0.24 (0.08 0.51)	0.22 (0.08 0.47)	0.24 (0.08 0.49)	0.18 (0.04 0.44)	0.14 (0.04 0.31)
E_{int}	Exponential(M=1.0)	11.29 (5.93 18.48)	10.61 (5.33 17.85)	21.86 (17.25 25.48)	8.13 (4.73 12.73)	5.59 (3.58 8.27)	3.12 (2.83 3.66)
Y_{int}	Exponential(M=1.0)	1.14e-02 (4.64e-03 2.60e-02)	7.76e-03 (2.49e-03 2.41e-02)	1.38e-02 (6.91e-03 2.49e-02)	3.29e-02 (1.32e-02 7.50e-02)	6.82e-02 (2.18e-02 1.74e-01)	4.82e-02 (2.75e-02 8.72e-02)

Supplementary Table 9: Model parameter priors and estimated values ($n = 100$)

Parameter	Prior	Posterior (Median (95% HPD))					
		$p_h = 0.02$	$p_h = 0.05$	$p_h = 0.10$	$p_h = 0.20$	$p_h = 0.50$	$p_h = 0.80$
Posterior		-46392 (-46447 -46341)	-46339 (-46399 -46293)	-46389 (-46435 -46316)	-46373 (-46436 -46321)	-46379 (-46424 -46334)	-46379 (-46431 -46324)
Tree height		0.375 (0.329 0.431)	0.435 (0.338 0.494)	0.398 (0.344 0.483)	0.397 (0.343 0.460)	0.421 (0.362 0.488)	0.471 (0.410 0.544)
Clock rate	Uniform(5.0e-4, 2.0e-3)	7.06e-04 (5.94e-04 8.61e-04)	6.03e-04 (5.17e-04 8.14e-04)	6.20e-04 (5.00e-04 7.27e-04)	6.33e-04 (5.42e-04 7.35e-04)	6.04e-04 (5.12e-04 6.88e-04)	5.38e-04 (5.00e-04 5.97e-04)
κ	Lognormal(M=1.0, SD=1.25)	3.699 (3.055 4.405)	3.718 (3.009 4.404)	3.724 (3.077 4.515)	3.739 (3.098 4.454)	3.691 (2.991 4.433)	3.703 (3.061 4.438)
γ	Exponential(M=1.0)	3.50e-02 (1.03e-03 8.47e-02)	3.59e-02 (1.39e-03 8.92e-02)	3.53e-02 (1.06e-03 8.63e-02)	3.72e-02 (1.14e-03 8.99e-02)	3.52e-02 (1.27e-03 9.11e-02)	3.39e-02 (1.03e-03 8.23e-02)
R_0	Lognormal(M=1.5, SD=0.5, MIN=1.0)	2.94 (2.57 3.31)	2.57 (2.29 2.85)	2.25 (2.00 2.72)	2.13 (1.95 2.34)	2.14 (1.95 2.31)	2.22 (2.07 2.42)
α	Uniform(0.0, 2.0)	0.27 (0.08 0.57)	0.29 (0.08 0.69)	0.28 (0.10 0.62)	0.18 (0.04 0.38)	0.15 (0.05 0.33)	0.15 (0.04 0.37)
E_{int}	Exponential(M=1.0)	11.22 (6.25 17.19)	18.17 (8.53 24.04)	19.96 (16.05 25.55)	11.80 (7.88 14.31)	5.33 (4.11 6.61)	4.17 (3.75 4.71)
Y_{int}	Exponential(M=1.0)	8.85e-03 (2.72e-03 2.13e-02)	4.56e-02 (2.61e-03 1.35e-01)	1.78e-02 (5.16e-03 1.12e-01)	1.57e-02 (3.12e-03 5.08e-02)	2.84e-02 (8.84e-03 8.63e-02)	9.58e-02 (3.68e-02 2.90e-01)

Supplementary Table 10: Model parameter priors and estimated values ($n = 1000$)

Parameter	Prior	Posterior (Median (95% HPD))					
		$p_h = 0.02$	$p_h = 0.05$	$p_h = 0.10$	$p_h = 0.20$	$p_h = 0.50$	$p_h = 0.80$
Posterior		-46378 (-46419 -46325)	-46356 (-46409 -46309)	-46361 (-46414 -46297)	-46373 (-46435 -46296)	-46405 (-46464 -46317)	-46481 (-46545 -46395)
Tree height		0.365 (0.336 0.400)	0.351 (0.325 0.380)	0.337 (0.323 0.366)	0.338 (0.323 0.358)	0.335 (0.322 0.350)	0.342 (0.322 0.366)
Clock rate	Uniform(5.0e-4, 2.0e-3)	6.80e-04 (5.94e-04 8.04e-04)	7.55e-04 (6.50e-04 8.52e-04)	7.89e-04 (6.73e-04 9.25e-04)	7.82e-04 (6.59e-04 9.04e-04)	7.63e-04 (6.65e-04 8.81e-04)	6.63e-04 (5.53e-04 7.97e-04)
κ	Lognormal(M=1.0, SD=1.25)	3.732 (3.088 4.535)	3.710 (3.079 4.476)	3.737 (3.064 4.491)	3.724 (3.049 4.480)	3.719 (3.081 4.480)	3.726 (3.053 4.414)
γ	Exponential(M=1.0)	3.53e-02 (1.00e-03 9.50e-02)	3.64e-02 (1.28e-03 9.05e-02)	3.56e-02 (1.12e-03 8.55e-02)	3.40e-02 (1.12e-03 8.97e-02)	3.71e-02 (1.07e-03 8.64e-02)	3.57e-02 (1.11e-03 8.62e-02)
R_0	Lognormal(M=1.5, SD=0.5, MIN=1.0)	3.15 (2.77 3.53)	2.57 (2.32 2.84)	2.20 (1.98 2.44)	2.06 (1.84 2.32)	1.94 (1.70 2.30)	2.07 (1.79 2.36)
α	Uniform(0.0, 2.0)	0.30 (0.08 0.81)	0.27 (0.13 0.51)	0.27 (0.12 0.49)	0.24 (0.11 0.47)	0.21 (0.12 0.36)	0.21 (0.10 0.40)
E_{int}	Exponential(M=1.0)	8.41 (5.17 14.35)	8.98 (5.18 13.40)	10.20 (5.42 16.84)	7.38 (4.43 10.23)	3.96 (1.25 6.39)	3.43 (0.78 5.47)
Y_{int}	Exponential(M=1.0)	1.18e-02 (6.39e-03 2.03e-02)	8.61e-03 (4.53e-03 1.44e-02)	5.91e-03 (3.89e-03 1.05e-02)	5.87e-03 (3.52e-03 1.00e-02)	6.36e-03 (4.12e-03 9.45e-03)	8.74e-03 (4.48e-03 1.69e-02)

Supplementary Table 11: Model parameter priors and estimated values ($n = 2500$)

Parameter	Prior	Posterior (Median (95% HPD))					
		$p_h = 0.02$	$p_h = 0.05$	$p_h = 0.10$	$p_h = 0.20$	$p_h = 0.50$	$p_h = 0.80$
Posterior		-46338 (-46385 -46296)	-46323 (-46371 -46275)	-46335 (-46400 -46275)	-46335 (-46412 -46262)	-46452 (-46525 -46388)	-46448 (-46510 -46390)
Tree height		0.348 (0.326 0.369)	0.341 (0.323 0.362)	0.340 (0.323 0.366)	0.340 (0.325 0.359)	0.417 (0.391 0.443)	0.417 (0.391 0.444)
Clock rate	Uniform(5.0e-4, 2.0e-3)	7.70e-04 (6.52e-04 8.90e-04)	7.81e-04 (6.84e-04 8.94e-04)	7.82e-04 (6.62e-04 9.20e-04)	7.68e-04 (6.39e-04 8.91e-04)	5.19e-04 (5.00e-04 5.79e-04)	5.15e-04 (5.00e-04 5.54e-04)
κ	Lognormal(M=1.0, SD=1.25)	3.739 (3.015 4.377)	3.721 (3.105 4.471)	3.713 (3.055 4.429)	3.686 (3.076 4.435)	3.681 (3.046 4.429)	3.688 (2.975 4.359)
γ	Exponential(M=1.0)	3.53e-02 (1.17e-03 8.13e-02)	3.56e-02 (1.05e-03 9.57e-02)	3.78e-02 (1.01e-03 9.14e-02)	3.79e-02 (1.23e-03 9.21e-02)	3.68e-02 (1.02e-03 9.42e-02)	3.75e-02 (1.08e-03 8.69e-02)
R_0	Lognormal(M=1.5, SD=0.5, MIN=1.0)	2.83 (2.58 3.17)	2.44 (2.18 2.69)	2.17 (1.91 2.38)	2.05 (1.79 2.37)	1.01 (1.00 1.05)	1.06 (1.00 1.14)
α	Uniform(0.0, 2.0)	0.27 (0.11 0.54)	0.27 (0.14 0.48)	0.30 (0.15 0.50)	0.29 (0.17 0.44)	0.55 (0.38 0.74)	0.41 (0.25 0.59)
E_{int}	Exponential(M=1.0)	10.88 (6.51 15.44)	10.56 (6.93 15.36)	9.31 (4.64 13.16)	4.80 (2.38 8.79)	2.01 (1.40 2.63)	1.82 (1.27 2.39)
Y_{int}	Exponential(M=1.0)	1.46e-02 (8.50e-03 2.38e-02)	1.10e-02 (6.63e-03 1.60e-02)	1.01e-02 (5.00e-03 1.75e-02)	9.90e-03 (5.06e-03 1.87e-02)	8.67e-02 (4.53e-02 1.38e-01)	9.12e-02 (5.60e-02 1.36e-01)

Supplementary Table 12: Model parameter priors and estimated values ($n = 5000$)

Parameter	Prior	Posterior (Median (95% HPD))					
		$p_h = 0.02$	$p_h = 0.05$	$p_h = 0.10$	$p_h = 0.20$	$p_h = 0.50$	$p_h = 0.80$
Posterior		-46335 (-46377 -46289)	-46327 (-46379 -46279)	-46326 (-46382 -46263)	-46306 (-46363 -46253)	-46365 (-46424 -46315)	-46428 (-46478 -46380)
Tree height		0.355 (0.327 0.381)	0.348 (0.328 0.370)	0.344 (0.326 0.364)	0.444 (0.425 0.466)	0.436 (0.412 0.464)	0.439 (0.414 0.463)
Clock rate	Uniform(5.0e-4, 2.0e-3)	7.21e-04 (6.21e-04 8.30e-04)	7.66e-04 (6.57e-04 8.80e-04)	7.87e-04 (6.71e-04 9.08e-04)	5.07e-04 (5.00e-04 5.30e-04)	5.07e-04 (5.00e-04 5.29e-04)	5.05e-04 (5.00e-04 5.22e-04)
κ	Lognormal(M=1.0, SD=1.25)	3.712 (3.017 4.416)	3.726 (3.050 4.425)	3.725 (3.073 4.472)	3.696 (3.057 4.427)	3.682 (3.055 4.400)	3.700 (3.058 4.495)
γ	Exponential(M=1.0)	3.96e-02 (1.12e-03 9.39e-02)	3.38e-02 (1.15e-03 8.39e-02)	3.49e-02 (1.26e-03 8.90e-02)	3.69e-02 (1.16e-03 9.11e-02)	3.67e-02 (1.02e-03 8.53e-02)	3.47e-02 (1.01e-03 8.95e-02)
R_0	Lognormal(M=1.5, SD=0.5, MIN=1.0)	2.86 (2.58 3.19)	2.39 (2.14 2.68)	2.25 (1.95 2.52)	1.02 (1.00 1.06)	1.03 (1.00 1.09)	1.11 (1.03 1.18)
α	Uniform(0.0, 2.0)	0.27 (0.11 0.52)	0.32 (0.16 0.54)	0.32 (0.19 0.54)	0.82 (0.62 0.99)	0.68 (0.49 0.88)	0.49 (0.34 0.68)
E_{int}	Exponential(M=1.0)	11.61 (6.50 17.27)	10.88 (4.52 17.09)	5.95 (2.84 9.63)	2.55 (2.12 2.82)	2.04 (1.51 2.60)	1.57 (1.14 2.10)
Y_{int}	Exponential(M=1.0)	2.22e-02 (1.37e-02 3.43e-02)	1.79e-02 (9.95e-03 2.86e-02)	1.27e-02 (8.02e-03 1.83e-02)	1.65e-01 (1.09e-01 2.48e-01)	1.49e-01 (9.60e-02 2.29e-01)	1.49e-01 (9.54e-02 2.21e-01)

Supplementary Table 13. Sequencing primer list

name	seq	length
nCoV-2019_1_LEFT	ACCAACCAACTTTCGATCTCTTGT	24
nCoV-2019_1_RIGHT	CATCTTTAAGATGTTGACGTGCCTC	25
nCoV-2019_2_LEFT	CTGTTTTACAGGTTGCGGACGT	22
nCoV-2019_2_RIGHT	TAAGGATCAGTGCCAAGCTCGT	22
nCoV-2019_3_LEFT	CGGTAATAAAGGAGCTGGTGGC	22
nCoV-2019_3_RIGHT	AAGGTGTCTGCAATTCATAGCTCT	24
nCoV-2019_4_LEFT	GGTGTATACTGCTGCCGTGAAC	22
nCoV-2019_4_RIGHT	CACAAGTAGTGGCACCTTCTTTAGT	25
nCoV-2019_5_LEFT	TGGTGAAACTTCATGGCAGACG	22
nCoV-2019_5_RIGHT	ATTGATGTTGACTTTCTCTTTTGGAGT	28
nCoV-2019_6_LEFT	GGTGTGTTGGAGAAGGTTCCG	22
nCoV-2019_6_RIGHT	TAGCGGCCTTCTGTAACACAG	22
nCoV-2019_7_LEFT	ATCAGAGGCTGCTCGTGTGTA	22
nCoV-2019_7_LEFT_alt0	CATTTGCATCAGAGGCTGCTCG	22
nCoV-2019_7_RIGHT	TGCACAGGTGACAATTTGTCCA	22
nCoV-2019_7_RIGHT_alt5	AGGTGACAATTTGTCCACCGAC	22
nCoV-2019_8_LEFT	AGAGTTTCTTAGAGACGGTTGGGA	24
nCoV-2019_8_RIGHT	GCTTCAACAGCTTACTAGTAGGT	24
nCoV-2019_9_LEFT	TCCCACAGAAGTGTTAACAGAGGA	24
nCoV-2019_9_LEFT_alt4	TTCCCACAGAAGTGTTAACAGAGG	24
nCoV-2019_9_RIGHT	ATGACAGCATCTGCCACAACAC	22
nCoV-2019_9_RIGHT_alt2	GACAGCATCTGCCACAACACAG	22
nCoV-2019_10_LEFT	TGAGAAGTGCTCTGCCTATACAGT	24
nCoV-2019_10_RIGHT	TCATCTAACCAATCTTCTTCTTGCTCT	27
nCoV-2019_11_LEFT	GGAATTTGGTGCCACTTCTGCT	22
nCoV-2019_11_RIGHT	TCATCAGATTCAACTTGCATGGCA	24
nCoV-2019_12_LEFT	AAACATGGAGGAGGTGTTGCAG	22
nCoV-2019_12_RIGHT	TTCACTTTCATTTCCAAAAAGCTTGA	27
nCoV-2019_13_LEFT	TCGCACAAATGTCTACTTAGCTGT	24
nCoV-2019_13_RIGHT	ACCACAGCAGTTAAAACACCCT	22
nCoV-2019_14_LEFT	CATCCAGATTCTGCCACTCTTGT	23
nCoV-2019_14_LEFT_alt4	TGGCAATCTTCATCCAGATTCTGC	24
nCoV-2019_14_RIGHT	AGTTTCCACACAGACAGGCATT	22
nCoV-2019_14_RIGHT_alt2	TGCGTGTTTCTTCTGCATGTGC	22
nCoV-2019_15_LEFT	ACAGTGCTTAAAAAGTGTAAGTGCC	27
nCoV-2019_15_LEFT_alt1	AGTGCTTAAAAAGTGTAAGTGCC	26
nCoV-2019_15_RIGHT	AACAGAACTGTAGCTGGCACT	22
nCoV-2019_15_RIGHT_alt3	ACTGTAGCTGGCACTTTGAGAGA	23
nCoV-2019_16_LEFT	AATTTGGAAGAAGCTGCTCGGT	22
nCoV-2019_16_RIGHT	CACAACCTGCGTGTGGAGGTTA	22
nCoV-2019_17_LEFT	CTTCTTTCTTTGAGAGAAGTGAGGACT	27
nCoV-2019_17_RIGHT	TTTGTTGGAGTGTTAACAATGCAGT	25
nCoV-2019_18_LEFT	TGGAATACCCACAAGTTAATGGTTTAAAC	29
nCoV-2019_18_LEFT_alt2	ACTTCTATTAATGGGCAGATAACAACCTGT	30
nCoV-2019_18_RIGHT	AGCTTGTTTACCACACGTACAAGG	24

nCoV-2019_18_RIGHT_alt1	GCTTGTTTACCACACGTACAAGG	23
nCoV-2019_19_LEFT	GCTGTTATGTACATGGGCACACT	23
nCoV-2019_19_RIGHT	TGTCCAACCTAGGGTCAATTTCTGT	25
nCoV-2019_20_LEFT	ACAAAGAAAACAGTTACACAACAACCA	27
nCoV-2019_20_RIGHT	ACGTGGCTTTATTAGTTGCATTGTT	25
nCoV-2019_21_LEFT	TGGCTATTGATTATAAACACTACACACCC	29
nCoV-2019_21_LEFT_alt2	GGCTATTGATTATAAACACTACACACCT	29
nCoV-2019_21_RIGHT	TAGATCTGTGTGGCCAACCTCT	22
nCoV-2019_21_RIGHT_alt0	GATCTGTGTGGCCAACCTCTC	22
nCoV-2019_22_LEFT	ACTACCGAAGTTGTAGGAGACATTATACT	29
nCoV-2019_22_RIGHT	ACAGTATTCTTTGCTATAGTAGTCGGC	27
nCoV-2019_23_LEFT	ACAACACTAACATAGTTACACGGTGT	27
nCoV-2019_23_RIGHT	ACCAGTACAGTAGGTTGCAATAGTG	25
nCoV-2019_24_LEFT	AGGCATGCCTTCTTACTGTAAGT	23
nCoV-2019_24_RIGHT	ACATTCTAACCATAGCTGAAATCGGG	26
nCoV-2019_25_LEFT	GCAATTGTTTTTCAGCTATTTTGCAGT	27
nCoV-2019_25_RIGHT	ACTGTAGTGACAAGTCTCTCGCA	23
nCoV-2019_26_LEFT	TTGTGATACATTCTGTGCTGGTAGT	25
nCoV-2019_26_RIGHT	TCCGCACTATCACCACATCAG	22
nCoV-2019_27_LEFT	ACTACAGTCAGCTTATGTGTCAACC	25
nCoV-2019_27_RIGHT	AATACAAGCACCAAGGTCACGG	22
nCoV-2019_28_LEFT	ACATAGAAGTTACTGGCGATAGTTGT	26
nCoV-2019_28_RIGHT	TGTTTAGACATGACATGAACAGGTGT	26
nCoV-2019_29_LEFT	ACTTGTGTTCTTTTTGTTGCTGC	24
nCoV-2019_29_RIGHT	AGTGTACTCTATAAGTTTTGATGGTGTGT	29
nCoV-2019_30_LEFT	GCACAACATAATGGTGACTTTTTGCA	25
nCoV-2019_30_RIGHT	ACCACTAGTAGATACACAAACACCAG	26
nCoV-2019_31_LEFT	TTCTGAGTACTGTAGGCACGGC	22
nCoV-2019_31_RIGHT	ACAGAATAAACACCAGGTAAGAATGAGT	28
nCoV-2019_32_LEFT	TGGTGAATACAGTCATGTAGTTGCC	25
nCoV-2019_32_RIGHT	AGCACATCACTACGCAACTTTAGA	24
nCoV-2019_33_LEFT	ACTTTTGAAGAAGCTGCGCTGT	22
nCoV-2019_33_RIGHT	TGGACAGTAACTACGTCATCAAGC	25
nCoV-2019_34_LEFT	TCCCATCTGGTAAAGTTGAGGGT	23
nCoV-2019_34_RIGHT	AGTGAAATTGGGCCTCATAGCA	22
nCoV-2019_35_LEFT	TGTTTCGCATTCAACCAGGACAG	22
nCoV-2019_35_RIGHT	ACTTCATAGCCACAAGGTTAAAGTCA	26
nCoV-2019_36_LEFT	TTAGCTTGGTTGTACGCTGCTG	22
nCoV-2019_36_RIGHT	GAACAAAGACCATTGAGTACTCTGGA	26
nCoV-2019_37_LEFT	ACACACCACTGGTTGTTACTCAC	23
nCoV-2019_37_RIGHT	GTCCACACTCTCCTAGCACCAT	22
nCoV-2019_38_LEFT	ACTGTGTTATGTATGCATCAGCTGT	25
nCoV-2019_38_RIGHT	CACCAAGAGTCAGTCTAAAGTAGCG	25
nCoV-2019_39_LEFT	AGTATTGCCCTATTTTCTTCATAACTGGT	29
nCoV-2019_39_RIGHT	TGTAACCTGGACACATTGAGCCC	22
nCoV-2019_40_LEFT	TGCACATCAGTAGTCTTACTCTCAGT	26
nCoV-2019_40_RIGHT	CATGGCTGCATCACGGTCAAAT	22
nCoV-2019_41_LEFT	GTTCCCTTCCATCATATGCAGCT	23

nCoV-2019_41_RIGHT	TGGTATGACAACCATTAGTTTGGCT	25
nCoV-2019_42_LEFT	TGCAAGAGATGGTTGTGTTCCC	22
nCoV-2019_42_RIGHT	CCTACCTCCCTTTGTTGTGTTGT	23
nCoV-2019_43_LEFT	TACGACAGATGTCTTGTGCTGC	22
nCoV-2019_43_RIGHT	AGCAGCATCTACAGCAAAAGCA	22
nCoV-2019_44_LEFT	TGCCACAGTACGTCTACAAGCT	22
nCoV-2019_44_LEFT_alt3	CCACAGTACGTCTACAAGCTGG	22
nCoV-2019_44_RIGHT	AACCTTTCCACATACCGCAGAC	22
nCoV-2019_44_RIGHT_alt0	CGCAGACGGTACAGACTGTGTT	22
nCoV-2019_45_LEFT	TACCTACAACCTGTGCTAATGACCC	25
nCoV-2019_45_LEFT_alt2	AGTATGTACAAATACCTACAACCTGTGCT	29
nCoV-2019_45_RIGHT	AAATTGTTTTCTTCATGTTGGTAGTTAGAGA	30
nCoV-2019_45_RIGHT_alt7	TTCATGTTGGTAGTTAGAGAAAGTGTGTC	29
nCoV-2019_46_LEFT	TGTCGCTTCCAAGAAAAGGACG	22
nCoV-2019_46_LEFT_alt1	CGCTTCCAAGAAAAGGACGAAGA	23
nCoV-2019_46_RIGHT	CACGTTACCTAAGTTGGCGTA	22
nCoV-2019_46_RIGHT_alt2	CACGTTACCTAAGTTGGCGTAT	23
nCoV-2019_47_LEFT	AGGACTGGTATGATTTTGTAGAAAACCC	28
nCoV-2019_47_RIGHT	AATAACGGTCAAAGAGTTTTAACCTCTC	28
nCoV-2019_48_LEFT	TGTTGACACTGACTTAACAAAGCCT	25
nCoV-2019_48_RIGHT	TAGATTACCAGAAGCAGCGTGC	22
nCoV-2019_49_LEFT	AGGAATTACTTGTGTATGCTGCTGA	25
nCoV-2019_49_RIGHT	TGACGATGACTTGGTTAGCATTAAATACA	28
nCoV-2019_50_LEFT	GTTGATAAGTACTTTGATTGTTACGATGGT	30
nCoV-2019_50_RIGHT	TAACATGTTGTGCCAACCA	22
nCoV-2019_51_LEFT	TCAATAGCCGCCACTAGAGGAG	22
nCoV-2019_51_RIGHT	AGTGCATTAACATTGGCCGTGA	22
nCoV-2019_52_LEFT	CATCAGGAGATGCCACAACCTGC	22
nCoV-2019_52_RIGHT	GTTGAGAGCAAAATTCATGAGGTCC	25
nCoV-2019_53_LEFT	AGCAAAATGTTGGACTGAGACTGA	24
nCoV-2019_53_RIGHT	AGCCTCATAAACTCAGGTTCCC	23
nCoV-2019_54_LEFT	TGAGTTAACAGGACACATGTTAGACA	26
nCoV-2019_54_RIGHT	AACCAAAAACCTGTCCATTAGCACA	25
nCoV-2019_55_LEFT	ACTCAACTTTACTTAGGAGGTATGAGCT	28
nCoV-2019_55_RIGHT	GGTGTACTCTCCTATTTGTACTTTACTGT	29
nCoV-2019_56_LEFT	ACCTAGACCACCACTTAACCGA	22
nCoV-2019_56_RIGHT	ACACTATGCGAGCAGAAGGGTA	22
nCoV-2019_57_LEFT	ATTCTACACTCCAGGGACCACC	22
nCoV-2019_57_RIGHT	GTAATTGAGCAGGGTCGCCAAT	22
nCoV-2019_58_LEFT	TGATTTGAGTGTGTTGCAATGCCAGA	25
nCoV-2019_58_RIGHT	CTTTTCTCCAAGCAGGGTTACGT	23
nCoV-2019_59_LEFT	TCACGCATGATGTTTCATCTGCA	23
nCoV-2019_59_RIGHT	AAGAGTCCTGTTACATTTTCAGCTTG	26
nCoV-2019_60_LEFT	TGATAGAGACCTTTATGACAAGTTGCA	27
nCoV-2019_60_RIGHT	GGTACCAACAGCTTCTCTAGTAGC	24
nCoV-2019_61_LEFT	TGTTTATCACCCGCGAAGAAGC	22
nCoV-2019_61_RIGHT	ATCACATAGACAACAGGTGCGC	22
nCoV-2019_62_LEFT	GGCACATGGCTTTGAGTTGACA	22

nCoV-2019_62_RIGHT	GTTGAACCTTTCTACAAGCCGC	22
nCoV-2019_63_LEFT	TGTTAAGCGTGTGACTGGACT	22
nCoV-2019_63_RIGHT	ACAAACTGCCACCATCACAACC	22
nCoV-2019_64_LEFT	TCGATAGATATCCTGCTAATTCATTGT	28
nCoV-2019_64_RIGHT	AGTCTTGTAAGTGTCCAGAGGT	25
nCoV-2019_65_LEFT	GCTGGCTTTAGCTTGTGGTTT	22
nCoV-2019_65_RIGHT	TGTCAGTCATAGAACAAACACCAATAGT	28
nCoV-2019_66_LEFT	GGGTGTGGACATTGCTGCTAAT	22
nCoV-2019_66_RIGHT	TCAATTTCCATTTGACTCCTGGGT	24
nCoV-2019_67_LEFT	GTTGTCCAACAATTACCTGAACTTACT	28
nCoV-2019_67_RIGHT	CAACCTTAGAACTACAGATAAATCTTGGG	30
nCoV-2019_68_LEFT	ACAGGTTTCATCTAAGTGTGTGTGT	24
nCoV-2019_68_RIGHT	CTCCTTATCAGAACCAGCACCA	23
nCoV-2019_69_LEFT	TGTCGCAAAATATACTCAACTGTGTCA	27
nCoV-2019_69_RIGHT	TCTTTATAGCCACGGAACCTCCA	23
nCoV-2019_70_LEFT	ACAAAAGAAAATGACTCTAAAGAGGGTTT	29
nCoV-2019_70_RIGHT	TGACCTTCTTTAAAGACATAACAGCAG	28
nCoV-2019_71_LEFT	ACAAATCCAATTCAGTTGTCTTCCTATTC	29
nCoV-2019_71_RIGHT	TGGAAAAGAAAGGTAAGAACAAGTCCT	27
nCoV-2019_72_LEFT	ACACGTGGTGTATTACCTGAC	24
nCoV-2019_72_RIGHT	ACTCTGAACACTTTCCATCCAAC	25
nCoV-2019_73_LEFT	CAATTTTGTAAATGATCCATTTTGGGTGT	29
nCoV-2019_73_RIGHT	CACCAGCTGTCCAACCTGAAGA	22
nCoV-2019_74_LEFT	ACATCACTAGGTTTCAAACCTTACTTGC	28
nCoV-2019_74_RIGHT	GCAACACAGTTGCTGATTCTCTTC	24
nCoV-2019_75_LEFT	AGAGTCCAACCAACAGAATCTATTGT	26
nCoV-2019_75_RIGHT	ACCACCAACCTTAGAATCAAGATTGT	26
nCoV-2019_76_LEFT	AGGGCAAACCTGGAAAGATTGCT	22
nCoV-2019_76_LEFT_alt3	GGGCAAACCTGGAAAGATTGCTGA	23
nCoV-2019_76_RIGHT	ACACCTGTGCCTGTAAACCAT	22
nCoV-2019_76_RIGHT_alt0	ACCTGTGCCTGTAAACCATGGA	23
nCoV-2019_77_LEFT	CCAGCAACTGTTTGTGGACCTA	22
nCoV-2019_77_RIGHT	CAGCCCTATTAACAGCCTGC	22
nCoV-2019_78_LEFT	CAACTTACTCCTACTTGGCGTGT	23
nCoV-2019_78_RIGHT	TGTGTACAAAACTGCCATATTGCA	25
nCoV-2019_79_LEFT	GTGGTGATTCAACTGAATGCAGC	23
nCoV-2019_79_RIGHT	CATTTTCATCTGTGAGCAAAGGTGG	24
nCoV-2019_80_LEFT	TTGCCTTGGTGATATTGCTGCT	22
nCoV-2019_80_RIGHT	TGGAGCTAAGTTGTTTAAACAAGCG	24
nCoV-2019_81_LEFT	GCACTTGAAAACTTCAAGATGTGG	25
nCoV-2019_81_RIGHT	GTGAAGTTCTTTCTTGTGCAGGG	24
nCoV-2019_82_LEFT	GGGCTATCATCTTATGTCCTCCCT	25
nCoV-2019_82_RIGHT	TGCCAGAGATGTCACCTAAATCAA	24
nCoV-2019_83_LEFT	TCCTTTGCAACCTGAATTAGACTCA	25
nCoV-2019_83_RIGHT	TTGACTCCTTTGAGCACTGGC	22
nCoV-2019_84_LEFT	TGCTGTAGTTGTCTCAAGGGCT	22
nCoV-2019_84_RIGHT	AGGTGTGAGTAACTGTTACAAACAAC	27
nCoV-2019_85_LEFT	ACTAGCACTCTCCAAGGGTGTT	22

nCoV-2019_85_RIGHT	ACACAGTCTTTTACTCCAGATTCCC	25
nCoV-2019_86_LEFT	TCAGGTGATGGCACAACAAGTC	22
nCoV-2019_86_RIGHT	ACGAAAGCAAGAAAAAGAAGTACGC	25
nCoV-2019_87_LEFT	CGACTACTAGCGTGCCTTTGTA	22
nCoV-2019_87_RIGHT	ACTAGGTTCCATTGTTCAAGGAGC	24
nCoV-2019_88_LEFT	CCATGGCAGATTCCAACGGTAC	22
nCoV-2019_88_RIGHT	TGGTCAGAATAGTGCCATGGAGT	23
nCoV-2019_89_LEFT	GTACGCGTTCATGTGGTCATT	22
nCoV-2019_89_LEFT_alt2	CGCGTTCCATGTGGTCATTCAA	22
nCoV-2019_89_RIGHT	ACCTGAAAGTCAACGAGATGAAACA	25
nCoV-2019_89_RIGHT_alt4	ACGAGATGAAACATCTGTTGTCCT	25
nCoV-2019_90_LEFT	ACACAGACCATTCCAGTAGCAGT	23
nCoV-2019_90_RIGHT	TGAAATGGTGAATTGCCCTCGT	22
nCoV-2019_91_LEFT	TCACTACCAAGAGTGTGTTAGAGGT	25
nCoV-2019_91_RIGHT	TTCAAGTGAGAACCAAAAGATAATAAGCA	29
nCoV-2019_92_LEFT	TTTGTGCTTTTTAGCCTTTCTGCT	24
nCoV-2019_92_RIGHT	AGGTTCTCTGGCAATTAATTGTAAGG	27
nCoV-2019_93_LEFT	TGAGGCTGGTTCTAAATCACCCA	23
nCoV-2019_93_RIGHT	AGGTCTTCCTTGCCATGTTGAG	22
nCoV-2019_94_LEFT	GGCCCCAAGGTTTACCCAATAA	22
nCoV-2019_94_RIGHT	TTTGGCAATGTTGTTCCCTTGAGG	23
nCoV-2019_95_LEFT	TGAGGGAGCCTTGAATACACCA	22
nCoV-2019_95_RIGHT	CAGTACGTTTTTGCCGAGGCTT	22
nCoV-2019_96_LEFT	GCCAACAACAACAAGGCCAAAC	22
nCoV-2019_96_RIGHT	TAGGCTCTGTTGGTGGGAATGT	22
nCoV-2019_97_LEFT	TGGATGACAAAGATCCAAATTTCAAAGA	28
nCoV-2019_97_RIGHT	ACACACTGATTAAGATTGCTATGTGAG	28
nCoV-2019_98_LEFT	AACAATTGCAACAATCCATGAGCA	24
nCoV-2019_98_RIGHT	TTCTCCTAAGAAGCTATTAATAATCACATGG	30

Chapter 6

Unrecognized introductions of SARS-CoV-2 into the US state of Georgia shaped the early epidemic

The following *Research Article*, published in *Virus Evolution* in February 2022 in collaboration with research teams across Emory University led by Dr. Anne Piantadosi. Our goal was to use consensus sequence data to characterize the spread of SARS-CoV-2 into the state of Georgia, USA early in the pandemic. We show that while there were many introductions into the state, a single introduction was responsible for the majority of the sampled lineages in our data. This lineage circulated within region for roughly three weeks prior to detection. Furthermore, as travel history was available for a number of the sequenced patients we were able to compare the viral sequences sampled from individuals to the viral lineages circulating both in Georgia and in their region of travel. Unfortunately, do to the sparsity of sequence data in many locales we were unable to draw definitive conclusions from this analysis.

6.1 M.A.M. Contributions

Conceptualization, Validation, Formal analysis (**Figure 1-5, Figure S3-14, Table S3, S5-10**), Investigation (**Figure 1-5, Figure S3-14, Table S3, S5-10**), Writing - Original Draft, Writing - Review & Editing, Visualization (**Figure 1-5, Figure S3-14**).

6.2 Published Manuscript

Reproduced with permission from the Oxford University Press.

Unrecognized introductions of SARS-CoV-2 into the US state of Georgia shaped the early epidemic

Ahmed Babiker,^{1,2,†,‡} Michael A. Martin,^{3,4,†,§} Charles Marvil,² Stephanie Bellman,⁵ Robert A. Petit III,¹ Heath L. Bradley,² Victoria D. Stittleburg,¹ Jessica Ingersoll,² Colleen S. Kraft,^{1,2} Yan Li,⁶ Jing Zhang,⁶ Clinton R. Paden,⁶ Timothy D. Read,¹ Jesse J. Waggoner,¹ Katia Koelle,^{3,††} and Anne Piantadosi^{1,2,*,‡‡}

¹Department of Medicine, Division of Infectious Diseases, Emory University School of Medicine, 201 Dowman Drive, Atlanta, GA 30322, USA, ²Department of Pathology and Laboratory Medicine, Emory University School of Medicine, 201 Dowman Drive, Atlanta, GA 30322, USA, ³Department of Biology, Emory University, 201 Dowman Drive, Atlanta, GA 30322, USA, ⁴Population Biology, Ecology, and Evolution Graduate Program, Laney Graduate School, Emory University, 201 Dowman Drive, Atlanta, GA 30322, USA, ⁵Environmental Health Sciences PhD Program, Laney Graduate School, Emory University, 201 Dowman Drive, Atlanta, GA 30322, USA and ⁶Division of Viral Diseases, Centers for Disease Control and Prevention, 1600 Clifton Road, Atlanta, GA 30333, USA

[†]These authors contributed equally.

[‡]<https://orcid.org/0000-0003-0578-4871>

[§]<https://orcid.org/0000-0002-9689-4066>

^{††}<https://orcid.org/0000-0002-0254-6141>

^{‡‡}<https://orcid.org/0000-0002-5942-1534>

*Corresponding author: E-mail: anne.piantadosi@emory.edu

Abstract

In early 2020, as diagnostic and surveillance responses for severe acute respiratory syndrome coronavirus 2 (SARS-CoV-2) ramped up, attention focused primarily on returning international travelers. Here, we build on existing studies characterizing early patterns of SARS-CoV-2 spread within the USA by analyzing detailed clinical, molecular, and viral genomic data from the state of Georgia through March 2020. We find evidence for multiple early introductions into Georgia, despite relatively sparse sampling. Most sampled sequences likely stemmed from a single or small number of introductions from Asia three weeks prior to the state's first detected infection. Our analysis of sequences from domestic travelers demonstrates widespread circulation of closely related viruses in multiple US states by the end of March 2020. Our findings indicate that the exclusive focus on identifying SARS-CoV-2 in returning international travelers early in the pandemic may have led to a failure to recognize locally circulating infections for several weeks and point toward a critical need for implementing rapid, broadly targeted surveillance efforts for future pandemics.

Key words: SARS-CoV-2; introductions; travel; Georgia.

1. Introduction

Phylogenetic studies have been critical to investigating the introduction and spread of severe acute respiratory syndrome coronavirus 2 (SARS-CoV-2) throughout the USA and globally. Understanding the source of viral introductions and the subsequent dynamics of viral spread is essential for evaluating the efficacy of public health interventions and informing the response to future outbreaks. For example, a phylogenetic analysis indicated that the first identified case of SARS-CoV-2 in the USA, in mid-January 2020, did not directly lead to the initial wave of infections in Washington State; instead, its transmission was stopped by public health interventions. By contrast, undetected introductions into Washington State, likely in early February, sparked significant downstream transmission, despite federal policies to limit travel from China beginning on 2nd February (Worobey et al. 2020).

On a broader scale, relatively uninterrupted travel in early 2020 allowed multiple introductions of SARS-CoV-2 into specific regions

of the USA. For example, in New York City, the epicenter of the US outbreak in Spring 2020, multiple undetected introductions of viral lineages, likely from Europe, sparked local transmission chains (Gonzalez-Reiche et al. 2020). These undetected introductions into the USA are thought to have resulted in a significant level of unobserved infection in early 2020 (Perkins et al. 2020).

Few studies have attempted to characterize early patterns of SARS-CoV-2 introduction and circulation in the southeastern USA, and none to date have focused on the state of Georgia, a major national and international travel hub due to Hartsfield-Jackson Atlanta International Airport. The first reported SARS-CoV-2 case in Georgia was on 2 March 2020 in Fulton County (Georgia Department of Public Health 2020) and reported cases rose slowly throughout the month, topping 100 per day for the first time on 20 March 2020. By the end of March, a total of 3,929 cases had been reported in the state (Dong, Du, and Gardner 2020).

Reported cases are a function of both underlying epidemiological dynamics and detection by the public health system: healthcare-seeking behavior, frequency of diagnostic testing, and completeness of reporting to public health. From January through March 2020, there were rapid shifts in the availability of and recommendations for SARS-CoV-2 diagnostic testing in Georgia and the USA as a whole. Due to limited availability of SARS-CoV-2 diagnostic tests and the assumption that viral transmission was largely restricted to China, testing was initially limited to individuals with recent travel history to mainland China or those who had contact with a known traveler or a diagnosed case of SARS-CoV-2 (Patel et al. 2020). As large outbreaks were identified outside of China and testing through clinical laboratories became possible, testing was expanded to include high-risk individuals with compatible illness and potential community exposure (Health Alert Network 2020; Schuchat 2020). Reflecting these national trends, SARS-CoV-2 testing for patients within the Emory Healthcare (EHC) system prior to 15 March 2020 required physician request, public health agency approval, and testing via the Georgia Department of Public Health (GADPH) or the Centers for Disease Control and Prevention (CDC) (Babiker et al. 2020b). Only 176 patients were tested for SARS-CoV-2 in the EHC system between 26 January 2020 and 16 March 2020. On 29 February 2020, guidelines from the Food and Drug Administration (CDC 2020) allowed certified labs to validate testing for SARS-CoV-2, and testing volumes nationwide increased considerably. On 15 March 2020, local testing at EHC began, and in the second half of March 2020 over 2,700 tests were performed at the Emory University Hospital Molecular and Microbiology Laboratories.

Changing test volumes can obfuscate underlying epidemiological dynamics, and case data alone cannot be used to evaluate the relative importance of viral introductions versus local transmission in sustaining viral spread within a region. To better understand the early epidemic in Georgia, we analyzed SARS-CoV-2 whole genome sequences sampled in Georgia from 29 February 2020 (the first available sequence) through 31 March 2020. We assessed the changing frequencies of viral clades and, by incorporating globally sampled sequences, estimated the number and timing of viral introductions into the state. Where available, we interrogated travel history to identify the contribution of international and domestic travel to SARS-CoV-2 spread within Georgia. Finally, we combined sequence data with detailed clinical meta-data to evaluate associations between viral genotype and clinical parameters. These results add to the growing body of work characterizing the spread of SARS-CoV-2 into and within the USA and provide insight into early events that shaped the outbreak in Georgia.

2. Results

2.1 One Hundred Eight (108) SARS-CoV-2 genomes from the first month of the pandemic in Georgia were sequenced

To understand the diversity and spread of SARS-CoV-2 in Georgia during early 2020, we sequenced forty-seven complete SARS-CoV-2 genomes from patients seen within the EHC system through 31 March 2020 (Supplementary Tables S1 and S2, Supplementary Figures S1 and S2) and combined them with the sixty-one publicly available SARS-CoV-2 sequences generated by other groups within this time frame (Supplementary Tables S3–S5). These 108 sequences represent 2.7 per cent of the 3,929 reported cases in Georgia through 31 March 2020 (Fig. 1A). They include two specimens from 29 February 2020, before the first officially reported

case, and at least ten samples per week throughout the month of March, with the exception of the week ending 29 March 2020. Thus, this dataset provides a temporally comprehensive sampling of the circulating viruses within the state at the time. County-level sampling location data were available for fifty-six sequences (Fig. 1B, C), which were largely sampled from the Atlanta metro area, the most densely populated region of the state, in which 46 per cent of the reported cases in this period occurred. Another significant portion of the reported cases occurred in Dougherty County and were associated with a funeral (Willis 2020). Sequences from this outbreak are not known to be included in our analysis; however, half of the included sequences did not have available county-level data. Nine sampled individuals are known to have traveled within two weeks prior to symptom onset (Supplementary Table S2).

2.2 Four major SARS-CoV-2 clades were present in the state of Georgia during early 2020

To assess the genetic diversity of the SARS-CoV-2 sequences circulating within Georgia during early 2020, we assigned each of them to a phylogenetic clade (Bedford, Hodcroft, and Neher 2020) (Fig. 2A). Among these sequences, the first identified clade was 20B, which was observed in two sequences sampled on 29 February 2020. Sequences in this clade harbor the canonical substitutions C14408T, A23403G (responsible for the widely reported D614G amino acid substitution in the spike protein (Volz et al. 2020)), G28881A, and G28882A relative to Wuhan/Hu-1 (EPI_ISL_402125 (Wu et al. 2020)). Clade 20B was prominent throughout Europe (Alm et al. 2020) and a number of US states (Zeller et al. 2021) throughout early 2020. Despite being the first identified clade in Georgia, local transmission of 20B appears to have been limited, and it was only sporadically ($N = 6/108$) identified throughout March 2020.

By contrast, clade 19B, a more ancestral clade, rapidly became dominant in Georgia throughout the spring of 2020. Sequences in this clade harbor the canonical substitutions 8782T and 28144C relative to Wuhan/Hu-1. This clade was first identified in Georgia on 3 March 2020, and nearly three-quarters ($N = 77/108$) of the analyzed Georgia sequences fell within clade 19B.

The remaining twenty-three available Georgia sequences from March 2020 were assigned to clades 20A ($N = 7/108$) and 20C ($N = 16/108$). Given the genetic diversity delimiting these clades and the global diversity of the clades at the time, these findings imply that there were multiple introductions of SARS-CoV-2 into GA, likely from multiple global sources. The temporal distribution of Pango lineages (Rambaut et al. 2020) mirrored these clade distributions (Supplementary Table S1, Supplementary Figure S3).

2.3 Multiple SARS-CoV-2 introductions into Georgia occurred by the end of March 2020

We reconstructed a maximum likelihood phylogenetic tree containing the 108 Georgia sequences, along with 4,514 global sequences, which were downsampled from all available sequences over the same time period to be geographically representative of case counts and to maximize phylogenetic resolution around the Georgia sequences (weighted downsampling strategy, Section 4). Sampling dates were used to exclude eleven sequences (one from Georgia) that did not follow the expected molecular clock and to estimate the dates of internal nodes based on a time-resolved tree. A significant temporal signal in these data was confirmed using root-to-tip regression (Supplementary Figure S4). The sequences from Georgia were distributed heterogeneously throughout the tree (Fig. 2B, Supplementary Figure S5,

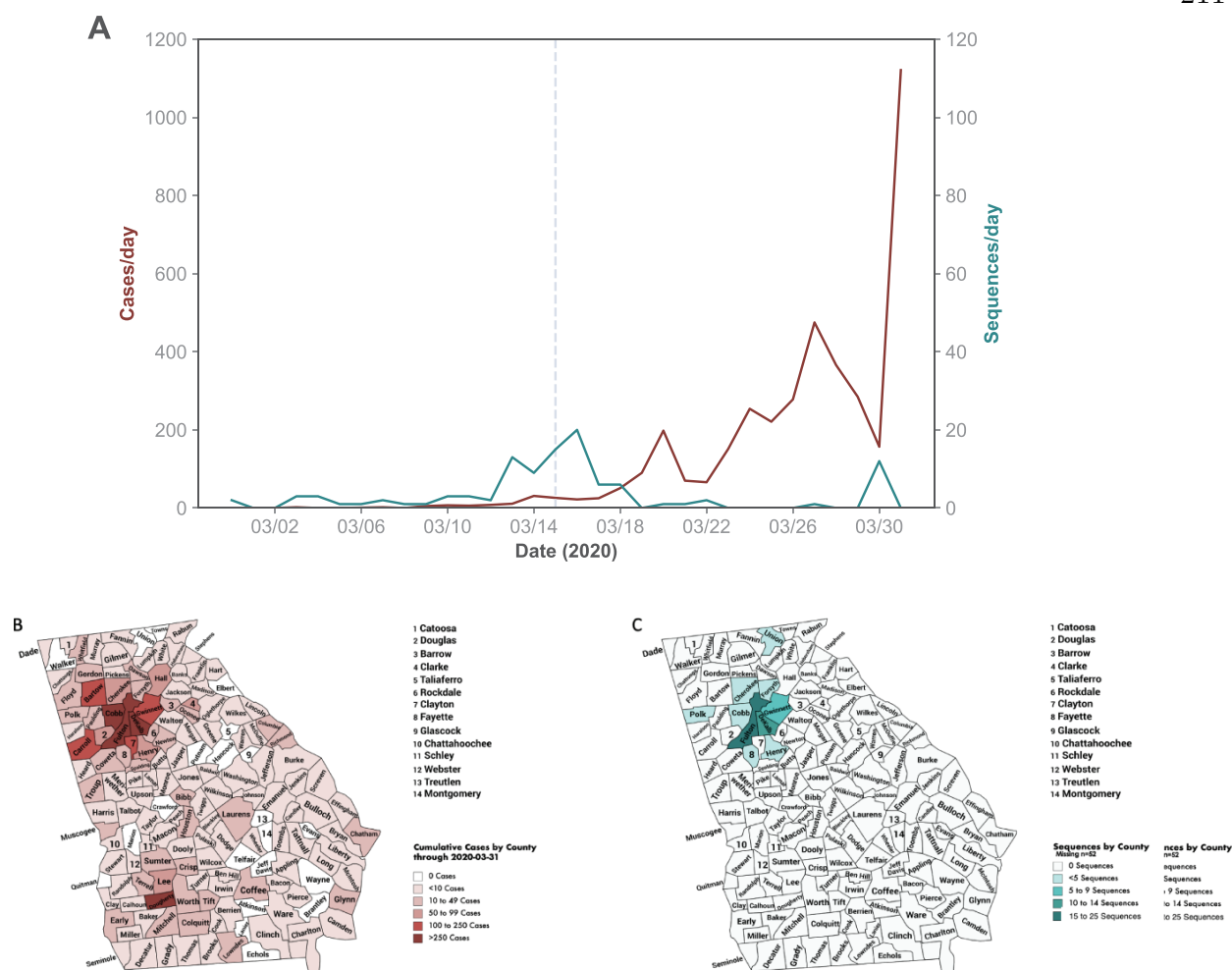


Figure 1. Temporal and spatial distribution of SARS-CoV-2 cases and sequences in the state of Georgia. (A) Daily numbers of reported cases within the state of Georgia (red) and daily number of available sequences (GISAID). The dashed line indicates 15 March 2020, the date that EHC received Emergency Use Authorization for diagnostic testing. (B) Cumulative number of reported cases as of 31 March 2020 by county. (C) County of residence for the patients from which viral sequences were sampled, where available ($N = 56$). County-level location data are unavailable for the remaining sequences. The Atlanta metro region comprises 10 counties within the Atlanta Regional Commission: Cherokee, Clayton, Cobb, DeKalb, Douglas, Fayette, Fulton, Gwinnett, Henry, and Rockdale.

Supplementary Table S5). The majority of Georgia sequences ($N = 69$) were closely related and clustered together within clade 19B (Pango lineage A), while the rest either did not cluster together or descended from highly polytomous nodes along with many other sequences.

To quantify the number of introductions into Georgia represented by this dataset, we inferred the discrete location of internal nodes using maximum likelihood ancestral state reconstruction. As undersampling of Georgia sequences can only bias the number of introductions downwards, this represents the lower limit of the number of true introductions through 31 March 2020. We conservatively estimate that there were at least 19 [95 per cent CI 17–21] introductions into Georgia in this time range (Fig. 2C). The earliest was estimated to have occurred in early to mid-February 2020 and gave rise to the sixty-nine closely related 19B sequences. Most introductions occurred in late February or early March 2020 and appear as singletons or doubletons in the tree. Highly consistent results were obtained using an alternative downsampling strategy designed to be temporally and geographically homogeneous (up to twenty sequences per county per week) (Supplement, Supplementary Figure S6).

2.4 The earliest lineage in Georgia was most likely introduced directly from Asia several weeks prior to SARS-CoV-2 detection in the state

To provide a more robust analysis of the evolutionary history of the sixty-nine closely related Georgia 19B sequences, we employed Bayesian phylogenetic reconstruction, which simultaneously estimates tree structure and discrete states of internal nodes and provides a posterior distribution of possible reconstructions. To provide context for the ancestral origins of the 19B subclade, we identified the shared mutations between it and its closest relatives (Fig. 2B, clade marked with red '+'): T26729C and G28077C (which are subclade-defining) and T28144C (which is clade 19B-defining). We then selected all available high-quality sequences that contained these mutations, which included 67 sequences from Georgia (two were removed due to the presence of ambiguous nucleotides at clade defining genome positions), 370 from other US states, and 91 from other countries (Supplementary Table S6). One sequence was excluded as it did not follow the expected molecular clock. A significant temporal signal in the remaining data was confirmed using root-to-tip regression (Supplementary Figure S7). For computational efficiency we excluded five US sequences

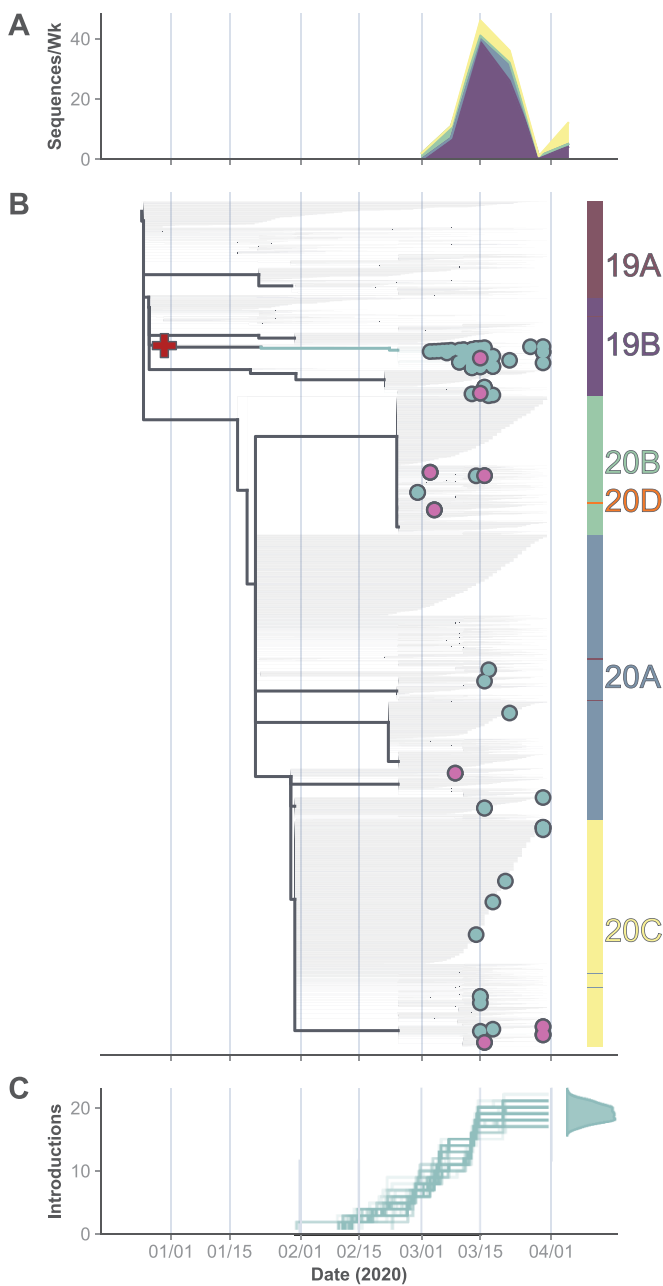


Figure 2. Presence of multiple clades and maximum likelihood phylogenetic analysis indicate multiple introductions of SARS-CoV-2 into Georgia. (A) Number of sequences from Georgia per clade, per week included in the phylogenetic analysis. (B) Time-resolved maximum likelihood tree of 4,611 globally sampled sequences rooted at Wuhan/Hu-1, downsampled based on the cumulative number of cases in a given country as of 31 March 2020 and genetic distance to Georgia sequences (weighted downsampling strategy). Internal nodes are colored based on their estimated location either inside (green) or outside (gray) of Georgia. Georgia tips are colored in green except for those with known travel history, which are shown in pink. The color bar at right shows the clade identity of each sequence in the tree. Branch widths are weighted for visual clarity. Red + indicates the phylogenetic clade used to select sequences for downstream Bayesian phylogenetic analyses. (C) Estimated cumulative number of introductions into Georgia (transition from a non-Georgia node to a Georgia-node/tip) based on the ancestral state reconstruction of internal nodes. Estimation was repeated on 100 bootstrap replicate trees and the timing of introduction events for each replicate is shown as an individual line. The Gaussian kernel density plot at right shows the estimated cumulative number of introduction events as of 31 March 2020.

without state metadata, eighteen sequences from US states with fewer than four sequences in this subclade and seventy-two international sequences sampled after 29 February 2020. The excluded international sequences either did not cluster with the US sequences ($N = 1$, sampled from China) or were evolutionarily descendant from the US sequences and are thus likely exportations from the USA to these international regions (Supplementary Figures S8 and S9). Therefore, 432 sequences were included in our Bayesian phylogenetic analysis including the 67 from Georgia, 346 from other US states, 12 from China (including Hong Kong), 5 from South Korea, and 2 from Vietnam (Supplementary Table S6).

Our analysis revealed that the US sequences in the 19B subclade were phylogenetically distinct from the ancestral sequences, consistent with a single or small number of introductions of this lineage into the USA (Fig. 3, Supplementary Table S7). To evaluate the source of introduction, we inferred the location of the most recent common ancestor (MRCA) of all US sequences in the 19B subclade. The MRCA was assigned to Georgia in 65 per cent of sampled trees (posterior probability of 0.65). The next most likely discrete state of the MRCA node was South Carolina, with posterior probability of 0.13. Thus, Georgia is the most likely site of introduction of the 19B subclade, with the important caveat that undersampling at the beginning of the epidemic makes it difficult to draw firm conclusions. Although we maximized our power to detect multiple introductions of this subclade into the state of Georgia by including nearly all available phylogenetically related domestic sequences, it is possible that the 19B subclade was originally introduced into a state with minimal genomic surveillance. Furthermore, it is possible that over-sampling of sequences within Georgia relative to other regions biased these results. To assess the impact of this possibility, we performed Bayesian phylogenetic (BEAST) analyses in which sequences were downsampled in a temporally and geographically homogeneous manner (Section 4). In each of these downsampled replicates, the MRCA of all US sequences was assigned to Georgia with the highest probability (Supplementary Figure S10A, Supplementary Table S7), consistent with our non-downsampled analysis. The next most probable ancestral state in these downsampled analyses was South Carolina, which indicates that if this clade was not first introduced into Georgia, it was likely introduced elsewhere in the southeastern USA. While the distribution of estimated number of introductions into Georgia in the downsampled alignments was slightly higher than the full alignment (Supplementary Figure S10B), these analyses consistently support a limited number of introductions into Georgia. Much of the genetic diversity of non-Georgia sequences appears nested within the genetic diversity of sequences from Georgia (Fig. 3, Supplementary Figure S8), consistent with one, or a small number of, introduction(s) into Georgia.

Importantly, there was a gap of approximately three weeks between the estimated time to most common ancestor (tMRCA) of the US sequences in this analysis (8 February 2020 [1 February 2020, 14 February 2020]) and the earliest sampled US sequence (1 March 2020), highlighting a relative lack of dense sampling of SARS-CoV-2 genomes throughout the USA during the spring of 2020. Although the earliest US sequence in this analysis was sampled in Mississippi on 1 March 2020 (EPI_ISL_648018), it had one additional single-nucleotide polymorphism (SNP) (G922A) relative to Wuhan/Hu-1 compared to the earliest Georgia sequence (EPI_ISL_420786, sampled 3 March 2020), supporting the

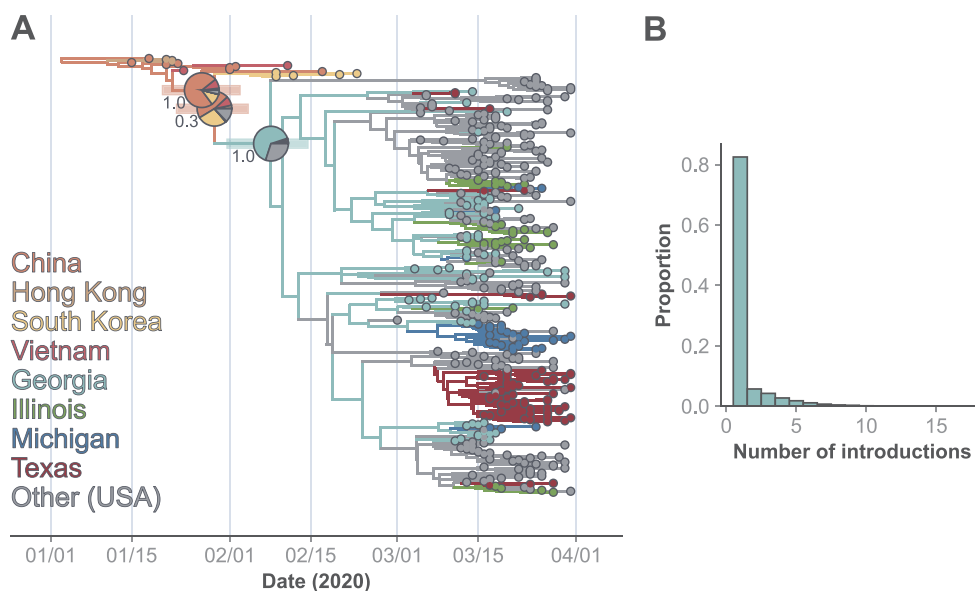


Figure 3. Bayesian phylogenetic analysis of genetically related Georgia 19B sequences and their phylogenetic neighbors reveals undetected circulation in February 2020. (A) Maximum clade credibility tree (median node heights) of select 19B sequences. Tips are colored by their state (USA) or country (intl.) of origin. Less abundant states are colored as 'Other (USA)' for visualization purposes only. Internal nodes are colored by their most probable location based on the set of estimated trees and ancestral state reconstruction. Select nodes annotated with their 95 per cent highest posterior density of estimated date (horizontal bar), location probabilities (pie chart), and posterior support (text). Negative branch lengths are manually set to 0 for visualization purposes. (B) Estimated number of introductions of the 19B subclade shown in (A) into the state of Georgia for each sampled tree in the Bayesian phylogenetic reconstruction.

hypothesis that this 19B subclade was likely first introduced into Georgia. As the first case in the state of Georgia was not reported until 2 March 2020, this analysis indicates that SARS-CoV-2 was likely spreading within the state for approximately three weeks prior to detection in either diagnostic or sequencing data.

While the source of the 19B subclade introduction was ambiguous in our phylogenetic reconstruction (posterior probabilities for China: 0.47, South Korea: 0.28, Vietnam: 0.09), the branching structure of this subclade relative to related sequences from China and South Korea was well-resolved by the data with posterior probability of 1. Overall, these results indicate that this subclade was most likely introduced from Asia in late January or early February and spread undetected throughout the USA for three to four weeks.

2.5 Analysis of sequence metadata identified a small number of travel-associated introductions

To assess the contribution of domestic and international travel to the introduction of SARS-CoV-2 into Georgia, we leveraged the extensive clinical and epidemiological data available for EHC patients in this study. Clinical data were available for forty-six of the forty-seven EHC patients from whom complete SARS-CoV-2 sequences were obtained, as well as an additional 8 patients without complete SARS-CoV-2 sequences (Table 1, Supplementary Table S2). Twenty-five of these 54 patients (46 per cent) were female and 29 (54 per cent) were male, and ages ranged from 21 to 92 years. Thirty (56 per cent) of these patients were African American, a larger proportion than the demographics of Georgia in general (United States Census Bureau 2019), likely owing to both the disproportionate representation of the Atlanta metro in these data and the disproportionate impact of the SARS-CoV-2 pandemic on people of color (Subbaraman 2020). The duration of symptoms prior to sample collection ranged from 1 to 28 days (median 6 days). Clinical severity ranged from mild (outpatient

Table 1. Demographic and clinical data from fifty-four EHC patients. One patient with no available data was excluded.

	N (%)
Age (mean [standard deviation])	53.0 [17.1]
Female sex	25 (46.3)
Race	
African American	30 (55.6)
Asian	4 (7.4)
White	17 (31.5)
Hispanic/Latino	3 (5.6)
Travel in preceding two weeks	9 (16.6)
Diabetes mellitus	13 (24.1)
Hypertension	25 (46.3)
Obesity	25 (46.3)
Lung disease	9 (16.7)
Immunosuppression	14 (25.9)
Days from symptom onset to sample collection (median [aq1-aq3])	5.5 [4,8]
SARS-CoV-2 disease severity ^a	
Mild	19 (35.2)
Moderate	23 (42.6)
Severe	12 (22.2)
In-hospital death	4 (7.4)

^aSARS-CoV-2 disease severity was classified as severe if the patient was admitted to an ICU, moderate if the patient was hospitalized without ICU admission, and mild if the patient had an outpatient or emergency department visit only.

or ED visit only, $N = 19$) to moderate (inpatient without intensive care unit (ICU) admission, $N = 23$) to severe (inpatient with ICU admission, $N = 12$), and four patients died. Although we did not specifically select samples from returning travelers, we found that nine patients (17 per cent) had traveled outside of Georgia within the two weeks prior to diagnosis. Four had traveled internationally, including three of the four patients with the earliest

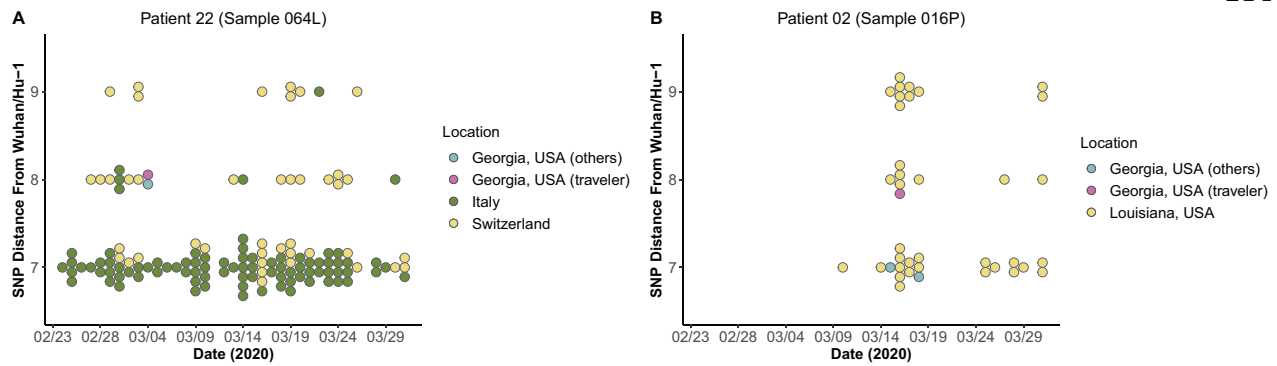


Figure 4. Analysis of SARS-CoV-2 whole genome sequences from EHC patients with recent travel provides examples of travel-associated infections of SARS-CoV-2 coming into Georgia. (A) The sequence from P22 (traveler) was compared to related sequences from Georgia (others) and the regions of travel. Sequences in this analysis were within the same ancestral lineage as the P22 sequence and differed from it by 0 or 1 SNPs compared to Wuhan/Hu-1 (y-axis). (B) The sequence from P02 (traveler) was compared to related sequences from Georgia (others) and the region of travel. As in (A), sequences in this analysis were within the same ancestral lineage as the P02 sequence and differed from it by 0 or 1 SNPs compared to Wuhan/Hu-1 (y-axis).

dates of testing, consistent with restrictions in place to prioritize SARS-CoV-2 testing from returning travelers in early March 2020.

In one patient (P22), there was strong SARS-CoV-2 genomic evidence that the infection had been acquired in the location of travel (Italy and Switzerland); the SARS-CoV-2 sequence from P22 was identical to 18 of the 1,657 publicly available sequences from Italy and Switzerland sampled within the same time frame. It matched one other sequence from Georgia, from a sample that had matching metadata (date of sample collection, patient age, and patient gender). We therefore presumed that these samples were from the same individual, with independent sequencing performed by our group and the GADPH. Further analysis of SARS-CoV-2 sequences within the same lineage demonstrated that there were many sequences ancestral to the P22 sequence by one SNP from Italy and Switzerland, but none from Georgia (Fig. 4A, Supplementary Table S8), consistent with travel-associated infection. Supporting this, the patient had been traveling in Europe for a month prior to symptom onset, encompassing the entire plausible incubation period for SARS-CoV-2. We were unable to draw definitive conclusions about where infection was acquired for the remaining patients with international travel, not only due to insufficient epidemiological and viral genomic data but also due to the limited diversity of circulating SARS-CoV-2 at the time (Supplementary Results, Supplementary Table S8, Supplementary Figure S11A).

Domestic travel to states with ongoing community transmission could also have introduced SARS-CoV-2 lineages into Georgia. For example, there is considerable genomic evidence that one patient in our study (P02) was infected while traveling to New Orleans. The sequence from P02 was distinct to all samples from Georgia but identical to seven SARS-CoV-2 sequences from Louisiana (Fig. 4B). This finding is consistent with a recently published study on the spread of SARS-CoV-2 into and within Louisiana (Zeller et al. 2021). By contrast, another patient in our study had also recently traveled to Louisiana (P39), yet the most closely related sequences were found in both Georgia ($N = 2$) and Louisiana ($N = 19$). These sequences were not identical to P39 but were three SNPs more ancestral to it. Thus, it is not clear based on viral genomic data whether P39 was infected in Georgia or Louisiana. This uncertainty could be resolved with detailed epidemiological data, e.g. if the patient had traveled to Louisiana outside of the plausible incubation period for SARS-CoV-2. However, travel dates were incompletely recorded in the medical record for this patient (Supplementary Table S8).

Inferring the location of infection for other domestic travelers was also challenging due to the circulation of highly similar viruses in multiple states and ambiguities in travel history. For example, the SARS-CoV-2 sequence from P14, who had traveled to Mississippi, was identical to not only one sequence from Mississippi but also six from Georgia (Supplementary Figure S11B), and the patient was in both locations during the potential incubation period. The SARS-CoV-2 sequence from P05, who had traveled to Colorado, was identical to not only two SARS-CoV-2 sequences from Colorado but also one from Georgia, and the dates of travel were incompletely documented in the medical record (Supplementary Figure S11C). The SARS-CoV-2 sequence from P27, who had traveled to North Carolina, had no identical matches but harbored an additional mutation to sequences from both North Carolina and Georgia (Supplementary Figure S11D), and the patient was in both locations during the potential incubation period. Overall, given higher rates of domestic travel as compared to international travel and the short tMRCA of all circulating SARS-CoV-2 sequences, it is unsurprising that the viral lineages circulating within US states in early 2020 were highly similar. This similarity prevented us from conclusively inferring the location of infection for domestic travelers.

An additional challenge to these analyses is that in all cases, highly similar SARS-CoV-2 sequences were present in widespread locations outside of Georgia and the region of travel (Supplementary Table S8), making it difficult to exclude the possibility that patients were infected through alternative mechanisms such as contact with another traveler or unreported travel themselves.

2.6 The 19B subclade disappeared by the end of April 2020

Given the genetic relationship of many Georgia sequences within clade 19B, we wanted to know to what extent this subclade seeded outbreaks beyond the timeframe of our phylogenetic analyses. We first identified the shared substitutions between these Georgia sequences to generate a subclade-defining mutational profile (Fig. 5A). These SNPs include T490A, C3177T, T18736C, C24034T, T26729C, G28077C, and A29700G as well as the two 19B defining SNPs C8782T and T28144C. Of these nine substitutions, five were non-synonymous: T490A (ORF1ab Asp75Glu), C3177T (ORF1ab Pro971Leu), T18736C (ORF1ab Phe6158Leu), G28077C (ORF8 Val62Leu), and T28144C (ORF8 Leu84Ser).

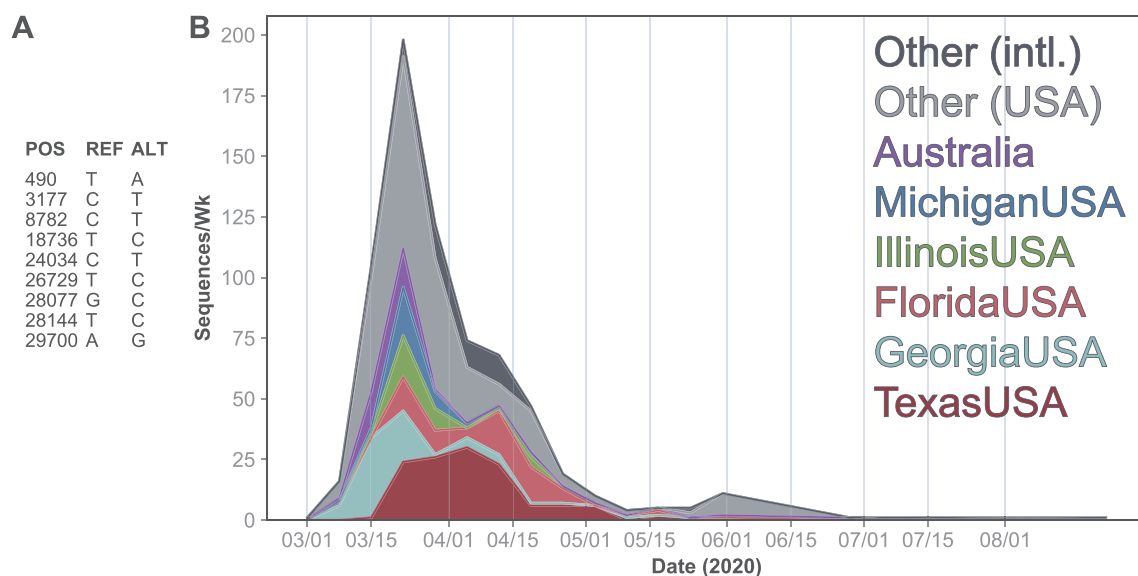


Figure 5. Shared mutations between related Georgia 19B sequences and global sequences harboring this mutational profile indicate its decline in early 2020. (A) Shared mutations (relative to Wuhan/Hu-1) of all the sixty-nine closely related Georgia 19B sequences, which define the 19B subclade. (B) Number of sequences per week with the mutational profile of the 19B subclade shown in (A). Sequences are colored by the region they were sampled from.

The total number of global high-quality sequences per week sharing the above subclade-defining mutational profile peaked in mid-March, within the timeframe of our phylogenetic analyses (Fig. 5B, Supplementary Table S9). The 19B subclade appeared to go extinct by the end of April; consequently, the number of Georgia sequences belonging to this subclade also dropped to zero shortly after its peak. The apparent extinction of the 19B subclade was consistent with the widely reported increase of sequences and clades harboring the D614G substitution in the spike protein (Volz et al. 2020). This subclade was most frequently detected domestically, as opposed to internationally. It was most prominently identified in Texas, where it was first identified on 11 March 2020 and was consistently observed from then until the end of April. Internationally, this 19B subclade was most frequently observed in Australia. Due to limited sequences, particularly from the state of Georgia in May 2020, we did not attempt to estimate the number of reported infections attributable to this subclade over time.

2.7 Samples with D614G substitution did not differ in CT value, subgenomic RNA level, or clinical severity

Due to the rapid decline of the 19B subclade, we wondered whether samples from that lineage displayed clinical or molecular features that could be associated with lower transmissibility. We focused our analysis on spike amino acid position 614. The D614G substitution is a defining substitution between 20X and 19X phylogenetic clades that has been associated with increased transmissibility (Volz et al. 2020), potentially due to higher viral loads (Plante et al. 2021). Sequence data at position 614 were available for 48 EHC patients in this study, 19 (40 per cent) of which carried the 614G amino acid residue and 29 (60 per cent) of which carried the D614 residue. There was no statistically significant difference in the SARS-CoV-2 C_T (cycle threshold) value between nasopharyngeal (NP) samples with the G residue ($n=18$) and D residue ($n=28$) (median: 24.0 vs. 24.2, $P=0.547$) (Supplementary Figure S12), including after adjustment for day of symptom onset and disease severity ($P=0.84$).

We also assessed whether there were differences in subgenomic RNA (sgRNA), which is a marker for active viral replication (Wölfel et al. 2020). sgRNA was detected in a similar proportion of samples with the D and G residues [30/32 (93.8 per cent) and 15/17 (88.2 per cent), respectively; $P=0.60$] (Supplementary Table S1), and the level of sgRNA was similar for samples with the D residue (mean C_T 28.6, SD 5.6) and G residue (mean C_T 27.3, SD 6.3; $P=0.50$). This did not differ when adjusted for the SARS-CoV-2 genomic RNA C_T value in these samples (D residue, mean C_T difference 4.7 cycles, SD 2.5; G residue, mean C_T difference 4.2 cycles, SD 1.7; $P=0.49$).

Finally, disease severity was similar between patients with the D residue (mild: 42.9 per cent, moderate: 35.7 per cent, severe: 21.4 per cent) and G residue (mild: 27.8 per cent, moderate: 44.4 per cent, severe: 27.8 per cent, $P=0.585$). More broadly, across all EHC patients, disease severity was not associated with age; other comorbidities were not assessed. Disease severity was associated with time since symptom onset; patients with severe disease had experienced a longer duration of symptoms prior to diagnosis (mean of 8.1 days) than those with mild disease (5.1 days, $P=0.01$) (Supplementary Figure S13A). Disease severity was not associated with the SARS-CoV-2 C_T value, as the mean C_T was 26.6 for patients with severe disease vs. 24.8 for moderate disease vs. 24.3 for mild disease (Supplementary Figure S13B), and there was no significant association after adjustment for symptom duration, age, and the C_T value ($P=0.42$).

3. Discussion

Despite its high domestic and international connectivity, Georgia was spared a large SARS-CoV-2 epidemic in early 2020. However, little is known about the viral evolutionary dynamics in the state during this time. Here, we detected at least 19 introductions of SARS-CoV-2 into Georgia from phylogenetic analysis of 108 sequences obtained through the end of March 2020. As this estimate includes only those lineages represented in the available sequencing data, the true number of introductions is certainly higher. Furthermore, observing roughly 19 introductions

among only 108 sequences implies that a large proportion of the sequences in this analysis were attributed to a novel introduction compared to local transmission. While phylogenetic studies focused specifically on the spread of SARS-CoV-2 in the south-eastern USA in early 2020 are relatively limited, studies from the region (broadly defined) consistently found multiple circulating lineages (Louisiana (Zeller et al. 2021), Maryland (Thielen et al. 2021), and North Carolina (McNamara et al. 2020)), indicative of multiple introductions, and this pattern is mirrored in US states in other regions (California (Deng et al. 2020), Connecticut (Fauver et al. 2020), Illinois (Lorenzo-Redondo et al. 2020), Massachusetts (Lemieux et al. 2021), New York (Gonzalez-Reiche et al. 2020), Washington (Bedford et al. 2020; Worobey et al. 2020), and Wisconsin (Moreno et al. 2020)). Existing studies that leverage genomic and travel data have shown that both international and domestic travel fueled the early domestic spread of SARS-CoV-2 (Fauver et al. 2020).

Notably, nearly 65 per cent of the SARS-CoV-2 sequences sampled from Georgia through March 2020 were highly genetically related and fell within a single 19B subclade. Bayesian phylogenetic reconstruction of these Georgia sequences, as well as globally sampled sequences within the same subclade and ancestral relatives, demonstrates that they were likely the result of a single or small number of introductions into the USA in early February. Based on our analysis, Georgia was the most likely site of introduction of this lineage into the USA, but because international SARS-CoV-2 genomic surveillance was fairly limited in early 2020, it is difficult to know this for certain. Importantly, the time to MRCA of the sequences in this subclade is estimated to have been two to four weeks before the first detected SARS-CoV-2 infection in Georgia, which was reported on 2 March 2020 (Georgia Department of Public Health 2020). Due to stochasticity in transmission dynamics at low infectious population sizes (Pekar et al. 2021), this lineage was likely introduced even earlier. The estimated detection lag of this lineage is therefore one to two weeks longer than was observed in the UK (du Plessis et al. 2021). Thus, SARS-CoV-2 was circulating within Georgia for a substantial period of time before being identified by clinical or genomic surveillance.

Finding a large number of sequences from a single or small number of introductions is consistent with the substantial transmission heterogeneity of SARS-CoV-2 that has been reported both within Georgia (Lau et al. 2020) and elsewhere (Miller et al. 2020; Popa et al. 2020; Lemieux et al. 2021). For example, a recent phylogenetic study of SARS-CoV-2 sequences from Louisiana estimated that a single introduction into Louisiana was responsible for the majority of transmission within the state following superspreading events associated with Mardi Gras (Zeller et al. 2021). Additionally, a study of genomes collected in the Boston area have identified large superspreading events associated with nursing facilities and an international business conference (Lemieux et al. 2021).

Our analysis of SARS-CoV-2 infection in domestic travelers returning to Georgia also underscores the fact that there was widespread unrecognized transmission in early 2020. In fact, due to the presence of identical viruses in multiple states, it was difficult to infer from viral genomic data alone whether returning travelers in this study were infected in Georgia or travel locations such as North Carolina, Mississippi, and Colorado. Taken together, these results emphasize that the early focus of diagnostic testing on returning international travelers, rather than more broad testing of patients with COVID-19 symptoms, led to under-recognition of existing infections in early 2020.

In addition, while our analysis of returning travelers highlights the need for more comprehensive genome sequencing of emerging pathogens, it also emphasizes the limited resolution of genomic epidemiology when the genetic diversity of a pathogen is low. Viral genomic analyses can be enhanced by the collection of finely resolved metadata. Our study benefited from linked clinical and epidemiological data for nearly half of the SARS-CoV-2 samples sequenced, but despite extensive chart review, we encountered limitations, e.g. in reporting specific dates of travel and symptom onset. Thus, there is a need for a dedicated infrastructure for data collection in the setting of outbreak analysis, beyond routinely collected clinical data.

Our study also provides information regarding the dynamics of early SARS-CoV-2 lineages in the USA. The 19B subclade, which caused most of the infections described in this study, appears to have spread from Georgia both domestically and internationally (e.g. to Australia) before dying out in April/May of 2020. The apparent extinction of this D614-containing 19B subclade occurred concurrently with the widely reported sweep of SARS-CoV-2 clades harboring the 614G mutation (Volz et al. 2020). The increased transmission of 614G-containing viruses may be due to their ability to cause infection with higher viral loads (Plante et al. 2021). We did not observe a difference in either viral load or subgenomic RNA in patients with D614 or 614G-containing viruses in this study, which may be due to small sample size.

While the 19B subclade reported here was associated with limited forward transmission, we did not find strong evidence for ongoing transmission from the other observed introductions of SARS-CoV-2 into Georgia. However, we primarily analyzed genomes collected through the end of March 2020, so it is possible that other observed introductions, particularly those that occurred later in the time frame of this analysis, seeded downstream transmission chains that are not described here.

Overall, our findings provide several key take-home messages about the early SARS-CoV-2 pandemic that may be applicable to future outbreaks. First, our study recognizes that, despite intensive effort, diagnostic testing capabilities lagged well behind SARS-CoV-2 transmission early in the pandemic. In addition, the focused effort on diagnosis in returning international travelers meant that substantial local and domestic transmission was occurring, but was missed. In a broader context, our findings highlight that highly transmissible pathogens may potentially spread faster than can be detected by the current surveillance infrastructure around the world. This lesson also applies to emerging variants of SARS-CoV-2 (Centers for Disease Control and Prevention 2021). When new variants with likely enhanced transmission are reported to be circulating widely in other countries, it is highly likely that community transmission is already occurring within the USA, given the mobility of the population. Therefore, success of public health policies and interventions countering these variants depends on early planning and implementation, prior to detection in the USA. Given the inevitable challenges in developing and rolling out diagnostic tests for a novel pathogen, these findings underscore the importance of early, empiric public health interventions to attenuate transmission while diagnostic and sequencing efforts 'catch up'.

Future pandemic responses will benefit from public health measures that presume early unrecognized transmission and act to mitigate it, while also implementing aggressive population-based surveillance, including prioritizing testing of asymptomatic contacts. These activities will be synergistic with the much needed, and now expanding, infrastructure for pathogen genomic

surveillance and enhanced collection of detailed clinical and epidemiological data.

4. Methods

4.1 Collection of clinical data and samples

This study was approved by the Emory University Institutional Review Board. Clinical data including demographics, comorbid conditions, duration of symptoms prior to testing, travel history, and severity of illness were extracted by chart review. Disease severity was classified as mild (ED or outpatient visit only), moderate (inpatient without ICU admission), or severe (inpatient with ICU admission).

Residual clinical samples (nasopharyngeal, oropharyngeal, swab samples, and bronchoalveolar lavage samples) were collected from EHC patients between 3 March 2020 and 31 March 2020, including from inpatient and outpatient sites across 8 hospitals and multiple clinics. Total nucleic acids were extracted and underwent testing in a SARS-CoV-2 triplex real-time reverse-transcriptase polymerase chain reaction (rRT-PCR), as described (Waggoner et al. 2020). Testing for subgenomic RNA was performed using a modified forward primer (5'-CGATCTCTGTAGATCTGTTCTC-3') and the reverse primer and probe for the N2 target used in the triplex SARS-CoV-2 rRT-PCR.

4.2 SARS-CoV-2 genome sequencing

Samples underwent DNase treatment (ArcticZymes), cDNA synthesis with random primers and Superscript III (Invitrogen), Nextera XT tagmentation (Illumina), and Illumina sequencing (Babiker et al. 2020a). A median of 36.4 million reads were obtained per sample, and individual results are listed in Supplementary Table S1. Reference-based SARS-CoV-2 genome assembly was performed using viral-ngs v.2.0.21 (Broad Institute 2020) with reference NC_045512 (Wu et al. 2020). Reads per million (RPM) was calculated by dividing the number of mapped reads by the total number of reads and multiplying by 1 million.

Lower titer viruses were sequenced using a multiplex PCR amplification strategy followed by amplicon sequencing as described (Paden et al. 2020). Briefly, RNA was reverse transcribed using random hexamers. The resulting cDNA was used as a template for four pools of SARS-CoV-2-specific multiplex PCR. PCR amplicons were purified and used to prepare sequencing libraries using the Illumina Nextera FLEX kit and sequenced on an Illumina NovaSeq instrument. Reads were trimmed for quality and primers were removed using BBDuk (Bushnell 2022) and assembled using the BETACORONAVIRUS module of IRMA v.1.0.2 (Shepard et al. 2016).

4.3 Clade assignment

We assigned all sequences in our dataset to a given clade using Nextclade v.0.13.0 (Hadfield et al. 2018; Bedford, Hodcroft, and Neher 2020). Pango lineages were assigned using the Pangolin COVID-19 Lineage Assigner with pangoLEARN v.2021-08-09 (Rambaut et al. 2020).

4.4 Statistical analysis

Comparison of categorical variables was performed by the Chi square test (or Fisher's when expected frequencies < 5). Comparison of continuous variables was performed by the Wilcoxon rank sum test or Kruskal–Wallis test when appropriate. Correlation of C_T values to logRPM was assessed by Poisson regression.

Statistical analysis was performed using R v.4.0.2 (Vienna, Austria) (R Core Team 2020) and the RStudio interface v.1.3.1073 (Boston, MA, USA) (RStudio Team 2020). Maps showing the number of cases and number of sequences per Georgia county were generated with <https://mapchart.net> accessed on 30 August 2021.

4.5 Global sequence data

To place the sequences from Georgia in a global context, we downloaded all sequences sampled through 31 March 2020 and labeled as 'complete', 'high coverage', and 'collection date complete' from the Global Initiative for Sharing All Influenza Data (GISAID) database (Shu and McCauley 2017) as of 27 March 2021. We excluded any sequences from non-human hosts, any sequences related to a cruise ship, and any sequences with known travel history (to avoid biasing the ancestral state reconstruction), as annotated in the NextMeta file. These sequences, as well as the new EHC sequences presented in this analysis (when multiple samples from the same subject were available, we only included the NP swab sample), were aligned to Wuhan/Hu-1 (EPI_ISL_402125) using MAFFT v7.464 (Katoh et al. 2002) and removing any insertions relative to Wuhan/Hu-1 (Wu et al. 2020). To account for the potential sequencing error, we masked the first and last 100 nucleotides of the genome as well as sites 11,083, 15,324, and 21,575, which were identified as 'highly homoplasic' in early SARS-CoV-2 sequencing data (De Maio et al. 2020). Sequences with less than 28,000 A, C, T, and G nucleotides after aligning were removed. The GISAID Acknowledgement Table is provided in Supplementary Table S3.

4.6 Maximum likelihood phylogenetic analysis

For our phylogenetic analyses, we first downsampled the available global sequence data to maintain a representative geographical distribution of sequences (weighted downsampling strategy). We downsampled the available sequences from each country based on the cumulative number of reported SARS-CoV-2 cases by 31 March 2020 (Dong, Du, and Gardner 2020) and a target alignment size of 6,000 sequences. For countries where the number of available sequences was greater than the product of the target alignment size and the relative number of cumulative cases in that country, we sampled sequences with weight $1/(1+D)$ where D is the minimum SNP distance of a given sequence to all available Georgia sequences. Only A, C, T, and G nucleotides were considered when calculating pairwise distances. NumPy v.1.19 (Harris et al. 2020) in Python v.3.9.4 (Python Software Foundation 2020) was used to calculate the pairwise distances. We manually included all Georgia sequences and Wuhan/Hu-1 in the final alignment. The alignment included 4,622 sequences, including 108 from Georgia (Supplementary Table S5). An alternative downsampling procedure, including a maximum of twenty sequences per country per week, was investigated to assess the robustness of our results (Supplementary Methods, Supplementary Figure S6A). Downsampling was conducted in Python using BioPython (Cock et al. 2009) and Pandas v.1.1 (Pandas Development Team 2020).

IQ-TREE v.2.1.3 (Nguyen et al. 2015) was used to generate maximum likelihood phylogenies with 1,000 ultrafast bootstrap replicates (Hoang et al. 2018), collapsing small branches, and using ModelFinder to identify the best fit nucleotide substitution model (Kalyaanamoorthy et al. 2017). A GTR + F + I + G4 model was chosen. TreeTime v.0.8.2 (Sagulenko, Puller, and Neher 2018) was used to remove any sequences falling outside four interquartile ranges of the expected molecular clock rate, rooting at Wuhan/Hu-1.

The date of internal nodes was estimated using TreeTime with a fixed clock rate of 0.001 (Duchene et al. 2020) and a coalescent skyline. TreeTime was run for a maximum of three iterations and polytomies were not resolved. Root-to-tip regression, conducted using SciPy v.1.5.4 (Virtanen et al. 2020), confirmed a significant clock rate ($P < 0.0001$) in the set of included sequences (Supplementary Figure S4).

TreeTime was also used to reconstruct the ancestral states of internal nodes (Georgia/Non-Georgia) with a sampling bias correction of 2.5. We used the reconstructed traits of internal nodes to estimate the number of introductions into Georgia (transition from a non-Georgia node to a Georgia node along a given lineage). To provide a conservative estimate, we attributed multiple Georgia nodes descending from a non-Georgia polytomous internal node to be the result of a single introduction. Furthermore, we only considered the earliest (in time) introduction into Georgia for each lineage giving rise to a Georgia sequence. In other words, we did not account for the reintroduction of a given lineage into Georgia when counting the number of introductions. This procedure was repeated on 100 bootstrap replica trees to account for phylogenetic uncertainty.

4.7 Bayesian phylogenetic analysis

For a more robust reconstruction of the timing and source of introduction for the highly related sequences belonging to clade 19B, we conducted a Bayesian discrete phylogeographic reconstruction. We identified the set of highly related Georgia sequences by calculating the pairwise phylogenetic distance between all Georgia sequences in the time-resolved maximum likelihood phylogeny using BioPython. SciPy was used to identify clusters in this distance matrix with a cutoff of 0.3 years. We identified sixty-nine Georgia sequences in the largest cluster.

As we wished to include the ancestral relatives to these sixty-nine sequences in our Bayesian phylogenetic analysis, we first identified their great-grandparent in the time-resolved maximum likelihood phylogeny. Next, we identified the set of nucleotide substitutions shared between all sequences that descended from that great-grandparent. We allowed for the presence of ambiguous nucleotides when identifying shared SNPs (e.g. an R nucleotide was assumed to match both A and G nucleotides). We identified three nucleotide substitutions shared between these sequences: T26729C, G28077C, and the 19B clade defining SNP T28144C. The other 19B clade defining SNP C8782T was identified in all sequences descending from this node except one, EPI_ISL_454974. Finally, we identified all ‘complete’, ‘high coverage’, and ‘sampling date complete’ sequences sampled through 31 March 2020 in GISAID as of 27 March 2021 that matched this mutational profile (excluding any with ambiguous nucleotides at any sites in the mutational profile) after aligning to Wuhan/Hu-1 as described above. Again, we excluded any sequences from non-human samples, related to cruise ships, or with travel history. IQ-Tree was used to generate a maximum likelihood phylogeny of these sequences with the same parameters as described above and TreeTime was used to remove any samples falling outside four interquartile ranges of the expected molecular clock rate, rooted at the best fit root as identified by least-squares regression. The final alignment included 527 sequences, of which 67 were from Georgia. Root-to-tip regression confirmed a significant clock rate ($P < 0.0001$) in the set of included sequences of sequences (Supplementary Figure S7).

To improve computational efficiency, we removed sequences from any states with fewer than four sequences in the data set

or US sequences without a specified state. Furthermore, international sequences sampled after 29 February 2020 were excluded as they were evolutionary descendant from the MRCA of all US sequences and therefore likely represent exportations of this subclade from the USA (Supplementary Figures S8 and S9). Furthermore, we generated five downsampled alignments in which at most five sequences per country/US state per week were randomly sampled, including Georgia. Each downsampled alignment included 226 sequences (Supplementary Table S6).

Bayesian phylogenetic inference was conducted using BEAST2 v2.6.6 (Bouckaert et al. 2019) with Beagle v3.1.2 (Ayres et al. 2012) and discrete trait estimation implemented in BEAST_CLASSIC v.1.50 (Lemey et al. 2009). We assumed an exponential population coalescent using a Laplace distribution for the growth rate prior ($\mu = 0.0$, $\text{scale} = 10.0$) and a Lognormal ($\mu = 1.0$, $\sigma = 2.0$) prior on the population size. We used an HKY + Γ_4 substitution model with a Lognormal ($\mu = 1.0$, $\sigma = 1.25$) prior on K . We used a relaxed molecular clock (Drummond et al. 2006) with a normal ($\mu = 1E-3$, $\sigma = 1E-4$) prior on the mean clock rate (Duchene et al. 2020), and an exponential ($\mu = 0.33$) prior on the standard deviation of the clock rate. Uniform priors were used for nucleotide frequencies and the proportion of invariant sites. We parameterized the discrete ancestral state reconstruction with a Poisson ($\lambda = (N_{\text{traits}} * N_{\text{traits}} - 1)/8$, $\text{offset} = N_{\text{traits}} - 1$) distribution for the number of non-zero rates, a Γ ($\alpha = 1.0$, $\beta = 1.0$) prior for the relative rates, and a Γ ($\alpha = 0.001$, $\beta = 1000$) prior on the rate of discrete trait changes. Rates were assumed to be symmetric. Included sequences were assigned to their country (international sequences) or state (US sequences) of origin. BEAST XML files were generated using a custom Python script and XML templates originally generated using Beauti v.2.6.3 and edited by hand. The MCMC chain was run for 285 M steps, saving every 5,000 steps. The first 10 per cent of MCMC steps were discarded as burn in. The ESS value of all parameters was >100 and >200 for parameters relevant to our conclusions as annotated by Tracer (Rambaut et al. 2018). The maximum clade credibility summary tree (with median node heights) was reconstructed using TreeAnnotator v.2.6.3. When tabulating the number of introductions of the 19B subclade into Georgia, we considered only the earliest (in time) introduction along a given lineage. In other words, we did not account for the reintroduction of a given lineage into Georgia when counting the number of introductions.

Downstream analysis of the TreeTime and BEAST output was conducted in Python using BioPython, Pandas, and NumPy. Results were visualized using Baltic v.0.1.6 (Dudas 2020), Matplotlib v.3.3.356 (Hunter 2007), and Seaborn v.0.11.157 (Waskom et al. 2020).

4.8 Georgia travel history

To assess the probability that patients with recent travel history were infected during travel, we compared the sequence from each traveler to sequences circulating in the region they were traveling to, sequences circulating in the state of Georgia, and sequences circulating globally. To ensure that our inferences were not biased by homoplastic artifacts in phylogenetic reconstruction, we generated a mutational profile for each traveler’s sequence by identifying the SNPs relative to Wuhan/Hu-1. Insertions and deletions were not considered in this analysis. Next, we identified all sequences that matched either Wuhan/Hu-1 or the traveler’s sequence at all positions in the mutational profile, not allowing for Ns or ambiguous nucleotides. We calculated the genetic distance from Wuhan/Hu-1 for the traveler’s sequence and

all sequences from a given region, considering only A, C, T, and G characters. Sequences with a smaller genetic distance than the traveler sequence harbored a subset of the mutations in the traveler sequence, while those with a larger genetic distance harbored all of the mutations in the traveler sequence plus additional mutations. This analysis was conducted in Python using NumPy and Pandas. Figures for this analysis were generated in R v.4.0.4 using RStudio v.1.4.1106 with GGplot2 v.3.3 (Wickham et al. 2021).

4.9 Mutational profile of closely related Georgia 19B sequences

First, the shared SNPs (relative to Wuhan/Hu-1) between the sixty-nine closely related Georgia 19B sequences were identified from the sequence alignment described above using BioPython. We allowed for the presence of ambiguous nucleotides when identifying shared SNPs. We refer to sequences harboring this mutational profile as belonging to the 'clade 19B subclade'. The variants in the mutational profile were annotated using snpEff v. 5.0 (Cingolani et al. 2012).

Next, we downloaded all 'complete', 'high coverage', and 'collection date complete' from GISAID sampled and uploaded through 27 March 2020 that shared the L84S amino acid (T28144C nucleotide) substitution, a clade defining mutation of 19B. We removed non-human samples, those related to cruise ships, and samples with travel history and aligned them to Wuhan/Hu-1 with MAFFT with the same parameters described above. We identified all sequences that non-ambiguously matched the Georgia 19B subclade mutational profile (Supplementary Table S9) using NumPy in Python. We summed the number of identified sequences per week for each US state as well as the total number of other countries using Pandas. Results were visualized using Matplotlib.

Data availability

All consensus sequence data used in this analysis are available from the GISAID (<https://www.gisaid.org>). Accession numbers are available in Supplementary Tables S1, S3, S5, S6, and S9. Sequence data newly generated for this project is available on NCBI under BioProject PRJNA634356, including both consensus sequences and raw reads (cleaned of human reads). Metadata for the Georgia, USA, sequences needed to replicate the analysis is available in Supplementary Tables S1, S2, S4, and S8 as well as at <https://zenodo.org/record/6038869>. Metadata for non-Georgia sequences is available via GISAID. Code necessary to replicate this analysis is available at <https://zenodo.org/record/6038869>. Output files from the BEAST analysis can be found at https://figshare.com/articles/dataset/Unrecognized_introductions_of_SARS-CoV-2_into_the_state_of_Georgia_shaped_the_early_epidemic_v_1_0/14935380.

Supplementary data

Supplementary data is available at *Virus Evolution* online.

Acknowledgements

We would like to acknowledge our laboratory colleagues at the Emory University Healthcare Microbiology, Molecular and Referral Laboratories, who have worked tirelessly to provide necessary care to our patients during this time. We thank the Emory Clinical

Virology Research Laboratory, the Georgia Clinical Research Centers, and the Yerkes NHP Genomics Core for support in sample collection and sequencing. We thank Audrey Kunkes and the Georgia Department of Public Health for their support. Publicly available SARS-CoV-2 sequences from Georgia were generously contributed by Mayo Clinic Laboratories, Quest Diagnostics, and the U.S. Air Force School of Aerospace Medicine. We gratefully acknowledge the authors from the originating laboratories responsible for obtaining the specimens, as well as the submitting laboratories where the genome data were generated and shared via GISAID, on which this research is based (Supplementary Table S3). All submitters of data may be contacted directly via www.gisaid.org.

Funding

This study was supported by the CDC contract 75D30121C10084 under BAA ERR 20-15-2997, the Pediatric Research Alliance Center for Childhood Infections and Vaccines and Children's Healthcare of Atlanta, and the Emory WHSC COVID-19 Urgent Research Engagement (CURE) Center, made possible by generous philanthropic support from the O. Wayne Rollins Foundation and the William Randolph Hearst Foundation. The Yerkes NHP Genomics Core is supported in part by NIH P51 OD011132, and sequence data were acquired on an Illumina NovaSeq6000 funded by NIH S10 OD 026799. Sample collection was supported by the National Center for Advancing Translational Sciences of the National Institutes of Health under Award Number UL1TR002378. Research reported in this publication was supported by the National Institute Of Allergy And Infectious Diseases of the National Institutes of Health under Award Number K08AI139348 (A.P.) and F31 AI154738 (M.A.M.). The content is solely the responsibility of the authors and does not necessarily represent the official views of the National Institutes of Health.

Conflict of interest: None declared.

Disclaimer

The findings and conclusions in this report are those of the authors and do not necessarily represent the official position of the Centers for Disease Control and Prevention. Use of trade names is for identification only and does not imply endorsement by the Centers for Disease Control and Prevention, the Public Health Service, or the US Department of Health and Human Services.

References

- Alm, E. et al. (2020) 'Geographical and Temporal Distribution of SARS-CoV-2 Clades in the WHO European Region, January to June 2020', *Eurosurveillance*, 25: pii=2001410.
- Ayres, D. L. et al. (2012) 'BEAGLE: An Application Programming Interface and High-Performance Computing Library for Statistical Phylogenetics', *Systematic Biology*, 61: 170–3.
- Babiker, A. et al. (2020a) 'Metagenomic Sequencing to Detect Respiratory Viruses in Persons under Investigation for COVID-19', *Journal of Clinical Microbiology*, 59: 1. (M. J. Loeffelholz, Ed.).
- Babiker, A. et al. (2020b) 'SARS-CoV-2 Testing', *American Journal of Clinical Pathology*, 153: 706–8.
- Bedford, T. et al. (2020) 'Cryptic Transmission of SARS-CoV-2 in Washington State', *Science*, 370: 571–5.

- Bedford, T., Hodcroft, E. B., and Neher, R. A. (2020), *Updated Nextstrain SARS-CoV-2 Clade Naming Strategy*. Nextstrain. <<https://nextstrain.org/blog/2021-01-06-updated-sars-cov-2-clade-naming>> accessed 8 Feb 2022.
- Bouckaert, R. et al. (2019) 'BEAST 2.5: An Advanced Software Platform for Bayesian Evolutionary Analysis', *PLoS Computational Biology*, 15: e1006650.
- Broad Institute. (2020), *Viral-Pipelines*. <<https://github.com/broadinstitute/viral-pipelines>> accessed 8 Feb 2022.
- Bushnel, B. (2022), BBDuk. Joint Genome Institute. <<https://sourceforge.net/projects/bbmap/>> accessed Feb 8, 2022.
- CDC. (2020), CDC 2019-Novel Coronavirus (2019-ncov) Real-Time RT-PCR Diagnostic Panel. Centers for Disease Control and Prevention. <<https://www.fda.gov/media/134922/download>> accessed 8 Feb 2022.
- Centers for Disease Control and Prevention. (2021), *SARS-CoV-2 Variant Classifications and Definitions*. <https://www.cdc.gov/coronavirus/2019-ncov/variants/variant-info.html?CDC_AA_refVal=https%3A%2F%2Fwww.cdc.gov%2Fcoronavirus%2F2019-ncov%2Fcases-updates%2Fvariant-surveillance%2Fvariant-info.html> accessed 8 Feb 2022.
- Cingolani, P. et al. (2012) 'A Program for Annotating and Predicting the Effects of Single Nucleotide Polymorphisms, SnpEff', *Fly*, 6: 80–92.
- Cock, P. J. A. et al. (2009) 'Biopython: Freely Available Python Tools for Computational Molecular Biology and Bioinformatics', *Bioinformatics*, 25: 1422–3.
- De Maio, N. et al. (2020), *Masking Strategies for SARS-CoV-2 Alignments*. *Virological*. <<https://virological.org/t/masking-strategies-for-sars-cov-2-alignments/480>> accessed 8 Feb 2022.
- Deng, X. et al. (2020) 'Genomic Surveillance Reveals Multiple Introductions of SARS-CoV-2 into Northern California', *Science*, 369: 582–7.
- Dong, E., Du, H., and Gardner, L. (2020) 'An Interactive Web-based Dashboard to Track COVID-19 in Real Time', *The Lancet Infectious Diseases*, 20: 533–4.
- Drummond, A. J. et al. (2006) 'Relaxed Phylogenetics and Dating with Confidence', *PLoS Biology*, 4: e88. (D. Penny, Ed.).
- du Plessis, L. et al. (2021) 'Establishment and Lineage Dynamics of the SARS-CoV-2 Epidemic in the UK', *Science*, 371: 708–12.
- Duchene, S. et al. (2020) 'Temporal Signal and the Phylodynamic Threshold of SARS-CoV-2', *Virus Evolution*, 6: veaa061.
- Dudas, G. (2020), *Baltic*. <<https://github.com/evogytis/baltic>> accessed 7 Mar 2022.
- Fauver, J. R. et al. (2020) 'Coast-to-Coast Spread of SARS-CoV-2 during the Early Epidemic in the United States', *Cell*, 181: 990–6.e5.
- Georgia Department of Public Health. (2020), *Gov. Kemp, Officials Confirm Two Cases of COVID-19 in Georgia*. Government of Georgia. <<https://dph.georgia.gov/press-releases/2020-03-02/gov-kemp-officials-confirm-two-cases-covid-19-georgia>> accessed 8 Feb 2022.
- Gonzalez-Reiche, A. S. et al. (2020) 'Introductions and Early Spread of SARS-CoV-2 in the New York City Area', *Science*, 369: 297–301.
- Hadfield, J. et al. (2018) 'Nextstrain: Real-time Tracking of Pathogen Evolution', *Bioinformatics*, 34: 4121–3. (J. Kelso, Ed.).
- Harris, C. R. et al. (2020) 'Array Programming with NumPy', *Nature*, 585: 357–62.
- Health Alert Network. (2020), *Updated Guidance on Evaluating and Testing Persons for Coronavirus Disease 2019 (COVID-19)*. Centers for Disease Control and Prevention. <<https://emergency.cdc.gov/han/2020/HAN00429.asp>> accessed 8 Mar 2022.
- Hoang, D. T. et al. (2018) 'UFBoot2: Improving the Ultrafast Bootstrap Approximation', *Molecular Biology and Evolution*, 35: 518–22.
- Hunter, J. D. (2007) 'Matplotlib: A 2D Graphics Environment', *Computing in Science & Engineering*, 9: 99–104.
- Kalyaanamoorthy, S. et al. (2017) 'ModelFinder: Fast Model Selection for Accurate Phylogenetic Estimates', *Nature Methods*, 14: 587–9.
- Katoh, K. et al. (2002) 'MAFFT: A Novel Method for Rapid Multiple Sequence Alignment Based on Fast Fourier Transform.', *Nucleic Acids Research*, 30: 3059–66.
- Lau, M. S. Y. et al. (2020) 'Characterizing Superspreading Events and Age-specific Infectiousness of SARS-CoV-2 Transmission in Georgia, USA', *Proceedings of the National Academy of Sciences*, 117: 22430–5.
- Lemey, P. et al. (2009) 'Bayesian Phylogeography Finds Its Roots', *PLoS Computational Biology*, 5: e1000520. (C. Fraser, Ed.).
- Lemieux, J. E. et al. (2021) 'Phylogenetic Analysis of SARS-CoV-2 in Boston Highlights the Impact of Superspreading Events', *Science*, 371: eabe3261.
- Lorenzo-Redondo, R. et al. (2020) 'A Clade of SARS-CoV-2 Viruses Associated with Lower Viral Loads in Patient Upper Airways', *EBioMedicine*, 62: 103112.
- McNamara, R. P. et al. (2020) 'High-Density Amplicon Sequencing Identifies Community Spread and Ongoing Evolution of SARS-CoV-2 in the Southern United States', *Cell Reports*, 33: 108352.
- Miller, D. et al. (2020) 'Full Genome Viral Sequences Inform Patterns of SARS-CoV-2 Spread into and within Israel', *Nature Communications*, 11: 5518.
- Moreno, G. K. et al. (2020) 'Revealing Fine-scale Spatiotemporal Differences in SARS-CoV-2 Introduction and Spread', *Nature Communications*, 11: 5558.
- Nguyen, L. T. et al. (2015) 'IQ-TREE: A Fast and Effective Stochastic Algorithm for Estimating Maximum-likelihood Phylogenies', *Molecular Biology and Evolution*, 32: 268–74.
- Paden, C. R. et al. (2020) 'Rapid, Sensitive, Full-Genome Sequencing of Severe Acute Respiratory Syndrome Coronavirus 2', *Emerging Infectious Diseases*, 26: 2401–5.
- Pandas Development Team. (2020), *Pandas*. NumFocus. <<https://pandas.pydata.org>> accessed 14 Nov 2020.
- Patel, A. et al. (2020) 'Initial Public Health Response and Interim Clinical Guidance for the 2019 Novel Coronavirus Outbreak — United States, December 31, 2019–February 4, 2020', *MMWR. Morbidity and Mortality Weekly Report*, 69: 140–6.
- Pekar, J. et al. (2021) 'Timing the SARS-CoV-2 Index Case in Hubei Province', *Science*, 372: 412–7.
- Perkins, T. A. et al. (2020) 'Estimating Unobserved SARS-CoV-2 Infections in the United States', *Proceedings of the National Academy of Sciences*, 117: 22597–602.
- Plante, J. A. et al. (2021) 'Spike Mutation D614G Alters SARS-CoV-2 Fitness', *Nature*, 592: 116–21.
- Popa, A. et al. (2020) 'Genomic Epidemiology of Superspreading Events in Austria Reveals Mutational Dynamics and Transmission Properties of SARS-CoV-2', *Science Translational Medicine*, 12: eabe2555.
- Python Software Foundation. (2020), *Python Language Reference*. <<http://www.python.org>> accessed 29 Mar 2022.
- R Core Team. (2020), *R: A Language and Environment for Statistical Computing*. Vienna, Australia. <<https://www.R-project.org/>> accessed 11 Dec 2020.
- Rambaut, A. et al. (2018) 'Posterior Summarization in Bayesian Phylogenetics Using Tracer 1.7', *Systematic Biology*, 67: 901–4. (E. Susko, Ed.).

- Rambaut, A. et al. (2020) 'A Dynamic Nomenclature Proposal for SARS-CoV-2 Lineages to Assist Genomic Epidemiology', *Nature Microbiology*, 5: 1403–7.
- RStudio Team. (2020) *RStudio: Integrated Development for R*. Boston, MA. <<https://www.rstudio.com>> accessed 11 Aug 2020.
- Sagulenko, P., Puller, V., and Neher, R. A. (2018) 'TreeTime: Maximum-likelihood Phylodynamic Analysis', *Virus Evolution*, 4: 1–9.
- Schuchat, A., CDC COVID-19 Response Team. (2020) 'Public Health Response to the Initiation and Spread of Pandemic COVID-19 in the United States, February 24–April 21, 2020', *MMWR. Morbidity and Mortality Weekly Report*, 69: 551–6.
- Shepard, S. S. et al. (2016) 'Viral Deep Sequencing Needs an Adaptive Approach: IRMA, the Iterative Refinement Meta-assembler', *BMC Genomics*, 17: 708.
- Shu, Y., and McCauley, J. (2017) 'GISAID: Global Initiative on Sharing All Influenza Data – from Vision to Reality', *Eurosurveillance*, 22: 2–4.
- Subbaraman, N. (2020) 'How to Address the Coronavirus's Outsized Toll on People of Colour', *Nature*, 581: 366–7.
- Thielen, P. M. et al. (2021) 'Genomic Diversity of SARS-CoV-2 during Early Introduction into the Baltimore–Washington Metropolitan Area', *JCI Insight*, 6: e144350.
- United States Census Bureau. (2019), *Georgia*. United States Government. <<https://data.census.gov/cedsci/profile?g=0400000US13>> accessed 8 Feb 2022.
- SciPy 1.0 Contributors, Virtanen, P. et al. (2020) 'SciPy 1.0: Fundamental Algorithms for Scientific Computing in Python', *Nature Methods*, 17: 261–72.
- Volz, E. M. et al. (2020) 'Evaluating the Effects of SARS-CoV-2 Spike Mutation D614G on Transmissibility and Pathogenicity', *Cell*, 184: 64–75.e11.
- Waggoner, J. J. et al. (2020) 'Triplex Real-Time RT-PCR for Severe Acute Respiratory Syndrome Coronavirus 2', *Emerging Infectious Diseases*, 26: 1633–35.
- Waskom, M. et al. (2020), *Seaborn*. <<https://seaborn.pydata.org/index.html>> accessed 21 Jan 2022.
- Wickham, H., et al. (2021), *Ggplot2: Elegant Graphics for Data Analysis*. Springer-Verlag. New York. <<http://ggplot2.org>> accessed 8 Feb 2022.
- Willis, H., and Williams, V. (2020). *A Funeral Is Thought to Have Sparked A Covid-19 Outbreak in Albany, Ga. — And Led to Many More Funerals*. Washington Post. <https://www.washingtonpost.com/politics/a-funeral-sparked-a-covid-19-outbreak—and-led-to-many-more-funerals/2020/04/03/546fa0cc-74e6-11ea-87da-77a8136c1a6d_story.html> accessed 8 Feb 2022.
- Wölfel, R. et al. (2020) 'Virological Assessment of Hospitalized Patients with COVID-2019', *Nature*, 581: 465–9.
- Worobey, M. et al. (2020) 'The Emergence of SARS-CoV-2 in Europe and North America', *Science*, 370: 564–70.
- Wu, F. et al. (2020) 'A New Coronavirus Associated with Human Respiratory Disease in China', *Nature*, 579: 265–9.
- Zeller, M., et al. (2021), *Emergence of an Early SARS-CoV-2 Epidemic in the United States* (Preprint). *Epidemiology*. <<http://medrxiv.org/lookup/doi/10.1101/2021.02.05.21251235>> accessed 26 Mar 2021.

6.3 Supplement

Reproduced with permission from Oxford University Press.

Supplement

Supplementary Methods

Maximum likelihood phylogenetic analysis

To estimate the number of introductions into Georgia, USA, sequences sampled from Georgia must be placed in the context of globally sampled sequences. In the main text, available sequences were downsampled by weighting based on the cumulative number of infections in a given country as of 2020-03-31 and the minimum genetic distance of a given sequence to all Georgia sequences. As a sensitivity analysis, we alternatively downsampled the available sequences (*Methods*) in a temporally homogeneous manner but taking a maximum of 20 samples per country per week. The alignment included 5079 sequences including 108 from Georgia (**Supplementary Table 10**). A maximum likelihood phylogenetic tree was inferred and the number of introductions into Georgia estimated as described in *Methods*. Of the 5079 sequences in the alignment, 29 failed the clock filter using the Maximum Likelihood phylogenetic tree.

Supplementary Results

Maximum likelihood phylogenetic analysis

A significant molecular clock rate was confirmed in the set of temporally downsampled sequences using root-to-tip regression ($p < 0.0001$, **Supplementary Figure 14**). Using this tree (**Supplementary Figure 6B**), we estimated slightly fewer introductions into Georgia (14 [13-19]) compared to the analysis using the weighted downsampling procedure presented in the main text. This is likely due to the fact that sequences in this tree were not sampled in proportion to their genetic relatedness to Georgia sequences, which reduces the resolution of phylogenetic clustering near the included Georgia sequences. In other words, clades which are attributed to one introduction in this analysis are attributed to multiple clades in the analysis presented in the main text due to the addition of a closely related non-Georgia sequence.

The estimated timing of introductions into Georgia is, in general, slightly earlier in this analysis compared to that in the main text (**Supplementary Figure 6C**). The earliest introduction is estimated to have occurred in late-January/early-February as opposed to mid-February. This is because a number of 20B sequences from the state of Georgia descend directly from a polytomous internal node which is dated in early February when using the weighted downsampling scheme but dated early January using the temporal downsampling scheme. These analyses are consistent in that roughly half of the introductions into Georgia are estimated to have occurred throughout the month of March, in line with the increased surveillance during this time period.

SARS-CoV-2 in returning international travelers

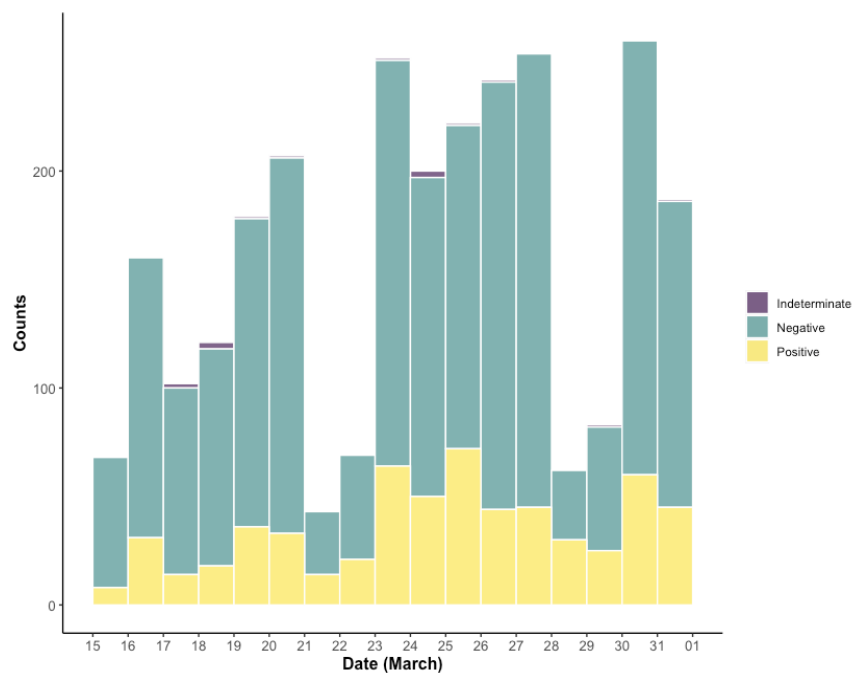
Viral genomic and epidemiologic information was used to evaluate potential SARS-CoV-2 introductions from other returning international travelers. In P33, there was genomic evidence suggesting that SARS-CoV-2 was more likely acquired in the location of travel (Italy and Poland) than Georgia. Specifically, there were 82 sequences from Italy and Poland that were ancestral to the P33 sequence by one SNP (**Supplementary Table 8**). Although there was one sequence from Georgia that was identical to the P33 sequence, based on news reports (Bluestein, G. & Oliviero, H. Officials confirm Georgia's first 2 cases of coronavirus. *Atlanta Journal-Constitution* <https://www.ajc.com/blog/politics/kemp-expected-address-coronavirus-late-night-press-conference/VqbHGt7Z0p8U9KTx6bCIJM/>) we have reason to believe these cases were epidemiologically linked and both associated with shared travel. Otherwise, there were no other Georgia sequences in the lineage. Supporting travel-associated infection, P33 had traveled to Italy and Poland from 8 days prior to symptom

onset until the day of symptom onset, encompassing the most likely incubation period for SARS-CoV-2.

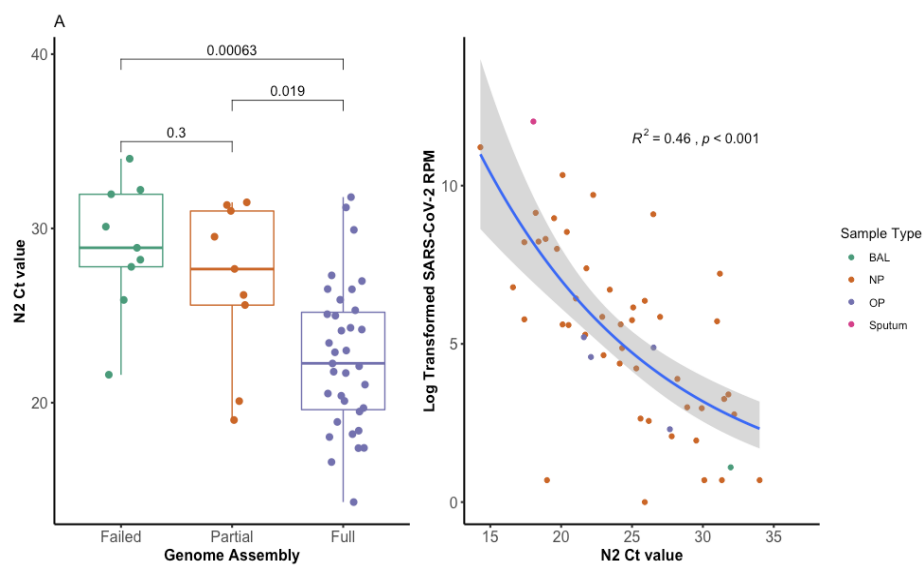
Results were less clear for P8, who had traveled to Nigeria. Among the 15 available sequences from Nigeria during this time period, none were in the same phylogenetic lineage as the sequence from P8. There was one sequence from Georgia in the same lineage, and it was one SNP more ancestral than the P8 sequence, making it plausible that this patient could have had a locally-acquired infection. Compatible with this, P8 returned from Nigeria 8 days prior to symptom onset, allowing time for exposure to and incubation of a locally-acquired infection. However, it is difficult to exclude the possibility that the patient was infected in Nigeria and related sequences were not captured due to undersampling.

Finally, the SARS-CoV-2 sequence from P23, who had traveled to Costa Rica, was equally related to sequences from both Costa Rica and Georgia (**Supplementary Figure 11A**), and the patient's travel spanned part, but not all, of the potential incubation period for infection, making it impossible to know where infection was acquired.

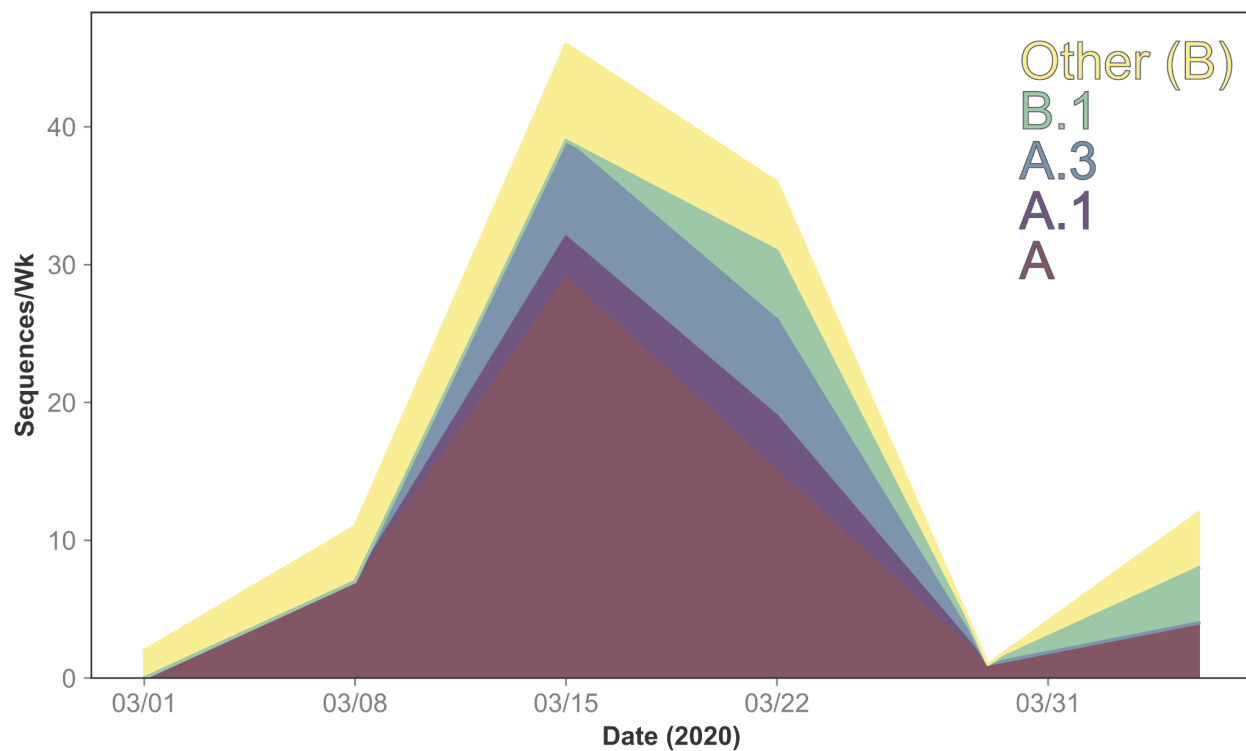
Supplementary Figures



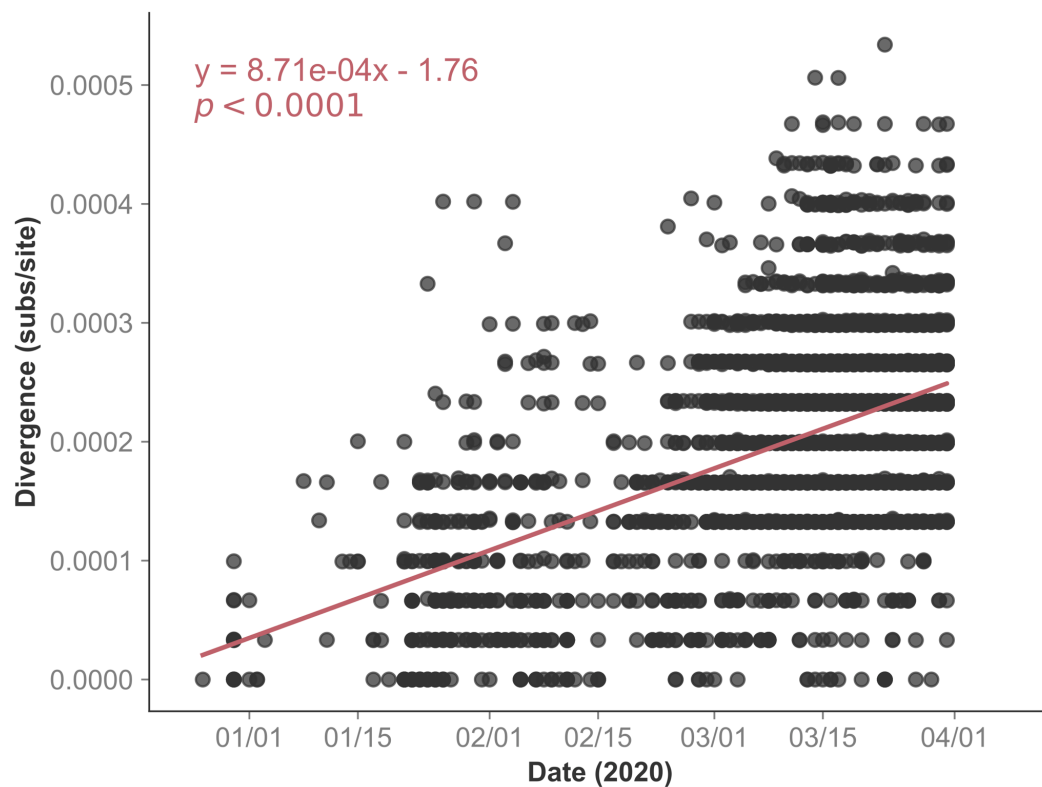
Supplementary Figure 1. SARS-CoV-2 diagnostic rRT-PCR tests performed by the EHC Molecular and Microbiology Laboratories between 2020-03-15 and 2020-03-31. Daily test results are colored by outcome. 610 (22.5%) of the 2,711 tests performed were positive for SARS-CoV-2.



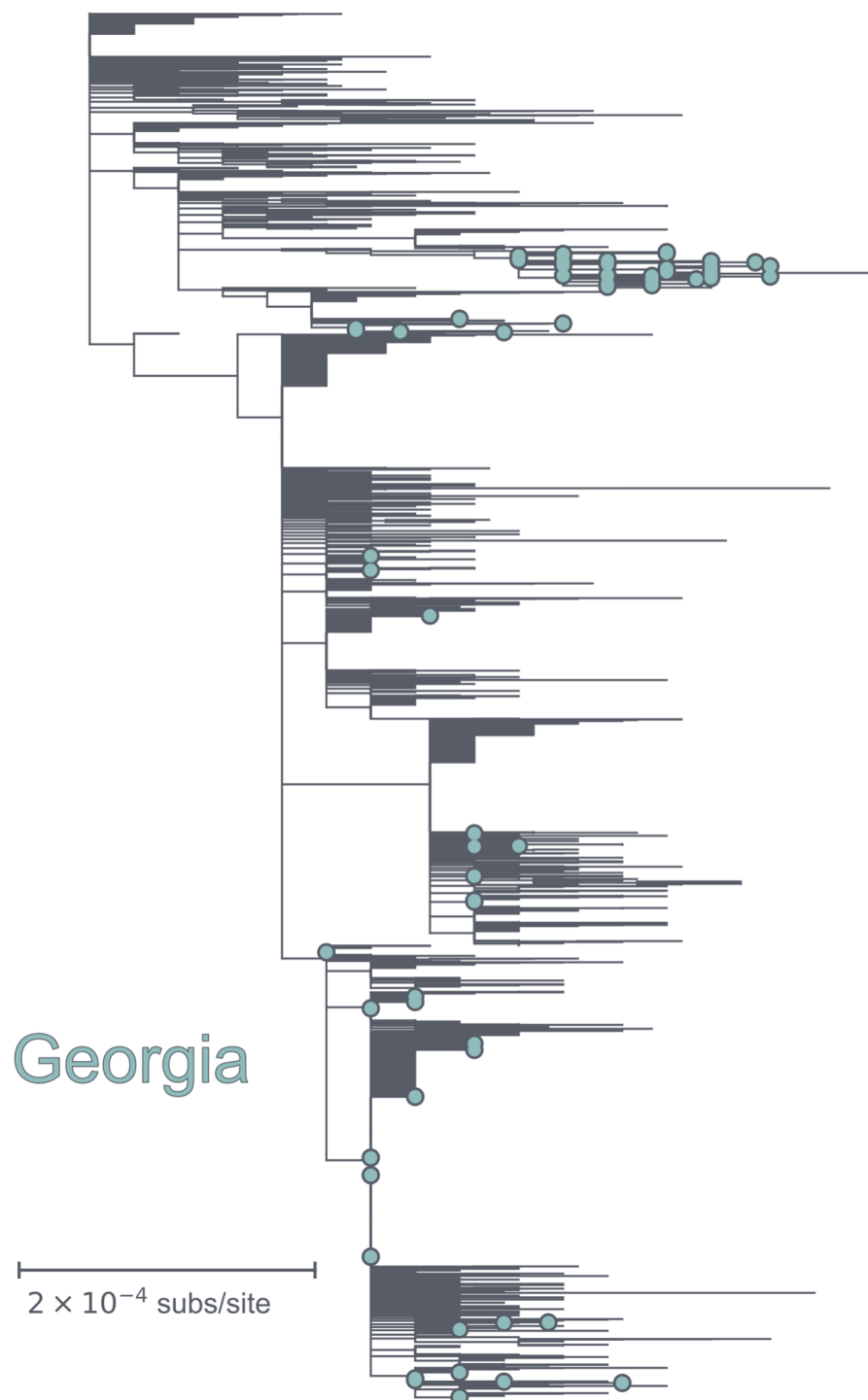
Supplementary Figure 2. Associations between C_T value and SARS-CoV-2 sequencing parameters. (A) SARS-CoV-2 C_T value by SARS-CoV-2 genome coverage for 50 positive nasopharyngeal specimens. (B) Log transformed SARS-CoV-2 reads per million total sequencing reads (RPM) for 52 positive bronchial alveolar lavage (BAL), nasopharyngeal (NP), oropharyngeal (OP), and sputum specimens.



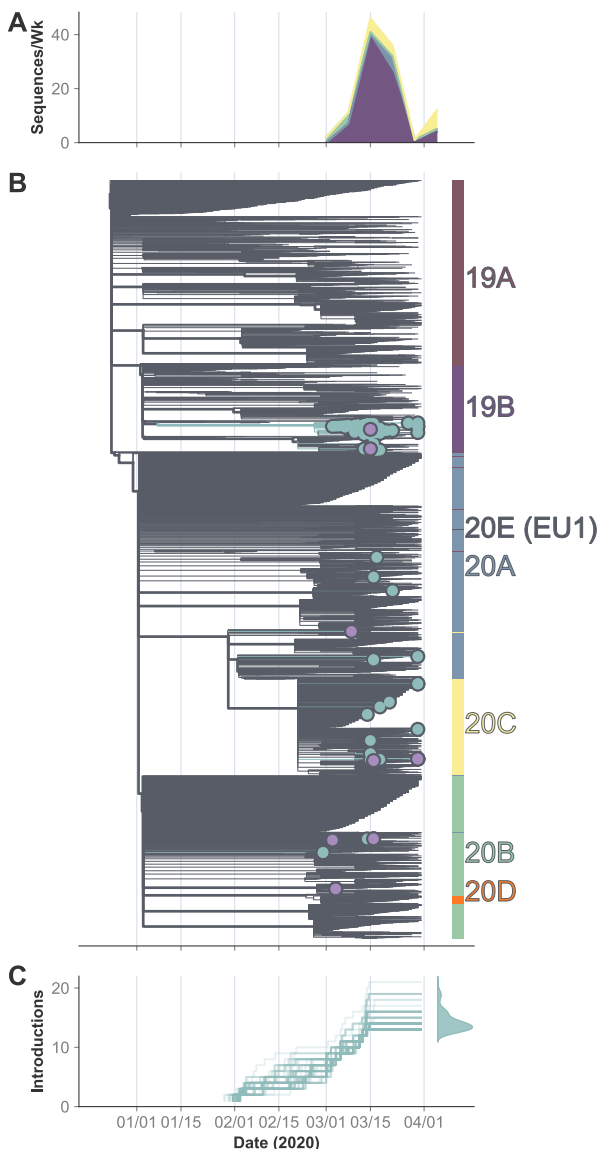
Supplementary Figure 3. Number of sequences from Georgia per lineage, per week included in the phylogenetic analysis. Sequences were grouped based on the last day of their date of sampling. Lineages with a total of less than seven sequences included into the dataset were grouped based on their parent lineage (A/B).



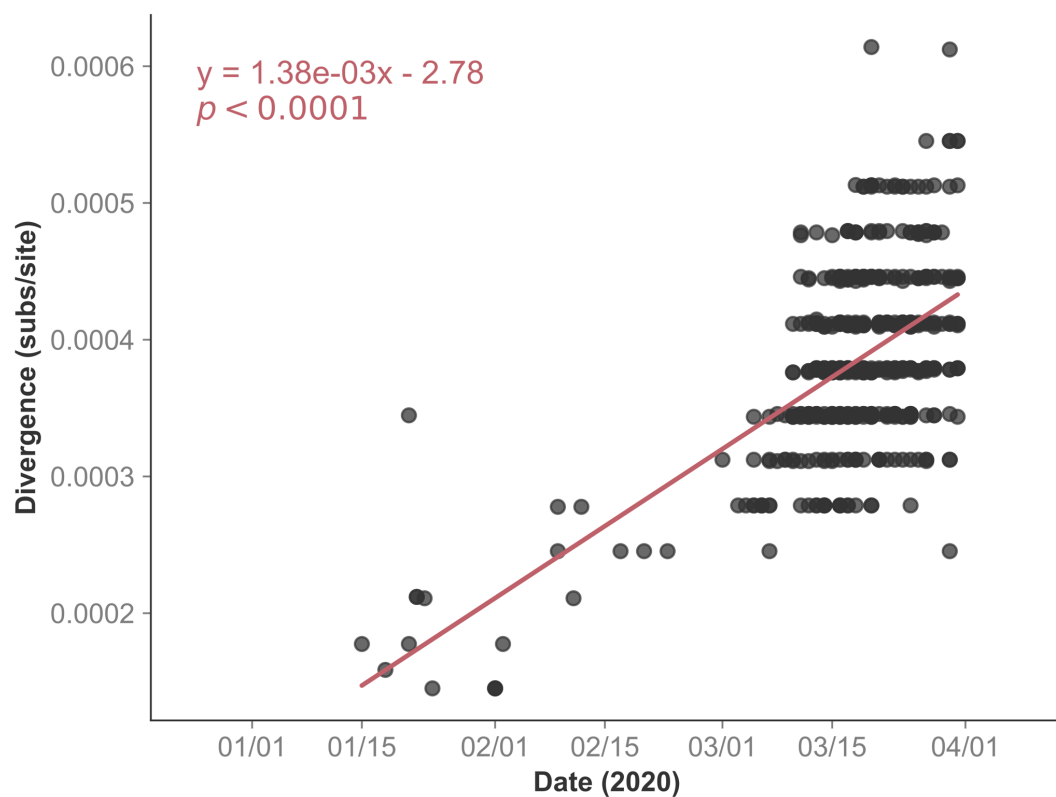
Supplementary Figure 4. Root-to-tip regression of global sequences selected using weighted downsampling. Root-to-tip regression of the 4611 downsampled sequences included in the maximum likelihood phylogenetic analysis that passed the TreeTime clock filter (four interquartile widths). Downsampling was based on per-country case counts and genetic distance to Georgia sequences. A linear regression line was fit and the p -value that the slope of that line is 0 is shown.



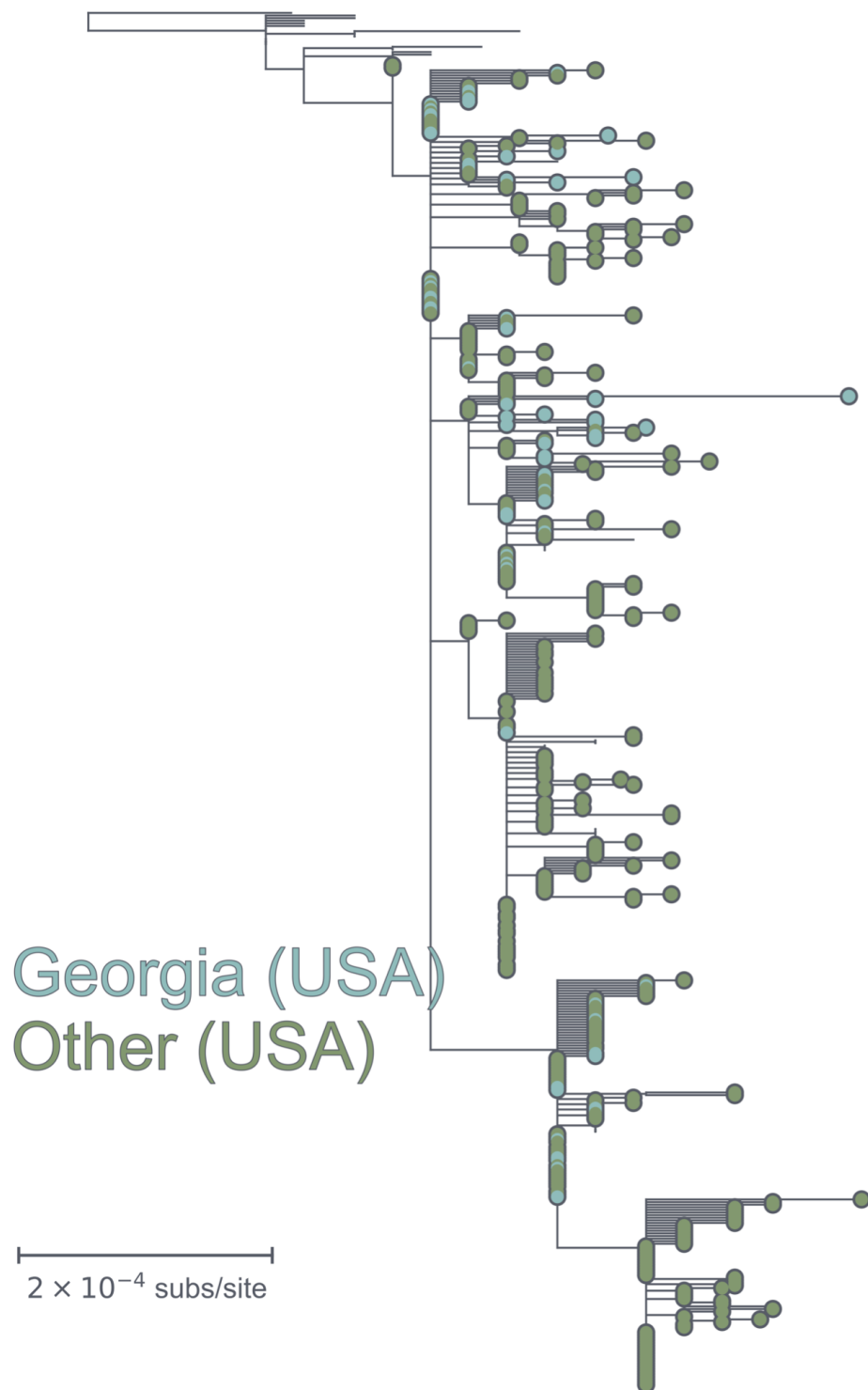
Supplementary Figure 5. Maximum likelihood divergence tree of sequences selected using weighted downsampling. Maximum likelihood phylogeny of the 4611 downsampled sequences which passed the TreeTime clock filter (four interquartile widths) with nucleotide divergence branch lengths. Tips from the state of Georgia are labelled in teal.



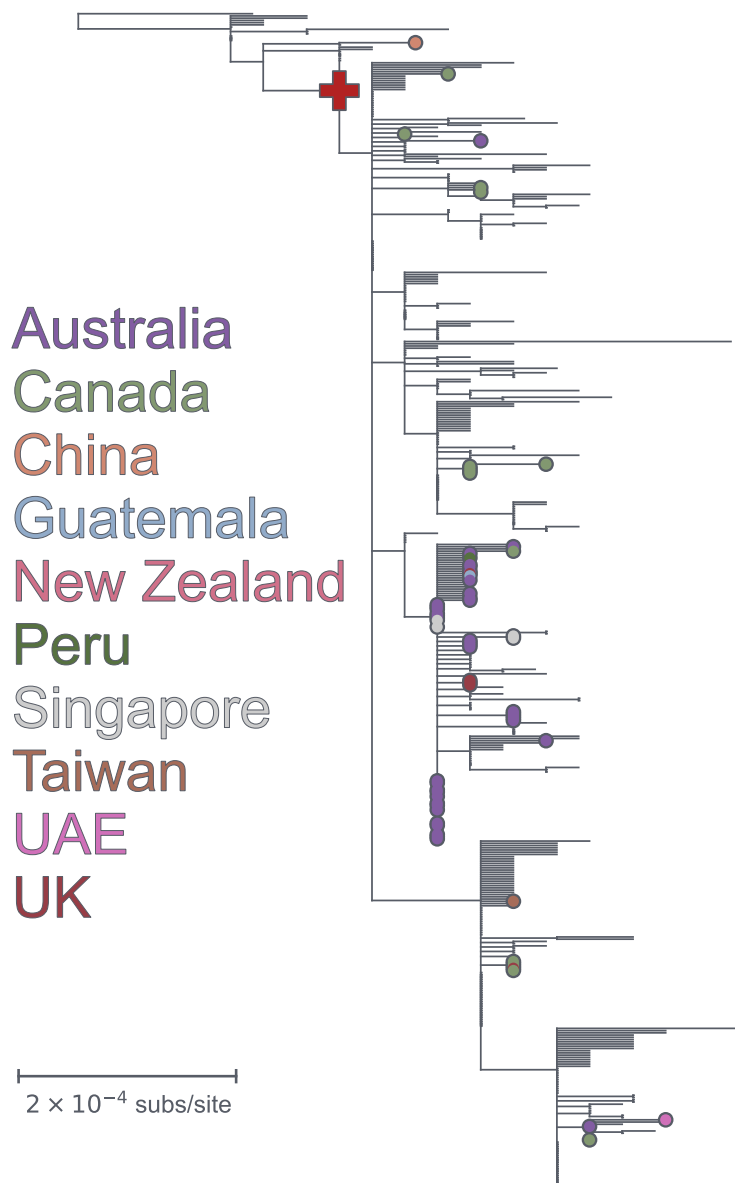
Supplementary Figure 6. Presence of multiple clades and maximum likelihood phylogenetic analysis indicates multiple introductions of SARS-CoV-2 into Georgia (temporally and geographically homogeneous downsampling). A) Number of sequences from Georgia per clade, per week included in the phylogenetic analysis. B) Time-resolved maximum likelihood tree of 5050 global temporally downsampled sequences (based on their date of isolation with a maximum of 20 sequences per country per week) and rooted at Wuhan/Hu-1. Includes sequences which passed the TreeTime clock filter (four interquartile widths). Internal nodes are colored based on their estimated location either inside (green) or outside (grey) of Georgia. Georgia tips are colored in green except for those with known travel history which are shown in pink. Color bar at right shows the clade identity of each sequence in the tree. Branch widths are weighted for visual clarity. B) Estimated cumulative number of introductions into Georgia (transition from a non-Georgia node to a Georgia-node/tip) based on the ancestral state reconstruction of internal nodes. Estimation was repeated on 100 bootstrap replicate trees and the timing of introduction events for each replicate is shown as an individual line. Gaussian kernel density plot at right shows the estimated cumulative number of introduction events as of 2020-03-31.



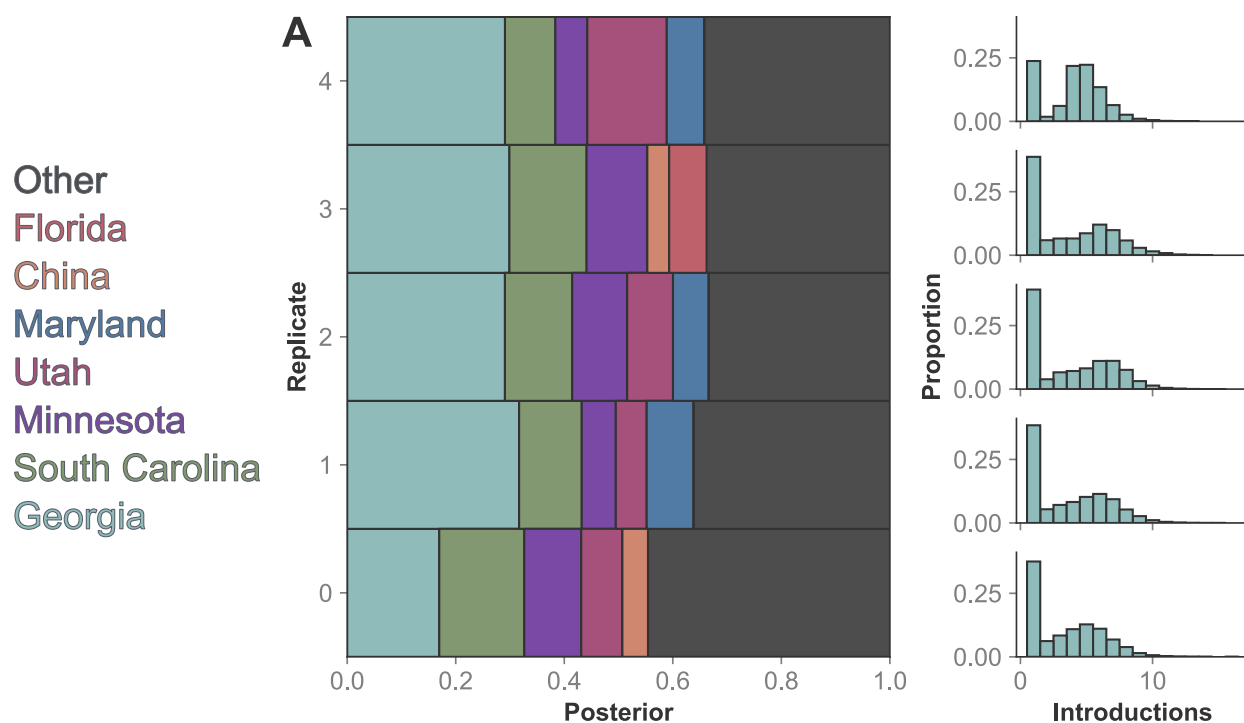
Supplementary Figure 7. Root-to-tip regression of select 19B sequences. Root-to-tip regression of 527 select 19B sequences which are genetically related to the 69 closely-related Georgia 19B sequences which passed the TreeTime clock filter (four interquartile widths). A linear regression line was fit and the p -value that the slope of that line is 0 is shown. A subset of these sequences was used in the Bayesian phylogenetic analysis.



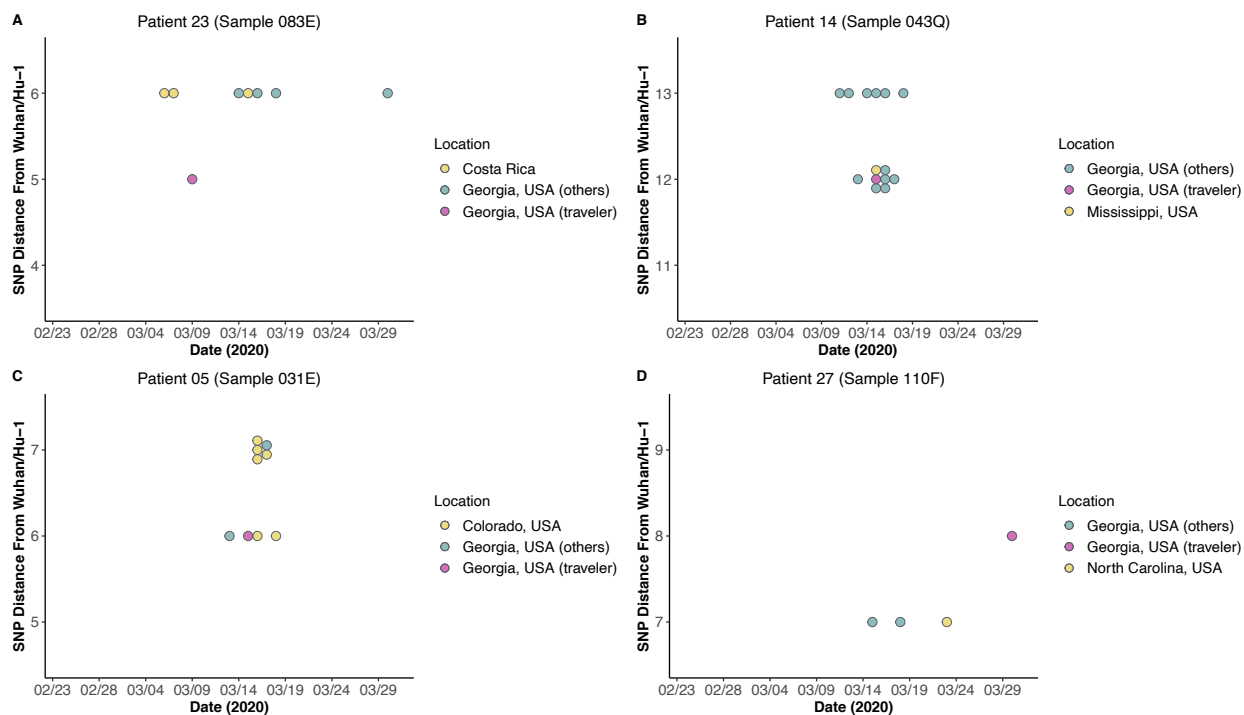
Supplementary Figure 8. Maximum likelihood divergence tree of select 19B sequences with U.S. sequences highlighted. Maximum likelihood phylogeny of 527 select 19B sequences which are genetically related to the 67 closely-related Georgia 19B sequences, which passed the TreeTime clock filter (four interquartile widths). Tips from the state of Georgia are labelled in teal and tips from other U.S. states are labelled in green. A subset of these sequences was used in the Bayesian phylogenetic analysis.



Supplementary Figure 9. Maximum likelihood divergence tree of select 19B sequences with non-U.S. sequences highlighted. Maximum likelihood phylogeny of 527 select 19B sequences which are genetically related to the 67 closely-related Georgia 19B sequences, which passed the TreeTime clock filter (four interquartile widths). Tips from outside of the United States sampled after 2020-02-29 are highlighted. The MRCA of all U.S. sequences in the tree is labelled with a red “+.” A subset of these sequences was used in the Bayesian phylogenetic analysis.

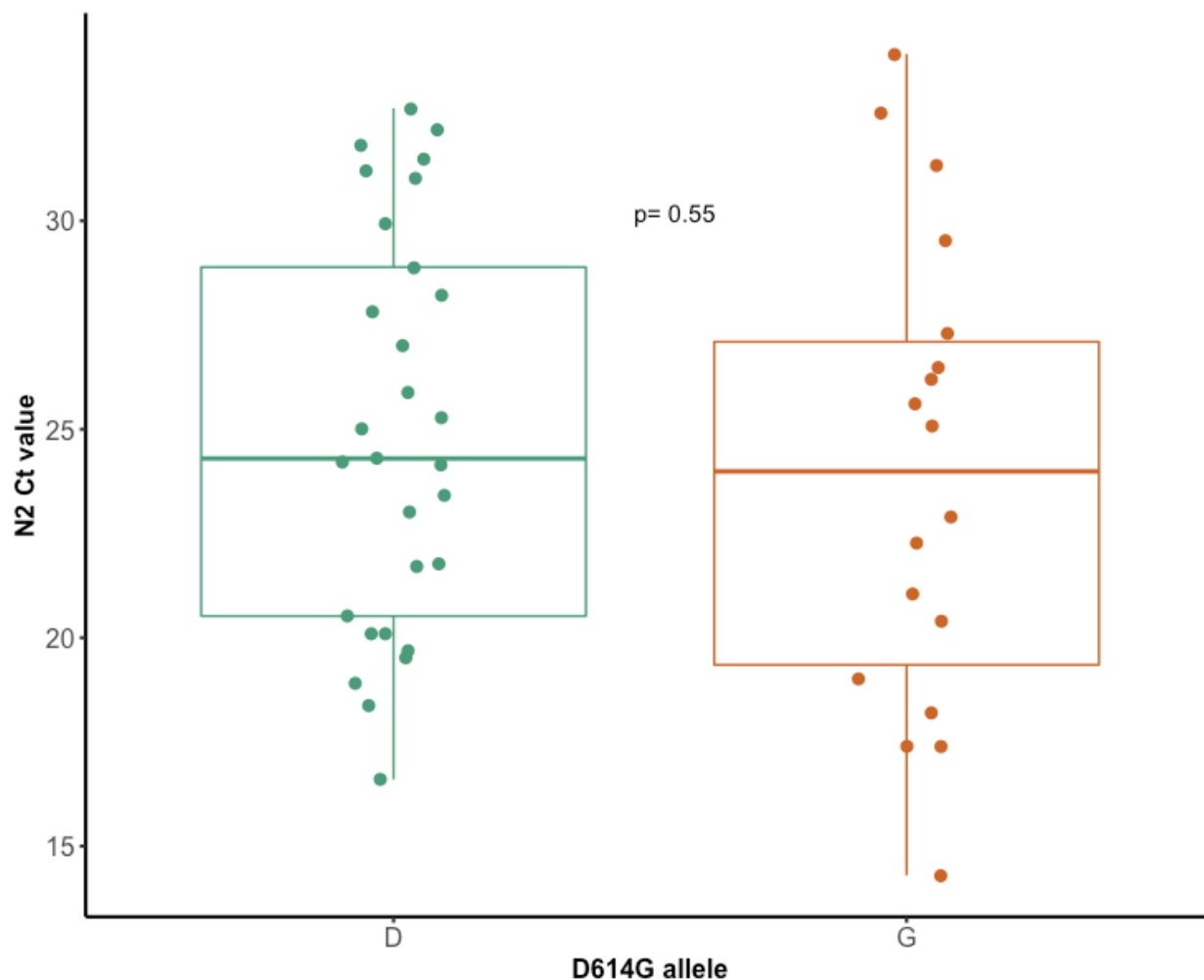


Supplementary Figure 10. Downsampled Bayesian phylogenetic analysis of genetically related Georgia 19B sequences and their phylogenetic neighbors. Sequences in the 19B subclade were randomly downsampled to at most five sequences per country/U.S. state per week, including Georgia. Bayesian discrete trait phylogenographic analysis was conducted on each replicate alignment. A) Discrete trait probabilities of the MRCA of all U.S. sequences in the maximum clade credibility tree for each replicate analysis. B) Estimated number of introductions into Georgia amongst the set of sampled trees for each replicate analysis.

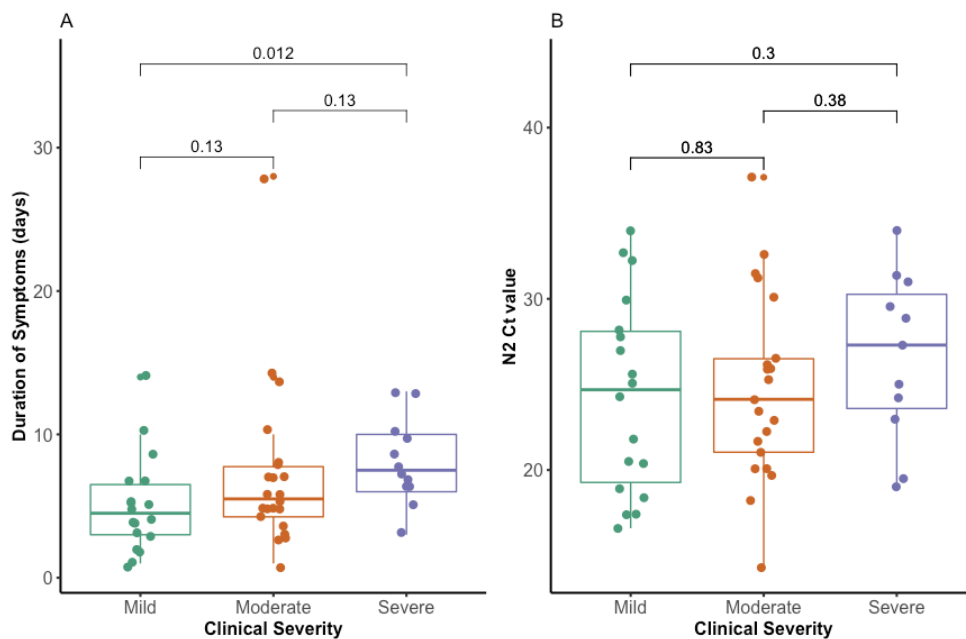


Supplementary Figure 11. Comparison of SARS-CoV-2 genomes from returning travelers.

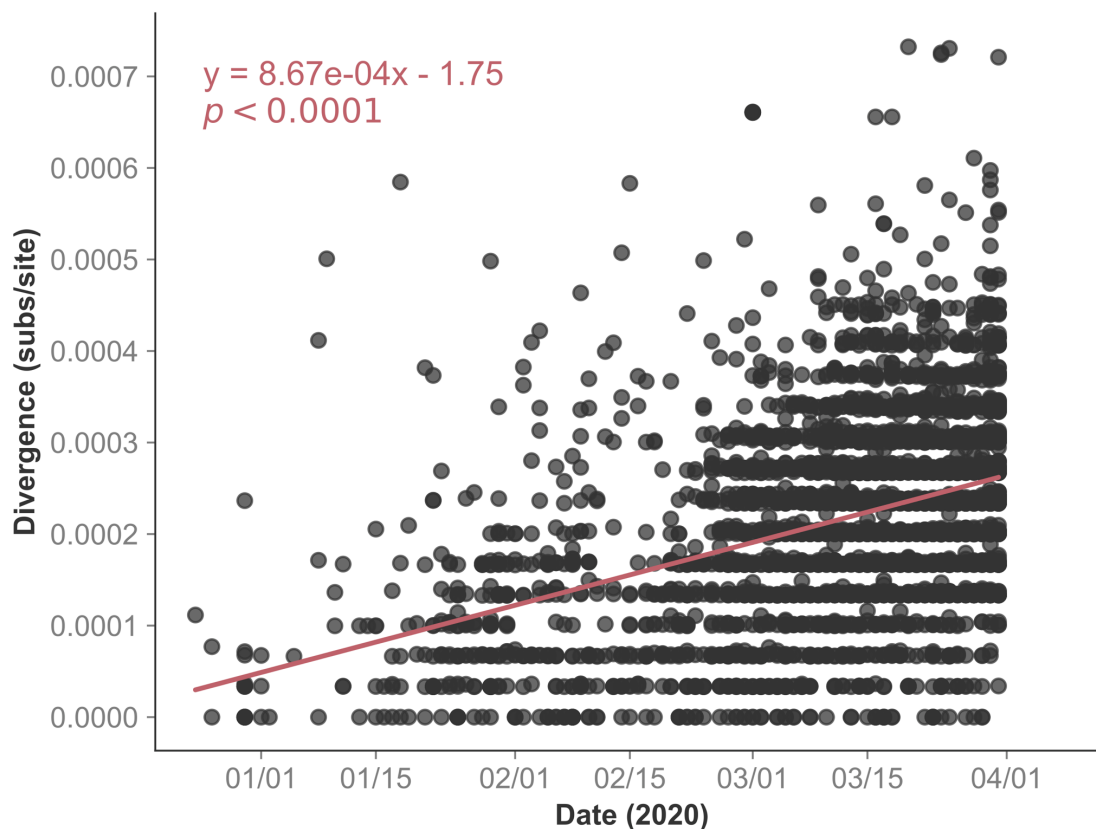
(A) The sequence from P23 was compared to related sequences from Georgia and Costa Rica
 (B) The sequence from P14 was compared to related sequences from Georgia and Mississippi
 (C) The sequence from P05 was compared to related sequences from Georgia and Colorado
 (D) The sequence from P27 was compared to related sequences from Georgia and North Carolina. Each patient sequence was compared to related sequence from Georgia and the region of travel within the same lineage and within 1 SNP (relative to Wuhan/Hu-1, y-axis) of the patient sequence.



Supplementary Figure 12. SARS-CoV-2 rRT-PCR C_T value by spike position 614 residue for 47 Nasopharyngeal (NP) samples. SARS-CoV-2 C_T value, measured using the nucleocapsid N2 target, for 47 positive nasopharyngeal specimens with sequence information available regarding spike amino acid position 614.



Supplementary Figure 13. Associations between molecular results and clinical parameters. (A) Duration of symptoms relative to date of testing across clinical severity for 52 patients with nasopharyngeal (NP) swabs available. (B) C_T value, measured using the nucleocapsid N2 target, across clinical severity for 50 patients with positive NP swabs available.



Supplementary Figure 14. Root-to-tip regression of global sequences selected using temporally and geographically homogeneous downsampling. Root-to-tip regression of 5050 globally sampled sequences downsampled based on their date of isolation (max 20 sequences per country per week) and rooted at Wuhan/Hu-1. Includes sequences which passed the TreeTime clock filter (four interquartile widths).

Table S1. Detailed SARS-CoV-2 sequencing metrics

Patient ID	Sample ID	GBRAD	Accession	Patient age	Patient gender	Sample Type	Sample date	Research	NC	CI	SeqNA	CI Total	mNGS sequencing reads	SARS-CoV-2 reads per million (RPM)	by mNGS	SARS-CoV-2 coverage by mNGS (%)	Depth by mNGS (Mean X)	Amplicon sequencing coverage	Nextstrain clade	PangoLineage	D614G	Included in phylogenetic analysis	19B	Subclade
P01	GA-EHC009	EPI_ISL_754755	40	F	NP	43905	19.8	22.27				7995524	765		0.49	0.49	12	19B	A.3	D	Yes	Yes	No	
P02	GA-EHC016P		40	F	NP	43906	26.2	29.61				98960176	13		NA	NA	1	20C	B.1.2	G	Yes	No	No	
P03	GA-EHC018R		52	F	NP	43901	31.5	41.45				63251868	26		0.52	0.52	1	19B	A.3	D	Yes	Yes	Yes	
P04	GA-EHC019S		63	M	NP	43903	Negative	N				40618205	1		NA	NA	0.997500253	19B	A.3	D	Yes	No	No	
P06	GA-EHC022V	EPI_ISL_1278059	64	F	NP	43901	17.4	23.37				335818	1364		0.99	0.99	36	19B	A.3	D	Yes	Yes	Yes	
P03	GA-EHC023W	EPI_ISL_754776	40	F	NP	43902	31.8	26.82				78160125	30		1	0.21	1	19B	A.3	D	Yes	Yes	Yes	
P04	GA-EHC030D	EPI_ISL_1503972	22	M	NP	43905	16.6	18.35				41362550	887		1	0.35	1	19B	A.3	D	Yes	Yes	Yes	
P05	GA-EHC031E	EPI_ISL_754749	63	M	NP	43905	21.8	25.92				416185	1615		0.98	0.98	12	19B	A.1	D	Yes	No	No	
P08	GA-EHC032F		37	F	NP	43906	27.8	31.77				24041504	8		NA	NA	0.99647651	19B	A.3	D	Yes	Yes	Yes	
P06	GA-EHC033G	EPI_ISL_754751	28	M	NP	43905	19.7	23.58				24797198	2896		1	0.56	1	19B	A.3	D	Yes	Yes	Yes	
P07	GA-EHC034H	EPI_ISL_754752	21	F	NP	43905	17.4	19.22				108659539	322		1	0.39	1	20C	B.1.369	G	Yes	No	No	
P47	GA-EHC035I		76	F	NP	43906	28.2	35.69				1088358	49		0.05	0.05	56	19B	A.3	D	Yes	Yes	Yes	
P08	GA-EHC036J	EPI_ISL_754753	72	M	NP	43906	22.8	26.27				22241214	348		1	0.20	1	20B	B.1.1.29	G	Yes	No	No	
P09	GA-EHC037K	EPI_ISL_754754	35	M	NP	43904	18.9	21.9				35062760	4087		1	0.76	1	19B	A.3	D	Yes	Yes	Yes	
P10	GA-EHC038L	EPI_ISL_754755	27	F	NP	43906	24.2	30.3				31698437	274		1	0.21	1	19B	A.3	D	Yes	Yes	Yes	
P43	GA-EHC039M		53	F	NP	43906	25.8	30.91				27921988	1		0.03	0.03	1	19B	A.3	D	Yes	No	No	
P11	GA-EHC040N	EPI_ISL_754756	71	M	NP	43906	24.3	27.81				24747845	130		1	0.12	1	19B	A.3	D	Yes	Yes	Yes	
P12	GA-EHC041O	EPI_ISL_754757	71	M	NP	43905	14.3	16.47				25143479	7389		1	1.50	1	20C	B.1	G	Yes	No	No	
P13	GA-EHC042P	EPI_ISL_754758	48	F	NP	43905	18.4	21.53				32914438	3757		1	0.70	1	19B	A.3	D	Yes	Yes	Yes	
P14	GA-EHC043Q	EPI_ISL_754759	74	M	NP	43905	28.3	28.79				42220931	68		1	0.10	1	19B	A.3	D	Yes	Yes	Yes	
P15	GA-EHC044R	EPI_ISL_754760	64	M	NP	43905	21.7	24.14				65193628	199		1	0.19	1	19B	A.3	D	Yes	Yes	Yes	
P48	GA-EHC045S		36	F	NP	43905	Negative	N				not done	not done		not done	not done	not done	not done	not done	not done	not done	No	No	No
P49	GA-EHC046T		65	M	NP	43906	35.1	37.72				31970680	2		0.08	0.08	1	19B	A.3	D	Yes	No	No	
P55	GA-EHC047U	EPI_ISL_1278100	25	F	NP	43905	21.9	25.87				2134445	30783		1	312	1	19B	A.3	D	Yes	Yes	Yes	
P49	GA-EHC048V		41	F	NP	43903	32.7	N				not done	not done		1	98	1	19B	A.3	D	Yes	No	No	
P16	GA-EHC049W	EPI_ISL_754761	21	F	NP	43905	17.4	19.62				59818725	3654		1	0.97047079	1	20C	B.1.369	G	Yes	No	No	
P35	GA-EHC050X		54	M	NP	43906	29.5	36.33				71223821	7		0.47	0.47	1	19B	A.3	D	Yes	No	No	
P50	GA-EHC051Y		54	M	NP	43906	31	33.23				1071845	303		0.43	0.43	1	19B	A.3	D	Yes	No	No	
P17	GA-EHC052Z	EPI_ISL_754762	60	M	NP	43906	24.1	36.4				31394448	80		1	0.20	1	19B	A.3	D	Yes	Yes	Yes	
P18	GA-EHC053A	EPI_ISL_754763	41	F	NP	43905	20.5	24.15				37807078	269		1	0.11	1	19B	A.3	D	Yes	Yes	Yes	
P19	GA-EHC054B	EPI_ISL_754764	38	M	NP	43905	23	24.81				82744830	104		1	0.12	1	19B	A.3	D	Yes	Yes	Yes	
P20	GA-EHC055C	EPI_ISL_754765	42	M	NP	43904	18.2	21.27				42982383	9320		1	130	1	20C	B.1	G	Yes	No	No	
P21	GA-EHC060H	EPI_ISL_754777	59	F	OP	43901	26.5	31.3				73241	132		1	0.24	1	19B	A.3	D	Yes	Yes	Yes	
P22	GA-EHC064L	EPI_ISL_754778	21	F	OP	43984	22.1	27.33				26393072	98		0.99	0.99	9	20B	B.1.1	G	Yes	No	No	
P33	GA-EHC069Q		48	M	NP	43903	25.6	N				222115615	14		0.79	0.79	1	20B	A.3	D	Yes	No	No	
P45	GA-EHC076X		47	M	BAL	43895	32	N				670023	3		<1%	<1%	1	19B	A.3	D	Yes	No	No	
P36	GA-EHC080B	EPI_ISL_2790700	58	M	NP	43900	28.9	34.45				834593	20		0.04	0.04	1	19B	A.3	D	Yes	Yes	Yes	
P36	GA-EHC081C		58	M	OP	43900	27.7	30.84				30895121	10		0.4	0.4	1	19B	B.1	D	Yes	No	No	
P23	GA-EHC083E	EPI_ISL_454690	60	F	NP	43899	20.4	26.95				47542787	5096		1	488	1	20A	B.1	G	Yes	No	No	
P44	GA-EHC084F		39	F	NP	43901	34	N				67601938	2		<1%	<1%	1	19B	A.3	D	Yes	No	No	
P44	GA-EHC085G		39	F	OP	43901	21.6	N				83861856	183		<1%	<1%	1	19B	A.3	D	Yes	No	No	
P24	GA-EHC086H	EPI_ISL_455356	62	M	NP	43900	25	29.09				48951189	314		1	29	1	19B	A.3	D	Yes	Yes	Yes	
P24	GA-EHC087I	EPI_ISL_455360	62	M	Sputum	43900	18	26.95				242735	161		1	161	1	19B	A.3	D	Yes	No	No	
P25	GA-EHC097S	EPI_ISL_754766	61	M	NP	43902	23.4	27.06				4161690	822		1	19	1	19B	A.3	D	Yes	Yes	Yes	
P21	GA-EHC106H		59	F	NP	43901	25.1	23.68				3891907	274		0.8	0.8	1	19B	A.3	D	Yes	Yes	Yes	
P26	GA-EHC108D	EPI_ISL_754750	75	M	NP	43920	27	32.53				28745368	348		1	12	1	19B	A.3	D	Yes	Yes	Yes	
P51	GA-EHC109E		51	M	NP	43920	34	N				not done	not done		1	20C	1	20C	B.1.1	G	Yes	No	No	
P27	GA-EHC110F	EPI_ISL_754767	61	M	NP	43920	25.1	30.11				26377907	469		1	21	1	20C	B.1	G	Yes	No	No	
P42	GA-EHC111G		49	M	NP	43920	32.2	40.32				7331914	16		0.05	0.05	1	19B	B.1.1	D	Yes	Yes	Yes	
P32	GA-EHC112H	EPI_ISL_2107431	85	F	NP	43920	21	27.88				68871545	623		1	99	1	20C	B.1.302	G	Yes	No	No	
P28	GA-EHC113J	EPI_ISL_754768	75	M	NP	43920	25.9	32.3				11346840	579		1	10	1	19B	A.3	D	Yes	Yes	Yes	
P52	GA-EHC114K		56	F	NP	43920	26.5	31.95				160832	8915		0.85	0.85	1	20C	B.1	G	Yes	No	No	
P29	GA-EHC115L	EPI_ISL_456361	62	F	NP	43920	22.3	27.8				1828980	312		1	312	1	20C	B.1	G	Yes	No	No	
P30	GA-EHC117N		45	M	NP	43920	29.9	N				67068013	19		0.82	0.82	1	19B	A.3	D	Yes	Yes	Yes	
P53	GA-EHC118O		47	F	NP	43920	32.6	N				not done	not done		1	20C	1	20C	B.1	G	Yes	No	No	
P31	GA-EHC119P	EPI_ISL_754747	92	F	NP	43920	27.3	31.47				52701235	42		0.56	0.56	5	20A	B.1	G	Yes	No	No	
P54	GA-EHC120Q		39	M	NP	43920	37.1	N				not done	not done		1	20C	1	20C	A	G	Yes	No	No	
P39	GA-EHC121R		47	F	NP	43920	31.3	39.39				61204786	1		0.1	0.1	1	20C	B.1	G	Yes	No	No	
P37	GA-EHC121Q		62	M	NP	43904	19	28.89				88826460	2		0.25	0.25	1	19B	A	G	Yes	No	No	

Table S2. Detailed clinical data for 54 EHC patients with SARS-CoV-2 infection

Patient number	Sample ID	Sample Type	Sample date	Research N2 Ct	Age	Gender	Race	Ethnicity	Duration of symptoms (days)	County of residence	Travel within 2 weeks prior to symptom onset	Severity	Death	serology	date of serology	DM	HTN	obesity (BMI>30)	lung disease	Immunosuppression condition	Included in phylogenetic analysis				
P01	GA-EHC-0399	NP	43903	19.2	57	F	Caucasian or White	Non-Hispanic or Latino	10	Cherokee	N	ICU	Y	N/A	N/A	Y	Y	Y	N	N	COVID Stage 3, ESLD	Yes			
P02	GA-EHC-016P	NP	43908	26.2	40	F	Asian	Non-Hispanic or Latino	8	Gwinnett	New Orleans, LA	Intensive	N	N/A	N/A	N	N	N	N	N	N	Yes			
P03	GA-EHC-023W	NP	43902	31.8	40	F	unknown	unknown	unknown	unknown	unknown	unknown	unknown	unknown	unknown	unknown	unknown	unknown	unknown	unknown	unknown	Yes			
P04	GA-EHC-020D	NP	43905	18.6	22	M	African American	Non-Hispanic or Latino	unknown	Forsyth	unknown	ED	N	N/A	N/A	N	N	N	N	N	N	Yes			
P05	GA-EHC-031E	NP	43905	21.8	63	M	Caucasian or White	Non-Hispanic or Latino	3	Fulton	Colorado	Clinic	N	IGG PoS	46034	N	N	N	N	N	N	N	Yes		
P06	GA-EHC-030S	NP	43905	19.7	28	M	Hispanic	Hispanic or Latino	5	Fulton	N	Intensive	N	N/A	N/A	N	N	N	Y	N	N	Yes			
P07	GA-EHC-034H	NP	43905	17.4	21	F	Caucasian or White	Non-Hispanic or Latino	4	Dekalb	N	ED	N	N/A	N/A	N	N	N	N	N	N	Yes			
P08	GA-EHC-036L	NP	43906	22.9	72	M	African American	Non-Hispanic or Latino	5	Fulton	Nigeria	Intensive	N	N/A	N/A	N	N	Y	N	N	N	Yes			
P09	GA-EHC-037K	NP	43904	18.9	36	M	Caucasian or White	Non-Hispanic or Latino	2	Dekalb	N	ED	N	N/A	N/A	N	N	N	N	N	N	Yes			
P10	GA-EHC-038L	NP	43906	24.2	27	F	Caucasian or White	Non-Hispanic or Latino	13	Cobb	unknown	ICU	N	N/A	N/A	N	N	Y	N	N	N	Yes			
P11	GA-EHC-040N	NP	43906	24.3	71	M	African American	Non-Hispanic or Latino	5	Gwinnett	unknown	ED	N	N/A	N/A	N	N	N	N	N	N	Yes			
P12	GA-EHC-041D	NP	43905	14.3	71	M	African American	Non-Hispanic or Latino	5	Dekalb	N	Intensive	N	N/A	N/A	N	Y	N	N	N	N	ESRD	Yes		
P13	GA-EHC-042P	NP	43905	18.4	48	F	African American	Non-Hispanic or Latino	5	Dekalb	N	ED	N	N/A	N/A	Y	N	Y	N	N	N	Yes			
P14	GA-EHC-043Q	NP	43905	25.3	74	M	African American	Non-Hispanic or Latino	6	Fulton	Mississippi	Intensive	N	N/A	N/A	N	Y	Y	Y	Y	Y	Obstructive Sleep apnea	COVID Stage 3	Yes	
P15	GA-EHC-044H	NP	43905	21.7	64	M	African American	Non-Hispanic or Latino	4	Fulton	N	Intensive	N	N/A	N/A	N	Y	Y	Y	Y	N	ESRD	Yes		
P16	GA-EHC-049W	NP	43905	17.4	21	F	Caucasian or White	Non-Hispanic or Latino	4	Dekalb	N	ED	N	N/A	N/A	N	N	N	N	N	N	N	Yes		
P17	GA-EHC-052Z	NP	43906	24.1	60	M	African American	Non-Hispanic or Latino	28	Fulton	N	Intensive	N	N/A	N/A	N	N	N	N	N	N	N	Yes		
P18	GA-EHC-053A	NP	43905	20.5	41	F	African American	Non-Hispanic or Latino	1	Fulton	N	ED	N	N/A	N/A	N	Y	Y	Y	N	N	N	Yes		
P19	GA-EHC-054B	NP	43905	23	38	M	African American	Non-Hispanic or Latino	8	Henry	N	ICU	N	N/A	N/A	N	Y	Y	Y	N	N	N	Yes		
P20	GA-EHC-055C	NP	43904	18.2	42	M	Hispanic	Hispanic or Latino	7	Fulton	N	Intensive	N	N/A	N/A	N	N	Y	Y	Y	Y	Chronic bronchitis	N	Yes	
P21	GA-EHC-059H	CP	43901	26.5	59	F	African American	Non-Hispanic or Latino	8	Fulton	N	Intensive	N	N/A	N/A	N	N	N	N	N	N	N	Multiple Sclerosis	Yes	
P22	GA-EHC-060B	NP	43901	21.9	59	F	African American	Non-Hispanic or Latino	8	Fulton	N	Intensive	N	N/A	N/A	N	N	N	N	N	N	N	Multiple Sclerosis	No	
P23	GA-EHC-063E	NP	43899	20.4	60	F	Caucasian or White	Non-Hispanic or Latino	3	Gwinnett	Italy, Switzerland	ED	N	N/A	N/A	N	N	N	N	N	N	N	N	Yes	
P24	GA-EHC-068H	NP	43900	25	62	M	African American	Non-Hispanic or Latino	6	Fulton	unknown	ICU	Y	N/A	N/A	Y	Y	Y	Y	Y	N	HFV	Yes		
P24	GA-EHC-087I	Sodium	43900	18	62	M	African American	Non-Hispanic or Latino	6	Fulton	unknown	ICU	Y	N/A	N/A	Y	Y	Y	Y	N	HFV	No			
P25	GA-EHC-097B	NP	43902	23.4	61	M	African American	Non-Hispanic or Latino	5	Cobb	N	Intensive	N	N/A	N/A	Y	Y	Y	Y	Y	N	HFV	Yes		
P26	GA-EHC-108D	NP	43920	27	76	M	African American	Non-Hispanic or Latino	14	Dekalb	unknown	Clinic	N	N/A	N/A	N	Y	N	N	N	N	N	Multiple Myeloma	Yes	
P27	GA-EHC-110F	NP	43920	25.1	61	M	Caucasian or White	Non-Hispanic or Latino	4	Fulton	North Carolina	Clinic	N	N/A	N/A	N	N	N	N	N	N	N	N	Yes	
P28	GA-EHC-113J	NP	43920	25.9	75	M	Caucasian or White	Non-Hispanic or Latino	10	Dekalb	N	Intensive	N	N/A	N/A	N	Y	N	N	N	N	N	N	Yes	
P29	GA-EHC-115L	NP	43920	22.3	62	F	African American	Non-Hispanic or Latino	3	Dekalb	N	Intensive	N	N/A	N/A	N	N	N	N	N	N	N	N	Yes	
P30	GA-EHC-117N	NP	43920	28.9	46	F	African American	Non-Hispanic or Latino	7	Fulton	N	ED	N	N/A	N/A	N	N	N	N	N	N	N	N	HFV	Yes
P31	GA-EHC-119P	NP	43920	27.3	92	F	African American	Non-Hispanic or Latino	1	Dekalb	N	ICU	Y	N/A	N/A	N	Y	Y	Y	Y	N	N	N	HFV	No
P32	GA-EHC-124H	NP	43920	21	85	F	African American	Non-Hispanic or Latino	3	Fulton	N	Intensive	N	N/A	N/A	N	Y	Y	Y	Y	N	N	N	Yes	
P33	GA-EHC-060E	NP	43903	25.6	48	M	Caucasian or White	Non-Hispanic or Latino	9	Cobb	Italy, Poland	Clinic	N	N/A	N/A	N	Y	Y	Y	N	N	N	N	Yes	
P34	GA-EHC-018R	NP	43901	31.5	52	F	African American	Non-Hispanic or Latino	14	Dekalb	N	Intensive	N	N/A	N/A	Y	Y	Y	Y	N	N	N	Yes		
P35	GA-EHC-050X	NP	43906	29.5	54	M	Caucasian or White	Non-Hispanic or Latino	7	Linton	N	ICU	N	N/A	N/A	N	N	N	N	N	N	N	N	Yes	
P36	GA-EHC-089B	NP	43900	28.9	58	M	African American	Non-Hispanic or Latino	9	Dekalb	unknown	ICU	N	N/A	N/A	N	Y	Y	Y	Y	N	N	N	Yes	
P36	GA-EHC-081C	CP	43900	27.7	58	M	African American	Non-Hispanic or Latino	9	Dekalb	unknown	ICU	N	N/A	N/A	N	Y	Y	Y	Y	N	N	N	Yes	
P37	GA-EHC-171D	NP	43904	19	62	M	African American	Non-Hispanic or Latino	7	Fulton	N	ICU	Y	N/A	N/A	Y	Y	Y	Y	N	N	N	HFV	No	
P38	GA-EHC-022P	NP	43906	27.8	37	F	African American	Non-Hispanic or Latino	5	Gwinnett	N	ED	N	N/A	N/A	N	Y	Y	Y	Y	N	N	N	Yes	
P39	GA-EHC-121R	NP	43920	31.3	47	F	African American	Non-Hispanic or Latino	5	Gwinnett	New Orleans, LA	Intensive	N	N/A	N/A	N	Y	Y	Y	Y	N	N	N	Yes	
P40	GA-EHC-048T	NP	43906	30.1	65	M	Caucasian or White	Non-Hispanic or Latino	5	Cobb	N	Intensive	N	N/A	N/A	Y	Y	Y	Y	Y	N	N	N	COVID Stage 3	Yes
P41	GA-EHC-119S	NP	43903	Negative	63	M	African American	Non-Hispanic or Latino	6	Fulton	N	Intensive	N	N/A	N/A	Y	Y	Y	Y	N	N	N	N	Yes	
P42	GA-EHC-111G	NP	43920	32.2	49	M	Asian	Non-Hispanic or Latino	7	Gwinnett	N	ED	N	N/A	N/A	N	N	Y	Y	N	N	N	N	Yes	
P43	GA-EHC-030M	NP	43906	26.9	53	F	Caucasian or White	Non-Hispanic or Latino	14	Gwinnett	N	Intensive	N	N/A	N/A	N	N	Y	Y	N	N	N	N	Yes	
P44	GA-EHC-084F	NP	43901	34	39	F	African American	Non-Hispanic or Latino	3	Fulton	N	ED	N	N/A	N/A	N	N	Y	Y	Y	N	N	N	No	
P44	GA-EHC-085G	CP	43901	21.6	39	F	African American	Non-Hispanic or Latino	3	Fulton	N	ED	N	N/A	N/A	N	N	Y	Y	Y	N	N	N	No	
P45	GA-EHC-078X	BAL	43895	32	47	M	Hispanic	Hispanic or Latino	13	Dekalb	N	Intensive	N	N/A	N/A	N	N	N	N	N	N	N	N	No	
P46	GA-EHC-027V	NP	43901	17.4	64	F	African American	Non-Hispanic or Latino	3	Fulton	N	Intensive	N	N/A	N/A	N	N	Y	Y	Y	N	N	N	SLE	Yes
P47	GA-EHC-035I	NP	43908	28.2	76	F	Caucasian or White	Non-Hispanic or Latino	2	Dekalb	N	ED	N	N/A	N/A	N	N	N	N	N	N	N	N	N	Yes
P48	GA-EHC-045S	NP	43905	Negative	36	F	Caucasian or White	Non-Hispanic or Latino	6	Dekalb	unknown	ICU	N	N/A	N/A	N	N	Y	Y	Y	N	N	N	No	
P49	GA-EHC-048V	NP	43903	32.7	41	F	Asian	Non-Hispanic or Latino	10	Dekalb	N	ED	N	N/A	N/A	Y	Y	Y	Y	N	N	N	N	No	
P50	GA-EHC-061Y	NP	43906	31	54	M	African American	Non-Hispanic or Latino	13	Fulton	N	ICU	N	N/A	N/A	Y	Y	Y	Y	N	N	N	No		
P51	GA-EHC-108E	NP	43920	34	51	M	Caucasian or White	Non-Hispanic or Latino	10	Fulton	N	ICU	N	N/A	N/A	N	Y	Y	Y	Y	N	N	N	No	
P52	GA-EHC-114K	NP	43920	26.5	56	F	African American	Non-Hispanic or Latino	7	Fulton	N	Intensive	N	N/A	N/A	N	N	Y	Y	Y	N	N	N	Yes	
P53	GA-EHC-116Q	NP	43920	32.6	47	F	Asian	Non-Hispanic or Latino	7	Gwinnett	N	Intensive	N	N/A	N/A	N	N	Y	Y	Y	N	N	N	No	
P54	GA-EHC-120Q	NP	43920	37.1	39	M	African American	Non-Hispanic or Latino	4	Cobb	N	Intensive	N	N/A	N/A	Y	Y	Y	Y	Y	N	N	N	No	
P55	GA-EHC-047U	NP	43906	20.1	25	F	African American	Non-Hispanic or Latino	3	Dekalb	N	Intensive	N	N/A	N/A	Y	Y	Y	Y	N	N	N	N	Heart transplant	Yes

Table S3. GISAID acknowledgements table for all sequences used in travel and phylogenetic analyses.

We gratefully acknowledge the following Authors from the Originating laboratories responsible for obtaining the specimens, as well as the Submitting laboratories where the genome data were generated and shared via GISAID, on which this research is based.

All Submitters of data may be contacted directly via www.gisaid.org

Authors are sorted alphabetically.

Accession ID	Originating Laboratory	Submitting Laboratory	Authors
EPI_ISL_875674	"1. AO Universitaria S. Giovanni di Dio e Ruggi D'Aragona, Scuola Medica Salernitana Hospital / 2.UO.C. di Virologia e Microbiologia, Università della Campania 1. Vanvitelli / 3. AO Universitaria "Federico II" Napoli Hospital / 4.AORN "San Giuseppe Moscati" Avellino Hospital / 5.AO "San Pio - presidio G. Rummo" Benevento Hospital / 6.AO "Sant'Anna e San Sebastiano" Caserta Hospital / 7.P.O Maria Santissima Adolorata Eboli Hospital / 8.Bogen Istituto di Ricerche Genetiche"	"1. Genome Research Center for Health (CRGS) / 2. Laboratory of Molecular Medicine and Genomics(LMMGE) / 3. Center for Research in Pure and Applied Mathematics (CRMPA)"	"Giorgio Giurato (Corresponding Author); Alessandro Weisz (Corresponding Author); Alessia Coscu; Aniello Gentile; Annamaria Salvati; Antonello Saccomanno; Arnolfo Petruzzello; Assunta Sellitto; Carlo Ferravante; Domenico Memoli; Domenico Palumbo; Elena Alexandrov; Emilia Vaccaro; Francesca Marciano; Francesca Rizzo (Corresponding Author); Gianluigi Franci; Giovanni Nassa; Giovanni Pecoraro; Giuseppe Fenza; Giuseppe Portella; Gregorio Goffredi; Ilana Terenzi; Jessica Lambert; Maddalena Schoppa; Maria Grazia Foti; Maria Landi; Marianna Scorma; Mariarosaria Ingino; Massimiliano Galdero; Maurizio Fumi; Michele Caraglia; Michele Cannamo; Oriana Strianese; Pasquale Pagliano; Rita Greco; Roberta Tarallo; Sonia Amabile; Teresa Rocco; Valeria Minci Cappa; Vincenzo Rocco; Viola Melone; Vittoria Letizia; Ylenia D'Agostino
EPI_ISL_985399, EPI_ISL_985400, EPI_ISL_985402, EPI_ISL_985404, EPI_ISL_985405, EPI_ISL_985406, EPI_ISL_985407, EPI_ISL_985410, EPI_ISL_985433, EPI_ISL_988352, EPI_ISL_989241, EPI_ISL_990198, EPI_ISL_991178, EPI_ISL_993930, EPI_ISL_994654, EPI_ISL_994655, EPI_ISL_994656, EPI_ISL_994657, EPI_ISL_994660, EPI_ISL_994661, EPI_ISL_994662, EPI_ISL_994663, EPI_ISL_994664, EPI_ISL_994665, EPI_ISL_994666, EPI_ISL_994667	"Dr. Andrija Stampar" Teaching Institute of Public Health, Department of Clinical Microbiology	Institute of Applied Genomics	Federica Cattonaro; Jasmina Vranes; Michele Morgante; Michele Morgante
EPI_ISL_683329, EPI_ISL_699656, EPI_ISL_699657, EPI_ISL_707791, EPI_ISL_707792	"1.Laboratory of Microbiology, National Reference Lab, Charles Nicolle Hospital - 2.University of Tunis ElManar, Faculty of Medicine of Tunis, LR99ES09, Tunis, Tunisia	"1.Clinical and Experimental Pharmacology Lab, LR16SP02 National Center of Pharmacovigilance, University of Tunis El Manar, Tunis, Tunisia. 2-Neurodegenerative diseases and psychiatric troubles, LR16SP03, Razi Hospital, University of Tunis El Manar, Tunis, Tunisia. 3- Ministry of Health, National Observatory of New and Emerging Diseases, 1006, Tunis, Tunisia	Alia Ben Khlija; Asma Ferjani; Awatef El MOussa; Gaies Emma; Guedi Benrabah; Habiba Ben Romdhane; Hanen El Jebari; Hanen ElJebari; Ithem Boutiba-Ben Boubaker; Ines Mndiri; Jallia Ben Khelli; Maher Kharrat; Mouna Ben Sassi; Mouna Sali; Nisaf Ben Alaya; Riadh Daghtout; Riadh Goudier; Salma Abid; Salwa Mabret; Sameh Trabelsi; Sana Ferjanj; Souissi Amira
EPI_ISL_451973, EPI_ISL_451975, EPI_ISL_451979, EPI_ISL_451982, EPI_ISL_451984, EPI_ISL_451985	"1. ViroGenetics - BSL3 Laboratory of Virology, Maopolska Centre of Biotechnology, Jagiellonian University; 2. II Department of Internal Medicine, Faculty of Medicine, Jagiellonian University Medical College; 3. DIAGNOSTYKA Ltd.	"1. ViroGenetics - BSL3 Laboratory of Virology, Maopolska Centre of Biotechnology, Jagiellonian University; 2. II Department of Internal Medicine, Faculty of Medicine, Jagiellonian University Medical College.	Jakub Swadba; Krzysztof Pyr; Marcin Surmiak; Marek Sanak; Marta Rogalska-Kupiec; Monika Giecka-Czapla; Pawe P abaj; Wojciech Branicki
EPI_ISL_455440, EPI_ISL_455442, EPI_ISL_455444, EPI_ISL_455445, EPI_ISL_455446, EPI_ISL_455447, EPI_ISL_455449, EPI_ISL_455450, EPI_ISL_455451, EPI_ISL_455452, EPI_ISL_455453, EPI_ISL_492067	"1. ViroGenetics - BSL3 Laboratory of Virology, Maopolska Centre of Biotechnology, Jagiellonian University; 2. II Department of Internal Medicine, Faculty of Medicine, Jagiellonian University Medical College; 3. Narodowy Instytut Zdrowia Publicznego - Pastwowy Zakad Higieny (NIZP-PZH)	"1. ViroGenetics - BSL3 Laboratory of Virology, Maopolska Centre of Biotechnology, Jagiellonian University; 2. II Department of Internal Medicine, Faculty of Medicine, Jagiellonian University Medical College; 3. Narodowy Instytut Zdrowia Publicznego - Pastwowy Zakad Higieny (NIZP-PZH).	Agnieszka Koalkowska-Kulesza; Aleksandra A. Zasada; Aleksandra Milewska; Ewelina Hallman-Szlezelska; Katarzyna Owczarek; Katarzyna Pancer; Katarzyna Zacharczuk; Krzysztof Pyr; Magdalena Rzecczkowska; Marek Sanak; Natalia Wolniuk; Pawe P abaj; Tomasz Wikowicz; Wojciech Branicki
EPI_ISL_876042, EPI_ISL_876043, EPI_ISL_876072, EPI_ISL_876077, EPI_ISL_876078, EPI_ISL_876082, EPI_ISL_876083, EPI_ISL_876092, EPI_ISL_876093, EPI_ISL_876094, EPI_ISL_876095, EPI_ISL_876096, EPI_ISL_876097, EPI_ISL_876098, EPI_ISL_876099, EPI_ISL_877000, EPI_ISL_877001, EPI_ISL_877002, EPI_ISL_877003, EPI_ISL_877004, EPI_ISL_877005, EPI_ISL_877006, EPI_ISL_877009, EPI_ISL_877010, EPI_ISL_877011, EPI_ISL_877012, EPI_ISL_877013, EPI_ISL_877014, EPI_ISL_877016, EPI_ISL_877036, EPI_ISL_883499, EPI_ISL_894218, EPI_ISL_918412, EPI_ISL_918413, EPI_ISL_918415, EPI_ISL_918416, EPI_ISL_918418, EPI_ISL_918419, EPI_ISL_918420, EPI_ISL_918421, EPI_ISL_934420, EPI_ISL_934421	"1 AO Universitaria S. Giovanni di Dio e Ruggi D'Aragona, Scuola Medica Salernitana Hospital / 2.UO.C. di Virologia e Microbiologia, Università della Campania 1. Vanvitelli / 3. AO Universitaria "Federico II" Napoli Hospital / 4.AORN "San Giuseppe Moscati" Avellino Hospital / 5.AO "San Pio - presidio G. Rummo" Benevento Hospital / 6.AO "Sant'Anna e San Sebastiano" Caserta Hospital / 7.P.O Maria Santissima Adolorata Eboli Hospital / 8.Bogen Istituto di Ricerche Genetiche	"1. Genome Research Center for Health (CRGS) / 2. Laboratory of Molecular Medicine and Genomics(LMMGE) / 3. Center for Research in Pure and Applied Mathematics (CRMPA)"	Alessandro Weisz; Alessandro Weisz (Corresponding Author); Alessia Coscu; Andreina Baj; Aniello Gentile; Annamaria Salvati; Antonello Saccomanno; Arnolfo Petruzzello; Assunta Sellitto; Carlo Ferravante; Domenico Memoli; Domenico Palumbo; Edmondo Adoriso; Elena Alexandrov; Emilia Vaccaro; Fausto Sessa; Francesca Marciano; Francesca Rizzo; Francesca Rizzo (Corresponding Author); Francesco Curcio; Gianluigi Franci; Giorgio Dirani; Giorgio Giurato; Giorgio Giurato (Corresponding Author); Giovanni Nassa; Giovanni Pecoraro; Giuseppe Fenza; Giuseppe Portella; Gregorio Goffredi; Ilana Terenzi; Jessica Lambert; Maddalena Schoppa; Maria Grazia Foti; Maria Landi; Marianna Scorma; Mariarosaria Ingino; Massimiliano Galdero; Maurizio Fumi; Michela Iacobelli; Michele Caraglia; Michele Cannamo; Oriana Strianese; Pasquale Pagliano; Rita Greco; Roberta Tarallo; Rosanna Plusio; Silvia Zanoli; Simona Semprini; Sonia Amabile; Stefania Marzotto; Teresa Rocco; Valeria Minci Cappa; Vincenzo Rocco; Viola Melone; Vittoria Letizia; Vittorio Sambri; Ylenia D'Agostino
EPI_ISL_1361596	"1 AO Universitaria S. Giovanni di Dio e Ruggi D'Aragona, Scuola Medica Salernitana Hospital / 2.UO.C. di Virologia e Microbiologia, Università della Campania 1. Vanvitelli / 3. AO Universitaria "Federico II" Napoli Hospital / 4.AORN "San Giuseppe Moscati" Avellino Hospital / 5.AO "San Pio - presidio G. Rummo" Benevento Hospital / 6.AO "Sant'Anna e San Sebastiano" Caserta Hospital / 7.P.O Maria Santissima Adolorata Eboli Hospital / 8.Bogen Istituto di Ricerche Genetiche / 9. U.O.C. di Genetica Medica e di Laboratorio A.O.R.N., Azienda Ospedaliera di Rilievo Nazionale Antonio Cardarelli, Napoli / 10. Centro di riferimento Oncologico della Basilicata (IROCC-CROB), Rionero in Vulture (FZ) / 11. Presidio Ospedaliero di Agropoli, Agropoli (SA).	"1. Genome Research Center for Health (CRGS) / 2. Laboratory of Molecular Medicine and Genomics(LMMGE) / 3. Center for Research in Pure and Applied Mathematics (CRMPA)"	Alessandro Weisz (Corresponding Author); Alessia Coscu; Andreina Baj; Aniello Gentile; Annamaria Salvati; Antonello Saccomanno; Arnolfo Petruzzello; Assunta Sellitto; Cavano Antonella; Carlo Ferravante; D'Auria Foresta; De Luca Luciano; Domenico Memoli; Domenico Palumbo; Edmondo Adoriso; Elena Alexandrov; Emilia Vaccaro; Fausto Sessa; Francesca Marciano; Francesca Rizzo (Corresponding Author); Francesco Curcio; Gianluigi Franci; Giorgio Dirani; Giorgio Giurato (Corresponding Author); Giovanni Nassa; Giovanni Pecoraro; Giuseppe Fenza; Giuseppe Portella; Guy Aioriano; Gregorio Goffredi; Ilana Terenzi; Jessica Lambert; Maddalena Schoppa; Marcello Ametrano; Maria Grazia Foti; Maria Landi; Marianna Scorma; Mariano Foronza; Mariarosaria Ingino; Maria Tarallo; Massimiliano Chetta; Massimiliano Galdero; Maurizio Fumi; Michela Iacobelli; Michele Caraglia; Michele Cannamo; Morena D'Avenia; Oriana Strianese; Pasquale Pagliano; Rita Greco; Roberta Tarallo; Rosanna Plusio; Silvia Zanoli; Simona Semprini; Sonia Amabile; Stefania Marzotto; Teresa Rocco; Valeria Minci Cappa; Vincenzo Rocco; Viola Melone; Vittoria Letizia; Vittorio Sambri; Ylenia D'Agostino
EPI_ISL_450444	20 Dongda Street, Fengtai District, Beijing, Beijing 100071, China	Dept. OPA, Beijing Institute of Microbiology and Epidemiology	Fan, H.; Fang, Gong, J.H.; L.Q. and Liu, W.; Qi, R.Z.; X.A.; Zhang, Zheng, K.; Zheng, W.
EPI_ISL_72361, EPI_ISL_729465, EPI_ISL_729468, EPI_ISL_729500, EPI_ISL_729501, EPI_ISL_729502, EPI_ISL_729503, EPI_ISL_729504, EPI_ISL_729505, EPI_ISL_729506, EPI_ISL_729507, EPI_ISL_729508, EPI_ISL_729510, EPI_ISL_729511, EPI_ISL_729512, EPI_ISL_729513, EPI_ISL_729515, EPI_ISL_729516, EPI_ISL_729517, EPI_ISL_729518, EPI_ISL_729519, EPI_ISL_729520, EPI_ISL_729521, EPI_ISL_729522, EPI_ISL_729523, EPI_ISL_729524, EPI_ISL_729525, EPI_ISL_729526, EPI_ISL_729527, EPI_ISL_729528, EPI_ISL_729529, EPI_ISL_729530, EPI_ISL_729531, EPI_ISL_729532, EPI_ISL_729533, EPI_ISL_729534, EPI_ISL_729535, EPI_ISL_729536, EPI_ISL_729537, EPI_ISL_729538, EPI_ISL_729539, EPI_ISL_729540, EPI_ISL_729541, EPI_ISL_729542, EPI_ISL_729543, EPI_ISL_729544, EPI_ISL_729545, EPI_ISL_729546, EPI_ISL_729547, EPI_ISL_729548	A. Krumholz, Labor Dr. Krause und Kollegen MVZ GmbH, Kiel	Charité Universitätsmedizin Berlin, Institut für Virologie	Barbara Mühlemann; Christian Drosten; Julia Schneider; Jörn Behlheim-Schwarzbach; Talitha Veith; Terry Jones; Victor M Corman
EPI_ISL_455042, EPI_ISL_455043, EPI_ISL_455050	ACT Pathology	NSW Health Pathology - Institute of Clinical Pathology and Medical Research; Westmead Hospital, University of Sydney	CIDM-PH et al.
EPI_ISL_498468, EPI_ISL_498472, EPI_ISL_498473, EPI_ISL_498477, EPI_ISL_498478, EPI_ISL_498480, EPI_ISL_498483, EPI_ISL_498485, EPI_ISL_498486, EPI_ISL_498489, EPI_ISL_498490, EPI_ISL_498491, EPI_ISL_498492, EPI_ISL_498493, EPI_ISL_498494, EPI_ISL_498495, EPI_ISL_498496, EPI_ISL_498497, EPI_ISL_498498, EPI_ISL_498499, EPI_ISL_498500, EPI_ISL_498501, EPI_ISL_498502, EPI_ISL_498503, EPI_ISL_498505, EPI_ISL_498506, EPI_ISL_498510, EPI_ISL_498511, EPI_ISL_498512, EPI_ISL_498513, EPI_ISL_498514, EPI_ISL_498515, EPI_ISL_498516, EPI_ISL_498518, EPI_ISL_498519, EPI_ISL_498520, EPI_ISL_498521, EPI_ISL_498522, EPI_ISL_498523, EPI_ISL_498524, EPI_ISL_498525, EPI_ISL_498526, EPI_ISL_498527, EPI_ISL_498528, EPI_ISL_498529, EPI_ISL_498531			

EPI_ISL_509713		Viral Diseases, Centers for Disease Control and Prevention	
EPI_ISL_631580, EPI_ISL_631804, EPI_ISL_631838, EPI_ISL_632068, EPI_ISL_632069, EPI_ISL_632098, EPI_ISL_632121, EPI_ISL_632136	Bellevue Hospital Center	New York City Public Health Laboratory	Jade Wang; et al
see above	Bellevue Hospital Center	New York City Public Health Laboratory	Jade Wang; et al
EPI_ISL_457824	Bezmi'alem Vakfi University, Dept Microbiology, Medical School, Fatih, Istanbul, Turkey	Bezmi'alem Vakfi University, Medical School & Beykoz Institute of Life Sciences & Biotechnology	Bilge Sumbul; Elif Karaaslan; Filiz Guney; Mehmet Z. Doymaz; Merve Kalkan; Nesibe Cetin
EPI_ISL_429992, EPI_ISL_429993, EPI_ISL_429994, EPI_ISL_429995, EPI_ISL_429996, EPI_ISL_429997, EPI_ISL_429998, EPI_ISL_429999, EPI_ISL_430000, EPI_ISL_430001, EPI_ISL_430002, EPI_ISL_430003, EPI_ISL_430004, EPI_ISL_430006, EPI_ISL_430007, EPI_ISL_430009, EPI_ISL_430011, EPI_ISL_430012, EPI_ISL_430014, EPI_ISL_430015, EPI_ISL_434516	see above	Andersen lab at Scripps Research	Ahmad Tibi; Amid Abdelnour with SEARCH Alliance San Diego; Issa Abu-Dayyeh; Lama Hussein; Lina Mohammad; Zein Naber
see above	Biological Sciences and Public Health, Polytechnic University of Marche	Biological Sciences and Public Health, Polytechnic University of Marche	Alessandrini, F.; Bagnarelli, P.; Caucci, S.; Di Sante, L.; Melchionda, F.; Menzo, S.; Onofri, V.; Tagliabracchi, A.; Turchi, C.
EPI_ISL_516079, EPI_ISL_516080, EPI_ISL_516081, EPI_ISL_516082, EPI_ISL_516083, EPI_ISL_516084, EPI_ISL_516085, EPI_ISL_516086, EPI_ISL_516087, EPI_ISL_516088	see above	Genetics Research Center, University of Social Welfare and Rehabilitation Sciences	Ali Jafarpour; Azam Ghaziasadi; Hossein Najmabadi; Khadijeh Jalalvand; Kinia Kahrizi; Marziyah Moheeni; Mohammad Khazeni; Shayed Amir Momeni; Seyed Mohammad Jazayeri; Seyedeh eham Mortazavi; Zohreh Fatahi
EPI_ISL_596453	Boccal laboratory, Com. Iran, Department of Virology, School of Public Health, Tehran University of Medical Sciences, Tehran, Iran.	Genetics Research Center, University of Social Welfare and Rehabilitation Sciences	Ali Jafarpour; Azam Ghaziasadi; Hossein Najmabadi; Khadijeh Jalalvand; Kinia Kahrizi; Marziyah Moheeni; Mohammad Khazeni; Shayed Amir Momeni; Seyed Mohammad Jazayeri; Seyedeh eham Mortazavi; Zohreh Fatahi
EPI_ISL_420799, EPI_ISL_420800, EPI_ISL_420801	Brian D. Allogood Army Community Hospital	Pathogen Discovery, Respiratory Viruses Branch, Division of Viral Diseases, Centers for Disease Control and Prevention	Alison S. Lauder Halpin; Anne Uehara; Christopher A. Elkins; Clinton R. Paden; Haibin Wang; Jasmine Padilla; Jing Zhang; Justin Lee; Krista Queen; Mary S. Keckler; Rachel Marine; Suziang Tong; Yan Li; Ying Tao
EPI_ISL_631563, EPI_ISL_631562, EPI_ISL_631565, EPI_ISL_631573, EPI_ISL_631800, EPI_ISL_631803, EPI_ISL_631805, EPI_ISL_631806, EPI_ISL_631807, EPI_ISL_631819, EPI_ISL_631829, EPI_ISL_631864, EPI_ISL_631976, EPI_ISL_631979, EPI_ISL_631981, EPI_ISL_631984, EPI_ISL_632077, EPI_ISL_632078, EPI_ISL_632100, EPI_ISL_632114, EPI_ISL_632123, EPI_ISL_632155, EPI_ISL_632156	see above	Brookdale University Hospital Medical Center	Jade Wang; et al
see above	Brookdale University Hospital Medical Center	New York City Public Health Laboratory	Jade Wang; et al
EPI_ISL_631508	Brooklyn Hospital Center	New York City Public Health Laboratory	Jade Wang; et al
EPI_ISL_414521, EPI_ISL_732541, EPI_ISL_732542, EPI_ISL_732544, EPI_ISL_732545, EPI_ISL_732546, EPI_ISL_732547, EPI_ISL_732548, EPI_ISL_732549, EPI_ISL_732550, EPI_ISL_732551, EPI_ISL_732552, EPI_ISL_732564	see above	Bundeswehr Institute of Microbiology	Alexandra Rehn; Enrico Georgi; Malena Bestehorn-Willmann; Markus Antwerpen; Markus H Antwerpen and Roman Wölfel; Mathias C Walter; Mathias Walter; Roman Wölfel; Sabine Zange
see above	Bundeswehr Institute of Microbiology	Bundeswehr Institute of Microbiology	Alexandra Rehn; Enrico Georgi; Malena Bestehorn-Willmann; Markus Antwerpen; Markus H Antwerpen and Roman Wölfel; Mathias C Walter; Mathias Walter; Roman Wölfel; Sabine Zange
EPI_ISL_524476	Bilach Hospital	Institute of Medical Virology, University of Zurich	Alexandra Trkola; Andrea Zbinden; Fiona Steiner; Gabriela Zlotner; Jon Huder; Jörg Böni; Maryam Zaheri; Michael Huber; Patrick Redi; Riccarda Capaul; Stefan Schmutz; Verena Kufner
EPI_ISL_445320	C.C.SALUD FAMILIAR PADRE FELIX DONOSO G.	Instituto de Salud Publica de Chile	Alejandra Acevedo; Andrés E Castillo; Bárbara Parra; Carolina Tamblay; Gabriel Leal; Jaime Lagos; Jorge Fernandez; Loredana Arata; Patricia Bustos; Paz Tapia; Rodrigo Fasce; Winston Andrade
EPI_ISL_445318	C.DE SALUD FAMILIAR PABLO NERUDA	Instituto de Salud Publica de Chile	Alejandra Acevedo; Andrés E Castillo; Bárbara Parra; Carolina Tamblay; Gabriel Leal; Jaime Lagos; Jorge Fernandez; Loredana Arata; Patricia Bustos; Paz Tapia; Rodrigo Fasce; Winston Andrade
EPI_ISL_539531	C.H.U Nuestra Señora de Candelaria	Instituto de Salud Carlos III	A. Monzón; F. Casas; I.; J. Jiménez; Iglesias-Caballero; M. Camarero; M. Cuesta; M. González-Esguevillas; M. Molinero Calamita; M. Zaballos; O. Diez; P. Jiménez; S. Juliá; S. Pozo; S. Varona
EPI_ISL_576177	CA, CDPH, Viral and Rickettsial Disease Laboratory	Pathogen Discovery, Respiratory Viruses Branch, Division of Viral Diseases, Centers for Disease Control and Prevention	Anna Uehara; Brian Lynch; Clinton R. Paden; Haibin Wang; Jing Zhang; Krista Queen; Peter Cook; Suziang Tong; Yan Li; Ying Tao
EPI_ISL_605780	CEIRS Data Processing and Coordinating Center, St. Jude Center of Excellence for Influenza Research and Surveillance (CEIRS)	CEIRS Data Processing and Coordinating Center, St. Jude Center of Excellence for Influenza Research and Surveillance (CEIRS)	A.E.; Ali; El-Guindy; El-Sayes, M.; El-Shesheny, R.; El-Taweel, A.; Gomaa, M.; Kamel; Kandell, A.; Kayali, G.; Kayed; Kutkat, O.; M.A.; M.N.; Mahmoud; Mahrous, N.; Mostasim, Y.; Mostafa, A.; N.M.; Naguib, A.; Roshdy; S.H.; Shehata, M.; Showky, S.; W.H.; Webby, R.
EPI_ISL_1303032	CEIRS Data Processing and Coordinating Center, Center for Research on Influenza Pathogenesis (CRIP)	CEIRS Data Processing and Coordinating Center, Center for Research on Influenza Pathogenesis (CRIP)	Adolfo Garcia-Sastre; Adriana van De Guchte; Ajay Ojha; Ana S. Gonzalez-Reiche; Breydi Altburguerque; Edward C. Holmes; Eileen Serrano; Erick Salinas; Hala Alshammary; Ham van Bakel; Jayeeta Dutta; Jorge Levican; Juan Soto; Leonardo I. Almonacid; Matthew M. Hernandez; Melissa Smith; Rafael A. Medina; Robert Sebra; Shwetha Hara Sridhar; Tamara Garcia-Salun; Viviana Simon; Ying-Chih Wang; Zenab Khan
EPI_ISL_445266, EPI_ISL_445267	CENTRO ONCOLOGICO DEL NORTE	Instituto de Salud Publica de Chile	Alejandra Acevedo; Andrés E Castillo; Bárbara Parra; Carolina Tamblay; Gabriel Leal; Jaime Lagos; Jorge Fernandez; Loredana Arata; Patricia Bustos; Paz Tapia; Rodrigo Fasce; Winston Andrade
EPI_ISL_644273, EPI_ISL_644310, EPI_ISL_644319, EPI_ISL_644321, EPI_ISL_644342, EPI_ISL_644343	CEPHR / Vincent's Hospital	Irish Coronavirus Sequencing Consortium - National Virus Reference Laboratory	Alejandro Abner Garcia Leon; Gabriel Gonzalez; Michael Carr; Patrick Mallon
EPI_ISL_445316	CESFAM BALMACEDA DE RENCA	Instituto de Salud Publica de Chile	Alejandra Acevedo; Andrés E Castillo; Bárbara Parra; Carolina Tamblay; Gabriel Leal; Jaime Lagos; Jorge Fernandez; Loredana Arata; Patricia Bustos; Paz Tapia; Rodrigo Fasce; Winston Andrade
EPI_ISL_421455, EPI_ISL_421479, EPI_ISL_421480, EPI_ISL_421485, EPI_ISL_421486	CH Barreiro Montijo	Instituto Nacional de Saude (INSA)	Guomar et al
EPI_ISL_420041, EPI_ISL_420049, EPI_ISL_420050, EPI_ISL_420056, EPI_ISL_420057, EPI_ISL_421500, EPI_ISL_421509, EPI_ISL_421510, EPI_ISL_421511, EPI_ISL_428353, EPI_ISL_428359, EPI_ISL_428360, EPI_ISL_443309, EPI_ISL_443316	see above	CH Compiègne Laboratoire de Biologie	Angela Brisebarre; Etienne Simon-Lorière; Flora Donati; Marion Barbet; Maud Vanpeene; Mélanie Albert; Meline Bizard; Olivia Raulin; Raulin Olivia; Sylvie Behilli; Sylvie van der Werf; Vincent Enouf
EPI_ISL_416403, EPI_ISL_420044, EPI_ISL_420053, EPI_ISL_428350	CH Jean de Navarre Laboratoire de Biologie	National Reference Center for Viruses of Respiratory Infections, Institut Pasteur, Paris	Angela Brisebarre; Etienne Simon-Lorière; Flora Donati; Marion Barbet; Maud Vanpeene; Mélanie Albert; Meline Bizard; Olivia Raulin; Raulin Olivia; Sylvie Behilli; Sylvie van der Werf; Vincent Enouf
EPI_ISL_428358, EPI_ISL_428366	CH Jeanne de Navarre Laboratoire de Biologie	National Reference Center for Viruses of Respiratory Infections, Institut Pasteur, Paris	Angela Brisebarre; Etienne Simon-Lorière; Flora Donati; Marion Barbet; Maud Vanpeene; Mélanie Albert; Meline Bizard; Olivia Raulin; Raulin Olivia; Sylvie Behilli; Sylvie van der Werf; Vincent Enouf
EPI_ISL_421482, EPI_ISL_421483, EPI_ISL_421484	CH VN Gaia - Espinho	Instituto Nacional de Saude (INSA)	Guomar et al
EPI_ISL_418006	CHBarreiro Montijo	Instituto Nacional de Saude (INSA)	Guomar et al
EPI_ISL_418017	CHMT	Instituto Nacional de Saude (INSA)	Guomar et al
EPI_ISL_418222	CHRU Bretonneau - Serv. Bacterio-Virol.	National Reference Center for Viruses of Respiratory Infections, Institut Pasteur, Paris	Angela Brisebarre; Etienne Simon-Lorière; Fabiana Gambaro; Flora Donati; Julien Marlet; Marion Barbet; Maud Vanpeene; Mélanie Albert; Meline Bizard; Sylvie Behilli; Sylvie van der Werf; Vincent Enouf
EPI_ISL_416502, EPI_ISL_416503, EPI_ISL_416504, EPI_ISL_416505, EPI_ISL_416506, EPI_ISL_416507, EPI_ISL_416508, EPI_ISL_416509, EPI_ISL_416510, EPI_ISL_416511, EPI_ISL_416512, EPI_ISL_416513, EPI_ISL_443289, EPI_ISL_443290	see above	CHRU Pontchaillou - Laboratoire de Virologie	Angela Brisebarre; Etienne Simon-Lorière; Flora Donati; Gisèle Lagathu; Marion Barbet; Maud Vanpeene; Mélanie Albert; Meline Bizard; Meline Albert; Sylvie Behilli; Sylvie van der Werf; Vincent Enouf
EPI_ISL_418027, EPI_ISL_421453, EPI_ISL_421464, EPI_ISL_421465	see above	CHTMDA	Guomar et al
EPI_ISL_418219, EPI_ISL_443266, EPI_ISL_443267, EPI_ISL_443268, EPI_ISL_443269, EPI_ISL_443270, EPI_ISL_443271, EPI_ISL_443272, EPI_ISL_443273, EPI_ISL_443274, EPI_ISL_443275, EPI_ISL_443276, EPI_ISL_443277, EPI_ISL_443282, EPI_ISL_443283	see above	CHU - Hôpital Cavale Blanche - Labo. de Virologie	Angela Brisebarre; Etienne Simon-Lorière; Fabiana Gambaro; Flora Donati; Léa Pilorge; Marion Barbet; Maud Vanpeene; Mélanie Albert; Meline Bizard;

Infections, Institut Pasteur, Paris				Sylvie Behilli; Sylvie van der Werf; Vincent Enouf			
EPI_ISL_645189, EPI_ISL_645170, EPI_ISL_645171, EPI_ISL_649954, EPI_ISL_649955, EPI_ISL_649956, EPI_ISL_649957, EPI_ISL_649958, EPI_ISL_649959, EPI_ISL_649960, EPI_ISL_649961, EPI_ISL_649962, EPI_ISL_649963, EPI_ISL_649964, EPI_ISL_649965, EPI_ISL_649966, EPI_ISL_649967, EPI_ISL_649968, EPI_ISL_649969, EPI_ISL_649970	see above	CHU Bordeaux	CNR Virus des Infections Respiratoires - France SUD	Antonin Bal; Bruno Lina; Camille Ciccone; Gregory Destras; Gwendolyne Burfin; Hadrien Rège; Isabelle Garrigue; Laurence Jossset; Marie-Edith Lafont; Martine Valette; Patxika Bellecave; Pascale Trimoulet; Quentin Semanas			
EPI_ISL_645188, EPI_ISL_645189, EPI_ISL_645190, EPI_ISL_645191, EPI_ISL_645192, EPI_ISL_645193, EPI_ISL_645194, EPI_ISL_660353, EPI_ISL_660354, EPI_ISL_660355, EPI_ISL_660356, EPI_ISL_660357, EPI_ISL_660358, EPI_ISL_660359, EPI_ISL_660360	see above	CHU Clermont-Ferrand	CNR Virus des Infections Respiratoires - France SUD	Amélie Breblion; Antonin Bal; Audrey Mirand; Bruno Lina; Christel Regagnon; Christine Archimbaud; Cécile Henquell; Gregory Destras; Gwendolyne Burfin; Hadrien Rège; Hélène Chabrolles; Laurence Jossset; Martine Chantoin; Martine Valette; Maxime Bisseux; Patricia Combes; Quentin Semanas			
EPI_ISL_418002		CHU Coimbra	Instituto Nacional de Saude (INSA)	Guomar et al			
EPI_ISL_418005		CHU Coimbra - Pediátrico	Instituto Nacional de Saude (INSA)	Guomar et al			
EPI_ISL_416751, EPI_ISL_416752		CHU Gabriel Montpied	CNR Virus des Infections Respiratoires - France SUD	Alexandre; Antonin Bal; Bouscambert-Duchamp; Bréngal-Pérez; Bruno; Cheymat; Destras; Florence; Gaymard; Gregory; Jossset; Karen; Laurence; Lina; Martine; Maude; Morfin-Sherpa; Valette; Valérie			
EPI_ISL_641556, EPI_ISL_644681, EPI_ISL_644682, EPI_ISL_644683, EPI_ISL_644684, EPI_ISL_644685, EPI_ISL_644686, EPI_ISL_644687, EPI_ISL_644688, EPI_ISL_644689, EPI_ISL_644690, EPI_ISL_644691, EPI_ISL_644692, EPI_ISL_644693, EPI_ISL_660672, EPI_ISL_660673, EPI_ISL_660674, EPI_ISL_660675, EPI_ISL_660676, EPI_ISL_660677, EPI_ISL_660678, EPI_ISL_660679, EPI_ISL_660680, EPI_ISL_660681, EPI_ISL_660682, EPI_ISL_660683, EPI_ISL_660684, EPI_ISL_660685, EPI_ISL_660686, EPI_ISL_660687, EPI_ISL_660688, EPI_ISL_660689, EPI_ISL_660690, EPI_ISL_660691, EPI_ISL_660692	see above	CHU Montpellier	CNR Virus des Infections Respiratoires - France SUD	Antonin Bal; Bruno Lina; Gregory Destras; Gwendolyne Burfin; Hadrien Rège; Laurence Jossset; Martine Valette; Michel Segondy; Quentin Semanas; Vincent Foulongne			
EPI_ISL_645217, EPI_ISL_649173, EPI_ISL_649174, EPI_ISL_649175, EPI_ISL_649176, EPI_ISL_649177, EPI_ISL_663249, EPI_ISL_663250, EPI_ISL_663251, EPI_ISL_663252, EPI_ISL_663253, EPI_ISL_663254, EPI_ISL_663255, EPI_ISL_663256, EPI_ISL_663257, EPI_ISL_663258, EPI_ISL_663259, EPI_ISL_663260, EPI_ISL_663261, EPI_ISL_663262, EPI_ISL_663263, EPI_ISL_663264, EPI_ISL_663265, EPI_ISL_663266, EPI_ISL_700371	see above	CHU Nantes	CNR Virus des Infections Respiratoires - France SUD	Antonin Bal; Bruno Lina; Céline Bressollette; Gregory Destras; Gwendolyne Burfin; Hadrien Rège; Laurence Jossset; Louise Castain; Martine Valette; Quentin Semanas; Virginie Ferré			
EPI_ISL_644689, EPI_ISL_644698, EPI_ISL_644699, EPI_ISL_644700, EPI_ISL_644701, EPI_ISL_644702, EPI_ISL_645197, EPI_ISL_645198, EPI_ISL_645199, EPI_ISL_645200, EPI_ISL_660710, EPI_ISL_660711, EPI_ISL_660712, EPI_ISL_660713, EPI_ISL_660714, EPI_ISL_660715, EPI_ISL_660716, EPI_ISL_660717, EPI_ISL_660718	see above	CHU Nîmes	CNR Virus des Infections Respiratoires - France SUD	Antonin Bal; Bruno Lina; Gregory Destras; Gwendolyne Burfin; Hadrien Rège; Jean-Philippe Lavigne; Laurence Jossset; Marie-Josée Carles; Martine Valette; Maxence Lotellier; Quentin Semanas; Stephan Robin			
EPI_ISL_645216, EPI_ISL_663227, EPI_ISL_663228, EPI_ISL_663229, EPI_ISL_663230, EPI_ISL_663231, EPI_ISL_663232, EPI_ISL_663233, EPI_ISL_663234, EPI_ISL_663235, EPI_ISL_707781, EPI_ISL_707782	see above	CHU Poitiers	CNR Virus des Infections Respiratoires - France SUD	Agnès Bety-Defaux; Antonin Bal; Bruno Lina; Clément Jousselet; Gregory Destras; Gwendolyne Burfin; Hadrien Rège; Laurence Jossset; Magali Garcia; Martine Valette; Nicolas Lévêque; Quentin Semanas			
EPI_ISL_671978		CHU Purpan - Laboratoire de Virologie - Institut Fédératif de Biologie	CHU Purpan - Laboratoire de Virologie - Institut Fédératif de Biologie	Boyer P.; Carcenac R.; Dubois M.; Harter A.; Izopet J.; Latour J.; Ranger N.; Tremeaux P.			
EPI_ISL_434626, EPI_ISL_434627		CHU Purpan - Laboratoire de Virologie - Institut Fédératif de Biologie	Laboratoire de virologie - École Nationale Vétérinaire de Toulouse	Guillaume Croville; Jacques Zippel; Jean-Luc Guérin			
EPI_ISL_535732, EPI_ISL_535801		CHU Sainte-Justine	Laboratoire de santé publique du Québec	Guillaume Bourque; Ioannis Ragoussis; Jesse Shapiro; Mark Lathrop and Michel Roger; Mark Lathrop and Michel Roger on behalf of the CoVSeQ research group; Sandrine Moreira			
EPI_ISL_641551, EPI_ISL_641552, EPI_ISL_641553, EPI_ISL_660373		CHU Toulouse	CNR Virus des Infections Respiratoires - France SUD	Antonin Bal; Bruno Lina; Gregory Destras; Gwendolyne Burfin; Hadrien Rège; Jean Michel Mansau; Laurence Jossset; Martine Valette; Quentin Semanas			
EPI_ISL_644673, EPI_ISL_644674, EPI_ISL_644675, EPI_ISL_645174, EPI_ISL_645175, EPI_ISL_645176, EPI_ISL_645177, EPI_ISL_645178, EPI_ISL_645179, EPI_ISL_645180, EPI_ISL_645181, EPI_ISL_645182, EPI_ISL_645183, EPI_ISL_663206, EPI_ISL_663207, EPI_ISL_663208, EPI_ISL_663209, EPI_ISL_663210, EPI_ISL_663211, EPI_ISL_663212, EPI_ISL_663213, EPI_ISL_663214, EPI_ISL_663215, EPI_ISL_663216, EPI_ISL_663217, EPI_ISL_663218, EPI_ISL_663219, EPI_ISL_663220, EPI_ISL_663221, EPI_ISL_663222, EPI_ISL_663223	see above	CHU de Limoges	CNR Virus des Infections Respiratoires - France SUD	Antonin Bal; Bruno Lina; Gregory Destras; Gwendolyne Burfin; Hadrien Rège; Laurence Jossset; Martine Valette; Quentin Semanas; Sylvie Rogez			
EPI_ISL_645173		CHU de Nice	CNR Virus des Infections Respiratoires - France SUD	Antonin Bal; Bruno Lina; Gregory Destras; Gwendolyne Burfin; Géraldine Gonfrier; Hadrien Rège; Laurence Jossset; Martine Valette; Quentin Semanas; Valérie Giordanengo			
EPI_ISL_641520, EPI_ISL_693387, EPI_ISL_693388, EPI_ISL_693389, EPI_ISL_693390		CHU de Nice - Hôpital Archet 2	CNR Virus des Infections Respiratoires - France SUD	Antonin Bal; Bruno Lina; Gregory Destras; Gwendolyne Burfin; Géraldine Gonfrier; Hadrien Rège; Laurence Jossset; Martine Valette; Quentin Semanas; Valérie Giordanengo			
EPI_ISL_641522		CHU de Nice - Hôpital Archet 3	CNR Virus des Infections Respiratoires - France SUD	Antonin Bal; Bruno Lina; Gregory Destras; Gwendolyne Burfin; Géraldine Gonfrier; Hadrien Rège; Laurence Jossset; Martine Valette; Quentin Semanas; Valérie Giordanengo			
EPI_ISL_641523		CHU de Nice - Hôpital Archet 4	CNR Virus des Infections Respiratoires - France SUD	Antonin Bal; Bruno Lina; Gregory Destras; Gwendolyne Burfin; Géraldine Gonfrier; Hadrien Rège; Laurence Jossset; Martine Valette; Quentin Semanas; Valérie Giordanengo			
EPI_ISL_641524		CHU de Nice - Hôpital Archet 5	CNR Virus des Infections Respiratoires - France SUD	Antonin Bal; Bruno Lina; Gregory Destras; Gwendolyne Burfin; Géraldine Gonfrier; Hadrien Rège; Laurence Jossset; Martine Valette; Quentin Semanas; Valérie Giordanengo			
EPI_ISL_641525		CHU de Nice - Hôpital Archet 6	CNR Virus des Infections Respiratoires - France SUD	Antonin Bal; Bruno Lina; Gregory Destras; Gwendolyne Burfin; Géraldine Gonfrier; Hadrien Rège; Laurence Jossset; Martine Valette; Quentin Semanas; Valérie Giordanengo			
EPI_ISL_641526		CHU de Nice - Hôpital Archet 7	CNR Virus des Infections Respiratoires - France SUD	Antonin Bal; Bruno Lina; Gregory Destras; Gwendolyne Burfin; Géraldine Gonfrier; Hadrien Rège; Laurence Jossset; Martine Valette; Quentin Semanas; Valérie Giordanengo			
EPI_ISL_641527		CHU de Nice - Hôpital Archet 9	CNR Virus des Infections Respiratoires - France SUD	Antonin Bal; Bruno Lina; Gregory Destras; Gwendolyne Burfin; Géraldine Gonfrier; Hadrien Rège; Laurence Jossset; Martine Valette; Quentin Semanas; Valérie Giordanengo			
EPI_ISL_641538, EPI_ISL_641539, EPI_ISL_641540, EPI_ISL_641541, EPI_ISL_641542, EPI_ISL_641543, EPI_ISL_641544, EPI_ISL_641545, EPI_ISL_645184, EPI_ISL_649942, EPI_ISL_649943, EPI_ISL_649944, EPI_ISL_649945, EPI_ISL_649946, EPI_ISL_649953, EPI_ISL_660326, EPI_ISL_660327, EPI_ISL_660328, EPI_ISL_660329, EPI_ISL_660330, EPI_ISL_660331, EPI_ISL_660332, EPI_ISL_660334, EPI_ISL_660335, EPI_ISL_660336, EPI_ISL_660337, EPI_ISL_660338, EPI_ISL_660339, EPI_ISL_660340, EPI_ISL_660341, EPI_ISL_660344, EPI_ISL_660345, EPI_ISL_660346, EPI_ISL_660347, EPI_ISL_660348, EPI_ISL_660349	see above	CHU de Saint-Etienne Hôpital Nord	CNR Virus des Infections Respiratoires - France SUD	Antonin Bal; Bruno Lina; Bruno Pozzetto; Gregory Destras; Gwendolyne Burfin; Hadrien Rège; Issam Bachri; Laurence Jossset; Manon Vogrig; Marine Delorme; Martine Valette; Quentin Semanas; Sylvie Gorzatio; Sylvie Pilet; Thomas Bourlet			
EPI_ISL_418024		CHUA - Faro	Instituto Nacional de Saude (INSA)	Guomar et al			
EPI_ISL_535736, EPI_ISL_535737, EPI_ISL_535741, EPI_ISL_535772, EPI_ISL_535773, EPI_ISL_535774, EPI_ISL_535775, EPI_ISL_535776, EPI_ISL_535777, EPI_ISL_535778, EPI_ISL_535779, EPI_ISL_535780, EPI_ISL_535781, EPI_ISL_535782, EPI_ISL_535822, EPI_ISL_535823, EPI_ISL_535824, EPI_ISL_535825, EPI_ISL_535826	see above	CHUL-LABO MULTI / MICRO	Laboratoire de santé publique du Québec	Guillaume Bourque; Ioannis Ragoussis; Jesse Shapiro; Mark Lathrop and Michel Roger; Mark Lathrop and Michel Roger on behalf of the CoVSeQ research group; Sandrine Moreira			
EPI_ISL_417988, EPI_ISL_417990, EPI_ISL_417991, EPI_ISL_417994, EPI_ISL_417995, EPI_ISL_417996, EPI_ISL_418010, EPI_ISL_418011, EPI_ISL_418012, EPI_ISL_418013, EPI_ISL_418014, EPI_ISL_418015, EPI_ISL_418016	see above	CHULC - H Curry Cabral	Instituto Nacional de Saude (INSA)	Guomar et al			
EPI_ISL_417992, EPI_ISL_417993		CHULC - H D Estefania	Instituto Nacional de Saude (INSA)	Guomar et al			
EPI_ISL_535726, EPI_ISL_535729, EPI_ISL_535735, EPI_ISL_535740, EPI_ISL_535753, EPI_ISL_535783, EPI_ISL_535789, EPI_ISL_535802, EPI_ISL_535806, EPI_ISL_535826, EPI_ISL_535827, EPI_ISL_535830, EPI_ISL_535832	see above	CHUM - Microbiologie - Hôpital Saint-Luc	Laboratoire de santé publique du Québec	Guillaume Bourque; Ioannis Ragoussis; Jesse Shapiro; Mark Lathrop and Michel Roger; Mark Lathrop and Michel Roger on behalf of the CoVSeQ			

EPI_ISL_445245, EPI_ISL_445248, EPI_ISL_445250, EPI_ISL_445254, EPI_ISL_445255, EPI_ISL_445258, EPI_ISL_445260	see above	CLINICA ALEMANA DE SANTIAGO S.A.	Instituto de Salud Publica de Chile	Alejandra Acevedo; Andrés E Castillo; Bárbara Parra; Carolina Tambley; Gabriel Leal; Jaime Lagos; Jorge Fernandez; Loredana Arata; Patricia Bustos; Paz Tapia; Rodrigo Fasce; Winston Andrade
EPI_ISL_445272, EPI_ISL_445285, EPI_ISL_445287		CLINICA CIUDAD DEL MAR	Instituto de Salud Publica de Chile	Alejandra Acevedo; Andrés E Castillo; Bárbara Parra; Carolina Tambley; Gabriel Leal; Jaime Lagos; Jorge Fernandez; Loredana Arata; Patricia Bustos; Paz Tapia; Rodrigo Fasce; Winston Andrade
EPI_ISL_445297		CLINICA INTEGRAL S.A.	Instituto de Salud Publica de Chile	Alejandra Acevedo; Andrés E Castillo; Bárbara Parra; Carolina Tambley; Gabriel Leal; Jaime Lagos; Jorge Fernandez; Loredana Arata; Patricia Bustos; Paz Tapia; Rodrigo Fasce; Winston Andrade
EPI_ISL_445299		CLINICA LAS CONDES S.A.	Instituto de Salud Publica de Chile	Alejandra Acevedo; Andrés E Castillo; Bárbara Parra; Carolina Tambley; Gabriel Leal; Jaime Lagos; Jorge Fernandez; Loredana Arata; Patricia Bustos; Paz Tapia; Rodrigo Fasce; Winston Andrade
EPI_ISL_445282, EPI_ISL_445283, EPI_ISL_445290, EPI_ISL_445292		CLINICA MAGALLANES S.A.	Instituto de Salud Publica de Chile	Alejandra Acevedo; Andrés E Castillo; Bárbara Parra; Carolina Tambley; Gabriel Leal; Jaime Lagos; Jorge Fernandez; Loredana Arata; Patricia Bustos; Paz Tapia; Rodrigo Fasce; Winston Andrade
EPI_ISL_445284		CLINICA REDSALUD VITACURA.	Instituto de Salud Publica de Chile	Alejandra Acevedo; Andrés E Castillo; Bárbara Parra; Carolina Tambley; Gabriel Leal; Jaime Lagos; Jorge Fernandez; Loredana Arata; Patricia Bustos; Paz Tapia; Rodrigo Fasce; Winston Andrade
EPI_ISL_445249		CLINICA SANTA MARIA S.A.	Instituto de Salud Publica de Chile	Alejandra Acevedo; Andrés E Castillo; Bárbara Parra; Carolina Tambley; Gabriel Leal; Jaime Lagos; Jorge Fernandez; Loredana Arata; Patricia Bustos; Paz Tapia; Rodrigo Fasce; Winston Andrade
EPI_ISL_445262		CLINICA TABANCURA	Instituto de Salud Publica de Chile	Alejandra Acevedo; Andrés E Castillo; Bárbara Parra; Carolina Tambley; Gabriel Leal; Jaime Lagos; Jorge Fernandez; Loredana Arata; Patricia Bustos; Paz Tapia; Rodrigo Fasce; Winston Andrade
EPI_ISL_445306, EPI_ISL_445312, EPI_ISL_445315, EPI_ISL_445361		CLINICA UC SAN CARLOS DE APOQUINDO	Instituto de Salud Publica de Chile	Alejandra Acevedo; Andrés E Castillo; Bárbara Parra; Carolina Tambley; Gabriel Leal; Jaime Lagos; Jorge Fernandez; Loredana Arata; Patricia Bustos; Paz Tapia; Rodrigo Fasce; Winston Andrade
EPI_ISL_445334		CLINICA UNIVERSITARIA DE PUERTO MONTE S.A.	Instituto de Salud Publica de Chile	Alejandra Acevedo; Andrés E Castillo; Bárbara Parra; Carolina Tambley; Gabriel Leal; Jaime Lagos; Jorge Fernandez; Loredana Arata; Patricia Bustos; Paz Tapia; Rodrigo Fasce; Winston Andrade
EPI_ISL_445330		CLINICA VESPUCCIO S. A.	Instituto de Salud Publica de Chile	Alejandra Acevedo; Andrés E Castillo; Bárbara Parra; Carolina Tambley; Gabriel Leal; Jaime Lagos; Jorge Fernandez; Loredana Arata; Patricia Bustos; Paz Tapia; Rodrigo Fasce; Winston Andrade
EPI_ISL_536310		CLSC et Centre d'Hébergement La Petite-Nation	Laboratoire de santé publique du Québec	Guillaume Bourque; Ioannis Ragoussis; Jesse Shapiro; Mark Lathrop and Michel Roger on behalf of the CoVSeQ research group; Sandrine Moreira
EPI_ISL_420043, EPI_ISL_420061		CMIP	National Reference Center for Viruses of Respiratory Infections, Institut Pasteur, Paris	Angela Brisebarre; Etienne Simon-Lorière; Flora Donati; Marion Barbet; Maud Vanpeene; Mélanie Albert; Méline Bizard; Sylvie Behilli; Sylvie van der Werf; Vincent Enouf
EPI_ISL_410486, EPI_ISL_416745, EPI_ISL_416746, EPI_ISL_508933, EPI_ISL_508937, EPI_ISL_508939, EPI_ISL_508940, EPI_ISL_508942, EPI_ISL_508945, EPI_ISL_508948, EPI_ISL_508951, EPI_ISL_508953, EPI_ISL_508954, EPI_ISL_508955, EPI_ISL_508956, EPI_ISL_508957, EPI_ISL_508959, EPI_ISL_509000, EPI_ISL_509001, EPI_ISL_509002, EPI_ISL_525536, EPI_ISL_525537, EPI_ISL_525540, EPI_ISL_525541, EPI_ISL_525542, EPI_ISL_525543, EPI_ISL_525544, EPI_ISL_525545, EPI_ISL_578176, EPI_ISL_578177, EPI_ISL_678494, EPI_ISL_678495, EPI_ISL_678496, EPI_ISL_678497, EPI_ISL_678498, EPI_ISL_678499,	see above	CNR Virus des Infections Respiratoires - France SUD	CNR Virus des Infections Respiratoires - France SUD	Alexandre; Alexandre Gaymard; Antonin; Antonin Bal; Bal; Bouscambert-Duchamp; Brengel-Pesce; Bruno Lina; Bruno.; Carine Moustaud; Cheynet; Destras; Emile Frobert; Florence; Florence Morfin-Sherpa; Gaymard; Gregory; Gregory Destras; Gregory Quaromes; Gwendolynne Burfin; Hadrien Regue; Josset; Karen; Laurence; Laurence Josset; Lina; Martine; Martine Valette; Maude; Maude Bouscambert-Duchamp; Morfin-Sherpa; Quentin Semanas; Raphaëlle Lamy; Solenne Brun; Valette; Valerie
EPI_ISL_452127, EPI_ISL_452128, EPI_ISL_452129, EPI_ISL_452130		CO Department of Public Health and Environment	Pathogen Discovery, Respiratory Viruses Branch, Division of Viral Diseases, Centers for Disease Control and Prevention	Alison S. Laufer Halpin; Anna Montmayeur; Anna Uehara; Christopher A. Ekins; Clinton R. Paden; Haibin Wang; Jing Zhang; Krista Queen; Mary S. Keckler; Rachel Mariner; Susiang Tong; Yan Li; Ying Tao; Zachary Weiner
EPI_ISL_416894, EPI_ISL_418248, EPI_ISL_418249		COMPLEJO ASISTENCIAL UNIVERSITARIO DE BURGOS	Instituto de Salud Carlos III	A. Morzón; F. Casas; G. Hospital; —; I. Jiménez; I. Magias-Lobón G.; Iglecias-Caballero; M. Camarero; M. Camarero S. Pozo; F. Casas; I. Jiménez; P. Jiménez; M. Zaballos A. Morzón; M. Cuesta; M. González-Eguez; M. Molinero Calamita; M. Zaballos; P. Jiménez; S. Juliá; S. Juliá M. Cuesta; I. Magias Lobón; S. Pozo; S. Varona
EPI_ISL_412981		CR&WISCO GENERAL HOSPITAL	Hubei Provincial Center for Disease Control and Prevention	Bin Fang; Bo Yang; Bo Yu; Faxian Zhan; Guojun Ye; Jing Li; Junqiang Xu; Kun Cai; Linlin Liu; Xiang Li; Xiao Yu; Xixiang Huo; Yongzhong Jiang.
EPI_ISL_447556, EPI_ISL_447557, EPI_ISL_447558, EPI_ISL_447559, EPI_ISL_447560, EPI_ISL_447561, EPI_ISL_447562, EPI_ISL_447563, EPI_ISL_447847, EPI_ISL_447862	see above	CSIR-Centre for Cellular and Molecular Biology	CSIR-Centre for Cellular and Molecular Biology	Archana Bharadwaj Siva; Dhivya Vedagiri; Divya Gupta; Divya Tej Sowpati; Karthik Bharadwaj Tallapaka; Krishnan Harinivas Harashan; Lamuk Zawer; Namani Gaur; Payel Mukherjee; Priya Singh; Purushotham Vodnal; Rakesh K Mishra; Sakshi Shambhavi; Santosh Kumar Kuncha; Shagutta Khan; Sofia Baru; Tulasi Nagabandi; Vishal Sah
EPI_ISL_450306, EPI_ISL_465687, EPI_ISL_465692, EPI_ISL_535799, EPI_ISL_535800, EPI_ISL_535813, EPI_ISL_535815, EPI_ISL_535876, EPI_ISL_535884, EPI_ISL_535902, EPI_ISL_535910, EPI_ISL_535928, EPI_ISL_535946, EPI_ISL_535948, EPI_ISL_536027, EPI_ISL_536028, EPI_ISL_536040, EPI_ISL_536042, EPI_ISL_536044, EPI_ISL_536150, EPI_ISL_536158, EPI_ISL_536160, EPI_ISL_536166, EPI_ISL_536181, EPI_ISL_536213, EPI_ISL_536215, EPI_ISL_536216, EPI_ISL_536237, EPI_ISL_536243, EPI_ISL_536272, EPI_ISL_536278, EPI_ISL_536286, EPI_ISL_536299, EPI_ISL_536301, EPI_ISL_536302, EPI_ISL_536304, EPI_ISL_536344, EPI_ISL_536361, EPI_ISL_536383	see above	CSSS Haut-Richelieu/Rouville (Hôpital)	Laboratoire de santé publique du Québec	Guillaume Bourque; Ioannis Ragoussis; Jesse Shapiro; Mark Lathrop and Michel Roger; Mark Lathrop and Michel Roger on behalf of the CoVSeQ research group; Sandrine Moreira
EPI_ISL_536109		CSSS de Port-Cartier	Laboratoire de santé publique du Québec	Guillaume Bourque; Ioannis Ragoussis; Jesse Shapiro; Mark Lathrop and Michel Roger on behalf of the CoVSeQ research group; Sandrine Moreira
EPI_ISL_536206, EPI_ISL_536260		CSSS de la Minganie	Laboratoire de santé publique du Québec	Guillaume Bourque; Ioannis Ragoussis; Jesse Shapiro; Mark Lathrop and Michel Roger on behalf of the CoVSeQ research group; Sandrine Moreira
EPI_ISL_426416, EPI_ISL_812141		CT-Dr. Katherine A. Kelley State Public Health Lab	Pathogen Discovery, Respiratory Viruses Branch, Division of Viral Diseases, Centers for Disease Control and Prevention	Alison S. Laufer Halpin; Anna Montmayeur; Anna Uehara; Brian Lynch; Christopher A. Ekins; Clinton R. Paden; Haibin Wang; Jing Zhang; Krista Queen; Mary S. Keckler; Peter Cook; Rachel Mariner; Susiang Tong; Yan Li; Ying Tao
EPI_ISL_468314		CTA Centro de Testagem e Aconselhamento	Instituto Adolfo Lutz, Interdisciplinary Procedures Center, Strategic Laboratory	Claudia Regina Gonçalves; Claudio Tavares Sacchi; Erica Vaessa Ramos Gomes
EPI_ISL_445303		CTRO.DE SALUD FAMILIAR DR. RAUL YAZIGI	Instituto de Salud Publica de Chile	Alejandra Acevedo; Andrés E Castillo; Bárbara Parra; Carolina Tambley; Gabriel Leal; Jaime Lagos; Jorge Fernandez; Loredana Arata; Patricia Bustos; Paz Tapia; Rodrigo Fasce; Winston Andrade
EPI_ISL_451935, EPI_ISL_452142		CUB Hospital Erasme Laboratoire d'Anatomie Pathologique	CUB Hospital Erasme Laboratoire d'Anatomie Pathologique	Dr. Nicky D'Haene; Isabelle Salmon; Niky D'Haene; Prof. Isabelle Salmon
EPI_ISL_535749, EPI_ISL_535761, EPI_ISL_535764, EPI_ISL_535765, EPI_ISL_535811, EPI_ISL_536337, EPI_ISL_536365, EPI_ISL_536366	see above	CUSM-Site Glen-LAB Microbiologie	Laboratoire de santé publique du Québec	Guillaume Bourque; Ioannis Ragoussis; Jesse Shapiro; Mark Lathrop and Michel Roger; Mark Lathrop and Michel Roger on behalf of the CoVSeQ research group; Sandrine Moreira
EPI_ISL_428367, EPI_ISL_443300, EPI_ISL_443301, EPI_ISL_443302, EPI_ISL_443311, EPI_ISL_443312, EPI_ISL_443313, EPI_ISL_443317	see above	Cabinet Médical	National Reference Center for Viruses of Respiratory Infections, Institut Pasteur, Paris	Angela Brisebarre; Etienne Simon-Lorière; Flora Donati; Marion Barbet; Maud Vanpeene; Mélanie Albert; Méline Bizard; Sylvie Behilli; Sylvie van der Werf; Vincent Enouf
EPI_ISL_418235		Cabinet médical	National Reference Center for Viruses of Respiratory Infections, Institut Pasteur, Paris	Angela Brisebarre; Etienne Simon-Lorière; Flora Donati; Marion Barbet; Maud Vanpeene; Mélanie Albert; Méline Bizard; Sylvie Behilli; Sylvie van der Werf; Vincent Enouf
EPI_ISL_418812, EPI_ISL_418813, EPI_ISL_429807, EPI_ISL_429817, EPI_ISL_429818, EPI_ISL_429819, EPI_ISL_429820, EPI_ISL_482474, EPI_ISL_482475, EPI_ISL_482478, EPI_ISL_482480, EPI_ISL_482481, EPI_ISL_482482, EPI_ISL_482483, EPI_ISL_482484	see above	Cadham Provincial Laboratory	National Microbiology Laboratory	: Anna Majer; David Alexander; Elsie Grudecki; Gary Van Domselaar; Grace Seo; Jared Bullard; Jennifer Tanner; Kerry Dutt; Kristyn Burak; Matthew Gilmour; Morag Graham; Natalie Knox; Nathalie Bastien; Paul Van Cateesele; Philip Madon; Rhannnon Huzarewich; Russell Mandes; Russell Mandes; Shan Tyson; Timothy Booth; Yan Lu

EPI_ISL_438109, EPI_ISL_438110, EPI_ISL_438111, EPI_ISL_438112, EPI_ISL_438113, EPI_ISL_438114, EPI_ISL_438115, EPI_ISL_438116, EPI_ISL_438117, EPI_ISL_438118, EPI_ISL_438119, EPI_ISL_438120, EPI_ISL_438121, EPI_ISL_438124, EPI_ISL_438125, EPI_ISL_475770, EPI_ISL_475771, EPI_ISL_475772, EPI_ISL_475773, EPI_ISL_475774, EPI_ISL_475775, EPI_ISL_475776, EPI_ISL_475777, EPI_ISL_475778, EPI_ISL_475779, EPI_ISL_475780, EPI_ISL_475781, EPI_ISL_475782, EPI_ISL_475783, EPI_ISL_475784, EPI_ISL_475785, EPI_ISL_475786, EPI_ISL_475787, EPI_ISL_475788, EPI_ISL_475789, EPI_ISL_475791, EPI_ISL_475792, EPI_ISL_475793, EPI_ISL_475794, EPI_ISL_475795, EPI_ISL_475796, EPI_ISL_475797, EPI_ISL_475798, EPI_ISL_475799, EPI_ISL_583665, EPI_ISL_583666, EPI_ISL_583667, EPI_ISL_583668, EPI_ISL_583669, EPI_ISL_583670, EPI_ISL_583671, EPI_ISL_583672, EPI_ISL_583673, EPI_ISL_583674, EPI_ISL_583675, EPI_ISL_583676, EPI_ISL_583677, EPI_ISL_583678, EPI_ISL_583679, EPI_ISL_583680, EPI_ISL_583681	see above	Center for Virology, Medical University of Vienna	Berghaler laboratory, CoMM Research Center for Molecular Medicine of the Austrian Academy of Sciences	Adi Steinrigl, Alexander Lercher, Alexandra Popa, Andreas Berghaler, Benedikt Agerer; Christian Paar; Christoph Bock; Daniela Schmid; Dorothee von Laer; Elisabeth Puchhammer-Stoeckl; Elisabeth Puchhammer-Stöckl; Franz Albertberger; Gernot Waldner; Gregor Hörmann; Guenter Weiss; Gunther Vogl; Henrike Colacco; Jakob-Wendelin Genger; Jan Laine; Judith Abele; Kings Rieger-Hohenwarter; Lukas Ender; Manfred Narz; Mark Smyth; Martin Senekowitsch; Michael Schuster; Peter Hufnagl; Peter Obrist; Rainer Gattringer; Sabine Sussitz-Rack; Stephan Aberle; Thomas Penz; Wegene Borena
EPI_ISL_523950	see above	Center of Medical Microbiology, Virology, and Hospital Hygiene, University of Duesseldorf	Center of Medical Microbiology, Virology, and Hospital Hygiene, Heinrich Heine University Duesseldorf	Alexander Dithley, Andreas Walker, Daniel Strelow, Hendrik Streeck, Jessica Nicolai, Jörg Timm; Klaus Pfeffer; Malte Kohns Vasconcelos; Marek Korencak; Maximilian Dماغنهز; Tobias Wienemann; Torsten Houwaart
EPI_ISL_413488, EPI_ISL_414487, EPI_ISL_414488, EPI_ISL_414489, EPI_ISL_414505, EPI_ISL_414506, EPI_ISL_414507, EPI_ISL_417457, EPI_ISL_417458, EPI_ISL_417459, EPI_ISL_417460, EPI_ISL_417461, EPI_ISL_417462, EPI_ISL_417463, EPI_ISL_417464, EPI_ISL_417465, EPI_ISL_417466, EPI_ISL_417467, EPI_ISL_417468, EPI_ISL_419541, EPI_ISL_419542, EPI_ISL_419543, EPI_ISL_419544, EPI_ISL_419545, EPI_ISL_419546, EPI_ISL_419547, EPI_ISL_419548, EPI_ISL_419549, EPI_ISL_419550, EPI_ISL_419551, EPI_ISL_419552, EPI_ISL_425121, EPI_ISL_425122, EPI_ISL_425123, EPI_ISL_425124, EPI_ISL_425125, EPI_ISL_425126, EPI_ISL_425127, EPI_ISL_425128, EPI_ISL_425130, EPI_ISL_425131, EPI_ISL_425132, EPI_ISL_425138, EPI_ISL_425139, EPI_ISL_523927, EPI_ISL_523929, EPI_ISL_523931, EPI_ISL_523932, EPI_ISL_523933, EPI_ISL_523934, EPI_ISL_523937, EPI_ISL_523938, EPI_ISL_523939, EPI_ISL_523940, EPI_ISL_523941, EPI_ISL_523942, EPI_ISL_523943, EPI_ISL_523944, EPI_ISL_523948, EPI_ISL_523949, EPI_ISL_602513, EPI_ISL_602517	see above	Center of Medical Microbiology, Virology, and Hospital Hygiene, University of Duesseldorf	Center of Medical Microbiology, Virology, and Hospital Hygiene, University of Duesseldorf	Alexander Dithley, Andreas Walker, Björn-Erik Jensen, Björn-Erik Jensen, Daniel Strelow, Detlef Knöding-Milias, Hendrik Streeck, Jessica Nicolai, Jörg Timm, Jörg Timm, Klaus Pfeffer, Lisanna Hulse, Malte Kohns Vasconcelos, Marek Korencak, Maximilian Dماغنهز, Nadine Lübke, Onwin Adams; Sandra Hauka, Tina Sentf, Tobias Wienemann; Torsten Feldt, Torsten Houwaart Ji Jiansong; Ji Qiaoying; Wang Xiaoguang; Ye Bifeng; Ye Ling
EPI_ISL_429852, EPI_ISL_429853, EPI_ISL_429854, EPI_ISL_495459	see above	Centers for Disease Control and Prevention of Lishui	Department of InspectionCenters for Disease Control and Prevention of Lishui	
EPI_ISL_406031, EPI_ISL_420082, EPI_ISL_420083, EPI_ISL_420084, EPI_ISL_420085, EPI_ISL_421641, EPI_ISL_421651, EPI_ISL_426488, EPI_ISL_428489, EPI_ISL_428490, EPI_ISL_428491, EPI_ISL_429882, EPI_ISL_429883, EPI_ISL_429884	see above	Centers for Disease Control, R.O.C. (Taiwan)	Centers for Disease Control, R.O.C. (Taiwan)	Ji-Rong Yang; Jung-Jung Mu; Ming-Tsan Liu; Ming-Tsan Liu; Shu-Ying Li; Yu-Chi Lin; Yu-Chi-Lin
EPI_ISL_457750, EPI_ISL_459964	see above	Centogene AG	Centogene AG	Dr. Krishna Kumar Kandaswamy, Prof. Dr. Peter Bauer
EPI_ISL_455583, EPI_ISL_455594	see above	Central Chest Institute of Thailand	National Institute of Health, Department of medical Sciences, Ministry of Public Health, Thailand	Chittaganpith; Malinee; Okada; Pammen; Phuygun; Pitaluk; Sripappom; Sitiporn; Sunthareeya; Thanadachakul; Thanutsapa; Waichareon; Warawan; Wongboot
EPI_ISL_794603, EPI_ISL_794604	see above	Central Laboratories, Egyptian Ministry of Health and Population	Central Laboratories, Egyptian Ministry of Health and Population	A.E.; Ali; El Guindy; El Sayes; El Taweel; A.; El-Sheshery, R.; Gomaa, M.; Kamel; Kandell, A.; Kayali, G.; Kayed; Khalifa; Kutkat, O.; M.A.; M.K.; M.N.; Mahmoud; Mahrous, N.; Mostasim, Y.; Mostafa, A.; N.M.; Naguib, A.; Roshdy; S.H.; Saleh, M.; Shawky, S.; Shehata, M.; W.H.
EPI_ISL_978502, EPI_ISL_978503, EPI_ISL_978504, EPI_ISL_978505, EPI_ISL_978506, EPI_ISL_978507, EPI_ISL_978508, EPI_ISL_978509, EPI_ISL_978510, EPI_ISL_978511, EPI_ISL_978512, EPI_ISL_978513, EPI_ISL_978514, EPI_ISL_978515, EPI_ISL_978516, EPI_ISL_978517, EPI_ISL_978518, EPI_ISL_978519, EPI_ISL_978520, EPI_ISL_978521, EPI_ISL_978522, EPI_ISL_978523	see above	Central Public Health Laboratory - LACEN-Bahia, Salvador, Brazil	Central Public Health Laboratory - LACEN-Bahia, Salvador, Brazil	Arabela Leal; Breno Dominguez; Felicidade Pereira; Jaqueline Gomes; Luciana Oliveira; Lúcia Alcântara; Marcela Gómez; Marta Giovanetti; Patricia Cajado; Stephane Tosta; Wagner Fonseca; Vanessa Nancy
EPI_ISL_429667, EPI_ISL_429669, EPI_ISL_429671, EPI_ISL_429676, EPI_ISL_429681, EPI_ISL_429687, EPI_ISL_429688, EPI_ISL_429695	see above	Central Public Health Laboratory/Octávio Magalhães Institute (IOM) from the Ezequiel Dias Foundation (FUNED)	Instituto Octávio Magalhães / Fundação Ezequiel Dias (IOM/Funed)	Jolison Xavier; Luiz Carlos Junior Alcântara; Marcos Vinícius Silva; Marluce Aparecida Assunção Oliveira; Marta Giovanetti; Talita Adeline; Vagner Fonseca
EPI_ISL_447251	see above	Central Virology Laboratory	Central Virology Laboratory	Dant Sofer; Efrat Bucris; Ella Mendelson; Michal Mandelboim; Neta Zuckerman; Oran Erster; Orna Mor
EPI_ISL_419211	see above	Central Virology Laboratory	Israel Institute for Biological Research	Adi Beth-Din; Anat Zvi; Boaz Polli; Dana Stein; Einat Viner; Gad Sagi; Gali Regav-Yochay; Hadass Tamir; Hagit Achdout; Inbar Cohen-Gihon; Liach Cheny; Michal Mandelboim; Nir Paran; Ofir Israeli; Orit Shliman; Oran Erster; Orly Laskar; Sharon Melamed; Shay Weiss; Shmuel S. Shapiro; Shmuel Yitzhaki; Tomer Israely; Yifat Yanahom Ronen
EPI_ISL_430842	see above	Central chest institute of Thailand	National Institute of Health, Department of medical Sciences, Ministry of Public Health, Thailand	Chittaganpith; Malinee; Okada; Pammen; Phuygun; Pitaluk; Sripappom; Sitiporn; Sunthareeya; Thanadachakul; Thanutsapa; Waichareon; Warawan; Wongboot
EPI_ISL_458000	see above	Centre For Biotechnology Research and Development	Centre For Biotechnology Research and Development	C.N. and Michuki; D.K.; G.N.; J.O.; Kimotho, J.; Matoke-Muha; Muuo; Ochwo, M.; S.L.; Symker; Waruhii; Zablon
EPI_ISL_414624, EPI_ISL_416494	see above	Centre Hospitalier Universitaire de Rouen Laboratoire de Virologie	National Reference Center for Viruses of Respiratory Infections, Institut Pasteur, Paris	Angela Brisebarre; Etienne Simon-Lorière; Flora Donati; Flora Donati Vincent Enouf; Jean-Christophe Planter; Marion Barbet; Maud Vanpee; Méline Bizard; Méline Albert; Sylvie Behilli; Sylvie van der Werf; Vincent Enouf
EPI_ISL_508958, EPI_ISL_509012	see above	Centre Hospitalier Alpes Leman	CNR Virus des Infections Respiratoires - France SUD	Alexandre Gaymard; Antonin Bal; Bruno Lina; Carine Moustaud; Florence Morfin-Sherpa; Gregory Destras; Gwendolynne Burfin; Laurence Jossot; Martine Valette; Maude Bouscambert-Duchamp; Raphaëlle Lamy; Solenne Brun
EPI_ISL_414627, EPI_ISL_414628, EPI_ISL_414629, EPI_ISL_414630, EPI_ISL_414634, EPI_ISL_414635, EPI_ISL_414636, EPI_ISL_414637, EPI_ISL_414638, EPI_ISL_415654, EPI_ISL_416495, EPI_ISL_416496, EPI_ISL_416497, EPI_ISL_418218, EPI_ISL_418220, EPI_ISL_418221, EPI_ISL_418222, EPI_ISL_418223, EPI_ISL_418227, EPI_ISL_418228, EPI_ISL_418229, EPI_ISL_418231, EPI_ISL_418236, EPI_ISL_418237, EPI_ISL_418238, EPI_ISL_418239, EPI_ISL_429968	see above	Centre Hospitalier Compègne Laboratoire de Biologie	National Reference Center for Viruses of Respiratory Infections, Institut Pasteur, Paris	Angela Brisebarre; Etienne Simon-Lorière; Fabiana Gambaro; Flora Donati; Flora Donati Vincent Enouf; Marion Barbet; Maud Vanpee; Méline Albert; Méline Bizard; Méline Albert; Sylvie Behilli; Sylvie van der Werf; Vincent Enouf
EPI_ISL_418428, EPI_ISL_508947	see above	Centre Hospitalier Lucien Husel	CNR Virus des Infections Respiratoires - France SUD	Alexandre Gaymard; Antonin Bal; Bruno Lina; Carine Moustaud; Florence Morfin-Sherpa; Gregory Destras; Gwendolynne Burfin; Laurence Jossot; Martine Valette; Maude Bouscambert-Duchamp; Raphaëlle Lamy; Solenne Brun
EPI_ISL_508998	see above	Centre Hospitalier Pierre Duodot	CNR Virus des Infections Respiratoires - France SUD	Alexandre Gaymard; Antonin Bal; Bruno Lina; Carine Moustaud; Florence Morfin-Sherpa; Gregory Destras; Gwendolynne Burfin; Laurence Jossot; Martine Valette; Maude Bouscambert-Duchamp; Raphaëlle Lamy; Solenne Brun
EPI_ISL_414633	see above	Centre Hospitalier René Dubois Laboratoire de Microbiologie - Bist A	National Reference Center for Viruses of Respiratory Infections, Institut Pasteur, Paris	Angela Brisebarre; Flora Donati Vincent Enouf; Marion Barbet; Maud Vanpee; Méline Bizard; Méline Albert; Sylvie Behilli; Sylvie van der Werf
EPI_ISL_414625	see above	Centre Hospitalier Régional Universitaire de Nantes Laboratoire de Virologie	National Reference Center for Viruses of Respiratory Infections, Institut Pasteur, Paris	Angela Brisebarre; Flora Donati Vincent Enouf; Marianne Coste-Burel; Marion Barbet; Maud Vanpee; Méline Bizard; Méline Albert; Sylvie Behilli; Sylvie van der Werf
EPI_ISL_535787, EPI_ISL_535788, EPI_ISL_535790, EPI_ISL_535842, EPI_ISL_535844, EPI_ISL_535871, EPI_ISL_535896, EPI_ISL_535907, EPI_ISL_535931, EPI_ISL_535932, EPI_ISL_535933, EPI_ISL_535934, EPI_ISL_535935, EPI_ISL_536002, EPI_ISL_536005, EPI_ISL_536006, EPI_ISL_536009, EPI_ISL_536010, EPI_ISL_536015, EPI_ISL_536016, EPI_ISL_536047, EPI_ISL_536050, EPI_ISL_536052, EPI_ISL_536053, EPI_ISL_536054, EPI_ISL_536059, EPI_ISL_536060, EPI_ISL_536063, EPI_ISL_536073, EPI_ISL_536074, EPI_ISL_536076, EPI_ISL_536079, EPI_ISL_536120, EPI_ISL_536126, EPI_ISL_536129, EPI_ISL_536130, EPI_ISL_536134, EPI_ISL_536138, EPI_ISL_536151, EPI_ISL_536153, EPI_ISL_536154, EPI_ISL_536391, EPI_ISL_560415	see above	Centre Hospitalier Régional de Lanaudière	Laboratoire de santé publique du Québec	Guillaume Bourque; Ioannis Ragoussis; Jesse Shapiro; Mark Lathrop and Michel Roger; Mark Lathrop and Michel Roger on behalf of the CoVSeQ research group; Sandrine Moreira
EPI_ISL_418418, EPI_ISL_418419, EPI_ISL_420617, EPI_ISL_508879, EPI_ISL_508880, EPI_ISL_508959, EPI_ISL_508960	see above	Centre Hospitalier Saint Joseph Saint Luc	CNR Virus des Infections Respiratoires - France SUD	Alexandre Gaymard; Antonin Bal; Bruno Lina; Carine Moustaud; Florence Morfin-Sherpa; Gregory Destras; Gwendolynne Burfin; Laurence Jossot; Martine Valette; Maude Bouscambert-Duchamp; Raphaëlle Lamy; Solenne Brun
EPI_ISL_416757, EPI_ISL_417340, EPI_ISL_418426, EPI_ISL_419183, EPI_ISL_419185, EPI_ISL_419186, EPI_ISL_420620, EPI_ISL_508938, EPI_ISL_508944, EPI_ISL_525539	see above	Centre Hospitalier de Bourg en Bresse	CNR Virus des Infections Respiratoires - France SUD	Alexandre; Alexandre Gaymard; Antonin; Antonin Bal; Bal; Bouscambert-Duchamp; Brengele-Peace; Bruno Lina; Bruno ; Carine Moustaud; Cheynet; Destras; Florence; Florence Morfin-Sherpa; Gaymard; Gregory; Gregory Destras; Gwendolynne Burfin; Jossot; Karen; Laurence; Laurence Jossot; Lina; Martine; Martine Valette; Maude; Maude Bouscambert-Duchamp; Morfin-Sherpa; Raphaëlle Lamy; Solenne Brun; Valette; Valérie
EPI_ISL_417338, EPI_ISL_418413, EPI_ISL_419174, EPI_ISL_419175, EPI_ISL_419176, EPI_ISL_419187, EPI_ISL_419188, EPI_ISL_420613, EPI_ISL_420614, EPI_ISL_508875, EPI_ISL_508876, EPI_ISL_508943, EPI_ISL_508945, EPI_ISL_508946, EPI_ISL_508949, EPI_ISL_508950, EPI_ISL_508952, EPI_ISL_509005	see above	Centre Hospitalier de Macon	CNR Virus des Infections Respiratoires - France SUD	Alexandre Gaymard; Antonin Bal; Bruno Lina; Carine Moustaud; Florence Morfin-Sherpa; Gregory Destras; Gwendolynne Burfin; Laurence Jossot; Martine Valette; Maude Bouscambert-Duchamp; Raphaëlle Lamy; Solenne Brun

EPI_ISL_416749, EPI_ISL_418414, EPI_ISL_418417, EPI_ISL_419168, EPI_ISL_508881, EPI_ISL_509006	Centre Hospitalier de Valence Centre Hospitalier de Villefranche	CNR Virus des Infections Respiratoires - France SUD CNR Virus des Infections Respiratoires - France SUD	Alexandre, Alexandre Gaymard; Antonin, Antonin Bal; Bal, Bouscambert-Duchamp; Brenzel-Peace; Bruno Lina; Bruno ; Carine Moustaud; Cheynet, Desras; Florence; Florence Morfin-Sherpa; Gaymard; Gregory; Gregory Desras; Gwendolyn Burfin; Jossot; Karen; Laurence; Laurence Jossot; Lina; Martine; Martine Valette; Maude; Maude Bouscambert-Duchamp; Morfin-Sherpa; Raphaëlle Lamy; Solenne Brun; Valette; Valérie
EPI_ISL_418412	Centre Hospitalier des Vals d'Ardeche	CNR Virus des Infections Respiratoires - France SUD	Alexandre Gaymard; Antonin Bal; Bruno Lina; Carine Moustaud; Florence Morfin-Sherpa; Gregory Desras; Gwendolyn Burfin; Laurence Jossot; Martine Valette; Maude Bouscambert-Duchamp; Raphaëlle Lamy; Solenne Brun
EPI_ISL_535753, EPI_ISL_535754, EPI_ISL_535755, EPI_ISL_535756, EPI_ISL_560413, EPI_ISL_560414, EPI_ISL_535724, EPI_ISL_535742, EPI_ISL_535743	Centre de Recherches Médicales de Lambarene (CERMEL) Centre de SSS d'Arhabakaka-et-de-Tèrabèri - Hôtel-Dieu Centre de SSS La Pommerie	Department of Emerging Infectious Diseases, Institute of Tropical Medicine, Nagasaki University Laboratoire de santé publique du Québec Laboratoire de santé publique du Québec	AKIM A. Adegnik; Bertrand Lell; Hanuka Abe; Jiro Yasuda; Rodrigue Bkangou; Yuri Ushijima Guillaume Bourque; Ioannis Ragoussi; Jesse Shapiro; Mark Lathrop and Michel Roger on behalf of the CoVSeQ research group; Sandrine Moreira Guillaume Bourque; Ioannis Ragoussi; Jesse Shapiro; Mark Lathrop and Michel Roger on behalf of the CoVSeQ research group; Sandrine Moreira
EPI_ISL_535747, EPI_ISL_535748, EPI_ISL_535916, EPI_ISL_535976, EPI_ISL_535979, EPI_ISL_536007, EPI_ISL_536034, EPI_ISL_536038	Centre de SSS de Trois-Rivières	Laboratoire de santé publique du Québec	Guillaume Bourque; Ioannis Ragoussi; Jesse Shapiro; Mark Lathrop and Michel Roger on behalf of the CoVSeQ research group; Sandrine Moreira
EPI_ISL_535727, EPI_ISL_535776, EPI_ISL_535777, EPI_ISL_535779, EPI_ISL_535780, EPI_ISL_535781, EPI_ISL_535804, EPI_ISL_535805, EPI_ISL_535806, EPI_ISL_535816, EPI_ISL_535854	Centre de SSS de la Haute-Yamaska	Laboratoire de santé publique du Québec	Guillaume Bourque; Ioannis Ragoussi; Jesse Shapiro; Mark Lathrop and Michel Roger; Mark Lathrop and Michel Roger on behalf of the CoVSeQ research group; Sandrine Moreira
EPI_ISL_471458	Centre de Virologie des Maladies Tropicales	Functional Genomic Platform/Service Analyses Biologique/MATRS/ Centre National Pour la Recherche Scientifique Et Technique (CNRS)	Abdellah LARAQJ; Abdelkader LAATIRIS; Ahmed REGGAD; Elmoustafa EL FAHIME; Farida HILALI; Hicham EL ANNAZ; Idriss-Amine LAHLLOU; Khalid ENNIB; Marouane MELLOULI; Mly Abiessezz ELALAOUI; Mostafa ELOUENASS; Naida TOULI; Rachid ABI; Réda TAGAJODI; Sataes ELKOCHRI; Sana ALAOUI-Amine; Tahar BALJOU; Yasmine SEKRSOKH; Youssaf AKHOUDJ; Zohour KASMY
EPI_ISL_535808, EPI_ISL_443310	Centre de santé Chibougamau Centre de santé Filières	Laboratoire de santé publique du Québec National Reference Center for Viruses of Respiratory Infections, Institut Pasteur, Paris	Guillaume Bourque; Ioannis Ragoussi; Jesse Shapiro; Mark Lathrop and Michel Roger; Sandrine Moreira Angela Brisabane; Elisme Simon-Lorère; Flora Donati; Marion Barbet; Maud Vanpeene; Mélanie Albert; Meline Bizard; Sylvie Behlil; Sylvie van der Wert; Vincent Enouf
EPI_ISL_465697, EPI_ISL_536353	Centre de santé Innuulivik	Laboratoire de santé publique du Québec	Guillaume Bourque; Ioannis Ragoussi; Jesse Shapiro; Mark Lathrop and Michel Roger on behalf of the CoVSeQ research group; Sandrine Moreira
EPI_ISL_483923, EPI_ISL_483931, EPI_ISL_483937, EPI_ISL_483945, EPI_ISL_483947, EPI_ISL_483948, EPI_ISL_483952, EPI_ISL_483959, EPI_ISL_483961, EPI_ISL_483964, EPI_ISL_483966, EPI_ISL_483967, EPI_ISL_483971, EPI_ISL_483973, EPI_ISL_483976, EPI_ISL_483980, EPI_ISL_483982, EPI_ISL_483985, EPI_ISL_483986, EPI_ISL_483987, EPI_ISL_483989, EPI_ISL_483992, EPI_ISL_483995, EPI_ISL_483999, EPI_ISL_484002, EPI_ISL_484005, EPI_ISL_484006, EPI_ISL_484012, EPI_ISL_484019, EPI_ISL_484020, EPI_ISL_484028, EPI_ISL_484034, EPI_ISL_484036, EPI_ISL_484053, EPI_ISL_484056, EPI_ISL_484059, EPI_ISL_484064, EPI_ISL_484070, EPI_ISL_484072, EPI_ISL_484079, EPI_ISL_484085, EPI_ISL_484087, EPI_ISL_484091, EPI_ISL_484093, EPI_ISL_484095, EPI_ISL_484096, EPI_ISL_484104, EPI_ISL_484110, EPI_ISL_484115, EPI_ISL_484117, EPI_ISL_484126, EPI_ISL_484129, EPI_ISL_484131, EPI_ISL_484134, EPI_ISL_484136, EPI_ISL_484145, EPI_ISL_484152, EPI_ISL_484169, EPI_ISL_484170, EPI_ISL_484174, EPI_ISL_484189, EPI_ISL_484191	COVID-19 Genomics UK (COG-UK) Consortium	All Raza Awan; Chloe Fisher; Jonathan Edgeworth; Luke Snell; Penny Cliff; Rahul Batra	
EPI_ISL_560550, EPI_ISL_560551, EPI_ISL_560552, EPI_ISL_560556, EPI_ISL_560558, EPI_ISL_560560, EPI_ISL_560566, EPI_ISL_560661, EPI_ISL_560668, EPI_ISL_560671, EPI_ISL_560702, EPI_ISL_560705, EPI_ISL_560712, EPI_ISL_560719, EPI_ISL_560722, EPI_ISL_560723, EPI_ISL_560678, EPI_ISL_560679, EPI_ISL_560684, EPI_ISL_560686, EPI_ISL_560695, EPI_ISL_560696, EPI_ISL_560697, EPI_ISL_560698, EPI_ISL_560699, EPI_ISL_560700, EPI_ISL_560703, EPI_ISL_560739, EPI_ISL_560740, EPI_ISL_560741, EPI_ISL_560737, EPI_ISL_560739, EPI_ISL_560740, EPI_ISL_561873	Centre for Clinical Infection and Diagnostics Research and Genomics Innovation Unit, Guy's and St. Thomas' NHS Trust Centre for Dengue Research	Centre for Clinical Infection and Diagnostics Research and Genomics Innovation Unit, Guy's and St. Thomas' NHS Trust Centre for Dengue Research	All Raza Awan; Chloe Fisher; Jonathan Edgeworth; Luke Snell; Rahul Batra Anand Wijewickrama; Chandima Jeewandara; Damsayanthi Kampanthi; Damsayanthi Tadmapthy; Deshri Jayathilaka; Dinuka Ariyaratne; Dinuka Ariyaratne; Dyanath Ransinghe; Eranga Nanangoda; Gathasara Neelika Malaviya; Lashin Gomes; Neelika Malaviya
EPI_ISL_428670, EPI_ISL_428671, EPI_ISL_428672, EPI_ISL_428673, EPI_ISL_525478, EPI_ISL_525479	Centre for Enzyme Innovation, University of Portsmouth / Translational Research Laboratory, Portsmouth Hospitals NHS Trust	COVID-19 Genomics UK (COG-UK) Consortium	Alyson Lloyd; Angela Beckett; Anoop Chauhan; Ethan Butcher; Garry Scarlett; Kelly Bicknell; Robert Impey; Samuel Robson; Sarah Wylie; Scott Elliott; Sharon Glayshear; Yann Bourgeois
EPI_ISL_475279, EPI_ISL_475280, EPI_ISL_475282, EPI_ISL_475283, EPI_ISL_475284, EPI_ISL_475285, EPI_ISL_475286, EPI_ISL_475287, EPI_ISL_475288, EPI_ISL_475289, EPI_ISL_475291, EPI_ISL_475292, EPI_ISL_475293, EPI_ISL_475296, EPI_ISL_475297, EPI_ISL_475298, EPI_ISL_475299, EPI_ISL_475300, EPI_ISL_475321, EPI_ISL_475322, EPI_ISL_475323, EPI_ISL_475325, EPI_ISL_475326, EPI_ISL_475327, EPI_ISL_475328, EPI_ISL_475329, EPI_ISL_475330, EPI_ISL_475341, EPI_ISL_479175, EPI_ISL_479176, EPI_ISL_479177, EPI_ISL_479178, EPI_ISL_479179, EPI_ISL_479180, EPI_ISL_479181, EPI_ISL_479184, EPI_ISL_479185, EPI_ISL_479186, EPI_ISL_479187, EPI_ISL_479188, EPI_ISL_479189, EPI_ISL_479190, EPI_ISL_479191, EPI_ISL_479192, EPI_ISL_479193, EPI_ISL_479194, EPI_ISL_484415, EPI_ISL_484416, EPI_ISL_484417, EPI_ISL_499302, EPI_ISL_499303, EPI_ISL_499304, EPI_ISL_499306, EPI_ISL_499308, EPI_ISL_507137, EPI_ISL_507139, EPI_ISL_507140, EPI_ISL_507141, EPI_ISL_507142, EPI_ISL_507143, EPI_ISL_507146, EPI_ISL_507147, EPI_ISL_507148, EPI_ISL_507149, EPI_ISL_507150, EPI_ISL_507155, EPI_ISL_512409, EPI_ISL_512410, EPI_ISL_512411, EPI_ISL_512412, EPI_ISL_514457, EPI_ISL_514459, EPI_ISL_514460, EPI_ISL_514461, EPI_ISL_514462, EPI_ISL_514463, EPI_ISL_514465, EPI_ISL_514466, EPI_ISL_514485, EPI_ISL_514486, EPI_ISL_514489, EPI_ISL_514490, EPI_ISL_526634, EPI_ISL_526635, EPI_ISL_526636, EPI_ISL_526642, EPI_ISL_613282, EPI_ISL_613284, EPI_ISL_613285, EPI_ISL_613287	Centre for Human Virology & Genomics, Nigerian Institute of Medical Research NSW Health Pathology - Institute of Clinical Pathology and Medical Research; Westmead Hospital, University of Sydney NSW Health Pathology - Institute of Clinical Pathology and Medical Research; Westmead Hospital, University of Sydney	Shaihu, J Carter I; Chen SC; Eden J-S; Gall; Gray K; Holmes EC; Kok J and Dwyer DE for the 2019-nCoV Study Group*; Lam C; M; Maddocks S; O'Sullivan MV; Rahman H; Rockett R; Sintcheko V; Timms V ; Alicia; Carter I; Chen SC; Eden J-S; Gall; Gray K; Holmes EC; Kok J and Dwyer DE for the 2019-nCoV Study Group*; Lam C; M; Maddocks S; O'Sullivan MV; Rahman H; Rockett R; Sintcheko V; Timms V	
EPI_ISL_413124, EPI_ISL_413594, EPI_ISL_413595, EPI_ISL_417030	Centre for Infectious Diseases and Microbiology Laboratory NSW Health Pathology - Institute of Clinical Pathology and Medical Research; Westmead Hospital, University of Sydney	Centre for Infectious Diseases and Microbiology Public Health NSW Health Pathology - Institute of Clinical Pathology and Medical Research; Westmead Hospital, University of Sydney	Arnot A; Arnot A and Sadaad R for the 2019-nCoV Study Group; Bachmann N; Basile K; Byun R; Carter I; Carter I and Rahman H for the 2019-nCoV Study Group; Chang S; Chen SC; Chen SC and Maddocks S for the 2019-nCoV Study Group; Draper J; Dwyer DE; Dwyer DE and Rockett R for the 2019-nCoV Study Group; Dwyer DE for the 2019-nCoV Study Group; Eden J-S; Eden J-S and Lam C for the 2019-nCoV Study Group; Eden J-S; Gall M; Gall M and Arnot A for the 2019-nCoV Study Group; Gray K; Gray K and Timms V for the 2019-nCoV Study Group; Holmes EC; Holmes EC and O'Sullivan MV for the 2019-nCoV Study Group; Kok J; Kok J and Dwyer DE for the 2019-nCoV Study Group; Lam C; Lam C and Gray K for the 2019-nCoV Study Group; Maddocks S; Maddocks S and Kok J for the 2019-nCoV Study Group; O'Sullivan MV; O'Sullivan MV and Sintcheko V for the 2019-nCoV Study Group; Propekn M; Rahman H; Rahman H and Holmes EC for the 2019-nCoV Study Group; Rockett R; Rockett R and Eden J-S for the 2019-nCoV Study Group; Sadaad R; Sadaad R and Carter I for the 2019-nCoV Study Group; Sim E; Sintcheko V; Sintcheko V and Chen SC for the 2019-nCoV Study Group; Sorrell T; Timms; Timms V; Timms V and Gall M for the 2019-nCoV Study Group; Y

EPI_ISL_911718, EPI_ISL_911719, EPI_ISL_911720, EPI_ISL_911721, EPI_ISL_911722, EPI_ISL_911723, EPI_ISL_911724, EPI_ISL_911725, EPI_ISL_911726, EPI_ISL_911727, EPI_ISL_911728, EPI_ISL_911729, EPI_ISL_911730, EPI_ISL_911731, EPI_ISL_911732, EPI_ISL_911733, EPI_ISL_911734, EPI_ISL_911735, EPI_ISL_911736, EPI_ISL_911737, EPI_ISL_911738, EPI_ISL_911739, EPI_ISL_911740, EPI_ISL_911741, EPI_ISL_911742, EPI_ISL_911743, EPI_ISL_911744, EPI_ISL_911745, EPI_ISL_911746, EPI_ISL_911747, EPI_ISL_911748, EPI_ISL_911749, EPI_ISL_911750, EPI_ISL_911751, EPI_ISL_911752, EPI_ISL_911753, EPI_ISL_911754, EPI_ISL_911755, EPI_ISL_911756, EPI_ISL_911757, EPI_ISL_911758, EPI_ISL_911759	see above	Clinical Diagnostics Laboratory, Diagnostic & Experimental Pathology, Lilly Research Laboratories	Clinical Diagnostics Laboratory, Diagnostic & Experimental Pathology, Lilly Research Laboratories	Andrew Schade; Angie Fulford; Erin Wray; Jeff Fill; Joe Oakley; John Calley; John McEwee; Leslie O'Neill Reising; Leslie O'Neill Reising; Mayuri Vaidya; Pat Finnegan; Phil Ebert; Rachael Redmond; Sam McNeely; Tim Holzer
EPI_ISL_424352		Clinical Laboratory, Fuyang City Center for Disease Control and Prevention	Clinical Laboratory, Fuyang City Center for Disease Control and Prevention	Ge, B.
EPI_ISL_416432		Clinical Microbiology Lab	Infectious Disease Research Department, King Abdulrahman International Medical Research Center (KAIMRC)	Abdulrahman Alswaji; Liliane Okdah; Majeed Alghoribi; Michel Doumit; Sadeem Athayfi; Sameera Al Johari
EPI_ISL_447441, EPI_ISL_447442, EPI_ISL_447443, EPI_ISL_447444, EPI_ISL_447445, EPI_ISL_447446, EPI_ISL_447447, EPI_ISL_447448, EPI_ISL_447449, EPI_ISL_447450	see above	Clinical Microbiology Laboratory, Sheba Medical Center	Stern Lab	Stern Lab
EPI_ISL_447384, EPI_ISL_447385, EPI_ISL_447386, EPI_ISL_447387, EPI_ISL_447388, EPI_ISL_447389, EPI_ISL_447391, EPI_ISL_447393, EPI_ISL_447394, EPI_ISL_447395, EPI_ISL_447396, EPI_ISL_447397, EPI_ISL_447399, EPI_ISL_447406, EPI_ISL_447417, EPI_ISL_447418	see above	Clinical Microbiology Laboratory, The Baruch Padah Medical Center, Poriya	Stern Lab	Stern Lab
EPI_ISL_877585, EPI_ISL_877586, EPI_ISL_877587, EPI_ISL_877588, EPI_ISL_877589, EPI_ISL_877590, EPI_ISL_877591, EPI_ISL_877592, EPI_ISL_877761	see above	Clinical Virology Laboratory, Institute of Liver and Biliary Sciences	ILBS - IGIB	Abhishek Padhi; Ekta Gupta; Jawinder Singh Maras; Reshu Agarwal; Sheetalath Roogo; Shridhar Sivasubbu; Shwetank Sharma; Vinod Scaria
EPI_ISL_605083, EPI_ISL_605811, EPI_ISL_605812, EPI_ISL_605816	see above	Clinical Virology Unit, Hadassah Hebrew University Medical Center	Stern Lab	Stern Lab
EPI_ISL_447408, EPI_ISL_447409, EPI_ISL_447410, EPI_ISL_447411, EPI_ISL_447412, EPI_ISL_447416	see above	Clinique AVERAY LA BROUSTE, Med. Polyvalente	National Reference Center for Viruses of Respiratory Infections, Institut Pasteur, Paris	Angela Brisebarre; Elsa Ngwem; Etienne Simon-Lorière; Flora Donati; Marion Barbat; Maud Vanpeene; Mélanie Albert; Méline Bizard; Sylvie Behilli; Sylvie van der Werf; Vincent Enouf
EPI_ISL_949248	see above	Cliniques universitaires Saint-Luc	UCLouvain/FRECMBLG	Benoit Kabamba Mukadi; Jean Ruette; Lysa Pinsmaye
EPI_ISL_949244, EPI_ISL_949245, EPI_ISL_949246, EPI_ISL_949247, EPI_ISL_949249, EPI_ISL_949250, EPI_ISL_949252, EPI_ISL_1029965, EPI_ISL_1029966, EPI_ISL_1029968, EPI_ISL_1029969, EPI_ISL_1029971, EPI_ISL_1029972, EPI_ISL_1029973	see above	Clinica Universidad de Navarra	Instituto de Salud Carlos III	Benoit Kabamba Mukadi; Jean Ruette; Lysa Pinsmaye
EPI_ISL_862652, EPI_ISL_862653	see above	Clinica Universidad de Navarra. Servicio de Enfermedades Infecciosas y Microbiología clínica	SeqCOVID-SPAIN consortium/IBV(CSIC)	Jose Luis del Pozo and SeqCOVID-SPAIN consortium; Miriam Fernández-Alonso
EPI_ISL_1040819, EPI_ISL_1040820, EPI_ISL_1040821	see above	CoVid WC Cape Town Metro	NHLSI/UCT	Arash Irzadeh; Bruna Galvão; Carolyn Williamson; Deelan Doolabh; Diana Hardie; Innocent Madau; Kruger Marais; Lynn Tyers; Marvin Hsiao; Stephan Korsman
EPI_ISL_677286, EPI_ISL_677287	see above	Colorado Department of Public Health and Environment	Colorado Department of Public Health and Environment	Emily A. Travanty; Laura Bankers; Molly Hetherington-Rauth; Sarah Elizabeth Totten; Shannon Ely; Shannon R. Matzinger
EPI_ISL_455329, EPI_ISL_455330, EPI_ISL_455331, EPI_ISL_578194	see above	Complejo Hospitalario Universitario La Coruna	Instituto de Salud Carlos III	A. Monzón; F. Casas; I. Jiménez; Iglesias-Caballero; J. López; M. Camarero; M. Cuesta; M. González-Esguevillas; M. Molinero Calamita; M. Zaballos; M.A. Canizares; P. Jiménez; S. Juliá; S. Pozo; S. Varona
EPI_ISL_455333	see above	Complejo Hospitalario Universitario de Santiago	Instituto de Salud Carlos III	A. Monzón; F. Casas; I. Jiménez; Iglesias-Caballero; J. Llovo; M. Camarero; M. Cuesta; M. González-Esguevillas; M. Molinero Calamita; M. Zaballos; P. Jiménez; S. Juliá; S. Pozo; S. Varona
EPI_ISL_539569, EPI_ISL_539570, EPI_ISL_539571, EPI_ISL_539572, EPI_ISL_862645, EPI_ISL_862646, EPI_ISL_862647, EPI_ISL_862648, EPI_ISL_862649, EPI_ISL_862650, EPI_ISL_862651	see above	Complejo Hospitalario de Navarra	Instituto de Salud Carlos III	A. Monzón; F. Casas; I. Jiménez; Iglesias-Caballero; J. López; M. Camarero; M. Cuesta; M. González-Esguevillas; M. Molinero Calamita; M. Zaballos; M. Camarero; P. Jiménez; S. Juliá; S. Molinero Calamita; S. Pozo; S. Varona
EPI_ISL_455334, EPI_ISL_455335, EPI_ISL_578195, EPI_ISL_435716	see above	Complejo Hospitalario de Orense	Instituto de Salud Carlos III	A. Monzón; F. Casas; I. Jiménez; Iglesias-Caballero; M. Camarero; M. Cuesta; M. García; M. González-Esguevillas; M. Molinero Calamita; M. Paz; M. Zaballos; P. Jiménez; S. Juliá; S. Pozo; S. Varona
EPI_ISL_536288	see above	Connecticut State Department of Public Health	Grubbaugh Lab - Yale School of Public Health	Adam Moore; Akiko Iwasaki; Albert Ko; Alice Lu; Allison Nelson; Anderson Brito; Anne Wylie; Arnau Casanovas; Catherine Muenker; Chaney Kalinich; Chantal Vogels; Charlee Dela Cruz; Cole Jensen; Isabel Ott; Joseph Fauver; Maria Tokuyama; Mary Petrone; Nathan Grubbaugh; Patrick Wong; Peiwen Lu; Richard Martello; Saad Omar; Sheik Farhadian; Tara Aperi
EPI_ISL_455327, EPI_ISL_539526, EPI_ISL_539527, EPI_ISL_539528, EPI_ISL_539529, EPI_ISL_539530, EPI_ISL_691681	see above	Conseil Cri de la SSS de la Baie-James	Laboratoire de santé publique du Québec	Guillaume Bourque; Ioannis Ragousias; Jesse Shapiro; Mark Lathrop and Michel Roger on behalf of the CoVSeQ research group; Sandrine Moreira
EPI_ISL_862641, EPI_ISL_862642, EPI_ISL_862643, EPI_ISL_862644	see above	Consejería de Sanidad y Asuntos Sociales	Instituto de Salud Carlos III	A. Monzón; F. Casas; G. Gutiérrez; I. I. Gutiérrez; G.; I. Jiménez; Iglesias-Caballero; M. Camarero; M. Cuesta; M. González-Esguevillas; M. Molinero Calamita; M. Pozo; M. Zaballos; P. Jiménez; S. Juliá; S. Molinero Calamita; S. Pozo; S. Varona
EPI_ISL_468615, EPI_ISL_468616, EPI_ISL_468617, EPI_ISL_468618, EPI_ISL_468621	see above	Contra Costa Public Health Lab	Chan-Zuckerberg Biohub	A. Monzón; F. Casas; I. Gutiérrez; G.; I. Jiménez; Iglesias-Caballero; M. Camarero; M. Cuesta; M. González-Esguevillas; M. Pozo; M. Zaballos; P. Jiménez; S. Juliá; S. Molinero Calamita; S. Varona
EPI_ISL_454635	see above	County Of San Luis Obispo Public Health Laboratory	Chan-Zuckerberg Biohub	CZB Ctlahub Consortium
EPI_ISL_468388, EPI_ISL_468389, EPI_ISL_468390, EPI_ISL_468391, EPI_ISL_468392, EPI_ISL_468393, EPI_ISL_468394, EPI_ISL_468395, EPI_ISL_468396, EPI_ISL_468397, EPI_ISL_468398, EPI_ISL_468399, EPI_ISL_468400, EPI_ISL_468401, EPI_ISL_468402, EPI_ISL_468403, EPI_ISL_468404, EPI_ISL_468405	see above	County of Santa Clara Public Health	Chan-Zuckerberg Biohub	CZB Ctlahub Consortium
EPI_ISL_437044	see above	County of Santa Clara Public Health Department	Chan-Zuckerberg Biohub	CZB Ctlahub Consortium
EPI_ISL_436641, EPI_ISL_436672, EPI_ISL_436674, EPI_ISL_513773	see above	County of Santa Clara Public Health Department	Chan-Zuckerberg Biohub	CZB Ctlahub Consortium

see above	Department of Health Technology and Informatics, The Hong Kong Polytechnic University	Department of Health Technology and Informatics, The Hong Kong Polytechnic University	A.K.-L.; A.Y.-M.; B.K.-C.; C.T.-M.; Chan; Chau; D.H.-K.; Fung; G.K.-H.; H.-Y.; Ho; J.S.-L.; K.-T.; K.K.-G.; K.S.-C.; K.S.-S.; L.-K.; Lai; Lao; Lee; Leung; Luk; K.; M.C.-Y.; Ng; Que; S.K.-Y.; S.P.; Shum; Su; T.-L.; T.T.-L.; Tam; To; W.-K.; W.G.; Wong; Wu; Y.-W.-M.; Yam; Yao; Yip
EPI_ISL_1289435, EPI_ISL_1289436, EPI_ISL_1289437, EPI_ISL_1289438, EPI_ISL_1289439, EPI_ISL_1289440, EPI_ISL_1289441, EPI_ISL_1289442, EPI_ISL_1289443, EPI_ISL_1289444, EPI_ISL_1289445	Department of Health Technology and Informatics, The Hong Kong Polytechnic University	Department of Health Technology and Informatics, The Hong Kong Polytechnic University	Alan Ka-Lun Wu, Alex Yat-Man Ho, Barry Kin-Chung Wong, Chio To-Mei Chan, David Ho-Kwong Shum, Denise Sze-Hang Wong, Gilman Kit-Hang Siu, Hui-Yin Liao, Jake Siu-Lun Leung, Kam-Tong Yip, Kenneth Siu-Sing Leung, Kingsley King-Gee Tam, Kitty Sau-Chun Fung, Kristine Luk, Lam-Kwong Lee, Miranda Chong-Yee Yau, Sandy Ka-Yee Chau, Shea Ping Yip, Tak-Lun Que, Timothy Ting-Leung Ng, Wing Cheong Yam, Wing-Kin To, Yvette Wai-Man Lai
EPI_ISL_529151, EPI_ISL_529162	Department of Immunology, The Scripps Research Institute	Andersen lab at Scripps Research	Allison Smithier, Antonette Bell, Arnaud Drouin, Dahlene Fusco, Gilberto Sabino-Santos, I. with SEARCH Alliance San Diego, Kaylynn Genemaras, Lilia Melnik, Mchardy, Patricia Snarski, Outgley, M., Robert Garry with SEARCH Alliance San Diego, Stefanski, E.
EPI_ISL_522407	Department of Infection Prevention and Infectious Diseases, University Hospital Regensburg	Department of Infection Prevention and Infectious Diseases, University Hospital Regensburg	Fritsch, J.; Holzmann, T.; Schneider-Brachert, W.
EPI_ISL_513298, EPI_ISL_513299, EPI_ISL_513300, EPI_ISL_513301, EPI_ISL_513302, EPI_ISL_513303, EPI_ISL_513304, EPI_ISL_513305, EPI_ISL_513306, EPI_ISL_513307	Department of Infection Prevention and Infectious Diseases, University Hospital Regensburg	Department of Infection Prevention and Infectious Diseases, University Hospital Regensburg	Fritsch, J.; Holzmann, T.; Schneider-Brachert, W.
EPI_ISL_605929, EPI_ISL_605930	Department of Infectious Disease Prevention and Control, Henan Provincial Center for Disease Control and Prevention	Department of Infectious Disease Prevention and Control, Henan Provincial Center for Disease Control and Prevention	Guo, W.; Hu, X.; Huang, X.; Li, D.; Li, X.; Lu, S.; Wu, B.; Ye, Y.
EPI_ISL_568556, EPI_ISL_568557, EPI_ISL_568558, EPI_ISL_568559, EPI_ISL_568560	Department of Infectious Diseases and Immunology, National Hospital Organization Nagoya Medical Center	Clinical Research Center, National Hospital Organization Nagoya Medical Center	Hirotaoka Ode; Kazuhiro Matsuoka; Mai Kubota; Masakazu Matsuda; Mayumi Imahashi; Miko Nakasui; Mikko Mori; Nakasui Mho; Yasumasa Iwatsuki; Yoshihiro Nakata; Yoshiyuki Yokomaku
EPI_ISL_524474, EPI_ISL_524480, EPI_ISL_524481	Department of Infectious Diseases, Cantonal Hospital Baden	Institute of Medical Virology, University of Zurich	Alexandra Trkola; Andrea Zbinden; Fiona Steiner; Gabriela Zillener; Jon Huder; Jürg Böni; Maryam Zaheri; Michael Huber; Patrick Redli; Riccarda Capaul; Stefan Schmutz; Verena Kufner
EPI_ISL_457699, EPI_ISL_457700, EPI_ISL_457721, EPI_ISL_457724, EPI_ISL_457728, EPI_ISL_457732, EPI_ISL_457736, EPI_ISL_457749	Department of Infectious Diseases, Istituto Superiore di Sanità, Roma, Italy	Army Medical and Veterinary Research Center	Alessandra Lo Presti; Anna Anselmo; Antonella Fortunato; Antonella Marchi; Concetta Fabiani Silvia Fillo; Concetta Fabiani Silvia Fillo; Eleonora Benedetti; Florio Lista; Francesco Giordani; Giovanni Faggioni; Nino D'Amore; Paola Stefanelli; Riccardo De Sanctis; Stefano Fiore; Vanessa Vera Faïn
EPI_ISL_412973	Department of Infectious Diseases, Istituto Superiore di Sanità, Roma, Italy	Virology Laboratory, Scientific Department, Army Medical Center	Andrea Ciaramacconi; Anna Anselmo; Antonella Fortunato; Antonella Marchi; Concetta Fabiani; Eleonora Benedetti; Florio Lista; Giovanni Faggioni; Paola Stefanelli; Riccardo De Sanctis; Silvia Fillo; Stefano Fiore; Stefano Palomba
EPI_ISL_856889, EPI_ISL_856904	Department of Infectious Diseases, Istituto Superiore di Sanità, Roma, Italy	Virology Laboratory, Scientific Department, Army Medical Center	Alessandra Lo Presti; Angela Di Martino; Anna Anselmo; Antonella Fortunato; Florio Lista; Francesco Giordani; Giovanni Faggioni; Nino D'Amore; Paola Stefanelli; Riccardo De Sanctis; Silvia Fillo; Stefano Fiore; Vanessa Vera Faïn
EPI_ISL_856888	Department of Infectious Diseases, Istituto Superiore di Sanità, Roma, Italy; A.O.R. San Carlo di Potenza, Laboratorio Microbiologia e Virologia, Potenza, Italy	Virology Laboratory, Scientific Department, Army Medical Center	Alessandra Lo Presti; Angela Di Martino; Anna Anselmo; Antonella Fortunato; Antonio Picerno; Florio Lista; Francesco Giordani; Giovanni Faggioni; Nino D'Amore; Paola Stefanelli; Riccardo De Sanctis; Silvia Fillo; Stefano Fiore; Vanessa Vera Faïn
EPI_ISL_856890	Department of Infectious Diseases, Istituto Superiore di Sanità, Roma, Italy; AO Annunziata, UOC Microbiologia e Virologia, Cosenza, Italy	Virology Laboratory, Scientific Department, Army Medical Center	Alessandra Lo Presti; Angela Di Martino; Anna Anselmo; Antonella Fortunato; Cristina Ginaldi; Florio Lista; Francesco Giordani; Giovanni Faggioni; Nino D'Amore; Paola Stefanelli; Riccardo De Sanctis; Silvia Fillo; Stefano Fiore; Vanessa Vera Faïn
EPI_ISL_856905, EPI_ISL_856906	Department of Infectious Diseases, Istituto Superiore di Sanità, Roma, Italy; AO S.M. della Misericordia, S.C. Microbiologia, Perugia, Italy	Virology Laboratory, Scientific Department, Army Medical Center	Alessandra Lo Presti; Angela Di Martino; Anna Anselmo; Antonella Fortunato; Barbara Camilloni; Florio Lista; Francesco Giordani; Giovanni Faggioni; Nino D'Amore; Paola Stefanelli; Riccardo De Sanctis; Silvia Fillo; Stefano Fiore; Vanessa Vera Faïn
EPI_ISL_856871, EPI_ISL_856891, EPI_ISL_856892	Department of Infectious Diseases, Istituto Superiore di Sanità, Roma, Italy; AORN dei Colli, UOC Microbiologia Virologia, Napoli, Italy	Virology Laboratory, Scientific Department, Army Medical Center	Alessandra Lo Presti; Angela Di Martino; Anna Anselmo; Antonella Fortunato; Florio Lista; Francesco Giordani; Giovanni Faggioni; Luigi Atripaldi; Nino D'Amore; Paola Stefanelli; Riccardo De Sanctis; Silvia Fillo; Stefano Fiore; Vanessa Vera Faïn
EPI_ISL_856900, EPI_ISL_856901	Department of Infectious Diseases, Istituto Superiore di Sanità, Roma, Italy; A.O.U.P. V. Emanuele di Catania, P.O. Gaspare Rodolico, Catania, Italy	Virology Laboratory, Scientific Department, Army Medical Center	Alessandra Lo Presti; Angela Di Martino; Anna Anselmo; Antonella Fortunato; Florio Lista; Francesco Giordani; Giovanni Faggioni; Guido Sciala; Nino D'Amore; Paola Stefanelli; Riccardo De Sanctis; Silvia Fillo; Stefano Fiore; Vanessa Vera Faïn
EPI_ISL_856902	Department of Infectious Diseases, Istituto Superiore di Sanità, Roma, Italy; AS Alto Adige, Microbiologia e Virologia, Bolzano, Italy	Virology Laboratory, Scientific Department, Army Medical Center	Alessandra Lo Presti; Angela Di Martino; Anna Anselmo; Antonella Fortunato; Elisabetta Pagani; Florio Lista; Francesco Giordani; Giovanni Faggioni; Nino D'Amore; Paola Stefanelli; Riccardo De Sanctis; Silvia Fillo; Stefano Fiore; Vanessa Vera Faïn
EPI_ISL_856898, EPI_ISL_856899	Department of Infectious Diseases, Istituto Superiore di Sanità, Roma, Italy; ASL Città di Torino, S.C. Microbiologia e Virologia, Torino, Italy	Virology Laboratory, Scientific Department, Army Medical Center	Alessandra Lo Presti; Angela Di Martino; Anna Anselmo; Antonella Fortunato; Florio Lista; Francesco Giordani; Giovanni Faggioni; Nino D'Amore; Paola Stefanelli; Riccardo De Sanctis; Silvia Fillo; Stefano Fiore; Valeria Ghisetti; Vanessa Vera Faïn
EPI_ISL_856893, EPI_ISL_856894	Department of Infectious Diseases, Istituto Superiore di Sanità, Roma, Italy; ASUITS - Ospedale Maggiore, S.C. UOC Igiene e Sanità Pubblica, Trieste, Italy	Virology Laboratory, Scientific Department, Army Medical Center	Alessandra Lo Presti; Angela Di Martino; Anna Anselmo; Antonella Fortunato; Florio Lista; Francesco Giordani; Giovanni Faggioni; Nino D'Amore; Paola Stefanelli; Pierfrancesco D'Agaro; Riccardo De Sanctis; Silvia Fillo; Stefano Fiore; Vanessa Vera Faïn
EPI_ISL_856887	Department of Infectious Diseases, Istituto Superiore di Sanità, Roma, Italy; AUOC Policlinico Bari, UOC Igiene, Bari, Italy	Virology Laboratory, Scientific Department, Army Medical Center	Alessandra Lo Presti; Angela Di Martino; Anna Anselmo; Antonella Fortunato; Florio Lista; Francesco Giordani; Giovanni Faggioni; Maria Chironna; Nino D'Amore; Paola Stefanelli; Riccardo De Sanctis; Silvia Fillo; Stefano Fiore; Vanessa Vera Faïn
EPI_ISL_856907	Department of Infectious Diseases, Istituto Superiore di Sanità, Roma, Italy; AUSL Valle d'Aosta, Aosta, Italy	Virology Laboratory, Scientific Department, Army Medical Center	Alessandra Lo Presti; Angela Di Martino; Anna Anselmo; Antonella Fortunato; Florio Lista; Francesco Giordani; Giovanni Faggioni; Massimo Di Benedetto; Nino D'Amore; Paola Stefanelli; Riccardo De Sanctis; Silvia Fillo; Stefano Fiore; Vanessa Vera Faïn
EPI_ISL_856880, EPI_ISL_856895, EPI_ISL_856896	Department of Infectious Diseases, Istituto Superiore di Sanità, Roma, Italy; Ospedale Riuniti, Laboratorio Virologia, Ancona, Italy	Virology Laboratory, Scientific Department, Army Medical Center	Alessandra Lo Presti; Angela Di Martino; Anna Anselmo; Antonella Fortunato; Florio Lista; Francesco Giordani; Giovanni Faggioni; Nino D'Amore; Paola Stefanelli; Patrizia Bagnarelli; Riccardo De Sanctis; Silvia Fillo; Stefano Fiore; Vanessa Vera Faïn
EPI_ISL_856881, EPI_ISL_856887	Department of Infectious Diseases, Istituto Superiore di Sanità, Roma, Italy; PO Cardarelli, Laboratorio Analisi Microbiologia e Virologia, Campobasso, Italy	Virology Laboratory, Scientific Department, Army Medical Center	Alessandra Lo Presti; Angela Di Martino; Anna Anselmo; Antonella Fortunato; Florio Lista; Francesco Giordani; Giovanni Faggioni; Massimiliano Sottelli; Nino D'Amore; Paola Stefanelli; Riccardo De Sanctis; Silvia Fillo; Stefano Fiore; Vanessa Vera Faïn
EPI_ISL_856908	Department of Infectious Diseases, Istituto Superiore di Sanità, Roma, Italy; PO Madre Teresa di Calcutta, UOC Laboratorio Analisi ULSS 6 Euganea, Padova, Italy	Virology Laboratory, Scientific Department, Army Medical Center	Alessandra Lo Presti; Angela Di Martino; Anna Anselmo; Antonella Fortunato; Florio Lista; Francesco Giordani; Giacomo Mezzapelle; Giovanni Faggioni; Nino D'Amore; Paola Stefanelli; Riccardo De Sanctis; Silvia Fillo; Stefano Fiore; Vanessa Vera Faïn
EPI_ISL_856884, EPI_ISL_856903	Department of Infectious Diseases, Istituto Superiore di Sanità, Roma, Italy; PO Santa Chiara, Microbiologia e Virologia, Trento, Italy	Virology Laboratory, Scientific Department, Army Medical Center	Alessandra Lo Presti; Angela Di Martino; Anna Anselmo; Antonella Fortunato; Florio Lista; Francesco Giordani; Giovanni Faggioni; Nino D'Amore; Paola Stefanelli; Paolo Lanzafame; Riccardo De Sanctis; Silvia Fillo; Stefano Fiore; Vanessa Vera Faïn
EPI_ISL_856886	Department of Infectious Diseases, Istituto Superiore di Sanità, Roma, Italy; PO Spirito Santo, UOC Microbiologia e Virologia Clinica, Pescara, Italy	Virology Laboratory, Scientific Department, Army Medical Center	Alessandra Lo Presti; Angela Di Martino; Anna Anselmo; Antonella Fortunato; Florio Lista; Francesco Giordani; Giovanni Faggioni; Nino D'Amore; Paola Stefanelli; Paolo Fazi; Riccardo De Sanctis; Silvia Fillo; Stefano Fiore; Vanessa Vera Faïn
EPI_ISL_856909	Department of Infectious Diseases, Istituto Superiore di	Virology Laboratory, Scientific Department, Army Medical	Alessandra Lo Presti; Angela Di Martino; Anna Anselmo; Antonella Fortunato; Florio Lista; Francesco Giordani; Giovanni Faggioni; Mario Rasseu; Nino

EPI_ISL_420785	FL Bureau of Health Laboratories Tampa	Pathogen Discovery, Respiratory Viruses Branch, Division of Viral Diseases, Centers for Disease Control and Prevention	Alison S. Lauffer Halpin; Anne Uehara; Christopher A. Elkins; Clinton R. Paden; Halbin Wang; Jasmine Padilla; Jing Zhang; Justin Lee; Krista Queen; Mary S. Keckler; Rachel Marine; Susang Tong; Yan Li; Ying Tao	
EPI_ISL_452110, EPI_ISL_452111, EPI_ISL_452132	FL Bureau of Public Health Laboratories	Pathogen Discovery, Respiratory Viruses Branch, Division of Viral Diseases, Centers for Disease Control and Prevention	Alison S. Lauffer Halpin; Anna Montmayeur; Anna Uehara; Christopher A. Elkins; Clinton R. Paden; Halbin Wang; Jing Zhang; Krista Queen; Mary S. Keckler; Rachel Marine; Susang Tong; Yan Li; Ying Tao; Zachary Weiner	
EPI_ISL_424853, EPI_ISL_424854	FL Bureau of Public Health Laboratories-Miami	Pathogen Discovery, Respiratory Viruses Branch, Division of Viral Diseases, Centers for Disease Control and Prevention	Alison S. Lauffer Halpin; Anna Uehara; Christopher A. Elkins; Clinton R. Paden; Halbin Wang; Jing Zhang; Krista Queen; Mary S. Keckler; Rachel Marine; Susang Tong; Yan Li; Ying Tao	
EPI_ISL_419559, EPI_ISL_419560, EPI_ISL_424855, EPI_ISL_447841, EPI_ISL_812138, EPI_ISL_812142, EPI_ISL_445277	FL Bureau of Public Health Laboratories-Tampa	Pathogen Discovery, Respiratory Viruses Branch, Division of Viral Diseases, Centers for Disease Control and Prevention	Alison S. Lauffer Halpin; Anna Montmayeur; Anna Uehara; Brian Lynch; Christopher A. Elkins; Clinton R. Paden; Halbin Wang; Jasmine Padilla; Jing Zhang; Justin Lee; Krista Queen; Mary S. Keckler; Peter Cook; Rachel Marine; Susang Tong; Yan Li; Ying Tao	
EPI_ISL_417010, EPI_ISL_418252	FUNDACION JIMENEZ DIAZ	Instituto de Salud Publica de Chile	Alejandro Acevedo; Andrés E Castillo; Bárbara Parra; Carolina Tambley; Gabriel Leal; Jaime Lagos; Jorge Fernandez; Loredana Arata; Patricia Bustos; Paz Tapia; Rodrigo Fasce; Winston Andrade	
EPI_ISL_526937, EPI_ISL_526938, EPI_ISL_526939, EPI_ISL_526940, EPI_ISL_526941, EPI_ISL_526943, EPI_ISL_526944	Fareose National Reference Laboratory for Fish and Animal Diseases	Fareose National Reference Laboratory for Fish and Animal Diseases	Debes Hammershaimb Christiansen; Maria Marjanodóttir Dahl; Petra Elisabeth Petersen	
EPI_ISL_451963, EPI_ISL_451966, EPI_ISL_451969, EPI_ISL_451970	Federal Budget Institution of Science, State Research Center for Applied Microbiology & Biotechnology	Federal Budget Institution of Science, State Research Center for Applied Microbiology & Biotechnology	Abaimova A; Bakhteva I; Blagodatskikh S; Bogun A; Borzillo A; Chekan I; Chernykh S; Denisenko E; Dentovskaya S; Detsushv K; Detsushva E; Dyatlov I; Firsova V; Frolov V; Fursov M; Fursova N; Galikina E; Gaspelchenkova T; Goncharova J; Gorbatov A; Hrybtseva A; Ivanov S; Kalmantayeva T; Kalmantayeva O; Kanashenko M; Kartayev N; Kartseva A; Khomyakova A; Khramov M; Kislchenko A; Kolchanova A; Koroleva-Ushakova A; Koslova I; Krasnikova E; Kuzin V; Kuzina E; Makarova M; Mann M; Novikova T; Piatonov M; Podkopaev Y; Ryabko A; Shaikhutdinova R; Shemyakin I; Shishkina L; Silina M; Sizova A; Skryabin Y; Slukin P; Slukina N; Solomentsev V; Solovieva A; Teymurtasov M; Timofeev V; Titareva G; Trunyakova A; Tyurin E; Vagayakaya A; Zemtsovskaya N; Zhuravskaya R	
EPI_ISL_480791, EPI_ISL_480796, EPI_ISL_480801, EPI_ISL_480802, EPI_ISL_480804, EPI_ISL_480805, EPI_ISL_480806, EPI_ISL_480812, EPI_ISL_489803, EPI_ISL_495332, EPI_ISL_495333, EPI_ISL_495334, EPI_ISL_495342, EPI_ISL_495344, EPI_ISL_495346, EPI_ISL_495347, EPI_ISL_495349, EPI_ISL_495350, EPI_ISL_495351, EPI_ISL_495355, EPI_ISL_495357, EPI_ISL_495359, EPI_ISL_495360, EPI_ISL_495363, EPI_ISL_495371, EPI_ISL_495388, EPI_ISL_495389, EPI_ISL_495390, EPI_ISL_495393, EPI_ISL_495394, EPI_ISL_495397, EPI_ISL_495398, EPI_ISL_495399, EPI_ISL_495400, EPI_ISL_495402, EPI_ISL_495403, EPI_ISL_495404, EPI_ISL_508743, EPI_ISL_508744, EPI_ISL_508745, EPI_ISL_508746, EPI_ISL_508748, EPI_ISL_508749, EPI_ISL_508755, EPI_ISL_508766, EPI_ISL_508767, EPI_ISL_508769, EPI_ISL_508771, EPI_ISL_508772, EPI_ISL_508773, EPI_ISL_508774, EPI_ISL_508775, EPI_ISL_508776, EPI_ISL_508777, EPI_ISL_508778, EPI_ISL_508779, EPI_ISL_508780, EPI_ISL_508781, EPI_ISL_508782, EPI_ISL_508784, EPI_ISL_508786, EPI_ISL_508787, EPI_ISL_508788, EPI_ISL_508790, EPI_ISL_508791, EPI_ISL_508792, EPI_ISL_508793, EPI_ISL_508794, EPI_ISL_508795, EPI_ISL_508796, EPI_ISL_508797, EPI_ISL_508798, EPI_ISL_508799, EPI_ISL_508800, EPI_ISL_508801, EPI_ISL_508802, EPI_ISL_508803, EPI_ISL_508805, EPI_ISL_508807, EPI_ISL_509716, EPI_ISL_509717, EPI_ISL_509718, EPI_ISL_509719, EPI_ISL_509721, EPI_ISL_509723, EPI_ISL_509724, EPI_ISL_509725, EPI_ISL_509726, EPI_ISL_509727, EPI_ISL_509728, EPI_ISL_509729, EPI_ISL_509730, EPI_ISL_509731, EPI_ISL_509732, EPI_ISL_509733, EPI_ISL_509734, EPI_ISL_509735, EPI_ISL_509736, EPI_ISL_509737, EPI_ISL_509738, EPI_ISL_509739, EPI_ISL_509740, EPI_ISL_509741, EPI_ISL_509742, EPI_ISL_509743, EPI_ISL_509745, EPI_ISL_509746, EPI_ISL_509747, EPI_ISL_509748, EPI_ISL_509749, EPI_ISL_509750, EPI_ISL_509751, EPI_ISL_509752, EPI_ISL_509753, EPI_ISL_509754, EPI_ISL_509755, EPI_ISL_509756, EPI_ISL_509757, EPI_ISL_509758, EPI_ISL_509759, EPI_ISL_509760, EPI_ISL_509761, EPI_ISL_509762, EPI_ISL_509763, EPI_ISL_509764, EPI_ISL_509765, EPI_ISL_509766, EPI_ISL_509767, EPI_ISL_509769, EPI_ISL_509771, EPI_ISL_509772, EPI_ISL_509773, EPI_ISL_509774, EPI_ISL_514140, EPI_ISL_514141, EPI_ISL_514142, EPI_ISL_514143, EPI_ISL_514144, EPI_ISL_517871, EPI_ISL_526580, EPI_ISL_526581, EPI_ISL_569681, EPI_ISL_653153, EPI_ISL_653157, EPI_ISL_653181, EPI_ISL_653185, EPI_ISL_653253, EPI_ISL_653254, EPI_ISL_653255, EPI_ISL_653256, EPI_ISL_653257, EPI_ISL_653258, EPI_ISL_653261, EPI_ISL_653262, EPI_ISL_653265, EPI_ISL_653266, EPI_ISL_653267, EPI_ISL_653268	Florida Bureau of Public Health Laboratories Florida Bureau of Public Health Laboratories, Florida Department of Health Florida Bureau of Public Health Laboratories Florida Bureau of Public Health Laboratories, Florida Department of Health	Jason Blanton; Sarah Schmedes Blanton, J.; Schmedes, S.		
EPI_ISL_455903, EPI_ISL_476139	see above EPI_ISL_470882 Foerde Hospital, Department of Microbiology	Flushing Hospital Medical Center New York City Public Health Laboratory Norwegian Institute of Public Health, Department of Virology The Public Health Agency of Sweden	Hilde Elishaug; Kamilla Heddeland Intestjord; Karoline Bragstad; Kathrine Stene-Johansen; Olav Hungnes; Rasmus Riis Kopperud Anna Risberg; Anna-Malin Linde; Karin Tegmark-Waell; Maria Lind Karlberg; Mattias Hauklund; Olov Svartstrom; Oskar Karlsson Lindjo; Petra Edquist; Reza Advani; Sandra Brodteson; Shamm Mursadskoi	
EPI_ISL_434650, EPI_ISL_475538	EPI_ISL_413587	Folling Halsocentral Foundation Elisabeth-Tweesteden Ziekenhuis	The Public Health Agency of Sweden Erasmus Medical Center	Anna Risberg; Anna-Malin Linde; Karin Tegmark-Waell; Kerstin Persson Moberg; Maria Lind Karlberg; Mattias Hauklund; Mia Byting; Olov Svartstrom; Oskar Karlsson Lindjo; Reza Advani; Sandra Brodteson; Theresa Ernkich Anne van der Linden; Anneliek van der Eijk; Aura Timen; Bas Oude Munnink; Claudia Schapendonk; Corien Swaan; Corine GeurtsvanKessel; David Nieuwenhuijse; Irina Chestakova; Jeroen van Kampen; Jolanda Voermans; Madelief Mullers; Manon Koopmans; Mark Pronk; Mart Stein; Pascal Leomond; Reina Sikkema; Richard Molenkamp; Sandra Kengma Mbouou; on behalf of the Dutch national COVID-19 response team.
EPI_ISL_411060, EPI_ISL_411066, EPI_ISL_431118, EPI_ISL_431180, EPI_ISL_431240, EPI_ISL_431782, EPI_ISL_431783, EPI_ISL_431784, EPI_ISL_431785	see above EPI_ISL_862839, EPI_ISL_862857	Fujian Center for Disease Control and Prevention Fujita Health University Bantane Hospital	Fujian Center for Disease Control and Prevention Fujita Health University, School of Medicine, Department of Microbiology	Chen Wei; He Wenxiang; Huang Xingmin; Lin Qi; Weng Yuwei; Zhang Yanhua Masahiro Suzuki; Yohei Doi
EPI_ISL_862837, EPI_ISL_862838, EPI_ISL_862840, EPI_ISL_862841, EPI_ISL_728000	EPI_ISL_728206, EPI_ISL_728207, EPI_ISL_728208	Fujita Health University Hospital Fujita Health University Okazaki Medical Center	Fujita Health University, School of Medicine, Department of Microbiology Department of Virology and Parasitology, Fujita Health University School of Medicine	Masahiro Suzuki; Yohei Doi Aki Sakurai; Masahiro Suzuki; Satoshi Komoto; Takayuki Murata; Takuma Ishihara; Tomihiko Ide; Yohei Doi
EPI_ISL_718273, EPI_ISL_727998, EPI_ISL_727999, EPI_ISL_728153, EPI_ISL_728154, EPI_ISL_728155, EPI_ISL_728156, EPI_ISL_728159	see above	Fujita Health University Okazaki Medical Center	Department of Virology and Parasitology, Fujita Health University School of Medicine	Aki Sakurai; Masahiro Suzuki; Satoshi Komoto; Takayuki Murata; Takuma Ishihara; Tomihiko Ide; Yohei Doi
EPI_ISL_479967, EPI_ISL_479968, EPI_ISL_479969, EPI_ISL_479970, EPI_ISL_479971, EPI_ISL_479972, EPI_ISL_479973, EPI_ISL_479974, EPI_ISL_479975, EPI_ISL_479976, EPI_ISL_479977, EPI_ISL_479978, EPI_ISL_480120, EPI_ISL_480121, EPI_ISL_480122, EPI_ISL_480123, EPI_ISL_480124, EPI_ISL_480125, EPI_ISL_480126, EPI_ISL_480129	see above	Fukui Prefectural Institute of Public Health and Environmental Science	Pathogen Genomics Center, National Institute of Infectious Diseases	Aki Sakurai; Masahiro Suzuki; Satoshi Komoto; Takayuki Murata; Takuma Ishihara; Tomihiko Ide; Yohei Doi Hajime Kamiya; Kentaro Itokawa; Makoto Kuroda; Masanori Hashino; Miho Toho; Motoki Suzuki; Rina Tanaka; Tsuyoshi Sekizuka
EPI_ISL_684421, EPI_ISL_684422, EPI_ISL_684425, EPI_ISL_684434, EPI_ISL_684435, EPI_ISL_684436, EPI_ISL_684437, EPI_ISL_684438, EPI_ISL_684439	see above	Fukuoka Institute of Health and Environmental Sciences	Pathogen Genomics Center, National Institute of Infectious Diseases	Kentaro Itokawa; Makoto Kuroda; Masanori Hashino; Rina Tanaka; Tsuyoshi Sekizuka
EPI_ISL_419235, EPI_ISL_419236, EPI_ISL_419237	EPI_ISL_482447, EPI_ISL_462448, EPI_ISL_462449	Fundacion Jimenez Diaz Fundació Lluís contra la SIDA (FLSida)/Hospital Universitari Germans Trias i Pujol	Instituto de Salud Carlos III IiSxixa AIDS Research Lab	Camarero, S.; Casas, I.; Cuesta, I.; Fernández, R.; González-Espiguelias, M.; Iglesias-Caballero, M.; Jiménez, M.; Jiménez, P.; Juliá, M.; Molinero Calamita, M.; Morón, S.; Pozo, F.; Varona, S.; Zaballós, A. Bonaventura Clotet; Joaquim Segalés; Jorge Carrillo; Julia Blanco; Lidia Ruiz; Marc Corbacho; Marc Noguera-Julian; Maria Pilar Armergot; Maria Ubals; Mariona Parera; Nuria Izquierdo; Oriol Miñá; Roger Paredes

EPI_ISL_462478	Fundación Jiménez Díaz	Instituto de Salud Carlos III	A. Monzón; F. Casas; I. J. Jiménez; Iglesias-Caballero; M. Camarero; M. Cuesta; M. González-Esguevillas; M. Molinero Calamita; M. Zaballos; P. Jiménez; R. Fernández; S. Juliá; S. Pozo; S. Varona
EPI_ISL_420313	Furst Medical Laboratory	Norwegian Institute of Public Health, Department of Virology	Hilde Elshaug; Kamilla Heddeland Instefjord; Karoline Bragstad; Kathrine Stene-Johansen; Olav Hungnes
EPI_ISL_522549	Félix Guyon Hospital	UMR PHMIT Université de La Réunion	Camille Lebarbenchon; David Wilkinson; Patrick Mavingui
EPI_ISL_420786, EPI_ISL_420787, EPI_ISL_420788	GA Department of Public Health	Pathogen Discovery, Respiratory Viruses Branch, Division of Viral Diseases, Centers for Disease Control and Prevention	Alison S. Lauffer Halpin; Anne Uehara; Christopher A. Elkins; Clinton R. Paden; Habin Wang; Jasmine Padilla; Jing Zhang; Justin Lee; Krista Queen; Mary S. Keckler; Rachel Marine; Suxiang Tong; Yan Li; Ying Tao
EPI_ISL_419556, EPI_ISL_419557, EPI_ISL_424858, EPI_ISL_424859, EPI_ISL_424861, EPI_ISL_424864, EPI_ISL_426417	GA Department of Public Health Laboratory	Pathogen Discovery, Respiratory Viruses Branch, Division of Viral Diseases, Centers for Disease Control and Prevention	Alison S. Lauffer Halpin; Anne Uehara; Christopher A. Elkins; Clinton R. Paden; Habin Wang; Jasmine Padilla; Jing Zhang; Justin Lee; Krista Queen; Mary S. Keckler; Rachel Marine; Suxiang Tong; Yan Li; Ying Tao
EPI_ISL_418416, EPI_ISL_508679, EPI_ISL_509003, EPI_ISL_509004	GH Les Portes du Sud	CNR Virus des Infections Respiratoires - France SUD	Alexandre Gaymard; Antonin Bal; Bruno Lina; Carine Moustaud; Florence Morfin-Sherpa; Gregory Desiras; Gwendolyne Burfin; Laurence Josset; Martine Valette; Maude Bouscambert-Duchamp; Raphaëlle Lamy; Solenne Brun
EPI_ISL_428351, EPI_ISL_428352, EPI_ISL_428363	GH Nord Essonne Service de Biologie clinique	National Reference Center for Viruses of Respiratory Infections, Institut Pasteur, Paris	Angela Brisebarre; Etienne Simon-Lorère; Flora Donati; Marion Barbet; Maud Vanpeene; Melanie Albert; Méline Bizard; Sylvie Behilli; Sylvie van der Werf; Vincent Enouf
EPI_ISL_583429, EPI_ISL_583434, EPI_ISL_583463, EPI_ISL_583464, EPI_ISL_583467	García-Sastre Laboratory, Department of Microbiology, Icahn School of Medicine at Mount Sinai	van Bavel Laboratory, Genetics and Genomics Sciences, Icahn School of Medicine at Mount Sinai	Adolfo García-Sastre; Adriana van de Guchte; Ajay Obla; Ana S. González-Reiche; Genovefa Papanicolaou; Gurjani Shah; Harm van Bavel; Jayeeta Dutta; Judith Aberg; Kent Sepkowitz; Miguei-Angel Perales; Ngolela Esther Babady; Sadaf Aslam; Teresa Aydllo; Tobias Hohl; Zenab Khan; and Mini Kambaj
EPI_ISL_475110, EPI_ISL_475115	Gavle klinisk mikrobiologi	The Public Health Agency of Sweden	Anna Risberg; Anna-Malin Lind; Karin Tegmark-Wisell; Maria Lind Karberg; Mattias Haukland; Olov Svarstom; Oskar Karlsson Lindskog; Petra Edquist; Reza Advani; Sandra Brodesson; Shamam Mularasoli
EPI_ISL_420855, EPI_ISL_420876, EPI_ISL_420877, EPI_ISL_430064	Geelong Centre for Emerging Infectious Diseases	Geelong Centre for Emerging Infectious Diseases	Alexandersen S.; Bhatta T.R.; Chamings A.; Chamings, A.; Raj Bhatta T.
EPI_ISL_406799, EPI_ISL_406800, EPI_ISL_406801	General Hospital of Central Theater Command of People's Liberation Army of China	BOI & Institute of Microbiology, Chinese Academy of Sciences & Shandong First Medical University & Shandong Academy of Medical Sciences & General Hospital of Central Theater Command of People's Liberation Army of China	Weileng Shi and Zhenhong Hu; Weijun Chen; Yuhai Bi
EPI_ISL_1167779, EPI_ISL_1167782, EPI_ISL_1167789, EPI_ISL_1167793, EPI_ISL_1167807, EPI_ISL_1167821, EPI_ISL_1167824, EPI_ISL_1167830	Genetica Molecular and Subdepartamento de Virología ISP Chile	Instituto de Salud Pública de Chile	Andrés Castillo; Barbara Parra; Giselle Barra; Jaime Lagos; Javier Tognarelli; Jorge Fernandez; Karen Orostica; Loredana Arata; Patricia Bustos; Rodrigo Fasce
EPI_ISL_452120, EPI_ISL_452125	Georgia Department of Health	Pathogen Discovery, Respiratory Viruses Branch, Division of Viral Diseases, Centers for Disease Control and Prevention	Alison S. Lauffer Halpin; Anna Montmayeur; Anna Uehara; Christopher A. Elkins; Clinton R. Paden; Habin Wang; Jing Zhang; Krista Queen; Mary S. Keckler; Rachel Marine; Suxiang Tong; Yan Li; Ying Tao; Zachary Weiner
EPI_ISL_594456	Georgia Public Health Laboratory	Pathogen Discovery, Respiratory Viruses Branch, Division of Viral Diseases, Centers for Disease Control and Prevention	Anna Uehara; Clinton Paden; Habin Wang; Jing Zhang; Julu Bhatnagar; Krista Queen; Suxiang Tong; Yan Li; Ying Tao
EPI_ISL_539504, EPI_ISL_862567, EPI_ISL_862640	Gerencia de Asistencia Sanitaria de Soria	Instituto de Salud Carlos III	A. Monzón; C. Aldes; F. Casas; I. J. Jiménez; Iglesias-Caballero; M. Camarero; M. Cuesta; M. González-Esguevillas; M. Molinero Calamita; M. Zaballos; P. Jiménez; S. Juliá; S. Pozo; S. Varona
EPI_ISL_539557	Gerencia del área de salud de Badajoz, Llerena y Zafra	Instituto de Salud Carlos III	A. Monzón; C. Pazos; F. Casas; I. J. Jiménez; Iglesias-Caballero; M. Camarero; M. Cuesta; M. González-Esguevillas; M. Molinero Calamita; M. Zaballos; P. Jiménez; S. Juliá; S. Pozo; S. Varona
EPI_ISL_480083, EPI_ISL_480084, EPI_ISL_480085, EPI_ISL_480086, EPI_ISL_480087, EPI_ISL_480088, EPI_ISL_480089	Gifu Prefectural Institute of Public Health and Environmental Sciences	Pathogen Genomics Center, National Institute of Infectious Diseases	Hajime Kamiya; Kentaro Itokawa; Makoto Kuroda; Masanori Hashino; Moto Suzuki; Rina Tanaka; Tsuyoshi Sekizuka; Yoshihiko Kameyama
EPI_ISL_452221	Goethe University Hospital Frankfurt	Institute for Medical Virology, Goethe University Hospital Frankfurt	Anemarie Berger; Björn Rotter; Denisa Bojkova; Jindrich Cinat; Klaus Hoffmeier; Sandra Westhaus; Sandra Ciesek; Sebastian Hoehli; Tuna Toptan; and Marek Widera
EPI_ISL_1225382	Gorgas Memorial Laboratory of Health Studies	Gorgas Memorial Laboratory of Health Studies	Adriana Weedon; Alejandra Valoy; Alexander Martinez; Ambar Moreno; Anyuri Ortiz; Brechla Moreno; Claudia Gonzalez; Daniel Castillo; Danilo Franco; Dave Beltran; Dimetza Arauz; Elimelec Valdespino; Gretel Vasquez; Ika Guerra; Isela Guerrero; Jessica Gondola; Jim Chang; Juan Miguel Pascale; Layda Abrego; Lisseth Saenz; Mabel Martinez-Montero; Maria Chai-German; Mariela Castillo; Melissa Gaitan; Oris Chavama; Rita Corrales; Rita Rodriguez; Sandra Lopez-Verges; Yamika Diaz; Yaneth Pitti; Zumara Chaverra
EPI_ISL_640040, EPI_ISL_640043, EPI_ISL_1040818, EPI_ISL_1040822	Groote Schuur Hospital w/ GSH	NHLS/UCT	Arash Iranzadeh; Bruna Galvão; Carolyn Williamson; Deelan Doolabh; Diana Hardie; Innocent Ndaband; Kruger Marais; Lynn Tyers; Marvin Hsiao; Stephen Korsman
EPI_ISL_447734, EPI_ISL_447735, EPI_ISL_447736, EPI_ISL_447738, EPI_ISL_447739, EPI_ISL_447740, EPI_ISL_447741, EPI_ISL_447742, EPI_ISL_447743, EPI_ISL_447744, EPI_ISL_447745, EPI_ISL_447746, EPI_ISL_447747, EPI_ISL_447748, EPI_ISL_447750, EPI_ISL_447754	Grupo de Investigaciones Microbiológicas-UR (GIMUR), Departamento de Biología, Facultad de Ciencias Naturales, Universidad del Rosario, Bogotá, Colombia	Grupo de Investigaciones Microbiológicas-UR (GIMUR), Departamento de Biología, Facultad de Ciencias Naturales, Universidad del Rosario, Bogotá, Colombia Icahn School of Medicine at Mount Sinai, New York, USA	Adriana Castillo; Alberto Paniz-Mondolfi; Ana S. González-Reiche; Angelica Rico; Anibal A. Tellerán; Carolina Florez; Carolina Hernandez; David Martinez; Emilia Mia Sordillo; Esther C. Barros; Harm van Bavel; Jesse E. James; Juan David Ramirez; Laura Vega; Lisseth Pardo; Marina Muñoz; Martha L. Ospina; Matthew M. Hernandez; Nathalia Ballesteros; Sergio Castañeda; Sergio Gomez; Viviana Simon
EPI_ISL_406531	Guangdong Provincial Center for Diseases Control and Prevention; Guangdong Provincial Public Health	Guangdong Provincial Center for Disease Control and Prevention	Baisheng Li; Changwen Ke; Feng Ruan; Guanhao He; Haojie Zhong; Huhong Deng; Jianfeng He; Jianpeng Xiao; Jianxiang Geng; Jianxiong Hu; Jie Wu; Jing Lu; Lifeng Lin; Lijun Liang; Lirong Zou; Min Kang; Qi Zhu; Shujang Mei; Songjian Xiao; Tao Liu; Tie Song; Weilin Zeng; Wenjun Ma; Xing Li; Xujuan Tang; Xue Zhuang; Xuguang Chen; Ying Wang; Yingchao Song; Yingtao Zhang; Yuhuang Liao; Zhe Liu
EPI_ISL_406533	Guangdong Provincial Center for Diseases Control and Prevention; Guangdong Provincial Public Health	Guangdong Provincial Center for Diseases Control and Prevention	Baisheng Li; Changwen Ke; Feng Ruan; Guanhao He; Haojie Zhong; Huhong Deng; Jianfeng He; Jianpeng Xiao; Jianxiang Geng; Jianxiong Hu; Jie Wu; Jing Lu; Lifeng Lin; Lijun Liang; Lirong Zou; Min Kang; Qi Zhu; Shujang Mei; Songjian Xiao; Tao Liu; Tie Song; Weilin Zeng; Wenjun Ma; Xing Li; Xujuan Tang; Xue Zhuang; Xuguang Chen; Ying Wang; Yingchao Song; Yingtao Zhang; Yuhuang Liao; Zhe Liu
EPI_ISL_403932, EPI_ISL_403933, EPI_ISL_403934, EPI_ISL_403935, EPI_ISL_403936, EPI_ISL_403937	Guangdong Provincial Center for Diseases Control and Prevention; Guangdong Provincial Public Health	Department of Microbiology, Guangdong Provincial Center for Diseases Control and Prevention	Baisheng Li; Changwen Ke; Feng Ruan; Guanhao He; Haojie Zhong; Huhong Deng; Jianfeng He; Jianpeng Xiao; Jianxiang Geng; Jianxiong Hu; Jie Wu; Jing Lu; Lifeng Lin; Lijun Liang; Lirong Zou; Min Kang; Qi Zhu; Shujang Mei; Songjian Xiao; Tao Liu; Tie Song; Weilin Zeng; Wenjun Ma; Xing Li; Xujuan Tang; Xue Zhuang; Xuguang Chen; Ying Wang; Yingchao Song; Yingtao Zhang; Yuhuang Liao; Zhe Liu
EPI_ISL_406534, EPI_ISL_406535, EPI_ISL_406536	Guangdong Provincial Center for Diseases Control and Prevention; Guangdong Provincial Public Health	Guangdong Provincial Center for Diseases Control and Prevention	Baisheng Li; Changwen Ke; Feng Ruan; Guanhao He; Haojie Zhong; Huhong Deng; Jianfeng He; Jianpeng Xiao; Jianxiang Geng; Jianxiong Hu; Jie Wu; Jing Lu; Lifeng Lin; Lijun Liang; Lirong Zou; Min Kang; Qi Zhu; Shujang Mei; Songjian Xiao; Tao Liu; Tie Song; Weilin Zeng; Wenjun Ma; Xing Li; Xujuan Tang; Xue Zhuang; Xuguang Chen; Ying Wang; Yingchao Song; Yingtao Zhang; Yuhuang Liao; Zhe Liu
EPI_ISL_406538	Guangdong Provincial Center for Diseases Control and Prevention; Guangdong Provincial Institute of Public Health	Guangdong Provincial Center for Diseases Control and Prevention	Baisheng Li; Changwen Ke; Feng Ruan; Guanhao He; Haojie Zhong; Huhong Deng; Jianfeng He; Jianpeng Xiao; Jianxiang Geng; Jianxiong Hu; Jie Wu; Jing Lu; Lifeng Lin; Lijun Liang; Lirong Zou; Min Kang; Qi Zhu; Shujang Mei; Songjian Xiao; Tao Liu; Tie Song; Weilin Zeng; Wenjun Ma; Xing Li; Xujuan Tang; Xue Zhuang; Xuguang Chen; Ying Wang; Yingchao Song; Yingtao Zhang; Yuhuang Liao; Zhe Liu
EPI_ISL_428441, EPI_ISL_428442, EPI_ISL_428443, EPI_ISL_428444, EPI_ISL_428445, EPI_ISL_428446, EPI_ISL_428447, EPI_ISL_428448, EPI_ISL_428449, EPI_ISL_428450, EPI_ISL_428451, EPI_ISL_428452, EPI_ISL_428453, EPI_ISL_428454, EPI_ISL_428455, EPI_ISL_428456, EPI_ISL_428457, EPI_ISL_428458, EPI_ISL_428459, EPI_ISL_428460, EPI_ISL_428461, EPI_ISL_428462, EPI_ISL_428463, EPI_ISL_428464, EPI_ISL_428465, EPI_ISL_428466, EPI_ISL_428467, EPI_ISL_428468, EPI_ISL_428469, EPI_ISL_428470, EPI_ISL_428471, EPI_ISL_428472, EPI_ISL_428473, EPI_ISL_428474, EPI_ISL_428475, EPI_ISL_428476, EPI_ISL_428477, EPI_ISL_428478	Guangdong Provincial Center for Diseases Control and Prevention; Guangdong Provincial Institute of Public Health	School of Public Health, The University of Hong Kong	Bosheng Li; Hann Zeng; Haoguo Gu; Hui-Ling Yen; Jie Wu; Leo L.M. Poon; Lijun Liang; Tie Song; Yao Hu; Yingchao Song; Zhenhui Li
EPI_ISL_413851, EPI_ISL_413852, EPI_ISL_413853, EPI_ISL_413854, EPI_ISL_413855, EPI_ISL_413856, EPI_ISL_413857, EPI_ISL_413858, EPI_ISL_413860, EPI_ISL_413861, EPI_ISL_413862, EPI_ISL_413863, EPI_ISL_413864, EPI_ISL_413866, EPI_ISL_413867, EPI_ISL_413875, EPI_ISL_413884			

see above	Guangdong Provincial Institution of Public Health, Guangdong Provincial Center for Disease Control and Prevention	Guangdong Provincial Institution of Public Health	Andrew Rambaut; Bo Peng; Changwen Ke; Chuming Liang; Huangying Zheng; Hufang Lin; Jing Lu; Jingju Peng; Jufeng Sun; Josh Quick; Juan Su; Kang Min; Kubiao Li; Liliang Zeng; Liu Zhe; Louis du Plessis; Mingfeng Liang; Moritz Kraemer; Nick Loman; Nuno Faria; Oliver Pybus; Pingping Zhou; Qianlin Xiong; Ru bai; Rulin Sun; Runyu Yuan; Sarah François; Sheng Fang; Song Tie; Tao Lu; Verity Hill; Wei Li; Wenjun Ma; Wenzhe Su; Xi Tang
EPI_ISL_509695, EPI_ISL_509696, EPI_ISL_509697, EPI_ISL_509698, EPI_ISL_509699, EPI_ISL_509700, EPI_ISL_509701, EPI_ISL_509702, EPI_ISL_509703, EPI_ISL_509710	Guatemala Ministry of Public Health	Pathogen Discovery, Respiratory Viruses Branch, Division of Viral Diseases, Centers for Disease Control and Prevention	Anna Uehara; Clinton Paden; Habibi Wang; Jing Zhang; Krista Queen; Suxiang Tong; Yan Li; Ying Tao
see above	Guatemala Ministry of Public Health	Kabara Cancer Research Institute	Craig S. Richmond & Parica A. Kenny
EPI_ISL_418186	Gundersen Molecular Diagnostic Laboratory	Kabara Cancer Research Institute	Craig S. Richmond; Craig S. Richmond & Parica A. Kenny; Parica A. Kenny
EPI_ISL_418184, EPI_ISL_418187, EPI_ISL_418188, EPI_ISL_419651, EPI_ISL_419652, EPI_ISL_422453, EPI_ISL_422465	Gundersen Molecular Diagnostic Laboratory	Kabara Cancer Research Institute	Craig S. Richmond; Craig S. Richmond & Parica A. Kenny; Parica A. Kenny
see above	Gundersen Molecular Diagnostic Laboratory	Kabara Cancer Research Institute	Craig S. Richmond; Craig S. Richmond & Parica A. Kenny; Parica A. Kenny
EPI_ISL_479850, EPI_ISL_479851, EPI_ISL_479853, EPI_ISL_479854, EPI_ISL_479896, EPI_ISL_479897, EPI_ISL_479898, EPI_ISL_479899, EPI_ISL_479900, EPI_ISL_479901, EPI_ISL_480015, EPI_ISL_480016, EPI_ISL_480017, EPI_ISL_480018, EPI_ISL_480019, EPI_ISL_480020	Gunma Prefectural Institute of Public Health and Environmental Sciences	Pathogen Genomics Center, National Institute of Infectious Diseases	Hajime Kamiya; Hiroyuki Tsukagoshi; Kentaro Itokawa; Makoto Kuroda; Masanori Hashino; Motoki Suzuki; Rina Tanaka; Tsuyoshi Sekizuka
see above	Gunma Prefectural Institute of Public Health and Environmental Sciences	Pathogen Genomics Center, National Institute of Infectious Diseases	Hajime Kamiya; Hiroyuki Tsukagoshi; Kentaro Itokawa; Makoto Kuroda; Masanori Hashino; Motoki Suzuki; Rina Tanaka; Tsuyoshi Sekizuka
EPI_ISL_421454, EPI_ISL_421458, EPI_ISL_421481, EPI_ISL_421487, EPI_ISL_421491	H Beatriz Angelo	Instituto Nacional de Saude (INSA)	Guiomar et al
EPI_ISL_418003, EPI_ISL_418007, EPI_ISL_418008, EPI_ISL_418019, EPI_ISL_418020, EPI_ISL_418021, EPI_ISL_418022	H Braga	Instituto Nacional de Saude (INSA)	Guiomar et al
see above	H Braga	Instituto Nacional de Saude (INSA)	Guiomar et al
EPI_ISL_421457	H Dr Nello Mendonca - Funchal	Instituto Nacional de Saude (INSA)	Guiomar et al
EPI_ISL_418026, EPI_ISL_421449, EPI_ISL_421459, EPI_ISL_421460, EPI_ISL_421461	H Dr. Nello Mendonca - Funchal	Instituto Nacional de Saude (INSA)	Guiomar et al
EPI_ISL_418023, EPI_ISL_421466, EPI_ISL_421467	H Evora	Instituto Nacional de Saude (INSA)	Guiomar et al
EPI_ISL_418018	H Garcia de Orta	Instituto Nacional de Saude (INSA)	Guiomar et al
EPI_ISL_421446, EPI_ISL_421447, EPI_ISL_421448	H Guimaraes	Instituto Nacional de Saude (INSA)	Guiomar et al
EPI_ISL_418025, EPI_ISL_421462, EPI_ISL_421468, EPI_ISL_421469, EPI_ISL_421470, EPI_ISL_421471, EPI_ISL_421488, EPI_ISL_421490, EPI_ISL_421492, EPI_ISL_421495	H Santarem	Instituto Nacional de Saude (INSA)	Guiomar et al
see above	H Santarem	Instituto Nacional de Saude (INSA)	Guiomar et al
EPI_ISL_455587	H.R.H. Maha Chakri Sirindhorn Medical Center	National Institute of Health, Department of medical Sciences, Ministry of Public Health, Thailand	Chittagangpich; Malinee; Okada; Pammen; Phuygun; Pitaluk; Siripaporn; Stipporn; Sunthareeya; Thanadachakul; Thanuapa; Waicharoen; Warawan; Wongboot
EPI_ISL_426420, EPI_ISL_426421	HI Dept. of Health, State Laboratories Division	Pathogen Discovery, Respiratory Viruses Branch, Division of Viral Diseases, Centers for Disease Control and Prevention	Alison S. Laifer Halpin; Anna Uehara; Christopher A. Elkins; Clinton R. Paden; Habibi Wang; Jing Zhang; Krista Queen; Mary S. Keckler; Rachel Marine; Suxiang Tong; Yan Li; Ying Tao
EPI_ISL_445323	HOSP. ENFERMEDADES INFECCIOSAS	Instituto de Salud Publica de Chile	Alejandra Acevedo; Andrés E Castillo; Bárbara Parra; Carolina Tambley; Gabriel Leal; Jaime Lagos; Jorge Fernandez; Loredana Arata; Patricia Bustos; Paz Tapia; Rodrigo Fasce; Winston Andrade
EPI_ISL_445321	HOSPITAL CLINICO DEL SUR	Instituto de Salud Publica de Chile	Alejandra Acevedo; Andrés E Castillo; Bárbara Parra; Carolina Tambley; Gabriel Leal; Jaime Lagos; Jorge Fernandez; Loredana Arata; Patricia Bustos; Paz Tapia; Rodrigo Fasce; Winston Andrade
EPI_ISL_445275	HOSPITAL CLINICO FUSAT	Instituto de Salud Publica de Chile	Alejandra Acevedo; Andrés E Castillo; Bárbara Parra; Carolina Tambley; Gabriel Leal; Jaime Lagos; Jorge Fernandez; Loredana Arata; Patricia Bustos; Paz Tapia; Rodrigo Fasce; Winston Andrade
EPI_ISL_445335	HOSPITAL DE CALBUCO	Instituto de Salud Publica de Chile	Alejandra Acevedo; Andrés E Castillo; Bárbara Parra; Carolina Tambley; Gabriel Leal; Jaime Lagos; Jorge Fernandez; Loredana Arata; Patricia Bustos; Paz Tapia; Rodrigo Fasce; Winston Andrade
EPI_ISL_445251, EPI_ISL_445305	HOSPITAL DE CARABINEROS	Instituto de Salud Publica de Chile	Alejandra Acevedo; Andrés E Castillo; Bárbara Parra; Carolina Tambley; Gabriel Leal; Jaime Lagos; Jorge Fernandez; Loredana Arata; Patricia Bustos; Paz Tapia; Rodrigo Fasce; Winston Andrade
EPI_ISL_419238	HOSPITAL DE CRUCES.	Instituto de Salud Carlos III	A. Monzón; F. Casas; I. Aranzamendi, M.; I. Jiménez; Iglesias-Caballero; M. Camarero; M. Cuesta; M. González-Eguavillas; M. Molinero Calamita; M. Zaballos; P. Jiménez; S. Juliá; S. Pozo; S. Varona
EPI_ISL_445300	HOSPITAL DE RANCAGUA	Instituto de Salud Publica de Chile	Alejandra Acevedo; Andrés E Castillo; Bárbara Parra; Carolina Tambley; Gabriel Leal; Jaime Lagos; Jorge Fernandez; Loredana Arata; Patricia Bustos; Paz Tapia; Rodrigo Fasce; Winston Andrade
EPI_ISL_445360, EPI_ISL_445368	HOSPITAL DEL PROFESOR	Instituto de Salud Publica de Chile	Alejandra Acevedo; Andrés E Castillo; Bárbara Parra; Carolina Tambley; Gabriel Leal; Jaime Lagos; Jorge Fernandez; Loredana Arata; Patricia Bustos; Paz Tapia; Rodrigo Fasce; Winston Andrade
EPI_ISL_445270, EPI_ISL_445340, EPI_ISL_445342, EPI_ISL_445343, EPI_ISL_445344, EPI_ISL_445345, EPI_ISL_445346, EPI_ISL_445347, EPI_ISL_445348, EPI_ISL_447119	HOSPITAL DR.HERNAN HENRIQUEZ ARAVENA	Instituto de Salud Publica de Chile	Alejandra Acevedo; Andrés E Castillo; Bárbara Parra; Carolina Tambley; Gabriel Leal; Jaime Lagos; Jorge Fernandez; Loredana Arata; Patricia Bustos; Paz Tapia; Rodrigo Fasce; Winston Andrade
see above	HOSPITAL DR.HERNAN HENRIQUEZ ARAVENA	Instituto de Salud Publica de Chile	Alejandra Acevedo; Andrés E Castillo; Bárbara Parra; Carolina Tambley; Gabriel Leal; Jaime Lagos; Jorge Fernandez; Loredana Arata; Patricia Bustos; Paz Tapia; Rodrigo Fasce; Winston Andrade
EPI_ISL_445310, EPI_ISL_445329, EPI_ISL_445365, EPI_ISL_445366, EPI_ISL_445371	HOSPITAL DR.SOTERO DEL RIO	Instituto de Salud Publica de Chile	Alejandra Acevedo; Andrés E Castillo; Bárbara Parra; Carolina Tambley; Gabriel Leal; Jaime Lagos; Jorge Fernandez; Loredana Arata; Patricia Bustos; Paz Tapia; Rodrigo Fasce; Winston Andrade
EPI_ISL_445313, EPI_ISL_445314, EPI_ISL_445364	HOSPITAL EL CARMEN DR.LUIS VALENTIN F.	Instituto de Salud Publica de Chile	Alejandra Acevedo; Andrés E Castillo; Bárbara Parra; Carolina Tambley; Gabriel Leal; Jaime Lagos; Jorge Fernandez; Loredana Arata; Patricia Bustos; Paz Tapia; Rodrigo Fasce; Winston Andrade
EPI_ISL_445372	HOSPITAL FF.AA. "CIRUJANO C. GUZMAN	Instituto de Salud Publica de Chile	Alejandra Acevedo; Andrés E Castillo; Bárbara Parra; Carolina Tambley; Gabriel Leal; Jaime Lagos; Jorge Fernandez; Loredana Arata; Patricia Bustos; Paz Tapia; Rodrigo Fasce; Winston Andrade
EPI_ISL_418247	HOSPITAL GENERAL DE SEGOVIA	Instituto de Salud Carlos III	A. Monzón; F. Casas; I. Hernando-Real S.; I. Jiménez; Iglesias-Caballero; M. Camarero; M. Cuesta; M. González-Eguavillas; M. Molinero Calamita; M. Zaballos; P. Jiménez; S. Juliá; S. Pozo; S. Varona
EPI_ISL_445286	HOSPITAL HANGA ROA	Instituto de Salud Publica de Chile	Alejandra Acevedo; Andrés E Castillo; Bárbara Parra; Carolina Tambley; Gabriel Leal; Jaime Lagos; Jorge Fernandez; Loredana Arata; Patricia Bustos; Paz Tapia; Rodrigo Fasce; Winston Andrade
EPI_ISL_445331, EPI_ISL_445332	HOSPITAL HERMINDA MARTIN CHILLAN	Instituto de Salud Publica de Chile	Alejandra Acevedo; Andrés E Castillo; Bárbara Parra; Carolina Tambley; Gabriel Leal; Jaime Lagos; Jorge Fernandez; Loredana Arata; Patricia Bustos; Paz Tapia; Rodrigo Fasce; Winston Andrade
EPI_ISL_445289	HOSPITAL NAVAL PUERTO WILLIAMS	Instituto de Salud Publica de Chile	Alejandra Acevedo; Andrés E Castillo; Bárbara Parra; Carolina Tambley; Gabriel Leal; Jaime Lagos; Jorge Fernandez; Loredana Arata; Patricia Bustos; Paz Tapia; Rodrigo Fasce; Winston Andrade
EPI_ISL_445327	HOSPITAL PADRE HURTADO	Instituto de Salud Publica de Chile	Alejandra Acevedo; Andrés E Castillo; Bárbara Parra; Carolina Tambley; Gabriel Leal; Jaime Lagos; Jorge Fernandez; Loredana Arata; Patricia Bustos; Paz Tapia; Rodrigo Fasce; Winston Andrade

EPI_ISL_445268, EPI_ISL_445269, EPI_ISL_445280, EPI_ISL_445284, EPI_ISL_445288, EPI_ISL_445293, EPI_ISL_445294	see above	HOSPITAL REG LAUTARO NAVARRO AVARIA	Instituto de Salud Publica de Chile	Alejandra Acevedo; Andrés E Castillo; Bárbara Parra; Carolina Tambley; Gabriel Leal; Jaime Lagos; Jorge Fernandez; Loredana Arata; Patricia Bustos; Paz Tapia; Rodrigo Fasce; Winston Andrade
EPI_ISL_445307		HOSPITAL SAN JOSE DE MAIPO	Instituto de Salud Publica de Chile	Alejandra Acevedo; Andrés E Castillo; Bárbara Parra; Carolina Tambley; Gabriel Leal; Jaime Lagos; Jorge Fernandez; Loredana Arata; Patricia Bustos; Paz Tapia; Rodrigo Fasce; Winston Andrade
EPI_ISL_445304		HOSPITAL SAN JUAN DE DIOS	Instituto de Salud Publica de Chile	Alejandra Acevedo; Andrés E Castillo; Bárbara Parra; Carolina Tambley; Gabriel Leal; Jaime Lagos; Jorge Fernandez; Loredana Arata; Patricia Bustos; Paz Tapia; Rodrigo Fasce; Winston Andrade
EPI_ISL_417007		HOSPITAL SANTA MARIA NAI	Instituto de Salud Carlos III	A. Monzón; I. García Costa, J.; Iglesias-Caballero; M. Camarero S. Pozo F.; Casas I. Jiménez; M. Cuesta; M. González-Esguevillas; M. Molinero Calamita; M. Zaballo; P. Jiménez; S. Juliá; S. Varona
EPI_ISL_418253, EPI_ISL_419240, EPI_ISL_419709		HOSPITAL TXAGORRITXU	Instituto de Salud Carlos III	A. Monzón; C. F. Casas; I. Gómez-González C.; I. Gómez; J. Jiménez; Iglesias-Caballero; M. Camarero; M. Camarero S. Pozo F.; Casas I. Jiménez; M. Cuesta; M. González-Esguevillas; M. Molinero Calamita; M. Zaballo; P. Jiménez; S. Juliá; S. Pozo; S. Varona
EPI_ISL_418251		HOSPITAL UNIVERSITARIO LA PAZ	Instituto de Salud Carlos III	A. Monzón; F. Casas; I. Jiménez; I. Romero P.; Iglesias-Caballero; M. Camarero; M. Cuesta; M. González-Esguevillas; M. Molinero Calamita; M. Zaballo; P. Jiménez; S. Juliá; S. Pozo; S. Varona
EPI_ISL_418243, EPI_ISL_418244		HOSPITAL UNIVERSITARIO VIRGEN DE LAS NIEVES	Instituto de Salud Carlos III	A. Monzón; F. Casas; I. Jiménez; I. Sanbornmatu S.; Iglesias-Caballero; M. Camarero; M. Cuesta; M. González-Esguevillas; M. Molinero Calamita; M. Zaballo; P. Jiménez; S. Juliá; S. Pozo; S. Varona
EPI_ISL_430847		HS mikrobiologi virus	The Public Health Agency of Sweden	Anna Risberg; Anna-Malin Linde; Karin Tegmark-Wisell; Maria Lind Karlberg; Mattias Haukland; Mia Blyting; Olov Svarstrom; Oskar Karlsson Lindjo; Shaman Muradrasoli; Zhibing Yun
EPI_ISL_418009, EPI_ISL_421463, EPI_ISL_421489, EPI_ISL_421494		HSE Iha Terceira - Angra do Heroismo	Instituto Nacional de Saude (INSA)	Guomar et al
EPI_ISL_454436, EPI_ISL_454437, EPI_ISL_454438, EPI_ISL_454439, EPI_ISL_454440, EPI_ISL_454441, EPI_ISL_454442, EPI_ISL_454443, EPI_ISL_454444, EPI_ISL_454445, EPI_ISL_454446, EPI_ISL_455902, EPI_ISL_469073, EPI_ISL_469074, EPI_ISL_475093, EPI_ISL_475094, EPI_ISL_475096, EPI_ISL_475097, EPI_ISL_475098, EPI_ISL_475100, EPI_ISL_475114, EPI_ISL_475116, EPI_ISL_475548, EPI_ISL_475553, EPI_ISL_475556, EPI_ISL_548247	see above	Halmstad klinisk mikrobiologi	The Public Health Agency of Sweden	Anna Risberg; Anna-Malin Linde; Karin Tegmark-Wisell; Maria Lind Karlberg; Mattias Haukland; Mia Blyting; Olov Svarstrom; Oskar Karlsson Lindjo; Petra Edqvist; Reza Advani; Sandra Brodesson; Shahan Muradrasoli; Shaman Muradrasoli
EPI_ISL_418510		Hangzhou Center for Disease Control and Prevention	Inspection Center of Hangzhou Center for Disease Control and Prevention	Li Jun; Pan Jingcao; Wang haoqi; Yu hua; Yu xinfeng
EPI_ISL_418506		Hangzhou Center for Disease Control and Prevention	Inspection Center of Hangzhou Center for Disease Control and Prevention	Li Jun; Pan Jingcao; Wang haoqi; Yu hua; Yu xinfeng
EPI_ISL_418441, EPI_ISL_418442, EPI_ISL_418502, EPI_ISL_418503, EPI_ISL_418504, EPI_ISL_418507, EPI_ISL_418508, EPI_ISL_418509, EPI_ISL_418511, EPI_ISL_418512, EPI_ISL_418513, EPI_ISL_418514, EPI_ISL_418515	see above	Hangzhou Center for Disease Control and Prevention	Inspection Center of Hangzhou Center for Disease Control and Prevention	Li Jun; Pan Jingcao; Wang haoqi; Yu hua; Yu xinfeng
EPI_ISL_421221, EPI_ISL_421222, EPI_ISL_421224, EPI_ISL_421225, EPI_ISL_421226, EPI_ISL_421227, EPI_ISL_421228, EPI_ISL_421229, EPI_ISL_421230, EPI_ISL_421231, EPI_ISL_421232, EPI_ISL_421233, EPI_ISL_421235, EPI_ISL_421236, EPI_ISL_421237, EPI_ISL_421238, EPI_ISL_421239, EPI_ISL_421240, EPI_ISL_421241, EPI_ISL_421242, EPI_ISL_421243, EPI_ISL_421244, EPI_ISL_421245, EPI_ISL_421246, EPI_ISL_421247, EPI_ISL_421248, EPI_ISL_421249, EPI_ISL_421250, EPI_ISL_421251, EPI_ISL_421252, EPI_ISL_421253, EPI_ISL_421254, EPI_ISL_421255, EPI_ISL_421256, EPI_ISL_421257, EPI_ISL_421258, EPI_ISL_421259, EPI_ISL_421260, EPI_ISL_421261, EPI_ISL_421262, EPI_ISL_421263, EPI_ISL_421264, EPI_ISL_421265, EPI_ISL_421266, EPI_ISL_421267, EPI_ISL_421268, EPI_ISL_421269, EPI_ISL_421270, EPI_ISL_421271, EPI_ISL_421272, EPI_ISL_421273, EPI_ISL_421274, EPI_ISL_421275, EPI_ISL_421276, EPI_ISL_421277, EPI_ISL_421278, EPI_ISL_421279, EPI_ISL_421280, EPI_ISL_421281, EPI_ISL_421282, EPI_ISL_421283, EPI_ISL_421284, EPI_ISL_421285, EPI_ISL_421286	see above	Hangzhou Center for Diseases Control and Prevention	Hangzhou Center for Diseases Control and Prevention	
EPI_ISL_421221, EPI_ISL_421222, EPI_ISL_421224, EPI_ISL_421225, EPI_ISL_421226, EPI_ISL_421227, EPI_ISL_421228, EPI_ISL_421229, EPI_ISL_421230, EPI_ISL_421231, EPI_ISL_421232, EPI_ISL_421233, EPI_ISL_421235, EPI_ISL_421236, EPI_ISL_421237, EPI_ISL_421238, EPI_ISL_421239, EPI_ISL_421240, EPI_ISL_421241, EPI_ISL_421242, EPI_ISL_421243, EPI_ISL_421244, EPI_ISL_421245, EPI_ISL_421246, EPI_ISL_421247, EPI_ISL_421248, EPI_ISL_421249, EPI_ISL_421250, EPI_ISL_421251, EPI_ISL_421252, EPI_ISL_421253, EPI_ISL_421254, EPI_ISL_421255, EPI_ISL_421256, EPI_ISL_421257, EPI_ISL_421258, EPI_ISL_421259, EPI_ISL_421260, EPI_ISL_421261, EPI_ISL_421262, EPI_ISL_421263, EPI_ISL_421264, EPI_ISL_421265, EPI_ISL_421266, EPI_ISL_421267, EPI_ISL_421268, EPI_ISL_421269, EPI_ISL_421270, EPI_ISL_421271, EPI_ISL_421272, EPI_ISL_421273, EPI_ISL_421274, EPI_ISL_421275, EPI_ISL_421276, EPI_ISL_421277, EPI_ISL_421278, EPI_ISL_421279, EPI_ISL_421280, EPI_ISL_421281, EPI_ISL_421282, EPI_ISL_421283, EPI_ISL_421284, EPI_ISL_421285, EPI_ISL_421286	see above	Hannover Medical School, Institute of Virology	Hannover Medical School, Institute of Virology	
EPI_ISL_883158, EPI_ISL_883159, EPI_ISL_883160, EPI_ISL_883161, EPI_ISL_883162, EPI_ISL_883163		Hannover Medical School, Institute of Virology	Hannover Medical School, Institute of Virology	Haoqi Wang; Hua Yu; Jun Li; Junfang Chen; Lingfeng Mao; Shuchang Chen; Xin Qian; Xinfen Yu; Xuchu Wang; Zhou Sun
EPI_ISL_413487		Harborview Medical Center	University of Washington Virology Lab	Alexander Greninger; Arun Nalla; Hong Xie; Keith Jerome; Pavitra Roychoudhury
EPI_ISL_429256		Health Sciences Technology Park, Avicena, 8, 18016 Granada, Spain	Sequencing and Bioinformatics Service FISABIO-Public Health	Almudena Rojas; Joaquin Mendoza; Pablo Mendoza
EPI_ISL_540993, EPI_ISL_540994, EPI_ISL_540995, EPI_ISL_540996, EPI_ISL_540997, EPI_ISL_540998, EPI_ISL_540999, EPI_ISL_541000, EPI_ISL_541001	see above	Health and Environmental Research Institute of Gwangju Metropolitan city	Health and Environmental Research Institute of Gwangju Metropolitan city	Ji-eun Lee; Min Ji Kim
EPI_ISL_451310, EPI_ISL_451311		Hellenic Pasteur Institute, National Influenza Reference Laboratory of Southern Greece & Unit of Bioinformatics and Applied Genomics	Hellenic Pasteur Institute, National Influenza Reference Laboratory of Southern Greece & Unit of Bioinformatics and Applied Genomics	Andreas Mentis; Androniki Voulgari-Kokota; Antonios Kalliaropoulos; Athanasios Kossyvakis; Evangelidou Maria; Horefti Elina; Timokratis Karamitros; Vasiliki Pogka
EPI_ISL_430469		Hellenic Pasteur Institute, Public Health Laboratories	Hellenic Pasteur Institute, Public Health Laboratories, Unit of Bioinformatics and Applied Genomics	Andreas Mentis; Androniki Voulgari-Kokota; Antonios Kalliaropoulos; Aspasia Kontou; Athanasios Kossyvakis; Evangelidou Maria; Horefti Elina; Timokratis Karamitros; Vasiliki Pogka
EPI_ISL_450525, EPI_ISL_450526, EPI_ISL_450527, EPI_ISL_450528, EPI_ISL_450529		Hematology Laboratory, Section of Molecular Diagnostics, University Clinical Centre, Medical University of Gdansk	Department of Virology, Faculty of Medicine, University of Helsinki, Helsinki, Finland	Aneta Szulc; Maciej Grzybek; Marlena Robakowska; Olii Vapalahti; Teemu Simura
EPI_ISL_1303471		Henry Mayo Newhall Hospital	Los Angeles County PHL	P. Hemarajata et al.
EPI_ISL_479903, EPI_ISL_479904, EPI_ISL_479905, EPI_ISL_479906, EPI_ISL_479907, EPI_ISL_479908, EPI_ISL_479909, EPI_ISL_479910, EPI_ISL_479911, EPI_ISL_479912	see above	Himeji City Institute of Environment and Health	Pathogen Genomics Center, National Institute of Infectious Diseases	Hajime Kamiya; Kentaro Itokawa; Makoto Kuroda; Masanori Hashino; Motoi Suzuki; Rina Tanaka; Tsuyoshi Sekizuka
EPI_ISL_480178, EPI_ISL_480179		Hiroshima City Institute of Public Health	Pathogen Genomics Center, National Institute of Infectious Diseases	Hajime Kamiya; Kentaro Itokawa; Kota Noritsune; Makoto Kuroda; Masanori Hashino; Motoi Suzuki; Rina Tanaka; Tsuyoshi Sekizuka
EPI_ISL_479812, EPI_ISL_479813, EPI_ISL_479814, EPI_ISL_479815, EPI_ISL_479816, EPI_ISL_479817, EPI_ISL_479818, EPI_ISL_479819, EPI_ISL_479820	see above	Hokkaido Institute of Public Health	Pathogen Genomics Center, National Institute of Infectious Diseases	Hajime Kamiya; Kentaro Itokawa; Makoto Kuroda; Masanori Hashino; Motoi Suzuki; Rika Komagome; Rina Tanaka; Tsuyoshi Sekizuka
EPI_ISL_412028, EPI_ISL_412030		Hong Kong Department of Health	School of Public Health, The University of Hong Kong	Daniel K.W. Chu; Dominic N.C. Tsang; Leo L.M. Poon; Malik Peris
EPI_ISL_414517, EPI_ISL_414519, EPI_ISL_414527, EPI_ISL_414528, EPI_ISL_414569, EPI_ISL_414571, EPI_ISL_476801, EPI_ISL_476802, EPI_ISL_476803, EPI_ISL_476804	see above	Hong Kong Department of Health	School of Public Health, The University of Hong Kong	Daniel K.W. Chu; Dominic N.C. Tsang; Leo L.M. Poon; Malik Peris
EPI_ISL_412029		Hong Kong Department of Health	The University of Hong Kong	Daniel K.W. Chu; Dominic N.C. Tsang; Leo L.M. Poon; Malik Peris
EPI_ISL_560581, EPI_ISL_560582, EPI_ISL_560583		Hospital	National Reference Center for Viruses of Respiratory Infections, Institut Pasteur, Paris	Etienne Simon-Lorière; Fabiana Gambaro; Maud Vanpeene; Sylvie Behilli; Sylvie van der Werf; Vincent Enouf
EPI_ISL_418427		Hopital Privé de l'Est Lyonnais	CNR Virus des Infections Respiratoires - France SUD	Alexandre Gaymard; Antonin Bal; Bruno Lina; Carine Moustaud; Florence Morfin-Sherpa; Gregory Destras; Gwendolyne Burtin; Laurence Jossot; Martine Valette; Maude Bouscambert-Duchamp; Raphaëlle Lamy; Solenne Brun
EPI_ISL_418229		Hopital franco britannique - Laboratoire	National Reference Center for Viruses of Respiratory Infections, Institut Pasteur, Paris	Angela Brisebarre; Etienne Simon-Lorière; Flora Donat; Marianne Asso Bonnet; Marion Barbet; Maud Vanpeene; Mélanie Albert; Meline Bizard; Sylvie Behilli; Sylvie van der Werf; Vincent Enouf

EPI_ISL_416501	Hopital franco britannique - Service des Urgences	National Reference Center for Viruses of Respiratory Infections, Institut Pasteur, Paris	Angela Brisebarre; Etienne Simon-Lorière; Flora Donati; Marion Barbet; Maud Vanpenne; Méline Bizard; Méline Albert; Sylvie Behilli; Sylvie van der Werf;
EPI_ISL_515564	Hosp. Municipal Prof. Dr. Alípio Corrêa Netto	Instituto Adolfo Lutz, Interdisciplinary Procedures Center, Strategic Laboratory	Claudia Regina Gonçalves; Claudio Tavares Sacchi; Erica Valessa Ramos Gomes
EPI_ISL_560620, EPI_ISL_560621, EPI_ISL_560622, EPI_ISL_560623, EPI_ISL_560624, EPI_ISL_560625, EPI_ISL_560626, EPI_ISL_560627	Hopital	National Reference Center for Viruses of Respiratory Infections, Institut Pasteur, Paris	Etienne Simon-Lorière; Fabiana Gambaro; Maud Vanpenne; Sylvie Behilli; Sylvie van der Werf; Vincent Enouf
EPI_ISL_434366, EPI_ISL_434368, EPI_ISL_434372, EPI_ISL_434373, EPI_ISL_434375, EPI_ISL_434376, EPI_ISL_450724, EPI_ISL_450725, EPI_ISL_450726, EPI_ISL_450727, EPI_ISL_450728, EPI_ISL_450729, EPI_ISL_450730, EPI_ISL_450731	Hopital AZ Riviereland	Institute of Tropical Medicine	; Colin Anthony; Philippe Seihorst
EPI_ISL_471554	Hopital Bosque da Saúde	Instituto Adolfo Lutz, Interdisciplinary Procedures Center, Strategic Laboratory	Claudia Regina Gonçalves; Claudio Tavares Sacchi; Erica Valessa Ramos Gomes
EPI_ISL_539559, EPI_ISL_539560	Hopital Campo Araúelo	Instituto de Salud Carlos III	A. Monzón; F. Casas; G. Rodríguez; I. I. Jiménez; Iglesias-Caballero; J. López; M. Camarero; M. Cuesta; M. González-Esguevillas; M. Molinero Calamita; M. Zaballos; P. Jiménez; S. Juliá; S. Pozo; S. Varona
EPI_ISL_462479	Hopital Clinic	Instituto de Salud Carlos III	A. Monzón; F. Casas; I. I. Jiménez; Iglesias-Caballero; M. Camarero; M. Cuesta; M. González-Esguevillas; M. Molinero Calamita; M. Zaballos; M.A. Marcos; P. Jiménez; S. Juliá; S. Pozo; S. Varona
EPI_ISL_491441, EPI_ISL_491442, EPI_ISL_491455	Hopital Clinica Bíblica	Incienza, Instituto Costarricense de Investigación y Enseñanza en Nutrición y Salud	Adriana Godínez & Melany Calderon; Claudio Soto-Garita; Estela Cordero; Francisco Duarte; Hebleen Brenes
EPI_ISL_539549, EPI_ISL_539550, EPI_ISL_539551, EPI_ISL_539552, EPI_ISL_539553, EPI_ISL_539554, EPI_ISL_539555, EPI_ISL_539556, EPI_ISL_862827, EPI_ISL_862828, EPI_ISL_862829, EPI_ISL_862830, EPI_ISL_862831, EPI_ISL_862832, EPI_ISL_862833, EPI_ISL_862834, EPI_ISL_862835, EPI_ISL_862836	Hopital Clinic	Instituto de Salud Carlos III	A. Monzón; F. Casas; I. I. Jiménez; I. Marcos; Iglesias-Caballero; M. Pozo; M. Camarero; M. Cuesta; M. González-Esguevillas; M. Molinero Calamita; M. Zaballos; M.A. Marcos; M.A.; M. Camarero; P. Jiménez; S. Juliá; S. Molinero Calamita; S. Pozo; S. Varona
EPI_ISL_539500, EPI_ISL_539501, EPI_ISL_539502, EPI_ISL_539509, EPI_ISL_539510, EPI_ISL_539511, EPI_ISL_539512, EPI_ISL_578190, EPI_ISL_578191	Hopital Clinico Universitario Lozano Blesa	Instituto de Salud Carlos III	A. Monzón; F. Casas; I. I. Jiménez; Iglesias-Caballero; M. Camarero; M. Cuesta; M. González-Esguevillas; M. Molinero Calamita; M. Zaballos; P. Jiménez; R. Benito; S. Juliá; S. Pozo; S. Varona
EPI_ISL_510288, EPI_ISL_510289, EPI_ISL_510291, EPI_ISL_510292, EPI_ISL_510293, EPI_ISL_510294, EPI_ISL_510296, EPI_ISL_510297, EPI_ISL_510298, EPI_ISL_510300, EPI_ISL_510301, EPI_ISL_510302, EPI_ISL_510303	Hopital Clinico Universitario de Santiago de Compostela	SeqCOVID-SPAIN consortium/IBV(CSIC)	Amparo Coira Nieto; Antonio Aguilera Guirao; Gema Barbeito Castañeira; José Javier Costa Alcalde; Mª Luisa Pérez del Molino Bernal; Rocío Trastry Pena and SeqCOVID-SPAIN consortium
EPI_ISL_455344, EPI_ISL_455345, EPI_ISL_455346, EPI_ISL_455347, EPI_ISL_455348, EPI_ISL_455349	Hopital Comarcal de Melilla	Instituto de Salud Carlos III	A. Monzón; F. Casas; I. I. Jiménez; I. Pérez; Iglesias-Caballero; M. Camarero; M. Cuesta; M. González-Esguevillas; M. Molinero Calamita; M. Zaballos; P. Jiménez; S. Juliá; S. Pozo; S. Varona
EPI_ISL_574592	Hopital Domingos Leonardo Ceravolo Presidente Prudente	Instituto Adolfo Lutz, Interdisciplinary Procedures Center, Strategic Laboratory	Claudia Regina Gonçalves; Claudio Tavares Sacchi; Erica Valessa Ramos Gomes; Karoline Rodrigues Campos
EPI_ISL_491447	Hopital Fernando Escalante Pradilla	Incienza, Instituto Costarricense de Investigación y Enseñanza en Nutrición y Salud	Adriana Godínez & Melany Calderon; Claudio Soto-Garita; Estela Cordero; Francisco Duarte; Hebleen Brenes
EPI_ISL_912273	Hopital General Universitario Gregorio Marañón	SeqCOVID-SPAIN consortium / IBV (CSIC)	Dario García de Viedma; Julia Suárez; Laura Pérez-Lago; Marta Herranz; Patricia Muñoz and SeqCOVID-SPAIN consortium; Pilar Catalán; Sergio Buenestado-Serrano; Victor Manuel de la Cueva
EPI_ISL_481043, EPI_ISL_481044, EPI_ISL_481051, EPI_ISL_481052, EPI_ISL_481054, EPI_ISL_481055, EPI_ISL_481056, EPI_ISL_481057, EPI_ISL_481058, EPI_ISL_481059, EPI_ISL_481060, EPI_ISL_481066, EPI_ISL_481075, EPI_ISL_481077, EPI_ISL_481083, EPI_ISL_481086, EPI_ISL_481087, EPI_ISL_481089, EPI_ISL_481094, EPI_ISL_481096, EPI_ISL_481097, EPI_ISL_481103, EPI_ISL_510113, EPI_ISL_510117, EPI_ISL_510122, EPI_ISL_510146, EPI_ISL_510148, EPI_ISL_510165, EPI_ISL_510166, EPI_ISL_510167, EPI_ISL_510168, EPI_ISL_510169, EPI_ISL_510170, EPI_ISL_510171, EPI_ISL_510172, EPI_ISL_510173, EPI_ISL_510174, EPI_ISL_510176, EPI_ISL_510178, EPI_ISL_510180, EPI_ISL_510182, EPI_ISL_510183, EPI_ISL_510185, EPI_ISL_510186, EPI_ISL_510190, EPI_ISL_510191, EPI_ISL_510192, EPI_ISL_510193, EPI_ISL_510194, EPI_ISL_510195, EPI_ISL_510196, EPI_ISL_510199, EPI_ISL_510201, EPI_ISL_510202, EPI_ISL_510203, EPI_ISL_510204, EPI_ISL_510205, EPI_ISL_510207, EPI_ISL_510211, EPI_ISL_510212, EPI_ISL_510213, EPI_ISL_510216, EPI_ISL_510217, EPI_ISL_510218, EPI_ISL_510220, EPI_ISL_510221, EPI_ISL_510222, EPI_ISL_510223, EPI_ISL_510224, EPI_ISL_510225, EPI_ISL_510226, EPI_ISL_510227, EPI_ISL_510228, EPI_ISL_510231, EPI_ISL_510232, EPI_ISL_510233, EPI_ISL_510236, EPI_ISL_510237, EPI_ISL_510238, EPI_ISL_510240, EPI_ISL_514878, EPI_ISL_654082, EPI_ISL_654083, EPI_ISL_654084, EPI_ISL_654187, EPI_ISL_654188	SeqCOVID-SPAIN consortium/IBV(CSIC)	Dario Garcia de Viedma; Dario Garcia de Viedma and SeqCOVID-SPAIN consortium; Jon Sicilia; Julia Suárez; Laura Pérez-Lago; Marta Herranz; Patricia Muñoz; Patricia Muñoz and SeqCOVID-SPAIN consortium; Pilar Catalán	
EPI_ISL_539523	Hopital General de Segovia	Instituto de Salud Carlos III	A. Monzón; F. Casas; I. I. Jiménez; Iglesias-Caballero; M. Camarero; M. Cuesta; M. González-Esguevillas; M. Molinero Calamita; M. Zaballos; P. Jiménez; S. Hernández; S. Juliá; S. Pozo; S. Varona
EPI_ISL_418245, EPI_ISL_418246	Hopital General y Universitario de Guadalajara	Instituto de Salud Carlos III	A. Monzón; F. Casas; I. González-Praetorius A.; I. Jiménez; Iglesias-Caballero; M. Camarero; M. Cuesta; M. González-Esguevillas; M. Molinero Calamita; M. Zaballos; P. Jiménez; S. Juliá; S. Pozo; S. Varona
EPI_ISL_523971	Hopital Geral Santa Marcelina	Instituto Adolfo Lutz, Interdisciplinary Procedures Center, Strategic Laboratory	Claudia Regina Gonçalves; Claudio Tavares Sacchi; Erica Valessa Ramos Gomes
EPI_ISL_861636	Hopital Geral de Sao Mateus São Paulo	Instituto Adolfo Lutz, Interdisciplinary Procedures Center, Strategic Laboratory	Claudia Regina Gonçalves; Claudio Tavares Sacchi; Erica Valessa Ramos Gomes; Karoline Rodrigues Campos
EPI_ISL_515555	Hopital Geral de Vila Nova Cachoeirinha	Instituto Adolfo Lutz, Interdisciplinary Procedures Center, Strategic Laboratory	Claudia Regina Gonçalves; Claudio Tavares Sacchi; Erica Valessa Ramos Gomes
EPI_ISL_574595	Hopital Geral de Vila Penteado Dr. Jose Pangelina	Instituto Adolfo Lutz, Interdisciplinary Procedures Center, Strategic Laboratory	Claudia Regina Gonçalves; Claudio Tavares Sacchi; Erica Valessa Ramos Gomes; Karoline Rodrigues Campos
EPI_ISL_871974, EPI_ISL_871975, EPI_ISL_871979	Hopital Infanta Cristina	Instituto de Salud Carlos III	A. Monzón; F. Casas; I. García, P.; I. Jiménez; Iglesias-Caballero; M. Camarero; M. Cuesta; M. González-Esguevillas; M. Pozo; M. Zaballos; P. Jiménez; S. Juliá; S. Molinero Calamita; S. Varona
EPI_ISL_524462	Hopital Metropolitano	Instituto Adolfo Lutz, Interdisciplinary Procedures Center, Strategic Laboratory	Claudia Regina Gonçalves; Claudio Tavares Sacchi; Erica Valessa Ramos Gomes
EPI_ISL_527739	Hopital Mexico [San Jose/San Jose]	Incienza, Instituto Costarricense de Investigación y Enseñanza en Nutrición y Salud	Adriana Godínez & Melany Calderon; Claudio Soto-Garita; Estela Cordero; Francisco Duarte; Hebleen Porras
EPI_ISL_515541	Hopital Montemagno	Instituto Adolfo Lutz, Interdisciplinary Procedures Center, Strategic Laboratory	Claudia Regina Gonçalves; Claudio Tavares Sacchi; Erica Valessa Ramos Gomes
EPI_ISL_468311, EPI_ISL_468312	Hopital Municipal Dr Ignacio Proença de Gouvea	Instituto Adolfo Lutz, Interdisciplinary Procedures Center, Strategic Laboratory	Claudia Regina Gonçalves; Claudio Tavares Sacchi; Erica Valessa Ramos Gomes
EPI_ISL_515521	Hopital Municipal Dr Waldemar Tebaldi	Instituto Adolfo Lutz, Interdisciplinary Procedures Center, Strategic Laboratory	Claudia Regina Gonçalves; Claudio Tavares Sacchi; Erica Valessa Ramos Gomes
EPI_ISL_515548	Hopital Municipal Dr. Jose Soares Hungria	Instituto Adolfo Lutz, Interdisciplinary Procedures Center, Strategic Laboratory	Claudia Regina Gonçalves; Claudio Tavares Sacchi; Erica Valessa Ramos Gomes
EPI_ISL_527862	Hopital Municipal de Urgência	Instituto Adolfo Lutz, Interdisciplinary Procedures Center,	Claudia Regina Gonçalves; Claudio Tavares Sacchi; Erica Valessa Ramos Gomes

Strategic Laboratory			
EPI_ISL_468308, EPI_ISL_515520, EPI_ISL_515538, EPI_ISL_515546, EPI_ISL_515551, EPI_ISL_491451	Hospital Municipal do Tatuape Carminio Caricchio	Instituto Adolfo Lutz, Interdisciplinary Procedures Center, Strategic Laboratory	Claudia Regina Gonçalves; Claudio Tavares Sacchi; Erica Valessa Ramos Gomes
EPI_ISL_539496	Hospital México	Incienza, Instituto Costarricense de Investigación y Enseñanza en Nutrición y Salud	Adriana Godínez & Melany Calderon; Claudio Soto-Garita; Estela Cordero; Francisco Duarte; Hebleen Brenes
EPI_ISL_539525, EPI_ISL_862637	Hospital Nuestra Señora de Meribéil	Instituto de Salud Carlos III	A. Monzón; F. Casas; F. Fernández; I. Jiménez; Iglesias-Caballero; M. Camarero; M. Cuesta; M. González-Esguevillas; M. Molinero Calamita; M. Zaballos; P. Jiménez; S. Julía; S. Pozo; S. Varona
EPI_ISL_419386, EPI_ISL_419387	Hospital Prof. Doutor Fernando Fonseca, EPE	Instituto Gulbenkian de Ciência	A. Monzón; A. San Pedro; F. Casas; I. Jiménez; Iglesias-Caballero; M. Camarero; M. Cuesta; M. González-Esguevillas; M. Molinero Calamita; M. Zaballos; P. Jiménez; S. Julía; S. Pozo; S. Varona
EPI_ISL_523956	Hospital Regional de Asais	Instituto Adolfo Lutz, Interdisciplinary Procedures Center, Strategic Laboratory	Cathy Paulino; Joao Sobral; Joao Costa; Ricardo Leite; Susana Ladeira
EPI_ISL_524463	Hospital Regional de Coia	Instituto Adolfo Lutz, Interdisciplinary Procedures Center, Strategic Laboratory	Claudia Regina Gonçalves; Claudio Tavares Sacchi; Erica Valessa Ramos Gomes
EPI_ISL_491456	Hospital San Juan de Dios	Incienza, Instituto Costarricense de Investigación y Enseñanza en Nutrición y Salud	Adriana Godínez & Melany Calderon; Claudio Soto-Garita; Estela Cordero; Francisco Duarte; Hebleen Brenes
EPI_ISL_419234, EPI_ISL_455336, EPI_ISL_455337, EPI_ISL_455338, EPI_ISL_455339, EPI_ISL_455340, EPI_ISL_455341, EPI_ISL_455342, EPI_ISL_455343, EPI_ISL_578196, EPI_ISL_578197, EPI_ISL_578198, EPI_ISL_578199, EPI_ISL_578200, EPI_ISL_578201	Hospital San Pedro	Instituto de Salud Carlos III	A. Monzón; Alonso, C.; C. Alonso; Camarero, S.; Casas, I.; Cuesta, I.; F. Casas; González-Esguevillas, M.; I. Jiménez; Iglesias-Caballero; Iglesias-Caballero, M.; J.M. Azcona; Jiménez, M.; Jiménez, P.; Julía, M.; M. Blasco; M. Camarero; M. Cuesta; M. González-Esguevillas; M. Molinero Calamita; M. Zaballos; Molinero Calamita, M.; Monzón, S.; P. Jiménez; Pozo, F.; S. Julía; S. Pozo; S. Varona; Varona, S.; Zaballos, A.
EPI_ISL_539558, EPI_ISL_539561, EPI_ISL_539562, EPI_ISL_862654	Hospital San Pedro de Alcántara	Instituto de Salud Carlos III	A. Monzón; E. Cerro; F. Casas; I. Jiménez; I. Rodríguez; G.; Iglesias-Caballero; J. López; M. Pozo; M. Camarero; M. Cuesta; M. González-Esguevillas; M. Molinero Calamita; M. Zaballos; M.A. Cañizares; M. Camarero; P. Jiménez; S. Julía; S. Molinero Calamita; S. Pozo; S. Varona
EPI_ISL_510312, EPI_ISL_510313, EPI_ISL_510314, EPI_ISL_510315, EPI_ISL_510316, EPI_ISL_510317, EPI_ISL_510318, EPI_ISL_510319, EPI_ISL_510320, EPI_ISL_510321, EPI_ISL_510322, EPI_ISL_510323, EPI_ISL_510324, EPI_ISL_510325, EPI_ISL_510326, EPI_ISL_510327, EPI_ISL_510328, EPI_ISL_510329	Hospital San Pedro de Alcántara (Cáceres)	SeqCOVID-SPAIN consortium/IBV(CSIC)	Cristina Muñoz Cuevas; Quadaupe Rodríguez Rodríguez and SeqCOVID-SPAIN consortium
EPI_ISL_491438, EPI_ISL_491440, EPI_ISL_491448, EPI_ISL_515527	Hospital San Rafael de Alajuela	Incienza, Instituto Costarricense de Investigación y Enseñanza en Nutrición y Salud	Adriana Godínez & Melany Calderon; Claudio Soto-Garita; Estela Cordero; Francisco Duarte; Hebleen Brenes
EPI_ISL_468310	Hospital Santa Clara	Instituto Adolfo Lutz, Interdisciplinary Procedures Center, Strategic Laboratory	Claudia Regina Gonçalves; Claudio Tavares Sacchi; Erica Valessa Ramos Gomes
EPI_ISL_471545, EPI_ISL_515528, EPI_ISL_515545, EPI_ISL_523969	Hospital Sao Paulo de Ensino da UNIFESP	Instituto Adolfo Lutz, Interdisciplinary Procedures Center, Strategic Laboratory	Claudia Regina Gonçalves; Claudio Tavares Sacchi; Erica Valessa Ramos Gomes
EPI_ISL_524484	Hospital Schwyz	Institute of Medical Virology, University of Zurich	Alexandra Trkola; Andrea Zbinden; Fiona Steiner; Gabriela Zlotner; Jon Huder; Jürg Böni; Maryam Zaheri; Michael Huber; Patrick Redl; Riccardo Capaul; Stefan Schmutz; Verena Kufner
EPI_ISL_414015, EPI_ISL_414016	Hospital São Joaquim Beneficência Portuguesa	Instituto Adolfo Lutz, Interdisciplinary Procedures Center, Strategic Laboratory	Audrey Cilli; Carlos Henrique Camargo; Claudia Regina Gonçalves; Claudio Tavares Sacchi; Daniela Bernardes Borges da Silva; Ester Cedeira Sabino; Fabiana Cristina Pereira dos Santos Terezinha Maria de Paiva; Maria do Carmo Sampaio Tavares Timenetsky; Simone Guadagnoni Morillo; Terezinha Maria de Paiva
EPI_ISL_455350, EPI_ISL_455351	Hospital Txagorritxu	Instituto de Salud Carlos III	A. Monzón; C. Gómez; F. Casas; I. Jiménez; Iglesias-Caballero; M. Camarero; M. Cuesta; M. González-Esguevillas; M. Molinero Calamita; M. Zaballos; P. Jiménez; S. Julía; S. Pozo; S. Varona
EPI_ISL_483059	Hospital Universitat Germans Trias i Pujol	IrsiCaixa AIDS Research Lab	A. Valencia; B. Clotet; C. Avila-Nieto; E. Vidal; G. Camarero; I. Blanco; J. Blanco; J. Carrillo; J. Rodon; J. Segalés; J. Vergara-Alert; M. Noguera-Julian; M. Pareja; M. Puig; M.T. Terrón; N. Izquierdo-Ustero; S. Cruz; V. Guallar
EPI_ISL_471472, EPI_ISL_510689	Hospital Universitat Germans Trias i Pujol(HUGTIP)/Fundació Lluita contra la SIDA (FLSida)/IRTA-CReSA	IrsiCaixa AIDS Research Lab	Albert Bensaïd; Bonaventura Clotet; Joaquim Segalés; Jordi Rodon; Jorge Carrillo; Julia Blanco; Julia Vergara; Lidia Ruiz; Marc Noguera-Julian; Nuria Izquierdo; Pilar Armengol; Roger Paredes
EPI_ISL_418860, EPI_ISL_418861, EPI_ISL_444977, EPI_ISL_444978, EPI_ISL_444979, EPI_ISL_444980, EPI_ISL_444981, EPI_ISL_444982, EPI_ISL_444983, EPI_ISL_444984, EPI_ISL_444985, EPI_ISL_444986, EPI_ISL_444987, EPI_ISL_444988, EPI_ISL_444989, EPI_ISL_444990, EPI_ISL_447532, EPI_ISL_447533, EPI_ISL_450337, EPI_ISL_458130, EPI_ISL_458132, EPI_ISL_819300, EPI_ISL_819301, EPI_ISL_819302, EPI_ISL_819303, EPI_ISL_819304, EPI_ISL_819305, EPI_ISL_819306, EPI_ISL_819307, EPI_ISL_819308, EPI_ISL_819309, EPI_ISL_819310, EPI_ISL_819311, EPI_ISL_819312, EPI_ISL_819313, EPI_ISL_819314, EPI_ISL_819315, EPI_ISL_819316	Hospital Universitat Vall d'Hebron - Vall d'Hebron Institut de Recerca	Hospital Universitat Vall d'Hebron - Vall d'Hebron Institut de Recerca	Andrés Antón; Ariadna Rando; Carla Castillo; Cristina Andrés; Damián Garcia-Cebic; Damián Garcia-Cebic; Josep F. Abril; Josep Gregori; Josep Quer; Juliana Esperalba; Maria Carmen Martín; Maria Carmen Martín; Maria Gema Codina; Maria Píñana; Mercedes Guerrero-Murilo; Tomás Pumarola
EPI_ISL_538012, EPI_ISL_538013, EPI_ISL_538014, EPI_ISL_538015, EPI_ISL_538016, EPI_ISL_538017, EPI_ISL_538018, EPI_ISL_538019, EPI_ISL_538020, EPI_ISL_538021, EPI_ISL_538022, EPI_ISL_538023, EPI_ISL_538024, EPI_ISL_538025, EPI_ISL_538026, EPI_ISL_538027, EPI_ISL_538028, EPI_ISL_538030, EPI_ISL_538033, EPI_ISL_538034, EPI_ISL_538035, EPI_ISL_538036, EPI_ISL_538037, EPI_ISL_538038, EPI_ISL_538039, EPI_ISL_538041, EPI_ISL_538042, EPI_ISL_538043, EPI_ISL_538044, EPI_ISL_538045, EPI_ISL_538046, EPI_ISL_538047, EPI_ISL_538048, EPI_ISL_538049, EPI_ISL_538050, EPI_ISL_538051, EPI_ISL_538052, EPI_ISL_538054	Hospital Universitat i Politècnic La Fe de València	SeqCOVID-SPAIN consortium/IBV(CSIC)	Ana Gil Brusola; Eva González Barbera; José Luis López Hontangas and SeqCOVID-SPAIN consortium; Maria Dolores Gómez Ruiz; Salvador Giner Almazaz
EPI_ISL_421171, EPI_ISL_421172, EPI_ISL_421173, EPI_ISL_421174, EPI_ISL_421175, EPI_ISL_421176, EPI_ISL_421177, EPI_ISL_421178, EPI_ISL_421179, EPI_ISL_421200, EPI_ISL_421201, EPI_ISL_421202, EPI_ISL_421203, EPI_ISL_421204, EPI_ISL_421205, EPI_ISL_421206, EPI_ISL_421207, EPI_ISL_421208, EPI_ISL_421209, EPI_ISL_421210, EPI_ISL_428711, EPI_ISL_430718, EPI_ISL_529982, EPI_ISL_529983, EPI_ISL_529984, EPI_ISL_529985, EPI_ISL_529986	Hospital Universitario 12 de Octubre	Hospital Universitario 12 de Octubre	Elias Dahhdou; Esther Viedma; Fernando Lázaro; Jesús Mingorance; Juan Carlos Galán; Julio Garcia; M° Dolores Folgueira; Natalia Stella; Rafael Cantón; Rafael Delgado; Raúl Recio; Sara González
EPI_ISL_417954, EPI_ISL_417961, EPI_ISL_417963, EPI_ISL_417967	Hospital Universitario 12 de Octubre	Hospital Universitario La Paz	Elias Dahhdou; Esther Viedma; Fernando Lázaro; Jesús Mingorance; Juan Carlos Galán; Julio Garcia; M° Dolores Folgueira; Natalia Stella; Rafael Cantón; Rafael Delgado; Sara Gonzalez
EPI_ISL_467092, EPI_ISL_467093, EPI_ISL_467094, EPI_ISL_467095, EPI_ISL_467096, EPI_ISL_467097, EPI_ISL_467098, EPI_ISL_467099, EPI_ISL_467100, EPI_ISL_467101, EPI_ISL_467102, EPI_ISL_467103, EPI_ISL_467104, EPI_ISL_467105, EPI_ISL_467106, EPI_ISL_467107, EPI_ISL_467108, EPI_ISL_467109, EPI_ISL_467110, EPI_ISL_467111, EPI_ISL_467113, EPI_ISL_467114, EPI_ISL_467115, EPI_ISL_467116, EPI_ISL_467117, EPI_ISL_467118, EPI_ISL_467119, EPI_ISL_467120, EPI_ISL_467121, EPI_ISL_467122, EPI_ISL_467123, EPI_ISL_467124, EPI_ISL_467125, EPI_ISL_467126, EPI_ISL_467127, EPI_ISL_467128, EPI_ISL_467129, EPI_ISL_467130, EPI_ISL_467131, EPI_ISL_467132, EPI_ISL_467134, EPI_ISL_467136, EPI_ISL_467137, EPI_ISL_467138, EPI_ISL_467139, EPI_ISL_467140, EPI_ISL_467141, EPI_ISL_467142, EPI_ISL_467143, EPI_ISL_467144, EPI_ISL_467145, EPI_ISL_467146, EPI_ISL_467147, EPI_ISL_467148, EPI_ISL_467149, EPI_ISL_467150, EPI_ISL_467151, EPI_ISL_467152, EPI_ISL_467153, EPI_ISL_467154, EPI_ISL_467155, EPI_ISL_467156, EPI_ISL_467157, EPI_ISL_467158, EPI_ISL_467159, EPI_ISL_467160, EPI_ISL_467161, EPI_ISL_467162, EPI_ISL_467163, EPI_ISL_467164, EPI_ISL_467165, EPI_ISL_467166, EPI_ISL_467167, EPI_ISL_467168, EPI_ISL_467169, EPI_ISL_467170, EPI_ISL_467171, EPI_ISL_467172, EPI_ISL_467173, EPI_ISL_467174, EPI_ISL_467175, EPI_ISL_467176, EPI_ISL_467177, EPI_ISL_467178, EPI_ISL_467179, EPI_ISL_467180, EPI_ISL_467181, EPI_ISL_467182, EPI_ISL_467183, EPI_ISL_509616, EPI_ISL_509617, EPI_ISL_509618	Hospital Universitario Araba. Vitoria-Gasteiz	SeqCOVID-SPAIN consortium/IBV(CSIC)	
EPI_ISL_452692, EPI_ISL_452693, EPI_ISL_452694, EPI_ISL_452695, EPI_ISL_452696, EPI_ISL_452698, EPI_ISL_452699, EPI_ISL_452700, EPI_ISL_452701, EPI_ISL_452702, EPI_ISL_452703, EPI_ISL_452704, EPI_ISL_452705, EPI_ISL_452706, EPI_ISL_452707, EPI_ISL_452708, EPI_ISL_452709, EPI_ISL_452710, EPI_ISL_452711, EPI_ISL_452712, EPI_ISL_452713, EPI_ISL_452714, EPI_ISL_452715, EPI_ISL_452716, EPI_ISL_452717, EPI_ISL_452718, EPI_ISL_452719, EPI_ISL_452720, EPI_ISL_452721, EPI_ISL_452722, EPI_ISL_452723, EPI_ISL_452724, EPI_ISL_452725, EPI_ISL_452726, EPI_ISL_452727, EPI_ISL_452728, EPI_ISL_452729, EPI_ISL_452730, EPI_ISL_452731, EPI_ISL_452732, EPI_ISL_452733, EPI_ISL_452735, EPI_ISL_452736, EPI_ISL_452737, EPI_ISL_452738, EPI_ISL_452739, EPI_ISL_452740, EPI_ISL_452741, EPI_ISL_452742, EPI_ISL_452743, EPI_ISL_452744, EPI_ISL_452745, EPI_ISL_452746, EPI_ISL_452747, EPI_ISL_452748, EPI_ISL_452749, EPI_ISL_452750	Hospital Universitario Araba. Vitoria-Gasteiz	SeqCOVID-SPAIN consortium/IBV(CSIC)	Amaia Aguirre Quiñero; Andrés Canut Blanco and SeqCOVID-SPAIN consortium; Andrés Canut Blanco and SeqCOVID-SPAIN consortium; Carmen Gómez González; Marina Fernández Torres; M° Concepción Lecaroz Agara; M° Rosario Almela Ferrer; Silvia Hemez Crespo

EPI_ISL_452751, EPI_ISL_452753, EPI_ISL_452754, EPI_ISL_452755, EPI_ISL_452756, EPI_ISL_452757, EPI_ISL_452758, EPI_ISL_452759, EPI_ISL_452760, EPI_ISL_452761, EPI_ISL_452762, EPI_ISL_452763, EPI_ISL_452764, EPI_ISL_452765, EPI_ISL_452766, EPI_ISL_452767, EPI_ISL_452768, EPI_ISL_452769, EPI_ISL_452770, EPI_ISL_452771, EPI_ISL_452772, EPI_ISL_452773, EPI_ISL_452774, EPI_ISL_452775, EPI_ISL_452777, EPI_ISL_452780, EPI_ISL_452782, EPI_ISL_452783, EPI_ISL_452784, EPI_ISL_452785, EPI_ISL_452786			
see above	Hospital Universitario Araba. Vitoria-Gasteiz,	SeqCOVID-SPAIN consortium/IBV(CSIC)	Amaia Aguirre Quifonero; Andrés Canut Blasco and SeqCOVID-SPAIN consortium; Carmen Gómez González; María Concepción Lecaroz Agara; María Rosario Almela Ferrer; Marina Fernández Torres; Silvia Hernández Crespo
EPI_ISL_455326	Hospital Universitario Insular de Gran Canaria	Instituto de Salud Carlos III	A. Hernández; A. Monzón; F. Casas; I. Jiménez; Iglesias-Caballero; M. Camarero; M. Cuesta; M. González-Esguevillas; M. Molinero Calamita; M. Zaballos; P. Jiménez; S. Juliá; S. Pozo; S. Varona
EPI_ISL_428674, EPI_ISL_428675, EPI_ISL_428676, EPI_ISL_428677, EPI_ISL_428678, EPI_ISL_428679, EPI_ISL_428680, EPI_ISL_428681, EPI_ISL_428682, EPI_ISL_430719, EPI_ISL_430720, EPI_ISL_430721, EPI_ISL_435144	Hospital Universitario La Paz	Hospital Universitario 12 de Octubre	Elias Dahdoh; Esther Viedma; Fernando Lázaro; Jesús Mingorance; Juan Carlos Galán; Julio García; M ^o Dolores Folgueira; Natalia Stella; Rafael Cantón; Rafael Delgado; Raúl Recio; Sara González
EPI_ISL_417969, EPI_ISL_417972, EPI_ISL_417975, EPI_ISL_417978, EPI_ISL_530041, EPI_ISL_530042	Hospital Universitario La Paz	Hospital Universitario La Paz	Elias Dahdoh; Esther Viedma; Fernando Lázaro; Jesús Mingorance; Juan Carlos Galán; Julio García; María Rodríguez; M ^o Dolores Folgueira; Natalia Stella; Rafael Cantón; Rafael Delgado; Raúl Recio; Sara González
EPI_ISL_831039	Hospital Universitario La Paz (Madrid)	SeqCOVID-SPAIN consortium/IBV(CSIC)	Elias Dahdoh; Fernando Lázaro-Perona; Jesús Mingorance and SeqCOVID-SPAIN consortium; María Rodríguez-Tejedor
EPI_ISL_871976, EPI_ISL_871977	Hospital Universitario Lozano Belsa	Instituto de Salud Carlos III	A. Monzón; F. Casas; I. Benito, R.; I. Jiménez; Iglesias-Caballero; M. Camarero; M. Cuesta; M. González-Esguevillas; M. Pozo; M. Zaballos; P. Jiménez; S. Juliá; S. Molinero Calamita; S. Varona
EPI_ISL_537809, EPI_ISL_537810	Hospital Universitario Marqués de Valdeilla (Santander), Servicio de Microbiología	SeqCOVID-SPAIN consortium/IBV(CSIC)	Daniel Pablo Marcos; Jesús Rodríguez Lozano; Jose Manuel Méndez Legaza; María Eleonor Cano García; María Siller Ruiz and SeqCOVID-SPAIN consortium; Mónica Gozalo Marguello
EPI_ISL_539503, EPI_ISL_539504, EPI_ISL_539505, EPI_ISL_539506, EPI_ISL_539507, EPI_ISL_539508, EPI_ISL_539513, EPI_ISL_539514, EPI_ISL_539515, EPI_ISL_539516, EPI_ISL_539517, EPI_ISL_539518, EPI_ISL_539519, EPI_ISL_578199, EPI_ISL_578192, EPI_ISL_871978, EPI_ISL_871980, EPI_ISL_871981, EPI_ISL_871982, EPI_ISL_871983	Hospital Universitario Miguel Servet	Instituto de Salud Carlos III	A. Monzón; A. Rezusta; F. Casas; I. Jiménez; I. Rezusta; A. Iglesias-Caballero; M. Camarero; M. Cuesta; M. González-Esguevillas; M. Molinero Calamita; M. Pozo; M. Zaballos; P. Jiménez; R. Benito; S. Juliá; S. Molinero Calamita; S. Pozo; S. Varona
EPI_ISL_452453, EPI_ISL_452454, EPI_ISL_452457, EPI_ISL_452459, EPI_ISL_452460, EPI_ISL_452461, EPI_ISL_452462, EPI_ISL_452464, EPI_ISL_452465, EPI_ISL_452466, EPI_ISL_452467, EPI_ISL_452468, EPI_ISL_452469, EPI_ISL_452470, EPI_ISL_452471, EPI_ISL_467064, EPI_ISL_467066, EPI_ISL_467068, EPI_ISL_467069, EPI_ISL_467070, EPI_ISL_467071, EPI_ISL_467072, EPI_ISL_467073, EPI_ISL_467074, EPI_ISL_467075, EPI_ISL_467076, EPI_ISL_467077, EPI_ISL_467078, EPI_ISL_467085, EPI_ISL_467086, EPI_ISL_467087	Hospital Universitario Puerta del Mar de Cádiz - INIBICA	SeqCOVID-SPAIN consortium/IBV(CSIC)	Fátima Galán-Sánchez; Manuel Rodríguez-Iglesias and SeqCOVID-SPAIN consortium; Manuel Rodríguez-Iglesias and SeqCOVID-SPAIN consortium; Salud Rodríguez-Palares
EPI_ISL_530004, EPI_ISL_530005, EPI_ISL_530006, EPI_ISL_530007, EPI_ISL_530008, EPI_ISL_530009	Hospital Universitario Ramón y Cajal	Hospital Universitario 12 de Octubre	Elias Dahdoh; Esther Viedma; Fernando Lázaro; Jesús Mingorance; Juan Carlos Galán; Julio García; M ^o Dolores Folgueira; Natalia Stella; Rafael Cantón; Rafael Delgado; Raúl Recio; Sara González
EPI_ISL_417979, EPI_ISL_417980, EPI_ISL_417981, EPI_ISL_530109, EPI_ISL_530110, EPI_ISL_530112, EPI_ISL_530113	Hospital Universitario Ramón y Cajal	Hospital Universitario La Paz	Elias Dahdoh; Esther Viedma; Fernando Lázaro; Jesús Mingorance; Juan Carlos Galán; Julio García; M ^o Dolores Folgueira; Natalia Stella; Rafael Cantón; Rafael Delgado; Raúl Recio; Sara González
EPI_ISL_871973	Hospital Universitario Severo Ochoa	Instituto de Salud Carlos III	A. Monzón; F. Casas; I. García; I. Jiménez; Iglesias-Caballero; M. Camarero; M. Cuesta; M. González-Esguevillas; M. Pozo; M. Zaballos; M.L.; P. Jiménez; S. Juliá; S. Molinero Calamita; S. Varona
EPI_ISL_419230	Hospital Universitario Virgen de las Nieves	Instituto de Salud Carlos III	Camarero, S.; Casas, I.; Cuesta, I.; González-Esguevillas, M.; Iglesias-Caballero, M.; Jiménez, P.; Juliá, M.; Molinero Calamita, M.; Monzón, S.; Pozo, F.; Sanbonmatsu, S.; Varona, S.; Zaballos, A.
EPI_ISL_467061, EPI_ISL_467062, EPI_ISL_474797, EPI_ISL_474833, EPI_ISL_474834, EPI_ISL_474841, EPI_ISL_474842, EPI_ISL_474843, EPI_ISL_474845, EPI_ISL_474851, EPI_ISL_474852, EPI_ISL_474854, EPI_ISL_474855, EPI_ISL_474856, EPI_ISL_474857, EPI_ISL_474859, EPI_ISL_474860, EPI_ISL_474861, EPI_ISL_474862, EPI_ISL_474863, EPI_ISL_474864, EPI_ISL_474865, EPI_ISL_474866, EPI_ISL_474867, EPI_ISL_474868, EPI_ISL_474869, EPI_ISL_474909, EPI_ISL_474920, EPI_ISL_474922, EPI_ISL_474923, EPI_ISL_474926, EPI_ISL_474927, EPI_ISL_474928, EPI_ISL_474930, EPI_ISL_474934, EPI_ISL_474936, EPI_ISL_474938, EPI_ISL_474943, EPI_ISL_510424, EPI_ISL_510444	Hospital Universitario Virgen de las Nieves de Granada-SAS	SeqCOVID-SPAIN consortium/IBV(CSIC)	Irene Pedrosa Corral; José M. Navarro-Mari and SeqCOVID-SPAIN consortium; Mercedes Pérez Ruiz; Sara Sanbonmatsu Gámez
EPI_ISL_471539	Hospital Universitario da USP Sao Paulo	Instituto Adolfo Lutz, Interdisciplinary Procedures Center, Strategic Laboratory	Claudia Regina Gonçalves; Claudio Tavares Sacchi; Erica Valessa Ramos Gomes
EPI_ISL_419233, EPI_ISL_455325, EPI_ISL_539532	Hospital Universitario de Canarias	Instituto de Salud Carlos III	A. Monzón; B. Castro; Camarero, S.; Casas, I.; Castro, B.; Cuesta, I.; F. Casas; González-Esguevillas, M.; I. Jiménez; Iglesias-Caballero; Iglesias-Caballero, M.; Jiménez, M.; Jiménez, P.; Juliá, M.; M. Camarero; M. Cuesta; M. González-Esguevillas; M. Molinero Calamita; M. Zaballos; Molinero Calamita, M.; Monzón, S.; P. Jiménez; Pozo, F.; S. Juliá; S. Pozo; S. Varona; Varona, S.; Zaballos, A.
EPI_ISL_539520, EPI_ISL_539521, EPI_ISL_539522, EPI_ISL_862655, EPI_ISL_862656, EPI_ISL_862657, EPI_ISL_862658	Hospital Universitario de Ceuta	Instituto de Salud Carlos III	A. Monzón; F. Casas; G. Sánchez; I. H. Hjana, S.; I. Jiménez; Iglesias-Caballero; J. López; M. Camarero; M. Cuesta; M. González-Esguevillas; M. Molinero Calamita; M. Pozo; M. Zaballos; P. Jiménez; S. Juliá; S. Molinero Calamita; S. Pozo; S. Varona
EPI_ISL_467086, EPI_ISL_467087, EPI_ISL_467088, EPI_ISL_467089, EPI_ISL_467090, EPI_ISL_467091, EPI_ISL_474910, EPI_ISL_474911, EPI_ISL_474912, EPI_ISL_474913, EPI_ISL_474914, EPI_ISL_474915, EPI_ISL_474916, EPI_ISL_474917, EPI_ISL_537683, EPI_ISL_537689, EPI_ISL_537700, EPI_ISL_537703, EPI_ISL_537706, EPI_ISL_537709, EPI_ISL_537709, EPI_ISL_537715, EPI_ISL_537715, EPI_ISL_537716, EPI_ISL_537716, EPI_ISL_561570	Hospital Universitario de Gran Canaria Dr. Negrín	SeqCOVID-SPAIN consortium/IBV(CSIC)	Ana Bordes Benítez and SeqCOVID-SPAIN consortium; Francisco J. Chamizo López; M. Carmen Pérez González
EPI_ISL_455315, EPI_ISL_455316, EPI_ISL_455317, EPI_ISL_455318, EPI_ISL_455319, EPI_ISL_455320, EPI_ISL_455321, EPI_ISL_455322, EPI_ISL_455324, EPI_ISL_539497	Hospital Virgen de las Nieves	Instituto de Salud Carlos III	A. Monzón; F. Casas; I. I. Jiménez; Iglesias-Caballero; J. Lepe; M. Camarero; M. Cuesta; M. González-Esguevillas; M. Molinero Calamita; M. Zaballos; P. Jiménez; S. Juliá; S. Pozo; S. Sanbonmatsu; S. Varona
EPI_ISL_455314	Hospital Virgen del Rocío	Instituto de Salud Carlos III	A. Monzón; F. Casas; I. I. Jiménez; Iglesias-Caballero; J. Lepe; M. Camarero; M. Cuesta; M. González-Esguevillas; M. Molinero Calamita; M. Zaballos; P. Jiménez; S. Juliá; S. Pozo; S. Varona
EPI_ISL_476435, EPI_ISL_476439, EPI_ISL_476445, EPI_ISL_476446, EPI_ISL_476469, EPI_ISL_476490, EPI_ISL_455352, EPI_ISL_455353, EPI_ISL_455354	Hospital da Clinicas da Faculdade de Medicina da Universidade de São Paulo	Instituto de Medicina Tropical da Universidade de São Paulo	Camila Alves Maia da Silva; Carolina S. Lazar; Cecília Salme Alencar; Darlan da Silva Candido; Erika Regina Manu; Ester Sabino; Flavia Cristina da Silva Sales; Gales Magalhães Ferreira; Jaqueleine Goes de Jesus; Julien Thezo; Mariana Severo Ramundo; Nuno Faria; Samples; Ingra Moraes Claro; Sequencing; Ingra Moraes Claro; Silvia F. Costa; Thais de Moura Coletti
EPI_ISL_414577, EPI_ISL_414578	Hospital de Cruces	Instituto de Salud Carlos III	A. Monzón; F. Casas; I. I. Jiménez; Iglesias-Caballero; M. Aranzamendi; M. Camarero; M. Cuesta; M. González-Esguevillas; M. Molinero Calamita; M. Zaballos; P. Jiménez; S. Juliá; S. Pozo; S. Varona
EPI_ISL_414577, EPI_ISL_414578	Hospital de Talca, Chile	Instituto de Salud Pública de Chile	Alejandra Acevedo; Andrés E. Castillo; Bárbara Barra; Carolina Tambly; Gabriel Lesi; Giselle Barra; Jaime Lagos; Javier Tognarelli; Jorge Fernández; Lorendi Arata; Patricia Bustos; Paz Topa; Rodrigo Fajos; Soledad Ulloa; Winston Andrade
EPI_ISL_510247, EPI_ISL_510248, EPI_ISL_510249, EPI_ISL_510250, EPI_ISL_510251, EPI_ISL_510252, EPI_ISL_510253, EPI_ISL_510256, EPI_ISL_510257, EPI_ISL_510258, EPI_ISL_510259, EPI_ISL_510260, EPI_ISL_510261, EPI_ISL_510262, EPI_ISL_510263, EPI_ISL_510264, EPI_ISL_510265, EPI_ISL_510266	Hospital de la Santa Creu i Sant Pau. Servicio de Microbiología	SeqCOVID-SPAIN consortium/IBV(CSIC)	Elsenda Miró and SeqCOVID-SPAIN consortium; Ferran Navarro; Núria Rabella
EPI_ISL_515565, EPI_ISL_523965, EPI_ISL_523982	Hospital do Servidor Público Estadual Francisco Morato de Oliveira	Instituto Adolfo Lutz, Interdisciplinary Procedures Center, Strategic Laboratory	Claudia Regina Gonçalves; Claudio Tavares Sacchi; Erica Valessa Ramos Gomes
EPI_ISL_861635	Hospital e Maternidade Madre Theodora	Instituto Adolfo Lutz, Interdisciplinary Procedures Center, Strategic Laboratory	Claudia Regina Gonçalves; Claudio Tavares Sacchi; Erica Valessa Ramos Gomes; Karoline Rodrigues Campos
EPI_ISL_893195	Hospital e Pronto Socorro Portinari	Instituto Adolfo Lutz, Interdisciplinary Procedures Center, Strategic Laboratory	Claudia Regina Gonçalves; Claudio Tavares Sacchi; Erica Valessa Ramos Gomes; Karoline Rodrigues Campos

see above	Hôpital Pierre-Le Gardeur	Laboratoire de santé publique du Québec	Guillaume Bourque; Ioannis Ragoussis; Jesse Shapiro; Mark Lathrop and Michel Roger; Mark Lathrop and Michel Roger on behalf of the CoVSeQ research group; Sandrine Moreira
EPI_ISL_414631, EPI_ISL_414632	Hôpital Robert Debré Laboratoire de Virologie	National Reference Center for Viruses of Respiratory Infections, Institut Pasteur, Paris	Angela Brisebarre; Flora Donat Vincent Enouf; Laurent Andreoletti; Marion Barbet; Maud Vanpeene; Méline Bizard; Méline Albert; Sylvie Behilli; Sylvie van der Werf
EPI_ISL_535810, EPI_ISL_535899, EPI_ISL_535969, EPI_ISL_536010, EPI_ISL_536011, EPI_ISL_536056, EPI_ISL_536057, EPI_ISL_536252	Hôpital Sainte-Croix	Laboratoire de santé publique du Québec	Guillaume Bourque; Ioannis Ragoussis; Jesse Shapiro; Mark Lathrop and Michel Roger; Mark Lathrop and Michel Roger on behalf of the CoVSeQ research group; Sandrine Moreira
see above	Hôpital d'Alma	Laboratoire de santé publique du Québec	Guillaume Bourque; Ioannis Ragoussis; Jesse Shapiro; Mark Lathrop and Michel Roger; Mark Lathrop and Michel Roger on behalf of the CoVSeQ research group; Sandrine Moreira
EPI_ISL_536046	Hôpital de Chicoufimi	Laboratoire de santé publique du Québec	Guillaume Bourque; Ioannis Ragoussis; Jesse Shapiro; Mark Lathrop and Michel Roger; Mark Lathrop and Michel Roger on behalf of the CoVSeQ research group; Sandrine Moreira
EPI_ISL_536056, EPI_ISL_536064, EPI_ISL_536107	Hôpital de Gatineau	Laboratoire de santé publique du Québec	Guillaume Bourque; Ioannis Ragoussis; Jesse Shapiro; Mark Lathrop and Michel Roger; Mark Lathrop and Michel Roger on behalf of the CoVSeQ research group; Sandrine Moreira
EPI_ISL_465601, EPI_ISL_535858, EPI_ISL_536266	Hôpital de Hull	Laboratoire de santé publique du Québec	Guillaume Bourque; Ioannis Ragoussis; Jesse Shapiro; Mark Lathrop and Michel Roger; Mark Lathrop and Michel Roger on behalf of the CoVSeQ research group; Sandrine Moreira
EPI_ISL_465686, EPI_ISL_535794, EPI_ISL_535809, EPI_ISL_535886, EPI_ISL_535887, EPI_ISL_535911, EPI_ISL_535995, EPI_ISL_536051, EPI_ISL_536117, EPI_ISL_536122, EPI_ISL_536124, EPI_ISL_536127, EPI_ISL_536132, EPI_ISL_536168, EPI_ISL_536169, EPI_ISL_536207, EPI_ISL_536208, EPI_ISL_536209, EPI_ISL_536230, EPI_ISL_536238, EPI_ISL_536239, EPI_ISL_536242, EPI_ISL_536244, EPI_ISL_536291, EPI_ISL_536312, EPI_ISL_536363, EPI_ISL_536367, EPI_ISL_536385, EPI_ISL_536386, EPI_ISL_536387, EPI_ISL_536392, EPI_ISL_536393	Hôpital de Lasalle	Laboratoire de santé publique du Québec	Guillaume Bourque; Ioannis Ragoussis; Jesse Shapiro; Mark Lathrop and Michel Roger; Mark Lathrop and Michel Roger on behalf of the CoVSeQ research group; Sandrine Moreira
see above	Hôpital de Maria	Laboratoire de santé publique du Québec	Guillaume Bourque; Ioannis Ragoussis; Jesse Shapiro; Mark Lathrop and Michel Roger; Mark Lathrop and Michel Roger on behalf of the CoVSeQ research group; Sandrine Moreira
EPI_ISL_535744	Hôpital de Mont-Laurier	Laboratoire de santé publique du Québec	Guillaume Bourque; Ioannis Ragoussis; Jesse Shapiro; Mark Lathrop and Michel Roger; Sandrine Moreira
EPI_ISL_465684, EPI_ISL_535885, EPI_ISL_536111, EPI_ISL_536112, EPI_ISL_536299	Hôpital de Papineau	Laboratoire de santé publique du Québec	Guillaume Bourque; Ioannis Ragoussis; Jesse Shapiro; Mark Lathrop and Michel Roger on behalf of the CoVSeQ research group; Sandrine Moreira
EPI_ISL_535945	Hôpital de Rouyn-Noranda	Laboratoire de santé publique du Québec	Guillaume Bourque; Ioannis Ragoussis; Jesse Shapiro; Mark Lathrop and Michel Roger on behalf of the CoVSeQ research group; Sandrine Moreira
EPI_ISL_535985, EPI_ISL_535986, EPI_ISL_535987	Hôpital de Saint-Eustache	Laboratoire de santé publique du Québec	Guillaume Bourque; Ioannis Ragoussis; Jesse Shapiro; Mark Lathrop and Michel Roger; Mark Lathrop and Michel Roger on behalf of the CoVSeQ research group; Sandrine Moreira
EPI_ISL_535793, EPI_ISL_535865, EPI_ISL_535926, EPI_ISL_535929, EPI_ISL_535930, EPI_ISL_535941, EPI_ISL_535942, EPI_ISL_535943, EPI_ISL_535947, EPI_ISL_535982	Hôpital de Verdun	Laboratoire de santé publique du Québec	Guillaume Bourque; Ioannis Ragoussis; Jesse Shapiro; Mark Lathrop and Michel Roger; Mark Lathrop and Michel Roger on behalf of the CoVSeQ research group; Sandrine Moreira
see above	Hôpital de l'Enfant-Jésus	Laboratoire de santé publique du Québec	Guillaume Bourque; Ioannis Ragoussis; Jesse Shapiro; Mark Lathrop and Michel Roger; Sandrine Moreira
EPI_ISL_535716, EPI_ISL_535723, EPI_ISL_535728	Hôpital du Centre-de-la-Mauricie	Laboratoire de santé publique du Québec	Guillaume Bourque; Ioannis Ragoussis; Jesse Shapiro; Mark Lathrop and Michel Roger; Mark Lathrop and Michel Roger on behalf of the CoVSeQ research group; Sandrine Moreira
EPI_ISL_535739	Hôpital du Sacré-Coeur de Montréal	Laboratoire de santé publique du Québec	Guillaume Bourque; Ioannis Ragoussis; Jesse Shapiro; Mark Lathrop and Michel Roger on behalf of the CoVSeQ research group; Sandrine Moreira
EPI_ISL_535914, EPI_ISL_535937, EPI_ISL_535971, EPI_ISL_535974, EPI_ISL_535978, EPI_ISL_535996, EPI_ISL_535998, EPI_ISL_535999, EPI_ISL_536001, EPI_ISL_536030	Hôpital de l'Enfant-Jésus	Laboratoire de santé publique du Québec	Guillaume Bourque; Ioannis Ragoussis; Jesse Shapiro; Mark Lathrop and Michel Roger; Mark Lathrop and Michel Roger on behalf of the CoVSeQ research group; Sandrine Moreira
see above	Hôpital du Suroit	Laboratoire de santé publique du Québec	Guillaume Bourque; Ioannis Ragoussis; Jesse Shapiro; Mark Lathrop and Michel Roger; Mark Lathrop and Michel Roger on behalf of the CoVSeQ research group; Sandrine Moreira
EPI_ISL_535812	Hôpital de Saint-Jérôme	Laboratoire de santé publique du Québec	Guillaume Bourque; Ioannis Ragoussis; Jesse Shapiro; Mark Lathrop and Michel Roger; Mark Lathrop and Michel Roger on behalf of the CoVSeQ research group; Sandrine Moreira
EPI_ISL_450307, EPI_ISL_450311, EPI_ISL_450313, EPI_ISL_465680, EPI_ISL_535913, EPI_ISL_535917, EPI_ISL_535918, EPI_ISL_535919, EPI_ISL_535988, EPI_ISL_536026, EPI_ISL_536095, EPI_ISL_536097, EPI_ISL_536098, EPI_ISL_536102, EPI_ISL_536105, EPI_ISL_536163, EPI_ISL_536198, EPI_ISL_536200, EPI_ISL_536201, EPI_ISL_536202, EPI_ISL_536228, EPI_ISL_536257, EPI_ISL_536259, EPI_ISL_536273, EPI_ISL_536274, EPI_ISL_536319, EPI_ISL_536349, EPI_ISL_536354, EPI_ISL_536355, EPI_ISL_536356, EPI_ISL_536357, EPI_ISL_536358, EPI_ISL_536359, EPI_ISL_536362, EPI_ISL_536390	Hôpital de Saint-Jérôme	Laboratoire de santé publique du Québec	Guillaume Bourque; Ioannis Ragoussis; Jesse Shapiro; Mark Lathrop and Michel Roger; Mark Lathrop and Michel Roger on behalf of the CoVSeQ research group; Sandrine Moreira
see above	Hôpital régional de Rimouski	Laboratoire de santé publique du Québec	Guillaume Bourque; Ioannis Ragoussis; Jesse Shapiro; Mark Lathrop and Michel Roger; Mark Lathrop and Michel Roger on behalf of the CoVSeQ research group; Sandrine Moreira
EPI_ISL_535901, EPI_ISL_536113, EPI_ISL_536114	Hôpital régional de Saint-Jérôme	Laboratoire de santé publique du Québec	Guillaume Bourque; Ioannis Ragoussis; Jesse Shapiro; Mark Lathrop and Michel Roger; Mark Lathrop and Michel Roger on behalf of the CoVSeQ research group; Sandrine Moreira
EPI_ISL_535720, EPI_ISL_535756, EPI_ISL_535757	Hôpital, CLSC et Centre d'Hébergement de Roberval	Laboratoire de santé publique du Québec	Guillaume Bourque; Ioannis Ragoussis; Jesse Shapiro; Mark Lathrop and Michel Roger on behalf of the CoVSeQ research group; Sandrine Moreira
EPI_ISL_536205	Hôtel-Dieu de Lévis	Laboratoire de santé publique du Québec	Guillaume Bourque; Ioannis Ragoussis; Jesse Shapiro; Mark Lathrop and Michel Roger; Mark Lathrop and Michel Roger on behalf of the CoVSeQ research group; Sandrine Moreira
EPI_ISL_535798, EPI_ISL_535838, EPI_ISL_536022	Hôtel-Dieu de Sorel	Laboratoire de santé publique du Québec	Guillaume Bourque; Ioannis Ragoussis; Jesse Shapiro; Mark Lathrop and Michel Roger; Mark Lathrop and Michel Roger on behalf of the CoVSeQ research group; Sandrine Moreira
EPI_ISL_536101	IA State Hygienic Laboratory	Pathogen Discovery, Respiratory Viruses Branch, Division of Viral Diseases, Centers for Disease Control and Prevention	Alison S. Lauffer Halpin; Anna Uehara; Brian Lynch; Christopher A. Elkins; Clinton R. Paden; Halbin Wang; Jasmine Padilla; Jing Zhang; Justin Lee; Krista Queen; Mary S. Keckler; Rachel Marine; Suxiang Tong; Yan Li; Ying Tao
EPI_ISL_535750, EPI_ISL_535751, EPI_ISL_535758, EPI_ISL_535759, EPI_ISL_535820, EPI_ISL_535821, EPI_ISL_535833, EPI_ISL_535834, EPI_ISL_535835, EPI_ISL_535836	ICMR-National Institute of Cholera and Enteric Diseases	National Institute of Biomedical Genomics	Ananya Chatterjee; Arindam Maitra; Hasina Banu; Mamta Chawla Sarkar; Saumitra Das; Shanta Dutta; Sreedhar Chinnaswamy
see above	IL Department of Public Health Chicago Laboratory	Pathogen Discovery, Respiratory Viruses Branch, Division of Viral Diseases, Centers for Disease Control and Prevention	Alison S. Lauffer Halpin; Anna Montmayeur; Anna Uehara; Christopher A. Elkins; Clinton R. Paden; Halbin Wang; Jing Zhang; Krista Queen; Mary S. Keckler; Rachel Marine; Suxiang Tong; Yan Li; Ying Tao; Zachary Weiner
EPI_ISL_535903, EPI_ISL_535904, EPI_ISL_535990, EPI_ISL_536121	IN State Department of Health Laboratory Services	Pathogen Discovery, Respiratory Viruses Branch, Division of Viral Diseases, Centers for Disease Control and Prevention	Alison S. Lauffer Halpin; Anna Montmayeur; Anna Uehara; Christopher A. Elkins; Clinton R. Paden; Halbin Wang; Jing Zhang; Krista Queen; Mary S. Keckler; Rachel Marine; Suxiang Tong; Yan Li; Ying Tao; Zachary Weiner
EPI_ISL_424865, EPI_ISL_424895, EPI_ISL_424896, EPI_ISL_424897, EPI_ISL_424898, EPI_ISL_424899, EPI_ISL_424900, EPI_ISL_447842, EPI_ISL_647990, EPI_ISL_647991, EPI_ISL_647992, EPI_ISL_647993, EPI_ISL_647994, EPI_ISL_647995, EPI_ISL_647996, EPI_ISL_647997, EPI_ISL_647998, EPI_ISL_647999, EPI_ISL_648000, EPI_ISL_648001	INMI Lazzaro Spallanzani IRCCS	INMI Lazzaro Spallanzani IRCCS	Antonino Di Caro; Barbara Bartolini; Cesare E. M. Gruber; Cesare Ernesto Maria Gruber; Concetta Castilletti; Daniele Lapa; Eleonora Lalle; Emanuela Giombini; Fabrizio Carletti; Francesca Colavita; Francesco Mesana; Giuseppe Ippolito; Licia Bordini; Maria R. Capobianchi; Maria Rosaria Capobianchi; Martina Ruesca
see above	INMI Lazzaro Spallanzani IRCCS	Laboratory of Virology, INMI Lazzaro Spallanzani IRCCS	Antonino Di Caro; Barbara Bartolini; Cesare E. M. Gruber; Cesare Ernesto Maria Gruber; Concetta Castilletti; Daniele Lapa; Eleonora Lalle; Emanuela Giombini; Fabrizio Carletti; Francesca Colavita; Francesco Mesana; Giuseppe Ippolito; Licia Bordini; Maria R. Capobianchi; Maria Rosaria Capobianchi; Martina Ruesca
EPI_ISL_826798, EPI_ISL_826800, EPI_ISL_826802, EPI_ISL_826804, EPI_ISL_826805, EPI_ISL_826807, EPI_ISL_826809, EPI_ISL_826811, EPI_ISL_826812, EPI_ISL_826814, EPI_ISL_826816, EPI_ISL_826818	INMI Lazzaro Spallanzani IRCCS	Laboratory of Virology, INMI Lazzaro Spallanzani IRCCS	Antonino Di Caro; Barbara Bartolini; Cesare E. M. Gruber; Cesare Ernesto Maria Gruber; Concetta Castilletti; Daniele Lapa; Eleonora Lalle; Emanuela Giombini; Fabrizio Carletti; Francesca Colavita; Francesco Mesana; Giuseppe Ippolito; Licia Bordini; Maria R. Capobianchi; Maria Rosaria Capobianchi; Martina Ruesca

	see above	INSPI-CRN DE INFLUENZA Y OTROS VIRUS RESPIRATORIOS	Instituto de Salud Publica de Chile	Alfredo Bruno; Andres Castillo; Barbara Parra; Domenica de Mora; Giselle Barra; Jaime Lagos; Javier Tognarelli; Jimmy Garce; Jorge Fernandez; Loredana Arata; Manuel Gonzalez; Maritza Ornela; Michelle Paez; Patricia Bustos; Rodrigo Fasce; Solon Narvaez
EPI_ISL_445302		INSTITUTO MEDICO LEGAL	Instituto de Salud Publica de Chile	Alejandra Acevedo; Andrés E Castillo; Bárbara Parra; Carolina Tambley; Gabriel Leal; Jaime Lagos; Jorge Fernandez; Loredana Arata; Patricia Bustos; Paz Tapia; Rodrigo Fasce; Winston Andrade
EPI_ISL_445261		INTEGRAMEDICA LAB. CLINICO LTDA.	Instituto de Salud Publica de Chile	Alejandra Acevedo; Andrés E Castillo; Bárbara Parra; Carolina Tambley; Gabriel Leal; Jaime Lagos; Jorge Fernandez; Loredana Arata; Patricia Bustos; Paz Tapia; Rodrigo Fasce; Winston Andrade
EPI_ISL_492980, EPI_ISL_492984, EPI_ISL_492985, EPI_ISL_492986, EPI_ISL_492987, EPI_ISL_751320, EPI_ISL_751347, EPI_ISL_751348, EPI_ISL_751349, EPI_ISL_751350, EPI_ISL_751351, EPI_ISL_751352, EPI_ISL_751353, EPI_ISL_751354, EPI_ISL_751355, EPI_ISL_751356, EPI_ISL_751357, EPI_ISL_751358, EPI_ISL_751359, EPI_ISL_751360, EPI_ISL_751361, EPI_ISL_751362, EPI_ISL_751363, EPI_ISL_751364, EPI_ISL_751365, EPI_ISL_751366, EPI_ISL_751367, EPI_ISL_751368, EPI_ISL_751369, EPI_ISL_751370, EPI_ISL_751371, EPI_ISL_751372, EPI_ISL_751373, EPI_ISL_751374, EPI_ISL_751375, EPI_ISL_751376, EPI_ISL_751377, EPI_ISL_751378, EPI_ISL_751379, EPI_ISL_751380, EPI_ISL_751381, EPI_ISL_751382, EPI_ISL_751383, EPI_ISL_751384, EPI_ISL_751385, EPI_ISL_751386, EPI_ISL_751387, EPI_ISL_751388, EPI_ISL_751389, EPI_ISL_751390, EPI_ISL_751391, EPI_ISL_751392, EPI_ISL_751393, EPI_ISL_751394, EPI_ISL_751395, EPI_ISL_751396, EPI_ISL_751397, EPI_ISL_751398, EPI_ISL_751399, EPI_ISL_751400, EPI_ISL_751401, EPI_ISL_751402, EPI_ISL_751403, EPI_ISL_751404, EPI_ISL_751405, EPI_ISL_751406, EPI_ISL_751407, EPI_ISL_751408, EPI_ISL_751409, EPI_ISL_751410, EPI_ISL_751411, EPI_ISL_751412, EPI_ISL_751413, EPI_ISL_751414, EPI_ISL_751415, EPI_ISL_751416, EPI_ISL_751417, EPI_ISL_751418, EPI_ISL_751419, EPI_ISL_751420, EPI_ISL_751421, EPI_ISL_751422, EPI_ISL_751423, EPI_ISL_751424, EPI_ISL_751425, EPI_ISL_751426, EPI_ISL_751427				
	see above	IRCCS Sacro Cuore Don Calabria Hospital, Department of Infectious, Tropical Diseases & Microbiology	University of Verona, Department of Biotechnology	Antonio Mori, Chiara Degli Esposti, Chiara Piubelli, Cristina Beltrami, Elena Romari, Emanuela Cosenin; Giulia Lopatniello; Luca Marcolongo; Massimo Delledonne; Michela Deiana
EPI_ISL_480961, EPI_ISL_480989		ISGlobal, Institut de Salut Global de Barcelona	SeqCOVID-SPAIN consortium/IBV(CSIC)	Alberto I. Garcia-Basteiro; Alfredo Mayor; Carola Dobao; Gemma Moneuncill; Pau Cisteró and SeqCOVID-SPAIN consortium
EPI_ISL_572324		IZSM	IZSM	Giovanna Fusco; Lorena Cardillo; Maurizio Viscardi
EPI_ISL_479936, EPI_ISL_479937, EPI_ISL_479938, EPI_ISL_479939, EPI_ISL_479940, EPI_ISL_479941, EPI_ISL_479942, EPI_ISL_479943, EPI_ISL_479944, EPI_ISL_479945, EPI_ISL_479946, EPI_ISL_479947, EPI_ISL_479948, EPI_ISL_479949, EPI_ISL_480001, EPI_ISL_480002, EPI_ISL_480003, EPI_ISL_480004, EPI_ISL_480025, EPI_ISL_480026, EPI_ISL_480027, EPI_ISL_480028, EPI_ISL_480180, EPI_ISL_480181				
	see above	Ibaraki Prefectural Institute of Public Health	Pathogen Genomics Center, National Institute of Infectious Diseases	Hajime Kamiya; Keiko Goto; Kentaro Itokawa; Makoto Kuroda; Masanori Hashino; Motoi Suzuki; Rina Tanaka; Tsuyoshi Sekizuka
EPI_ISL_683658, EPI_ISL_683659, EPI_ISL_683663, EPI_ISL_683664, EPI_ISL_683669, EPI_ISL_683670, EPI_ISL_683672, EPI_ISL_683673, EPI_ISL_683674, EPI_ISL_779716, EPI_ISL_779717, EPI_ISL_779718, EPI_ISL_779719, EPI_ISL_779720, EPI_ISL_779721, EPI_ISL_779722, EPI_ISL_779723, EPI_ISL_779724, EPI_ISL_779725, EPI_ISL_779726, EPI_ISL_779727, EPI_ISL_779728, EPI_ISL_779729, EPI_ISL_779754, EPI_ISL_779755, EPI_ISL_779756, EPI_ISL_779757, EPI_ISL_779758, EPI_ISL_779759, EPI_ISL_779760, EPI_ISL_779761, EPI_ISL_779762, EPI_ISL_779763, EPI_ISL_779764, EPI_ISL_779765, EPI_ISL_779766, EPI_ISL_779767, EPI_ISL_779768, EPI_ISL_779769, EPI_ISL_779770, EPI_ISL_779771, EPI_ISL_779772, EPI_ISL_779773, EPI_ISL_855403				
	see above	IDISSC/Hospital Clinico San Carlos de Madrid	SeqCOVID-SPAIN consortium/IBV(CSIC)	Alberto Delgado-Imbarren; Esther Culebras Lopez; Esther Culebras Lopez; Jorge Matias-Guiu; Luis Ortega Medina; Silvia Sánchez Ramón; Ulises Gómez-Pinedo and SeqCOVID-SPAIN consortium; Vicente Estrada Pérez
EPI_ISL_632847, EPI_ISL_632848, EPI_ISL_632849, EPI_ISL_632850, EPI_ISL_632851, EPI_ISL_632852, EPI_ISL_632853, EPI_ISL_632854, EPI_ISL_632855, EPI_ISL_632856, EPI_ISL_632857, EPI_ISL_632858, EPI_ISL_632859, EPI_ISL_632861, EPI_ISL_632862, EPI_ISL_632863, EPI_ISL_632864, EPI_ISL_632865, EPI_ISL_632866, EPI_ISL_632867, EPI_ISL_632868, EPI_ISL_632869, EPI_ISL_632870, EPI_ISL_632871, EPI_ISL_632872, EPI_ISL_632873, EPI_ISL_632874, EPI_ISL_632875				
	see above	Idaho Bureau of Laboratories	Center for Global Health, University of New Mexico Health Sciences Center	Christopher Ball; Darrell Dinwiddie; Daryl Domman; Kurt Schwalim; Matthew Burns; Robert Voermans
EPI_ISL_1164798, EPI_ISL_1164813		Idaho Bureau of Laboratories	IBL	"R. Beukeلمان; Aimee Censerios; Christopher Ball"; Matthew C. Burns; Robert L. Voermans
EPI_ISL_848466		Illinois Department of Public Health	Gagnon Lab, Southern Illinois University	Keith Gagnon
EPI_ISL_420789, EPI_ISL_420790		Illinois Department of Public Health Chicago Laboratory	Pathogen Discovery, Respiratory Viruses Branch, Division of Viral Diseases, Centers for Disease Control and Prevention	Ailson S. Lauffer Halpin; Anne Uehara; Christopher A. Elkins; Clinton R. Paden; Habtin Waud; Jasmine Padilla; Jing Zhang; Justin Lee; Krista Queen; Mary S. Keckler; Rachel Martinez; Suzang Tong; Yan Li; Ying Tao
EPI_ISL_475572		Imperial College London	Imperial College London	Je Zhou; Wendy Barclay
EPI_ISL_637009, EPI_ISL_637100, EPI_ISL_637101, EPI_ISL_637103, EPI_ISL_637104		Indian Council of Medical Research-National Institute of Virology, Microbial Containment Complex	Indian Council of Medical Research-National Institute of Virology, Microbial Containment Complex	Anita Shele-Aich; Dimpal A. Nyeayanit; Gururaj Rao Deshpande; Padijaramoorthy Thankann Ullas; Pragya D. Yadav; Prasad Sarkale; Priya Abraham; Varsha Potdar
EPI_ISL_413518, EPI_ISL_413519, EPI_ISL_413520, EPI_ISL_413521, EPI_ISL_514752		Infectious Disease Control Center, Center for Disease Control and Prevention of PLA	Infectious Disease Control Center, Center for Disease Control and Prevention of PLA	Li, L. J.; Li, L.; Li, P.; Li, Z. P.; Liu, S.; Qiu, S.; Song, H.
EPI_ISL_962528, EPI_ISL_962529, EPI_ISL_962530, EPI_ISL_962531, EPI_ISL_962532, EPI_ISL_962533, EPI_ISL_962534, EPI_ISL_962535, EPI_ISL_962536, EPI_ISL_962537, EPI_ISL_962538, EPI_ISL_962539, EPI_ISL_962540, EPI_ISL_962541, EPI_ISL_962542, EPI_ISL_962543, EPI_ISL_962544, EPI_ISL_962545, EPI_ISL_962546, EPI_ISL_962547, EPI_ISL_962548, EPI_ISL_962549, EPI_ISL_962550, EPI_ISL_962551, EPI_ISL_962552, EPI_ISL_962553, EPI_ISL_962554, EPI_ISL_962555, EPI_ISL_962556, EPI_ISL_962557, EPI_ISL_962558, EPI_ISL_962559, EPI_ISL_962560, EPI_ISL_962561, EPI_ISL_962562, EPI_ISL_962563, EPI_ISL_962564, EPI_ISL_962565, EPI_ISL_962566, EPI_ISL_962567, EPI_ISL_962568, EPI_ISL_962569, EPI_ISL_962570, EPI_ISL_962571, EPI_ISL_962572, EPI_ISL_962573, EPI_ISL_962574, EPI_ISL_962575, EPI_ISL_962576, EPI_ISL_962577, EPI_ISL_962578, EPI_ISL_962579, EPI_ISL_962580, EPI_ISL_962581, EPI_ISL_962582, EPI_ISL_962583, EPI_ISL_962584, EPI_ISL_962586, EPI_ISL_962589, EPI_ISL_962609, EPI_ISL_962870, EPI_ISL_962871, EPI_ISL_962873, EPI_ISL_962874, EPI_ISL_962875				
	see above	Infectious Disease Control and Prevention Institute	Infectious Disease Control and Prevention Institute	Bo Pang; Jianxing Wang; Julong Wu; Mingxiao Yao; Ti Liu; Xiaolin Jiang; Yan Li; Yujie He; Yuwei Zhang; Zengqiang Kou
EPI_ISL_596454		Infectious Disease and Tropical Medicine Research Center, Resistant Tuberculosis Institute, Zhejidian University of Medical Sciences, Zhejiang, Iran.	Genetics Research Center, University of Social Welfare and Rehabilitation Sciences	Ali Jafarpour; Azam Ghaziassadi; Ebrahim Kord; Hossein Najmabadi; Khadijeh Jalavand; Kimia Kahzizi; Marziyeh Moheini; Seyed Mohammad Hashemi-Shahi; Seyed Mohammad Jazayeri; Seyedeh Elham Mortazavi; Zohreh Fattahi
EPI_ISL_856712, EPI_ISL_856716		Infectious Diseases Unit, Department of Internal Medicine, Azienda Ospedaliera-Universitaria di Padova	Laboratory of Infectious Diseases, Department of Biomedical and Clinical Sciences L. Sacco, University of Milan	Alessia Lai; Anna Maria Cattelan; Annalisa Bergna; Carlo Della Ventura; Claudia Balotta; Davide Lenzi; Giangiulielmo Zehender on behalf of SARS-CoV-2 ITALIAN RESEARCH ENTERPRISE (SCIRE) Collaborative Group; Lolita Sasset; Massimo Galli
EPI_ISL_541970		Influenza Centre, University of Bergen	Norwegian Institute of Public Health, Department of Virology	Bjorn Blomborg; Fan Zhou; Hilde Ellehaug; Hilde Synnove Vøllan; Kamilla Heddeland Inefjord; Karl A Brokstad; Karoline Bragstad; Kathrine Stene-Johansen; Olav Hungnes; Rasmus Riis Kopperud; Rebecca J Cox
EPI_ISL_470900		Influenza etiology and epidemiology laboratory	Pathogenic Microorganisms Variability Laboratory	Alexander Gintsburg; Alexey Shchekhin; Andrey Botikov; Daria Grousova; Denis Logunov; Elena Burtseva; Elena Shidlovskaya; Inna Dolzhikova; Kirill Krasnoshchikov; Ludmila Kobukhina; Maria Nefedova; Nadezhda Kuznetsova; Svetlana Smetanova; Svetlana Trushakova; Vladimir Gutshchin
EPI_ISL_418215		Institut Pasteur Dakar	Institut Pasteur de Dakar	Amadou Alpha Sall; Ndongo Dia; Ousmane Faye
EPI_ISL_416408, EPI_ISL_428355, EPI_ISL_428356, EPI_ISL_428357		Institut Médico légal- Hop R. Poincaré	National Reference Center for Viruses of Respiratory Infections, Institut Pasteur, Paris	Angela Brisebare; Etienne Simon-Lorière; Flora Donati; Marion Barbet; Maud Vanpeene; Mélanie Albert; Moline Bizard; Sylvie Behilli; Sylvie van der Werf; Vincent Enouf
EPI_ISL_1293351, EPI_ISL_1303031, EPI_ISL_1321604		Institut National d'Hygiène (INH)	Unité Mixte Internationale TransVIHMI (UMI 233 IRD - U1175 INSERM - Université de Montpellier)IRD (institut de recherche pour le développement)	Abla A. KONOU; Adodo SADJI; Ahidjo AYOUBA; Akoaé SILADIN; Alassane OURO-MEDEL; Amvi EHLAN; Amélyo DORKENOO; Anoumou DAGNRA; Christelle BUTEL; Diéma MABA; Eric DELAPORTE; Issaka Maman; Kokou TEGUENI; Laetitia SERRANO; Marine PEETERS; Messanh DOUFFAN; Mirielle PRINCE-DAVID; Mounrou SALOU; Sidonie A. M. KACONISSOUE; Sika DOSSIM; Wembo A. HALATOKO
EPI_ISL_418206, EPI_ISL_418207, EPI_ISL_418208, EPI_ISL_418209, EPI_ISL_418210, EPI_ISL_418211, EPI_ISL_418212, EPI_ISL_418213, EPI_ISL_418214, EPI_ISL_418215, EPI_ISL_418216, EPI_ISL_418217, EPI_ISL_420069, EPI_ISL_420070, EPI_ISL_420072, EPI_ISL_420073, EPI_ISL_420074, EPI_ISL_420075, EPI_ISL_420076, EPI_ISL_420077, EPI_ISL_420078, EPI_ISL_480554, EPI_ISL_480556, EPI_ISL_480763, EPI_ISL_480787				
	see above	Institut Pasteur Dakar	Institut Pasteur de Dakar	Amadou Alpha Sall; Amadou Alpha Sall.; Amadou Alpha Sall.; Amadou Diop; Mamadou Malado Jallow; Marie Henriette Dior Ndioue; Moussa Moise Diagne; Ndongo Dia; Ousmane Faye; Saifouou Sanke
EPI_ISL_613418, EPI_ISL_613420, EPI_ISL_613421, EPI_ISL_613422, EPI_ISL_613423, EPI_ISL_613424, EPI_ISL_613425, EPI_ISL_613426, EPI_ISL_613427, EPI_ISL_613428, EPI_ISL_613429, EPI_ISL_613430, EPI_ISL_613431, EPI_ISL_613432, EPI_ISL_613433, EPI_ISL_613434, EPI_ISL_613435, EPI_ISL_613436, EPI_ISL_613437, EPI_ISL_613438, EPI_ISL_613439, EPI_ISL_613440, EPI_ISL_613441, EPI_ISL_613442, EPI_ISL_613443, EPI_ISL_613444, EPI_ISL_613445, EPI_ISL_613446, EPI_ISL_613447, EPI_ISL_613448, EPI_ISL_613449, EPI_ISL_613450, EPI_ISL_613451, EPI_ISL_613452				
	see above	Institut Pasteur de la Guadeloupe	Institut Pasteur de la Guadeloupe	Angela Brisebare; Antoine Talarmin; Camille Capel; Cherina Fleming; Etienne Simon-Lorière; Marion Barbet; Maud Vanpeene; Méline Bizard; Radjiv Steingrover; Stéphanie Guymard; Sylvie Behilli; Sylvie van der Werf; Sébastien Breurec; Vincent Enouf
EPI_ISL_459965, EPI_ISL_459966, EPI_ISL_459967, EPI_ISL_459968, EPI_ISL_459972, EPI_ISL_459973, EPI_ISL_459974, EPI_ISL_459975, EPI_ISL_459976		Institut Pasteur du Maroc	Institut Pasteur du Maroc	Abdellah Fouzi; Anass Abbad; Anderahmane Maaroufi; Angela Brisebare; Camille Capel; Etienne Simon-Lorière; Jalal Nourli; Latifa Anga; Marion Barbet; Maud Vanpeene; Mjid Etoualkil; Méline Bizard; Sylvie Behilli; Sylvie van der Werf; Vincent Enouf

EPI_ISL_417880	Slovak Academy of Sciences, Bratislava Institute of Virology, Biomedical Research Center of the Slovak Academy of Sciences, Bratislava, Public Health Authority of the Slovak Republic, Bratislava	Institute of Virology, Biomedical Research Center of the Slovak Academy of Sciences, Bratislava, Comenius University Science Park, Bratislava	Neboháňová, Monika Slávková; Sabina Fumaová Havliková; Tomáš Vlna; Viktória Hodorová; Viktória abanová; ubomira Lukalíková Boris Klempa; Diana Rusaková; Edita Staroňová; Elena Tichá; Jaroslav Bubiš; Juraj Kopáček; Juraj Koi; Martina Liková; Miroslav Böhmer; Monika Slávková; Sabina Fumaová Havliková; Tomáš Szemiel; Werner Krampfl	
EPI_ISL_852668, EPI_ISL_852669, EPI_ISL_852670, EPI_ISL_852671, EPI_ISL_852672, EPI_ISL_852673, EPI_ISL_852674, EPI_ISL_852675, EPI_ISL_852676, EPI_ISL_852677, EPI_ISL_852678, EPI_ISL_852679, EPI_ISL_852680, EPI_ISL_852681, EPI_ISL_852682, EPI_ISL_852683, EPI_ISL_852684, EPI_ISL_852685, EPI_ISL_852686, EPI_ISL_852687, EPI_ISL_852688, EPI_ISL_852689, EPI_ISL_852690, EPI_ISL_852691, EPI_ISL_852692, EPI_ISL_852693, EPI_ISL_852694, EPI_ISL_852695, EPI_ISL_852696, EPI_ISL_852697, EPI_ISL_852698, EPI_ISL_852699, EPI_ISL_852700, EPI_ISL_852701, EPI_ISL_852702, EPI_ISL_852703, EPI_ISL_852704, EPI_ISL_852705, EPI_ISL_852706, EPI_ISL_852707, EPI_ISL_852708, EPI_ISL_852709, EPI_ISL_852710, EPI_ISL_852711, EPI_ISL_852712, EPI_ISL_852713, EPI_ISL_852714, EPI_ISL_852715, EPI_ISL_852716, EPI_ISL_852717, EPI_ISL_852718, EPI_ISL_852719, EPI_ISL_852720, EPI_ISL_852721, EPI_ISL_852722, EPI_ISL_852723, EPI_ISL_852724, EPI_ISL_852725, EPI_ISL_852726, EPI_ISL_852727, EPI_ISL_852728, EPI_ISL_852729, EPI_ISL_852730, EPI_ISL_852731, EPI_ISL_852732, EPI_ISL_852733, EPI_ISL_852734, EPI_ISL_852735, EPI_ISL_852736, EPI_ISL_852737, EPI_ISL_852738, EPI_ISL_852739, EPI_ISL_852740, EPI_ISL_852741, EPI_ISL_852742, EPI_ISL_852743, EPI_ISL_852744, EPI_ISL_852745, EPI_ISL_852746, EPI_ISL_852747, EPI_ISL_852748, EPI_ISL_852749, EPI_ISL_852750, EPI_ISL_852751, EPI_ISL_852752, EPI_ISL_852753, EPI_ISL_852754, EPI_ISL_852755, EPI_ISL_852756, EPI_ISL_852757, EPI_ISL_852758, EPI_ISL_852759, EPI_ISL_852760, EPI_ISL_852761, EPI_ISL_852762, EPI_ISL_852763, EPI_ISL_852764, EPI_ISL_852765, EPI_ISL_852766, EPI_ISL_852767, EPI_ISL_852768, EPI_ISL_852769, EPI_ISL_852770, EPI_ISL_852771, EPI_ISL_852772, EPI_ISL_852773, EPI_ISL_852774, EPI_ISL_852775, EPI_ISL_852776, EPI_ISL_852777, EPI_ISL_852778, EPI_ISL_852779, EPI_ISL_852780, EPI_ISL_852781, EPI_ISL_852782, EPI_ISL_852783, EPI_ISL_852784, EPI_ISL_852785, EPI_ISL_852786, EPI_ISL_852787, EPI_ISL_852788, EPI_ISL_852789, EPI_ISL_852790, EPI_ISL_852791, EPI_ISL_852792, EPI_ISL_852793, EPI_ISL_852794, EPI_ISL_852795, EPI_ISL_852796, EPI_ISL_852797, EPI_ISL_852798, EPI_ISL_852799, EPI_ISL_852800, EPI_ISL_852801, EPI_ISL_852802, EPI_ISL_852803, EPI_ISL_852810, EPI_ISL_852811, EPI_ISL_852812	Institute of Virology, Medical Center, University of Freiburg, Freiburg, Germany	Institute of Virology, Clinical Virus Genomics, Medical Center, University of Freiburg, Freiburg, Germany	Hajo Grundmann; Jonas Fuchs; Lisa Kern; Marcus Panning; Sandra Reuter	
EPI_ISL_983566, EPI_ISL_983567, EPI_ISL_983568, EPI_ISL_983569, EPI_ISL_983570, EPI_ISL_983571, EPI_ISL_983572, EPI_ISL_983573, EPI_ISL_983574, EPI_ISL_983575, EPI_ISL_983576, EPI_ISL_983577, EPI_ISL_983578, EPI_ISL_983579, EPI_ISL_983580, EPI_ISL_983581, EPI_ISL_983582, EPI_ISL_983583	EPI_ISL_983566, EPI_ISL_983567, EPI_ISL_983568, EPI_ISL_983569, EPI_ISL_983570, EPI_ISL_983571, EPI_ISL_983572, EPI_ISL_983573, EPI_ISL_983574, EPI_ISL_983575, EPI_ISL_983576, EPI_ISL_983577, EPI_ISL_983578, EPI_ISL_983579, EPI_ISL_983580, EPI_ISL_983581, EPI_ISL_983582, EPI_ISL_983583	Institute of Virology, University Hospital, University of Bonn and German Center for Infection Research (DZIF), Bonn-Cologne, Bonn, Germany	Institute of Virology, University Hospital, University of Bonn and German Center for Infection Research (DZIF), Bonn-Cologne, Bonn, Germany	Marek Korenecak et al
EPI_ISL_455680	Institute of pathogenic microbiology, Jiangsu Provincial Center for Disease Control and Prevention	Institute of pathogenic microbiology, Jiangsu Provincial Center for Disease Control and Prevention	Cui, L.	
EPI_ISL_776751, EPI_ISL_776752, EPI_ISL_776753, EPI_ISL_776754, EPI_ISL_776760, EPI_ISL_776761, EPI_ISL_776762, EPI_ISL_776763, EPI_ISL_792101, EPI_ISL_792102, EPI_ISL_792104, EPI_ISL_792105, EPI_ISL_792106, EPI_ISL_792107, EPI_ISL_833152, EPI_ISL_833153, EPI_ISL_861626, EPI_ISL_861627, EPI_ISL_861633	Instituto Adolfo Lutz - Central	Instituto Adolfo Lutz, Interdisciplinary Procedures Center, Strategic Laboratory	Claudia Regina Gonçalves; Claudio Tavares Saachi; Erica Valeasa Ramos Gomes; Karoline Rodrigues Campos	
EPI_ISL_792103	Instituto Adolfo Lutz - Regional de Santo Andre	Instituto Adolfo Lutz, Interdisciplinary Procedures Center, Strategic Laboratory	Claudia Regina Gonçalves; Claudio Tavares Saachi; Erica Valeasa Ramos Gomes; Karoline Rodrigues Campos	
EPI_ISL_426364	Instituto Nacional de Ciencias Medicas y Nutricion Salvador Zubiran	Instituto Nacional de Ciencias Medicas y Nutricion Zubiran	Adnan Araiza Rodríguez; Alejandro Sánchez; Alfredo Ponce de León Garduño; Blanca Taboada; Carlos F. Arias; Carolina González Torres; Celia Boukadida; Cesar Raúl González Bonilla; Concepción Grajales Muñoz; Edgar Mendietta Condado; Eduardo Becerri Vargas; Fabiola Garcés Ayala; Fernando Ledesma Barrientos; Francisco Javier Gaytán Cervantes; Francisco Pulido; Gisela Barrera Badillo; Gloria Vázquez; Guillermo M. Ruiz-Palacios; Irma López Martínez; Joel Armando Vázquez Pérez; José Arturo Martínez Orozco; José Ernesto Ramírez González; José Esteban Muñoz Medina; Lucia Hernández Rivas; Luis Alberto García Andrade; Mario Mujica Sánchez; Pavel Isa; Pilar Ramos Cervantes; Ricardo García; Santiago Avila Rios; Victor Hugo Borja Aburto; Violeta Ibarra González	
EPI_ISL_426361, EPI_ISL_426362, EPI_ISL_426363, EPI_ISL_426365	Instituto Nacional de Ciencias Medicas y Nutricion Salvador Zubiran	Instituto Nacional de Ciencias Medicas y Nutricion Zubiran	Adnan Araiza Rodríguez; Alejandro Sánchez; Alfredo Ponce de León Garduño; Blanca Taboada; Carlos F. Arias; Carolina González Torres; Celia Boukadida; Cesar Raúl González Bonilla; Concepción Grajales Muñoz; Edgar Mendietta Condado; Eduardo Becerri Vargas; Fabiola Garcés Ayala; Fernando Ledesma Barrientos; Francisco Javier Gaytán Cervantes; Francisco Pulido; Gisela Barrera Badillo; Gloria Vázquez; Guillermo M. Ruiz-Palacios; Irma López Martínez; Joel Armando Vázquez Pérez; José Arturo Martínez Orozco; José Ernesto Ramírez González; José Esteban Muñoz Medina; Lucia Hernández Rivas; Luis Alberto García Andrade; Mario Mujica Sánchez; Pavel Isa; Pilar Ramos Cervantes; Ricardo García; Santiago Avila Rios; Victor Hugo Borja Aburto; Violeta Ibarra González	
EPI_ISL_424627	Instituto Nacional de Enfermedades Respiratorias	Instituto Nacional de Enfermedades Respiratorias	Adnan Araiza Rodríguez; Alejandro Sánchez; Alfredo Ponce de León Garduño; Blanca Taboada; Carlos F. Arias; Carolina González Torres; Celia Boukadida; Cesar Raúl González Bonilla; Concepción Grajales Muñoz; Edgar Mendietta Condado; Eduardo Becerri Vargas; Fabiola Garcés Ayala; Fernando Ledesma Barrientos; Francisco Javier Gaytán Cervantes; Francisco Pulido; Gisela Barrera Badillo; Gloria Vázquez; Guillermo M. Ruiz-Palacios; Irma López Martínez; Joel Armando Vázquez Pérez; Jorge Salas Hernández; José Arturo Martínez Orozco; José Ernesto Ramírez González; José Esteban Muñoz Medina; Lucia Hernández Rivas; Luis Alberto García Andrade; Mario Mujica Sánchez; Pavel Isa; Pilar Ramos Cervantes; Ricardo García; Santiago Avila Rios; Victor Hugo Borja Aburto; Violeta Ibarra González	
EPI_ISL_837608, EPI_ISL_837609, EPI_ISL_837610, EPI_ISL_837611, EPI_ISL_837612, EPI_ISL_837613, EPI_ISL_837614, EPI_ISL_837615, EPI_ISL_837616, EPI_ISL_837617, EPI_ISL_837618, EPI_ISL_837619, EPI_ISL_837620	Instituto Nacional de Enfermedades Respiratorias (INER)	Instituto Nacional de Enfermedades Respiratorias (INER)	Alejandra Hernández-Terán; Alma Rincón-Rubio; Celia Boukadida; Edgar Sevilla-Reyes; Eduardo Becerri-Vargas; Fidencio Mejía-Nepomuceno; Hector Esteban Paz-Juarez; Joel Armando Vázquez Pérez; Jorge Salas-Hernández; José Arturo Martínez-Orozco; Margarita Matias-Florentino; Mario Mujica-Sánchez; Olivia Briceño; Santiago Avila-Rios	
EPI_ISL_1301717, EPI_ISL_1301718, EPI_ISL_1301731	Instituto Nacional de Enfermedades Respiratorias (INER)	Instituto de Biotecnología de la UNAM	Alejandra Hernández-Terán; Alejandro Sanchez-Flores; Alma Rincón-Rubio; Andrea Santos Coy-Archavealtes; Authors from IBT; Blanca Taboada; Celia Boukadida; Clara Esperanza Santacruz-Tinoco; Edgar Mendietta-Condado; Eduardo Becerri-Vargas; Fidencio Mejía-Nepomuceno; Francisco Pulido; Gisela Barrera-Badillo; Gloria Vázquez; Hector Esteban Paz-Juarez; IMSS, INDRF and INER (in alphabetical order); Carlos F. Arias; Irma Lopez-Martinez; Jerome Jean Verleyen; Joel Armando Vázquez-Pérez; Jorge Salas-Hernández; José Arturo Martínez-Orozco; José Ernesto Ramírez-González; José Esteban Muñoz-Medina; Larissa Fernandes-Matano; Lucia Hernandez-Rivas; Luis Alberto Ochoa-Carrera; Margarita Matias-Florentino; Mario Mujica-Sánchez; Natividad Cruz-Ortiz; Pavel Isa; Ricardo Grande; Santiago Avila-Rios; Tatiana Nunez-Garcia; Teresa Rojas-Mendoza	
EPI_ISL_536527, EPI_ISL_536529, EPI_ISL_536531, EPI_ISL_536533, EPI_ISL_536534, EPI_ISL_536537, EPI_ISL_536538, EPI_ISL_536539, EPI_ISL_536540, EPI_ISL_536541, EPI_ISL_536542, EPI_ISL_536543, EPI_ISL_536544, EPI_ISL_536545, EPI_ISL_536546, EPI_ISL_536549, EPI_ISL_536550, EPI_ISL_536551, EPI_ISL_536552, EPI_ISL_536553, EPI_ISL_536554, EPI_ISL_536555, EPI_ISL_536556, EPI_ISL_536557, EPI_ISL_536558, EPI_ISL_536559, EPI_ISL_536560, EPI_ISL_536561	Instituto Nacional de Salud	Laboratorio de Infecciones Respiratorias Agudas	David Tarazona; Dennis Carhuarica; Eduardo Juscamayta Lopez; Faviola Valdivia Guerrero; Lenin Maturano Hernandez; Nancy Rojas Serrano; Ronnie Gavilan Chavez	
EPI_ISL_456117, EPI_ISL_456119, EPI_ISL_456120, EPI_ISL_456126, EPI_ISL_456127, EPI_ISL_456138, EPI_ISL_456145, EPI_ISL_456146, EPI_ISL_456148, EPI_ISL_456149, EPI_ISL_456150, EPI_ISL_456151, EPI_ISL_456155	Instituto Nacional de Salud - Unidad de Secuenciación y Análisis Genómico	Instituto Nacional de Salud, Universidad Cooperativa de Colombia, Instituto Alexander von Humboldt, Imperial College-London, London School of Hygiene & Tropical Medicine	Astrid C. Flórez; Carlos Franco-Muñoz; Christian Julian Villabona-Arenas; Diana Marcela Walteros-Acero; Diego A. Álvarez-Díaz; Erika Ospitia; Gloria Puerto; Jose A. Usme-Ciro; Juliana Barbosa; Katherine Lalton-Donato; Liz Villabona-Arenas; Luz Dary Rodriguez; Maily A Gonzalez; Marcela Mercado-Reyes; Martha Lucia Ospina Martinez; Nicolas D. Franco-Sierra; Sergio Gomez-Rangel; Sussy Echeverria; Zulma M. Cucunubá	
EPI_ISL_447755, EPI_ISL_447756, EPI_ISL_447757, EPI_ISL_447759, EPI_ISL_447760, EPI_ISL_447761, EPI_ISL_447762, EPI_ISL_447763, EPI_ISL_447765, EPI_ISL_447766, EPI_ISL_447768	Instituto Nacional de Salud, Bogotá, Colombia	Grupo de Investigaciones Microbiológicas-UIR (GIMUIR), Departamento de Biología, Facultad de Ciencias Naturales, Universidad del Rosario, Bogotá, Colombia Instituto Nacional de Salud, Bogotá, Colombia Iahn School of Medicine at Mount Sinai, New York, USA	Adriana Castillo; Alberto Paniz-Mondolfi; Ana S. Gonzalez-Reiche; Angelica Rico; Anibal A. Teherán; Carolina Florez; Carolina Hernandez; David Martinez; Emilio Mili Sordillo; Esther O. Barros; Harm van Bakel; Jessie E. James; Juan David Ramirez; Laura Vega; Lisseth Pardo; Marina Muñoz; Martha L. Ospina; Matthew M. Hernandez; Nathalia Ballesteros; Sergio Castañeda; Sergio Gomez; Viviana Simon	
EPI_ISL_497736, EPI_ISL_497738, EPI_ISL_497744, EPI_ISL_497745, EPI_ISL_498152, EPI_ISL_498153, EPI_ISL_498154, EPI_ISL_498155, EPI_ISL_498156, EPI_ISL_498157, EPI_ISL_498158, EPI_ISL_498159, EPI_ISL_498160, EPI_ISL_498161, EPI_ISL_498162, EPI_ISL_498166, EPI_ISL_498168, EPI_ISL_498170, EPI_ISL_653750, EPI_ISL_653751, EPI_ISL_653752	Instituto Nacional de Salud, Bogotá, Colombia	Instituto Nacional de Salud, Bogotá, Colombia	Astrid C. Flórez; Carlos Andrés Durán; Carlos Franco-Muñoz; Carolina Fero; Christian Julian Villabona-Arenas; Diana Marcela Walteros-Acero; Diego A. Álvarez-Díaz; Diego Andrés Prada; Franklin Prieto; Jonathan Reales; Jose A. Usme-Ciro; Katherine Lalton-Donato; Liz Villabona-Arenas; Marcela Mercado-Reyes; Martha Lucia Ospina Martinez; Mauricio Pacheco-Montealegre; Nicolas D. Franco-Sierra; Sussy Echeverria; Zulma M. Cucunubá	

EPI_ISL_475144, EPI_ISL_475145, EPI_ISL_475146, EPI_ISL_475147, EPI_ISL_510818	Klinisk mikrobiologi Västernorrland	The Public Health Agency of Sweden	Anna Risberg; Anna-Malin Linde; Karin Tegmark-Wisell; Maria Lind Karlberg; Mattias Haukand; Mia Brytting; Olov Svartstrom; Oskar Karlsson Lindjo; Petra Edquist; Reza Advani; Sandra Brodesson; Shannan Mursadrasol
EPI_ISL_429115, EPI_ISL_429116, EPI_ISL_429117, EPI_ISL_429118, EPI_ISL_429119, EPI_ISL_429120, EPI_ISL_429121, EPI_ISL_429122, EPI_ISL_429123, EPI_ISL_429124, EPI_ISL_429125, EPI_ISL_430848, EPI_ISL_430849, EPI_ISL_430850, EPI_ISL_430851, EPI_ISL_430852, EPI_ISL_430853, EPI_ISL_430854, EPI_ISL_430855, EPI_ISL_450834	see above Klinisk mikrobiologi och vardhygien Halmstad	The Public Health Agency of Sweden	Anna Risberg; Anna-Malin Linde; Arne Kotz; Karin Tegmark-Wisell; Maria Lind Karlberg; Mia Brytting; Olov Svartstrom; Oskar Karlsson Lindjo; Shannan Mursadrasol; Theresa Enkrich
EPI_ISL_424703, EPI_ISL_428148, EPI_ISL_428201, EPI_ISL_549024, EPI_ISL_549176	Klinisk mikrobiologi, Region Västerbotten	Unit for Biological Agents, Department for CBRN Defence and Security, Swedish Defence Research Agency	FOI Bioinformatics team; FOI Bioinformatics team
EPI_ISL_454903, EPI_ISL_455904, EPI_ISL_455905, EPI_ISL_455906, EPI_ISL_455907	Klinisk mikrobiologi, UAS	The Public Health Agency of Sweden	Anna Risberg; Anna-Malin Linde; Karin Tegmark-Wisell; Maria Lind Karlberg; Mattias Haukand; Olov Svartstrom; Oskar Karlsson Lindjo; Petra Edquist; Reza Advani; Shannan Mursadrasol
EPI_ISL_913323, EPI_ISL_934322	Klinisk mikrobiologi, Viruslab	The Public Health Agency of Sweden	Anna Risberg; Anna-Malin Linde; Carlo Berg; Karin Tegmark-Wisell; Maria Lind Karlberg; Mattias Haukand; Mia Brytting; Noura Walai; Oskar Karlsson Lindjo; Petra Edquist; Reza Advani; Sofia Stamouli
EPI_ISL_660384, EPI_ISL_660385, EPI_ISL_660386, EPI_ISL_660387, EPI_ISL_660388, EPI_ISL_660389, EPI_ISL_660390, EPI_ISL_660391, EPI_ISL_660392, EPI_ISL_660393, EPI_ISL_660394, EPI_ISL_660395, EPI_ISL_660396	see above Klinisk mikrobiologi Linköping	The Public Health Agency of Sweden	Anna Risberg; Anna-Malin Linde; Karin Tegmark-Wisell; Maria Lind Karlberg; Mattias Haukand; Mia Brytting; Olov Svartstrom; Oskar Karlsson Lindjo; Petra Edquist; Reza Advani; Sandra Brodesson
EPI_ISL_479823	Kochi Prefectural Institute of Public Health	Pathogen Genomics Center, National Institute of Infectious Diseases	Akihiko Tokaji; Hajime Kamiya; Kentaro Itokawa; Makoto Kuroda; Masanori Hashino; Motol Suzuki; Rina Tanaka; Tsuyoshi Sekizuka
EPI_ISL_407193	Korea Centers for Disease Control & Prevention (KCDC) Center for Laboratory Control of Infectious Diseases Division of Viral Diseases	Korea Centers for Disease Control & Prevention (KCDC) Center for Laboratory Control of Infectious Diseases Division of Viral Diseases	Heui Man Kim; Hye-Joon Jo; Jeong-Min Kim; Mi-Seon Kim; Myung Kuk Han; Namjoo Lee; SangHee Woo; Seehk Park; Yoon-Seok Chung
EPI_ISL_480103, EPI_ISL_480104, EPI_ISL_480105, EPI_ISL_480106, EPI_ISL_480107, EPI_ISL_480108	Koshigaya City Public Health Center	Pathogen Genomics Center, National Institute of Infectious Diseases	Aya Tamura; Hajime Kamiya; Kentaro Itokawa; Kyohel Sakata; Makoto Kuroda; Masanori Hashino; Motol Suzuki; Rina Tanaka; Takumi Daimon; Tsuyoshi Sekizuka; Yoko Togawa; Yoshiko Hamada; Yuka Furui
EPI_ISL_434651	Krokorns Halocentral	The Public Health Agency of Sweden	Anna Risberg; Anna-Malin Linde; Karin Tegmark-Wisell; Maria Lind Karlberg; Martin Ersson; Mia Brytting; Olov Svartstrom; Oskar Karlsson Lindjo; Theresa Enkrich
EPI_ISL_479991, EPI_ISL_479992, EPI_ISL_479993, EPI_ISL_479994, EPI_ISL_479995, EPI_ISL_479996	Kumamoto City Public Health Research Institute	Pathogen Genomics Center, National Institute of Infectious Diseases	Hajime Kamiya; Kaori Tashiro; Kentaro Itokawa; Makoto Kuroda; Masanori Hashino; Motol Suzuki; Rina Tanaka; Tsuyoshi Sekizuka
EPI_ISL_479824	Kumamoto Prefectural Institute of Public Health and Environmental Science	Pathogen Genomics Center, National Institute of Infectious Diseases	Hajime Kamiya; Kentaro Itokawa; Makoto Kuroda; Masanori Hashino; Motol Suzuki; Rina Tanaka; Shunsuke Yahiro; Tsuyoshi Sekizuka
EPI_ISL_515181, EPI_ISL_515182, EPI_ISL_515183	Kumasi Centre for Collaborative Research in Tropical Medicine, Kumasi	Institute of Virology, Charité - Universitätsmedizin Berlin	Augustina Sylverken; Christian Drosten; Eric Adu; Jesse Addo Asamoah; Julia Schneider; Jörn Beheim-Schwarzbach; Michael Owusu; Philip El-Duah; Richard Phillips.; Richmond Gorman; Richmond Yeboah; Shehane Arseyey; Victor Max Corman
EPI_ISL_434644, EPI_ISL_450809	Kungsholmsdoktor	The Public Health Agency of Sweden	Anna Risberg; Anna-Malin Linde; Karin Tegmark-Wisell; Linus Hammar; Maria Lind Karlberg; Mia Brytting; Olov Svartstrom; Oskar Karlsson Lindjo; Theresa Enkrich
EPI_ISL_420039, EPI_ISL_420040	L'Air du Temps	National Reference Center for Viruses of Respiratory Infections, Institut Pasteur, Paris	Angela Brisebane; Etienne Simon-Lorière; Flora Donati; Marion Barbet; Maud Vanpeene; Mélanie Albert; Méline Bizard; Sylvie Behilli; Sylvie van der Werf; Vincent Enouf
EPI_ISL_424688, EPI_ISL_452106, EPI_ISL_452107	LA Office of Public Health Laboratories	Pathogen Discovery, Respiratory Viruses Branch, Division of Viral Diseases, Centers for Disease Control and Prevention	Alison S. Lauffer Halpin; Anna Montmayeur; Anna Uehara; Christopher A. Elkins; Clinton R. Paden; Habin Wang; Jing Zhang; Krista Queen; Mary S. Keckler; Rachel Marine; Susiang Tong; Yan Li; Ying Tao; Zachary Weiner
EPI_ISL_416499, EPI_ISL_416500, EPI_ISL_416234, EPI_ISL_416240	LABM GH nord Essonne	National Reference Center for Viruses of Respiratory Infections, Institut Pasteur, Paris	Angela Brisebane; Christine Lambert; Etienne Simon-Lorière; Flora Donati; Marion Barbet; Maud Vanpeene; Mélanie Albert; Méline Bizard; Méline Albert; Antonin Bal; Bruno Lina; Gregory Destras; Gwendolyne Burfin; Hadrien Regue; Laurence Josset; Martine Valette; Quentin Semanas
EPI_ISL_428354, EPI_ISL_428361, EPI_ISL_428365	LABM GH nord Essonne de Longjumeau - BP 125	National Reference Center for Viruses of Respiratory Infections, Institut Pasteur, Paris	Angela Brisebane; Etienne Simon-Lorière; Flora Donati; Marion Barbet; Maud Vanpeene; Mélanie Albert; Méline Bizard; Sylvie Behilli; Sylvie van der Werf; Vincent Enouf
EPI_ISL_1359983	LABORATOIRE BOUVIER	CNR Virus des Infections Respiratoires - France SUD	Antonin Bal; Bruno Lina; Gregory Destras; Gwendolyne Burfin; Hadrien Regue; Laurence Josset; Martine Valette; Quentin Semanas
EPI_ISL_445271	LABORATORIO CLINICA CHILLAN	Instituto de Salud Publica de Chile	Alejandra Acevedo; Andrés E Castillo; Bárbara Parra; Carolina Tambley; Gabriel Leal; Jaime Lagos; Jorge Fernandez; Loredana Arata; Patricia Bustos; Paz Tapia; Rodrigo Fasce; Winston Andrade
EPI_ISL_445333	LABORATORIO CLINICA UNIVERSITARIA DE CONCEPCION	Instituto de Salud Publica de Chile	Alejandra Acevedo; Andrés E Castillo; Bárbara Parra; Carolina Tambley; Gabriel Leal; Jaime Lagos; Jorge Fernandez; Loredana Arata; Patricia Bustos; Paz Tapia; Rodrigo Fasce; Winston Andrade
EPI_ISL_445279	LABORATORIO INMUNOLAB SPA	Instituto de Salud Publica de Chile	Alejandra Acevedo; Andrés E Castillo; Bárbara Parra; Carolina Tambley; Gabriel Leal; Jaime Lagos; Jorge Fernandez; Loredana Arata; Patricia Bustos; Paz Tapia; Rodrigo Fasce; Winston Andrade
EPI_ISL_445273, EPI_ISL_445274, EPI_ISL_445278	LABORATORIO TORRE MEDICA LTDA.	Instituto de Salud Publica de Chile	Alejandra Acevedo; Andrés E Castillo; Bárbara Parra; Carolina Tambley; Gabriel Leal; Jaime Lagos; Jorge Fernandez; Loredana Arata; Patricia Bustos; Paz Tapia; Rodrigo Fasce; Winston Andrade
EPI_ISL_1139065, EPI_ISL_1139066, EPI_ISL_1139067, EPI_ISL_1139068, EPI_ISL_1201883	LACEN do Mato Grosso do Sul	Instituto Adolfo Lutz, Interdisciplinary Procedures Center, Strategic Laboratory	Caio Vinicius Dias Lopes; Claudia Regina Gonçalves; Claudio Tavares Sacchi; Erica Valessa Ramos Gomes; Karoline Rodrigues Campos
EPI_ISL_861869, EPI_ISL_861874, EPI_ISL_861879, EPI_ISL_861890, EPI_ISL_861893, EPI_ISL_861900, EPI_ISL_861902, EPI_ISL_861906, EPI_ISL_861907, EPI_ISL_861912, EPI_ISL_861913, EPI_ISL_861915	see above LATE - Laboratório de Técnicas Especiais - Hospital Israelita Albert Einstein	LATE - Laboratório de Técnicas Especiais - Hospital Israelita Albert Einstein	Ana Paula Moreira Salles; Deyvid Amgarten; Fernanda de Mello Malta; João Renato Rebelo Pinho; Pedro Henrique Sebe Rodrigues; Raquel Rlyuzo
EPI_ISL_469049, EPI_ISL_469052, EPI_ISL_469053	LNR National Reference Laboratory, Mohammed VI University of Health Sciences	Medical Biotechnology Laboratory, Rabat Medical and Pharmacy School, Mohammed VI University in Rabat	Chakib NEJARI; Houda BENRAHMA; Idrissa Diawara; Imane SMYEL; Jallil El Atar; Jallia RAHOU; Lahcen BELYAMANI and Azeddine IBRAHIMI; Laila SBABOU; Louina ALLAM; M.W. CHEMAO-EL-FIRRI; Mersien LAAMARTI; Mauna OUAADHRI; Rachid EL JAOUDI; Rachid MENTAG; Rokias LAAMARTI; Saaid AMZAZ; Souad KARTTI
EPI_ISL_455980, EPI_ISL_455981, EPI_ISL_455982, EPI_ISL_455983, EPI_ISL_455984, EPI_ISL_455985, EPI_ISL_455986, EPI_ISL_455987, EPI_ISL_455988, EPI_ISL_455989, EPI_ISL_455990, EPI_ISL_455991, EPI_ISL_455992, EPI_ISL_455993	see above LSUH3 Emerging Viral Threat Laboratory	Microbial Genome Sequencing Center	Abida Siddiq; Adam Greer; Andrew D. Yurochko; Byeong-Jae Lee; Camille F. Abshire; Chan-ki Min; Christopher G. Kevill; Daniel J. Snyder; Edna Ondari; Jason M. Bodily; Jeremy P. Karni; John A. Vanchiere; Katarzyna Zwolinska; Malgorzata Bienkowska-Haba; Martin J. Sapp; Md Maksudul Alam; Michelle M. Arnold; Monica Gestal-Carsté; Paul M. Weinberger; Rona S. Scott; Vaughn S. Cooper
EPI_ISL_528637, EPI_ISL_528638	LVMUFRJ	Bioinformatics Laboratory / LNCC	Amílcar Tanuri; Ana Teresa R. Vasconcelos; Bruno B. Bezerra; Diana Marianni; Elene Cobos; Fabio Limonte; Gustavo D. P. Silva; Isadora A. Correa; Luciana B. Aruda; Luciana J. Costa; Lucio A. Caldas; Luiz Almeida; Luiza Higgs; Marcelo Bozza; Orlando Ferreira; Sharton V. A. Coelho; Terezinha M. Castineiras; Wanderley de Souza
EPI_ISL_528539	LVMUFRJ	LNCC	Amílcar Tanuri; Ana Teresa R. Vasconcelos; Bruno B. Bezerra; Diana Marianni; Elene Cobos; Fabio Limonte; Gustavo M. Romário M. de Souza; Isadora A. Correa; Luciana B. Aruda; Luciana J. Costa.; Lucio A. Caldas; Luiz Almeida; Luiza Higgs; Marcelo Bozza; Orlando Ferreira; Sharton V. A. Coelho;

EPI_ISL_890761, EPI_ISL_890762, EPI_ISL_890763, EPI_ISL_890764, EPI_ISL_890765, EPI_ISL_890766, EPI_ISL_890767, EPI_ISL_890768, EPI_ISL_890769, EPI_ISL_890770, EPI_ISL_890771, EPI_ISL_890772, EPI_ISL_890773, EPI_ISL_890774, EPI_ISL_890775, EPI_ISL_890776, EPI_ISL_890777, EPI_ISL_890778, EPI_ISL_890779, EPI_ISL_890780, EPI_ISL_890781, EPI_ISL_890782, EPI_ISL_890783, EPI_ISL_890784, EPI_ISL_890785, EPI_ISL_890786, EPI_ISL_890787, EPI_ISL_890788, EPI_ISL_890789, EPI_ISL_890790, EPI_ISL_890791, EPI_ISL_890792, EPI_ISL_890793, EPI_ISL_890794, EPI_ISL_890795, EPI_ISL_890796, EPI_ISL_890797, EPI_ISL_890798, EPI_ISL_890799, EPI_ISL_890800, EPI_ISL_890801, EPI_ISL_890802, EPI_ISL_890803, EPI_ISL_890804, EPI_ISL_890805, EPI_ISL_890806, EPI_ISL_890807, EPI_ISL_890808, EPI_ISL_890809, EPI_ISL_890810, EPI_ISL_890811, EPI_ISL_890812, EPI_ISL_890813, EPI_ISL_890814, EPI_ISL_890815, EPI_ISL_890816, EPI_ISL_890817, EPI_ISL_890818, EPI_ISL_890819, EPI_ISL_890820, EPI_ISL_890821, EPI_ISL_890822, EPI_ISL_890823, EPI_ISL_890824, EPI_ISL_890825, EPI_ISL_890826, EPI_ISL_890827, EPI_ISL_890828, EPI_ISL_890829, EPI_ISL_890830, EPI_ISL_890831, EPI_ISL_890832, EPI_ISL_890833, EPI_ISL_890834, EPI_ISL_890835, EPI_ISL_890836, EPI_ISL_890837, EPI_ISL_890838, EPI_ISL_890839, EPI_ISL_890840, EPI_ISL_890841, EPI_ISL_890842, EPI_ISL_890843, EPI_ISL_890844, EPI_ISL_890845, EPI_ISL_890846, EPI_ISL_890847, EPI_ISL_890848, EPI_ISL_890849, EPI_ISL_890850, EPI_ISL_890851, EPI_ISL_890852, EPI_ISL_890853, EPI_ISL_890854, EPI_ISL_890855, EPI_ISL_890856, EPI_ISL_890857, EPI_ISL_890858, EPI_ISL_890859, EPI_ISL_890860, EPI_ISL_890861, EPI_ISL_890862, EPI_ISL_890863, EPI_ISL_890864, EPI_ISL_890865, EPI_ISL_890866, EPI_ISL_890867, EPI_ISL_890868, EPI_ISL_890869, EPI_ISL_890870, EPI_ISL_890871, EPI_ISL_890872, EPI_ISL_890873, EPI_ISL_890874, EPI_ISL_890875, EPI_ISL_890876, EPI_ISL_890877, EPI_ISL_890878, EPI_ISL_890879, EPI_ISL_890880, EPI_ISL_890881, EPI_ISL_890882, EPI_ISL_890883, EPI_ISL_890884, EPI_ISL_890885, EPI_ISL_890886, EPI_ISL_890887, EPI_ISL_890888, EPI_ISL_890889, EPI_ISL_890890, EPI_ISL_890891, EPI_ISL_890892, EPI_ISL_890893, EPI_ISL_890894, EPI_ISL_890895, EPI_ISL_890896, EPI_ISL_890897, EPI_ISL_890898, EPI_ISL_890899, EPI_ISL_890900, EPI_ISL_890901, EPI_ISL_890902, EPI_ISL_890903, EPI_ISL_890904, EPI_ISL_890905, EPI_ISL_890906, EPI_ISL_890907, EPI_ISL_890908, EPI_ISL_890909, EPI_ISL_890910, EPI_ISL_890911, EPI_ISL_890912, EPI_ISL_890913, EPI_ISL_890914, EPI_ISL_890915, EPI_ISL_890916, EPI_ISL_890917, EPI_ISL_890918, EPI_ISL_890919, EPI_ISL_890920, EPI_ISL_890921, EPI_ISL_890922, EPI_ISL_890923, EPI_ISL_890924, EPI_ISL_890925, EPI_ISL_890926, EPI_ISL_890927, EPI_ISL_890928, EPI_ISL_890929, EPI_ISL_890930, EPI_ISL_890931, EPI_ISL_890932, EPI_ISL_890933, EPI_ISL_890934, EPI_ISL_890935, EPI_ISL_890936, EPI_ISL_890937, EPI_ISL_890938, EPI_ISL_890939, EPI_ISL_890940, EPI_ISL_890941, EPI_ISL_890942, EPI_ISL_890943, EPI_ISL_890944, EPI_ISL_890945, EPI_ISL_890946, EPI_ISL_890947, EPI_ISL_890948, EPI_ISL_890949, EPI_ISL_890950, EPI_ISL_890951, EPI_ISL_890952, EPI_ISL_890953, EPI_ISL_890954, EPI_ISL_890955, EPI_ISL_890956, EPI_ISL_890957, EPI_ISL_890958, EPI_ISL_890959, EPI_ISL_890960, EPI_ISL_890961, EPI_ISL_890962, EPI_ISL_890963, EPI_ISL_890964, EPI_ISL_890965, EPI_ISL_890966, EPI_ISL_890967, EPI_ISL_890968, EPI_ISL_890969, EPI_ISL_890970, EPI_ISL_890971, EPI_ISL_890972, EPI_ISL_890973, EPI_ISL_890974, EPI_ISL_890975, EPI_ISL_890976, EPI_ISL_890977, EPI_ISL_890978, EPI_ISL_890979, EPI_ISL_890980, EPI_ISL_890981, EPI_ISL_890982, EPI_ISL_890983, EPI_ISL_890984, EPI_ISL_890985, EPI_ISL_890986, EPI_ISL_890987, EPI_ISL_890988, EPI_ISL_890989, EPI_ISL_890990, EPI_ISL_890991, EPI_ISL_890992, EPI_ISL_890993, EPI_ISL_890994, EPI_ISL_890995, EPI_ISL_890996, EPI_ISL_890997, EPI_ISL_890998, EPI_ISL_890999, EPI_ISL_891000	see above	Laboratoire de santé publique du Québec	Laboratoire de santé publique du Québec	Guillaume Bourque; Ioannis Ragoussia; Jesse Shapiro; Mark Lathrop and Michel Roger on behalf of the CoVSeQ research group; Mark Lathrop and Michel Roger on behalf of the CoVSeQ research group (http://covseq.ca/researchgroup); Sandrine Moreira
EPI_ISL_634818, EPI_ISL_700349	Laboratoire de virologie, CHU de Grenoble - CS 10217 - 38043 Grenoble cedex 10	CNR Virus des Infections Respiratoires - France SUD	Antoin Bal; Bruno Lina; Gregory Destras; Gwendolynne Burfin; Hadrien Règue; Laurence Josset; Martine Valette; Quentin Semanas; Sylvie Larrat	
EPI_ISL_634819, EPI_ISL_700350	Laboratoire de virologie, CHU de Grenoble - CS 10217 - 38043 Grenoble cedex 11	CNR Virus des Infections Respiratoires - France SUD	Antoin Bal; Bruno Lina; Gregory Destras; Gwendolynne Burfin; Hadrien Règue; Laurence Josset; Martine Valette; Quentin Semanas; Sylvie Larrat	
EPI_ISL_634820	Laboratoire de virologie, CHU de Grenoble - CS 10217 - 38043 Grenoble cedex 12	CNR Virus des Infections Respiratoires - France SUD	Antoin Bal; Bruno Lina; Gregory Destras; Gwendolynne Burfin; Hadrien Règue; Laurence Josset; Martine Valette; Quentin Semanas; Sylvie Larrat	
EPI_ISL_634821	Laboratoire de virologie, CHU de Grenoble - CS 10217 - 38043 Grenoble cedex 13	CNR Virus des Infections Respiratoires - France SUD	Antoin Bal; Bruno Lina; Gregory Destras; Gwendolynne Burfin; Hadrien Règue; Laurence Josset; Martine Valette; Quentin Semanas; Sylvie Larrat	
EPI_ISL_634822	Laboratoire de virologie, CHU de Grenoble - CS 10217 - 38043 Grenoble cedex 14	CNR Virus des Infections Respiratoires - France SUD	Antoin Bal; Bruno Lina; Gregory Destras; Gwendolynne Burfin; Hadrien Règue; Laurence Josset; Martine Valette; Quentin Semanas; Sylvie Larrat	
EPI_ISL_634823	Laboratoire de virologie, CHU de Grenoble - CS 10217 - 38043 Grenoble cedex 15	CNR Virus des Infections Respiratoires - France SUD	Antoin Bal; Bruno Lina; Gregory Destras; Gwendolynne Burfin; Hadrien Règue; Laurence Josset; Martine Valette; Quentin Semanas; Sylvie Larrat	
EPI_ISL_700359	Laboratoire de virologie, CHU de Grenoble - CS 10217 - 38043 Grenoble cedex 20	CNR Virus des Infections Respiratoires - France SUD	Antoin Bal; Bruno Lina; Gregory Destras; Gwendolynne Burfin; Hadrien Règue; Laurence Josset; Martine Valette; Quentin Semanas; Sylvie Larrat	
EPI_ISL_700360	Laboratoire de virologie, CHU de Grenoble - CS 10217 - 38043 Grenoble cedex 21	CNR Virus des Infections Respiratoires - France SUD	Antoin Bal; Bruno Lina; Gregory Destras; Gwendolynne Burfin; Hadrien Règue; Laurence Josset; Martine Valette; Quentin Semanas; Sylvie Larrat	
EPI_ISL_700361	Laboratoire de virologie, CHU de Grenoble - CS 10217 - 38043 Grenoble cedex 22	CNR Virus des Infections Respiratoires - France SUD	Antoin Bal; Bruno Lina; Gregory Destras; Gwendolynne Burfin; Hadrien Règue; Laurence Josset; Martine Valette; Quentin Semanas; Sylvie Larrat	
EPI_ISL_634833	Laboratoire de virologie, CHU de Grenoble - CS 10217 - 38043 Grenoble cedex 25	CNR Virus des Infections Respiratoires - France SUD	Antoin Bal; Bruno Lina; Gregory Destras; Gwendolynne Burfin; Hadrien Règue; Laurence Josset; Martine Valette; Quentin Semanas; Sylvie Larrat	
EPI_ISL_634834	Laboratoire de virologie, CHU de Grenoble - CS 10217 - 38043 Grenoble cedex 26	CNR Virus des Infections Respiratoires - France SUD	Antoin Bal; Bruno Lina; Gregory Destras; Gwendolynne Burfin; Hadrien Règue; Laurence Josset; Martine Valette; Quentin Semanas; Sylvie Larrat	
EPI_ISL_634835	Laboratoire de virologie, CHU de Grenoble - CS 10217 - 38043 Grenoble cedex 27	CNR Virus des Infections Respiratoires - France SUD	Antoin Bal; Bruno Lina; Gregory Destras; Gwendolynne Burfin; Hadrien Règue; Laurence Josset; Martine Valette; Quentin Semanas; Sylvie Larrat	
EPI_ISL_634817, EPI_ISL_700348	Laboratoire de virologie, CHU de Grenoble - CS 10217 - 38043 Grenoble cedex 9	CNR Virus des Infections Respiratoires - France SUD	Antoin Bal; Bruno Lina; Gregory Destras; Gwendolynne Burfin; Hadrien Règue; Laurence Josset; Martine Valette; Quentin Semanas; Sylvie Larrat	
EPI_ISL_476822, EPI_ISL_476824	Laboratoire des Fièvres Hémorragiques Virales du Benin	Charité-Universitätsmedizin Berlin	Anges; Drexler; Jan Felix; Moreira-Soto Andres; Sander Anna-Lena; Yadoulaton	
EPI_ISL_629081, EPI_ISL_629082, EPI_ISL_629083, EPI_ISL_629084, EPI_ISL_629085, EPI_ISL_629086, EPI_ISL_629087, EPI_ISL_629088, EPI_ISL_629089, EPI_ISL_629090, EPI_ISL_629091, EPI_ISL_629092, EPI_ISL_629093, EPI_ISL_629094, EPI_ISL_629095, EPI_ISL_666554, EPI_ISL_666556, EPI_ISL_666557, EPI_ISL_666559, EPI_ISL_666660, EPI_ISL_666661, EPI_ISL_666662, EPI_ISL_666664, EPI_ISL_683331, EPI_ISL_683332, EPI_ISL_683333	Laboratoire du Centre Hospitalier Annecy Genevois	CNR Virus des Infections Respiratoires - France SUD	Antoin Bal; Bruno Chanzy; Bruno Lina; Gregory Destras; Gwendolynne Burfin; Hadrien Règue; Hélène Peltre; Laurence Josset; Martine Valette; Quentin Semanas	
EPI_ISL_739897, EPI_ISL_740199, EPI_ISL_740242, EPI_ISL_740405, EPI_ISL_740444, EPI_ISL_740510, EPI_ISL_744233, EPI_ISL_744478, EPI_ISL_744723, EPI_ISL_744843, EPI_ISL_745011	Laboratoire national de santé, Microbiology, Virology	Laboratoire national de santé, Microbiology, Microbial Genomics Platform	Anke Wiencke-Baldachino; Catherine Regimbaut; Fatu Djabi; Jessica Tapp; Tamir Abdelrahman	
EPI_ISL_429129, EPI_ISL_429130, EPI_ISL_429131, EPI_ISL_429132, EPI_ISL_429133, EPI_ISL_429134, EPI_ISL_430856, EPI_ISL_430857, EPI_ISL_434641, EPI_ISL_434642	Laboratoriermedicin	The Public Health Agency of Sweden	Anna Risberg; Anna-Malin Linde; Karin Tegmark-Wisell; Maria Lind Karlberg; Olov Svartstrom; Oskar Karlsson Lindjö; Shaman Muradrasoli	
EPI_ISL_637108	Laboratorio Biologia Molecolare Sara Cov-2 - UOC Laboratorio Analisi - Servizio Medicina di Laboratorio, Ospedale "San Francesco" - ATS-ASSL Nuoro	Laboratorio specialistico UOC Ematologia - Ospedale "San Francesco" - ATS-ASSL Nuoro	Asproni Rosanna; Casu Gavino; Fancello Tatiana; Fiama Maura; Floris Anna Rita; Lo Maglio Iana; Mammì Giuseppe; Monne Maria Iritia; Palmas Angelo Domenico; Piras Giovanna; Sanna Filomena; Toja Alessandro	
EPI_ISL_792478, EPI_ISL_792482, EPI_ISL_792484	Laboratorio Central Mg. Luis Alfredo Pianiola	Hospital Regional Uthushua - Centro Austral De Investigaciones Cientificas - Universidad Nacional De Tierra Del Fuego on behalf of Proyecto Argentino Interinstitucional de genómica de SARS-CoV-2 (PAIS Consortium)	C; CF; Ceballos; F; Gallego; Gramund; ID; M; MC; Mazzeo; Nardi; Pianiola, L.; Pinto; SG; Ziehm	
EPI_ISL_1301620, EPI_ISL_1301621, EPI_ISL_1301622	Laboratorio Central de Epidemiologia IMSS	Instituto de Biotecnología de la UNAM	Alejandra Hernández-Terán; Alejandro Sanchez-Flores; Alma Rincón-Rubio; Andrea Santos Coy-Arechavala; Authors from IBT; Blanca Taboada; Celia Boukadda; Clara Esperanza Santacruz-Tinoco; Edgar Méndez-Condado; Eduardo Becerra-Vargas; Fidencio Mejía-Nepomuceno; Francisco Pulido; Gisela Barrera-Badillo; Gloria Vazquez; Hector Esteban Paz-Juárez; IMSS; INDRÉ and INER (in alphabetical order); Carlos F. Arias; Irma Lopez-Martínez; Jérôme Jean Verleyen; Joel Armando Vázquez-Pérez; Jorge Salas-Hernández; José Arturo Martínez-Crocco; José Ernesto Ramírez-González; José Esteban Muñoz-Medina; Larissa Fernández-Matano; Lucia Hernández-Rivas; Luis Alberto Ochoa-Carrera; Margarita Matias-Florentino; Mario Mujica-Sanchez; Natividad Cruz-Ortiz; Pavel Isa; Ricardo Grande; Santiago Avila-Rios; Tatiana Nunez-Garcia; Teresita Rojas-Mendoza	
EPI_ISL_1181609, EPI_ISL_1181610, EPI_ISL_1181614, EPI_ISL_1181615, EPI_ISL_1181616, EPI_ISL_1181617, EPI_ISL_1181618, EPI_ISL_1181619	Laboratorio Central de Saude Publica do Estado do Parana (LACEN-PR)	Laboratory of Respiratory Viruses and Measles, Oswaldo Cruz Institute, FIOCRUZ	Alice Sampaio Rocha; Ana Carolina Mendonca; Anna Carolina Paiva; Fernando Motta; Irina Nastassja Riediger; Luociana Appolinario; Maria do Carmo Debur; Marilda Siqueira on behalf of the FioCruz COVID-19 Genomic Surveillance Network; Paola Resende; Renata Serrano Lopes	
EPI_ISL_1181620	Laboratorio Central de Saude Publica do Estado do Rio Grande do Sul (LACEN-RS)	Laboratory of Respiratory Viruses and Measles, Oswaldo Cruz Institute, FIOCRUZ	Alice Sampaio Rocha; Ana Carolina Mendonca; Anna Carolina Paiva; Fernando Motta; Luociana Appolinario; Marilda Siqueira on behalf of the FioCruz COVID-19 Genomic Surveillance Network; Paola Resende; Renata Serrano Lopes; Tatiana Schaffer Gregarian	
EPI_ISL_1181611, EPI_ISL_1181612, EPI_ISL_1181613	Laboratorio Central de Saude Publica do Estado do Rio de Janeiro (LACEN-RJ)	Laboratory of Respiratory Viruses and Measles, Oswaldo Cruz Institute, FIOCRUZ	Alice Sampaio Rocha; Ana Carolina Mendonca; Andrea Cony Cavalcanti; Anna Carolina Paiva; Fernando Motta; Luociana Appolinario; Marilda Siqueira on behalf of the FioCruz COVID-19 Genomic Surveillance Network; Paola Resende; Renata Serrano Lopes	
EPI_ISL_792528, EPI_ISL_792527	Laboratorio Central, Ministerio de Salud Córdoba	Instituto de Patologia Vegetal (CIAP-INTA) on behalf of	Barbas, G.; Castro, G.; Debat, H.J.; FD; Fernández; MB; Piasno; Re; V	

EPI_ISL_792528, EPI_ISL_792531, EPI_ISL_792532, EPI_ISL_792535		Proyecto Argentino Interinstitucional de genómica de SARS-CoV-2 (PAIS Consortium)		
EPI_ISL_424667	Laboratorio Estatal de Salud Pública del Estado de México	Instituto de Diagnóstico y Referencia Epidemiológicos	Adnan Araiza Rodríguez; Alejandro Sánchez; Alfredo Ponce de León Garduño; Blanca Taboada; Carlos F. Arias; Carolina González Torres; Celia Boukadida; Cesar Raúl González Bonilla; Concepción Grajales Muñiz; Edgar Mendietta Condado; Eduardo Becerri Vargas; Fabiola Garcés Ayala; Fernando Ledesma Barrantes; Francisco Javier Gaytán Cervantes; Francisco Pulido; Gisela Barrera Badillo; Gloria Vázquez; Guillermo M. Ruiz-Palacios; Irma López Martínez; Joel Armando Vázquez Pérez; José Arturo Martínez Orozco; José Ernesto Ramírez González; José Esteban Muñoz Medina; Lucía Hernández Rivas; Luis Alberto García Andrade; Mario Mujica Sánchez; Pavel Isa; Pilar Ramos Cervantes; Ricardo Grande; Santiago Avila Rios; Victor Hugo Borja Aburto; Violeta Ibarra González	
EPI_ISL_424672	Laboratorio Estatal de Salud Pública del Estado de Puebla	Instituto de Diagnóstico y Referencia Epidemiológicos	Adnan Araiza Rodríguez; Alejandro Sánchez; Alfredo Ponce de León Garduño; Blanca Taboada; Carlos F. Arias; Carolina González Torres; Celia Boukadida; Cesar Raúl González Bonilla; Concepción Grajales Muñiz; Edgar Mendietta Condado; Eduardo Becerri Vargas; Fabiola Garcés Ayala; Fernando Ledesma Barrantes; Francisco Javier Gaytán Cervantes; Francisco Pulido; Gisela Barrera Badillo; Gloria Vázquez; Guillermo M. Ruiz-Palacios; Irma López Martínez; Joel Armando Vázquez Pérez; José Arturo Martínez Orozco; José Ernesto Ramírez González; José Esteban Muñoz Medina; Lucía Hernández Rivas; Luis Alberto García Andrade; Mario Mujica Sánchez; Pavel Isa; Pilar Ramos Cervantes; Ricardo Grande; Santiago Avila Rios; Victor Hugo Borja Aburto; Violeta Ibarra González	
EPI_ISL_424670	Laboratorio Estatal de Salud Pública del Estado de Querétaro	Instituto de Diagnóstico y Referencia Epidemiológicos	Adnan Araiza Rodríguez; Alejandro Sánchez; Alfredo Ponce de León Garduño; Blanca Taboada; Carlos F. Arias; Carolina González Torres; Celia Boukadida; Cesar Raúl González Bonilla; Concepción Grajales Muñiz; Edgar Mendietta Condado; Eduardo Becerri Vargas; Fabiola Garcés Ayala; Fernando Ledesma Barrantes; Francisco Javier Gaytán Cervantes; Francisco Pulido; Gisela Barrera Badillo; Gloria Vázquez; Guillermo M. Ruiz-Palacios; Irma López Martínez; Joel Armando Vázquez Pérez; José Arturo Martínez Orozco; José Ernesto Ramírez González; José Esteban Muñoz Medina; Lucía Hernández Rivas; Luis Alberto García Andrade; Mario Mujica Sánchez; Pavel Isa; Pilar Ramos Cervantes; Ricardo Grande; Santiago Avila Rios; Victor Hugo Borja Aburto; Violeta Ibarra González	
EPI_ISL_861628	Laboratorio Municipal de Guarulhos	Instituto Adolfo Lutz, Interdisciplinary Procedures Center, Strategic Laboratory	Claudia Regina Gonçalves; Claudio Tavares Sacchi; Erica Valeasa Ramos Gomes; Karoline Rodrigues Campos	
EPI_ISL_457946, EPI_ISL_457948, EPI_ISL_457952, EPI_ISL_457953, EPI_ISL_457956, EPI_ISL_457957, EPI_ISL_457958, EPI_ISL_457959, EPI_ISL_457961, EPI_ISL_457963	see above	Laboratorio de Biología Molecular Asociación Española Primera en Salud	Departments of Pathology and Medicine, New York University School of Medicine	
EPI_ISL_417034, EPI_ISL_911148, EPI_ISL_1069078	Laboratorio de Ecología de Doenças Transmissíveis na Amazonia, Instituto Leonidas e Maria Deane - Fiocruz Amazonia	Laboratório de Ecologia de Doenças Transmissíveis na Amazonia, Instituto Leonidas e Maria Deane - Fiocruz Amazonia	André Corado; Debora Duarte; Felipe Naveas on behalf of the Fiocruz COVID-19 Genomic Surveillance Network; Fernanda Nascimento; George Silva; Karina Pessoa; Luciana Gonçalves; Maria Júlia Brandão; Matilde Mejía; Michele Jesus; Sérgio Luz; Valdeine Nascimento; Victor Souza; Agatha Costa	
EPI_ISL_648595	Laboratorio de Infectología Servicio de Infectología Hospital Universitario Dr. José Eleuterio González - Universidad Autónoma de Nuevo León	Laboratorio de Infectología Molecular Departamento de Bioquímica y Medicina Molecular Facultad de Medicina - Universidad Autónoma de Nuevo León	Adrian Camacho-Ortiz; Ana M. Rivas-Estilla; Consuelo Treviño-Garza; Daniel Arellano-Soto; Eduardo Pérez-Alba; Elvira Garza-González; Kame A. Galán-Huerta; Laura Nuzzolo-Shihadeh; Manuel E. de-Is-O-Cavazos; María F. Herrera-Saldívar; Natalia Martínez-Acuña; Paola Boacanegra-Ibaras; Roberto Montede-Oca; Samantha M. Flores-Treviño; Sonia A. Lozano-Sepúlveda	
EPI_ISL_779169, EPI_ISL_779170, EPI_ISL_779171	Laboratorio de Infectología, Servicio de Infectología, Hospital Universitario Dr. José Eleuterio González - Universidad Autónoma de Nuevo León	Laboratorio de Infectología Molecular, Departamento de Bioquímica y Medicina Molecular Facultad de Medicina - Universidad Autónoma de Nuevo León	Adrian Camacho-Ortiz; Ana M. Rivas-Estilla; Daniel Arellano-Soto; Eduardo Pérez-Alba; Elvira Garza-González; Kame A. Galán-Huerta; Laura Nuzzolo-Shihadeh; María F. Herrera-Saldívar; Natalia Martínez-Acuña; Paola Boacanegra-Ibaras; Samantha M. Flores-Treviño; Sonia A. Lozano-Sepúlveda	
EPI_ISL_517770	Laboratorio de Referencia Nacional de Virus Respiratorio, Centro Nacional de Salud Pública, Instituto Nacional de Salud Perú	Laboratorio de Referencia Nacional de Biotecnología y Biología Molecular, Centro Nacional de Salud Pública, Instituto Nacional de Salud Perú	Carlos Padilla Rojas; Henri Bailon Calderon; Johanna Balbuena Torres; Karolyn Vega Chozo; Marco Galarza Perez; Maribel Huaranga Nuñez; Nancy Rojas Serrano; Omar Cáceres Rey; Priscila Lope Pan	
EPI_ISL_516626, EPI_ISL_516987, EPI_ISL_517958, EPI_ISL_523810, EPI_ISL_523954, EPI_ISL_523979, EPI_ISL_523994, EPI_ISL_524471, EPI_ISL_525206	see above	Laboratorio de Referencia Nacional de Virus Respiratorio, Centro Nacional de Salud Pública, Instituto Nacional de Salud Perú	Laboratorio de Referencia Nacional de Biotecnología y Biología Molecular, Centro Nacional de Salud Pública, Instituto Nacional de Salud Perú	Carlos Padilla Rojas; Henri Bailon Calderon; Johanna Balbuena Torres; Karolyn Vega Chozo; Marco Galarza Perez; Maribel Huaranga Nuñez; Nancy Rojas Serrano; Omar Cáceres Rey; Priscila Lope Pan
EPI_ISL_489836, EPI_ISL_489837, EPI_ISL_489838, EPI_ISL_489839, EPI_ISL_489987, EPI_ISL_489988, EPI_ISL_489989, EPI_ISL_489990, EPI_ISL_490209, EPI_ISL_490315, EPI_ISL_490316, EPI_ISL_490975, EPI_ISL_490976, EPI_ISL_491427, EPI_ISL_491428, EPI_ISL_491429, EPI_ISL_491430, EPI_ISL_491462	see above	Laboratorio de Referencia Nacional de Virus Respiratorio, Instituto Nacional de Salud Perú	Laboratorio de Referencia Nacional de Biotecnología y Biología Molecular, Instituto Nacional de Salud Perú	Carlos Padilla Rojas; Henri Bailon Calderon; Johanna Balbuena Torres; Karolyn Vega Chozo; Marco Galarza Perez; Maribel Huaranga Nuñez; Nancy Rojas Serrano; Omar Cáceres Rey; Priscila Lope Pan
EPI_ISL_491172	Laboratorio de Referencia Nacional de Virus Respiratorio, Instituto Nacional de Salud Perú	Laboratorio de Referencia Nacional de Biotecnología y Biología Molecular, Instituto Nacional de Salud Perú	Carlos Padilla Rojas; Henri Bailon Calderon; Johanna Balbuena Torres; Karolyn Vega Chozo; Marco Galarza Perez; Maribel Huaranga Nuñez; Nancy Rojas Serrano; Omar Cáceres Rey; Priscila Lope Pan	
EPI_ISL_1111075, EPI_ISL_1111076, EPI_ISL_1111077, EPI_ISL_1111078, EPI_ISL_1111079, EPI_ISL_1111080, EPI_ISL_1111081, EPI_ISL_1111087, EPI_ISL_1111088, EPI_ISL_1111089, EPI_ISL_1111090, EPI_ISL_1111091, EPI_ISL_1111092, EPI_ISL_1111093, EPI_ISL_1111094, EPI_ISL_1111095, EPI_ISL_1111096, EPI_ISL_1111097, EPI_ISL_1111098, EPI_ISL_1111099, EPI_ISL_1111100, EPI_ISL_1111101, EPI_ISL_1111102, EPI_ISL_1111103, EPI_ISL_1111104, EPI_ISL_1111105, EPI_ISL_1111106, EPI_ISL_1111107, EPI_ISL_1111108, EPI_ISL_1111109, EPI_ISL_1111110, EPI_ISL_1111111, EPI_ISL_1111112, EPI_ISL_1111113, EPI_ISL_1111114, EPI_ISL_1111115, EPI_ISL_1111116, EPI_ISL_1111117, EPI_ISL_1111118, EPI_ISL_1111119, EPI_ISL_1111200, EPI_ISL_1111201, EPI_ISL_1111202, EPI_ISL_1111203, EPI_ISL_1111204, EPI_ISL_1111205, EPI_ISL_1111206, EPI_ISL_1111207, EPI_ISL_1111208, EPI_ISL_1111209, EPI_ISL_1111210, EPI_ISL_1111211, EPI_ISL_1111212, EPI_ISL_1111213, EPI_ISL_1111214, EPI_ISL_1111215, EPI_ISL_1111216, EPI_ISL_1111217, EPI_ISL_1111218, EPI_ISL_1111219, EPI_ISL_1111220, EPI_ISL_1111221, EPI_ISL_1111222, EPI_ISL_1111223, EPI_ISL_1111224, EPI_ISL_1111225, EPI_ISL_1111226, EPI_ISL_1111228, EPI_ISL_1111229, EPI_ISL_1111230, EPI_ISL_1111231, EPI_ISL_1111232, EPI_ISL_1111233, EPI_ISL_1111234, EPI_ISL_1111235, EPI_ISL_1111237, EPI_ISL_1111238, EPI_ISL_1111239	see above	Laboratorio de Referencia Nacional de Virus Respiratorio, Instituto Nacional de Salud Perú	Laboratorio de Referencia Nacional de Enteropatógenos, Instituto Nacional de Salud Perú	Florella Orellana Peralta; Iris Silva Molina; Junior Caro Castro; Ronnie Gavilan Chavez; Veronica Hurtado Vela; Will Quino Sifuentes
EPI_ISL_487269	Laboratorio de Referencia Nacional de Virus Respiratorio, Instituto Nacional de Salud	Laboratorio de Referencia Nacional de Biotecnología y Biología Molecular, Instituto Nacional de Salud	Carlos Padilla Rojas; Henri Bailon Calderon; Johanna Balbuena Torres; Karolyn Vega Chozo; Marco Galarza Perez; Maribel Huaranga Nuñez; Nancy Rojas Serrano; Omar Cáceres Rey; Priscila Lope Pan	
EPI_ISL_415787	Laboratorio de Referencia Nacional de Virus Respiratorio, Instituto Nacional de Salud, Peru	Laboratorio de Referencia Nacional de Biotecnología y Biología Molecular, Instituto Nacional de Salud, Peru	Carlos Padilla Rojas; Henri Bailon Calderon; Johanna Balbuena Torres; Karolyn Vega Chozo; Marco Galarza Perez; Maribel Huaranga Nuñez; Nancy Rojas Serrano; Omar Cáceres Rey; Priscila Lope Pan	
EPI_ISL_514264	Laboratorio de Referencia Nacional de Virus Respiratorio, Instituto Nacional de Salud, Peru	Laboratorio de Referencia Nacional de Biotecnología y Biología Molecular, Instituto Nacional de Salud, Peru	Carlos Padilla Rojas; Henri Bailon Calderon; Johanna Balbuena Torres; Karolyn Vega Chozo; Marco Galarza Perez; Maribel Huaranga Nuñez; Nancy Rojas Serrano; Omar Cáceres Rey; Priscila Lope Pan	
EPI_ISL_491431	Laboratorio de Referencia Nacional de Virus Respiratorio, Instituto Nacional de Salud, Peru	Laboratorio de Referencia Nacional de Biotecnología y Biología Molecular, Instituto Nacional de Salud, Peru	Carlos Padilla Rojas; Henri Bailon Calderon; Johanna Balbuena Torres; Karolyn Vega Chozo; Marco Galarza Perez; Maribel Huaranga Nuñez; Nancy Rojas Serrano; Omar Cáceres Rey; Priscila Lope Pan	
EPI_ISL_520988, EPI_ISL_540924, EPI_ISL_540986, EPI_ISL_540987, EPI_ISL_540988, EPI_ISL_568515, EPI_ISL_568516	see above	Laboratorio de Referencia Nacional de Virus Respiratorios, Instituto Nacional de Salud Peru	Laboratorio de Genómica Microbiana, Universidad Peruana Cayetano Heredia	Alejandra Dávila-Bardley; Brenda Ayzano; Camila Castillo-Vilcachuanan; Guillermo Salvatierra; Janet Huancachoque; Luis González; Maribel Huaranga; Pablo Tsukayama; Pedro E. Romero; Pool Marcos
EPI_ISL_482468	Laboratorio de Referencia Nacional de Virus Respiratorios, Instituto Nacional de Salud Peru	Laboratorio de Referencia Nacional de Biotecnología y Biología Molecular, Instituto Nacional de Salud Peru	Carlos Padilla Rojas; Henri Bailon Calderon; Johanna Balbuena Torres; Karolyn Vega Chozo; Marco Galarza Perez; Maribel Huaranga Nuñez; Nancy Rojas Serrano; Omar Cáceres Rey; Priscila Lope Pan	
EPI_ISL_792364	Laboratorio de Virología - HIEAYC San Juan de Dios	Área de Secuenciación del Laboratorio de Virología del Hospital de Niños Dr. Ricardo Gutiérrez on behalf of Proyecto Argentino Interinstitucional de genómica de SARS-CoV-2 (PAIS Consortium)	A; Colmeiro; Ercole; Ferioli; Gatelli; Goya; LE; Lusso; M; M; MS; Nabae; Jodar; Nalae; R; S; Valinotto; Viegas, M.	
EPI_ISL_623138	Laboratorio de Virología Molecular / UFRJ	Bioinformatics Laboratory / LNCC	Alexandra S. Gerber; Amílcar Tanuri; Ana Paula de C Guimarães; Ana Tereza R de Vasconcelos; Carolina M Voloch; Covid19-UFRJ Workgroup; Cynthia C	

			Cardoso; Diana Mariani; Luiz G P de Almeida; Luis Cristóvão Pórtio; Orlando C. Ferreira; Otávio J. Brustolini; Renato S Aguiar; Ronaldo S Francisco Jr; Terezinha M P Castilheiras
EPI_ISL_430799, EPI_ISL_430800	Laboratorio de Virologia del Hospital de Niños Dr. Ricardo Gutiérrez	Área de Secuenciación del Laboratorio de Virología del Hospital de Niños Dr. Ricardo Gutiérrez on behalf of 'Proyecto Argentino Interinstitucional de genómica de SARS-CoV-2' (PAIS Consortium)	AS; E; Goya; Gravia; LE; Lusso; MI; MS; Mstchenko; Nabaeas Jodar; Natale; S; Valinoto; Viegas, M.
EPI_ISL_792451, EPI_ISL_792454, EPI_ISL_792463, EPI_ISL_792471	Laboratorio del Hospital Regional Ushuaia Gdor. Ernesto Campos	Hospital Regional Ushuaia - Centro Austral de Investigaciones Científicas - Universidad Nacional De Tierra Del Fuego on behalf of 'Proyecto Argentino Interinstitucional de genómica de SARS-CoV-2' (PAIS Consortium)	Boutureira, MF.; CA; CB; CF; Castro; Ceballos; Cáceres; De Rocío; F; G; Gallego; Gramundi; ID; Nardi; SB; SG; Yulan
EPI_ISL_413489	Laboratorio di Microbiologia e Virologia, Università Vita-Salute San Raffaele, Milano	Laboratorio di Microbiologia e Virologia, Università Vita-Salute San Raffaele, Milano	C. Di Resta; E. Boeri; E. Criscuolo; G. Lo Raso; I. Negri; M. Castelli; M. Clementi; M. Sampaolo; N. Mancini & N. Clementi; R. Burioni; R. Ferrarese; RA Diotti; V. Amato; V. Caputo
EPI_ISL_476221	Laboratory Fleury	Instituto de Medicina Tropical da Universidade de São Paulo	Camila Alves Maia da Silva; Darlan da Silva Candido; Erika Regina Manuli; Ester Sabino; Flavia Cristina da Silva Sales; Giulia Magalhães Ferreira; Jaqueline Goes de Jesus; Julien Theze; Mariana Severo Ramundo; Nuno Faria; Sampaes; Celso Granato; Sequencing: Ingra Moraes Claro; Thais de Moura Coletti
EPI_ISL_415741, EPI_ISL_415742, EPI_ISL_415743, EPI_ISL_417519, EPI_ISL_417520, EPI_ISL_417521, EPI_ISL_417522, EPI_ISL_417523, EPI_ISL_417524, EPI_ISL_417525, EPI_ISL_424969, EPI_ISL_424970, EPI_ISL_424971, EPI_ISL_424972, EPI_ISL_424973, EPI_ISL_424974, EPI_ISL_424975, EPI_ISL_424976, EPI_ISL_424977, EPI_ISL_444276, EPI_ISL_444277, EPI_ISL_444278, EPI_ISL_464092, EPI_ISL_667807, EPI_ISL_667808	see above	Laboratory Medicine	Cheng-Hsun Chiu; Cheng-Ta Yang; Chi-Hsien Huang; Chung-Guei Huang; Guang-Wu Chen; Kuang-Tso Le; Kuo-Chien Tsao; Kuo-Ming Lee; Mei-Jen Hsiao; Peng-Nien Huang; Po-Wei Huang; Shin-Ru Shih; Shu-Li Yang; Shu-Min Lin; Yi-Chun Liu; Yu-Nong Gong
EPI_ISL_411915	Laboratory Medicine	Department of Laboratory Medicine, Lin-Kou Chang Gung Memorial Hospital, Taoyuan, Taiwan	Chung-Guei Huang; Kuo-Chien Tsao; Shin-Ru Shih; Shu-Li Yang; Yuh-Cherng Huang; Yi-Chun Li; Yu-Nong Gong
EPI_ISL_529208, EPI_ISL_529209, EPI_ISL_529210, EPI_ISL_529211, EPI_ISL_529212	Laboratory Medicine, University of Washington	University of Washington, Laboratory Medicine	Greninger, A.; Jerome, K.; Roychoudhury, P.
EPI_ISL_437699	Laboratory for Urgent Response to Biological Threats	Institut Pasteur CIBU / ERI	A. Kwasiborski; C. Balliere; C. Batsijet; J. Vanhormwegen; JC. Manuguerra; V. Caru; V. Houredel
EPI_ISL_437699	Laboratory for Urgent Response to Biological Threats	Institut Pasteur CIBU / ERI	A. Kwasiborski; C. Balliere; C. Batsijet; H. Houredel; J. Vanhormwegen; JC. Manuguerra; V. Caru
EPI_ISL_435045, EPI_ISL_435046, EPI_ISL_435047	Laboratory of Genomics & Bioinformatics, Institute of Immunology and Experimental Therapy, Polish Academy of Sciences Oddział Mikrobiologii (Wojewodzkiej Szpitali Sanitarnej-Epidemiologicznej)	RSE "National Center for Biotechnology"	Alexandr Shevtsov; Asylan Amirgazin; Ilyas Akhmetollayev; Ruslan Kalendar; Viktoriya Lutsay; Yerlan Ramanculov
EPI_ISL_437625	Laboratory of Genomics & Bioinformatics, Institute of Immunology and Experimental Therapy, Polish Academy of Sciences Oddział Mikrobiologii (Wojewodzkiej Szpitali Sanitarnej-Epidemiologicznej)	Laboratory of Genomics & Bioinformatics, Institute of Immunology and Experimental Therapy, Polish Academy of Sciences	Aleksandra Herud; Dariusz Martynowski; Dorota Kujawa; Grazyna Zalewska; Joanna Sikorska; Krzysztof Jakub Pawlik; Oskar Karpinski and Lukasz Laczmani; Paulina Zebrowska
EPI_ISL_536399	Laboratory of Immunovirology, Universidad de Antioquia	Instituto Nacional de Salud - Unidad de Secuenciación y Genómica	Carlos Franco-Muñoz; Diego Álvarez-Díaz and Marcela Mercado-Reyes; Francisco J. Díaz; Katherine Lalton-Donato; Lizdany Florez; Wbeimar Agular-Jimenez
EPI_ISL_452358, EPI_ISL_452359, EPI_ISL_452361, EPI_ISL_452364	Laboratory of Infectious Diseases Center of Beijing Ditan Hospital	Laboratory of Infectious Diseases Center of Beijing Ditan Hospital	Chengjie Jie; Fengting Yu; Linghang Wang; Liting Yan; Siyuan Yang; Yunxia Tang
EPI_ISL_417445, EPI_ISL_417447, EPI_ISL_779704, EPI_ISL_779709, EPI_ISL_779712, EPI_ISL_779713, EPI_ISL_779714, EPI_ISL_780378, EPI_ISL_780381, EPI_ISL_780413	see above	Laboratory of Infectious Diseases, Department of Biomedical and Clinical Sciences L. Sacco, University of Milan	Agostino Riva; Alessia Lai; Annalisa Bergna; Arianna Gabrieli; Carla Della Ventura; Claudia Balotta; Dario Bernacchia; Gianguglielmo Zehender; Gianguglielmo Zehender on behalf of SARS-CoV-2 ITALIAN RESEARCH ENTERPRISE (SCIRE) Collaborative Group; Giuliano Rizzardini; Luca Meroni; Maciej Tarkowski; Massimo Galli; Spinello Antonini; Stefano Rusconi
EPI_ISL_418263, EPI_ISL_418264, EPI_ISL_418265	Laboratory of Microbiology, Department of Medicine, National and Kapodistrian University of Athens, Greece	Laboratory of Biology, Department of Medicine, Democritus University of Thrace, Greece	Elisavet Gatzidou; Ioannis Karakasilotis; Maria Bampali; Nikolaos Dovrolis; Nikolaos Spanakis; Stavroula Veletza
EPI_ISL_427043, EPI_ISL_434455, EPI_ISL_434456, EPI_ISL_434457, EPI_ISL_434458, EPI_ISL_434459, EPI_ISL_434460, EPI_ISL_434461, EPI_ISL_434462, EPI_ISL_434463, EPI_ISL_434464, EPI_ISL_434465, EPI_ISL_434467, EPI_ISL_434468, EPI_ISL_434470, EPI_ISL_434471, EPI_ISL_434472, EPI_ISL_434473, EPI_ISL_434474, EPI_ISL_434475, EPI_ISL_434476, EPI_ISL_434477, EPI_ISL_434478, EPI_ISL_434479, EPI_ISL_434480, EPI_ISL_434481, EPI_ISL_434482, EPI_ISL_434483, EPI_ISL_434484, EPI_ISL_434485, EPI_ISL_434486, EPI_ISL_434487, EPI_ISL_434488, EPI_ISL_434489, EPI_ISL_434490, EPI_ISL_434491, EPI_ISL_434492, EPI_ISL_434493, EPI_ISL_434494, EPI_ISL_434495, EPI_ISL_434496, EPI_ISL_434497, EPI_ISL_434498, EPI_ISL_434499, EPI_ISL_434500, EPI_ISL_434501, EPI_ISL_434502, EPI_ISL_434503, EPI_ISL_434504, EPI_ISL_434505, EPI_ISL_434506, EPI_ISL_434507, EPI_ISL_434508, EPI_ISL_434509, EPI_ISL_434510, EPI_ISL_434511	see above	Laboratory of Microbiology, Medical School, National and Kapodistrian University of Athens	Bampali, M.; Dovrolis, N.; Froukala, E.; Gatzidou, E.; Kasselis K.; N. and Karakasilotis, I.; Spanakis; Stavropoulou, A.; Tsakris, A.; Veletza, S.
EPI_ISL_654016	Laboratory of Microbiology, National Reference Lab, Charles Nicolle Hospital, 2-University of Tunis ElManar, Faculty of Medicine of Tunis, LR99ES09, Tunis, Tunisia	1-Clinical and Experimental Pharmacology Lab, LR16SP02, National Center of Pharmacovigilance, University of Tunis El Manar, Tunis, Tunisia. 2-Neurodegenerative diseases and psychiatric troubles, LR18SP03, Razi Hospital, University of Tunis El Manar, Tunis, Tunisia. 3- Ministry of Health, National Observatory of New and Emerging Diseases, 1005, Tunis, Tunisia	Alia Ben Kahla; Gaies Emma; Ilhem Boutba-Ben Boubaker; Imen Kaocem; Imen Mkada; Jalila Ben Khelli; Maher Kharrat; Mouna Ben Sassi; Mouna Safer; Nisaf Ben Alaya; Riadh Daghdous; Riadh Gouider.; Salma Abid; Sameh Trabelsi; Sana Ferjani; Soumaya Rammeh
EPI_ISL_811145	Laboratory of Microbiology, National Reference Lab, Charles Nicolle Hospital, 2-University of Tunis ElManar, Faculty of Medicine of Tunis, LR99ES09, Tunis, Tunisia	Clinical and Experimental Pharmacology Lab, LR16SP02, National Center of Pharmacovigilance, University of Tunis El Manar, Tunis, Tunisia. 2-Neurodegenerative diseases and psychiatric troubles, LR18SP03, Razi Hospital, University of Tunis El Manar, Tunis, Tunisia. 3- Ministry of Health, National Observatory of New and Emerging Diseases, 1005, Tunis, Tunisia	Alia Ben Kahla; Asma Ferjani; Awatef El Moussi; Gaies Emma; Habiba Ben Romdhan; Hanen El Jebari; Ilhem Boutba-Ben Boubaker; Ines Mdnii; Jalila Ben Khelli; Maher Kharrat; Mouna Ben Sassi; Mouna Safer; Nisaf Ben Alaya; Riadh Daghdous; Riadh Gouider.; Salma Abid; Sameh Trabelsi; Sana Ferjani; Soussi Amra
EPI_ISL_613707	Laboratory of Molecular Biology, Blood Center of Ribeirão Preto	Laboratory of Molecular Biology, Blood Center of Ribeirão Preto, Faculty of Medicine of Ribeirão Preto, University of São Paulo	Aparecida Y Yamamoto; Diego Villa Clé; Dimas T Covas; Elaine V Santos; Evandra S Rodrigues; Glaucou de Carvalho Pereira; Jolison Xavier; Luiz CJ Alcantara; Marta Giovanetti; Rodrigo T Calado; Simone Kashima; Svetoslav N Slavov; Talita Adeline; Vagner Fonseca
EPI_ISL_613709	Laboratory of Molecular Biology, Blood Center of Ribeirão Preto, Faculty of Medicine of Ribeirão Preto, University of São Paulo	Laboratory of Molecular Biology, Blood Center of Ribeirão Preto, Faculty of Medicine of Ribeirão Preto, University of São Paulo	Aparecida Y Yamamoto; Diego Villa Clé; Dimas T Covas; Elaine V Santos; Evandra S Rodrigues; Glaucou de Carvalho Pereira; Jolison Xavier; Luiz CJ Alcantara; Marta Giovanetti; Rodrigo T Calado; Simone Kashima; Svetoslav N Slavov; Talita Adeline; Vagner Fonseca
EPI_ISL_425228, EPI_ISL_425229, EPI_ISL_426051, EPI_ISL_426356, EPI_ISL_426357, EPI_ISL_426358, EPI_ISL_426359, EPI_ISL_426360	see above	Laboratory of Molecular Genetics, 2nd Faculty of Medicine, Charles University in Prague, Prague, Czech Republic	Katerina Polackova; Kateřina Poláková; Lenka Kramma; Lenka Kramná; Ondřej Cinek; Ondřej Cinek
EPI_ISL_417419, EPI_ISL_417421, EPI_ISL_428854	Laboratory of Molecular Virology International Center for Genetic Engineering and Biotechnology (ICGEB)	ARGO Open Lab Platform for Genome sequencing	D'Agaro P; Dal Monego S; Licastro D; Marcello A; Rajasekharan S; Segat L
EPI_ISL_417418	Laboratory of Molecular Virology International Center fro	ARGO Open Lab Platform for Genome sequencing	D'Agaro P; Dal Monego S; Licastro D; Marcello A; Rajasekharan S; Segat L

Genetic Engineering and Biotechnology (ICGEB)			
EPI_ISL_479618, EPI_ISL_479617, EPI_ISL_477971	Laboratory of Molecular Virology of the International Centre for Genetic Engineering and Biotechnology (ICGEB)	ARGO Open Lab Platform for Genome Sequencing	Confalonieri M; Confalonieri M Marcello A; Confalonieri P; D; D'Agaro P; Dal Monego S; Licastro; Marcello A; Rajasekharan S; Salton F; Segat L
EPI_ISL_584048, EPI_ISL_584049	Laboratory of Molecular Virology, Department of Biomedical, Surgical and Dental Sciences University of Milano	Laboratory of Molecular Virology, Department of Biomedical, Surgical and Dental Sciences University of Milano	Basilico, N.; Bianchi, M.; C. and Ferrante, P.; D'Alessandro, S.; Deibue, S.; Fattori, M.; Galli, Modenese, A.; Pariani, E.
EPI_ISL_415658, EPI_ISL_415660, EPI_ISL_415661, EPI_ISL_801549, EPI_ISL_801581, EPI_ISL_801582, EPI_ISL_801583, EPI_ISL_801586, EPI_ISL_801587, EPI_ISL_801588, EPI_ISL_801589, EPI_ISL_801590, EPI_ISL_801591, EPI_ISL_801596, EPI_ISL_801599, EPI_ISL_801600, EPI_ISL_801601, EPI_ISL_801602, EPI_ISL_801603, EPI_ISL_801604, EPI_ISL_801605, EPI_ISL_801606, EPI_ISL_801607, EPI_ISL_801608, EPI_ISL_801609, EPI_ISL_801610, EPI_ISL_801611, EPI_ISL_801612, EPI_ISL_801613, EPI_ISL_801614, EPI_ISL_801615, EPI_ISL_801616, EPI_ISL_801617, EPI_ISL_801618, EPI_ISL_801619, EPI_ISL_801620, EPI_ISL_801621, EPI_ISL_801622, EPI_ISL_801623, EPI_ISL_801624, EPI_ISL_801625, EPI_ISL_801626, EPI_ISL_801627, EPI_ISL_801628, EPI_ISL_801629, EPI_ISL_801630, EPI_ISL_801631, EPI_ISL_801632, EPI_ISL_801633, EPI_ISL_801634, EPI_ISL_801635, EPI_ISL_801636, EPI_ISL_801637, EPI_ISL_801638, EPI_ISL_801639, EPI_ISL_801640, EPI_ISL_801641, EPI_ISL_801642, EPI_ISL_801643, EPI_ISL_801644, EPI_ISL_801645, EPI_ISL_801646, EPI_ISL_801647, EPI_ISL_801648, EPI_ISL_801649, EPI_ISL_801650, EPI_ISL_801651, EPI_ISL_801652, EPI_ISL_801653, EPI_ISL_801654, EPI_ISL_801655, EPI_ISL_801656, EPI_ISL_801657, EPI_ISL_801658, EPI_ISL_801659, EPI_ISL_801660, EPI_ISL_801661, EPI_ISL_801662, EPI_ISL_801663, EPI_ISL_801664, EPI_ISL_801665, EPI_ISL_801666, EPI_ISL_801667, EPI_ISL_801668, EPI_ISL_801669, EPI_ISL_801670, EPI_ISL_801671, EPI_ISL_801672, EPI_ISL_801673, EPI_ISL_801674, EPI_ISL_801675, EPI_ISL_801676, EPI_ISL_801677			
see above	Laboratory of Molecular Virology, Pontificia Universidad Católica de Chile	MSHS Pathogen Surveillance Program	Adolfo Garcia-Sastre; Adriana van De Guchte; Ajay Obta; Ana Maria Contreras; Ana S. Gonzalez-Reiche; Ana Silvia Gonzalez-Reiche; Brenny Albuquerque; Carlos Palma; Constanza Maldonado; Edward C. Holmes; Eileen Serrano; Erick Salinas; Hala Alshammy; Harm van Bakel; Jayeeta Dutta; Jorge Levcian; Juan Soto; Leonardo I. Almonacid; M. Belen Leyton; Marcela Ferras; Matthew Hernandez; Matthew M. Hernandez; Melissa Smith; Mitchell Sullivan; Pablo Val; Rafael A. Medina; Rafael A. Medina; Robert Sotir; Shwetha Hara Sridhar; Shwetha Sridhar Hara; Tamara Garcia; Tamara Garcia-Salum; Viviana Simon; Ying-Chih Wang; Zenab Khan
EPI_ISL_427294, EPI_ISL_427295, EPI_ISL_427296, EPI_ISL_427297, EPI_ISL_427298, EPI_ISL_427299, EPI_ISL_427300, EPI_ISL_427301, EPI_ISL_427302, EPI_ISL_427303, EPI_ISL_427304, EPI_ISL_456071, EPI_ISL_456072, EPI_ISL_1181608	see above	Laboratory of Respiratory Viruses and Measles, Oswaldo Cruz Institute, FIOCRUZ	Laboratory of Respiratory Viruses and Measles, Oswaldo Cruz Institute, FIOCRUZ
EPI_ISL_451303, EPI_ISL_451304	Laboratory of Virology, INMI Lazzaro Spallanzani IRCCS	Laboratory of Virology, INMI Lazzaro Spallanzani IRCCS	Antonio Di Caro; Barbara Bartolini; Cesare E. M. Gruber; Francesco Messina; Giuseppe Ippolito; Maria R. Capobianchi; Martina Rueca
EPI_ISL_1341150	Laboratory of Virology, National center of expertise	RSE "National Center of Expertise" and RSE "National center for Biotechnology"	Abdalayev Askar; Amirgazin Asylhan; Balykbaev Kanat; Kamalova Dina; Ramankulov Erjan; Sharipova Saule; Shevtsov Alexander; Tungushbayev Talgat
EPI_ISL_1165139, EPI_ISL_1165140, EPI_ISL_1165141	Laboratory of virology and molecular diagnostics	Laboratory of virology and molecular diagnostics	Boshevska Golubinka; Elizabeta Janchevska; Kuzmanovska Maja
EPI_ISL_1334575, EPI_ISL_1334576, EPI_ISL_1334600, EPI_ISL_1335390, EPI_ISL_1335758, EPI_ISL_1335759, EPI_ISL_1335760	see above	Laboratory of virology, National center of expertise	RSE "National Center for Biotechnology" and RSE "National Center of Expertise"
EPI_ISL_414045, EPI_ISL_459076, EPI_ISL_456077	Laboratório Central de Saúde Pública Noel Nutels (LACEN-RJ)	Laboratory of Respiratory Viruses and Measles, Oswaldo Cruz Institute, FIOCRUZ	Aline Mattos; Alison Fabri; Bráulio Caetano; Cristiana Garcia; Fernando Motta; Jolison Xavier; Jonathan Lopes; Luciana Appolinario; Maria Nóbrega; Maria Ogzwevska; Marilda Siqueira on behalf of the FioCruz COVID-19 Genomic Surveillance Network; Marilda Siqueira/FioCruz COVID-19 Genomic Surveillance Network; Milene Miranda; Paola Resende; Sunando Roy
EPI_ISL_415105, EPI_ISL_427293	Laboratório Central de Saúde Pública Professor Gonçalo Moniz (LACEN-BA)	Laboratory of Respiratory Viruses and Measles, Oswaldo Cruz Institute, FIOCRUZ	Aline Mattos; Alison Fabri; Bráulio Caetano; Cristiana Garcia; Fernando Motta; Jolison Xavier; Jonathan Lopes; Luciana Appolinario; Marilda Siqueira on behalf of the FioCruz COVID-19 Genomic Surveillance Network; Marilda Siqueira on behalf of the FioCruz COVID-19 Genomic Surveillance Network; Milene Miranda; Paola Resende; Priscila Bom; Sunando Roy
EPI_ISL_427292	Laboratório Central de Saúde Pública do Estado de Alagoas (LACEN-AL)	Laboratory of Respiratory Viruses and Measles, Oswaldo Cruz Institute, FIOCRUZ	Aline Mattos; Bráulio Caetano; Cristiana Garcia; Fernando Motta; Jonathan Lopes; Jonathan Lopes; Luciana Appolinario; Maria Ogzwevska; Marilda Siqueira on behalf of the FioCruz COVID-19 Genomic Surveillance Network; Milene Miranda; Paola Resende; Priscila Bom; Sunando Roy
EPI_ISL_427305, EPI_ISL_427306	Laboratório Central de Saúde Pública do Estado de Santa Catarina (LACEN-SC)	Laboratory of Respiratory Viruses and Measles, Oswaldo Cruz Institute, FIOCRUZ	Aline Mattos; Bráulio Caetano; Cristiana Garcia; Fernando Motta; Jonathan Lopes; Luciana Appolinario; Maria Ogzwevska; Marilda Siqueira on behalf of the FioCruz COVID-19 Genomic Surveillance Network; Milene Miranda; Paola Resende; Priscila Bom; Sunando Roy
EPI_ISL_541372, EPI_ISL_541373, EPI_ISL_541374, EPI_ISL_541376	Laboratório Central de Saúde Pública do Estado de Sergipe (LACEN-SE)	Laboratory of Respiratory Viruses and Measles, Oswaldo Cruz Institute, FIOCRUZ	Ana Carolina Mendonça; Anna Carolina Paixão; Clomira Santos; Fernando Motta; Jonathan Lopes; Luciana Appolinario; Marilda Siqueira on behalf of the FioCruz COVID-19 Genomic Surveillance Network; Paola Resende
EPI_ISL_415128	Laboratório Central de Saúde Pública do Estado do Espírito Santo (LACEN-ES)	Laboratory of Respiratory Viruses and Measles, Oswaldo Cruz Institute, FIOCRUZ	Aline Mattos; Alison Fabri; Bráulio Caetano; Cristiana Garcia; Fernando Motta; Jolison Xavier; Jonathan Lopes; Luciana Appolinario; Maria Nóbrega; Maria Ogzwevska; Marilda Siqueira on behalf of the FioCruz COVID-19 Genomic Surveillance Network; Milene Miranda; Paola Resende; Priscila Bom; Sunando Roy
EPI_ISL_541340	Laboratório Central de Saúde Pública do Estado do Paraná (LACEN-PR)	Laboratory of Respiratory Viruses and Measles, Oswaldo Cruz Institute, FIOCRUZ	Ana Carolina Mendonça; Anna Carolina Paixão; Fernando Motta; Inna Riediger; Jonathan Lopes; Luciana Appolinario; Maria do Carmo Debur; Marilda Siqueira on behalf of the FioCruz COVID-19 Genomic Surveillance Network; Paola Resende
EPI_ISL_729804, EPI_ISL_729805, EPI_ISL_729806, EPI_ISL_729807, EPI_ISL_729808, EPI_ISL_729809, EPI_ISL_729810, EPI_ISL_729811, EPI_ISL_729812, EPI_ISL_729813, EPI_ISL_729814, EPI_ISL_729815, EPI_ISL_729816	see above	Laboratório Central de Saúde Pública do Estado do Rio Grande do Sul (LACEN-RS)	Ana Carolina Mendonça; Anna Carolina Paixão; Fernando Motta; Luciana Appolinario; Marilda Siqueira on behalf of the FioCruz COVID-19 Genomic Surveillance Network; Marilda Tereza Mar da Rosa; Paola Resende; Tatiana Schaffer Gregniani
EPI_ISL_636834	Laboratório de Imunofarmacologia - Instituto Oswaldo Cruz	Laboratório de Imunofarmacologia - Instituto Oswaldo Cruz	A.D.; C.Q.; De Paula; F.B.; Ferreira; Fintelman-Rodrigues, N.; M.A. and Sacramento; Saraiva; Souza; T.M.
EPI_ISL_437089, EPI_ISL_437090, EPI_ISL_437091, EPI_ISL_437092, EPI_ISL_437093, EPI_ISL_437094, EPI_ISL_437095, EPI_ISL_437096, EPI_ISL_466422, EPI_ISL_466423, EPI_ISL_466424, EPI_ISL_466425, EPI_ISL_466426, EPI_ISL_466428, EPI_ISL_466429, EPI_ISL_466430, EPI_ISL_466431, EPI_ISL_466432, EPI_ISL_466433, EPI_ISL_466434, EPI_ISL_466435, EPI_ISL_466436	see above	Latvijas Infektoloģijas centrs	Latvian Biomedical Research and Study Centre
EPI_ISL_451489, EPI_ISL_451545, EPI_ISL_451572, EPI_ISL_451602, EPI_ISL_451609, EPI_ISL_451611, EPI_ISL_451612, EPI_ISL_455041, EPI_ISL_455044, EPI_ISL_455063	see above	Laverty Pathology	NSW Health Pathology - Institute of Clinical Pathology and Medical Research; Westmead Hospital; University of Sydney
EPI_ISL_421507, EPI_ISL_421508	Le Château de Seine-Port	National Reference Center for Viruses of Respiratory Infections, Institut Pasteur, Paris	Angela Brisebarre; Etienne Simon-Lorière; Flora Donati; Marion Barbet; Maud Vanpenne; Mélanie Albert; Méline Bizard; Sylvie Behilli; Sylvie van der Werf; Vincent Enouf
EPI_ISL_498551, EPI_ISL_498552, EPI_ISL_498554, EPI_ISL_447588	Lebanese American University	Lebanese American University	Abdallah, J.; Abi Habib, W.; El Shesheny, R.; Goldstein, J. and Kayali, G.; Mokhatib, J. R. J.; Webyy
EPI_ISL_434638	Lednický Lab	Lednický lab	Alan, C.J.; Elbadry; Gibson; J.A.; J.C.; J.G. Jr. and Lednický, M.A.; M.M.; Morris; Stephenson; Subramaniam, K.; T.B.; Waltzek
EPI_ISL_434637	Lednický Laboratory, Emerging Pathogens Institute, University of Florida	Lednický Laboratory at Emerging Pathogens Institute, University of Florida	Alan, M.; C.J.; Elbadry; Gibson; J.A.; J.C.; J.G. Jr. and Lednický, M.A.; Morris; Stephenson; Subramaniam, K.; T.B.; Waltzek
EPI_ISL_539782, EPI_ISL_539783, EPI_ISL_539784, EPI_ISL_539785, EPI_ISL_539786, EPI_ISL_539787, EPI_ISL_539788, EPI_ISL_539789, EPI_ISL_539790, EPI_ISL_539791, EPI_ISL_539792, EPI_ISL_539793, EPI_ISL_539794, EPI_ISL_539795, EPI_ISL_539796, EPI_ISL_539797, EPI_ISL_539798, EPI_ISL_539799, EPI_ISL_539800, EPI_ISL_539801, EPI_ISL_539802, EPI_ISL_539803, EPI_ISL_539804, EPI_ISL_539805, EPI_ISL_539806, EPI_ISL_539807, EPI_ISL_539808, EPI_ISL_539809, EPI_ISL_539810, EPI_ISL_539811, EPI_ISL_539812, EPI_ISL_539813, EPI_ISL_539814, EPI_ISL_539815, EPI_ISL_539816, EPI_ISL_539817, EPI_ISL_539818, EPI_ISL_539819, EPI_ISL_539820, EPI_ISL_539821, EPI_ISL_539822, EPI_ISL_539823, EPI_ISL_539824, EPI_ISL_539825, EPI_ISL_539826, EPI_ISL_539827, EPI_ISL_539828, EPI_ISL_539829, EPI_ISL_539830, EPI_ISL_539831, EPI_ISL_539832, EPI_ISL_539833, EPI_ISL_539834, EPI_ISL_539835, EPI_ISL_539836, EPI_ISL_539837, EPI_ISL_539838, EPI_ISL_539839, EPI_ISL_539840, EPI_ISL_539841, EPI_ISL_539842, EPI_ISL_539843, EPI_ISL_539844, EPI_ISL_539845, EPI_ISL_539846, EPI_ISL_539847, EPI_ISL_539848, EPI_ISL_539849, EPI_ISL_539850, EPI_ISL_539851, EPI_ISL_539852, EPI_ISL_539853, EPI_ISL_539854, EPI_ISL_539855, EPI_ISL_539856, EPI_ISL_539857, EPI_ISL_539858, EPI_ISL_539859, EPI_ISL_539860, EPI_ISL_539861, EPI_ISL_539862, EPI_ISL_539863, EPI_ISL_539864, EPI_ISL_539865, EPI_ISL_539866, EPI_ISL_539867, EPI_ISL_539868, EPI_ISL_539869, EPI_ISL_539870, EPI_ISL_539871, EPI_ISL_539872, EPI_ISL_539873, EPI_ISL_539874, EPI_ISL_539875, EPI_ISL_539876, EPI_ISL_539877, EPI_ISL_539878, EPI_ISL_539879, EPI_ISL_539880, EPI_ISL_539881, EPI_ISL_539882, EPI_ISL_539883, EPI_ISL_539884, EPI_ISL_539885, EPI_ISL_539886, EPI_ISL_539887, EPI_ISL_539888, EPI_ISL_539889, EPI_ISL_539890, EPI_ISL_539891, EPI_ISL_539892, EPI_ISL_539893, EPI_ISL_539894, EPI_ISL_539895, EPI_ISL_539896, EPI_ISL_539897, EPI_ISL_539898, EPI_ISL_539899, EPI_ISL_539900, EPI_ISL_539901, EPI_ISL_539902, EPI_ISL_539903, EPI_ISL_539904, EPI_ISL_539905, EPI_ISL_539906, EPI_ISL_539907, EPI_ISL_539908, EPI_ISL_539909, EPI_ISL_539910, EPI_ISL_539911, EPI_ISL_539912, EPI_ISL_539913, EPI_ISL_539914, EPI_ISL_539915, EPI_ISL_539916, EPI_ISL_539917, EPI_ISL_539918, EPI_ISL_539919, EPI_ISL_539920, EPI_ISL_539921, EPI_ISL_539922, EPI_ISL_539923, EPI_ISL_539924, EPI_ISL_539925, EPI_ISL_539926, EPI_ISL_539927, EPI_ISL_539928, EPI_ISL_539929, EPI_ISL_539930, EPI_ISL_539931, EPI_ISL_539932, EPI_ISL_539933, EPI_ISL_539934, EPI_ISL_539935, EPI_ISL_539936, EPI_ISL_539937, EPI_ISL_539938, EPI_ISL_539939, EPI_ISL_539940, EPI_ISL_539941, EPI_ISL_539942, EPI_ISL_539943, EPI_ISL_539944, EPI_ISL_539945, EPI_ISL_539946, EPI_ISL_539947, EPI_ISL_539948, EPI_ISL_539949, EPI_ISL_539950, EPI_ISL_539951, EPI_ISL_539952, EPI_ISL_539953, EPI_ISL_539954, EPI_ISL_539955, EPI_ISL_539956, EPI_ISL_539957, EPI_ISL_539958, EPI_ISL_539959, EPI_ISL_539960, EPI_ISL_539961, EPI_ISL_539962, EPI_ISL_539963, EPI_ISL_539964, EPI_ISL_539965, EPI_ISL_539966, EPI_ISL_539967, EPI_ISL_539968, EPI_ISL_539969, EPI_ISL_539970, EPI_ISL_539971, EPI_ISL_539972, EPI_ISL_539973, EPI_ISL_539974, EPI_ISL_539975, EPI_ISL_539976, EPI_ISL_539977, EPI_ISL_539978, EPI_ISL_539979, EPI_ISL_539980, EPI_ISL_539981, EPI_ISL_539982, EPI_ISL_539983, EPI_ISL_539984, EPI_ISL_539985, EPI_ISL_539986, EPI_ISL_539987, EPI_ISL_539988, EPI_ISL_539989, EPI_ISL_539990, EPI_ISL_539991, EPI_ISL_539992, EPI_ISL_539993, EPI_ISL_539994, EPI_ISL_539995, EPI_ISL_539996, EPI_ISL_539997, EPI_ISL_539998, EPI_ISL_539999, EPI_ISL_600000	Lednický Laboratory, Emerging Pathogens Institute, University of Florida		

Table with 4 columns: Accession IDs (EPI_ISL), Laboratory Name, Country, and PI. Includes entries from Leeds Teaching Hospitals NHS Trust and Wellcome Sanger Institute.

Table with 4 columns: Accession IDs (EPI_ISL), Laboratory Name, Country, and PI. Includes entries from Wellcome Sanger Institute and Anthony Hale and Alex Alderton.

Table with 4 columns: Accession IDs (EPI_ISL), Laboratory Name, Country, and PI. Includes entries from Liverpool Clinical Laboratories and COVID-19 Genomics UK Consortium.

Table with 4 columns: Accession IDs (EPI_ISL), Laboratory Name, Country, and PI. Includes entries from Long Island Jewish Medical Center and New York City Public Health Laboratory.

Table with 4 columns: Accession IDs (EPI_ISL), Laboratory Name, Country, and PI. Includes entries from M Health Fairview and Minnesota Department of Health.

Table with 4 columns: Accession IDs (EPI_ISL), Laboratory Name, Country, and PI. Includes entries from MA State Public Health Laboratory and Pathogen Discovery.

Table with 4 columns: Accession IDs (EPI_ISL), Laboratory Name, Country, and PI. Includes entries from MB-Canton Provincial Laboratory and National Microbiology Laboratory.

Table with 4 columns: Accession IDs (EPI_ISL), Laboratory Name, Country, and PI. Includes entries from MD DOH Laboratories Administration and Instituto de Salud Pública de Chile.

Table with 4 columns: Accession IDs (EPI_ISL), Laboratory Name, Country, and PI. Includes entries from MEPHI, Aix Marseille University.

Table with 4 columns: Accession IDs (EPI_ISL), Laboratory Name, Country, and PI. Includes entries from M Health Fairview and Minnesota Department of Health.

Table with 4 columns: Accession IDs (EPI_ISL), Laboratory Name, Country, and PI. Includes entries from MA State Public Health Laboratory and Pathogen Discovery.

Table with 4 columns: Accession IDs (EPI_ISL), Laboratory Name, Country, and PI. Includes entries from MB-Canton Provincial Laboratory and National Microbiology Laboratory.

Table with 4 columns: Accession IDs (EPI_ISL), Laboratory Name, Country, and PI. Includes entries from MD DOH Laboratories Administration and Instituto de Salud Pública de Chile.

Table with columns for laboratory names, EPIS/ISL identifiers, and personnel/affiliations. Includes institutions like Charles University, Motol University Hospital, Mount Sinai Hospital, and various research centers.

EPI_ISL_605058, EPI_ISL_605059, EPI_ISL_605060, EPI_ISL_605061, EPI_ISL_605062, EPI_ISL_605063, EPI_ISL_605064, EPI_ISL_605065, EPI_ISL_605066, EPI_ISL_605067, EPI_ISL_605068, EPI_ISL_605069, EPI_ISL_605070, EPI_ISL_605071, EPI_ISL_605072, EPI_ISL_605073, EPI_ISL_605074, EPI_ISL_605077, EPI_ISL_605080, EPI_ISL_605123
see above National Virus Reference Laboratory Irish Coronavirus Sequencing Consortium - Helixworks Conor Crosbie; Nimesh Pinnamaneni; Sachin Chalapati
EPI_ISL_848153, EPI_ISL_848154, EPI_ISL_848155, EPI_ISL_848156, EPI_ISL_848157, EPI_ISL_848158, EPI_ISL_848159, EPI_ISL_848160, EPI_ISL_848161, EPI_ISL_848162, EPI_ISL_848163, EPI_ISL_848164, EPI_ISL_848165, EPI_ISL_848166
see above National Virus Reference Laboratory Irish Coronavirus Sequencing Consortium - National University of Ireland Galway Grainne Mc Andrew; Kate Reddington; Simone Coughlan
EPI_ISL_671373, EPI_ISL_671374, EPI_ISL_671375, EPI_ISL_671376, EPI_ISL_671377, EPI_ISL_671378, EPI_ISL_671379, EPI_ISL_671380, EPI_ISL_671381, EPI_ISL_671382, EPI_ISL_671383, EPI_ISL_671384, EPI_ISL_671385, EPI_ISL_671386, EPI_ISL_671387, EPI_ISL_671388, EPI_ISL_671389, EPI_ISL_671390, EPI_ISL_671391, EPI_ISL_671392, EPI_ISL_671393, EPI_ISL_671394, EPI_ISL_671395, EPI_ISL_671396, EPI_ISL_671397, EPI_ISL_671398, EPI_ISL_671399, EPI_ISL_671400, EPI_ISL_671401, EPI_ISL_671402, EPI_ISL_671403, EPI_ISL_671404, EPI_ISL_671405, EPI_ISL_671406, EPI_ISL_671407, EPI_ISL_671408, EPI_ISL_671409, EPI_ISL_671410, EPI_ISL_671411, EPI_ISL_671412, EPI_ISL_671413, EPI_ISL_671414, EPI_ISL_671415, EPI_ISL_671416, EPI_ISL_671417, EPI_ISL_671418, EPI_ISL_671419, EPI_ISL_671420, EPI_ISL_671421, EPI_ISL_671422, EPI_ISL_671423, EPI_ISL_671424, EPI_ISL_671425, EPI_ISL_671426, EPI_ISL_671427, EPI_ISL_671428, EPI_ISL_671429, EPI_ISL_671430, EPI_ISL_671431, EPI_ISL_671432, EPI_ISL_671433, EPI_ISL_671434, EPI_ISL_671435, EPI_ISL_671436, EPI_ISL_671437, EPI_ISL_671438, EPI_ISL_671439, EPI_ISL_671440, EPI_ISL_671441, EPI_ISL_671442, EPI_ISL_671443, EPI_ISL_671444, EPI_ISL_671445, EPI_ISL_671446, EPI_ISL_671447, EPI_ISL_671448, EPI_ISL_671449, EPI_ISL_671450, EPI_ISL_671451, EPI_ISL_671452, EPI_ISL_671453, EPI_ISL_671454, EPI_ISL_671455, EPI_ISL_671456, EPI_ISL_671457, EPI_ISL_671458, EPI_ISL_671459, EPI_ISL_671460, EPI_ISL_671461, EPI_ISL_671462, EPI_ISL_671463, EPI_ISL_671464, EPI_ISL_671465, EPI_ISL_671466, EPI_ISL_671467, EPI_ISL_671468, EPI_ISL_671469, EPI_ISL_671470, EPI_ISL_671471, EPI_ISL_671472, EPI_ISL_671473, EPI_ISL_671474, EPI_ISL_671475, EPI_ISL_671476, EPI_ISL_671477, EPI_ISL_671478, EPI_ISL_671479, EPI_ISL_671480, EPI_ISL_671481, EPI_ISL_671482, EPI_ISL_671483, EPI_ISL_671484, EPI_ISL_671485, EPI_ISL_671486, EPI_ISL_671487, EPI_ISL_671488, EPI_ISL_671489, EPI_ISL_671490, EPI_ISL_671491, EPI_ISL_671492, EPI_ISL_671493, EPI_ISL_671494, EPI_ISL_671495, EPI_ISL_671496, EPI_ISL_671497, EPI_ISL_671498, EPI_ISL_671499, EPI_ISL_671500, EPI_ISL_671501, EPI_ISL_671502, EPI_ISL_671503, EPI_ISL_671504, EPI_ISL_671505, EPI_ISL_671506, EPI_ISL_671507, EPI_ISL_671508, EPI_ISL_671509, EPI_ISL_671510, EPI_ISL_671511, EPI_ISL_671512, EPI_ISL_671513, EPI_ISL_671514, EPI_ISL_671515, EPI_ISL_671516, EPI_ISL_671517, EPI_ISL_671518, EPI_ISL_671519, EPI_ISL_671520, EPI_ISL_671521, EPI_ISL_671522, EPI_ISL_671523, EPI_ISL_671524, EPI_ISL_671525, EPI_ISL_671526, EPI_ISL_671527, EPI_ISL_671528, EPI_ISL_671529, EPI_ISL_671530, EPI_ISL_671531, EPI_ISL_671532, EPI_ISL_671533, EPI_ISL_671534, EPI_ISL_671535, EPI_ISL_671536, EPI_ISL_671537, EPI_ISL_671538, EPI_ISL_671539, EPI_ISL_671540, EPI_ISL_671541, EPI_ISL_671542, EPI_ISL_671543, EPI_ISL_671544, EPI_ISL_671545, EPI_ISL_671546, EPI_ISL_671547, EPI_ISL_671548, EPI_ISL_671549, EPI_ISL_671550, EPI_ISL_671551, EPI_ISL_671552, EPI_ISL_671553, EPI_ISL_671554, EPI_ISL_671555, EPI_ISL_671556, EPI_ISL_671557, EPI_ISL_671558, EPI_ISL_671559, EPI_ISL_671560, EPI_ISL_671561, EPI_ISL_671562, EPI_ISL_671563, EPI_ISL_671564, EPI_ISL_671565, EPI_ISL_671566, EPI_ISL_671567, EPI_ISL_671568, EPI_ISL_671569, EPI_ISL_671570, EPI_ISL_671571, EPI_ISL_671572, EPI_ISL_671573, EPI_ISL_671574, EPI_ISL_671575, EPI_ISL_671576, EPI_ISL_671577, EPI_ISL_671578, EPI_ISL_671579, EPI_ISL_671580, EPI_ISL_671581, EPI_ISL_671582, EPI_ISL_671583, EPI_ISL_671584, EPI_ISL_671585, EPI_ISL_671586, EPI_ISL_671587, EPI_ISL_671588, EPI_ISL_671589, EPI_ISL_671590, EPI_ISL_671591, EPI_ISL_671592, EPI_ISL_671593, EPI_ISL_671594, EPI_ISL_671595, EPI_ISL_671596, EPI_ISL_671597, EPI_ISL_671598, EPI_ISL_671599, EPI_ISL_671600, EPI_ISL_671601, EPI_ISL_671602, EPI_ISL_671603, EPI_ISL_671604, EPI_ISL_671605, EPI_ISL_671606, EPI_ISL_671607, EPI_ISL_671608, EPI_ISL_671609, EPI_ISL_671610, EPI_ISL_671611, EPI_ISL_671612, EPI_ISL_671613, EPI_ISL_671614, EPI_ISL_671615, EPI_ISL_671616, EPI_ISL_671617, EPI_ISL_671618, EPI_ISL_671619, EPI_ISL_671620, EPI_ISL_671621, EPI_ISL_671622, EPI_ISL_671623, EPI_ISL_671624, EPI_ISL_671625, EPI_ISL_671626, EPI_ISL_671627, EPI_ISL_671628, EPI_ISL_671629, EPI_ISL_671630, EPI_ISL_671631, EPI_ISL_671632, EPI_ISL_671633, EPI_ISL_671634, EPI_ISL_671635, EPI_ISL_671636, EPI_ISL_671637, EPI_ISL_671638, EPI_ISL_671639, EPI_ISL_671640, EPI_ISL_671641, EPI_ISL_671642, EPI_ISL_671643, EPI_ISL_671644, EPI_ISL_671645, EPI_ISL_671646, EPI_ISL_671647, EPI_ISL_671648, EPI_ISL_671649, EPI_ISL_671650, EPI_ISL_671651, EPI_ISL_671652, EPI_ISL_671653, EPI_ISL_671654, EPI_ISL_671655, EPI_ISL_671656, EPI_ISL_671657, EPI_ISL_671658, EPI_ISL_671659, EPI_ISL_671660, EPI_ISL_671661, EPI_ISL_671662, EPI_ISL_671663, EPI_ISL_671664, EPI_ISL_671665, EPI_ISL_671666, EPI_ISL_671667, EPI_ISL_671668, EPI_ISL_671669, EPI_ISL_671670, EPI_ISL_671671, EPI_ISL_671672, EPI_ISL_671673, EPI_ISL_671674, EPI_ISL_671675, EPI_ISL_671676, EPI_ISL_671677, EPI_ISL_671678, EPI_ISL_671679, EPI_ISL_671680, EPI_ISL_671681, EPI_ISL_671682, EPI_ISL_671683, EPI_ISL_671684, EPI_ISL_671685, EPI_ISL_671686, EPI_ISL_671687, EPI_ISL_671688, EPI_ISL_671689, EPI_ISL_671690, EPI_ISL_671691, EPI_ISL_671692, EPI_ISL_671693, EPI_ISL_671694, EPI_ISL_671695, EPI_ISL_671696, EPI_ISL_671697, EPI_ISL_671698, EPI_ISL_671699, EPI_ISL_671700, EPI_ISL_671701, EPI_ISL_671702, EPI_ISL_671703, EPI_ISL_671704, EPI_ISL_671705, EPI_ISL_671706, EPI_ISL_671707
National Virus Reference Laboratory Irish Coronavirus Sequencing Consortium - Teagasc Moorspark Calum Walsh; Fiona Crispie; Genuity Ireland; John Kenny; Matthew McCabe; Paul Cotter
National Virus Resource Center, Chinese Academy of Sciences, Wuhan 430071, China Computational Virology Group, Center for Bacteria and Viruses Resources and Bioinformatics, Wuhan Institute of Virology, Chinese Academy of Sciences/Wuhan 430071, China Di Liu; Hongping Wei; Jianjun Chen; Jin Xiong; Yi Huang; Yi Yan
Naval Health Research Center Naval Medical Research Center Biological Defense Research Directorate Adrian Paskey; Chris Myers; Desirée Pena-Gomez; Ewell Hollis; Kimberly Bishop-Lilly; Kyle Long; Logan Voegtly; Melinda Balansay-Ames; Nathaniel Christy; Regina Cer; Roger Pan
Naval Infectious Diseases Diagnostic Laboratory Naval Medical Research Center Biological Defense Research Directorate Adrian Paskey; Desirée Pena-Gomez; Francisco Malgon Bautista; Hua Wei Chen; Kimberly Bishop-Lilly; Kyle Long; Lindsay Glang; Logan Voegtly; Mark Simons; Megan Schilling; Regina Cer; Victor Sugharto
Nevada State Public Health Laboratory Nevada State Public Health Laboratory Andrew Gorzalski; Chris Laverdure; Cyprian Rossetto; David Jackson; Heather Kerwin; Joel R. Seivinsky; Mark Pandori; Natalie Crawford; Paul Hartley; Richard Tillet; Stephanie Van Hooser; Subhash C. Verma; and Mark Pandori
New Mexico Department of Health Scientific Laboratory Division Center for Global Health, University of New Mexico Health Sciences Center Darrell Dinwiddie; Daryl Domman; Joseph Hicks; Kurt Schwalim; Michael Edwards; Twila Kunde
New York Community Hospital New York City Public Health Laboratory Jade Wang; et al.
New York Presbyterian Lower Manhattan New York City Public Health Laboratory Jade Wang; et al.
New York Presbyterian Queens New York City Public Health Laboratory Jade Wang; et al.
New York Presbyterian-Brooklyn Methodist Hospital New York City Public Health Laboratory Jade Wang; et al.
New York Presbyterian/Weill Cornell Medical Center New York City Public Health Laboratory Jade Wang; et al.
New York-Presbyterian-Columbia University Medical Center New York City Public Health Laboratory Jade Wang; et al.
New York-Presbyterian & Mason Lab Mason Lab Alon Shalber; Arryn Craney; Benjamin Young; Cem Meydan; Chandrima Bhattacharya; Christopher E. Mason; Christopher Mozsary; Craig D. Westover; Daniel J. Butler; David Danko; Dmitry Meleshko; Dong Xu; Ebrahim Afshinnekoo; Fritz J. Sedlaczek; Hanna Rennert; Imran Hajrasouliha; Jenny Xiang; Joel Rosiene; John Siple; Jonathan Fox; Justyna Gawnys; Krista Ryon; Lars F. Westblade; Lin Cong; Marcin Imielinski; Maria Sierra; Massimo Loda; Matthew Mackay; Melissa Gusting; Mirela Sultovic; Nikolay A. Ivanov; Phyllis Ruggiero; Priya Velu; Shawn Levy
Nigeria Centre for Disease Control African Centre of Excellence for Genomics of Infectious Diseases (ACEGID), Redeemer's University, Ede, Osun State, Nigeria Ajogbasile F.V.; Folarin O.A.; Happei C.T.; Ihekweazu C.; Kayode A.; Oguzie J.; Olowoye I.; Olumade T.; Oluniji P.E.; Uwanibe J.
Nigeria Centre for Disease Control (NCDC) African Centre of Excellence for Genomics of Infectious Diseases (ACEGID), Redeemer's University, Ede, Osun State, Nigeria Ajogbasile F.V.; Folarin O.A.; Happei C.T.; Ihekweazu C.; Kayode A.; Oguzie J.; Olowoye I.; Olumade T.; Oluniji P.E.; Uwanibe J.
Niigata City Public Health Research Institute Pathogen Genomics Center, National Institute of Infectious Diseases Hajime Kamiya; Kentaro Itokawa; Makoto Kuroda; Masanori Hashino; Motoi Suzuki; Rina Tanaka; Tsuyoshi Sekizuka; Yurie Takahashi
Niigata Prefectural Institute of Public Health and Environmental Sciences Pathogen Genomics Center, National Institute of Infectious Diseases Hajime Kamiya; Kentaro Itokawa; Makoto Kuroda; Masanori Hashino; Motoi Suzuki; Reiko Arai; Rina Tanaka; Tsuyoshi Sekizuka
Nordland Hospital - Bodo, Laboratory Department, Molecular Biology Unit Norwegian Institute of Public Health, Department of Virology Hilde Elshaug; Kamilla Heddeland Instefjord; Karoline Bragstad; Kathrine Stene-Johansen; Olav Hungnes
North Dakota Department of Health, Public Health Laboratory North Dakota Department of Health, Public Health Laboratory Liza Wingenter

EPI_ISL_596502, EPI_ISL_596503, EPI_ISL_596504, EPI_ISL_596506, EPI_ISL_596508, EPI_ISL_596509, EPI_ISL_596510, EPI_ISL_596511, EPI_ISL_596512, EPI_ISL_596513, EPI_ISL_596515, EPI_ISL_596516, EPI_ISL_596517, EPI_ISL_596518	see above	Palestinian Ministry of Health	Molecular Genetics Lab	Damien Richard, Dana Najjar, Francois Balloux, Hisham Darwish, Husam Sallam, Issa Shateh, Lucy van Dorp, Mahmoud Ruzayqat, Nouar Outob, Osama Najjar, Zaidoun Salah												
EPI_ISL_968080	EPI_ISL_455605	EPI_ISL_434701	EPI_ISL_421502, EPI_ISL_421503	EPI_ISL_448222	EPI_ISL_654866, EPI_ISL_654867, EPI_ISL_654868, EPI_ISL_654869, EPI_ISL_654870, EPI_ISL_654871, EPI_ISL_654872, EPI_ISL_654873, EPI_ISL_654874, EPI_ISL_654875, EPI_ISL_654876, EPI_ISL_654877, EPI_ISL_654878, EPI_ISL_654879, EPI_ISL_654880, EPI_ISL_654881	see above	EPI_ISL_442523	EPI_ISL_456163, EPI_ISL_456171, EPI_ISL_456194, EPI_ISL_456195, EPI_ISL_456215, EPI_ISL_456221, EPI_ISL_456222, EPI_ISL_456223, EPI_ISL_456224	see above	EPI_ISL_420456, EPI_ISL_470830, EPI_ISL_470840, EPI_ISL_470841, EPI_ISL_470842, EPI_ISL_470843, EPI_ISL_470844, EPI_ISL_470845, EPI_ISL_470846, EPI_ISL_470847, EPI_ISL_470848, EPI_ISL_470849, EPI_ISL_470851, EPI_ISL_470852, EPI_ISL_470853, EPI_ISL_470854, EPI_ISL_470855, EPI_ISL_470856, EPI_ISL_470857, EPI_ISL_470858, EPI_ISL_470859, EPI_ISL_470860, EPI_ISL_470861, EPI_ISL_470862, EPI_ISL_470863, EPI_ISL_470864, EPI_ISL_470865, EPI_ISL_470866, EPI_ISL_470867, EPI_ISL_470868, EPI_ISL_470869, EPI_ISL_470872, EPI_ISL_470873	see above	EPI_ISL_512738, EPI_ISL_512739, EPI_ISL_512741, EPI_ISL_512742, EPI_ISL_512743, EPI_ISL_512744, EPI_ISL_512745, EPI_ISL_512746, EPI_ISL_512747, EPI_ISL_512748, EPI_ISL_512749, EPI_ISL_512750, EPI_ISL_512751, EPI_ISL_512752, EPI_ISL_512753, EPI_ISL_512754, EPI_ISL_512755, EPI_ISL_512756, EPI_ISL_512757, EPI_ISL_512758, EPI_ISL_512759, EPI_ISL_512760, EPI_ISL_512761, EPI_ISL_512762, EPI_ISL_512763, EPI_ISL_512764, EPI_ISL_512765, EPI_ISL_512766, EPI_ISL_512767, EPI_ISL_512768, EPI_ISL_512769, EPI_ISL_512770, EPI_ISL_512771, EPI_ISL_512772, EPI_ISL_512773, EPI_ISL_512774, EPI_ISL_512775, EPI_ISL_512776, EPI_ISL_512777, EPI_ISL_512778, EPI_ISL_512779, EPI_ISL_512780, EPI_ISL_512781, EPI_ISL_512782, EPI_ISL_512783, EPI_ISL_512784, EPI_ISL_512785, EPI_ISL_512786, EPI_ISL_512787, EPI_ISL_512788, EPI_ISL_512789, EPI_ISL_512790, EPI_ISL_512791, EPI_ISL_512792, EPI_ISL_512793, EPI_ISL_512794, EPI_ISL_512795, EPI_ISL_512796, EPI_ISL_512797, EPI_ISL_512798, EPI_ISL_512799, EPI_ISL_512800, EPI_ISL_512801, EPI_ISL_512802, EPI_ISL_512803, EPI_ISL_512804, EPI_ISL_512805, EPI_ISL_512806, EPI_ISL_512807, EPI_ISL_512808, EPI_ISL_512809, EPI_ISL_512810, EPI_ISL_512811, EPI_ISL_512812, EPI_ISL_512813, EPI_ISL_512814, EPI_ISL_512815, EPI_ISL_512816, EPI_ISL_512817, EPI_ISL_512818, EPI_ISL_512819, EPI_ISL_512820, EPI_ISL_512821, EPI_ISL_512822, EPI_ISL_512823, EPI_ISL_512824, EPI_ISL_512825, EPI_ISL_512826, EPI_ISL_512827, EPI_ISL_512828, EPI_ISL_512829, EPI_ISL_512830, EPI_ISL_512831, EPI_ISL_512832, EPI_ISL_512833, EPI_ISL_512834, EPI_ISL_512835, EPI_ISL_512836, EPI_ISL_512837, EPI_ISL_512838, EPI_ISL_512839, EPI_ISL_512840, EPI_ISL_512841, EPI_ISL_512842, EPI_ISL_512843, EPI_ISL_512844, EPI_ISL_512845, EPI_ISL_512846, EPI_ISL_512847, EPI_ISL_512848, EPI_ISL_512849, EPI_ISL_512850, EPI_ISL_512851, EPI_ISL_512852, EPI_ISL_512853, EPI_ISL_512854, EPI_ISL_512855, EPI_ISL_512856, EPI_ISL_512857, EPI_ISL_512858, EPI_ISL_512859, EPI_ISL_512860, EPI_ISL_512861, EPI_ISL_512862, EPI_ISL_512863, EPI_ISL_512864, EPI_ISL_512865, EPI_ISL_512866, EPI_ISL_512867, EPI_ISL_512868, EPI_ISL_512869, EPI_ISL_512870, EPI_ISL_512871, EPI_ISL_512872, EPI_ISL_512873, EPI_ISL_512874, EPI_ISL_512875, EPI_ISL_512876, EPI_ISL_512877, EPI_ISL_512878, EPI_ISL_512879, EPI_ISL_512880, EPI_ISL_512881, EPI_ISL_512882, EPI_ISL_512883, EPI_ISL_512884, EPI_ISL_512885, EPI_ISL_512886, EPI_ISL_512887, EPI_ISL_512888, EPI_ISL_512889, EPI_ISL_512890, EPI_ISL_512891, EPI_ISL_512892, EPI_ISL_512893, EPI_ISL_512894, EPI_ISL_512895, EPI_ISL_512896, EPI_ISL_512897, EPI_ISL_512898, EPI_ISL_512899, EPI_ISL_512900, EPI_ISL_512901, EPI_ISL_512902, EPI_ISL_512903, EPI_ISL_512904, EPI_ISL_512905, EPI_ISL_512906, EPI_ISL_512907, EPI_ISL_512908, EPI_ISL_512909, EPI_ISL_512910, EPI_ISL_512911, EPI_ISL_512912, EPI_ISL_512913, EPI_ISL_512914, EPI_ISL_512915, EPI_ISL_512916, EPI_ISL_512917, EPI_ISL_512918, EPI_ISL_512919, EPI_ISL_512920, EPI_ISL_512921, EPI_ISL_512922, EPI_ISL_512923, EPI_ISL_512924, EPI_ISL_512925, EPI_ISL_512926, EPI_ISL_512927, EPI_ISL_512928, EPI_ISL_512929, EPI_ISL_512930, EPI_ISL_512931, EPI_ISL_512932, EPI_ISL_512933, EPI_ISL_512934, EPI_ISL_512935, EPI_ISL_512936, EPI_ISL_512937, EPI_ISL_512938, EPI_ISL_512939, EPI_ISL_512940, EPI_ISL_512941, EPI_ISL_512942, EPI_ISL_512943, EPI_ISL_512944, EPI_ISL_512945, EPI_ISL_512946, EPI_ISL_512947, EPI_ISL_512948, EPI_ISL_512949, EPI_ISL_512950, EPI_ISL_512951, EPI_ISL_512952, EPI_ISL_512953, EPI_ISL_512954, EPI_ISL_512955, EPI_ISL_512956, EPI_ISL_512957, EPI_ISL_512958, EPI_ISL_512959, EPI_ISL_512960, EPI_ISL_512961, EPI_ISL_512962, EPI_ISL_512963, EPI_ISL_512964, EPI_ISL_512965, EPI_ISL_512966, EPI_ISL_512967, EPI_ISL_512968, EPI_ISL_512969, EPI_ISL_512970, EPI_ISL_512971, EPI_ISL_512972, EPI_ISL_512973, EPI_ISL_512974, EPI_ISL_512975, EPI_ISL_512976, EPI_ISL_512977, EPI_ISL_512978, EPI_ISL_512979, EPI_ISL_512980, EPI_ISL_512981, EPI_ISL_512982, EPI_ISL_512983, EPI_ISL_512984, EPI_ISL_512985, EPI_ISL_512986, EPI_ISL_512987, EPI_ISL_512988, EPI_ISL_512989, EPI_ISL_512990, EPI_ISL_512991, EPI_ISL_512992, EPI_ISL_512993, EPI_ISL_512994, EPI_ISL_512995, EPI_ISL_512996, EPI_ISL_512997, EPI_ISL_512998, EPI_ISL_512999, EPI_ISL_530000	see above	EPI_ISL_451487, EPI_ISL_451488, EPI_ISL_451552, EPI_ISL_451604	EPI_ISL_478673, EPI_ISL_478674	see above

Table with columns for EPI ID, Country/Region, and Contact Person. It lists various EPI programs including COVID-19 Genomics UK, Ministry of Public Health, Thailand, and various research units in China and the UK. The table contains hundreds of rows of EPI IDs and associated contact information.

EPI_ISL_417924	Secretaría de Salud Medellín	Instituto Nacional de Salud, Universidad Cooperativa de Colombia, Instituto Alexander von Humboldt, Imperial College-London, London School of Hygiene & Tropical Medicine	Astrid C. Flórez; Carlos Franco-Muñoz; Christian Julian Villabona Arenas; Diana Marcela Watteros-Acero; Diego A. Álvarez-Díaz; Erika Ospitia; Gloria Puerto, Jose A. Usme-Ciro; Juliana Barbosa; Katherine Labor-Donato; Liz Villazona-Arenas; Luz Dary Rodríguez; Maleny A. González; Marcela Mercado-Reyes; Martha Lucia Ospina Martínez; Nicolás D. Franco-Sierra; Sergio Gómez Rangel; Susy Echeverría-Londoño; Zulma M. Cucunubá
EPI_ISL_420038, EPI_ISL_420045, EPI_ISL_420055, EPI_ISL_421514	Sentinelles network	National Reference Center for Viruses of Respiratory Infections, Institut Pasteur, Paris	Angela Brisebare; Etienne Simon-Lorière; Flora Donati; Marion Barbet; Maud Vanpeene; Mélanie Albert; Méline Bizard; Sylvie Behilli; Sylvie van der Werf; Vincent End
EPI_ISL_420048, EPI_ISL_420058, EPI_ISL_420059, EPI_ISL_420060, EPI_ISL_420064, EPI_ISL_421501, EPI_ISL_421504, EPI_ISL_421505, EPI_ISL_421506, EPI_ISL_421512, EPI_ISL_428347, EPI_ISL_428348	Service de Biologie Médicale - BP 125	National Reference Center for Viruses of Respiratory Infections, Institut Pasteur, Paris	Angela Brisebare; Christine Lambert; Etienne Simon-Lorière; Flora Donati; Marion Barbet; Maud Vanpeene; Mélanie Albert; Méline Bizard; Sylvie Behilli; Sylvie van der Werf; Vincent End
EPI_ISL_420042, EPI_ISL_421513	Service de Biologie clinique	National Reference Center for Viruses of Respiratory Infections, Institut Pasteur, Paris	Angela Brisebare; Christine Lambert; Etienne Simon-Lorière; Flora Donati; Marion Barbet; Maud Vanpeene; Mélanie Albert; Méline Bizard; Sylvie Behilli; Sylvie van der Werf; Vincent End
EPI_ISL_469283, EPI_ISL_469284	Service de Virologie Hôpital Saint-Louis	Laboratory Cell Biology of Viral Infection-INSEERM unit 944	All Amara; Constance Delaunay; Laurent Meertens; Lucie Bonnet-Madain; SAUD MALMONA; Séverine Mercier-Delaurie
EPI_ISL_469282	Service de Virologie Hôpital Saint-Louis	Laboratory of Cell Biology of viral infection, Unit INSEERM-U64	All Amara; Constance Delaunay; Laurent Meertens; Lucie Bonnet-Madain
EPI_ISL_418232, EPI_ISL_418233	Service des Urgences	National Reference Center for Viruses of Respiratory Infections, Institut Pasteur, Paris	Angela Brisebare; Boukber; Etienne Simon-Lorière; Flora Donati; Marion Barbet; Maud Vanpeene; Mélanie Albert; Méline Bizard; Sylvie Behilli; Sylvie van der Werf; Vincent End
EPI_ISL_414598	Servicio Microbiología, Hospital Clínico Universitario, Valencia	Sequencing and Bioinformatics Service and Molecular Epidemiology Research Group, FISABIO-Public Health.	David Navarro; Fernando Gonzalez-Candelas; Giuseppe D'Auria; Griselda De Marco; Maria Alma Bracho; Neris Garcia-Gonzalez
EPI_ISL_414495	Servicio Microbiología, Hospital Clínico Universitario, Valencia.	Sequencing and Bioinformatics Service and Molecular Epidemiology Laboratory, FISABIO-Public Health	David Navarro; Fernando Gonzalez-Candelas; Giuseppe D'Auria; Griselda De Marco; Maria Alma Bracho; Neris Garcia-Gonzalez
EPI_ISL_420598, EPI_ISL_420599, EPI_ISL_420600	Servicio Virois Respiratorias-Departamento Virología-INEI	Instituto Nacional Enfermedades Infecciosas C.G. Malbran	Avaro M.; Baumeister E.; Benedetti E.; Campos J.; Cisterna D.; Dattoro ME; Lorenzo F.; Molina V.; Perandones C.; Popkevitch T.; Pontoriero A.; Russo M.; Tuduri E.
EPI_ISL_416485	Servicio de Microbiología, Consorcio Hospital General Universitario de Valencia	Sequencing and Bioinformatics Service and Molecular Epidemiology Research Group, FISABIO-Public Health	Concepcion Gimeno; Fernando Gonzalez-Candelas; Giuseppe D'Auria; Griselda De Marco; Maria Alma Bracho; Maria Dolores Ocete; Neris Garcia-Gonzalez
EPI_ISL_420125, EPI_ISL_420126, EPI_ISL_420127, EPI_ISL_420128, EPI_ISL_420129, EPI_ISL_420130, EPI_ISL_420131, EPI_ISL_420132, EPI_ISL_421515, EPI_ISL_421519, EPI_ISL_425201, EPI_ISL_425202, EPI_ISL_425203, EPI_ISL_425204, EPI_ISL_425205, EPI_ISL_425206, EPI_ISL_425207, EPI_ISL_425208, EPI_ISL_425209, EPI_ISL_425210, EPI_ISL_425211, EPI_ISL_425212, EPI_ISL_425213, EPI_ISL_425214, EPI_ISL_425215, EPI_ISL_425216, EPI_ISL_425217, EPI_ISL_425218, EPI_ISL_425219, EPI_ISL_425220, EPI_ISL_425221, EPI_ISL_425222, EPI_ISL_425223, EPI_ISL_425224, EPI_ISL_425225, EPI_ISL_425226, EPI_ISL_425227, EPI_ISL_425228, EPI_ISL_425229, EPI_ISL_425230, EPI_ISL_425231, EPI_ISL_425232, EPI_ISL_425233, EPI_ISL_425234, EPI_ISL_425235, EPI_ISL_425236, EPI_ISL_425237, EPI_ISL_425238, EPI_ISL_425239, EPI_ISL_425240, EPI_ISL_425241, EPI_ISL_425242, EPI_ISL_425243, EPI_ISL_425244, EPI_ISL_425245, EPI_ISL_425246, EPI_ISL_425247, EPI_ISL_425248, EPI_ISL_425249, EPI_ISL_425250, EPI_ISL_425251, EPI_ISL_425252, EPI_ISL_425253, EPI_ISL_425254, EPI_ISL_425255, EPI_ISL_425256, EPI_ISL_425257, EPI_ISL_425258, EPI_ISL_425259, EPI_ISL_425260, EPI_ISL_425261, EPI_ISL_425262, EPI_ISL_425263, EPI_ISL_425264, EPI_ISL_425265, EPI_ISL_425266, EPI_ISL_425267, EPI_ISL_425268, EPI_ISL_425269, EPI_ISL_425270, EPI_ISL_425271, EPI_ISL_425272, EPI_ISL_425273, EPI_ISL_425274, EPI_ISL_425275, EPI_ISL_425276, EPI_ISL_425277, EPI_ISL_425278, EPI_ISL_425279, EPI_ISL_425280, EPI_ISL_425281, EPI_ISL_425282, EPI_ISL_425283, EPI_ISL_425284, EPI_ISL_425285, EPI_ISL_425286, EPI_ISL_425287, EPI_ISL_425288, EPI_ISL_425289, EPI_ISL_425290, EPI_ISL_425291, EPI_ISL_425292, EPI_ISL_425293, EPI_ISL_425294, EPI_ISL_425295, EPI_ISL_425296, EPI_ISL_425297, EPI_ISL_425298, EPI_ISL_425299, EPI_ISL_425300, EPI_ISL_425301, EPI_ISL_425302, EPI_ISL_425303, EPI_ISL_425304, EPI_ISL_425305, EPI_ISL_425306, EPI_ISL_425307, EPI_ISL_425308, EPI_ISL_425309, EPI_ISL_425310, EPI_ISL_425311, EPI_ISL_425312, EPI_ISL_425313, EPI_ISL_425314, EPI_ISL_425315, EPI_ISL_425316, EPI_ISL_425317, EPI_ISL_425318, EPI_ISL_425319, EPI_ISL_425320, EPI_ISL_425321, EPI_ISL_425322, EPI_ISL_425323, EPI_ISL_425324, EPI_ISL_425325, EPI_ISL_425326, EPI_ISL_425327, EPI_ISL_425328, EPI_ISL_425329, EPI_ISL_425330, EPI_ISL_425331, EPI_ISL_425332, EPI_ISL_425333, EPI_ISL_425334, EPI_ISL_425335, EPI_ISL_425336, EPI_ISL_425337, EPI_ISL_425338, EPI_ISL_425339, EPI_ISL_425340, EPI_ISL_425341, EPI_ISL_425342, EPI_ISL_425343, EPI_ISL_425344, EPI_ISL_425345, EPI_ISL_425346, EPI_ISL_425347, EPI_ISL_425348, EPI_ISL_425349, EPI_ISL_425350, EPI_ISL_425351, EPI_ISL_425352, EPI_ISL_425353, EPI_ISL_425354, EPI_ISL_425355, EPI_ISL_425356, EPI_ISL_425357, EPI_ISL_425358, EPI_ISL_425359, EPI_ISL_425360, EPI_ISL_425361, EPI_ISL_425362, EPI_ISL_425363, EPI_ISL_425364, EPI_ISL_425365, EPI_ISL_425366, EPI_ISL_425367, EPI_ISL_425368, EPI_ISL_425369, EPI_ISL_425370, EPI_ISL_425371, EPI_ISL_425372, EPI_ISL_425373, EPI_ISL_425374, EPI_ISL_425375, EPI_ISL_425376, EPI_ISL_425377, EPI_ISL_425378, EPI_ISL_425379, EPI_ISL_425380, EPI_ISL_425381, EPI_ISL_425382, EPI_ISL_425383, EPI_ISL_425384, EPI_ISL_425385, EPI_ISL_425386, EPI_ISL_425387, EPI_ISL_425388, EPI_ISL_425389, EPI_ISL_425390, EPI_ISL_425391, EPI_ISL_425392, EPI_ISL_425393, EPI_ISL_425394, EPI_ISL_425395, EPI_ISL_425396, EPI_ISL_425397, EPI_ISL_425398, EPI_ISL_425399, EPI_ISL_425400, EPI_ISL_425401, EPI_ISL_425402, EPI_ISL_425403, EPI_ISL_425404, EPI_ISL_425405, EPI_ISL_425406, EPI_ISL_425407, EPI_ISL_425408, EPI_ISL_425409, EPI_ISL_425410, EPI_ISL_425411, EPI_ISL_425412, EPI_ISL_425413, EPI_ISL_425414, EPI_ISL_425415, EPI_ISL_425416, EPI_ISL_425417, EPI_ISL_425418, EPI_ISL_425419, EPI_ISL_425420, EPI_ISL_425421, EPI_ISL_425422, EPI_ISL_425423, EPI_ISL_425424, EPI_ISL_425425, EPI_ISL_425426, EPI_ISL_425427, EPI_ISL_425428, EPI_ISL_425429, EPI_ISL_425430, EPI_ISL_425431, EPI_ISL_425432, EPI_ISL_425433, EPI_ISL_425434, EPI_ISL_425435, EPI_ISL_425436, EPI_ISL_425437, EPI_ISL_425438, EPI_ISL_425439, EPI_ISL_425440, EPI_ISL_425441, EPI_ISL_425442, EPI_ISL_425443, EPI_ISL_425444, EPI_ISL_425445, EPI_ISL_425446, EPI_ISL_425447, EPI_ISL_425448, EPI_ISL_425449, EPI_ISL_425450, EPI_ISL_425451, EPI_ISL_425452, EPI_ISL_425453, EPI_ISL_425454, EPI_ISL_425455, EPI_ISL_425456, EPI_ISL_425457, EPI_ISL_425458, EPI_ISL_425459, EPI_ISL_425460, EPI_ISL_425461, EPI_ISL_425462, EPI_ISL_425463, EPI_ISL_425464, EPI_ISL_425465, EPI_ISL_425466, EPI_ISL_425467, EPI_ISL_425468, EPI_ISL_425469, EPI_ISL_425470, EPI_ISL_425471, EPI_ISL_425472, EPI_ISL_425473, EPI_ISL_425474, EPI_ISL_425475, EPI_ISL_425476, EPI_ISL_425477, EPI_ISL_425478, EPI_ISL_425479, EPI_ISL_425480, EPI_ISL_425481, EPI_ISL_425482, EPI_ISL_425483, EPI_ISL_425484, EPI_ISL_425485, EPI_ISL_425486, EPI_ISL_425487, EPI_ISL_425488, EPI_ISL_425489, EPI_ISL_425490, EPI_ISL_425491, EPI_ISL_425492, EPI_ISL_425493, EPI_ISL_425494, EPI_ISL_425495, EPI_ISL_425496, EPI_ISL_425497, EPI_ISL_425498, EPI_ISL_425499, EPI_ISL_425500, EPI_ISL_425501, EPI_ISL_425502, EPI_ISL_425503, EPI_ISL_425504, EPI_ISL_425505, EPI_ISL_425506, EPI_ISL_425507, EPI_ISL_425508, EPI_ISL_425509, EPI_ISL_425510, EPI_ISL_425511, EPI_ISL_425512, EPI_ISL_425513, EPI_ISL_425514, EPI_ISL_425515, EPI_ISL_425516, EPI_ISL_425517, EPI_ISL_425518, EPI_ISL_425519, EPI_ISL_425520, EPI_ISL_425521, EPI_ISL_425522, EPI_ISL_425523, EPI_ISL_425524, EPI_ISL_425525, EPI_ISL_425526, EPI_ISL_425527, EPI_ISL_425528, EPI_ISL_425529, EPI_ISL_425530, EPI_ISL_425531, EPI_ISL_425532, EPI_ISL_425533, EPI_ISL_425534, EPI_ISL_425535, EPI_ISL_425536, EPI_ISL_425537, EPI_ISL_425538, EPI_ISL_425539, EPI_ISL_425540, EPI_ISL_425541, EPI_ISL_425542, EPI_ISL_425543, EPI_ISL_425544, EPI_ISL_425545, EPI_ISL_425546, EPI_ISL_425547, EPI_ISL_425548, EPI_ISL_425549, EPI_ISL_425550, EPI_ISL_425551, EPI_ISL_425552, EPI_ISL_425553, EPI_ISL_425554, EPI_ISL_425555, EPI_ISL_425556, EPI_ISL_425557, EPI_ISL_425558, EPI_ISL_425559, EPI_ISL_425560, EPI_ISL_425561, EPI_ISL_425562, EPI_ISL_425563, EPI_ISL_425564, EPI_ISL_425565, EPI_ISL_425566, EPI_ISL_425567, EPI_ISL_425568, EPI_ISL_425569, EPI_ISL_425570, EPI_ISL_425571, EPI_ISL_425572, EPI_ISL_425573, EPI_ISL_425574, EPI_ISL_425575, EPI_ISL_425576, EPI_ISL_425577, EPI_ISL_425578, EPI_ISL_425579, EPI_ISL_425580, EPI_ISL_425581, EPI_ISL_425582, EPI_ISL_425583, EPI_ISL_425584, EPI_ISL_425585, EPI_ISL_425586, EPI_ISL_425587, EPI_ISL_425588, EPI_ISL_425589, EPI_ISL_425590, EPI_ISL_425591, EPI_ISL_425592, EPI_ISL_425593, EPI_ISL_425594, EPI_ISL_425595, EPI_ISL_425596, EPI_ISL_425597, EPI_ISL_425598, EPI_ISL_425599, EPI_ISL_425600, EPI_ISL_425601, EPI_ISL_425602, EPI_ISL_425603, EPI_ISL_425604, EPI_ISL_425605, EPI_ISL_425606, EPI_ISL_425607, EPI_ISL_425608, EPI_ISL_425609, EPI_ISL_425610, EPI_ISL_425611, EPI_ISL_425612, EPI_ISL_425613, EPI_ISL_425614, EPI_ISL_425615, EPI_ISL_425616, EPI_ISL_425617, EPI_ISL_425618, EPI_ISL_425619, EPI_ISL_425620, EPI_ISL_425621, EPI_ISL_425622, EPI_ISL_425623, EPI_ISL_425624, EPI_ISL_425625, EPI_ISL_425626, EPI_ISL_425627, EPI_ISL_425628, EPI_ISL_425629, EPI_ISL_425630, EPI_ISL_425631, EPI_ISL_425632, EPI_ISL_425633, EPI_ISL_425634, EPI_ISL_425635, EPI_ISL_425636, EPI_ISL_425637, EPI_ISL_425638, EPI_ISL_425639, EPI_ISL_425640, EPI_ISL_425641, EPI_ISL_425642, EPI_ISL_425643, EPI_ISL_425644, EPI_ISL_425645, EPI_ISL_425646, EPI_ISL_425647, EPI_ISL_425648, EPI_ISL_425649, EPI_ISL_425650, EPI_ISL_425651, EPI_ISL_425652, EPI_ISL_425653, EPI_ISL_425654, EPI_ISL_425655, EPI_ISL_425656, EPI_ISL_425657, EPI_ISL_425658, EPI_ISL_425659, EPI_ISL_425660, EPI_ISL_425661, EPI_ISL_425662, EPI_ISL_425663, EPI_ISL_425664, EPI_ISL_425665, EPI_ISL_425666, EPI_ISL_425667, EPI_ISL_425668, EPI_ISL_425669, EPI_ISL_425670, EPI_ISL_425671, EPI_ISL_425672, EPI_ISL_425673, EPI_ISL_425674, EPI_ISL_425675, EPI_ISL_425676, EPI_ISL_425677, EPI_ISL_425678, EPI_ISL_425679, EPI_ISL_425680, EPI_ISL_425681, EPI_ISL_425682, EPI_ISL_425683, EPI_ISL_425684, EPI_ISL_425685, EPI_ISL_425686, EPI_ISL_425687, EPI_ISL_425688, EPI_ISL_425689, EPI_ISL_425690, EPI_ISL_425691, EPI_ISL_425692, EPI_ISL_425693, EPI_ISL_425694, EPI_ISL_425695, EPI_ISL_425696, EPI_ISL_425697, EPI_ISL_425698, EPI_ISL_425699, EPI_ISL_425700, EPI_ISL_425701, EPI_ISL_425702, EPI_ISL_425703, EPI_ISL_425704, EPI_ISL_425705, EPI_ISL_425706, EPI_ISL_425707, EPI_ISL_425708, EPI_ISL_425709, EPI_ISL_425710, EPI_ISL_425711, EPI_ISL_425712, EPI_ISL_425713, EPI_ISL_425714, EPI_ISL_425715, EPI_ISL_425716, EPI_ISL_425717, EPI_ISL_425718, EPI_ISL_425719, EPI_ISL_425720, EPI_ISL_425721, EPI_ISL_425722, EPI_ISL_425723, EPI_ISL_425724, EPI_ISL_425725, EPI_ISL_425726, EPI_ISL_425727, EPI_ISL_425728, EPI_ISL_425729, EPI_ISL_425730, EPI_ISL_425731, EPI_ISL_425732, EPI_ISL_425733, EPI_ISL_425734, EPI_ISL_425735, EPI_ISL_425736, EPI_ISL_425737, EPI_ISL_425738, EPI_ISL_425739, EPI_ISL_425740, EPI_ISL_425741, EPI_ISL_425742, EPI_ISL_425743, EPI_ISL_425744, EPI_ISL_425745, EPI_ISL_425746, EPI_ISL_425747, EPI_ISL_425748, EPI_ISL_425749, EPI_ISL_425750, EPI_ISL_425751, EPI_ISL_425752, EPI_ISL_425753, EPI_ISL_425754, EPI_ISL_425755, EPI_ISL_425756, EPI_ISL_425757, EPI_ISL_425758, EPI_ISL_425759, EPI_ISL_425760, EPI_ISL_425761, EPI_ISL_425762, EPI_ISL_425763, EPI_ISL_425764, EPI_ISL_425765, EPI_ISL_425766, EPI_ISL_425767, EPI_ISL_425768, EPI_ISL_425769, EPI_ISL_425770, EPI_ISL_425771, EPI_ISL_425772, EPI_ISL_425773, EPI_ISL_425774, EPI_ISL_425775, EPI_ISL_425776, EPI_ISL_425777, EPI_ISL_425778, EPI_ISL_425779, EPI_ISL_425780, EPI_ISL_425781, EPI_ISL_425782, EPI_ISL_425783, EPI_ISL_425784, EPI_ISL_425785, EPI_ISL_425786, EPI_ISL_425787, EPI_ISL_425788, EPI_ISL_425789, EPI_ISL_425790, EPI_ISL_425791, EPI_ISL_425792, EPI_ISL_425793, EPI_ISL_425794, EPI_ISL_425795, EPI_ISL_425796, EPI_ISL_425797, EPI_ISL_425798, EPI_ISL_425799, EPI_ISL_425800, EPI_ISL_425801, EPI_ISL_425802, EPI_ISL_425803, EPI_ISL_425804, EPI_ISL_425805, EPI_ISL_425806, EPI_ISL_425807, EPI_ISL_425808, EPI_ISL_425809, EPI_ISL_425810, EPI_ISL_425811, EPI_ISL_425812, EPI_ISL_425813, EPI_ISL_425814, EPI_ISL_425815, EPI_ISL_425816, EPI_ISL_425817, EPI_ISL_425818, EPI_ISL_425819, EPI_ISL_425820, EPI_ISL_425821, EPI_ISL_425822, EPI_ISL_425823, EPI_ISL_425824, EPI_ISL_425825, EPI_ISL_425826, EPI_ISL_425827, EPI_ISL_425828, EPI_ISL_425829, EPI_ISL_425830, EPI_ISL_425831, EPI_ISL_425832, EPI_ISL_425833, EPI_ISL_425834, EPI_ISL_425835, EPI_ISL_425836, EPI_ISL_425837, EPI_ISL_425838, EPI_ISL_425839, EPI_ISL_425840, EPI_ISL_425841, EPI_ISL_425842, EPI_ISL_425843, EPI_ISL_425844, EPI_ISL_425845, EPI_ISL_425846, EPI_ISL_425847, EPI_ISL_425848, EPI_ISL_425849, EPI_ISL_425850, EPI_ISL_425851, EPI_ISL_425852, EPI_ISL_425853, EPI_ISL_425854, EPI_ISL_425855, EPI_ISL_425856, EPI_ISL_425857, EPI_ISL_425858, EPI_ISL_425859, EPI_ISL_425860, EPI_ISL_425861, EPI_ISL_425862, EPI_ISL_425863, EPI_ISL_425864, EPI_ISL_425865, EPI_ISL_425866, EPI_ISL_425867, EPI_ISL_425868, EPI_ISL_425869, EPI_ISL_425870, EPI_ISL_425871, EPI_ISL_425872, EPI_ISL_425873, EPI_ISL_425874, EPI_ISL_425875, EPI_ISL_425876, EPI_ISL_425877, EPI_ISL_425878, EPI_ISL_425879, EPI_ISL_425880, EPI_ISL_425881, EPI_ISL_425882, EPI_ISL_425883, EPI_ISL_425884, EPI_ISL_425885, EPI_ISL_425886, EPI_ISL_425887, EPI_ISL_425888, EPI_ISL_425889, EPI_ISL_425890, EPI_ISL_425891, EPI_ISL_425892, EPI_ISL_425893, EPI_ISL_425894, EPI_ISL_425895, EPI_ISL_425896, EPI_ISL_425897, EPI_ISL_425898, EPI_ISL_425899, EPI_ISL_425900, EPI_ISL_425901, EPI_ISL_425902, EPI_ISL_425903, EPI_ISL_425904, EPI_ISL_425905, EPI_ISL_425906, EPI_ISL_425907, EPI_ISL_425908, EPI_ISL_425909, EPI_ISL_425910, EPI_ISL_425911, EPI_ISL_425912, EPI_ISL_425913, EPI_ISL_425914, EPI_ISL_425915, EPI_ISL_425916, EPI_ISL_425917, EPI_ISL_425918, EPI_ISL_425919, EPI_ISL_425920, EPI_ISL_425921, EPI_ISL_425922, EPI_ISL_425923, EPI_ISL_425924, EPI_ISL_425925, EPI_ISL_425926, EPI_ISL_425927, EPI_ISL_425928, EPI_ISL_425929, EPI_ISL_425930, EPI_ISL_425931, EPI_ISL_425932, EPI_ISL_425933, EPI_ISL_425934, EPI_ISL_425935, EPI_ISL_425936, EPI_ISL_425937, EPI_ISL_425938, EPI_ISL_425939, EPI_ISL_425940, EPI_ISL_425941, EPI_ISL_425942, EPI_ISL_425943, EPI_ISL_425944, EPI_ISL_425945, EPI_ISL_425946, EPI_ISL_425947, EPI_ISL_425948, EPI_ISL_425949, EPI_ISL_425950, EPI_ISL_425951, EPI_ISL_425952, EPI_ISL_425953, EPI_ISL_425954, EPI_ISL_425955, EPI_ISL_425956, EPI_ISL_425957, EPI_ISL_425958, EPI_ISL_425959, EPI_ISL_425960, EPI_ISL_425961, EPI_ISL_425962, EPI_ISL_425963, EPI_ISL_425964, EPI_ISL_425965, EPI_ISL_425966, EPI_ISL_425967, EPI_ISL_425968, EPI_ISL_425969, EPI_ISL_425970, EPI_ISL_425971, EPI_ISL_425972, EPI_ISL_425973, EPI_ISL_425974, EPI_ISL_425975, EPI_ISL_425976, EPI_ISL_425977, EPI_ISL_425978, EPI_ISL_425979, EPI_ISL_425980, EPI_ISL_425981, EPI_ISL_425982, EPI_ISL_425983, EPI_ISL_425984, EPI_ISL_425985, EPI_ISL_425986, EPI_ISL_425987, EPI_ISL_425988, EPI_ISL_425989, EPI_ISL_425990, EPI_ISL_425991, EPI_ISL_425992, EPI_ISL_425993, EPI_ISL_425994, EPI_ISL_425995, EPI_ISL_425996, EPI_ISL_425997, EPI_ISL_425998, EPI_ISL_425999, EPI_ISL_430000			

EPI_ISL_452448, EPI_ISL_452449, EPI_ISL_452452, EPI_ISL_509619, EPI_ISL_509620, EPI_ISL_509621, EPI_ISL_509622, EPI_ISL_509623, EPI_ISL_509624, EPI_ISL_509625, EPI_ISL_509626, EPI_ISL_509627, EPI_ISL_509628, EPI_ISL_509629, EPI_ISL_509630, EPI_ISL_509631, EPI_ISL_509632				
see above	Servicio de Microbiología, HfRU de Málaga. Servicio Andaluz de Salud	SeqCOVID-SPAIN consortium/IBV(CSIC)	Begoña Palop Borrás and SeqCOVID-SPAIN consortium; Inmaculada de Toro Peinado; Inmaculada de Toro Peinado, M ^o Concepción Mediavilla Gradohoff	
EPI_ISL_539284, EPI_ISL_539285, EPI_ISL_539286, EPI_ISL_539287, EPI_ISL_654469, EPI_ISL_654470, EPI_ISL_654471, EPI_ISL_654472, EPI_ISL_654473, EPI_ISL_654474, EPI_ISL_654475, EPI_ISL_654476, EPI_ISL_654477, EPI_ISL_654478, EPI_ISL_796070, EPI_ISL_796071, EPI_ISL_796072, EPI_ISL_796073, EPI_ISL_796103, EPI_ISL_796104, EPI_ISL_796105, EPI_ISL_796106, EPI_ISL_796107, EPI_ISL_796108, EPI_ISL_796109, EPI_ISL_796110, EPI_ISL_796111, EPI_ISL_796112, EPI_ISL_796113, EPI_ISL_796114, EPI_ISL_796115, EPI_ISL_796116, EPI_ISL_796117, EPI_ISL_796118, EPI_ISL_796119, EPI_ISL_796120, EPI_ISL_796121, EPI_ISL_796122, EPI_ISL_796123, EPI_ISL_796124, EPI_ISL_796125, EPI_ISL_796126, EPI_ISL_796127, EPI_ISL_796128, EPI_ISL_796129, EPI_ISL_796130, EPI_ISL_796131, EPI_ISL_796132, EPI_ISL_796133				
see above	Servicio de Microbiología, Hospital General Universitario de Castellón	SeqCOVID-SPAIN consortium/IBV(CSIC)	María Dolores Tirado Balaguer and SeqCOVID-SPAIN consortium; María Dolores Tirado and SeqCOVID-SPAIN consortium; Rosario Moreno; Rosario Moreno Muñoz	
EPI_ISL_1014733	Servicio de Microbiología, Hospital Ramón y Cajal (CIBERESP)	SeqCOVID-SPAIN consortium/IBV(CSIC)	Jose M ^o González-Abta; Juan C Galán and SeqCOVID-SPAIN consortium; L. Olivarieta; Val Fernández	
EPI_ISL_480952, EPI_ISL_480953, EPI_ISL_480954, EPI_ISL_480955, EPI_ISL_480956, EPI_ISL_480957, EPI_ISL_480958, EPI_ISL_480959, EPI_ISL_480960, EPI_ISL_480961, EPI_ISL_480962, EPI_ISL_480963, EPI_ISL_480964, EPI_ISL_480965, EPI_ISL_480966, EPI_ISL_480967, EPI_ISL_480968, EPI_ISL_480969, EPI_ISL_480970, EPI_ISL_480971, EPI_ISL_480972, EPI_ISL_480973, EPI_ISL_480974, EPI_ISL_480975, EPI_ISL_480976, EPI_ISL_480977, EPI_ISL_480978, EPI_ISL_480979, EPI_ISL_480980, EPI_ISL_480981, EPI_ISL_480982, EPI_ISL_480983, EPI_ISL_480984, EPI_ISL_480985, EPI_ISL_480986, EPI_ISL_480987, EPI_ISL_480988, EPI_ISL_480989, EPI_ISL_480990, EPI_ISL_480991, EPI_ISL_480992, EPI_ISL_480993, EPI_ISL_480994, EPI_ISL_480995, EPI_ISL_480996, EPI_ISL_480997, EPI_ISL_480998, EPI_ISL_480999, EPI_ISL_481000, EPI_ISL_481001, EPI_ISL_481002, EPI_ISL_481003, EPI_ISL_481004, EPI_ISL_481005, EPI_ISL_481006, EPI_ISL_481007, EPI_ISL_481008, EPI_ISL_481009, EPI_ISL_481010, EPI_ISL_481011, EPI_ISL_481012, EPI_ISL_481013, EPI_ISL_481014, EPI_ISL_481015, EPI_ISL_481016, EPI_ISL_481017, EPI_ISL_481018, EPI_ISL_481019, EPI_ISL_481020, EPI_ISL_481021, EPI_ISL_481022, EPI_ISL_481023, EPI_ISL_481024, EPI_ISL_481025, EPI_ISL_481026, EPI_ISL_481027, EPI_ISL_481028, EPI_ISL_481029, EPI_ISL_481030, EPI_ISL_481031, EPI_ISL_481032, EPI_ISL_481033, EPI_ISL_481034, EPI_ISL_481035, EPI_ISL_481036, EPI_ISL_481037, EPI_ISL_481038, EPI_ISL_481039, EPI_ISL_481040				
see above	Servicio de Microbiología, Hospital Universitario Donostia. OSI Donostialdea, Área de Enfermedades Infecciosas, Grupo de Infección Respiratoria y Resistencia Antimicrobiana, Instituto de Investigación Sanitaria BIODONOSTIA	SeqCOVID-SPAIN consortium/IBV(CSIC)	Gustavo Cilla; Jose Maria Marimón and SeqCOVID-SPAIN consortium; Luis Piñeiro; Milagrosa Montes	
EPI_ISL_452618, EPI_ISL_452620, EPI_ISL_452621, EPI_ISL_452622, EPI_ISL_452623, EPI_ISL_452624, EPI_ISL_452625, EPI_ISL_452626, EPI_ISL_452627, EPI_ISL_452628, EPI_ISL_452629, EPI_ISL_452630, EPI_ISL_452631, EPI_ISL_452632, EPI_ISL_452633, EPI_ISL_452634, EPI_ISL_452635, EPI_ISL_452636, EPI_ISL_452637, EPI_ISL_452638, EPI_ISL_452639, EPI_ISL_452640, EPI_ISL_452641, EPI_ISL_452642, EPI_ISL_452643, EPI_ISL_452644, EPI_ISL_452645, EPI_ISL_452646, EPI_ISL_452647, EPI_ISL_452648, EPI_ISL_452649, EPI_ISL_452650, EPI_ISL_452651, EPI_ISL_452652, EPI_ISL_452653, EPI_ISL_452654, EPI_ISL_452655, EPI_ISL_452656, EPI_ISL_452657, EPI_ISL_452658, EPI_ISL_452659, EPI_ISL_452660, EPI_ISL_452661, EPI_ISL_452662, EPI_ISL_452663, EPI_ISL_452664, EPI_ISL_452665, EPI_ISL_452666, EPI_ISL_452667, EPI_ISL_452668, EPI_ISL_452669, EPI_ISL_452670, EPI_ISL_452671, EPI_ISL_452672, EPI_ISL_452673, EPI_ISL_452674, EPI_ISL_452675, EPI_ISL_452676, EPI_ISL_452677, EPI_ISL_452678, EPI_ISL_452679, EPI_ISL_452680, EPI_ISL_452681, EPI_ISL_452682, EPI_ISL_452683, EPI_ISL_452684, EPI_ISL_452685, EPI_ISL_452686, EPI_ISL_452687, EPI_ISL_452688, EPI_ISL_452689, EPI_ISL_452690				
see above	Servicio de Microbiología, Hospital Universitario Donostia. OSI Donostialdea, Área de Enfermedades Infecciosas, Grupo de Infección Respiratoria y Resistencia Antimicrobiana, Instituto de Investigación Sanitaria BIODONOSTIA.	SeqCOVID-SPAIN consortium/IBV(CSIC)	Gustavo Cilla; Jose Maria Marimón and SeqCOVID-SPAIN consortium; Luis Piñeiro; Milagrosa Montes	
EPI_ISL_414936, EPI_ISL_414937, EPI_ISL_414938, EPI_ISL_414939, EPI_ISL_414940, EPI_ISL_414941	Shandong Provincial Center for Disease Control and Prevention	Beijing Institute of Microbiology and Epidemiology	Bo Pang; Can-Fang Lin; Cun-Bao Li; Dian-Ming Kang; Feng Gao; Guo-Lin Wang; Ji Lei; Li-Jun Duan; Lin Yao; Mai-Juan Ma; Ming-Xiao Yao; Sheng-Xiang Ji; Wen-Kui Sun; Xiang-Na Zhao; Xiao Wei; Xiao-Li Zhang; Xiao-Lin Jiang; Yang Hang; Zeng-Qiang Kou	
EPI_ISL_416316, EPI_ISL_416317, EPI_ISL_416318, EPI_ISL_416319, EPI_ISL_416320, EPI_ISL_416321, EPI_ISL_416322, EPI_ISL_416323, EPI_ISL_416324, EPI_ISL_416325, EPI_ISL_416326, EPI_ISL_416327, EPI_ISL_416328, EPI_ISL_416329, EPI_ISL_416330, EPI_ISL_416331, EPI_ISL_416332, EPI_ISL_416333, EPI_ISL_416334, EPI_ISL_416335, EPI_ISL_416336, EPI_ISL_416337, EPI_ISL_416338, EPI_ISL_416339, EPI_ISL_416340, EPI_ISL_416341, EPI_ISL_416342, EPI_ISL_416343, EPI_ISL_416344, EPI_ISL_416345, EPI_ISL_416346, EPI_ISL_416347, EPI_ISL_416348, EPI_ISL_416349, EPI_ISL_416350, EPI_ISL_416351, EPI_ISL_416352, EPI_ISL_416353, EPI_ISL_416354, EPI_ISL_416355, EPI_ISL_416356, EPI_ISL_416357, EPI_ISL_416358, EPI_ISL_416359, EPI_ISL_416360, EPI_ISL_416361, EPI_ISL_416362, EPI_ISL_416363, EPI_ISL_416364, EPI_ISL_416365, EPI_ISL_416366, EPI_ISL_416367, EPI_ISL_416368, EPI_ISL_416369, EPI_ISL_416370, EPI_ISL_416371, EPI_ISL_416372, EPI_ISL_416373, EPI_ISL_416374, EPI_ISL_416375, EPI_ISL_416376, EPI_ISL_416377, EPI_ISL_416378, EPI_ISL_416379, EPI_ISL_416380, EPI_ISL_416381, EPI_ISL_416382, EPI_ISL_416383, EPI_ISL_416384, EPI_ISL_416385, EPI_ISL_416386, EPI_ISL_416387, EPI_ISL_416388, EPI_ISL_416389, EPI_ISL_416390, EPI_ISL_416391, EPI_ISL_416392, EPI_ISL_416393, EPI_ISL_416394, EPI_ISL_416395, EPI_ISL_416396, EPI_ISL_416397, EPI_ISL_416398, EPI_ISL_416399, EPI_ISL_416400, EPI_ISL_416401, EPI_ISL_416402, EPI_ISL_416403, EPI_ISL_416404, EPI_ISL_416405, EPI_ISL_416406, EPI_ISL_416407, EPI_ISL_416408, EPI_ISL_416409				
see above	Shanghai Public Health Clinical Center, Shanghai Medical College, Fudan University	National Research Center for Translational Medicine (Shanghai), Ruijin Hospital affiliated to Shanghai Jiao Tong University School of Medicine & Shanghai Public Health Clinical Center	Gang Lu; Hongzhou Lu; Saijuan Chen; Shengyue Wang; Xiaonan Zhang; Yun Ling; Yun Tan	
EPI_ISL_463889, EPI_ISL_463894, EPI_ISL_463895, EPI_ISL_463896, EPI_ISL_463897, EPI_ISL_463901	Shaoying Center for Disease Control and Prevention	Department of Pathology and Laboratory Medicine, University of California Los Angeles	Evann E. Hill; Fan Li; Huan Wu; Jilang Wang; Jialiang Tang; Jinkun Chen; QinChao Zhang; Shanzhen Yang; Yifang Wang; Zhuojing Jiang; Ziqin Li	
EPI_ISL_582125, EPI_ISL_582126, EPI_ISL_582608, EPI_ISL_582613, EPI_ISL_582620, EPI_ISL_582624, EPI_ISL_582625	Sheikh Khalifa Medical City Sheikh Khalifa Medical City	Molecular Surveillance lab Sheikh Khalifa Medical City Molecular Surveillance lab Sheikh Khalifa Medical City	Amirtharaj Francis; Hala Imambacous; Hiba Saud; Sahar Almarzooq; Sajeed Abdul; Stefan Weber Amirtharaj Francis; Hala Imambacous; Hiba Saud; Sahar Almarzooq; Sajeed Abdul; Stefan Weber	
EPI_ISL_406593	Shenzhen Key Laboratory of Pathogen and Immunity, National Clinical Research Center for Infectious Disease, Shenzhen Third People's Hospital	Shenzhen Key Laboratory of Pathogen and Immunity, National Clinical Research Center for Infectious Disease, Shenzhen Third People's Hospital	Chenguang Shen; Haixia Zheng; Li Xing; Yang Yang; Yingxia Lu; Zhixiang Xu	
EPI_ISL_406592	Shenzhen Third People's Hospital	Shenzhen Key Laboratory of Pathogen and Immunity, National Clinical Research Center for Infectious Disease, Shenzhen Third People's Hospital	Chenguang Shen; Haixia Zheng; Li Xing; Yang Yang; Yingxia Lu; Zhixiang Xu	
EPI_ISL_480074, EPI_ISL_480075, EPI_ISL_480076, EPI_ISL_480077, EPI_ISL_480078, EPI_ISL_480079, EPI_ISL_480080, EPI_ISL_480081				
see above	Shizuoka City Institute of Environmental Sciences and Public Health	Pathogen Genomics Center, National Institute of Infectious Diseases	Hajime Kamiya; Kenji Yagi; Kentaro Itokawa; Makoto Kuroda; Masanori Hashino; Motoki Suzuki; Rina Tanaka; Sou Okamura; Takaharu Maezawa; Tsuyoshi Sekizuka; Yui Kanazawa	
EPI_ISL_437187	Siloam Hospitals	Institute of Tropical Disease, Universitas Airlangga	Aldise M Nasti; Gatot Soejiarto; Jozzy R Dewantari; Kazufumi Shimizu; Krisnadi Rahardjo; Lakemi Wulandari; Maria I Lusida; Maria M Padminie; Mitsuhiro Nishimura; Resti Y Meliana; Retno A Setyoningrum; Rima R Prasetya; Soetjipto; Yasuko Mori; Yoiko K Shimizu	
EPI_ISL_482672, EPI_ISL_482677, EPI_ISL_482680	Singapore General Hospital	Department of Microbiology	Chenhao Li; Karrie Ko; Kern Rei Chng; Kian Sing Chan; Kun Lee Lim; Lynette Oon; Niranjan Nagarajan; Nurdyana Abdul Rahman	
EPI_ISL_407987	Singapore General Hospital	Programme in Emerging Infectious Diseases, Duke-NUS Medical School	Danielle E Anderson; Gavin JD Smith; Jayanthi Jayakumar; Jenny GH Low; Kian Sing Chan; Linfa Wang; Lynette LE Oon; Martin Linster; Yan Zhuang	
EPI_ISL_410536, EPI_ISL_410537	Singapore General Hospital, Molecular Laboratory, Division of Pathology	Programme in Emerging Infectious Diseases, Duke-NUS Medical School	Danielle E Anderson; Gavin JD Smith; Jayanthi Jayakumar; Jenny GH Low; Kian Sing Chan; Lynette LE Oon; Martin Linster; Shrim Kalimuddin; Yan Zhuang	
EPI_ISL_455586	Siriraj hospital	National Institute of Health, Department of medical Sciences, Ministry of Public Health, Thailand	Chittaganpich; Malinee; Okada; Pammen; Phuyung; Pitaluk; Sippapom; Sittiporn; Sunthareeya; Thanadachakul; Thanatsapa; Waichareon; Warawan; Wongboot	
EPI_ISL_454404, EPI_ISL_454405, EPI_ISL_454406, EPI_ISL_455842, EPI_ISL_455843, EPI_ISL_455844, EPI_ISL_455845, EPI_ISL_475085, EPI_ISL_475092, EPI_ISL_475099, EPI_ISL_475105, EPI_ISL_475106, EPI_ISL_475107, EPI_ISL_475108, EPI_ISL_475109, EPI_ISL_475110, EPI_ISL_475111, EPI_ISL_475112, EPI_ISL_475113, EPI_ISL_475549, EPI_ISL_475550, EPI_ISL_475554, EPI_ISL_475555, EPI_ISL_476143, EPI_ISL_476144, EPI_ISL_476145, EPI_ISL_548245, EPI_ISL_548246, EPI_ISL_710584				
see above	Skovde/Unilabs	The Public Health Agency of Sweden	Anna Risberg; Anna-Malin Linde; Department of Microbiology; Karin Tegmark-Wisell; Maria Lind Karlberg; Mattias Haukland; Mia Brytting; Olov Svartstrom; Oskar Karlsson Lindajo; Petra Edquist; Reza Advani; Sandra Brodsson; Shaman Muradasoli; Shaman Muradasoli; The Public Health Agency of Sweden	
EPI_ISL_1145037	Sonic - MVZ Medizinisches Labor Bremen GmbH	Robert Koch Institute	*Jolene Bowers; Ashlyn Pfeiffer; Chris French; Darrin Lemmer; Dave Engelthaler; Hayley Yaglom; Megan Folkerts; The Arizona COVID Genomics Union (ACGU)*	
EPI_ISL_1113261, EPI_ISL_1113276, EPI_ISL_1113446, EPI_ISL_1113457	Sonora Quest Laboratories	TGen North		
EPI_ISL_696223, EPI_ISL_696224, EPI_ISL_696225, EPI_ISL_696226, EPI_ISL_696227, EPI_ISL_696228, EPI_ISL_696229, EPI_ISL_696230, EPI_ISL_696231, EPI_ISL_696232, EPI_ISL_696233				
see above	Sonora Quest Laboratories, Laboratory Sciences of Arizona	TGen North	Ashlyn Pfeiffer; Chris French; Darrin Lemmer; Dave Engelthaler; Hayley Yaglom; Jolene Bowers; Megan Folkerts; The Arizona COVID Genomics Union	

(AGCU)

EPI_ISL_408431	Sorbonne Université, Inserm et Assistance Publique-Hôpitaux de Paris (Pôle Sérologie)	National Reference Center for Viruses of Respiratory Infections, Institut Pasteur, Paris	Angela Brisebane, Anne-Geneviève Marcelin; David Boutolleau; Elise Klément; Eric Caumes.; Flora Donati; Marion Barbet; Maud Vanpeene; Mélanie Albert; Maline Bizard; Sonia Burnel; Sylvie Behilli; Sylvie van der Werf; Valérie Pourcher; Vincent Calvez; Vincent Enouf
EPI_ISL_529171, EPI_ISL_529173, EPI_ISL_529174, EPI_ISL_529175	South Carolina Department of Health and Environmental Control	South Carolina Department of Health and Environmental Control	Haley V. Flores
EPI_ISL_451517, EPI_ISL_451518, EPI_ISL_451519, EPI_ISL_451521, EPI_ISL_451632, EPI_ISL_451633, EPI_ISL_451634, EPI_ISL_451635, EPI_ISL_451636, EPI_ISL_455036, EPI_ISL_455075, EPI_ISL_455076, EPI_ISL_455077, EPI_ISL_455078, EPI_ISL_455079, EPI_ISL_455080, EPI_ISL_455081, EPI_ISL_455082, EPI_ISL_455087, EPI_ISL_455088, EPI_ISL_455089, EPI_ISL_455096, EPI_ISL_455098	South Eastern Area Laboratory Services	NSW Health Pathology - Institute of Clinical Pathology and Medical Research, Westmead Hospital, University of Sydney	CIDM-PH et al.
see above	South Eastern Area Laboratory Services (SEALS)	NSW Health Pathology - Institute of Clinical Pathology and Medical Research, Westmead Hospital, University of Sydney	CIDM-PH et al.
EPI_ISL_478683, EPI_ISL_478684, EPI_ISL_478685, EPI_ISL_478686, EPI_ISL_478687, EPI_ISL_478688, EPI_ISL_478689, EPI_ISL_478690, EPI_ISL_478691, EPI_ISL_478692, EPI_ISL_478693, EPI_ISL_478694, EPI_ISL_478695, EPI_ISL_478696, EPI_ISL_478697, EPI_ISL_478698, EPI_ISL_478699, EPI_ISL_478700, EPI_ISL_478702, EPI_ISL_478703, EPI_ISL_478704, EPI_ISL_478706, EPI_ISL_490017, EPI_ISL_490018, EPI_ISL_490032, EPI_ISL_490034, EPI_ISL_490035, EPI_ISL_498751, EPI_ISL_513317, EPI_ISL_526697, EPI_ISL_593683	South Eastern Area Laboratory Services (SEALS)	NSW Health Pathology - Institute of Clinical Pathology and Medical Research, Westmead Hospital, University of Sydney	CIDM-PH et al.
see above	South Eastern Area Laboratory Services (SEALS)	NSW Health Pathology - Institute of Clinical Pathology and Medical Research, Westmead Hospital, University of Sydney	CIDM-PH et al.
EPI_ISL_456159, EPI_ISL_456167, EPI_ISL_456181, EPI_ISL_456217, EPI_ISL_456218, EPI_ISL_456219, EPI_ISL_456220, EPI_ISL_456225, EPI_ISL_456228, EPI_ISL_456230, EPI_ISL_456233, EPI_ISL_456234, EPI_ISL_456236, EPI_ISL_456237, EPI_ISL_456238, EPI_ISL_456242, EPI_ISL_456243, EPI_ISL_456244, EPI_ISL_456245, EPI_ISL_456246, EPI_ISL_456247, EPI_ISL_456248, EPI_ISL_456249, EPI_ISL_456250, EPI_ISL_456251, EPI_ISL_456252, EPI_ISL_456253, EPI_ISL_456254, EPI_ISL_456255, EPI_ISL_456256, EPI_ISL_456257, EPI_ISL_456258, EPI_ISL_456259, EPI_ISL_456260, EPI_ISL_456261, EPI_ISL_456262, EPI_ISL_456263, EPI_ISL_456264, EPI_ISL_456265, EPI_ISL_456266, EPI_ISL_456267, EPI_ISL_456268, EPI_ISL_456270, EPI_ISL_456271, EPI_ISL_456272, EPI_ISL_456273, EPI_ISL_456274, EPI_ISL_456275, EPI_ISL_456276, EPI_ISL_456277, EPI_ISL_456278, EPI_ISL_456279, EPI_ISL_456280, EPI_ISL_456281, EPI_ISL_456282, EPI_ISL_456283, EPI_ISL_456284, EPI_ISL_456285, EPI_ISL_456286, EPI_ISL_456287, EPI_ISL_456288, EPI_ISL_456289, EPI_ISL_456290, EPI_ISL_456291, EPI_ISL_456292, EPI_ISL_456308, EPI_ISL_536789, EPI_ISL_579125, EPI_ISL_579126, EPI_ISL_579127, EPI_ISL_579128, EPI_ISL_579129, EPI_ISL_579130, EPI_ISL_579131, EPI_ISL_579132, EPI_ISL_579133, EPI_ISL_579134, EPI_ISL_579135, EPI_ISL_579136, EPI_ISL_579137, EPI_ISL_579138, EPI_ISL_579139, EPI_ISL_579140, EPI_ISL_579141, EPI_ISL_579142, EPI_ISL_579143, EPI_ISL_579144, EPI_ISL_579145, EPI_ISL_579146, EPI_ISL_579147, EPI_ISL_579148, EPI_ISL_579149, EPI_ISL_579150, EPI_ISL_579151, EPI_ISL_579152, EPI_ISL_579153, EPI_ISL_579154, EPI_ISL_579155, EPI_ISL_579163	Institute of Environmental Science and Research (ESR)	Anja Werno; Antje van der Linden; Arto Upton; Chris Mansell; David Hammer; Dragana Drinkovic; Erasmus Smit; Gary McAuliffe; Hana Sofia Andersson; Hermes Perez; James Usher; Jill Sherwood; Jing Wang; Joep de Lig; Josh Freeman; Julia Howard; Juliet Elvy; Lauren Jolly; Mary De Almeida; Matt Bleakton; Matt Storey; Matthew Rogers; Max Bloomfield; Michael Adzide; Michelle Bain; Muhammad Faisal; Niko Fried; Olin Stander; Sally Roberts; Sarah Jeffrey; Sharmil Mutayyah; Susan Morphet; Susan Taylor; Timothy Blackmore; Vani Sarthyendran; Veronica Playle; Virginia Hope; Xiaoyun Ren	
EPI_ISL_469241, EPI_ISL_469242, EPI_ISL_469243, EPI_ISL_469244, EPI_ISL_469245, EPI_ISL_469246, EPI_ISL_469247, EPI_ISL_469248, EPI_ISL_469249, EPI_ISL_469250, EPI_ISL_469251, EPI_ISL_469252	Special Infectious Agents Unit	Special Infectious Agents Unit	A.M.; Al-Sobahy; Azhar; E.I.; El-Kafrawy; Farraj; Hassan; N.A.; S.A.; T.L.; Tolah; Uthman
see above	St Barnabas Hospital	New York City Public Health Laboratory	Jade Wang; et al.
EPI_ISL_631888, EPI_ISL_631917, EPI_ISL_631952, EPI_ISL_631971, EPI_ISL_631990	St. John's Episcopal Hospital	New York City Public Health Laboratory	Jade Wang; et al.
EPI_ISL_631529	St. Luke's Hospital	Minnesota Department of Health, Public Health Laboratory	Jacob Garlin; Matt Phibb; and Xiong Wang
EPI_ISL_514641, EPI_ISL_514646	St. Vincent's University Hospital	Institute of Genomics Core Facility, University of Tartu	Aleksandr Inevskii; Denis Kainov; Janne-Fossium Malmring; Svein Arne Nordbø; Tuuli Reilein
EPI_ISL_450346, EPI_ISL_450347, EPI_ISL_450348, EPI_ISL_450349, EPI_ISL_450350, EPI_ISL_450351, EPI_ISL_450352	St. Vincent's University Hospital	St. Vincent's University Hospital	Aisling Purcell; Gabriel Gonzalez; Guerin Macon; Kirsten Schaffer; Liza Fendley; Mary Lucy; Niamh Mullane; Suzie Coughlan; Séamus Fanning; Una Sutton-Fitzpatrick
see above	St. Vincent's University Hospital	St. Vincent's University Hospital	Aisling Purcell; Gabriel Gonzalez; Guerin Macon; Kirsten Schaffer; Liza Fendley; Mary Lucy; Niamh Mullane; Suzie Coughlan; Séamus Fanning; Una Sutton-Fitzpatrick
EPI_ISL_596646, EPI_ISL_596648, EPI_ISL_596653, EPI_ISL_596665, EPI_ISL_596668, EPI_ISL_596675	St. Vincent's University Hospital	St. Vincent's University Hospital	Aisling Purcell; Gabriel Gonzalez; Guerin Macon; Kirsten Schaffer; Liza Fendley; Mary Lucy; Niamh Mullane; Suzie Coughlan; Séamus Fanning; Una Sutton-Fitzpatrick
EPI_ISL_450445, EPI_ISL_450446, EPI_ISL_450447, EPI_ISL_450448, EPI_ISL_450449, EPI_ISL_450450, EPI_ISL_450451, EPI_ISL_450452, EPI_ISL_450453, EPI_ISL_450454, EPI_ISL_450455, EPI_ISL_450456, EPI_ISL_450457, EPI_ISL_450458, EPI_ISL_450459, EPI_ISL_450460, EPI_ISL_450461, EPI_ISL_450462, EPI_ISL_450463, EPI_ISL_450464, EPI_ISL_450465, EPI_ISL_450466, EPI_ISL_450467, EPI_ISL_450468, EPI_ISL_450469, EPI_ISL_450470, EPI_ISL_450471, EPI_ISL_450472, EPI_ISL_450473, EPI_ISL_450474, EPI_ISL_450475, EPI_ISL_450476, EPI_ISL_450477, EPI_ISL_450478, EPI_ISL_450479, EPI_ISL_450480, EPI_ISL_450481, EPI_ISL_476768, EPI_ISL_476772, EPI_ISL_476773, EPI_ISL_476774, EPI_ISL_476775, EPI_ISL_476776, EPI_ISL_476777, EPI_ISL_476778, EPI_ISL_476779, EPI_ISL_476780, EPI_ISL_476781, EPI_ISL_476782, EPI_ISL_476783, EPI_ISL_476784, EPI_ISL_476785, EPI_ISL_476786, EPI_ISL_476787, EPI_ISL_476788	Stanford clinical virology lab	Chan-Zuckerberg Biohub	Benjamin Pinky; Carlos Bustamante; Euan Ashley; Hannah N. DeJong; Jason Andrews; John Gorzynski; Katharine Walter; Manuel Rivas; Matthew T. Wheeler; Victoria N. Parkh; with CZB C14hub Consortium
EPI_ISL_418990, EPI_ISL_418991	State Key Laboratory for Diagnosis and Treatment of Infectious Diseases, National Clinical Research Center for Infectious Diseases, First Affiliated Hospital, Zhejiang University School of Medicine, Hangzhou, China 310003	State Key Laboratory for Diagnosis and Treatment of Infectious Diseases, National Clinical Research Center for Infectious Diseases, First Affiliated Hospital, Zhejiang University School of Medicine, Hangzhou, China 310003	Changzhong Jin; Chao Jiang; Fumin Liu; Haibo Wu; Hangqing Yao; Lanjuan Li; Lirfang Cheng; Min Zheng; Nanping Wu; Xiangyun Lu; Zhigang Wu
EPI_ISL_417443	State Key Laboratory for Emerging Infectious Diseases Department of Microbiology Li Ka Shing Faculty of Medicine The University of Hong Kong	State Key Laboratory for Emerging Infectious Diseases Department of Microbiology Li Ka Shing Faculty of Medicine The University of Hong Kong	Bobo Wing-Yee Mok; Honglin Chen; Kwok-Yung Yuen; Pui Wang; Shaofeng Deng; Siu-Ying Lau; Wenjun Song
EPI_ISL_444273	State Key Laboratory of Respiratory Disease, National Clinical Research Center for Respiratory Disease, Guangzhou Institute of Respiratory Health, the First Affiliated Hospital of Guangzhou Medical University	State Key Laboratory of Respiratory Disease, National Clinical Research Center for Respiratory Disease, Guangzhou Institute of Respiratory Health, the First Affiliated Hospital of Guangzhou Medical University	Huang; J. and Zhao, J.; Shi, Y.; Sun, J.; Zheng, K.
EPI_ISL_414663, EPI_ISL_414666, EPI_ISL_414689, EPI_ISL_414690, EPI_ISL_414691, EPI_ISL_414692	State Key Laboratory of Respiratory Disease, National Clinical Research Center for Respiratory Disease, Guangzhou Institute of Respiratory Health, the First Affiliated Hospital of Guangzhou Medical University	The First Affiliated Hospital of Guangzhou Medical University & BGI-Shenzhen	Zhao et al
EPI_ISL_414687	State Key Laboratory of Respiratory Disease, National Clinical Research Center for Respiratory Disease, Guangzhou Institute of Respiratory Health, the First Affiliated Hospital of Guangzhou Medical University	the First Affiliated Hospital of Guangzhou Medical University & BGI-Shenzhen	Zhao et al
EPI_ISL_406716, EPI_ISL_406717	State Key Laboratory of Virology, Wuhan University	State Key Laboratory of Virology, Wuhan University	Chen, L.; Chen, Y.; K. and Liu, Y.; Lan, L. Y.; Liu, F.; Liu, W.; Mei, Y.; Shi, M.; Sun, Z.; Wu, K.; Wu, W.; Xu, K.; Ye, G.; Zhang, Q.; Zhang, W.
EPI_ISL_752608, EPI_ISL_752609, EPI_ISL_752612, EPI_ISL_752614, EPI_ISL_752615, EPI_ISL_752616, EPI_ISL_752617, EPI_ISL_752618, EPI_ISL_752619, EPI_ISL_752620, EPI_ISL_752627, EPI_ISL_752628, EPI_ISL_752660, EPI_ISL_752700, EPI_ISL_752710, EPI_ISL_752711, EPI_ISL_752845	State Laboratories Division, Hawaii State Department of Health	State Laboratories Division, Hawaii State Department of Health	Drew Kuwazaki; Edward Desmond; Pamela O'Brien; Razvan Sultana; Sabrina Diemert
see above	State Laboratories Division, Hawaii State Department of Health	State Laboratories Division, Hawaii State Department of Health	Drew Kuwazaki; Edward Desmond; Pamela O'Brien; Razvan Sultana; Sabrina Diemert
EPI_ISL_428960, EPI_ISL_428961, EPI_ISL_428962, EPI_ISL_428963, EPI_ISL_428964, EPI_ISL_428965, EPI_ISL_428966, EPI_ISL_428967, EPI_ISL_428968, EPI_ISL_428969, EPI_ISL_428970, EPI_ISL_428971, EPI_ISL_428972, EPI_ISL_428973, EPI_ISL_428974, EPI_ISL_428975, EPI_ISL_428976, EPI_ISL_428977, EPI_ISL_428978, EPI_ISL_428979, EPI_ISL_428980, EPI_ISL_428981, EPI_ISL_428982, EPI_ISL_428983, EPI_ISL_428984, EPI_ISL_428985, EPI_ISL_428986, EPI_ISL_428987, EPI_ISL_428988, EPI_ISL_428989, EPI_ISL_428990, EPI_ISL_428991, EPI_ISL_428992, EPI_ISL_428993, EPI_ISL_428994, EPI_ISL_428995, EPI_ISL_428996, EPI_ISL_428997, EPI_ISL_428998, EPI_ISL_428999, EPI_ISL_429000, EPI_ISL_429001, EPI_ISL_429002, EPI_ISL_429003, EPI_ISL_429004, EPI_ISL_429005, EPI_ISL_429006, EPI_ISL_429007, EPI_ISL_429008, EPI_ISL_429009, EPI_ISL_429010, EPI_ISL_429011, EPI_ISL_429012, EPI_ISL_429013, EPI_ISL_429014, EPI_ISL_429015, EPI_ISL_429016, EPI_ISL_429017, EPI_ISL_429018, EPI_ISL_429019, EPI_ISL_429020, EPI_ISL_429021, EPI_ISL_429022, EPI_ISL_429023, EPI_ISL_429024	State Research Center of Virology and Biotechnology VECTOR, Department of Collection of Microorganisms	State Research Center of Virology and Biotechnology VECTOR, Department of Collection of Microorganisms	Alexander N. Shvalov; Anastasiya A. Nazarenko; Anastasiya M. Srinmova; Elena V. Gavrilova; Oleg V. Pyankov; Rinat A. Maksyutov; Sergey A. Bodnev; Tat'yana V. Tregubchuk
see above	State Research Center of Virology and Biotechnology VECTOR, Department of Collection of Microorganisms	State Research Center of Virology and Biotechnology VECTOR, Department of Collection of Microorganisms	Alexander N. Shvalov; Anastasiya A. Nazarenko; Anastasiya M. Srinmova; Elena V. Gavrilova; Oleg V. Pyankov; Rinat A. Maksyutov; Sergey A. Bodnev; Tat'yana V. Tregubchuk
EPI_ISL_417033	Sullivan Nicolaides Pathology	Public Health Virology Laboratory	Alyssa Pyke; Amanda De Jong; Andrew Van Den Hurk; Bixing Huang; Carmel Taylor; David Warrlow; Doris Genge; Elisabeth Gamez; Glen Hewitson; Ian Maxwell Mackay; Inga Sultana; Jamie McMahon; Jean Barcelon; Judy North; Mitchell Finger; Natalie Simpson; Neelima Nair; Peter Burtonclay; Peter Moore; Sarah Wheatley; Sean Moody; Sonja Hall-Mendelin; Timothy Gardam; and Frederick Moore
EPI_ISL_445225, EPI_ISL_475564	Surbunns VC	The Public Health Agency of Sweden	Anna Risberg; Anna-Malin Linde; Erik Embring; Karin Tegmark-Wisell; Maria Lind Karlberg; Mattias Haukild; Mia Brytting; Olov Svartstrom; Oskar Karlsson Lindajo; Reza Adyani; Sandra Brodbecksson; Theresa Erikson

EPI_ISL_434645, EPI_ISL_434649	Svarjdoz VC	The Public Health Agency of Sweden	Anna Risberg; Anna-Malin Linde; Karin Tegmark-Wisell; Maria Lind Karlberg; Mia Brytting; Olov Svartstrom; Oskar Karlsson Lindajo; Theresa Enkrich; Tommy Janers
EPI_ISL_478675, EPI_ISL_478676, EPI_ISL_478677, EPI_ISL_478678, EPI_ISL_478679, EPI_ISL_478680, EPI_ISL_478681, EPI_ISL_478682, EPI_ISL_478706, EPI_ISL_490037, EPI_ISL_593755, EPI_ISL_593756, EPI_ISL_593757, EPI_ISL_593758, EPI_ISL_593759	see above	Sydney South West Pathology Service (SSWPS) - Liverpool Hospital - NSW Health Pathology	NSW Health Pathology - Institute of Clinical Pathology and Medical Research; Westmead Hospital; University of Sydney
EPI_ISL_426500, EPI_ISL_426501, EPI_ISL_426502, EPI_ISL_426503, EPI_ISL_426504, EPI_ISL_426505, EPI_ISL_426506, EPI_ISL_426507, EPI_ISL_426508, EPI_ISL_426510, EPI_ISL_426511, EPI_ISL_426520, EPI_ISL_426521, EPI_ISL_426522, EPI_ISL_426523, EPI_ISL_426524, EPI_ISL_426525, EPI_ISL_426526, EPI_ISL_426532, EPI_ISL_426533, EPI_ISL_426534, EPI_ISL_426535, EPI_ISL_426536, EPI_ISL_694047, EPI_ISL_694048, EPI_ISL_694049, EPI_ISL_694052	see above	TGen North	TGen North
EPI_ISL_540432, EPI_ISL_540433, EPI_ISL_540434, EPI_ISL_576172, EPI_ISL_576175, EPI_ISL_576176	see above	TN Division of Laboratory Services	Pathogen Discovery, Respiratory Viruses Branch, Division of Viral Diseases, Centers for Disease Control and Prevention
EPI_ISL_426629, EPI_ISL_426630, EPI_ISL_426632, EPI_ISL_427392, EPI_ISL_427393, EPI_ISL_427394, EPI_ISL_427395, EPI_ISL_427398, EPI_ISL_428223, EPI_ISL_428230, EPI_ISL_428231, EPI_ISL_436101, EPI_ISL_436102, EPI_ISL_436104, EPI_ISL_436106, EPI_ISL_436107, EPI_ISL_447252, EPI_ISL_447253, EPI_ISL_447255, EPI_ISL_447257, EPI_ISL_447592, EPI_ISL_457726, EPI_ISL_457730, EPI_ISL_457733, EPI_ISL_458029	see above	TSQH-CP molecular lab	TSQH-CP molecular lab
EPI_ISL_411926, EPI_ISL_411927	see above	Taiwan Centers for Disease Control	Taiwan Centers for Disease Control
EPI_ISL_412968, EPI_ISL_420889, EPI_ISL_420890, EPI_ISL_445183	see above	Takayuki Hishiki Kanagawa Prefectural Institute of Public Health	Takayuki Hishiki Kanagawa Prefectural Institute of Public Health
EPI_ISL_1379444, EPI_ISL_1379445, EPI_ISL_1379446, EPI_ISL_1379447, EPI_ISL_1379448, EPI_ISL_1379449, EPI_ISL_1379450, EPI_ISL_1379451, EPI_ISL_1379452, EPI_ISL_1379453, EPI_ISL_1379454, EPI_ISL_1379455, EPI_ISL_1379456, EPI_ISL_1379457, EPI_ISL_1379458, EPI_ISL_1379459, EPI_ISL_1379460, EPI_ISL_1379461, EPI_ISL_1379462, EPI_ISL_1379463, EPI_ISL_1379464, EPI_ISL_1379465, EPI_ISL_1379466, EPI_ISL_1379467, EPI_ISL_1379468, EPI_ISL_1379469, EPI_ISL_1379470, EPI_ISL_1379471, EPI_ISL_1379472, EPI_ISL_1379473, EPI_ISL_1379474, EPI_ISL_1379475, EPI_ISL_1379476, EPI_ISL_1379477, EPI_ISL_1379478, EPI_ISL_1379481, EPI_ISL_1379482, EPI_ISL_1379483, EPI_ISL_1379484, EPI_ISL_1379485, EPI_ISL_1379486, EPI_ISL_1379487, EPI_ISL_1379488, EPI_ISL_1379489, EPI_ISL_1379490, EPI_ISL_1379491, EPI_ISL_1379492, EPI_ISL_1379493, EPI_ISL_1379494, EPI_ISL_1379495, EPI_ISL_1379496, EPI_ISL_1379497, EPI_ISL_1379498, EPI_ISL_1379499, EPI_ISL_1379500, EPI_ISL_1379501, EPI_ISL_1379502, EPI_ISL_1379503, EPI_ISL_1379504, EPI_ISL_1379505, EPI_ISL_1379506	see above	Tampa General Hospital Esoteric Lab	Tampa General Hospital Esoteric Research & Development Lab
EPI_ISL_529149, EPI_ISL_529150	see above	Technology Centre, Guangzhou Customs	Technology Centre, Guangzhou Customs
EPI_ISL_412966	see above	Technology Centre, Guangzhou Customs	Technology Centre, Guangzhou Customs
EPI_ISL_420796, EPI_ISL_420797, EPI_ISL_420798, EPI_ISL_452105, EPI_ISL_452112, EPI_ISL_452115	see above	Texas DSHS Lab Services	Pathogen Discovery, Respiratory Viruses Branch, Division of Viral Diseases, Centers for Disease Control and Prevention
EPI_ISL_525763, EPI_ISL_631660, EPI_ISL_631661, EPI_ISL_631662, EPI_ISL_644168, EPI_ISL_644176	see above	Texas Department of State Health Services	Texas Department of State Health Services
EPI_ISL_918160, EPI_ISL_918161, EPI_ISL_918162, EPI_ISL_918163, EPI_ISL_937531, EPI_ISL_937534, EPI_ISL_937539, EPI_ISL_937540, EPI_ISL_937541, EPI_ISL_937542, EPI_ISL_937543, EPI_ISL_937544, EPI_ISL_976893, EPI_ISL_976894, EPI_ISL_976895, EPI_ISL_976896, EPI_ISL_976897, EPI_ISL_976898, EPI_ISL_976899, EPI_ISL_976901, EPI_ISL_976902, EPI_ISL_976903, EPI_ISL_976904, EPI_ISL_976905, EPI_ISL_1296442, EPI_ISL_1296443, EPI_ISL_1296444, EPI_ISL_1296445, EPI_ISL_1296446, EPI_ISL_1296447, EPI_ISL_1296448, EPI_ISL_1296449, EPI_ISL_1296451, EPI_ISL_1296452, EPI_ISL_1296453, EPI_ISL_1296454, EPI_ISL_1296457	see above	Thai Red Cross Emerging Infectious Diseases Health Science Centre, Chulalongkorn Hospital, Faculty of Medicine, Chulalongkorn University	Thai Red Cross Emerging Infectious Diseases Center and Faculty of Medicine, Chulalongkorn University
EPI_ISL_672153, EPI_ISL_672154, EPI_ISL_672155, EPI_ISL_672157, EPI_ISL_672158, EPI_ISL_672159, EPI_ISL_672160, EPI_ISL_672161, EPI_ISL_672162, EPI_ISL_672172, EPI_ISL_857039	see above	The Ashley Laboratory, Stanford University	Chan-Zuckerberg Biohub
EPI_ISL_412978	see above	The Central Hospital Of Wuhan	Hubei Provincial Center for Disease Control and Prevention
EPI_ISL_450442	see above	The Department of Infectious Disease Prevention and Control, Henan Provincial Center for Disease Control and Prevention	The Department of Infectious Disease Prevention and Control, Henan Provincial Center for Disease Control and Prevention
EPI_ISL_429074, EPI_ISL_429075, EPI_ISL_429076, EPI_ISL_429077, EPI_ISL_429078, EPI_ISL_429079, EPI_ISL_429080, EPI_ISL_429081, EPI_ISL_429082, EPI_ISL_429083, EPI_ISL_429084, EPI_ISL_429085, EPI_ISL_429086, EPI_ISL_429087, EPI_ISL_429088, EPI_ISL_429089, EPI_ISL_429090, EPI_ISL_429091, EPI_ISL_429092, EPI_ISL_429093, EPI_ISL_429094, EPI_ISL_429095, EPI_ISL_429096, EPI_ISL_429097, EPI_ISL_429098, EPI_ISL_429099, EPI_ISL_429100, EPI_ISL_429101, EPI_ISL_429102, EPI_ISL_429103, EPI_ISL_429104, EPI_ISL_429105	see above	The First Affiliated Hospital of Guangzhou Medical University	BGI-shenzhen & The First Affiliated Hospital of Guangzhou Medical University
EPI_ISL_457687, EPI_ISL_457688, EPI_ISL_457689, EPI_ISL_457690, EPI_ISL_457691, EPI_ISL_457692, EPI_ISL_457693, EPI_ISL_457694, EPI_ISL_457695, EPI_ISL_457696, EPI_ISL_457697, EPI_ISL_457698	see above	The First Affiliated Hospital of Guangzhou Medical University, Guangzhou, China	BGI-shenzhen & The First Affiliated Hospital of Guangzhou Medical University
EPI_ISL_491092, EPI_ISL_530348, EPI_ISL_530349, EPI_ISL_530494	see above	The National Institute of Public Health	State Veterinary Institute Prague
EPI_ISL_471540, EPI_ISL_471544, EPI_ISL_471547, EPI_ISL_471553, EPI_ISL_471555, EPI_ISL_476067	see above	The National Institute of Public Health	State Veterinary Institute Prague and The National Institute of Public Health
EPI_ISL_489706, EPI_ISL_489709, EPI_ISL_490112, EPI_ISL_491093, EPI_ISL_491094, EPI_ISL_491095, EPI_ISL_491117, EPI_ISL_513314, EPI_ISL_513511, EPI_ISL_513512	see above	The National Institute of Public Health	The National Institute of Public Health and State Veterinary Institute Prague
EPI_ISL_422636	see above	The National Institute of Public Health Center for Epidemiology and Microbiology	State Veterinary Institute Prague
EPI_ISL_437519	see above	The National Institute of Public Health Center for Epidemiology and Microbiology	The National Institute of Public Health Center for Epidemiology and Microbiology
EPI_ISL_426379	see above	The National Laboratory of Health, Environment and Food, Maribor, Slovenia	The National Laboratory of Health, Environment and Food, Maribor, Slovenia
EPI_ISL_417551, EPI_ISL_417553, EPI_ISL_417555, EPI_ISL_417556, EPI_ISL_417557, EPI_ISL_417558, EPI_ISL_417560, EPI_ISL_417561, EPI_ISL_417562, EPI_ISL_417563, EPI_ISL_417564, EPI_ISL_417565, EPI_ISL_417566, EPI_ISL_417567, EPI_ISL_417568, EPI_ISL_417569, EPI_ISL_417570, EPI_ISL_417571, EPI_ISL_417572, EPI_ISL_417573, EPI_ISL_417574, EPI_ISL_417575, EPI_ISL_417576, EPI_ISL_417577, EPI_ISL_417578, EPI_ISL_417579, EPI_ISL_417580, EPI_ISL_417581, EPI_ISL_417582, EPI_ISL_417583, EPI_ISL_417584, EPI_ISL_417585, EPI_ISL_417586, EPI_ISL_417587, EPI_ISL_417588, EPI_ISL_417589, EPI_ISL_417590, EPI_ISL_417591, EPI_ISL_417592, EPI_ISL_417593, EPI_ISL_417594, EPI_ISL_417595, EPI_ISL_417596, EPI_ISL_417597, EPI_ISL_417598, EPI_ISL_417599, EPI_ISL_417600, EPI_ISL_417601, EPI_ISL_417602, EPI_ISL_417603, EPI_ISL_417604, EPI_ISL_417605, EPI_ISL_417606, EPI_ISL_417607, EPI_ISL_417608, EPI_ISL_417609, EPI_ISL_417610, EPI_ISL_417611, EPI_ISL_417612, EPI_ISL_417613, EPI_ISL_417614, EPI_ISL_417615, EPI_ISL_417616, EPI_ISL_417617, EPI_ISL_417618, EPI_ISL_417619, EPI_ISL_417620, EPI_ISL_417621, EPI_ISL_417622, EPI_ISL_417623, EPI_ISL_417624, EPI_ISL_417625, EPI_ISL_417626, EPI_ISL_417627, EPI_ISL_417628, EPI_ISL_417629, EPI_ISL_417630, EPI_ISL_417631, EPI_ISL_417632, EPI_ISL_417633, EPI_ISL_417634, EPI_ISL_417635, EPI_ISL_417636, EPI_ISL_417637, EPI_ISL_417638, EPI_ISL_417639, EPI_ISL_417640, EPI_ISL_417641, EPI_ISL_417642, EPI_ISL_417643, EPI_ISL_417644, EPI_ISL_417645, EPI_ISL_417646, EPI_ISL_417647, EPI_ISL_417648, EPI_ISL_417649, EPI_ISL_417650, EPI_ISL_417651, EPI_ISL_417652, EPI_ISL_417653, EPI_ISL_417654, EPI_ISL_417655, EPI_ISL_417656, EPI_ISL_417657, EPI_ISL_417658, EPI_ISL_417659, EPI_ISL_417660, EPI_ISL_417661, EPI_ISL_417662, EPI_ISL_417663, EPI_ISL_417664, EPI_ISL_417665, EPI_ISL_417666, EPI_ISL_417667, EPI_ISL_417668, EPI_ISL_417669, EPI_ISL_417670, EPI_ISL_417671, EPI_ISL_417672, EPI_ISL_417673, EPI_ISL_417674, EPI_ISL_417675, EPI_ISL_417676, EPI_ISL_417677, EPI_ISL_417678, EPI_ISL_417679, EPI_ISL_417680, EPI_ISL_417681, EPI_ISL_417682, EPI_ISL_417683, EPI_ISL_417684, EPI_ISL_417685, EPI_ISL_417686, EPI_ISL_417687, EPI_ISL_417688, EPI_ISL_417689, EPI_ISL_417690, EPI_ISL_417691, EPI_ISL_417692, EPI_ISL_417693, EPI_ISL_417694, EPI_ISL_417695, EPI_ISL_417696, EPI_ISL_417697, EPI_ISL_417698, EPI_ISL_417699, EPI_ISL_417700, EPI_ISL_417701, EPI_ISL_417702, EPI_ISL_417703, EPI_ISL_417704, EPI_ISL_417705, EPI_ISL_417706, EPI_ISL_417707, EPI_ISL_417708, EPI_ISL_417709, EPI_ISL_417710, EPI_ISL_417711, EPI_ISL_417712, EPI_ISL_417713, EPI_ISL_417714, EPI_ISL_417715, EPI_ISL_417716, EPI_ISL_417717, EPI_ISL_417718, EPI_ISL_417719, EPI_ISL_417720, EPI_ISL_417721, EPI_ISL_417722, EPI_ISL_417723, EPI_ISL_417724, EPI_ISL_417725, EPI_ISL_417726, EPI_ISL_417727, EPI_ISL_417728, EPI_ISL_417729, EPI_ISL_417730, EPI_ISL_417731, EPI_ISL_417732, EPI_ISL_417733, EPI_ISL_417734, EPI_ISL_417735, EPI_ISL_417736, EPI_ISL_417737, EPI_ISL_417738, EPI_ISL_417739, EPI_ISL_417740, EPI_ISL_417741, EPI_ISL_417742, EPI_ISL_417743, EPI_ISL_417744, EPI_ISL_417745, EPI_ISL_417746, EPI_ISL_417747, EPI_ISL_417748, EPI_ISL_417749, EPI_ISL_417750, EPI_ISL_417751, EPI_ISL_417752, EPI_ISL_417753, EPI_ISL_417754, EPI_ISL_417755, EPI_ISL_417756, EPI_ISL_417757, EPI_ISL_417758, EPI_ISL_417759, EPI_ISL_417760, EPI_ISL_417761, EPI_ISL_417762, EPI_ISL_417763, EPI_ISL_417764, EPI_ISL_417765, EPI_ISL_417766, EPI_ISL_417767, EPI_ISL_417768, EPI_ISL_417769, EPI_ISL_417770, EPI_ISL_417771, EPI_ISL_417772, EPI_ISL_417773, EPI_ISL_417774, EPI_ISL_417775, EPI_ISL_417776, EPI_ISL_417777, EPI_ISL_417778, EPI_ISL_417779, EPI_ISL_417780, EPI_ISL_417781, EPI_ISL_417782, EPI_ISL_417783, EPI_ISL_417784, EPI_ISL_417785, EPI_ISL_417786, EPI_ISL_417787, EPI_ISL_417788, EPI_ISL_417789, EPI_ISL_417790, EPI_ISL_417791, EPI_ISL_417792, EPI_ISL_417793, EPI_ISL_417794, EPI_ISL_417795, EPI_ISL_417796, EPI_ISL_417797, EPI_ISL_417798, EPI_ISL_417799, EPI_ISL_417800, EPI_ISL_417801, EPI_ISL_417802, EPI_ISL_417803, EPI_ISL_417804, EPI_ISL_417805, EPI_ISL_417806, EPI_ISL_417807, EPI_ISL_417808, EPI_ISL_417809, EPI_ISL_417810, EPI_ISL_417811, EPI_ISL_417812, EPI_ISL_417813, EPI_ISL_417814, EPI_ISL_417815, EPI_ISL_417816, EPI_ISL_417817, EPI_ISL_417818, EPI_ISL_417819, EPI_ISL_417820, EPI_ISL_417821, EPI_ISL_417822, EPI_ISL_417823, EPI_ISL_417824, EPI_ISL_417825, EPI_ISL_417826, EPI_ISL_417827, EPI_ISL_417828, EPI_ISL_417829, EPI_ISL_417830, EPI_ISL_417831, EPI_ISL_417832, EPI_ISL_417833, EPI_ISL_417834, EPI_ISL_417835, EPI_ISL_417836, EPI_ISL_417837, EPI_ISL_417838, EPI_ISL_417839, EPI_ISL_417840, EPI_ISL_417841, EPI_ISL_417842, EPI_ISL_417843, EPI_ISL_417844, EPI_ISL_417845, EPI_ISL_417846, EPI_ISL_417847, EPI_ISL_417848, EPI_ISL_417849, EPI_ISL_417850, EPI_ISL_417851, EPI_ISL_417852, EPI_ISL_417853, EPI_ISL_417854, EPI_ISL_417855, EPI_ISL_417856, EPI_ISL_417857, EPI_ISL_417858, EPI_ISL_417859, EPI_ISL_417860, EPI_ISL_417861, EPI_ISL_417862, EPI_ISL_417863, EPI_ISL_417864, EPI_ISL_417865, EPI_ISL_417866, EPI_ISL_417867, EPI_ISL_417868, EPI_ISL_417869, EPI_ISL_417870, EPI_ISL_417871, EPI_ISL_417872, EPI_ISL_417873, EPI_ISL_417874, EPI_ISL_417875, EPI_ISL_417876, EPI_ISL_417877, EPI_ISL_417878, EPI_ISL_417879, EPI_ISL_417880, EPI_ISL_417881, EPI_ISL_417882, EPI_ISL_417883, EPI_ISL_417884, EPI_ISL_417885, EPI_ISL_417886, EPI_ISL_417887, EPI_ISL_417888, EPI_ISL_417889, EPI_ISL_417890, EPI_ISL_417891, EPI_ISL_417892, EPI_ISL_417893, EPI_ISL_417894, EPI_ISL_417895, EPI_ISL_417896, EPI_ISL_417897, EPI_ISL_417898, EPI_ISL_417899, EPI_ISL_417900, EPI_ISL_417901, EPI_ISL_417902, EPI_ISL_417903, EPI_ISL_417904, EPI_ISL_417905, EPI_ISL_417906, EPI_ISL_417907, EPI_ISL_417908, EPI_ISL_417909, EPI_ISL_417910, EPI_ISL_417911, EPI_ISL_417912, EPI_ISL_417913, EPI_ISL_417914, EPI_ISL_417915, EPI_ISL_417916, EPI_ISL_417917, EPI_ISL_417918, EPI_ISL_417919, EPI_ISL_417920, EPI_ISL_417921, EPI_ISL_417922, EPI_ISL_417923, EPI_ISL_417924, EPI_ISL_417925, EPI_ISL_417926, EPI_ISL_417927, EPI_ISL_417928, EPI_ISL_417929, EPI_ISL_417930, EPI_ISL_417931, EPI_ISL_417932, EPI_ISL_417933, EPI_ISL_417934, EPI_ISL_417935, EPI_ISL_417936, EPI_ISL_417937, EPI_ISL_417938, EPI_ISL_417939, EPI_ISL_417940, EPI_ISL_417941, EPI_ISL_417942, EPI_ISL_417943, EPI_ISL_417944, EPI_ISL_417945, EPI_ISL_417946, EPI_ISL_417947, EPI_ISL_417948, EPI_ISL_417949, EPI_ISL_417950, EPI_ISL_417951, EPI_ISL_417952, EPI_ISL_417953, EPI_ISL_417954, EPI_ISL_417955, EPI_ISL_417956, EPI_ISL_417957, EPI_ISL_417958, EPI_ISL_417959, EPI_ISL_417960, EPI_ISL_417961, EPI_ISL_417962, EPI_ISL_417963, EPI_ISL_417964, EPI_ISL_417965, EPI_ISL_417966, EPI_ISL_417967, EPI_ISL_417968, EPI_ISL_417969, EPI_ISL_417970, EPI_ISL_417971, EPI_ISL_417972, EPI_ISL_417973, EPI_ISL_417974, EPI_ISL_417975, EPI_ISL_417976, EPI_ISL_417977, EPI_ISL_417978, EPI_ISL_417979, EPI_ISL_417980, EPI_ISL_417981, EPI_ISL_417982, EPI_ISL_417983, EPI_ISL_417984, EPI_ISL_417985, EPI_ISL_417986, EPI_ISL_417987, EPI_ISL_417988, EPI_ISL_417989, EPI_ISL_417990, EPI_ISL_417991, EPI_ISL_417992, EPI_ISL_417993, EPI_ISL_417994, EPI_ISL_417995, EPI_ISL_417996, EPI_ISL_417997, EPI_ISL_417998, EPI_ISL_417999	see above	Blazun Vosner H.; Duh D.; Hedzet S.; Janezic S.; Mahnic A.; Rupnik M.; Završnik J.	

EPI_ISL_455332	Xerencia de Xestión Integrada de Pontevedra e o Saúde	Instituto de Salud Carlos III	A. Monzón; F. Casas; I. J. Jiménez; Iglesias-Caballero; M. Camarero; M. Cuesta; M. Garcia; M. González-Esguevillas; M. Molinero Calamita; M. Zaballos; P. Jiménez; S. Júlita; S. Pizzo; S. Varona
EPI_ISL_428387, EPI_ISL_431080, EPI_ISL_435709	Yale COVID-19 Biorepository	Grubaug Lab - Yale School of Public Health	Adam Moore; Akiko Iwasaki; Albert Ko; Alice Lu; Allison Nelson; Anderson Brito; Anne Wylie; Arnu Casanovas; Catherine Muenker; Chaney Kalinich; Chantal Vogels; Charlese Dela Cruz; Cole Jensen; Isabel Ott; Joseph Fauver; Maria Tokuyama; Mary Petrone; Nathan Grubaug; Patrick Wong; Peiwen Lu; Richard Martinello; Saad Omer; Shelli Farhadian; Tara Alpert
EPI_ISL_419517, EPI_ISL_419518, EPI_ISL_419524, EPI_ISL_419525, EPI_ISL_419526, EPI_ISL_419527, EPI_ISL_419528, EPI_ISL_419529, EPI_ISL_419531, EPI_ISL_419532, EPI_ISL_419533, EPI_ISL_419534, EPI_ISL_419535, EPI_ISL_419536, EPI_ISL_419537, EPI_ISL_419538, EPI_ISL_419539, EPI_ISL_419540, EPI_ISL_419541, EPI_ISL_419542, EPI_ISL_419543, EPI_ISL_419544, EPI_ISL_419545, EPI_ISL_419546, EPI_ISL_419547, EPI_ISL_419548, EPI_ISL_419549, EPI_ISL_419550, EPI_ISL_419551, EPI_ISL_419552, EPI_ISL_419553, EPI_ISL_419554, EPI_ISL_419555, EPI_ISL_419556, EPI_ISL_419557, EPI_ISL_419558, EPI_ISL_419559, EPI_ISL_419560, EPI_ISL_419561, EPI_ISL_419562, EPI_ISL_419563, EPI_ISL_419564, EPI_ISL_419565, EPI_ISL_419566, EPI_ISL_419567, EPI_ISL_419568, EPI_ISL_419569, EPI_ISL_419570, EPI_ISL_419571, EPI_ISL_419572, EPI_ISL_419573, EPI_ISL_419574, EPI_ISL_419575, EPI_ISL_419576, EPI_ISL_419577, EPI_ISL_419578, EPI_ISL_419579, EPI_ISL_419580, EPI_ISL_419581, EPI_ISL_419582, EPI_ISL_419583, EPI_ISL_419584, EPI_ISL_419585, EPI_ISL_419586, EPI_ISL_419587, EPI_ISL_419588, EPI_ISL_419589, EPI_ISL_419590, EPI_ISL_419591, EPI_ISL_419592, EPI_ISL_419593, EPI_ISL_419594, EPI_ISL_419595, EPI_ISL_419596, EPI_ISL_419597, EPI_ISL_419598, EPI_ISL_419599	Yale Clinical Virology Laboratory	Grubaug Lab - Yale School of Public Health	Adam Moore; Akiko Iwasaki; Albert Ko; Alice Lu; Allison Nelson; Anderson Brito; Anne Wylie; Arnu Casanovas; Catherine Muenker; Chaney Kalinich; Chantal Vogels; Charlese Dela Cruz; Cole Jensen; Ellen Foxman; Isabel Ott; Joseph Fauver; Maria Tokuyama; Marie Landry; Mary Petrone; Nathan Grubaug; Patrick Wong; Peiwen Lu; Richard Martinello; Saad Omer; Shelli Farhadian; Tara Alpert
EPI_ISL_684796, EPI_ISL_684799	Yamagata Prefectural Institute of Public Health	Pathogen Genomics Center, National Institute of Infectious Diseases	Kentarō Itokawa; Makoto Kuroda; Masanori Hashino; Rina Tanaka; Tsuyoshi Sekizuka
EPI_ISL_408478	Yongchuan District Center for Disease Control and Prevention	Chongqing Municipal Center for Disease Control and Prevention	Chen Shuang; Li Qing; Ling Hua; Rong Rong; Su Kun; Tan ZhangPing; Tang Wenge; Tang Yun; Ye Sheng; Yu zhen
EPI_ISL_475889, EPI_ISL_475890, EPI_ISL_475891, EPI_ISL_475892, EPI_ISL_475893, EPI_ISL_475894, EPI_ISL_475895, EPI_ISL_475896, EPI_ISL_475897, EPI_ISL_475898, EPI_ISL_475899	Zentralinstitut für medizinische und chemische Labordiagnostik, Universitätsklinikum Innsbruck	Berghaler laboratory, CeMM Research Center for Molecular Medicine of the Austrian Academy of Sciences	Alexander Lercher; Alexandra Popa; Andreas Berghaler; Benedikt Agerer; Christoph Bock; Daniela Schmid; Dorothee von Laer; Elisabeth Puchhammer-Sodeik; Franz Allerberger; Gregor Hörmann; Guenther Weiss; Henrike Colacci; Jakob-Wendelin Genger; Jan Laine; Judith Aberle; Kinga Rieger-Höhenwarter; Lukas Ender; Mairied Naurz; Mark Smyth; Martin Senekowitsch; Michael Schuster; Peter Hufnagl; Rainer Guttringer; Stephan Aberle; Thomas Penz; Wegene Borena
EPI_ISL_404227, EPI_ISL_404228	Zhejiang Provincial Center for Disease Control and Prevention	Department of Microbiology, Zhejiang Provincial Center for Disease Control and Prevention	Chen Chen; Chonghao Hu; Enlu Chen; Fang Xu; Haiyan Mao; Hangping Zhu; Hao Yan; Jian Gao; Jianmin Jiang; Junhang Pan; Juying Yan; Liming Gong; Qiong Ge; Wen Shi; Wenwu Yao; Xinying Wang; Xiyu Lou; Yan Feng; Yanjun Zhang; Yi Sun; Yin Chen; Yisheng Sun; Yuyu Lu; Zhangng Yang; Zhen Li; Zhen Wang; Zhiping Chen
EPI_ISL_422425	Zhejiang Provincial Center for Disease Control and Prevention	Zhejiang Provincial Center for Disease Control and Prevention	Yanjun Zhang; Yi Sun
EPI_ISL_408479	Zhongxian Center for Disease Control and Prevention	Chongqing Municipal Center for Disease Control and Prevention	Chen Shuang; Li Qing; Ling Hua; Rong Rong; Su Kun; Tan ZhangPing; Tang Wenge; Tang Yun; Ye Sheng; Yu zhen; Zhang Hong
EPI_ISL_467430	Zoonotic and Exotic Infection Diseases Division	Zoonotic and Exotic Infection Diseases Division	Jinlang Wang; Zhigao Bu
EPI_ISL_459909	Zoonotic and Exotic Infection Diseases Division, Harbin Veterinary Research Institute, CAAS	Zoonotic and Exotic Infection Diseases Division, Harbin Veterinary Research Institute, CAAS	Jinlang Wang; Zhigao Bu
EPI_ISL_468134, EPI_ISL_468135, EPI_ISL_468136, EPI_ISL_468137, EPI_ISL_468138, EPI_ISL_468139, EPI_ISL_468140, EPI_ISL_468141, EPI_ISL_468142, EPI_ISL_468143, EPI_ISL_468144, EPI_ISL_468145	see above	[Romania, Bucharest] National Institute for Infectious Diseases "Prof. Dr. Matei Bal"	Corina Casangiu; Leontina Banica; Marius Cotic; Marius Surlesac; Simona Paraschiv
EPI_ISL_450196	burnrungrad international hospital	National Institute of Health, Department of Medical Sciences, Ministry of Public Health, Thailand	Chittaganpitch; Malinee; Okada; Pammen; Phuygun; Pitaluk; Sirippam; Stittorn; Sunthareeya; Thanadsachakul; Thanutsapa; Waicharon; Warawan; Wongboot
EPI_ISL_417536, EPI_ISL_417537, EPI_ISL_417538, EPI_ISL_417539, EPI_ISL_417540, EPI_ISL_417541, EPI_ISL_417542, EPI_ISL_417543, EPI_ISL_417544, EPI_ISL_417545, EPI_ISL_417546, EPI_ISL_417547, EPI_ISL_417548, EPI_ISL_417549, EPI_ISL_417550, EPI_ISL_417551, EPI_ISL_417552, EPI_ISL_417553, EPI_ISL_417554, EPI_ISL_417555, EPI_ISL_417556, EPI_ISL_417557, EPI_ISL_417558, EPI_ISL_417559, EPI_ISL_417560, EPI_ISL_417561, EPI_ISL_417562, EPI_ISL_417563, EPI_ISL_417564, EPI_ISL_417565, EPI_ISL_417566, EPI_ISL_417567, EPI_ISL_417568, EPI_ISL_417569, EPI_ISL_417570, EPI_ISL_417571, EPI_ISL_417572, EPI_ISL_417573, EPI_ISL_417574, EPI_ISL_417575, EPI_ISL_417576, EPI_ISL_417577, EPI_ISL_417578, EPI_ISL_417579, EPI_ISL_417580, EPI_ISL_417581, EPI_ISL_417582, EPI_ISL_417583, EPI_ISL_417584, EPI_ISL_417585, EPI_ISL_417586, EPI_ISL_417587, EPI_ISL_417588, EPI_ISL_417589, EPI_ISL_417590, EPI_ISL_417591, EPI_ISL_417592, EPI_ISL_417593, EPI_ISL_417594, EPI_ISL_417595, EPI_ISL_417596, EPI_ISL_417597, EPI_ISL_417598, EPI_ISL_417599	deCODE genetics	deCODE genetics	Agnar Helgason; Alma Moller; Ama B Agustsdottir; Arnaldur Gylfason; Asgeir Sigurdsson; Adalau Jonasdottir; Berglind Eiriksdottir; Bjarni Thorbjornsson; Brynjolfur J. Jonsson; Daniel F Gudbjartsson; Droplaug N Magnúsdóttir; Elisabet E Gardarsdóttir; Emil A Thorarinn; Gardar Sveinbjornsson; Gisli Masson; Gudmundur Georgsson; Gudmundur L Norddahl; Gudrun Sigmundsdóttir; Hakon Jonsson; Hilma Holm; Ingileif Jonasdóttir; Jóna Saemundsdóttir; Kamilla S Josefsdóttir; Karl Stefansson; Karl G Kristinnsson; Kjartan R Gudmundsson; Kristín E Sveinsdóttir; Louise le Roux; Maney Sveinsdóttir; Oelga S Gretarsdóttir; Ólafur T Magnússon; Pall Melsted; Patrick Sulem; Run Fridrikdóttir; Thora R Gunnarsdóttir; Thorudur Kristjánsson; Thorodur Gudnason; Unnur Thorsteinsdóttir
EPI_ISL_560591, EPI_ISL_560592, EPI_ISL_560593, EPI_ISL_560594, EPI_ISL_560596	hospital	National Reference Center for Viruses of Respiratory Infections, Institut Pasteur, Paris	Etienne Simon-Lorière; Fabiana Gambaro; Maud Vanpeene; Sylvie Behilli; Sylvie van der Werf; Vincent Enouf
EPI_ISL_560589, EPI_ISL_560570, EPI_ISL_560573, EPI_ISL_560574, EPI_ISL_560577, EPI_ISL_560578	hôpital	National Reference Center for Viruses of Respiratory Infections, Institut Pasteur, Paris	Etienne Simon-Lorière; Fabiana Gambaro; Maud Vanpeene; Sylvie Behilli; Sylvie van der Werf; Vincent Enouf
EPI_ISL_447909, EPI_ISL_447910, EPI_ISL_447911, EPI_ISL_447912, EPI_ISL_447913, EPI_ISL_447914, EPI_ISL_447915, EPI_ISL_447916, EPI_ISL_447917, EPI_ISL_447918, EPI_ISL_447919, EPI_ISL_447920, EPI_ISL_447921	see above	nia	National Institute of Health, Department of Medical Sciences, Ministry of Public Health, Thailand
EPI_ISL_458286	unknown	Bundeswehr Institute of Microbiology	Antwerpen; Bestehom-Willmann; Eckstein, S.; Handrick, S.; M.C.; M.H.; M.S.; Najja, H.; R. and Ben Moussa, M.; Rehn, A.; Stoecker, K.; Walter; Woelfel
EPI_ISL_450500, EPI_ISL_450501, EPI_ISL_450502, EPI_ISL_450503, EPI_ISL_450504	unknown	CAS Key Laboratory of Special Pathogens and Biosafety and Center for Emerging Infectious Diseases	Lin, H.; Shi, Z.; Si, H.; Xie, S.; Zhou, P.; Zhu, Y.
EPI_ISL_486429	unknown	Clinical Laboratory, Hospital Israelita Albert Einstein	Angarten, D.; C.L. and Pinho; F.G.; Guedes; J.R.; Malta, F.; Manguiera; R.A.; R.L.; Santana; de Menezes
EPI_ISL_483001, EPI_ISL_483002, EPI_ISL_483003, EPI_ISL_483005, EPI_ISL_483006	unknown	Clinical virology	Fares, W.; Triki, H.
EPI_ISL_488063, EPI_ISL_488064, EPI_ISL_488065	unknown	Computer Science and Engineering	A.B.; Adcock; Alejandro, B.; Arnold; Carrico, R.; Chariker; Chung, D.; E.O.; F.; Hwang; J.H.; J.W.; J.Y.; K.E.; L.A.; Lasnik; Palmer; Park; R.S.; Ramirez, J.; Roudsari; Walgel, S.; Wolf; Zacharias, W.; Zhang, M.
EPI_ISL_450484, EPI_ISL_450485, EPI_ISL_450486, EPI_ISL_450487	unknown	Data Science	C.J.; Carroll; Cohen; Miller, N.K.; S.H.; T.D.; Tran
EPI_ISL_447635, EPI_ISL_447636, EPI_ISL_447637, EPI_ISL_447638, EPI_ISL_447639, EPI_ISL_447640, EPI_ISL_447641, EPI_ISL_447642, EPI_ISL_447643, EPI_ISL_447644, EPI_ISL_447645, EPI_ISL_447646, EPI_ISL_447647, EPI_ISL_447648, EPI_ISL_447649, EPI_ISL_447650, EPI_ISL_447651, EPI_ISL_447652, EPI_ISL_447653, EPI_ISL_447654, EPI_ISL_447655, EPI_ISL_447656, EPI_ISL_447657, EPI_ISL_447658, EPI_ISL_447659, EPI_ISL_447660, EPI_ISL_447661, EPI_ISL_447662, EPI_ISL_447663, EPI_ISL_447664, EPI_ISL_447665, EPI_ISL_447666, EPI_ISL_447667, EPI_ISL_447668, EPI_ISL_447669, EPI_ISL_447670, EPI_ISL_447671, EPI_ISL_447672, EPI_ISL_447673, EPI_ISL_447674, EPI_ISL_447675, EPI_ISL_447676, EPI_ISL_447677, EPI_ISL_447678, EPI_ISL_447679, EPI_ISL_447680, EPI_ISL_447681, EPI_ISL_447682, EPI_ISL_447683, EPI_ISL_447684, EPI_ISL_447685, EPI_ISL_447686, EPI_ISL_447687, EPI_ISL_447688, EPI_ISL_447689, EPI_ISL_447690, EPI_ISL_447691, EPI_ISL_447692, EPI_ISL_447693, EPI_ISL_447694, EPI_ISL_447695, EPI_ISL_447696, EPI_ISL_447697, EPI_ISL_447698, EPI_ISL_447699	unknown	Department of Medicine	Bampali, M.; Dvoritis, N.; Froukala, E.; Gatzidou, E.; Kassel, K.; N. and Karakasilotis, I.; Spanakis; Stavropoulou, A.; Tsakris, A.; Veletza, S.
EPI_ISL_455683, EPI_ISL_455684, EPI_ISL_455685, EPI_ISL_455686, EPI_ISL_455687, EPI_ISL_455688, EPI_ISL_455689, EPI_ISL_455690, EPI_ISL_455691, EPI_ISL_455692, EPI_ISL_455693, EPI_ISL_455694, EPI_ISL_455695, EPI_ISL_455696, EPI_ISL_455697, EPI_ISL_455698, EPI_ISL_455699, EPI_ISL_455700, EPI_ISL_455701, EPI_ISL_455702, EPI_ISL_455703, EPI_ISL_455704, EPI_ISL_455705, EPI_ISL_455706, EPI_ISL_455707, EPI_ISL_455708, EPI_ISL_455709, EPI_ISL_455710, EPI_ISL_455711, EPI_ISL_455712, EPI_ISL_455713, EPI_ISL_455714, EPI_ISL_455715, EPI_ISL_455716, EPI_ISL_455717, EPI_ISL_455718, EPI_ISL_455719, EPI_ISL_455720, EPI_ISL_455721, EPI_ISL_455722, EPI_ISL_455723, EPI_ISL_455724, EPI_ISL_455725, EPI_ISL_455726, EPI_ISL_455727, EPI_ISL_455728, EPI_ISL_455729, EPI_ISL_455730, EPI_ISL_455731, EPI_ISL_455732, EPI_ISL_455733, EPI_ISL_455734, EPI_ISL_455735, EPI_ISL_455736, EPI_ISL_455737, EPI_ISL_455738, EPI_ISL_455739, EPI_ISL_455740, EPI_ISL_455741, EPI_ISL_455742, EPI_ISL_455743, EPI_ISL_455744, EPI_ISL_455745, EPI_ISL_455746, EPI_ISL_455747, EPI_ISL_455748, EPI_ISL_455749, EPI_ISL_455750, EPI_ISL_455751, EPI_ISL_455752, EPI_ISL_455753, EPI_ISL_455754, EPI_ISL_455755, EPI_ISL_455756, EPI_ISL_455757, EPI_ISL_455758, EPI_ISL_455759, EPI_ISL_455760, EPI_ISL_455761, EPI_ISL_455762, EPI_ISL_455763, EPI_ISL_455764, EPI_ISL_455765, EPI_ISL_455766, EPI_ISL_455767, EPI_ISL_455768, EPI_ISL_455769, EPI_ISL_455770, EPI_ISL_455771, EPI_ISL_455772, EPI_ISL_455773, EPI_ISL_455774, EPI_ISL_455775, EPI_ISL_455776, EPI_ISL_455777, EPI_ISL_455778, EPI_ISL_455779, EPI_ISL_455780, EPI_ISL_455781, EPI_ISL_455782, EPI_ISL_455783, EPI_ISL_455784, EPI_ISL_455785, EPI_ISL_455786, EPI_ISL_455787, EPI_ISL_455788, EPI_ISL_455789, EPI_ISL_455790, EPI_ISL_455791, EPI_ISL_455792, EPI_ISL_455793, EPI_ISL_455794, EPI_ISL_455795, EPI_ISL_455796, EPI_ISL_455797, EPI_ISL_455798, EPI_ISL_455799	see above	Department of Microbiology	Bao, L.; Cai, F.; Deng, W.; Gao, H.; Gao, Q.; Ge, X.; Gong, X.; Hu, Y.; Jiang, D.; Jiang, L.; Kan, B.; Li, C.; Li, J.; Li, Y.; Liu, J.; Lou, X.; Lu, J.; Lv, Z.; Mao, H.; Peng, H.; Qi, Z.; Qin, C.; Shi, W.; Sun, Y.; Tang, H.; Wang, L.; Wang, N.; Wang, X.; Wu, D.; Xu, K.; Yang, M.; Yan, W.; Yao, Y.; Zhang, H.; Zhang, Y.; Zhao, P.; Zhu, L.
EPI_ISL_449480, EPI_ISL_449481, EPI_ISL_449484, EPI_ISL_449486	unknown	Department of Respiratory and Critical Care	Bai, X.; Chang, Y.; Deng, T.; Gao, Y.; He, Y.; Jiang, N.; Liang, L.; Liu, L.; Liu, W.; Ma, M.; Ma, L.; Ma, X.; Pan, T.; Shi, H.; W.L. and Gao, Z.; Wang, G.; Wang, X.; Wei, X.; Xu, Y.; Yang, B.; Yang, D.; Zhai, B.; Zhang, J.; Zhang, Z.; Zheng, Y.; Zhou, Q.

Table S4. County data for non-EHC sequences.

Sequence ID	County
EPI_ISL_420786	Polk
EPI_ISL_420787	Cobb
EPI_ISL_424859	Fulton
EPI_ISL_424861	Fulton
EPI_ISL_424864	Fayette
EPI_ISL_426417	Fulton
EPI_ISL_419556	Fulton
EPI_ISL_419557	Fulton
EPI_ISL_420788	Fulton
EPI_ISL_424858	Gwinnett

Table S1. Sequence name and accession numbers to the reference database at the weighted downsampling maximum likelihood analysis.

Table with 10 columns: Sequence Name, GISAID Accession, Pass, M, Clust, File, Sequence Name, GISAID Accession, Pass, M, Clust, File, Sequence Name, GISAID Accession, Pass, M, Clust, File. The table lists various influenza virus sequences from different countries and regions, including Argentina, Australia, Austria, Azerbaijan, Bahrain, Bangladesh, Belgium, Bolivia, Bulgaria, Burkina Faso, Cambodia, Canada, Chile, China, Colombia, Costa Rica, Czechia, Denmark, Dominican Republic, Ecuador, Egypt, El Salvador, Estonia, Georgia, Germany, Greece, Guatemala, Haiti, Honduras, Hungary, India, Indonesia, Iran, Iraq, Israel, Italy, Japan, Kazakhstan, Kenya, Korea, Kuwait, Kyrgyzstan, Laos, Latvia, Lebanon, Lithuania, Luxembourg, Macedonia, Malawi, Malaysia, Maldives, Mali, Mexico, Moldova, Mongolia, Myanmar, Namibia, Nepal, Netherlands, New Zealand, Nicaragua, Niger, Nigeria, Norway, Oman, Pakistan, Panama, Paraguay, Peru, Philippines, Poland, Portugal, Romania, Russia, Rwanda, Saudi Arabia, Senegal, Serbia, Singapore, Slovakia, Slovenia, South Africa, South Korea, Spain, Sri Lanka, Sweden, Switzerland, Taiwan, Tajikistan, Thailand, Timor-Leste, Tunisia, Turkey, Uganda, Ukraine, United Kingdom, United States, Uruguay, Uzbekistan, Venezuela, Vietnam, West Bank, and Yemen.

Table with multiple columns listing various entities, their identifiers, and associated details. The table is organized into several vertical sections, each containing a list of entries with varying column widths and content.

Table S7. Select parameter prior and posterior estimates from the Bayesian phylogenetic analysis including select-19B sequences

Analysis	Parameter	Prior	Estimate (95% HPD)
Full	Posterior		-45680 (-45787 -45582)
Full	Tree height		0.240 (0.216 0.274)
Full	Proportion invariant	Uniform(0, 1)	0.764 (0.483 0.897)
Full	UCLD Mean	Normal(1.0e-3, 1.0e-4)	1.17e-03 (1.02e-03 1.32e-03)
Full	UCLD σ	Exponential(0.33)	0.64 (0.40 0.88)
Full	κ	Lognormal(1.0, 1.25)	6.513 (5.058 8.292)
Full	γ	Exponential(1.0)	4.93e-01 (1.03e-03 2.38e+00)
Rep 0	Posterior		-43577 (-43652 -43508)
Rep 0	Posterior		0.245 (0.216 0.287)
Rep 0	Tree height	Uniform(0, 1)	0.593 (0.098 0.883)
Rep 0	Proportion invariant	Normal(1.0e-3, 1.0e-4)	1.05e-03 (8.91e-04 1.20e-03)
Rep 0	UCLD Mean	Exponential(0.33)	0.68 (0.31 1.00)
Rep 0	UCLD σ	Lognormal(1.0, 1.25)	6.303 (4.514 8.585)
Rep 0	κ	Exponential(1.0)	4.58e-01 (1.55e-03 2.56e+00)
Rep 0	γ		
Rep 1	Posterior		-43851 (-43926 -43780)
Rep 1	Posterior		0.245 (0.218 0.285)
Rep 1	Tree height	Uniform(0, 1)	0.715 (0.301 0.911)
Rep 1	Proportion invariant	Uniform(0, 1)	0.715 (0.301 0.911)
Rep 1	UCLD Mean	Normal(1.0e-3, 1.0e-4)	1.08e-03 (9.26e-04 1.24e-03)
Rep 1	UCLD σ	Exponential(0.33)	0.60 (0.24 0.93)
Rep 1	κ	Lognormal(1.0, 1.25)	6.103 (4.512 8.079)
Rep 1	γ	Exponential(1.0)	5.03e-01 (1.15e-03 2.36e+00)
Rep 2	Posterior		-43821 (-43893 -43753)
Rep 2	Posterior		0.249 (0.219 0.293)
Rep 2	Tree height	Uniform(0, 1)	0.781 (0.455 0.920)
Rep 2	Proportion invariant	Uniform(0, 1)	0.781 (0.455 0.920)
Rep 2	UCLD Mean	Normal(1.0e-3, 1.0e-4)	1.06e-03 (9.12e-04 1.22e-03)
Rep 2	UCLD σ	Exponential(0.33)	0.62 (0.21 0.94)
Rep 2	κ	Lognormal(1.0, 1.25)	6.644 (4.818 8.941)
Rep 2	γ	Exponential(1.0)	4.57e-01 (1.09e-03 2.18e+00)
Rep 3	Posterior		-43741 (-43812 -43675)
Rep 3	Posterior		0.249 (0.218 0.291)
Rep 3	Tree height	Uniform(0, 1)	0.758 (0.409 0.923)
Rep 3	Proportion invariant	Uniform(0, 1)	0.758 (0.409 0.923)
Rep 3	UCLD Mean	Normal(1.0e-3, 1.0e-4)	1.09e-03 (9.33e-04 1.24e-03)
Rep 3	UCLD σ	Exponential(0.33)	0.66 (0.35 0.95)
Rep 3	κ	Lognormal(1.0, 1.25)	6.220 (4.446 8.205)
Rep 3	γ	Exponential(1.0)	4.69e-01 (1.14e-03 2.41e+00)
Rep 4	Posterior		-43673 (-43742 -43604)
Rep 4	Posterior		0.248 (0.217 0.291)
Rep 4	Tree height	Uniform(0, 1)	0.776 (0.442 0.920)
Rep 4	Proportion invariant	Uniform(0, 1)	0.776 (0.442 0.920)
Rep 4	UCLD Mean	Normal(1.0e-3, 1.0e-4)	1.08e-03 (9.22e-04 1.24e-03)
Rep 4	UCLD σ	Exponential(0.33)	0.55 (0.05 0.85)
Rep 4	κ	Lognormal(1.0, 1.25)	6.196 (4.545 8.296)
Rep 4	γ	Exponential(1.0)	4.43e-01 (1.03e-03 2.35e+00)

Table S8. Traveler data

Patient ID	Sample ID	Travel region	Compared to sequences in travel region			Compared to sequences in Georgia, USA			Compared to all publicly available sequences, excluding travel region and excluding Georgia, USA			
			Number of days prior to symptom onset during which travel occurred	Minimum number of SNPs (and direction ^a)	Sequences with the minimum number of SNPs	Total sequences	Minimum number of SNPs (and direction ^a)	Sequences with the minimum number of SNPs	Total sequences	Minimum number of SNPs (and direction ^a)	Sequences with the minimum number of SNPs	Total sequences
2	GA-EHC-016P	Louisiana, USA	unknown to 2	0	2	85	1 (ancestral)	2	106	0	51	35150
39	GA-EHC-111H	Louisiana, USA	20 to unknown	3 (ancestral)	19	85	3 (ancestral)	2	106	2 (ancestral)	1	24599
5	GA-EHC-031E	Colorado, USA	5 to 1	0	2	45	0	1	107	0	132	35934
14	GA-EHC-033Q	Mississippi, USA	8 to 3	0	1	20	0	6	103	0	28	35037
27	GA-EHC-110F	North Carolina, USA	8 to 6	1 (ancestral)	1	16	1 (ancestral)	2	105	1 (ancestral, descendant)	134 (ancestral), 1 (descendant)	35264
22	GA-EHC-064L	Italy	34 to 0	0	5	847	0	1	106	0	85	34451
22	GA-EHC-064L	Switzerland	34 to 0	0	13	810	0	1	106	0	47	34448
23	GA-EHC-063E	Costa Rica	9 to 1	1 (descendant)	3	21	1 (descendant)	4	107	0	48	35312
8	GA-EHC-065J	Nigeria	14 to 0	no sequences in lineage	8	15	1 (descendant)	1	105	1 (ancestral, descendant), 2 (descendant)	1264 (ancestral), 2 (descendant)	25166
33	GA-EHC-069Q	Italy	8 to 2	1 (ancestral)	1	847	0	1	106	1 (ancestral)	1185	34461
33	GA-EHC-069Q	Poland	2 to 0	1 (ancestral)	1	45	0	1	106	1 (ancestral)	1266	35263

^adirectionality only factors in when not identical; ancestral means the sequence(s) contain all mutations of the traveler sequence except one while child indicates the sequence(s) contain all mutations of the traveler sequence plus one additional

Patient ID	Sample ID	Travel region(s) and Georgia, USA (alphabetical)
2	GA-EHC-016P	Florida, USA; Illinois, USA; Michigan, USA; Minnesota, USA; Texas, USA; Utah, USA; Washington, USA; Wisconsin, USA
39	GA-EHC-111H	Mississippi, USA
5	GA-EHC-031E	Arizona, USA; Australia; California, USA; Canada; Florida, USA; Iceland; Indiana, USA; Kansas, USA; Maryland, USA; Massachusetts, USA; Michigan, USA; Minnesota, USA; Missouri, USA; Nevada, USA; New Jersey, USA; New Mexico, USA; New York, USA; New Zealand; Ohio, USA; Pennsylvania, USA
14	GA-EHC-033Q	California, USA; Delaware, USA; Florida, USA; Illinois, USA; Indiana, USA; Louisiana, USA; Maryland, USA; Massachusetts, USA; Michigan, USA; Minnesota, USA; Missouri, USA; New York, USA; Pennsylvania, USA; Texas, USA; USA; Utah, USA; Virgin Islands, USA; Virginia, USA; Washington, USA
27	GA-EHC-110F	Arizona, USA; California, USA; Canada; Louisiana, USA; Michigan, USA; Minnesota, USA; Missouri, USA; New York, USA; Pennsylvania, USA; Rhode Island, USA; Texas, USA; United Kingdom; Utah, USA; Washington, USA
22	GA-EHC-064L	Arizona, USA; Austria; Austria; Belgium; Canada; China; Colombia; France; Mexico; New Mexico, USA; Peru; Portugal; Romania; Singapore; Spain; Switzerland; United Kingdom
23	GA-EHC-063E	Argentina; Australia; Austria; Belgium; Bolivia; Brazil; California, USA; Canada; Chile; Colorado, USA; Connecticut, USA; Cyprus; Czech Republic; Denmark; Ecuador; Finland; Florida, USA; France; Germany; Greece; Guadeloupe; Hong Kong; Hungary; Iceland; Illinois, USA; India; Ireland; Israel; Italy; Japan; Latvia; Maine, USA; Maryland, USA; Massachusetts, USA; Michigan, USA; Minnesota, USA; Missouri, USA; Morocco; Netherlands; Nevada, USA; New York, USA; New Zealand; Oman; Pennsylvania, USA; Peru; Poland; Portugal; Puerto Rico, USA; Russia; Saudi Arabia; Sierra Leone; Singapore; Slovakia; South Africa; South Korea; Spain; Sri Lanka; Sweden; Switzerland; Taiwan; Texas, USA; Turkey, USA, USA; United Arab Emirates; United Kingdom; Utah, USA; Vietnam; Virgin Islands, USA; Washington, USA; Wisconsin, USA
8	GA-EHC-065J	Argentina; Arizona, USA; Australia; Austria; Belgium; Bolivia; Brazil; California, USA; Canada; Chile; Colorado, USA; Connecticut, USA; Cyprus; Czech Republic; Denmark; Ecuador; Finland; Florida, USA; France; Germany; Greece; Guadeloupe; Hong Kong; Hungary; Iceland; Illinois, USA; India; Ireland; Israel; Japan; Latvia; Maine, USA; Maryland, USA; Massachusetts, USA; Michigan, USA; Minnesota, USA; Missouri, USA; Morocco; Netherlands; Nevada, USA; New York, USA; New Zealand; Oman; Pennsylvania, USA; Peru; Poland; Portugal; Puerto Rico, USA; Russia; Saudi Arabia; Sierra Leone; Singapore; Slovakia; South Africa; South Korea; Spain; Sri Lanka; Sweden; Switzerland; Taiwan; Texas, USA; Turkey, USA, USA; United Arab Emirates; United Kingdom; Utah, USA; Vietnam; Virgin Islands, USA; Washington, USA; Wisconsin, USA
33	GA-EHC-069Q	Argentina; Arizona, USA; Australia; Austria; Belgium; Bolivia; Brazil; California, USA; Canada; Chile; Colorado, USA; Connecticut, USA; Cyprus; Czech Republic; Denmark; Ecuador; Finland; Florida, USA; France; Germany; Greece; Guadeloupe; Hong Kong; Hungary; Iceland; Illinois, USA; India; Ireland; Israel; Italy; Japan; Latvia; Maine, USA; Maryland, USA; Massachusetts, USA; Michigan, USA; Minnesota, USA; Missouri, USA; Morocco; Netherlands; Nevada, USA; New York, USA; New Zealand; Oman; Pennsylvania, USA; Peru; Portugal; Puerto Rico, USA; Russia; Saudi Arabia; Sierra Leone; Singapore; Slovakia; South Africa; South Korea; Spain; Sri Lanka; Sweden; Switzerland; Taiwan; Texas, USA; Turkey, USA, USA; United Arab Emirates; United Kingdom; Utah, USA; Vietnam; Virgin Islands, USA; Washington, USA; Wisconsin, USA
33	GA-EHC-069Q	Poland

Table B9: 198 Subside

Table with 4 columns: Sequence Name, GISAID Accession, Sequence Name, GISAID Accession. The table lists various influenza virus sequences and their corresponding GISAID accession numbers, organized into four main columns.

Table S10. Temporal & geographic homogeneity demographic sequences

Table with 10 columns: Sequence Name, GSAD Accession, Pass, M, Clock Filter, Sequence Name, GSAD Accession, Pass, M, Clock Filter, Sequence Name, GSAD Accession, Pass, M, Clock Filter, Sequence Name, GSAD Accession, Pass, M, Clock Filter. The table lists numerous demographic sequences such as Demomk-C1000-2000, Demomk-C1000-2000, Demomk-C1000-2000, etc., with their corresponding accession numbers and filter settings.

Supplementary Tables

Supplementary Table 1: Detailed SARS-CoV-2 sequencing metrics. A total of 54 samples were sequenced using a metagenomic next-generation sequencing (mNGS) approach (from 50 patients). A total of 10 samples were sequenced using a SARS-CoV-2 multiplex amplicon approach, including 5 samples with low coverage by mNGS and an additional 5 samples that were not attempted by mNGS. Abbreviations: BAL: bronchoalveolar lavage, Ct: cycle threshold, sgRNA: subgenomic RNA, mNGS: metagenomic next-generation sequencing, NP: nasopharyngeal, OP: oropharyngeal

Supplementary Table 2: Detailed clinical data for 54 EHC patients with SARS-CoV-2 infection in March 2020. Abbreviations: BAL: bronchoalveolar lavage, BMI: body mass index, CKD: chronic kidney disease, Ct: cycle threshold, DM: diabetes mellitus, ED: emergency department, ESLD: end-stage liver disease, ESRD: end-stage renal disease, F: female, HIV: human immunodeficiency virus, HTN: hypertension, ICU: intensive care unit, IgG: immunoglobulin G, M: male, N/A: not applicable, NP: nasopharyngeal, OP: oropharyngeal, SLE: systemic lupus erythematosus.

Supplementary Table 3: GISAID acknowledgements table for all sequences used in travel and phylogenetic analyses. We gratefully acknowledge all Authors from the Originating laboratories responsible for obtaining the specimens, as well as the submitting laboratories where the genome data were generated and shared via GISAID, on which this research is based. All Submitters of data may be contacted directly via GISAID.

Supplementary Table 4: County data for non-EHC sequences. Sequence data and additional metadata for included sequences can be accessed via www.gisaid.org.

Supplementary Table 5: Sequence names and accession numbers for sequences included in the weighted downsampling maximum likelihood analysis presented in **Figure 2**, **Supplementary Figure 4**, and **Supplementary Figure 5**. Sequence data and additional metadata for included sequences can be accessed via www.gisaid.org.

Supplementary Table 6: Sequence names and accession numbers for sequences included in the Bayesian phylogenetic analysis including select 19B sequences presented in **Figure 3**, **Supplementary Figure 7**, **Supplementary Figure 8**, **Supplementary Figure 9**, and **Supplementary Table 7**. Sequence data and additional metadata for included sequences can be accessed via www.gisaid.org.

Supplementary Table 7: Select parameter prior and posterior estimates from the Bayesian phylogenetic analysis including select-19B sequences presented in **Figure 3**, **Supplementary Figure 7**, and **Supplementary Figure 8**.

Supplementary Table 8: Travel data and mutational profile for 9 patients who had traveled in the 2 weeks preceding symptom onset. For each patient, the SARS-CoV-2 sequence was compared to other sequences in its ancestral lineage that had been obtained from the region of travel, the state of Georgia, and globally. Columns indicate the minimum number of SNPs between the traveler sequence and any sequence in its lineage, the number of sequences in the lineage that contained the minimum number of SNPs, and the total number of sequences available from the region. For sequences that are not identical, ancestral means the sequence(s) contain all mutations of the traveler sequence except one while child indicates the

sequence(s) contain all mutations of the traveler sequence plus one additional. Abbreviations: SNP: single nucleotide polymorphism

Supplementary Table 9: Sequence names and accession numbers for sequences which match the mutational profile of the 69 closely related 19B Georgia sequences presented in Figure 5. Sequence data and additional metadata for included sequences can be accessed via www.gisaid.org.

Supplementary Table 10: Sequence names and accession numbers for sequences included in the temporally homogeneous downsampling maximum likelihood analysis presented in Supplementary Figure 6 and Supplementary Figure 14. Sequence data and additional metadata for included sequences can be accessed via www.gisaid.org.

Main Figure Alt Text (for screen readers)

Figure 1

Multi-panel figure with two rows. First row contains a single figure, labelled A, and the second row contains two figures, B and C.

The top panel, A, shows both the number of reported cases in Georgia in red, and the number of sequences included in the analysis shown in green. Data is shown between 29 February 2020 and 31 March, 2020. A vertical dotted line is shown at 15 March 2020, the date on which the FDA allowed certified labs to validate tests for SARS-CoV-2.

The number of reported cases in Georgia are as follows: 03 March 2020: 2, 06 March 2020: 1, 07 March 2020: 2, 09 March 2020: 5, 10 March 2020: 7, 11 March 2020: 6, 12 March 2020: 8, 13 March 2020: 11, 14 March 2020: 31, 15 March 2020: 26, 16 March 2020: 22, 17 March 2020: 25, 18 March 2020: 51, 19 March 2020: 90, 20 March 2020: 198, 21 March 2020: 70, 22 March 2020: 66, 23 March 2020: 151, 24 March 2020: 254, 25 March 2020: 221, 26 March 2020: 278, 27 March 2020: 475, 28 March 2020: 366, 29 March 2020: 285, 30 March 2020: 157, 31 March 2020: 1121.

The number of included sequences sampled in Georgia are as follows: 29 February 2020: 2, 3 March 2020: 3, 4 March 2020: 3, 5 March 2020: 1, 6 March 2020: 1, 7 March 2020: 2, 8 March 2020: 1, 9 March 2020: 1, 10 March 2020: 3, 11 March 2020: 3, 12 March 2020: 2, 13 March 2020: 13, 14 March 2020: 9, 15 March 2020: 15, 16 March 2020: 20, 17 March 2020: 6, 18 March 2020: 6, 20 March 2020: 1, 21 March 2020: 1, 22 March 2020: 2, 27 March 2020: 1, 30 March 2020: 12.

The bottom left panel, B, shows a map of Georgia and counties are shaded by the cumulative number of reported cases as of 31 March 2020. The top 10 counties with the most cases are as follows: Fulton: 3409, Dougherty: 1980, DeKalb: 1949, Cobb: 1794, Bartow: 1137, Gwinnett: 1090, Carroll: 548, Cherokee: 514, Clayton: 480, Lee: 396. A total of 1582 cases were reported without county data.

The bottom right panel, C, shows a map of Georgia and counties are shaded by the cumulative number of sampled sequences as of 31 March 2020. County level data is missing for 52 sequences. Amongst those with county-level data, 23 are from Fulton County, 14 from DeKalb, 8 from Gwinnett, 4 from Cobb, 2 from Fayette, 1 from Union, 1 from Polk, 1 from Henry, 1 from Forsyth, and 1 from Cherokee.

Figure 2

Multi-panel figure with three vertically stacked panels. The x-axis for panels A, B, and C is time.

The top panel, A, shows the number of Georgia sequences per-clade per-week. Weeks are assumed to start on Monday. In the week ending 2020-03-01 there are two sequences in

clade 20B and no sequences in other clades. In the second week, ending 2020-03-08 there are seven sequences in clade 19B, four sequences in clade 20B, and no sequences in other clades. In the week ending 2020-03-15 there are 39 sequences in clade 19B, one sequence in clade 20A, one sequence in 20B, and 5 sequences in 20C. In the week ending 2020-03-22 there are 26 sequences in 19B, five sequences in 20A, one sequence in 20B, and four sequences in 20C. In the week ending 2020-03-29 there is one sequence in clade 19B and no sequences in other clades. Finally, in the week ending 2020-04-05 there are four sequences in clade 19B, one in 20A, and seven sequences in clade 20C.

The middle panel, B, shows a maximum-likelihood time aligned phylogenetic tree of 4611 globally sampled sequences which includes 107 sequences from the state of Georgia. Branches are colored based on maximum-likelihood ancestral state reconstruction (inside/outside of Georgia). Georgia tips are colored based on whether they are sampled from an individual with known travel history. Sequences are labelled by clade in a heatmap to the right. Of the 107 Georgia sequences, 69 (including one traveler) are in a single subclade of clade 19B which appears to have been introduced in mid-late February 2020 based on the ancestral state reconstruction. Seven Georgia sequences, including one traveler, are in another subclade of 19B. There are seven Georgia sequences in clade 20A, including one traveler. Most do not cluster together. There are eight Georgia sequences in clade 20B, including two travelers. Two sequences cluster together: one traveler and one non-traveler. Finally, there are 16 Georgia sequences in clade 20C, including three outliers. They do not appear to cluster together, with the exception of tips that descend from large polytomous internal nodes.

The bottom panel, C, is a step plot which shows the cumulative number of introductions into the state of Georgia. The analysis is repeated on 100 bootstrap replicate trees and thus there are 100 individual lines on the figure. The earliest introduction for most lines is mid February (~2020-02-10) and is associated with a set of 69 closely related Georgia tips. The cumulative number of introductions increases relatively linearly from late February through mid-March when it plateaus at roughly 19 introductions. At right is a density plot showing the cumulative number of introductions at the end of the time series (2020-03-31). The density peaks at 19 with a 95% highest-posterior density between 17 and 21.

Figure 3

Two panel figure with the panel at left showing a maximum clade credibility Bayesian time-resolved phylogenetic tree with median node heights of 430 globally sampled sequences which are part of clade 19B. Time is displayed on the x-axis. All sequences share the following genome substitutions: T26729C, G28077C, and T28144C. Median branch lengths are shown and negative branch lengths have manually been adjusted to 0 for the purposes of visualization. Ancestral branches and nodes are annotated based on their sampling region. International sequences are assigned to their country of origin and U.S. sequences are assigned to their state of origin. The MRCA of all sequences in the tree is assigned to China and is dated in early January. The MRCA of all U.S. sequences in the tree is dated between 2020-02-01 and 2020-02-14 (portrayed as a horizontal bar over the node) with a median date of 2020-02-08 and is assigned to Georgia with a posterior probability of 0.65 (portrayed as a pie chart over the node). The direct ancestor of this node is assigned to China with posterior probability of 0.47 probability (portrayed as a pie chart over the node). The posterior probability for the grouping of the U.S. sequences in a distinct clade from the ancestral sequences is 1. Sequences from other U.S. states are nested within the sequences sampled from Georgia. Besides Georgia the most prominent U.S. states with sequences in this subclade are Illinois, Michigan, and Texas. Sequences from Texas fall within a largely monophyletic clade as do sequences from Michigan. Sequences from Illinois are largely found in one of three clades. Panel at right shows a bar plot with the estimated number of introductions of the 19B subclade shown at left into the state of Georgia. The proportion of sampled trees is shown on the y-axis. In 82.5% of the sampled trees

there is only a single introduction into Georgia, there are two estimated introductions in 5.7% of trees, three estimated introductions in 4.3% of sampled trees, four estimated introductions in 0.03% of sampled trees, five estimated introductions in 0.02% of sampled trees, six estimated introductions in 0.01% of sampled trees, six estimated introductions in 0.01% of sampled trees. There is support from less than 0.01% of sampled trees for numbers of introductions greater than six.

Figure 4

Two panel figure with the panels arranged horizontally. Both figures are scatter plots showing sequences related to the sequences sampled from known travelers. Each plot shows the sequence sampled from the traveler, sequences sampled from the region/s the individual traveled to, and sequences sampled from Georgia. The x-axis shows the date of sample collection and the y-axis shows the distance of sequences relative to Wuhan/Hu-1. The x-axis spans from 2020-02-23 to 2020-03-31. Only sequences in the same evolutionary lineage as the traveler's sequence is shown. Only sequences within 1 SNP of the travelers sequence are shown.

The left panel, A, shows data for Patient 22 (Sample 046L) who had known travel history to both Italy and Switzerland and was sampled on 2020-03-04. The sequence sampled from Patient 22 harbors eight SNPs relative to Wuhan/Hu-1 and thus the figure shows sequences in the same lineage that are seven, eight, and nine SNPs from Wuhan/Hu-1. There are 81 sequences sampled from Italy that have seven SNPs relative to Wuhan/Hu-1 distributed throughout the time span. There are five sequences sampled from Italy that are eight SNPs relative to Wuhan/Hu-1, three sampled on 2020-02-29, one sampled on 2020-03-15, and one sampled on 2020-03-30. There is one sequence sampled from Italy that has 9 SNPs and is sampled on 2020-03-22. There are 21 sequences sampled from Switzerland that have seven SNPs, distributed throughout the time frame. There are thirteen sequences sampled from Switzerland that have eight SNPs, distributed throughout the time frame. There are eight sequences sampled from Switzerland that have 9 SNPs, distributed throughout the time frame. Only a single sequence from Georgia besides Patient 22 is shown and it harbors eight SNPs and was sampled on 2020-03-04.

The right panel, B, shows data for Patient 2 (Sample 016P) who had known travel history to Louisiana and was sampled on 2020-03-16. The sequence sampled from Patient 2 also harbors eight SNPs relative to Wuhan/Hu-1 and therefore sequences in the same lineage that harbor seven, eight, and nine SNPs are shown. There are 19 sequences from Louisiana with seven SNPs, sampled between 2020-03-10 and 2020-03-31. There are seven sequences from Louisiana with eight SNPs, sampled between 2020-03-14 and 2020-03-31. There are nine sequences from Louisiana with nine SNPs, also sampled between 2020-03-14 and 2020-03-31. There are only two other samples from Georgia shown, both with seven SNPs sampled on 2020-03-15 and 2020-03-18.

Figure 5

Multi-panel figure with two panels arranged horizontally.

The left panel, A, shows a table of the substitutions shared between all Georgia sequences in the tree shown in A. The substitutions are: T490A, C3177T, C8782T, T18736C, C24034T, T26729C, G28077C, T28144C, A29700G.

The right panel, B, stretches the full width of the figure and shows the number of globally sampled sequences per week which possess the mutational profile shown in panel B over time. The top six locations are shown and the remainder are grouped in Other (USA) or Other (intl.).

In the first week (week ending 2020-03-01) there was one sequence in Other (USA). In the second week (week ending 2020-03-08) there were six sequences from Georgia, two from Florida, one from Australia, and seven from Other (USA). In the week ending 2020-03-15 there

were 33 sequences from Georgia, 15 from Australia, two from Illinois, two from Michigan, one from Texas, 47 from Other (USA), and five from Other (Intl.). In the week ending 2020-03-22 there were 24 sequences from Texas, 21 from Georgia, 20 from Michigan, 17 from Illinois, 16 from Australia, 14 from Florida, 79 from Other (USA), and seven from Other (intl.). For the week ending 2020-03-29 there were 26 sequences from Texas, 10 from Florida, 9 from Illinois, 7 from Michigan, 1 from Australia, 1 from Georgia, 54 from Other (USA), and 14 from Other (intl.). For the week ending 2020-04-05 there were 30 sequences from Texas, 4 sequences from Florida, 4 from Georgia, 2 from Michigan, 23 from Other (USA), and 11 from Other (intl.). For the week ending 2020-04-12 there were 23 sequences from Texas, 18 sequences from Florida, four from Georgia, one from Illinois, one from Michigan, 9 from Other (USA), and 12 from Other (intl.). For the week ending 2020-04-19 there were 15 sequences from Florida, six from Texas, four from Illinois, two from Michigan, one from Georgia, 17 from Other (USA), and two from Other (intl.). For the week ending 2020-04-26 there were six sequences from Florida, six from Texas, one from Georgia, one from Illinois, and five from Other (USA). For the week ending 2020-05-03 there were six sequences from Texas, one from Illinois, three from Other (USA). For the week ending 2020-05-10 there was one sequence from Florida, one from Georgia, and two from Other (USA). For the week ending 2020-05-17 there were two sequences from Florida, two from Texas, and from Illinois. For the week ending 2020-05-24 there was one sequence from Texas, two from Other (USA), and two from Other (intl.). For the week ending 2020-05-31 there was one sequence from Illinois, one from Texas, and nine from Other (USA). For the week ending 2020-06-28 there was one sequence from Illinois. For the week ending 2020-07-05 there was one sequence from Georgia. For the week ending 2020-08-23 there was one sequence from Texas.

Chapter 7

Discussion

As viral pathogens replicate within-hosts and are transmitted between-hosts, they accumulate mutations in their genomes due to errors by the RNA polymerase. Many of these are lethal to the virus and unlikely to be observed and a very small subset improve viral fitness [1]. The remainder, however, are neutral or slightly deleterious (quasi-neutral) to viral fitness. Nevertheless the collection of these quasi-neutral mutations contains clues as to the processes which gave rise to the sampled genetic diversity. Here, I interrogate the patterns in influenza A and SARS-CoV-2 sequence data to reveal the ecological, epidemiological, and evolutionary forces which have shaped these populations.

Within human hosts, the amount of genetic diversity in the form of single nucleotide polymorphisms (SNPs) has been shown to be relatively minimal [2], which limits our understanding of the forces shaping within-host influenza diversity. As a result, in **Chapter 2**, I propose using alternative signal, that which is present in the genomic diversity. Specifically, I focus on the defective viral genomes (DVGs) generated during infection. DVGs are virions which harbor a large internal deletion in at least one segment, rendering them incapable of replicating on their own. Coinfection of cells with wild-type virus allows DVGs to proliferate throughout an infection. Based on this reliance on coinfection and the spatial structure of *in vivo* infections [3] I expect the dynamics of DVG diversity to mimic those of wild-type virus.

I identify DVGs in the deep sequencing data from nearly every sample, primarily in the three polymerase segments consistent with previous findings in the field [4]. The majority of the DVGs I identified have the canonical DVG breakpoints in which the packaging signals on the 5' and 3' ends of the genome are retained and all or the majority of the coding region is deleted. By looking at longitudinal data I show that DVG populations are highly dynamic across time points. However, DVG populations are more similar across shorter time intervals and more abundant DVGs are more likely to persist across time points. These dynamics are consistent with the dominance of genetic drift and consistent with the within-host dynamics of SNPs [2].

To investigate how within-host dynamics translate to dynamics observed at the host population scale, we turn to sequence data from the ongoing SARS-CoV-2 pandemic (reviewed in **Chapter 3**). First, I specifically focus on quantifying the transmission bottleneck, or the number of virions transmitted between a donor and recipient host (**Chapter 4**). By fitting a model to deep sequencing data from 39 transmission pairs, I estimate the bottleneck to be on the order of 1-3 virions. From an evolutionary perspective, this implies that population sizes are extremely small early in infection, which means that genetic drift will dominate the evolutionary dynamics. This will promote the fixation of novel variants either at transmission due to the stochastic transmission of low-frequency donor variations or shortly after transmission due to the fixation of *de novo* variants in the recipient. Consequently, very little genetic diversity is transmitted across chains and within-host selection on beneficial mutations must essentially reset at each transmission event.

Finally, I take advantage of the collection of substitutions present in host-population scale consensus sequence data to reveal the underlying epidemiological scenarios shaping the SARS-CoV-2 pandemic in early 2020. In Israel (**Chapter 5**) I use a Bayesian phylodynamic model to first show that non-pharmaceutical interventions were associated with a significant decrease in the reproductive number of the virus. However, arguably more interestingly, I show that transmission is highly heterogeneous: less than 10% of infected individuals are

responsible for more than 80% of transmissions. I find a consistent pattern in the state of Georgia, USA (**Chapter 6**). While I identify many independent introductions of SARS-CoV-2 into the state, the vast majority of sampled sequences were from a single introduction. This implies that while the transmission chains sparked by the majority of introductions stochastically died out, the successful introduction was likely disseminated throughout the population due to a superspreading event or a high-contact subset of the social network within the state.

Taken together, my results highlight the importance of stochasticity and heterogeneity in disease dynamics, across biological scales. This has important implications for our understanding of how infectious agents spread between people and how their genomes change throughout this spread. My findings that genetic drift is a strong driver of viral dynamics within hosts and transmission bottlenecks are small indicate that selection is likely very inefficient in this context. While not explicitly analyzed here, this hints at the importance of chronic infections (where selection has more time to fix beneficial mutations [5, 6]) or reservoir species (where the evolutionary context may be different [7, 8]) as a source for beneficial viral genotypes. For example, these explanations are currently widely accepted as the most likely source of novel SARS-CoV-2 variants of concern [9].

Epidemiologically, the stochasticity introduced by transmission heterogeneity results in a number of analysis and policy challenges. This long-acknowledged phenomenon decreases the probability that any given introduction of a pathogen into a region will spark sustained transmission (as observed in **Chapter 6**), but increases the speed of an outbreak, given it does not stochastically go extinct [10]. It has been proposed that by “chopping the tail,” that is eliminating the scenarios where superspreading occurs, the spread of SARS-CoV-2 could be controlled with relatively limited disruption to most daily activities [11]. However, implementing such strategies differs if superspreading occurs due to superspreaders, i.e. highly infectious individuals, or superspreading events, i.e. social gatherings particularly likely to promote transmission. From my results, I cannot disentangle the contribution of

these two distinct forces to the transmission heterogeneity of SARS-CoV-2. Recent data, however implies that variation in infectiousness between individuals plays at least some role in the superspreading dynamics of SARS-CoV-2 [12]. From a modeling perspective, the effects of superspreading make forecasting disease dynamics difficult [10]. The realized disease trajectory follows only one of the many possible stochastic realizations of the epidemic process. The more superspreading that exists in the transmission process the more variation that exists within these possible realizations. This issue also affects our ability to predict the emergence of new viral lineages which harbor fitness advantages compared to existing lineages. A lineage which stochastically finds itself transmitted during a superspreading event may appear to harbor a genuine fitness advantage based on its increased prevalence in the population (e.g. as described in [13]) regardless of its selective advantage. Alternatively stated, superspreading will increase transient variations in the lineage makeup of a given population which hinders our ability to detect genuine lineages with an evolutionary advantage.

On a different note, our analysis in **Chapter 4** provides a cautionary tale to computational modelers. Initial analyses of the same dataset identified a large transmission bottleneck for SARS-CoV-2 [14]. This finding, however was largely driven by the presence of spurious variants in the deep sequencing data. Similarly, a study out of the U.K. initially reported a large SARS-CoV-2 transmission bottleneck [15], but the estimates were ultimately revised during peer view to support a much smaller bottleneck [16]. Thus, it is not enough to simply apply inference methods to data. One must understand potential sources of error and bias in the data and be familiar with how the inference method can be affected by these biases. Rigorous inference methods applied to biased or error-prone data can, and often will, provide researchers with invalid results.

While great strides in our understanding of human RNA virus ecology, epidemiology, and evolution in recent years, there are a number of important open questions and methodological challenges in the field that remain to be tackled. From a methods standpoint, the number

of SARS-CoV-2 sequenced genomes has greatly eclipsed previous pandemics. This presents considerable challenges, particularly for traditional phylodynamic methods [17, 18], which are incredibly resource intensive. As a result, downsampling the available data has become commonplace [19]. This procedure inherently reduces the signal in the data which leaves considerable opportunity for methods that can operate directly on the scale of available data. In a similar vein, traditional phylodynamic methods (e.g. [20]) are too slow for real-time monitoring of the emergence of lineages with fitness advantages over ancestral lineages. As a result, most monitoring is currently being done by fitting models to the relative proportion of sequences in different lineages [21]. This, however, is inherently a reactive procedure that requires prior identification of the lineages under monitoring. Furthermore, these methods do not account for the underlying genetic diversity within a set of sequences and therefore can provide misleading results if sampling is non-representative. Additionally, most methods for host population scale monitoring of viral evolution rely only on consensus level data and therefore do not consider genetic variation within hosts. This may limit the sensitivity to identifying the selective pressures which act within hosts, as evidenced by the independent within-host evolution of D614G reported in [22]. Finally, my findings in **Chapter 4** indicate that transmission itself fixes mutations in the viral genome. This finding affords an alternative framing to the popular “molecular clock” framing which states that mutations are acquired at a given rate per unit of calendar time [23]. We propose that this finding can be leveraged to infer the number of transmission and hence epidemiological parameters, from the number of novel mutations in the viral genome [24].

The technology to sequence viral genomes has been transformative in our understanding of their ecology, epidemiology, and evolution. These data are particularly valuable when coupled with quantitative modeling approaches that can tease apart the ecological and evolutionary processes driving viral evolution. Here, I present analyses of influenza and SARS-CoV-2 sequence data with a focus on what the signals in accumulation can tell us about the underlying viral population dynamics. I feel that these studies complement existing and

ongoing work in the field and add to our growing understanding of how viral pathogens change within, between, and amongst human hosts.

Chapter 7 References

- [1] R. Sanjuan, A. Moya, and S. F. Elena, “The distribution of fitness effects caused by single-nucleotide substitutions in an RNA virus,” *Proceedings of the National Academy of Sciences*, vol. 101, pp. 8396–8401, June 2004.
- [2] J. T. McCrone, R. J. Woods, E. T. Martin, R. E. Malosh, A. S. Monto, and A. S. Llaure, “Stochastic processes constrain the within and between host evolution of influenza virus,” *eLife*, vol. 7, pp. 1–19, 2018.
- [3] M. E. Gallagher, C. B. Brooke, R. Ke, and K. Koelle, “Causes and Consequences of Spatial Within-Host Viral Spread,” *Viruses*, vol. 10, no. 11, pp. 1–23, 2018.
- [4] L. Pelz, D. Rüdiger, T. Dogra, F. G. Alnaji, Y. Genzel, C. B. Brooke, S. Y. Kupke, and U. Reichl, “Semi-continuous Propagation of Influenza A Virus and Its Defective Interfering Particles: Analyzing the Dynamic Competition To Select Candidates for Antiviral Therapy,” *Journal of Virology*, vol. 95, pp. e01174–21, Nov. 2021.
- [5] K. S. Xue, T. Stevens-Ayers, A. P. Campbell, J. A. Englund, S. A. Pergam, M. Boeckh, and J. D. Bloom, “Parallel evolution of influenza across multiple spatiotemporal scales,” *eLife*, vol. 6, pp. 1–16, 2017.
- [6] The CITIID-NIHR BioResource COVID-19 Collaboration, The COVID-19 Genomics UK (COG-UK) Consortium, S. A. Kemp, D. A. Collier, R. P. Datir, I. A. T. M. Ferreira, S. Gayed, A. Jahun, M. Hosmillo, C. Rees-Spear, P. Mlcochova, I. U. Lumb,

- D. J. Roberts, A. Chandra, N. Temperton, K. Sharrocks, E. Blane, Y. Modis, K. E. Leigh, J. A. G. Briggs, M. J. van Gils, K. G. C. Smith, J. R. Bradley, C. Smith, R. Doffinger, L. Ceron-Gutierrez, G. Barcenas-Morales, D. D. Pollock, R. A. Goldstein, A. Smielewska, J. P. Skittrall, T. Gouliouris, I. G. Goodfellow, E. Gkrania-Klotsas, C. J. R. Illingworth, L. E. McCoy, and R. K. Gupta, “SARS-CoV-2 evolution during treatment of chronic infection,” *Nature*, vol. 592, pp. 277–282, Apr. 2021.
- [7] V. L. Hale, P. M. Dennis, D. S. McBride, J. M. Nolting, C. Madden, D. Huey, M. Ehrlich, J. Grieser, J. Winston, D. Lombardi, S. Gibson, L. Saif, M. L. Killian, K. Lantz, R. M. Tell, M. Torchetti, S. Robbe-Austerman, M. I. Nelson, S. A. Faith, and A. S. Bowman, “SARS-CoV-2 infection in free-ranging white-tailed deer,” *Nature*, vol. 602, pp. 481–486, Feb. 2022.
- [8] L. Lu, R. S. Sikkema, F. C. Velkers, D. F. Nieuwenhuijse, E. A. J. Fischer, P. A. Meijer, N. Bouwmeester-Vincken, A. Rietveld, M. C. A. Wegdam-Blans, P. Tolsma, M. Koppelman, L. A. M. Smit, R. W. Hakze-van der Honing, W. H. M. van der Poel, A. N. van der Spek, M. A. H. Spierenburg, R. J. Molenaar, J. d. Rond, M. Augustijn, M. Woolhouse, J. A. Stegeman, S. Lycett, B. B. Oude Munnink, and M. P. G. Koopmans, “Adaptation, spread and transmission of SARS-CoV-2 in farmed minks and associated humans in the Netherlands,” *Nature Communications*, vol. 12, p. 6802, Dec. 2021.
- [9] S. P. Otto, T. Day, J. Arino, C. Colijn, J. Dushoff, M. Li, S. Mechai, G. Van Domselaar, J. Wu, D. J. Earn, and N. H. Ogden, “The origins and potential future of SARS-CoV-2 variants of concern in the evolving COVID-19 pandemic,” *Current Biology*, vol. 31, pp. R918–R929, July 2021.
- [10] J. O. Lloyd-Smith, S. J. Schreiber, P. E. Kopp, and W. M. Getz, “Superspreading and the effect of individual variation on disease emergence,” *Nature*, vol. 438, pp. 355–359, Nov. 2005.

- [11] M. P. Kain, M. L. Childs, A. D. Becker, and E. A. Mordecai, “Chopping the tail: How preventing superspreading can help to maintain COVID-19 control,” *Epidemics*, vol. 34, p. 100430, Mar. 2021.
- [12] R. Ke, P. P. Martinez, R. L. Smith, L. L. Gibson, A. Mirza, M. Conte, N. Gallagher, C. H. Luo, J. Jarrett, R. Zhou, A. Conte, T. Liu, M. Farjo, K. K. O. Walden, G. Rendon, C. J. Fields, L. Wang, R. Fredrickson, D. C. Edmonson, M. E. Baughman, K. K. Chiu, H. Choi, K. R. Scardina, S. Bradley, S. L. Gloss, C. Reinhart, J. Yedetore, J. Quicksall, A. N. Owens, J. Broach, B. Barton, P. Lazar, W. J. Heetderks, M. L. Robinson, H. H. Mostafa, Y. C. Manabe, A. Pekosz, D. D. McManus, and C. B. Brooke, “Daily longitudinal sampling of SARS-CoV-2 infection reveals substantial heterogeneity in infectiousness,” *Nature Microbiology*, vol. 7, pp. 640–652, May 2022.
- [13] E. B. Hodcroft, M. Zuber, S. Nadeau, T. G. Vaughan, K. H. D. Crawford, C. L. Althaus, M. L. Reichmuth, J. E. Bowen, A. C. Walls, D. Corti, J. D. Bloom, D. Veessler, D. Mateo, A. Hernando, I. Comas, F. González-Candelas, SeqCOVID-SPAIN consortium, F. González-Candelas, G. A. Goig, . Chiner-Oms, I. Cancino-Muñoz, M. G. López, M. Torres-Puente, I. Gomez-Navarro, S. Jiménez-Serrano, L. Ruiz-Roldán, M. A. Bracho, N. García-González, L. Martínez-Priego, I. Galán-Vendrell, P. Ruiz-Hueso, G. De Marco, M. L. Ferrús, S. Carbó-Ramírez, G. D’Auria, M. Coscollá, P. Ruiz-Rodríguez, F. J. Roig-Sena, I. Sanmartín, D. Garcia-Souto, A. Pequeno-Valtierra, J. M. C. Tubio, J. Rodríguez-Castro, N. Rabella, F. Navarro, E. Miró, M. Rodríguez-Iglesias, F. Galán-Sanchez, S. Rodriguez-Pallares, M. de Toro, M. B. Escudero, J. M. Azcona-Gutiérrez, M. B. Alberdi, A. Mayor, A. L. García-Basteiro, G. Moncunill, C. Dobaño, P. Cisteró, D. García-de Viedma, L. Pérez-Lago, M. Herranz, J. Sicilia, P. Catalán-Alonso, P. Muñoz, C. Muñoz-Cuevas, G. Rodríguez-Rodríguez, J. Alberola-Enguidanos, J. M. Nogueira, J. J. Camarena, A. Rezusta, A. Tristancho-Baró, A. Milagro, N. F. Martínez-Cameo, Y. Gracia-Grataloup, E. Martró, A. E. Bor-

doy, A. Not, A. Antuori-Torres, R. Benito, S. Algarate, J. Bueno, J. L. del Pozo, J. A. Boga, C. Castelló-Abietar, S. Rojo-Alba, M. E. Alvarez-Argüelles, S. Melon, M. Aranzamendi-Zaldumbide, A. Vergara-Gómez, J. Fernández-Pinero, M. J. Martínez, J. Vila, E. Rubio, A. Peiró-Mestres, J. Navero-Castillejos, D. Posada, D. Valverde, N. Estévez-Gómez, I. Fernandez-Silva, L. de Chiara, P. Gallego-García, N. Varela, R. Moreno, M. D. Tirado, U. Gomez-Pinedo, M. Gozalo-Margüello, M. Eliecer-Cano, J. M. Méndez-Legaza, J. Rodríguez-Lozano, M. Siller, D. Pablo-Marcos, A. Oliver, J. Reina, C. López-Causapé, A. Canut-Blasco, S. Hernáez-Crespo, M. L. A. Cordón, M.-C. Lecároz-Agara, C. Gómez-González, A. Aguirre-Quñonero, J. I. López-Mirones, M. Fernández-Torres, M. R. Almela-Ferrer, N. Gonzalo-Jiménez, M. M. Ruiz-García, A. Galiana, J. Sanchez-Almendro, G. Cilla, M. Montes, L. Piñeiro, A. Sorarrain, J. M. Marimón, M. D. Gomez-Ruiz, J. L. López-Hontangas, E. M. González Barberá, J. M. Navarro-Marí, I. Pedrosa-Corral, S. Sanbonmatsu-Gámez, C. Pérez-González, F. Chamizo-López, A. Bordes-Benítez, D. Navarro, E. Albert, I. Torres, I. Gascón, C. J. Torregrosa-Hetland, E. Pastor-Boix, P. Cascales-Ramos, B. Fuster-Escrivá, C. Gimeno-Cardona, M. D. Ocete, R. Medina-Gonzalez, J. González-Cantó, O. Martínez-Macias, B. Palop-Borrás, I. de Toro, M. C. Mediavilla-Gradolph, M. Pérez-Ruiz, . González-Recio, M. Gutiérrez-Rivas, E. Simarro-Córdoba, J. Lozano-Serra, L. Robles-Fonseca, A. de Salazar, L. Viñuela-González, N. Chueca, F. García, C. Gómez-Camarasa, A. Carvajal, R. de la Puente, V. Martín-Sánchez, J.-M. Fregeneda-Grandes, A. J. Molina, H. Argüello, T. Fernández-Villa, M. A. Farga-Martí, V. Domínguez-Márquez, J. J. Costa-Alcalde, R. Trastoy, G. Barbeito-Castiñeiras, A. Coira, M. L. Pérez-del Molino, A. Aguilera, A. M. Planas, A. Soriano, I. Fernandez-Cádenas, J. Pérez-Tur, M. . Marcos, A. Moreno-Docón, E. Viedma, J. Mingorance, J. C. Galán-Montemayor, M. Parra-Grande, T. Stadler, and R. A. Neher, “Spread of a SARS-CoV-2 variant through Europe in the summer of 2020,” *Nature*, vol. 595, pp. 707–712, July 2021.

[14] A. Popa, J.-W. Genger, M. D. Nicholson, T. Penz, D. Schmid, S. W. Aberle, B. Agerer,

- A. Lercher, L. Endler, H. Colaço, M. Smyth, M. Schuster, M. L. Grau, F. Martínez-Jiménez, O. Pich, W. Borena, E. Pawelka, Z. Keszei, M. Senekowitsch, J. Laine, J. H. Aberle, M. Redlberger-Fritz, M. Karolyi, A. Zoufaly, S. Maritschnik, M. Borkovec, P. Hufnagl, M. Nairz, G. Weiss, M. T. Wolfinger, D. von Laer, G. Superti-Furga, N. Lopez-Bigas, E. Puchhammer-Stöckl, F. Allerberger, F. Michor, C. Bock, and A. Bergthaler, “Genomic epidemiology of superspreading events in Austria reveals mutational dynamics and transmission properties of SARS-CoV-2,” *Science Translational Medicine*, vol. 12, p. eabe2555, Dec. 2020.
- [15] K. A. Lythgoe, M. Hall, L. Ferretti, M. de Cesare, A. Trebes, M. Andersson, N. Otecko, E. L. Wise, N. Moore, J. Lynch, S. Kidd, N. Cortes, M. Mori, A. Green, M. A. Ansari, L. Abeler-Dörner, C. E. Moore, R. Shaw, P. Simmonds, D. Buck, and J. A. Todd, “Shared SARS-CoV-2 diversity suggests localised transmission of minority variants,” p. 42, June 2020.
- [16] K. A. Lythgoe, M. Hall, L. Ferretti, M. de Cesare, G. MacIntyre-Cockett, A. Trebes, M. Andersson, N. Otecko, E. L. Wise, N. Moore, J. Lynch, S. Kidd, N. Cortes, M. Mori, R. Williams, G. Vernet, A. Justice, A. Green, S. M. Nicholls, M. A. Ansari, L. Abeler-Dörner, C. E. Moore, T. E. A. Peto, D. W. Eyre, R. Shaw, P. Simmonds, D. Buck, J. A. Todd, on behalf of the Oxford Virus Sequencing Analysis Group (OVSG), T. R. Connor, S. Ashraf, A. da Silva Filipe, J. Shepherd, E. C. Thomson, The COVID-19 Genomics UK (COG-UK) Consortium, D. Bonsall, C. Fraser, and T. Golubchik, “SARS-CoV-2 within-host diversity and transmission,” *Science*, vol. 372, p. eabg0821, Apr. 2021.
- [17] A. J. Drummond and A. Rambaut, “CEAST: Cayesian evolutionary analysis by sampling trees,” *CMC Evolutionary Biology*, vol. 7, no. 1, p. 214, 2007.
- [18] R. Couckaert, J. Heled, D. Kühnert, T. Vaughan, C.-H. Wu, D. Xie, M. A. Suchard, A. Rambaut, and A. J. Drummond, “CEAST 2: A Software Platform for Cayesian Evolutionary Analysis,” *PLoS Computational Biology*, vol. 10, p. e1003537, Apr. 2014.

- [19] E. Colyen, M. R. Dillon, N. A. Bokulich, J. T. Ladner, B. B. Larsen, C. M. Hepp, D. Lemmer, J. W. Sahl, A. Sanchez, C. Holdgraf, C. Sewell, A. G. Choudhury, J. Stachurski, M. McKay, D. M. Engelthaler, M. Worobey, P. Keim, and J. G. Caporaso, “Reproducibly sampling SARS-CoV-2 genomes across time, geography, and viral diversity,” *F1000Research*, vol. 9, p. 657, June 2020.
- [20] E. Volz, V. Hill, J. T. McCrone, A. Price, D. Jorgensen, . O’Toole, J. Southgate, R. Johnson, B. Jackson, F. F. Nascimento, S. M. Rey, S. M. Nicholls, R. M. Colquhoun, A. da Silva Filipe, J. Shepherd, D. J. Pascall, R. Shah, N. Jesudason, K. Li, R. Jarrett, N. Pacchiarini, M. Bull, L. Geidelberg, I. Siveroni, I. Goodfellow, N. J. Loman, O. G. Pybus, D. L. Robertson, E. C. Thomson, A. Rambaut, T. R. Connor, C. Koshy, E. Wise, N. Cortes, J. Lynch, S. Kidd, M. Mori, D. J. Fairley, T. Curran, J. P. McKenna, H. Adams, C. Fraser, T. Golubchik, D. Bonsall, C. Moore, S. L. Caddy, F. A. Khokhar, M. Wantoch, N. Reynolds, B. Warne, J. Maksimovic, K. Spellman, K. McCluggage, M. John, R. Beer, S. Affi, S. Morgan, A. Marchbank, A. Price, C. Kitchen, H. Gulliver, I. Merrick, J. Southgate, M. Guest, R. Munn, T. Workman, T. R. Connor, W. Fuller, C. Bresner, L. B. Snell, T. Charalampous, G. Nebbia, R. Batra, J. Edgeworth, S. C. Robson, A. Beckett, K. F. Loveson, D. M. Aanensen, A. P. Underwood, C. A. Yeats, K. Abudahab, B. E. Taylor, M. Menegazzo, G. Clark, W. Smith, M. Khakh, V. M. Fleming, M. M. Lister, H. C. Howson-Wells, L. Berry, T. Boswell, A. Joseph, I. Willingham, P. Bird, T. Helmer, K. Fallon, C. Holmes, J. Tang, V. Raviprakash, S. Campbell, N. Sheriff, M. W. Loose, N. Holmes, C. Moore, M. Carlile, V. Wright, F. Sang, J. Debebe, F. Coll, A. W. Signell, G. Betancor, H. D. Wilson, T. Feltwell, C. J. Houldcroft, S. Eldirdiri, A. Kenyon, T. Davis, O. Pybus, L. du Plessis, A. Zarebski, J. Raghvani, M. Kraemer, S. Francois, S. Attwood, T. Vasylyeva, M. E. Torok, W. L. Hamilton, I. G. Goodfellow, G. Hall, A. S. Jahun, Y. Chaudhry, M. Hosmillo, M. L. Pinckert, I. Georgana, A. Yakovleva, L. W. Meredith, S. Moses, H. Lowe, F. Ryan, C. L. Fisher, A. R. Awan, J. Boyes, J. Breuer, K. A. Harris, J. R. Brown, D. Shah, L. Atkinson, J. C.

Lee, A. Alcolea-Medina, N. Moore, N. Cortes, R. Williams, M. R. Chapman, L. J. Levett, J. Heaney, D. L. Smith, M. Bashton, G. R. Young, J. Allan, J. Loh, P. A. Randell, A. Cox, P. Madona, A. Holmes, F. Bolt, J. Price, S. Mookerjee, A. Rowan, G. P. Taylor, M. Ragonnet-Cronin, F. F. Nascimento, D. Jorgensen, I. Siveroni, R. Johnson, O. Boyd, L. Geidelberg, E. M. Volz, K. Brunker, K. L. Smollett, N. J. Loman, J. Quick, C. McMurray, J. Stockton, S. Nicholls, W. Rowe, R. Poplawski, R. T. Martinez-Nunez, J. Mason, T. I. Robinson, E. O'Toole, J. Watts, C. Breen, A. Cowell, C. Ludden, G. Sluga, N. W. Machin, S. S. Ahmad, R. P. George, F. Halstead, V. Sivaprakasam, E. C. Thomson, J. G. Shepherd, P. Asamaphan, M. O. Niebel, K. K. Li, R. N. Shah, N. G. Jesudason, Y. A. Parr, L. Tong, A. Broos, D. Mair, J. Nichols, S. N. Carmichael, K. Nomikou, E. Aranday-Cortes, N. Johnson, I. Starinskij, A. da Silva Filipe, D. L. Robertson, R. J. Orton, J. Hughes, S. Vattipally, J. B. Singer, A. D. Hale, L. R. Macfarlane-Smith, K. L. Harper, Y. Taha, B. A. Payne, S. Burton-Fanning, S. Waugh, J. Collins, G. Eltringham, K. E. Templeton, M. P. McHugh, R. Dewar, E. Wastenge, S. Dervisevic, R. Stanley, R. Prakash, C. Stuart, N. Elumogo, D. K. Sethi, E. J. Meader, L. J. Coupland, W. Potter, C. Graham, E. Barton, D. Padgett, G. Scott, E. Swindells, J. Greenaway, A. Nelson, W. C. Yew, P. C. Resende Silva, M. Andersson, R. Shaw, T. Peto, A. Justice, D. Eyre, D. Crooke, S. Hoosdally, T. J. Sloan, N. Duckworth, S. Walsh, A. J. Chauhan, S. Glaysher, K. Bicknell, S. Wyllie, E. Butcher, S. Elliott, A. Lloyd, R. Impney, N. Levene, L. Monaghan, D. T. Bradley, E. Allara, C. Pearson, P. Muir, I. B. Vipond, R. Hopes, H. M. Pymont, S. Hutchings, M. D. Curran, S. Parmar, A. Lackenby, T. Mbisa, S. Platt, S. Miah, D. Bibby, C. Manso, J. Hubb, M. Chand, G. Dabrera, M. Ramsay, D. Bradshaw, A. Thornton, R. Myers, U. Schaefer, N. Groves, E. Gallagher, D. Lee, D. Williams, N. Ellaby, I. Harrison, H. Hartman, N. Manesis, V. Patel, C. Bishop, V. Chalker, H. Osman, A. Bosworth, E. Robinson, M. T. Holden, S. Shaaban, A. Birchley, A. Adams, A. Davies, A. Gaskin, A. Plimmer, B. Gatica-Wilcox, C. McKerr, C. Moore, C. Williams, D. Heyburn, E. De Lacy, E. Hilvers, F. Downing,

G. Shankar, H. Jones, H. Asad, J. Coombes, J. Watkins, J. M. Evans, L. Fina, L. Gifford, L. Gilbert, L. Graham, M. Perry, M. Morgan, M. Bull, M. Cronin, N. Pacchiarini, N. Craine, R. Jones, R. Howe, S. Corden, S. Rey, S. Kumziene-Summerhayes, S. Taylor, S. Cottrell, S. Jones, S. Edwards, J. O'Grady, A. J. Page, J. Wain, M. A. Webber, A. E. Mather, D. J. Baker, S. Rudder, M. Yasir, N. M. Thomson, A. Aydin, A. P. Tedim, G. L. Kay, A. J. Trotter, R. A. Gilroy, N.-F. Alikhan, L. de Oliveira Martins, T. Le-Viet, L. Meadows, A. Kolyva, M. Diaz, A. Bell, A. V. Gutierrez, I. G. Charles, E. M. Adriaenssens, R. A. Kingsley, A. Casey, D. A. Simpson, Z. Molnar, T. Thompson, E. Acheson, J. A. Masoli, B. A. Knight, A. Hattersley, S. Ellard, C. Auckland, T. W. Mahungu, D. Irish-Tavares, T. Haque, Y. Bourgeois, G. P. Scarlett, D. G. Partridge, M. Raza, C. Evans, K. Johnson, S. Liggett, P. Baker, S. Essex, R. A. Lyons, L. G. Caller, S. Castellano, R. J. Williams, M. Kristiansen, S. Roy, C. A. Williams, P. L. Dyal, H. J. Tutill, Y. N. Panchbhaya, L. M. Forrest, P. Niola, J. Findlay, T. T. Brooks, A. Gavriil, L. Mestek-Boukhibar, S. Weeks, S. Pandey, L. Berry, K. Jones, A. Richter, A. Beggs, C. P. Smith, G. Bucca, A. R. Hesketh, E. M. Harrison, S. J. Peacock, S. Palmer, C. M. Churcher, K. L. Bellis, S. T. Girgis, P. Naydenova, B. Blane, S. Sridhar, C. Ruis, S. Forrest, C. Cormie, H. K. Gill, J. Dias, E. E. Higginson, M. Maes, J. Young, L. M. Kermack, N. F. Hadjirin, D. Aggarwal, L. Griffith, T. Swingler, R. K. Davidson, A. Rambaut, T. Williams, C. E. Balcazar, M. D. Gallagher, . O'Toole, S. Rooke, B. Jackson, R. Colquhoun, J. Ashworth, V. Hill, J. McCrone, E. Scher, X. Yu, K. A. Williamson, T. D. Stanton, S. L. Michell, C. M. Bewshea, B. Temper-ton, M. L. Michelsen, J. Warwick-Dugdale, R. Manley, A. Farbos, J. W. Harrison, C. M. Sambles, D. J. Studholme, A. R. Jeffries, A. C. Darby, J. A. Hiscox, S. Paterson, M. Iturriza-Gomara, K. A. Jackson, A. O. Lucaci, E. E. Vamos, M. Hughes, L. Rainbow, R. Eccles, C. Nelson, M. Whitehead, L. Turtle, S. T. Haldenby, R. Gregory, M. Gemmell, D. Kwiatkowski, T. I. de Silva, N. Smith, A. Angyal, B. B. Lindsey, D. C. Groves, L. R. Green, D. Wang, T. M. Freeman, M. D. Parker, A. J. Keeley, P. J.

Parsons, R. M. Tucker, R. Brown, M. Wyles, C. Constantinidou, M. Unnikrishnan, S. Ott, J. K. Cheng, H. E. Bridgewater, L. R. Frost, G. Taylor-Joyce, R. Stark, L. Baxter, M. T. Alam, P. E. Brown, P. C. McClure, J. G. Chappell, T. Tsoleridis, J. Ball, D. Gramatopoulos, D. Buck, J. A. Todd, A. Green, A. Trebes, G. MacIntyre-Cockett, M. de Cesare, C. Langford, A. Alderton, R. Amato, S. Goncalves, D. K. Jackson, I. Johnston, J. Sillitoe, S. Palmer, M. Lawniczak, M. Berriman, J. Danesh, R. Livett, L. Shirley, B. Farr, M. Quail, S. Thurston, N. Park, E. Betteridge, D. Weldon, S. Goodwin, R. Nelson, C. Beaver, L. Letchford, D. A. Jackson, L. Foulser, L. McMinn, L. Prestwood, S. Kay, L. Kane, M. J. Dorman, I. Martincorena, C. Puethe, J.-P. Keatley, G. Tonkin-Hill, C. Smith, D. Jamrozy, M. A. Beale, M. Patel, C. Ariani, M. Spencer-Chapman, E. Drury, S. Lo, S. Rajatileka, C. Scott, K. James, S. K. Buddenborg, D. J. Berger, G. Patel, M. V. Garcia-Casado, T. Dibling, S. McGuigan, H. A. Rogers, A. D. Hunter, E. Souster, and A. S. Neaverson, “Evaluating the Effects of SARS-CoV-2 Spike Mutation D614G on Transmissibility and Pathogenicity,” *Cell*, vol. 184, pp. 64–75.e11, Jan. 2021.

- [21] M. D. Figgins and T. Bedford, “SARS-CoV-2 variant dynamics across US states show consistent differences in effective reproduction numbers,” Dec. 2021.
- [22] G. Tonkin-Hill, I. Martincorena, R. Amato, A. R. Lawson, M. Gerstung, I. Johnston, D. K. Jackson, N. Park, S. V. Lensing, M. A. Quail, S. Goncalves, C. Ariani, M. Spencer Chapman, W. L. Hamilton, L. W. Meredith, G. Hall, A. S. Jahun, Y. Chaudhry, M. Hosmillo, M. L. Pinckert, I. Georgana, A. Yakovleva, L. G. Caller, S. L. Caddy, T. Feltwell, F. A. Khokhar, C. J. Houldcroft, M. D. Curran, S. Parmar, The COVID-19 Genomics UK (COG-UK) Consortium, A. Alderton, R. Nelson, E. M. Harrison, J. Sillitoe, S. D. Bentley, J. C. Barrett, M. E. Torok, I. G. Goodfellow, C. Langford, D. Kwiatkowski, and Wellcome Sanger Institute COVID-19 Surveillance Team, “Patterns of within-host genetic diversity in SARS-CoV-2,” *eLife*, vol. 10, p. e66857, Aug.

2021.

- [23] L. Cromham and D. Penny, “The modern molecular clock,” *Nature Reviews Genetics*, vol. 4, pp. 216–224, Mar. 2003.
- [24] Y. Park, M. Martin, and K. Koelle, “Phylodynamic inference for emerging viruses using segregating sites,” July 2021.